technische universität
dortmund

MAX-PLANCK-INSTITUT
FÜR KOHLENFORSCHUNG

Kollektive Totalsynthese
der Casban Diterpene:
Eine Strategie − Diverse Naturstoffe

Dissertation

zur Erlangung des akademischen Grades
eines Doktors der Naturwissenschaften (Dr. rer. nat.)
der Fakultät für Chemie und Chemische Biologie
der Technischen Universität Dortmund

vorgelegt von

Lorenz Ewan Löffler

Mülheim an der Ruhr
2021

Eidesstattliche Versicherung (Affidavit)

Löffler, Lorenz Ewan
‾‾‾‾‾‾‾‾‾‾‾‾‾‾‾‾‾‾‾‾‾‾‾‾‾‾‾‾‾‾
Name, Vorname
(Surname, first name)

‾‾‾‾‾‾‾‾‾‾‾‾‾‾‾‾‾‾‾‾‾‾‾‾‾‾‾‾‾‾
Matrikel-Nr.
(Enrolment number)

Belehrung:

Wer vorsätzlich gegen eine die Täuschung über Prüfungsleistungen betreffende Regelung einer Hochschulprüfungsordnung verstößt, handelt ordnungswidrig. Die Ordnungswidrigkeit kann mit einer Geldbuße von bis zu 50.000,00 € geahndet werden. Zuständige Verwaltungsbehörde für die Verfolgung und Ahndung von Ordnungswidrigkeiten ist der Kanzler/die Kanzlerin der Technischen Universität Dortmund. Im Falle eines mehrfachen oder sonstigen schwerwiegenden Täuschungsversuches kann der Prüfling zudem exmatrikuliert werden, § 63 Abs. 5 Hochschulgesetz NRW.

Die Abgabe einer falschen Versicherung an Eides statt ist strafbar.

Wer vorsätzlich eine falsche Versicherung an Eides statt abgibt, kann mit einer Freiheitsstrafe bis zu drei Jahren oder mit Geldstrafe bestraft werden, § 156 StGB. Die fahrlässige Abgabe einer falschen Versicherung an Eides statt kann mit einer Freiheitsstrafe bis zu einem Jahr oder Geldstrafe bestraft werden, § 161 StGB.

Die oben stehende Belehrung habe ich zur Kenntnis genommen:

Official notification:

Any person who intentionally breaches any regulation of university examination regulations relating to deception in examination performance is acting improperly. This offence can be punished with a fine of up to EUR 50,000.00. The competent administrative authority for the pursuit and prosecution of offences of this type is the chancellor of the TU Dortmund University. In the case of multiple or other serious attempts at deception, the candidate can also be unenrolled, Section 63, paragraph 5 of the Universities Act of North Rhine-Westphalia.

The submission of a false affidavit is punishable.

Any person who intentionally submits a false affidavit can be punished with a prison sentence of up to three years or a fine, Section 156 of the Criminal Code. The negligent submission of a false affidavit can be punished with a prison sentence of up to one year or a fine, Section 161 of the Criminal Code.

I have taken note of the above official notification.

‾‾‾‾‾‾‾‾‾‾‾‾‾‾‾‾‾‾‾‾‾‾
Ort, Datum
(Place, date)

‾‾‾‾‾‾‾‾‾‾‾‾‾‾‾‾‾‾‾‾‾‾
Unterschrift
(Signature)

Titel der Dissertation:
(Title of the thesis):

Kollektive Totalsynthese der Casban Diterpene:
Eine Strategie – Diverse Naturstoffe
‾‾‾

‾‾‾

Ich versichere hiermit an Eides statt, dass ich die vorliegende Dissertation mit dem Titel selbstständig und ohne unzulässige fremde Hilfe angefertigt habe. Ich habe keine anderen als die angegebenen Quellen und Hilfsmittel benutzt sowie wörtliche und sinngemäße Zitate kenntlich gemacht.
Die Arbeit hat in gegenwärtiger oder in einer anderen Fassung weder der TU Dortmund noch einer anderen Hochschule im Zusammenhang mit einer staatlichen oder akademischen Prüfung vorgelegen.

I hereby swear that I have completed the present dissertation independently and without inadmissible external support. I have not used any sources or tools other than those indicated and have identified literal and analogous quotations.

The thesis in its current version or another version has not been presented to the TU Dortmund University or another university in connection with a state or academic examination.*

---

*Please be aware that solely the German version of the affidavit ("Eidesstattliche Versicherung") for the PhD thesis is the official and legally binding version.

‾‾‾‾‾‾‾‾‾‾‾‾‾‾‾‾‾‾‾‾‾‾‾‾‾‾‾‾‾‾
Ort, Datum
(Place, date)

‾‾‾‾‾‾‾‾‾‾‾‾‾‾‾‾‾‾‾‾‾‾‾‾‾‾
Unterschrift
(Signature)

1. Berichterstatter: Prof. Dr. Alois Fürstner
2. Berichterstatter: Prof. Dr. Norbert Krause

Die vorliegende Arbeit entstand unter Anleitung von Prof. Dr. Alois Fürstner in der Zeit von Juli 2017 bis September 2021 am Max-Planck-Institut für Kohlenforschung in Mülheim an der Ruhr. Teile dieser Arbeit wurden bereits in folgenden Beiträgen veröffentlicht:

L. E. Löffler*, M. Buchsteiner*, L. R. Collins, F. P. Caló, S. Singha and A. Fürstner, *Helv. Chim. Acta,* **2021**, *104*, e2100042.

L. E. Löffler, C. Wirtz and A. Fürstner, *Angew. Chem. Int. Ed.* **2021**, *60*, 5316–5322.

Die praktischen Arbeiten erfolgten zum Teil in Zusammenarbeit mit Jasmin Blenk, Dr. Lee R. Collins, Michael Buchsteiner, Dr. Johanna Novacek, Philipp Müller und Phillip Schlathölter. Zur NMR-spektroskopischen Strukturaufklärung wurden einige Verbindungen von Cornelia Wirtz aus der NMR-Abteilung des Max-Planck-Instituts für Kohlenforschung unabhängig kontrolliert und bestätigt. Die Einkristallstrukturanalysen wurden von Nils Nöthling und Jörg Rust durchgeführt. Die beschriebenen Ergebnisse bilden eine vollständige Darstellung dieser gemeinsamen Arbeiten. Die von diesen Mitarbeitern alleinverantwortlich erzielten Ergebnisse wurden als solche an entsprechender Stelle vermerkt.

* Diese Autoren trugen in gleichem Maße zu dieser Arbeit bei.

Danksagung

Inhalt

Terpene sind eine imposante Gruppe sekundärer Naturstoffe mit einer großen Vielfalt an verschiedenen ungesättigten Kohlenstoffgerüsten. Die Familie der Casbane gehört zu den makrozyklischen Diterpenen und weist diverse biologische Aktivitäten auf. Einige Casbane-produzierende Pflanzen finden in der traditionellen chinesischen Medizin Anwendung. Interessanterweise wurden diese seltenen Metaboliten weltweit aus biologisch unabhängigen Organismen isoliert. Trotz ihrer vielversprechenden Eigenschaften und ihres großräumigen Auftretens wurden Casbane bisher weder synthetisiert noch ihre biologischen Aktivitäten weitergehend erforscht. Basierend auf einer modularen Konstruktion des Grundgerüstes und einer vielseitigen Diversifizierungssequenz gelang die konvergente Darstellung diverser Casbane: *in nuce* eine Strategie – diverse Naturstoffe (Abbildung 1).

Die Naturstofffamilie der Casbane besitzt als charakteristische Grundstruktur einen 14-gliedrigen ungesättigten Makrozyklus sowie ein anelliertes *gem*-Dimethylzyklopropan, welches in allen vier Konfigurationen in der Natur präsent ist.

Dieses Motiv wurde mithilfe einer Rhodium-katalysierten Zyklopropanierung enantioselektiv zum *cis*-System aufgebaut. Das entsprechende *trans*-Derivat wurde mittels anschließender Epimerisierung erzielt. Unter Alkinmetathese Bedingungen wurde der 14-gliedrige Makrozyklus in Gegenwart mehrerer Alkene geschlossen. Dies stellt einen Beleg für die Orthogonalität der Alkin- zur Alkenmetathese dar. Erstmalig wurde gezeigt, dass ein Zyklopropan in Konjugation zu einer C≡C Dreifachbindung, die an einer Ringschließenden Alkinmetathese beteiligt ist, unverändert bleibt. Abschließend wurden durch Anwendung regio- und stereoselektiver Folgechemie diverse Naturstoffe (Depressin, Euphorhylonal A und Yuexiandajisu A) dargestellt. Dies demonstriert die Vielseitigkeit der hier entwickelten Synthesestrategie.

Beim Vergleich der analytischen Daten des isolierten Naturstoffes Euphorhylonal A mit denen der postulierten und dargestellten Diastereomere zeigten sich Diskrepanzen zwischen den NMR Daten. Dies offenbarte die in der Literatur fehlerhaft zugeordnete Stereochemie. In einem computerchemischen Ansatz konnten zum einen die erhaltenen spektroskopischen Daten verifiziert und zum anderen die korrekte relative Stereochemie mit einer hohen Wahrscheinlichkeit vorausgesagt werden. Die postulierte Struktur von Euphorhylonal A konnte *via* Totalsynthese verifiziert und die absolute Konfiguration bestimmt werden.

Nach dem erfolgreichen Aufbau des Terpengerüstes wurde der Zugang zu zweifach oxygenierten Casbanen, basierend auf der zuvor entwickelten Baukastenstrategie, untersucht. Zum Einbau einer Hydroxyfunktionalität im „südlichen" Sektor war die Synthese eines neuen Bausteines erforderlich. Diesbezüglich ermöglichte die enantioselektive Bisborylierung mit anschließender chemoselektiver Oxygenierung die Installation dieser Hydroxyfunktionalität und stellt einen Schlüsselschritt auf dem Weg zur ersten Totalsynthese von 2-*epi*-10-Hydroxydepressin dar. Zukünftige Arbeiten zum Aufbau des 14-gliedrigen Makrozyklus und Darstellung weiterer Casbane sollen die Robustheit, der hier entwickelten Synthesestrategie, unterstreichen.
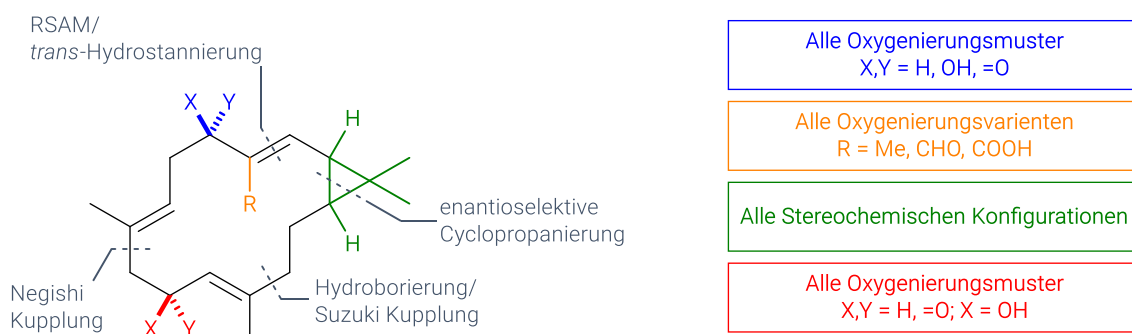
Abbildung 1. Allgemeine retrosynthetische Analyse der Casban Naturstofffamilie.

Der Aufbau des *gem*-Dimethylzyklopropans basierte auf den Rh-Katalysatoren [Rh$_2$(5*R*-MEPY)$_4$] oder [Rh$_2$(5*S*-MEPY)$_4$], welche zuerst von Doyle und Mitarbeitern beschrieben wurden. Um ausreichend Katalysator zur Verfügung zu stellen, sollte der Zugang zu diesen Katalysatorsystemen verbessert werden. In einem weiteren methodischen Ansatz sollte die zugrundeliegende Reaktivität der Rhodium-Rhodium-Katalysatoren mit der Reaktivität der analogen Wismut-Rhodium-Komplexe untersucht werden.

Basierend auf synthetischen Vorarbeiten innerhalb der Gruppe konnte durch ein effizienteres Verfahren die Ausbeute des [Rh$_2$(5*S*-MEPY)$_4$] Katalysators gesteigert sowie die Darstellung jenes vereinfacht werden. Im Vergleich zu diesen Rhodium-Rhodium Schaufelrad-Katalysatoren zeigte der nah verwandte heterodinukleare [BiRh(5*S*-MEPY)$_4$] Komplex, entgegen der Erwartung, keinerlei Reaktivität bei der Zyklopropanierung von Diazoverbindungen. Dieser unerwartete Unterschied wurde mit theoretischen Berechnungen der elektronischen Strukturen auf Dichtefunktionaltheorie (DFT) Niveau und dem Vergleich der erhaltenen Kristallstrukturen untersucht.

Als der strukturell signifikanteste Unterschied der verwandten Schaufelrad-Komplexe stellte sich die Ausrichtung der Liganden dar. Dies führt beim Wismut-Rhodium Komplex zu einer Verengung der Reaktionstasche am aktiven Rhodium-Zentrum. Die Analyse der elektronischen Strukturen zeigte eine deutlich veränderte energetische Verteilung der Molekülorbitale sowie eine Vergrößerung der HOMO/LUMO Lücke. Diese Grenzorbitale weisen zudem signifikant verschiedene Populationen an den Metallzentren auf (Abbildung 2).
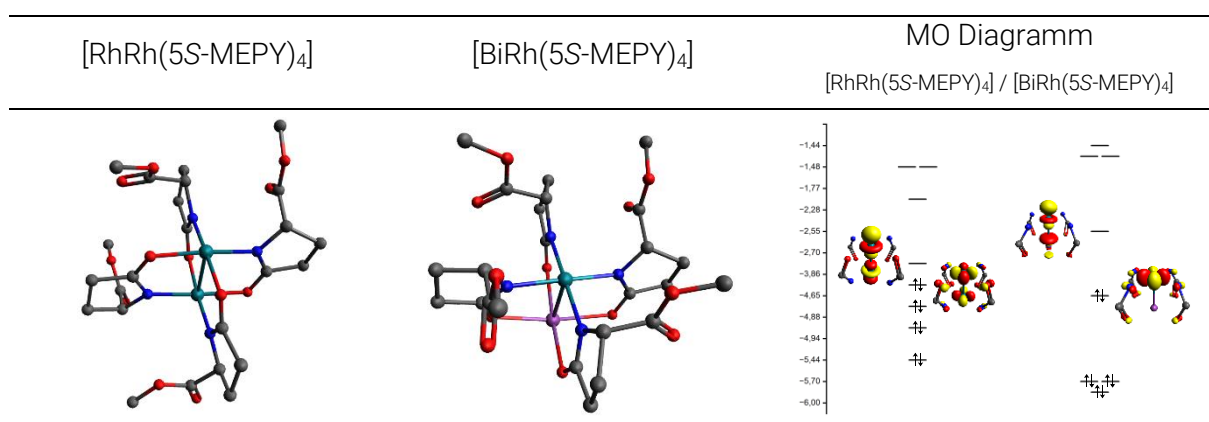

Abbildung 2. DFT-basierte geometrische Strukturoptimierungen und MO Diagramm der [RhRh(5*S*-MEPY)$_4$] und [BiRh(5*S*-MEPY)$_4$] Komplexe.

Abstract

Terpenes are a class of secondary natural products containing a fascinating diversity of unsaturated carbon skeletons. The casbane family belongs to the macrocyclic diterpenes and exhibit various biological activities. Some casbane diterpene producing plants are used in traditional Chinese medicine. These rare metabolites have been isolated from biologically unrelated organisms all over the world. Despite their promising biological activities and their structural diversity, only preliminary biological activity studies were conducted; previous classic total synthesis approaches were limited to the simplest member, the parent casbene. Based on a modular construction of the macrocyclic diterpene framework in combination with a versatile late-stage diversification, the convergent synthesis of several family members was accomplished: *in nuce* One Strategy – Multiple Targets.

The casbane natural product family is structurally characterised by its 14-membered unsaturated macrocycle with a fused *gem*-dimethyl cyclopropane, which naturally appears in all four configurations.

The *cis*-configured cyclopropane motif was prepared enantioselectively by a rhodium catalyst-controlled cyclopropanation. The corresponding *trans* derivative was accessed by subsequent epimerisation. The ring-closing alkyne metathesis enabled the cyclisation towards the 14-membered macrocycle in the presence of several alkenes and the cyclopropane unit. This demonstrated the orthogonality of alkyne metathesis towards alkene metathesis. Furthermore, the tolerance towards the cyclopropane unit, which was in conjugation with the catalytically transformed C≡C triple bond, was shown for the first time. Several natural products (depressin, euphorhylonal A, and yuexiandajisu A) were obtained after subjecting the resulting macrocyclic alkynes to regio- and stereoselective semi-reductive manipulations and late-stage diversifications. This synthesis of these natural products established the versatility of the herein developed synthetic strategy.

Comparison of the analytical data of the natural product euphorhylonal A with those of the synthesised diastereomers showed significant divergences. The configuration of euphorhylonal A was found to be misassigned. Using computational chemistry, the correct configuration (relative) of euphorhylonal A was predicted in high confidence and the absolute configuration was clarified by total synthesis.

The successful preparation of the terpene framework enabled the synthetic approach of twice oxygenated casbane diterpenes, including a hydroxy functionality in the "southern" sector. An enantioselective bisborylation with subsequent mono-oxidation was employed to incorporate the hydroxy functionality. This introduction marked a key step towards the total synthesis of 2-*epi*-10-hydroxydepressin. Future investigations towards the 14-membered macrocycle and synthesis of additional casbane diterpenes are expected to demonstrate the robustness of this synthetic strategy.
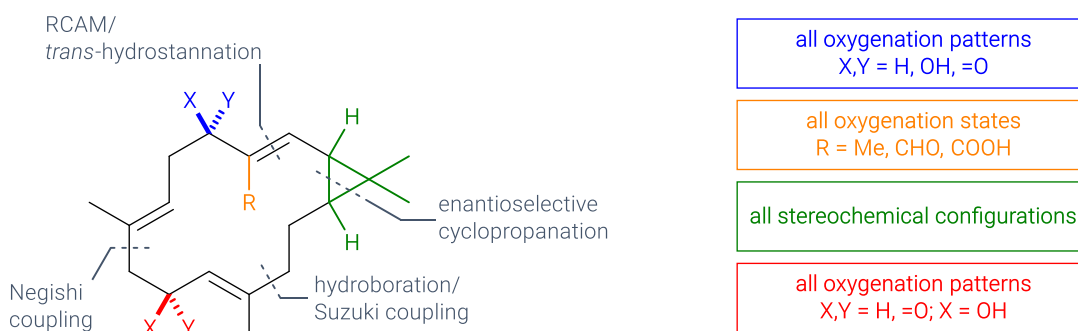
Figure 3. General retrosynthetic analysis of casbane diterpene natural product family.

The preparation of the *gem*-dimethyl cyclopropane using the dirhodium catalyst, [Rh$_2$(5*S*-MEPY)$_4$], was first described by Doyle and co-worker. The synthesis of these important catalysts was optimised in terms of yield and practicality, following previous achievements of the group.

In contrast to the [Rh$_2$(5*S*-MEPY)$_4$] catalyst, the closely related bismuth-rhodium carboxamidate complex [BiRh(5*S*-MEPY)$_4$] showed no observable reactivity in cyclopropanations with diazoacetate compounds. This surprising difference in reactivity was investigated by simulating their electronic structures using a computational approach and by comparing their structures in the solid state.

The geometric structures of both complexes showed dissimilar ligand orientations, forming a narrow environment at the binding site of the bismuth-rhodium complex. The computed molecular orbitals and the corresponding energy levels showed varied energetic distribution as well as a significant increase of the HOMO/LUMO gap. Furthermore, the frontier orbitals exhibit a dissimilar population at the metal centres (Figure 4). This constitution disfavours the diazo decomposition and carbene formation.

[RhRh(5*S*-MEPY)$_4$]	[BiRh(5*S*-MEPY)$_4$]	MO Diagram [RhRh(5*S*-MEPY)$_4$] / [BiRh(5*S*-MEPY)$_4$]
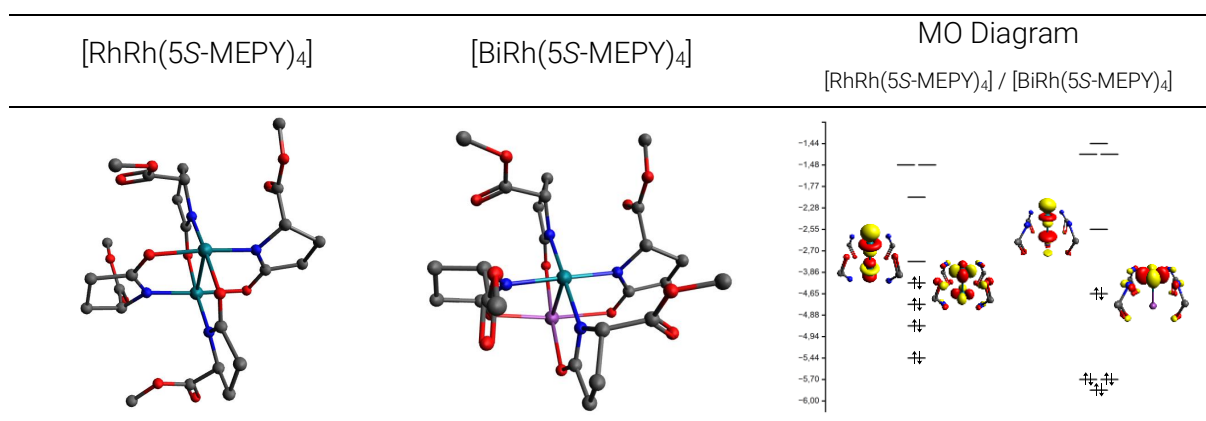
Figure 4. DFT-based geometric structure optimisation und MO diagram of [RhRh(5S-MEPY)$_4$] und [BiRh(5S-MEPY)$_4$] complexes.

Collective Total Synthesis of Casbane Diterpenes:

One Strategy – Multiple Targets

Contents

A GENERAL PART

1 INTRODUCTION

Nature generates an immense number of natural products with a diverse array of chemical structures and properties. This variety cannot be matched by either any manmade creativity or by artificial libraries. These molecules, not least because of their biological activities, have always fascinated chemists. Hence, it is no wonder that the field of natural product synthesis is so absorbing.

This research field commenced with the German chemist Friedrich Wöhler in 1828: "I cannot, so to say, hold my chemical water, and must tell you that I can make urea, without thereby needing to have kidneys, or anyhow, an animal, be it human or dog."[1]

Since then, the world and chemistry research have changed. The purposes of natural product synthesis have shifted from structural elucidation of small molecules to artistic and scientific synthesis of highly complex molecules. Especially, in the 20th and 21st century, the decades of scientific progression,[2] scientists such as R. B. Woodward and E. J. Corey made significant contributions to the field of organic chemistry and total synthesis. Their general understanding of reactivity and selectivity of reactions as well as the conceptual design of complex molecule synthesis remain popular until now.

To date, chemistry research is conducted at a very high level, combining different fields and utilising the benefits of digitalisation and computational chemistry. Thus, today's challenge is synthesising highly complex natural products in high quantity and selectivity with a minimum number of steps and material expenses, while aiming for several derivatives at once.

The herein discussed casbane natural product family is structurally characterised by a 14-membered macrocycle with a fused *gem*-dimethyl cyclopropane. Despite the impressive structural diversity and interesting biological activities of the casbane diterpene family members, their potential remains underrepresented in the synthetic research community. Therefore, the casbane diterpene family is an inspiring target for a collective total synthesis project.

The key steps of the total synthesis are ring-closing alkyne metathesis and post-metathetic late-stage diversification, both developed in the Fürstner group, in combination with a dirhodium catalysed *gem*-dimethyl cyclopropanation.

2 THE CASBANE FAMILY OF NATURAL PRODUCTS

2.1 STRUCTURAL DIVERSITY

The casbane family belongs to the largest class of natural products, the terpenes.[3] Their main structural characteristics are a 14-membered unsaturated macrocycle and a fused *gem*-dimethyl cyclopropyl unit (bicyclo[12.1.0]pentadecane framework, Figure 5). The casbane diterpene derivatives are produced by sessile soft corals as well as higher plants. Due to the variety of casbane diterpene producing species, casbane derivatives have been isolated around the world, even though they are extremely rare in nature. The majority of derivatives are generated by three organisms:

1) The *Alcyoniidae* family, a soft coral from the South China Sea, East China Sea and Red Sea.[4–10]
2) The *Euphorbiaceae* family (spurge), a flower collected in Africa, Asia, South America, and Australia.[11,12,21–26,13–20]
3) The *Poaceae* family, belonging to the Asian rice plants.[27,28]

The isolation of casbane diterpenes from soft corals and unrelated higher plants is noteworthy, as it invokes the question of how different organisms evolved metabolites of the same natural product family and whether this observation is based on a more general aspect?

The hydrocarbon (−)-casbene ((−)-**1**) was the first member of this natural product family isolated from an enzymatic preparation of the castor bean seedlings (*Ricinus communis* L.).[29–31] It represents the simplest casbane family member.

Since then, an enormous number of casbane natural products has been isolated and characterised by various research groups around the world. These casbane diterpenes illustrate a structurally diverse family, which varies by the oxygenation pattern and the stereochemical configurations at the fused *gem*-dimethyl cyclopropane. As a curiosity of casbane natural products, both *antipodal cis* configurations are present, as demonstrated by 10-hydroxydepressin (**2**)[4,6] and sinularcasbane A (**3**)[7] (Figure 5). Additionally, the *trans*-cyclopropane also appears in both enantiomeric forms. This "pseudo-enantiomeric" relationship is illustrated by 1-*epi*-10-hydroxydepressin (**4**)[6] and 2-*epi*-10-hydroxydepressin (**5**)[4] (Figure 5). However, in nature, the more common relative configuration of the cyclopropane is *cis*. Another interesting detail is the isolation of all four possible permutations of the cyclopropane from the single genus *Sinularia* sp. More interestingly, the *cis/trans* derivatives, 10-hydroxydepressin (**2**)[6], 1-*epi*-10-hydroxydepressin (**4**)[6], and 2-*epi*-10-hydroxydepressin (**5**)[4] were isolated from the single species *Sinularia depressa* (Figure 5).
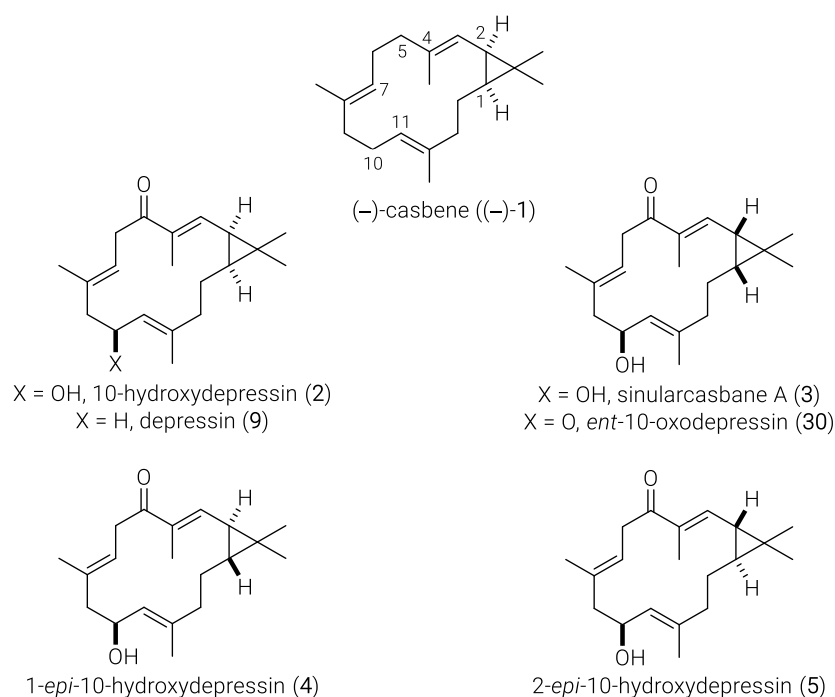
Figure 5. A selection of casbane natural products with all naturally occurring cyclopropane configurations.

Aside from the cyclopropane, the variation of oxygenation patterns around the macrocycle, including all oxidation levels, is noteworthy. The manifold oxidation levels are represented by alcohol groups at almost every position of the bicycle (sapidisin C (**6**)[32]), by epoxide (hookerianolide A (**7**)[33]), by aldehyde (pekinenal (**8**)[15,34]) as well as by ketone and lactone functionalities (depressin (**9**)[6], hookerianolide A (**7**)[33], & sapidisin C (**6**)[32]). In the recent years, even hydroperoxide and peroxide functionalities (EBC-320 (**10**)[22] & sinuereperoxide A (**11**)[8]) were found. In addition to the complex oxygenation pattern, the structural diversity further increases upon consideration of the geometric configuration of the unsaturated C=C bonds. This variable configuration (agrostistachin (**12**)[35], pekinenal (**8**)[15,34], koumbalone A (**13**)[36]) and partial saturation (10-oxo-11,12-dihydrodepressin (**14**)[6]) patterns are illustrated Figure 6. An overview of the casbane diterpene natural products is provided in Appendix G.
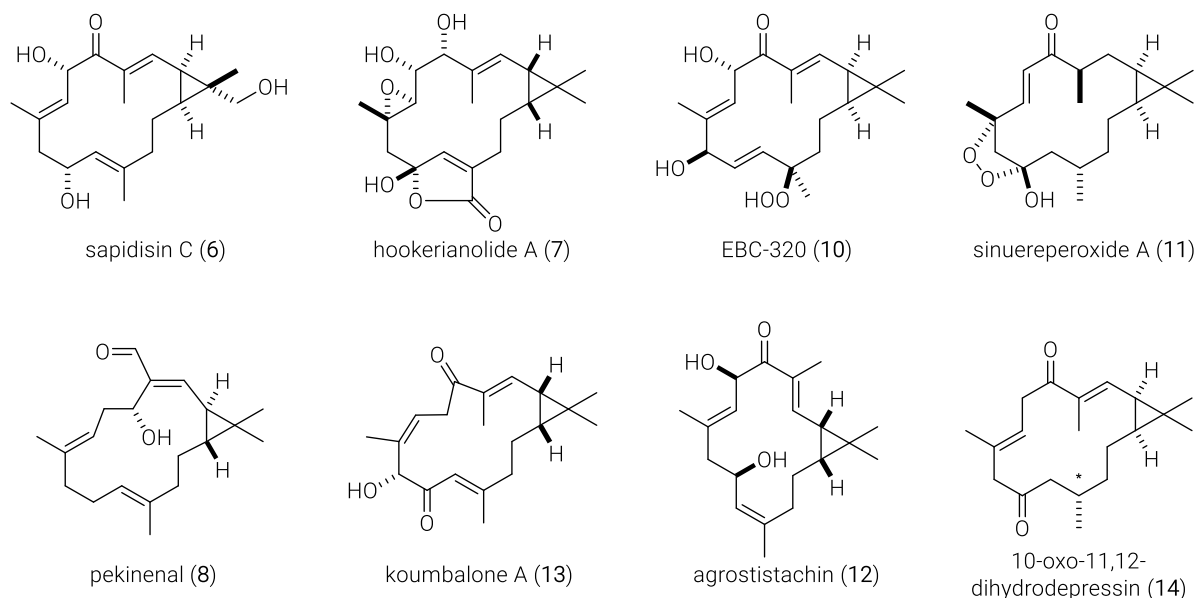
Figure 6. Selection of oxygenated casbane natural products (*configuration tentatively assigned).

In the 1980s and 1990s, the lack of highly accurate spectroscopy made the structural elucidation of the polyoxygenated casbane natural products challenging, especially with respect to the relative and absolute configuration. For this reason, some stereochemical assignments in the older literature are missing. In the recent literature, configurations were elucidated by methods such as nOe experiments, circular dichroism spectroscopy,[6] and Mosher ester analysis.[16] In some cases, the authors even provided X-ray structures with absolute configuration.[8] In many cases, however, the configuration was tentatively assigned based on NMR data,[6] by comparison with known structures,[37] or by biogenetic considerations. Considering the scarcity of reliable analytical data, asymmetric total synthesis is still an indispensable tool for structure elucidation. In this thesis, the synthesis of casbane diterpenes with a diverse oxygenation pattern at the C5 and the C18 position depressin (**9**), nominal euphorhylonal A (**15**), pekinenin C (**16**), and yuexiandajisu A (**17**) is discussed (Figure 7). These structures were ideal synthetic targets to challenge the ring-closing alkyne metathesis (RCAM) methodology developed in Mülheim followed by a *trans*-hydrostannation and late-stage functionalisation sequence.[38]
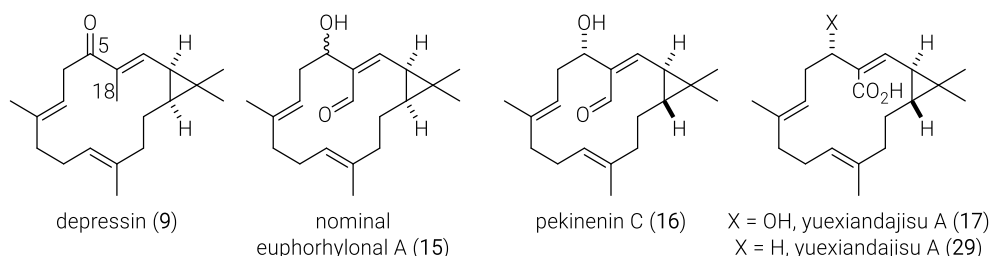
Figure 7. Synthetically interesting casbane natural products.

2.2 BIOLOGICAL BACKGROUND OF THE CASBANE FAMILY

2.2.1 BIOSYNTHESIS OF CASBANE DITERPENES

The (−)-casbene ((−)-**1**) synthase from mevalonate or geranylgeranyl pyrophosphate (GGPP) was achieved by employing an enzyme extract from castor bean seedlings in 1970, which demonstrates that GGPP is a key intermediate in its biosynthesis.[29,30,39] In 1976, the first total synthesis of (±)-casbene ((±)-**1**) confirmed the bicyclo[12.1.0]pentadecane framework.[40]

Twelve years later, the stereochemistry at C2 and the stereochemical course of macrocyclisation in the case of (−)-casbene ((−)-**1**) bearing a *cis-gem*-dimethyl cyclopropane was investigated. To this end, the enzyme extract (S-150 fraction) from the castor bean seedling was used in combination with deuterium-labelled GGPP (^{2}H-**18**) and carbon-labelled GGPP (^{13}C-**18**).[41] These investigations revealed a suprafacial intramolecular ring closure on the *re,re*-face of the 1,15 double bond and a 1*S*,2*R* configuration (−)-**1** (Scheme 1).[41] The cyclisation mechanism of GGPP with the castor bean seedlings' enzyme extract involves cleavage of the allylic pyrophosphate by a divalent metal ion, leading to an allylic carbocation, which subsequently forms the cyclopropane by alkylation and deprotonation.[39,42−46]

4
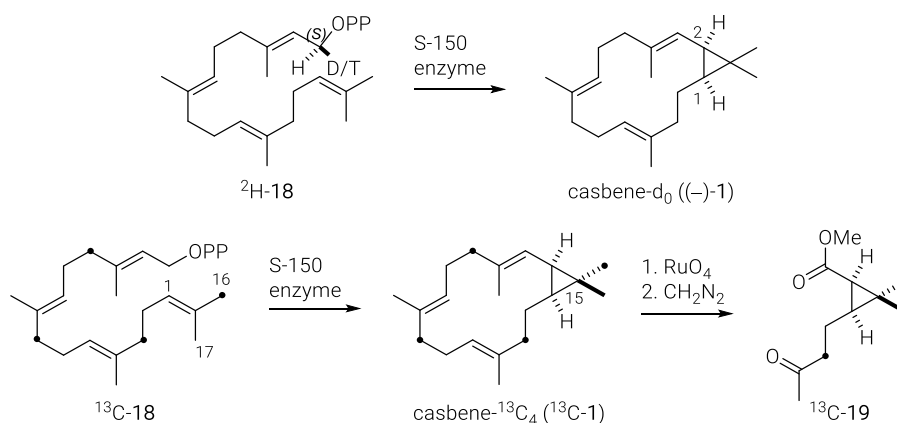
Scheme 1. Labelling experiments towards the mechanistic understanding of the biosynthesis.

Although the biosynthetic cyclopropanation leading to (−)-casbene ((−)-**1**) was studied, many details of the biosynthesis remain unclear.[43] However, GGPP was clearly identified as a key intermediate in the biosynthetic pathway of casbanes.[29,47,48]

Understanding this "double" cyclisation is of great interest since the casbane framework is most likely the progenitor of many polycyclic diterpene natural product families containing a cyclopropane unit, such as euphoractine (**20**), jatropholane (**21**), lathyrane (**22**), premyrsinane (**23**), tigliane (**24**), and ingenane (**25**) (Figure 8), as well as of linear products like seco-casbanes and seco-lathyranes.[42,49] Casbane diterpenes are likely biosynthetically also related to diterpene families missing the cyclopropane like cembrane (**26**), daphnane (**27**), jatrophane (**28**) families (Figure 8).

The interesting biological profiles of the ingenane (**25**) or tigliane (**24**) natural products families, as proinflammatory agents and as protein kinase C (PKC) activators, might be based on the ring strain energy of the cyclopropane and therefore are seen as potential alkylation agents.[42] Treatment of actinic keratosis with 3-*O*-angeloylingenol (PEP-005, Picato®, Leo Pharma) demonstrates the pharmacological relevance of these polycyclic diterpenes.[50] Since casbane diterpenes also contain this *gem*-dimethyl cyclopropane unit, it might also be relevant for their biological activity.
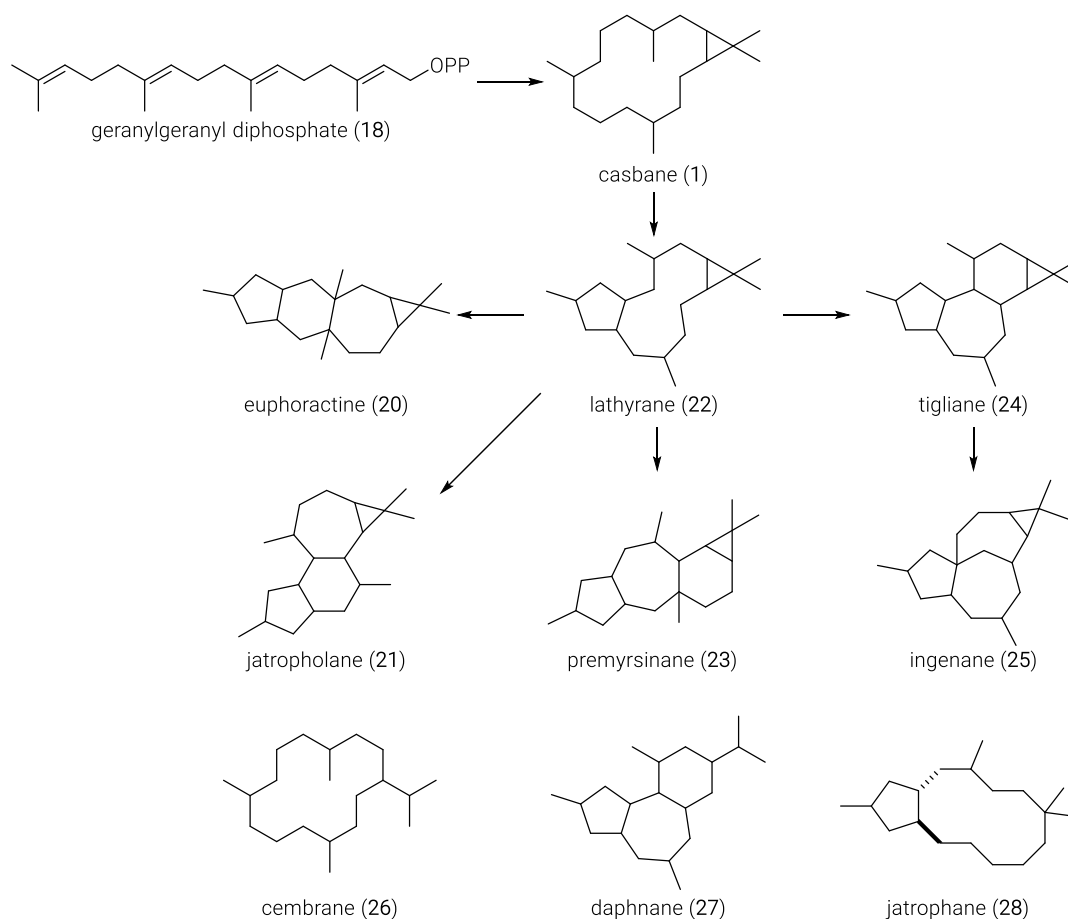
Figure 8. Related carbon skeletons of casbane.[42]

2.2.2 HISTORY OF CASBANE DITERPENES' BIOLOGICAL ACTIVITY PROFILES

Euphorbia is the largest genus of *Euphorbiaceae* family with more than 2000 species. It is characterised by the presence of milky latex and ranging from annuals to trees with unique flower structure.[51] The Greek Euphorbus was the eponym of the *Euphorbia* genus and the personal physician of Juba II (c. 48 BC – AD 23), the Romanised king of Mauretania. Euphorbus is supposed to have utilised *Euphorbia* species' as an ingredient in his medicine.[51] This report shows that already the Romans were aware of the pharmalogical power of the *Euphorbia* plant family. Other reports of traditional Chinese medicine "Lang Du" demonstrated the utilisation of *Euphorbiaceae* and *Thymelaeaceae* plant families for the treatment of various ailments. In further reports it was also mentioned as a pesticide and expectorant.[12,52] Recent studies of the "Lang Du" extract showed interesting inhibitory effects in growth of melanoma cells.[53] Regarding these biological activities, a deeper understanding was gained by investigating the isolated natural products of *Euphorbia ebracteolata, E. fischeriana* (both *Euphorbiaceae* family) and *Stellera chamaejasme* (*Thymelaeaceae* family).[12,52] Determination of the biologically active compounds from "Lang Du" by G.-W. Qin and co-worker was focused on *E. fischeriana* sp.[52,54,55] and the *E. ebracteolata* sp.[12] The only isolated casbane diterpenes, yuexiandajisu A (**17**) and B (**29**) exhibited antibacterial activity and inhibited proliferation of B lymphocytes, respectively (Figure 7).[12] In addition, Chinese pharmacology reports on utilisation of another five *Euphorbia* sp. (*E. pekinensis, E. kansui, E. lathyris, E. humifusa,* and *E. maculate*) containing several casbane natural products.[15]

Especially, the specie *Euphorbia pekinensis* was frequently used in traditional Chinese medicine and is known for its poisonous and stimulating effects.[13,14] Up to now, eight casbane diterpenes were isolated from *E. pekinensis*[16,17,34] with impressive biological activities.[11,14,15,18,34,42]

In addition, the structure-activity relationship regarding cytotoxicity was studied, indicating that the 3,4-double bond configuration does not have a significant effect. Contrary, the presence of hydroxy or ketone groups at the C5 position increased this activity.[16,17] Casbane diterpenes bearing an epoxide or lacking the cyclopropane were much less active.[16,17]

Aside the *Euphorbia* genus, the species *Croton nepetaefolius* from Brazil also produces a biologically active casbane with antimicrobial effects on planktonic forms and biofilms.[56−58]

In 2005, casbanes also have been isolated from the soft coral genus *Sinularia* with biological profiles like anti-inflammatory, cytotoxic, and anti-microbial activities.[6,7,59]

UV-irradiated Asian rice leaves (*Oryza sativa*) produced the casbane *ent*-10-oxodepressin (**30**), representing another genetically unrelated and higher casbane-producing plant (Figure 5).[28] Moreover, the *ent*-10-oxodepressin (**30**) was identified as a phytoalexin,[27,28,60] as well as (−)-casbene ((−)-**1**).[29−31,61,62] Especially, since rice represents an important nutrition for the world population, the fungicidal activity of *ent*-10-oxodepressin (**30**) from the Asian rice plant is relevant and requires detailed investigations in the future.[38]

2.3 PREVIOUS SYNTHETIC APPROACHES

Up to now, parent casbene (**1**) is the only member of the casbane diterpene family, which has been prepared by classic total synthesis. The number of biosynthetic investigations towards casbane diterpenes increased in the recent years.[43,45,47,63,64]

In 1970, the material of (−)-casbene ((−)-**1**) isolated by West and co-workers was not sufficient for full characterisation.[29,30] Therefore, Crombie *et al.* performed the first total synthesis of (±)-casbene ((±)-**1**) in 1976, which enabled the structure elucidation (Scheme 2).[29,30,40] A nickel carbonyl mediated marcocyclisation of **33** was utilised as the key step. Accordingly, chrysanthemate (±)-**31** was transformed through a multi-step sequence to alcohol **32** followed by oxidation and Wittig homologation. An additional homologation and bromination sequence afforded bisallylic dibromide **33**, which was then subjected to the nickel carbonyl mediated macrocyclisation to obtain (±)-casbene ((±)-**1**) (Scheme 2). The NMR data of the synthetic and the naturally derived casbene sample showed close similarity and confirmed the proposed relative stereochemistry.[40]
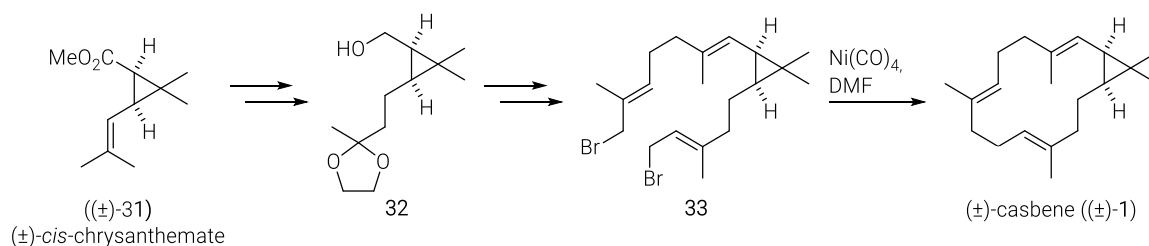
Scheme 2. Summary of the total synthesis of (±)-casbene ((±)-**1**) *via* a nickel carbonyl mediated cyclisation by Crombie *et al.* (1976)[40]

In 1980, Crombie *et al.* published a chiral pool synthetic version of the previous total synthesis. Both stereocentres were introduced from the naturally occurring 1*R*,3*S*-(+)-*cis*-chrysanthemic acid ((+)-**31**). This total synthesis gave (−)-casbene ((−)-**1**).

While the synthesis of casbene reported by Crombie *et al.* relied on traditional bond disconnections, in 1982 Takahashi and co-workers reported a biomimetic total synthesis of (±)-casbene ((±)-**1**) *via* an intramolecular bicyclisation (Scheme 3). The all-*trans*-geranylgeraniol **34** was converted into allylic diazo compound **35**, which subsequently underwent a copper mediated cyclisation upon slow addition to mixture of copper(I) iodide in THF at 0° C (Scheme 3).[65] This procedure represented a concise synthetic strategy towards (±)-casbene ((±)-**1**) with 14% overall yield, which was later used by Pattenden *et al.* to synthesise cembrenes *via* radical-mediated alkenyl cyclopropane ring-opening of casbene.[65,66]
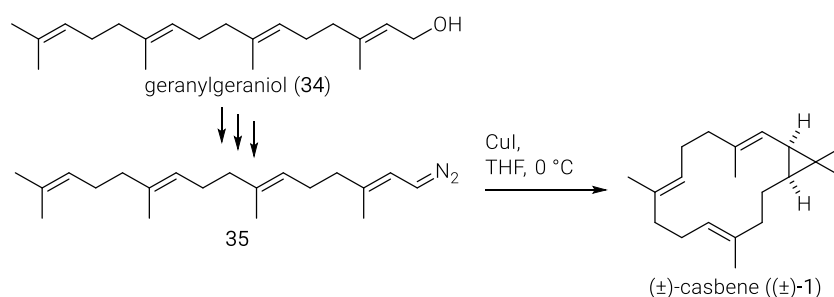
Scheme 3. Summary of (±)-casbene ((±)-**1**) total synthesis *via* intramolecular carbene bicyclisation by T. Takahashi co-workers (1982).[65]

Another chiral pool based total synthesis of (+)-casbene ((+)-**1**) was published by McMurry and Bosch (Scheme 4). Their macrocyclisation step was carried out through a titanium-induced intramolecular carbonyl coupling. The total synthesis commenced with (+)-2-carene (**36**), bearing the desired chiral centres and the cyclopropane. Followed by a three step sequence, the obtained *E*-alkenyl iodide **37** was cross-coupled with organozinc reagent **38** under Negishi conditions. This multi-step sequence afforded the desired dicarbonyl cyclisation precursor **39**. The subsequent cyclisation was carried out by slow addition of **39** to a refluxing mixture of TiCl₃/Zn-Cu in dimethoxyethane and gave a mixture of *E*/*Z*-isomers ((+)-**1** & **40**) in 75% yield (Scheme 4).
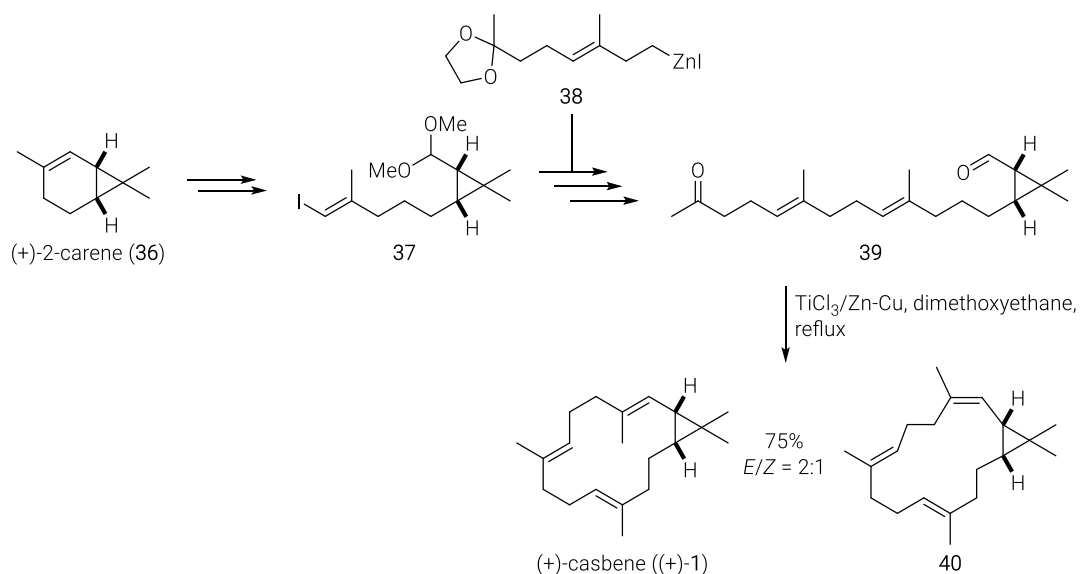
Scheme 4. Summary of (+)-casbene ((+)-**1**) total synthesis *via* intramolecular carbonyl cyclisation by McMurry and Bosch (1987).[67]

Motherwell and co-worker developed an intramolecular bicyclisation of an aldehyde and a trisubstituted alkene, mediated by 1,2-bis(chlorodimethylsilyl)ethane and zinc. This methodology was used in the total synthesis of casbene ((±)-**1**). Application of geranylgeranial **41** to these cyclisation conditions led to the formation of the side-product **42** in 46% yield and to the desired (±)-casbene ((±)-**1**) in 30% yield (Scheme 5).[68]
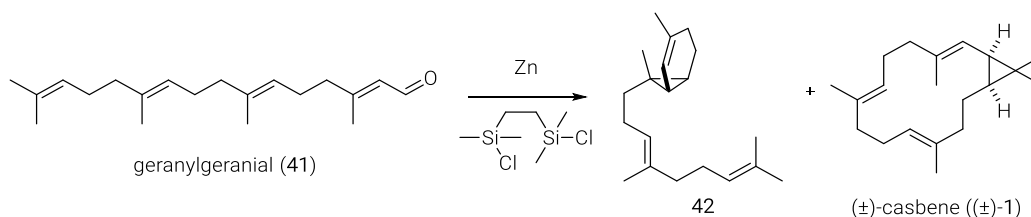
Scheme 5. Summary of (±)-casbene total synthesis *via* intramolecular bicyclisation by Motherwell and Roberts (1995).[68]

The total synthesis approach of Doyle and co-workers included a similar strategy as reported by Takahashi and co-workers (Scheme 3). Instead of utilising copper(I) iodide, Doyle and co-workers employed a dirhodium(II) carboxamidate catalysts for the intramolecular bicyclisation.[69] Geranylgeraniol **34** was converted into allyl diazo compound **35** (Scheme 6). Under Doyle's cyclisation conditions, the major products were pyrazole **43** and dimer **44**. In addition, an inseparable mixture of the desired (±)-casbene ((±)-**1**) and two different bicyclic side-products (**45** & **46**) was obtained.[70]

geranylgeraniol (**34**)   **35**

Rh$_2$L$_N$
CH$_2$Cl$_2$

pyrazole (**43**)   dimer **44**   **45**   **46**   (±)-casbene ((±)-**1**)
(cycloaddition)

R =
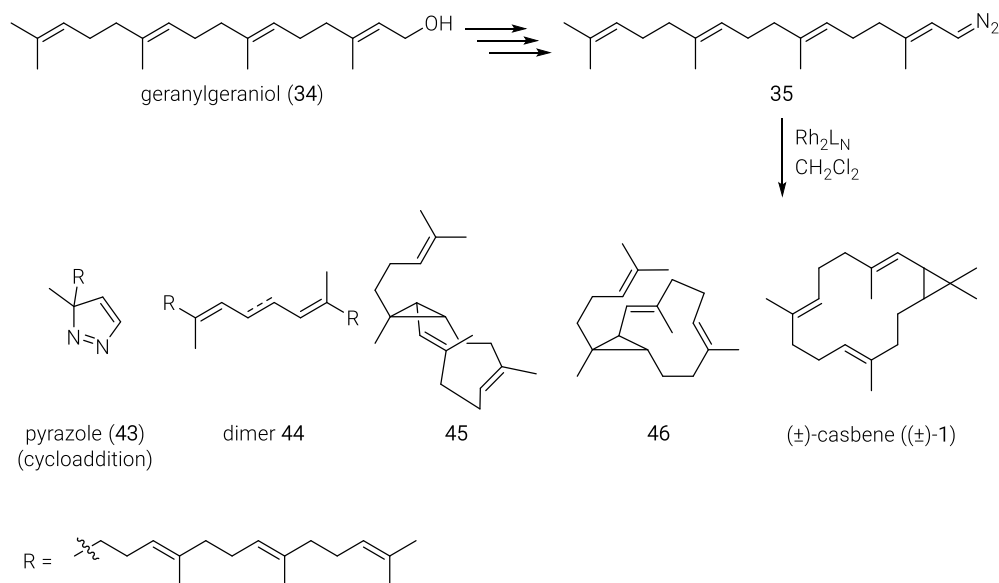
Scheme 6. Attempted synthesis of casbene by intramolecular cyclopropanation by Doyle and co-workers (2002).

Two main strategies were employed in the previous synthesis approaches.

1) The cyclopropane unit was introduced as a building block from a natural pool and stayed untouched throughout the syntheses. The macrocyclisation was carried out under different conditions with low to moderate yields.

2) Geranylgeraniol was processed into the corresponding cyclisation precursor, which was then converted into the bicyclo[12.1.0]pentadecane framework in one step. The challenge of this strategy was to avoid formation of six or ten membered rings during the macrocyclisation.

The low yielding macrocyclisations and narrow target selection of these approaches motivated us to develop a different strategy.

3 MOLYBDENUM CATALYSED RING-CLOSING ALKYNE METATHESIS

The interest in macrocyclic structures, as casbane diterpenes, comes in part from the enormous number of such natural products and their biochemical functionalities, which led to the development of macrocyclic pharmaceuticals. In this regard, the macrocyclic motif combines the benefits of large biomolecules with those of small molecules. This provides high affinity and selectivity for protein targets, whereas bioavailability is sufficiently preserved to reach the intracellular matrix. Therefore, diversity-oriented total synthesis of macrocyclic structures is important for initial target validation, structure-activity relationship establishment, and final development of derivatives with ideal pharmacokinetic properties.[71–73]

During the synthesis of macrocyclic natural products, the cyclisation represents a key design element. Therefore, a large variety of macrocyclisation approaches and methodologies were developed.[74,75] Among these, alkene and alkyne ring-closing metathesis play an important role to establish the macrocyclic architectures.[74] Unlike alkyne metathesis, alkene metathesis has been more widely investigated over the years and was awarded with the Nobel prizes in 2005.[76–78] This is mainly due to the availability of user-friendly catalysts and the great compatibility with a broad range of functional groups. A major drawback of ring-closing alkene metathesis (RCM) is the low stereoselectivity, in some cases.[79–82] On the other hand, alkyne metathesis, when combined with partial reduction of the alkyne, enables a more elegant construction of large ring sizes with full stereocontrol. For example, Lindlar reduction or *trans*-hydrostannation can be applied as post-metathetic transformations.

3.1 DEVELOPMENT OF EFFICIENT ALKYNE METATHESIS CATALYST SYSTEMS

In 1968, Pennella and co-workers reported the first alkyne metathesis by a heterogeneous tungsten trioxide catalyst on silica. This system caused the conversion of pent-2-yne into but-2-yne, hex-3-yne, and polymeric materials at 200 to 450 °C.[83] Shortly thereafter, Mortreux and Blanchard noted that a mixture of molybdenum hexacarbonyl and resorcinol enabled the first alkyne metathesis by a homogeneous catalyst system.[84]

Katz and McGinnis proposed the generally accepted alkyne metathesis mechanism, proceeding similarly to Chauvin's catalytic alkene metathesis cycle. The reaction is initiated by a formal [2+2] cycloaddition of a metal alkylidyne complex **A** and an alkyne **B**, generating a metallacyclobutadiene intermediate **C**. Cycloreversion from the tautomer **D** leads to the product **F** and regeneration of the metal alkylidyne complex **E** (Scheme 7).[85–87]
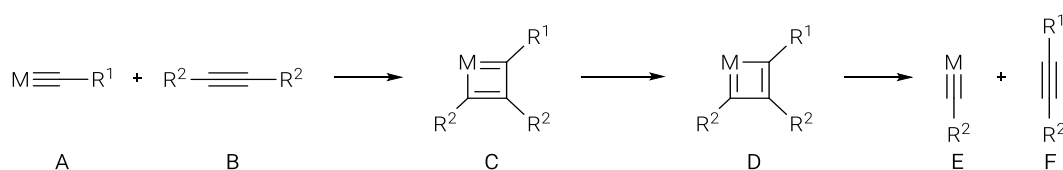
Scheme 7. Basic mechanism of alkyne metathesis catalysis by alkylidyne complexes.[85,88]

The mechanistic proposal was experimentally confirmed by Schrock and co-workers, using high oxidation state metal alkylidyne complexes of molybdenum(VI), tungsten(VI), and rhenium(VII).[89,90] Further mechanistic studies revealed the importance and reactivity of metallacyclobutadiene moieties as key intermediates in the catalytic cycle.[91-93]

In 1998, Cummins and co-workers reported the synthesis and reactivity of trisamido molybdenum(III) complex **47**, which reacts with dinitrogen (N_2) to the nitrido molybdenum(VI) product [N≡Mo{(^{t}Bu)(Ar)N}$_3$].[94-96] After *in situ* activation of **47** with CH_2Cl_2, alkyne metathesis was observed, which is based on the active complexes [ClMo{(^{t}Bu)(Ar)N}$_3$] and [HC≡Mo{(^{t}Bu)(Ar)N}$_3$]. While the molybdenum halide complex showed catalytic activity, the terminal alkylidyne complex only performed one turnover due to instability.[97-99]

The catalytic activity of such trisamido alkylidyne molybdenum complexes was improved by Moore and co-workers, avoiding the formation of unstable terminal alkylidyne and halide species (Scheme **8**). To this end, the trisamido molybdenum(III) complex **47** was activated with 1,2-dichloropropane, resulting in the formation of molybdenum halide complex **48** and propylidyne molybdenum(VI) complex **49**. The halide species **48** can be reductively recycled with magnesium to the trisamido molybdenum complex **47**.[100-102]
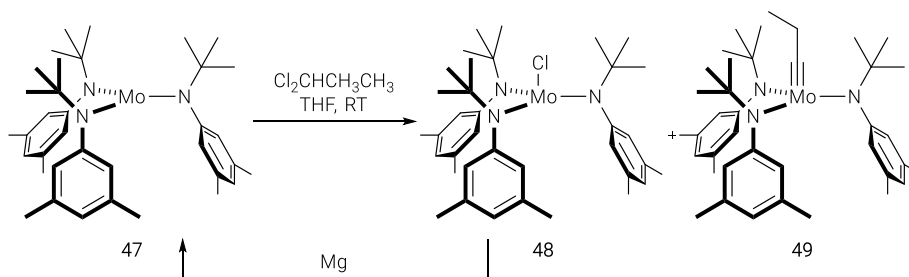
Scheme 8. 'Reductive recycle' strategy of molybdenum alkylidyne complexes synthesis by Moore and co-workers.

In 2010, Fürstner and co-workers published a new generation of molybdenum-based alkyne metathesis catalysts **50** bearing triphenylsilanolate ligands. The 1,10-phenanthroline adduct **51** represents an air-stable and therefore user-friendly pre-catalyst, which can be reactivated with $MnCl_2$ at 80 °C (Scheme 9).[88] The functional group tolerance and broad scope of this catalyst was investigated in a series of alkyne homometathesis, cross metathesis (ACM), and RCAM reactions.
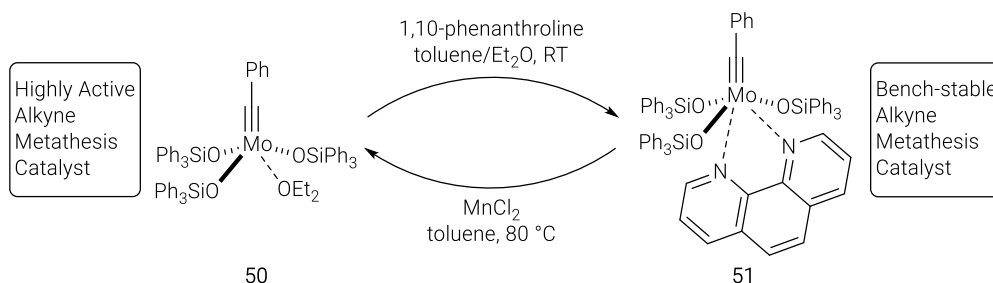
Scheme 9. Bench-stable alkyne metathesis catalyst: Reversible coordination of 1,10-phenanthroline.

In addition, Fürstner and co-workers reported a significant rate enhancement by addition of 5 Å molecular sieves (MS) of alkyne metathesis reactions with methyl-capped alkynes at room temperature. This effect is based on the adsorption of the by-product 2-butyne, which shifts the equilibrium towards the products and hinders the readmittance of 2-butyne into the catalytic

cycle.[88] This modification avoids the need for elevated temperature or gentle vacuum to remove these by-products.[88]

The application of ancillary silanolate ligands to molybdenum alkylidyne complexes led to the formation of alkyne metathesis catalysts with an extended functional group tolerance and a broad substrate scope. These improvements are deriving from the electronic and steric features of these ligand spheres, which are bulky enough to block undesired reactivity (bimolecular and an associative decomposition), but flexible enough to allow the desired alkyne metathesis to proceed.

In terms of the electronic properties, the π and σ donating character of these silanolate ligands enables the tuning of the Lewis acidity of the metal centre, satisfying the demands of the catalytic cycle.[103,104] However, recent theoretical studies of the metal−ligand binding profile revealed that linearisation of the M−O−Si bond angle would lead to a weaker M−O donor strength and not as previously hypothesised to an increase of electron donation.[105]

In the bent conformation, one σ-bond and one π-bond was found for each M−O binding, where the σ-bond contributed the larger O → M electron donation. The linearisation of this M−O−Si bond, considering a tripodal ligand system, leads to a second weak M−O π-bond, which contributes to the O → M electron donation. The simultaneous decrease of the orbital overlap of the σ-bond results in a much weaker O → M electron donation. Consequently, the linearisation weakens the M−O bond (Figure 9).
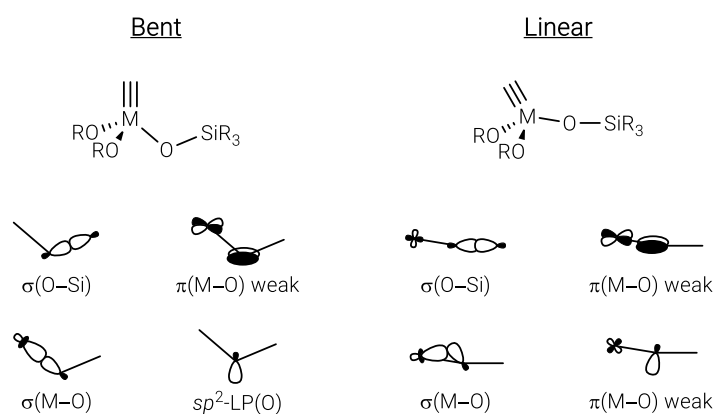
Figure 9. Bent vs linearised metal − ligand binding motifs.[105]

While the combination of molybdenum and these triarylsilanolate ligand spheres forms well-defined and highly active alkyne metathesis catalysts, functional group tolerance was still a challenge. Particularly substrates, which contain primary and propargylic alcohols, were often met with decomposition in RCAM.[106] The catalysts belong to the class of Schrock alkylidynes containing an early transition metal in its highest possible oxidation state (+VI) if one counts the alkylidyne ligand as trianionic.[88,107−109]

Two main deactivation pathways of alkylidyne complexes with protic functional groups have to be considered.

A) If the central metal is inappropriately sheltered, the Lewis acidic central metal endangers substituents at any activated position, leading to a ligand substitution and formation of a resonance-stabilised cation (Figure 10 A).

B) Even when the alkylidyne intermediate was formed, the propargylic alcohol, next to the nucleophilic carbon, might turn into a leaving group (Figure 10 B).
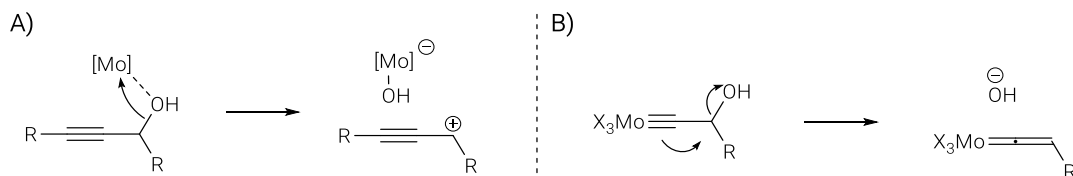
Figure 10. Deactivation/decomposition pathway of alkyne metathesis catalyst with propargylic alcohols.[106]

This limitation can be overcome, at least in part, by introducing a tridentate silanolate ligand to molybdenum alkylidyne complexes (Figure 11).[106] This approach combined the virtues of electronic and steric features of the silanolate ligands in an envisaged podand ligand sphere that shields the metal centre and prevents ligand substitution due to its chelating effect. Therefore, two versions with differently tethered backbones were synthesised in a few scalable steps. These catalytically active species are generated *in situ* by mixing the activated trisamido molybdenum alkylidyne complex **49** with either of the two ligands (**52** & **53**). The resulting alkyne metathesis catalysts are characterised by a broad substrate scope and superb functional group tolerance. More specifically this two-component alkyne metathesis catalyst system can tolerate secondary and primary alcohols as well as propargylic alcohols.[106]

Similarly, Zhang and co-workers developed an alkyne metathesis catalyst (**54**) with tridentate phenol ligand scaffold (**55**) generated in a similar manner (Figure 11).[110–113] However, the major drawbacks are the use of carbon tetrachloride as the solvent and the limited substrate scope.
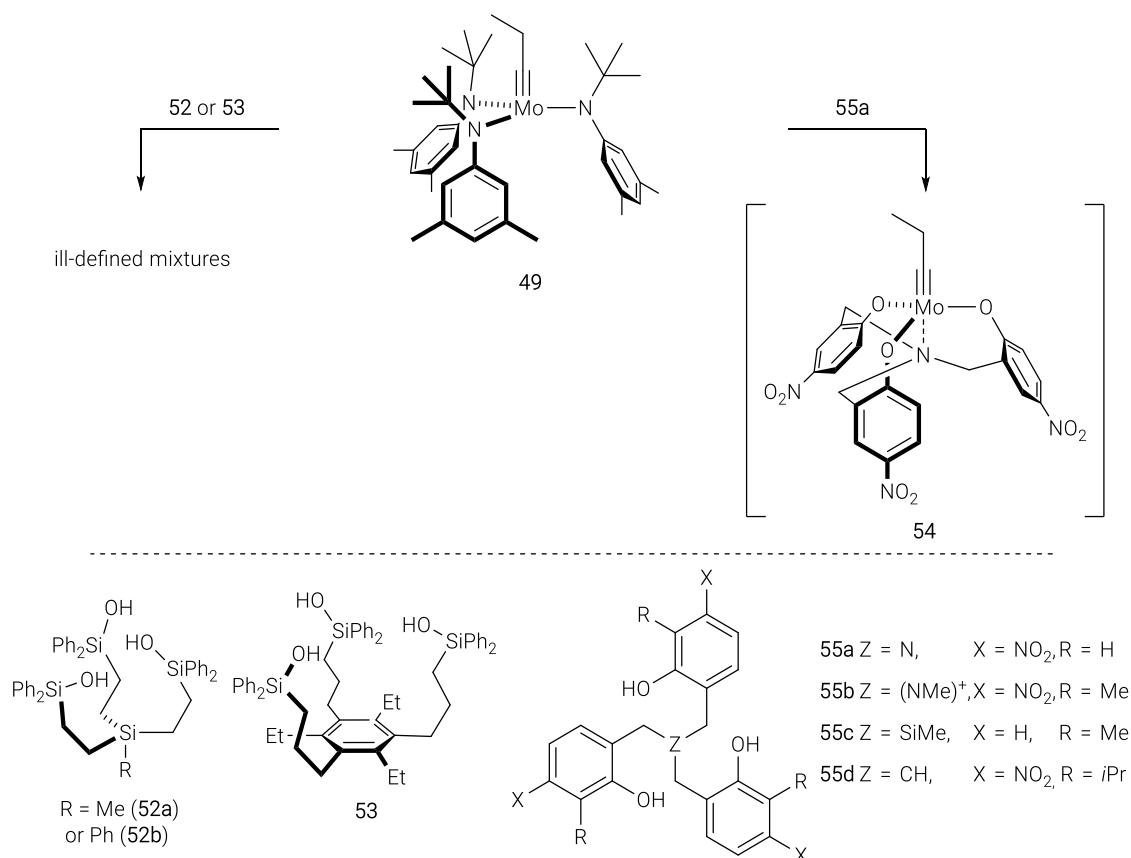
Figure 11. Two-component alkyne metathesis catalyst system.[106,110–113]

The latest generation of alkyne metathesis catalyst, also termed the canopy catalyst, was disclosed by Fürstner and co-workers (Figure 12).[114] The complexes **56**, **57**, and **58** exhibit a unique reactivity and selectivity profile that stems from the podand silanolate ligand spheres. Slight modification at the ligand sphere revealed a significant reaction rate acceleration with **58**. The excellent performance of these catalysts is illustrated by their broad functional group tolerance including unprotected primary alcohols as well as molecules with donor sites like basic nitrogen or heterocycles. In addition, this robustness gives the opportunity to use technical grade solvents.[115] Gratifying results were obtained by applying the canopy catalysts to macrocyclisation of demanding architectures, as en-route to the total synthesis of the marine toxin amphidinolide F.[115]

anisol phenyl canopy catalyst system (56)

phenyl canopy catalyst system (57)

methyl canopy catalyst system (58)
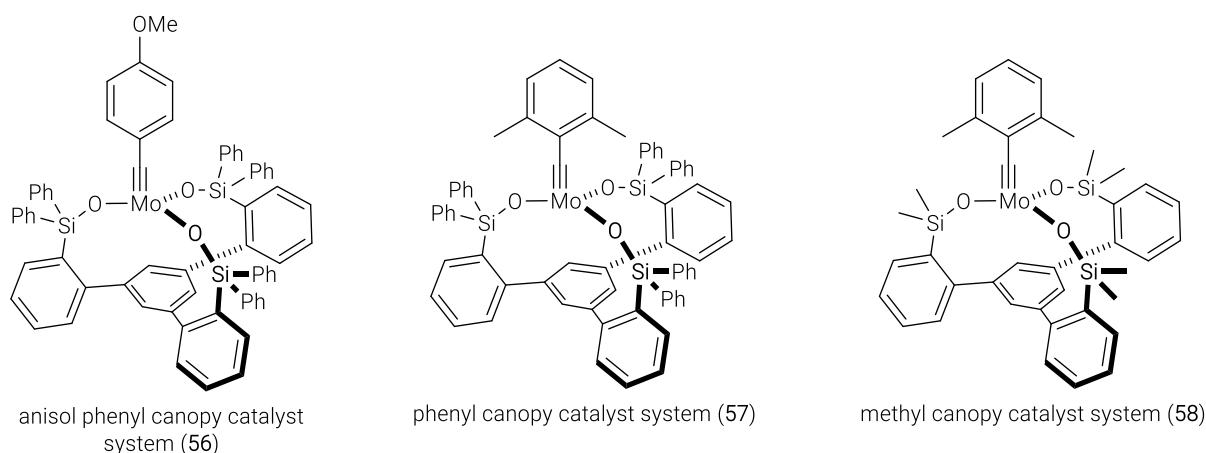
Figure 12. Canopy alkyne metathesis catalyst systems.

3.2 TERMINAL ALKYNE METATHESIS

Despite the success of alkyne metathesis with alkyl-capped alkynes, terminal alkynes are a known limitation. The trisilanolate alkylidyne molybdenum catalyst **50** showed significant deactivation in reactions with p-MeOC$_6$H$_4$C≡CH. This is due to decomposition of Schrock alkylidyne complexes *via* deprotiometallacyclobutadiene formation.[104] Nevertheless, also the decomposition *via* a bimolecular collision needs to be considered (Scheme 10):[103,109,116–118]

1. Formation of metallacycle **H**, followed by a transannular C−H activation might generate deprotiometallacyclobutadiene **I** by loss of one ligand (Scheme 10, left).[104,119] This deactivation is favoured by donor ligands, like alkoxides and silanolates.
2. Formation of metallacycle **J**, followed by cycloreversion might form the unstable methylidyne complex **K** and dimetallatetrahedranes **L** (Scheme 10, right).[104,119–123] Such µ-bridging acetylene complexes are able to open a polymerisation channel.

Despite these challenges, Fürstner and co-workers successfully utilised the trisilanolate alkylidyne molybdenum catalyst **50** for the RCAM of methyl-capped/terminal alkynes in the total synthesis of mandelalide A and for cross metathesis of methyl-capped/terminal alkynes.[119,124,125]
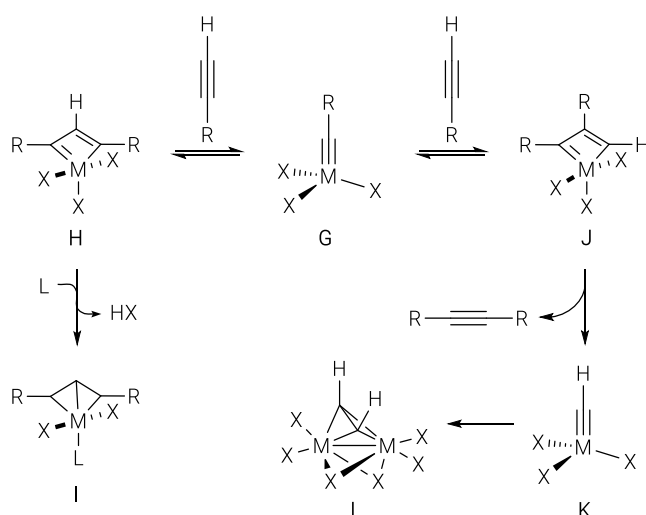
Scheme 10. Basic scenarios in terminal alkyne metathesis reactions; L = neutral ligand; M = Mo, W; X = anionic ligand.[119]

The limitation presented by terminal alkynes was addressed by Tamm and co-workers by application of the 2,4,6-trimethylbenzylidyne catalysts ([MesC≡M{OC(CF$_3$)$_2$(CH$_3$)}$_3$], M = Mo, W). These catalysts bearing highly fluorinated alkoxide ligands show advanced reaction profiles, which are owed by the significantly accelerated reaction rates, the less basic fluorinated alkoxide ligands, and the sterically demanding benzylidyne ligand.[126–129]

B   RESULTS AND DISCUSSION

B.1   COLLECTIVE TOTAL SYNTHESIS OF CASBANE DITERPENES: ONE STRATEGY – MULTIPLE TARGETS

Remark: Dr. Johanna Novacek initiated the total synthesis project of casbane diterpenes and explored a different approach towards the casbane diterpenes, including preliminary attempts of the RCAM/*trans*-hydrostannation/diversification. Parts of this research were carried out in collaboration. Her accomplishments helped to redesign the route and to develop the herein described total synthesis approaches.

1   FIRST APPROACH – STUDIES TOWARDS THE TOTAL SYNTHESIS OF 2-*EPI*-HYDROXYDEPRESSIN AND SINULARCASBANE A

1.1   ISOLATION AND STRUCTURAL ELUCIDATION

1-*epi*-10-Hydroxydepressin and 2-*epi*-10-hydroxydepressin

1-*epi*-10-Hydroxydepressin (**4**)[6] and 2-*epi*-10-hydroxydepressin (**5**)[4] (Figure 13) were first isolated from the South China Sea soft coral *Sinularia depressa*, which was collected at a depth of 20 m in the Lingshui Bay, Hainan Province, China. Extraction of the natural materials (510 g) and chromatographic purification of the dark brown residue gave 1-*epi*-hydroxydepressin (**4**, 1.6 mg) and 2-*epi*-10-hydroxydepressin (**5**, 1.9 mg) as a colourless oil each.

The casbane framework of 1-*epi*-10-hydroxydepressin (**4**) was elucidated by 2D-NMR analysis.[6] The *trans* configuration of the cyclopropane was determined by nOe analysis in combination with the ^{13}C NMR chemical shifts. The absolute stereochemistry of the C10−OH stereocentre was determined by Mosher ester analysis. No conclusive stereochemical relationship between the C10−OH group and the absolute configuration at the cyclopropane was identified based on NMR analysis. Therefore, CD analysis was conducted, which revealed the absolute configuration as 1*R*,2*S*,10*S*.[6]

The structure of 2-*epi*-10-hydroxydepressin (**5**)[4] was elucidated by 2D-NMR analysis and by comparison of analytical data with 1-*epi*-10-hydroxydepressin (**4**)[6]. Unfortunately, the Mosher ester analysis was unsuccessful, due to the limited amount of isolated material.[4] The *trans* configuration of the cyclopropane was determined by ^{13}C NMR and ROESY spectra analysis, as well as by comparison to related casbane diterpenes from *Sinularia* sp. and *S. depressa*.[6,7] Due to the flexibility of the macrocycle, the relative configuration at C10 could not be elucidated by nOe experiments. Consequently, the configuration of C10−OH group was tentatively assigned by comparing the ^{13}C NMR chemical shift (C10, δ = 65.1 ppm) with those of sinularcasbane A (**3**)[7] (C10, δ = 66.2 ppm) and 10-hydroxydepressin (**2**)[6] (C10, δ = 67.5 ppm),

in combination with biogenetic considerations. The absolute configuration was then determined as 1*S*,2*R*,10*S* by CD and comparison to structurally similar casbanes.[4]

Sinularcasbane A

Sinularcasbane A (**3**) (Figure 13) was first isolated together with five new casbanes and six known analogues from a South China Sea soft coral *Sinularia* sp,[7] which were collected at a depth of 8 m off the coast of Ximao island, Hainan Province, China. Extraction of the natural materials (2.7 kg) and chromatographic purification of the residue gave sinularcasbane A (**3**) as a colourless oil (2.1 mg). The structure was elucidated by 2D-NMR analysis and by comparison to 10-hydroxydepressin (**2**).[6]

The initial NMR data analysis revealed the similarity of sinularcasbane A (**3**) and 10-hydroxydepressin (**2**). The only significant deviation was the upfield shifted C20 signal (δ = 15.0 ppm) compared to that of 10-hydroxydepressin (**2**, δ = 18.3 ppm). Consequently, the isolation team suggested a diastereomeric relationship, in which both casbane diterpenes possess a *cis*-configured cyclopropane. The absolute configuration of C10−OH was assigned by biogenetic considerations and by comparison to 10-hydroxydepressin (**2**). The absolute configuration of the cyclopropane was assigned, based on the absolute configuration of C10−OH and the diastereomeric relationship to 10-hydroxydepressin (**2**).

As illustrated in Figure 13, this selection of the casbane natural products only differs in the configuration of the cyclopropane, which appears in all four possible permutations.

10-hydroxydepressin (2)   sinularcasbane A (3)   1-*epi*-10-hydroxydepressin (4)   2-*epi*-10-hydroxydepressin (5)
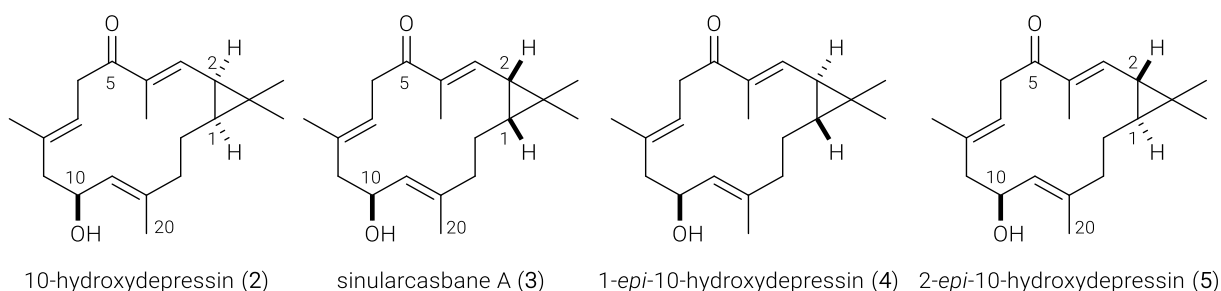
Figure 13. Selection of casbane natural products as synthetic targets 10-hydroydepressin (**2**)[6], sinularcasbane A (**3**)[7], 1-*epi*-10-hydroydepressin (**4**)[6], 2-*epi*-10-hydroxydepressin (**5**)[4].

1.2 OBJECTIVES

The casbane diterpenes are extremely rare in nature.[4] The discovery of these four casbanes demonstrates a fascinating structural similarity within the natural product family (Figure 13).

None of these casbanes has been approached by classic total synthesis, yet. In addition, the stereochemical assignments of 1-*epi*-10-hydroxydepressin (**4**), 2-*epi*-10-hydroxydepressin (**5**), and sinularcasbane A (**3**) are based more on assumptions than on data-driven conclusions. Therefore, the first total synthesis of these natural products with a diversity-oriented strategy would not only clarify the relative and absolute configuration, but also would bring at least four casbane derivatives into reach, and provide material for biological assays. The resulting synthetic plan should be concise, efficient and flexible in order to address all four permutations at the cyclopropane in one strategy. This flexibility should be catalytically achieved, rather than obtaining these motives from the narrow chiral natural pool[130] or utilising a masked *gem*-dimethyl unit.[131]

1.3 RETROSYNTHETIC ANALYSIS OF SINULARCASBANE A

This approach was based on the employment of RCAM to form the unsaturated macrocycle, followed by a hydroxy-directed *trans*-hydrostannation of the resulting cyclic alkyne. The resulting alkenyl stannane, which would contain the desired double bond geometry, would be used in late-stage diversification as a platform to access the desired oxygenation pattern in the "northern" sector. This late-stage diversification strategy was already successfully applied to several complex natural product syntheses.[74,132−134]

The total synthesis of sinularcasbane A (**3**) would be completed by oxidation of the alcohol at C5, followed by deprotection of the C10−OH (Scheme 11). The C5−OH group was envisioned as a directing group for the *trans*-hydrostannation of macrocyclic alkyne **59**, introducing the required alkene geometry. Then, the resulting stannane would be subjected to formal Stille cross coupling with methyl iodide to install the missing methyl group at the C18 position.

Macrocyclic alkyne **59** would be formed by RCAM of the terminal/methyl-capped diyne **60**, which would contain the *gem*-dimethyl cyclopropane in conjugation to the C≡C triple bond. This motif is an interesting structural pattern for RCAM and late-stage diversification of the resulting macrocyclic alkyne. The terminal alkyne of the RCAM precursor **60** would be introduced by oxidation and subsequent Bestmann-Ohira homologation of the corresponding aldehyde. The elongated cyclopropyl fragment **62** was envisaged to be coupled with western fragment **61**, after the secondary boronic ester would be selectively mono-oxidised to the corresponding alcohol. Cyclopropane fragment **63** would be elongated by carbometalation of the terminal alkyne and subsequent palladium catalysed coupling with vinyl bromide. The formed diene would then be subjected to an enantioselective bisborylation to afford the elongated cyclopropyl fragment **62**.[135] The western fragment synthesis (**61**) would commence from pentynol **64** followed by a hydroboration and bromination sequence to furnish *E*-alkenyl bromide **65**. The subsequent oxidation of **65** and introduction of the methyl-capped alkyne unit on treatment with the corresponding Grignard reagent would afford the desired western fragment **61**.
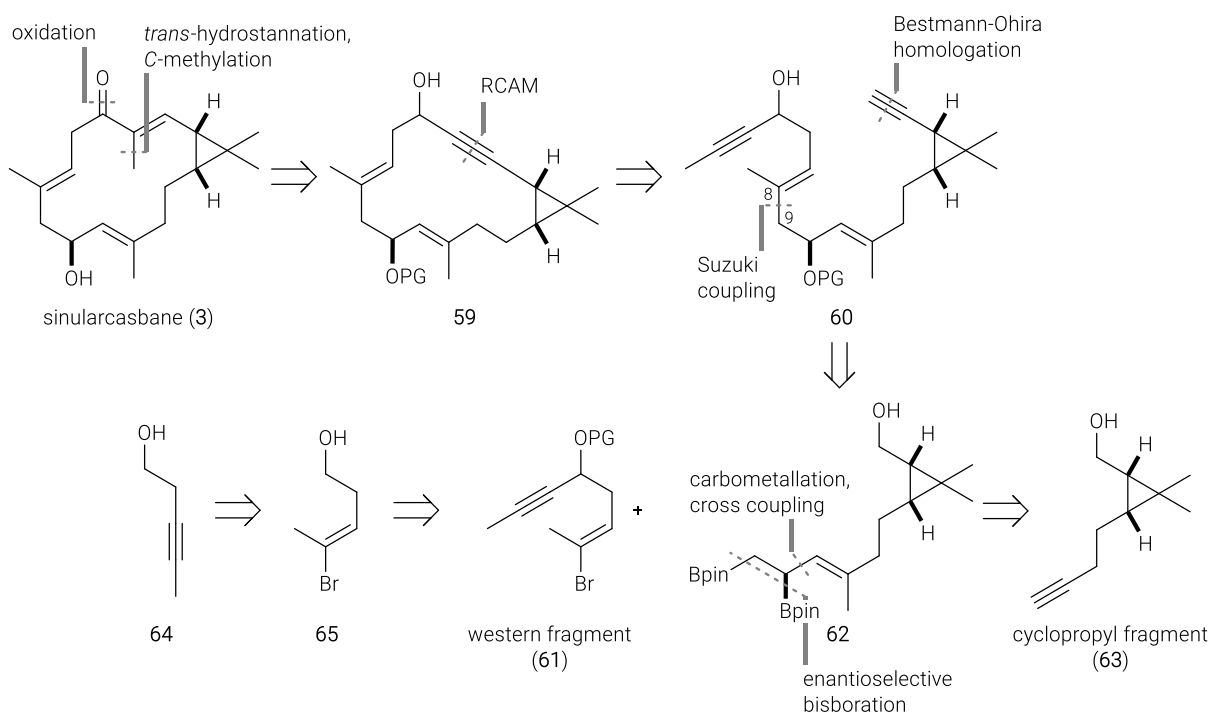
Scheme 11. Retrosynthetic analysis of sinalurcasbane A (**3**) − second approach.

The cyclopropyl fragment synthesis (**63**) would be accomplished by a multi-step sequence including hydrogenation of the electron poor alkene **66** in presence of the cyclopropane, selective ester reduction and subsequent Bestmann-Ohira homologation of the resulting aldehyde to introduce the terminal alkyne (Scheme 12). The reduction of bicyclic lactone **67** to bicyclic lactol **68**, which is in equilibrium with the open monocyclic aldehyde **69**, would allow for the introduction of unsaturated ester (**66**) by Wittig homologation. The key intermediate **67**, would be accessed via an enantioselective cyclopropanation of allyl diazoester **70**, which in turn would be readily available in two steps from prenyl alcohol **71** and diketene **72** (Scheme 12). The intramolecular cyclopropanation and the synthesis of the diazoester **70** are literature-known.[69]
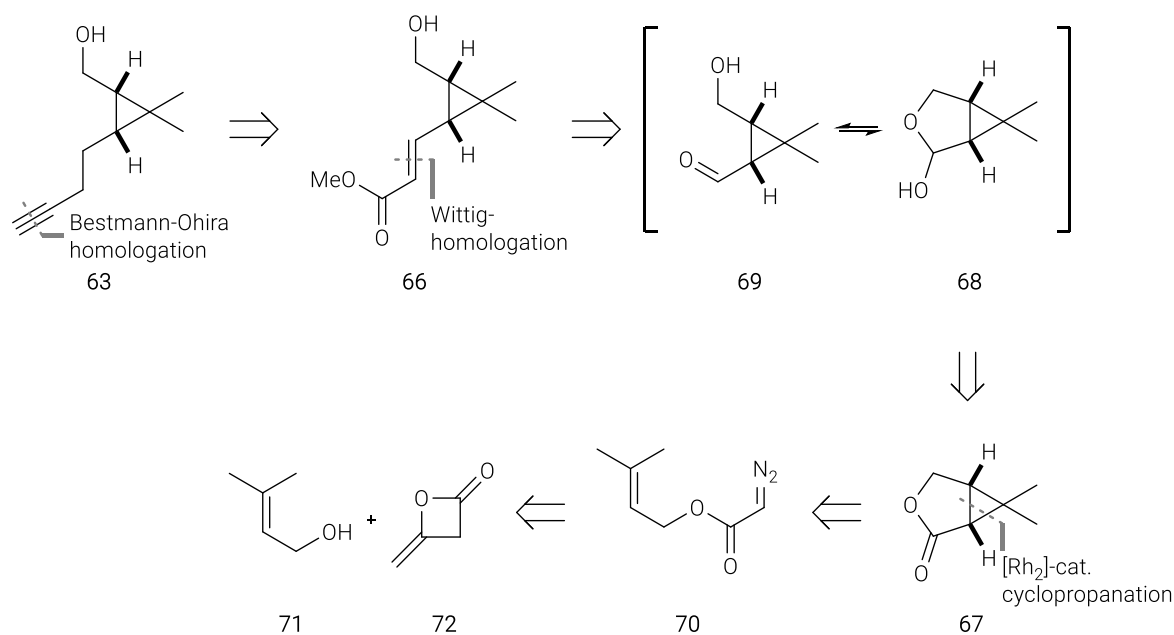
Scheme 12. The retrosynthetic analysis incorporating Doyle's intramolecular dirhodium catalysed cyclopropanation.

1.4 SYNTHESIS OF THE CYCLOPROPYL FRAGMENT

1.4.1 ENANTIOSELECTIVE CYCLOPROPANATION – SIMMONS-SMITH APPROACH

Initially, an enantioselective Simmons-Smith cyclopropanation of allylic alcohol **73** with 2,2-diiodo propane **74** *via* the Denmark-Kobayashi or Charette modification was investigated (Table **1**).

In terms of the Denmark-Kobayashi variant, the order of addition as well as the equivalents of Et$_2$Zn and chiral promotor **75** were varied. These attempts resulted in up 59% yield of the desired cyclopropane **76** with no induced chirality. In addition, the Charette modification at different temperatures, employing boronic ester **77** as chiral promotor, either led to no reaction or decomposition (Table 1). Therefore, a literature-known intramolecular catalyst-controlled cyclopropanation was employed.

Table 1. Simmons-Smith cyclopropanation – summary.

Methodology	Result
Denmark-Kobayashi Modification	Racemic, up to 59%
Charette Modification	No Reaction or Decomposition
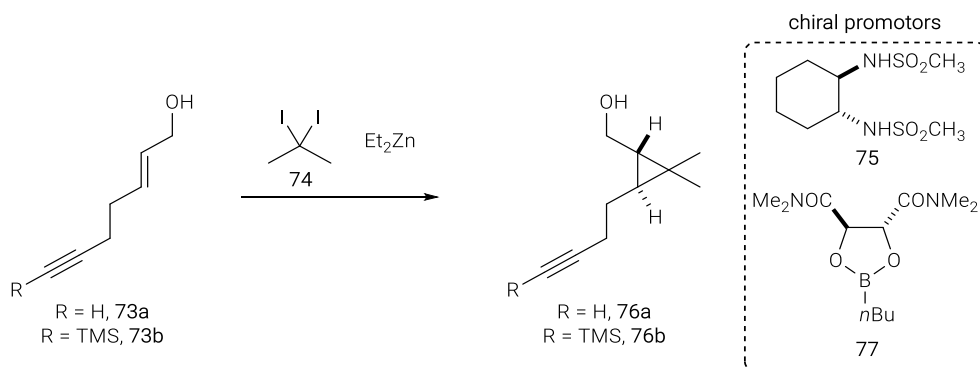
1.4.2 ENANTIOSELECTIVE CYCLOPROPANATION – [RH₂(MEPY)₄] CATALYSED CYCLOPROPANATION

[Rh$_2$(MEPY)$_4$] was discovered as a novel catalyst for the enantioselective intramolecular cyclopropanation of allyl diazoesters by M. P. Doyle and co-workers 30 years ago. The desired *cis-gem*-dimethyl cyclopropane is exclusively formed in very good yield with excellent enantioselectivity, while employing very low catalyst loading (0.1-1.0 mol%, Scheme 13).[69] Both enantiomers of the dirhodium(II) carboxamidate paddlewheel complex are literature-known ([Rh$_2$(5*R*-MEPY)$_4$] (**78**) and [Rh$_2$(5*S*-MEPY)$_4$] (**79**)) and enable the synthesis of both cyclopropane enantiomers (1*S*,2*R*-**80** & 1*R*,2*S*-**67**) (Scheme 13). The *trans* cyclopropane motives would be accessible by epimerising one of the bridging carbon stereocentres in the course of the total synthesis. Nevertheless, the [Rh$_2$(MEPY)$_4$] catalysts show an impressive reactivity profile including (intramolecular) cyclopropanation and intramolecular C−H insertion. Thus, these are applied in some total syntheses.[38,69,143−147,70,136−142]
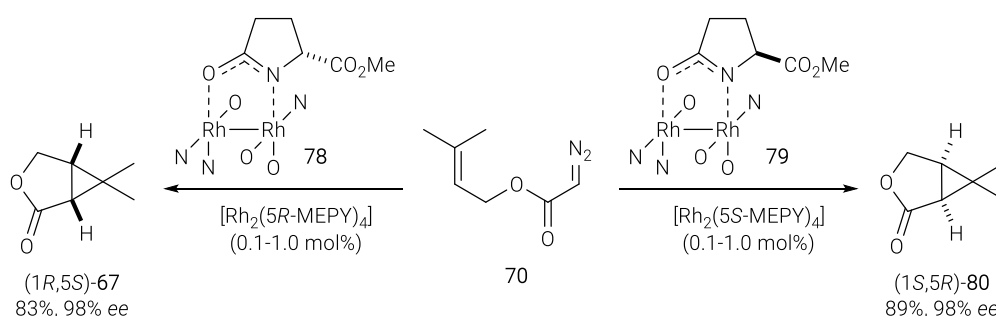
Scheme 13. Enantioselectivity of Doyle's [Rh$_2$(5*R*-MEPY)$_4$] **78** and [Rh$_2$(5*S*-MEPY)$_4$] **79** catalysts.[137,143]

The synthesis of the cyclopropyl fragment **63** commenced by NaOAc catalysed formation of β-ketoester **81** from prenyl alcohol **71** and diketene **72** in 70% yield. The subsequent Regitz diazotransfer under basic conditions with 4-acetamidobenzenesulfonyl azide (*p*-ABSA) and hydrolysis of the terminal ketone generated diazoester **70** in 75% yield. If diketene is not

available, a different protocol reported by Danheiser and co-workers might be used to access diazoester **70**.[148–150]
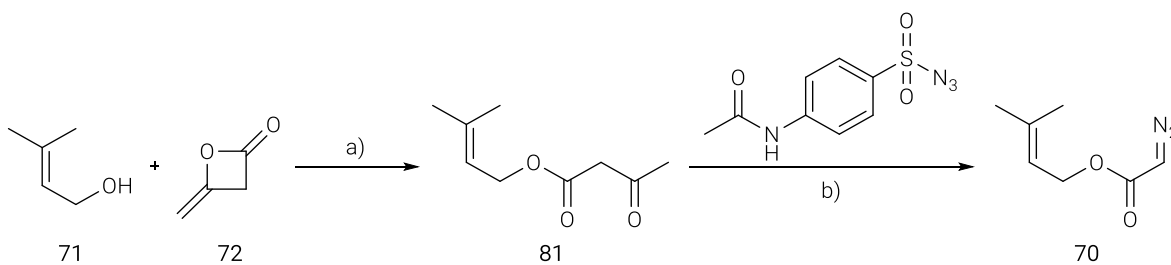
Scheme 14. Synthesis of allyl diazoester **70**. Conditions: a) **72** (1.2 equiv), NaOAc (0.12 equiv), THF, reflux, 70%; b) *i)* *p*-ABSA (1.3 equiv), Et$_3$N (1.3 equiv), MeCN, RT, *ii)* LiOH (5.5 equiv), H$_2$O, RT, 75% over 2 steps.

The intramolecular cyclopropanation was performed according to the procedure of Doyle and co-workers.[69,137,143] A mixture of diazoester **70** in CH$_2$Cl$_2$ was added over 30 hours, to prevent any dimerisation, to a refluxing mixture of [Rh$_2$(5*R*-MEPY)$_4$] catalyst **78** (0.5 mol%) in CH$_2$Cl$_2$. The desired lactone **67** was obtained in 89% yield with an enantioselectivity of 94% *ee* on multigram scale.
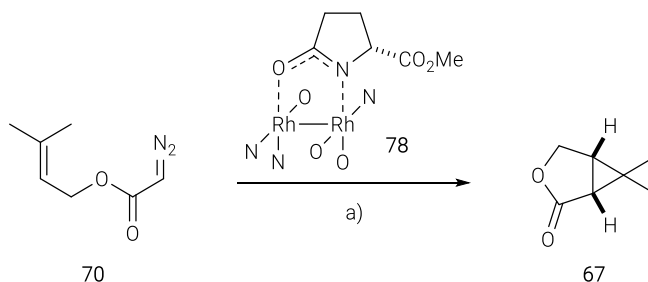
Scheme 15. Cyclopropanation of allyl diazoester **70** by Doyle's [Rh$_2$(5*R*-MEPY)$_4$] catalyst. Conditions: a) **70** (in CH$_2$Cl$_2$, addition over 30 h), [Rh$_2$(5*R*-MEPY)$_4$] (0.5 mol%), CH$_2$Cl$_2$, reflux, 89% (94% *ee*).

The reduction of lactone **67** to the corresponding lactol **68** was carried out by slow addition of DIBAL-H at −78 °C (Scheme 16).[151] This procedure avoided any over-reduction to the undesired diol. The resulting bicyclic lactol **68** was expected to be in an equilibrium with the monocyclic aldehyde **69**, which was converted into **66** by a Wittig homologation in 80% yield over two steps. The electron deficient alkene **66** was selectively hydrogenated in the presence of the strained cyclopropane with catalytic amounts of cobalt(II) chloride, using sodium borohydride as reducing agent under a hydrogen atmosphere, instead of an inert gas atmosphere.[152,153] These slightly modified conditions afforded the saturated ester **82** in 94% yield. The ester functionality was then reduced to the corresponding aldehyde **83** with DIBAL-H in CH$_2$Cl$_2$ at −78 °C. The resulting aldehyde was subjected to Bestmann-Ohira homologation to give cyclopropyl fragment **63** in 68% yield over two steps. In conclusion, the synthesis of fragment **63** was completed in eight steps and 24% overall yield (Scheme 16).
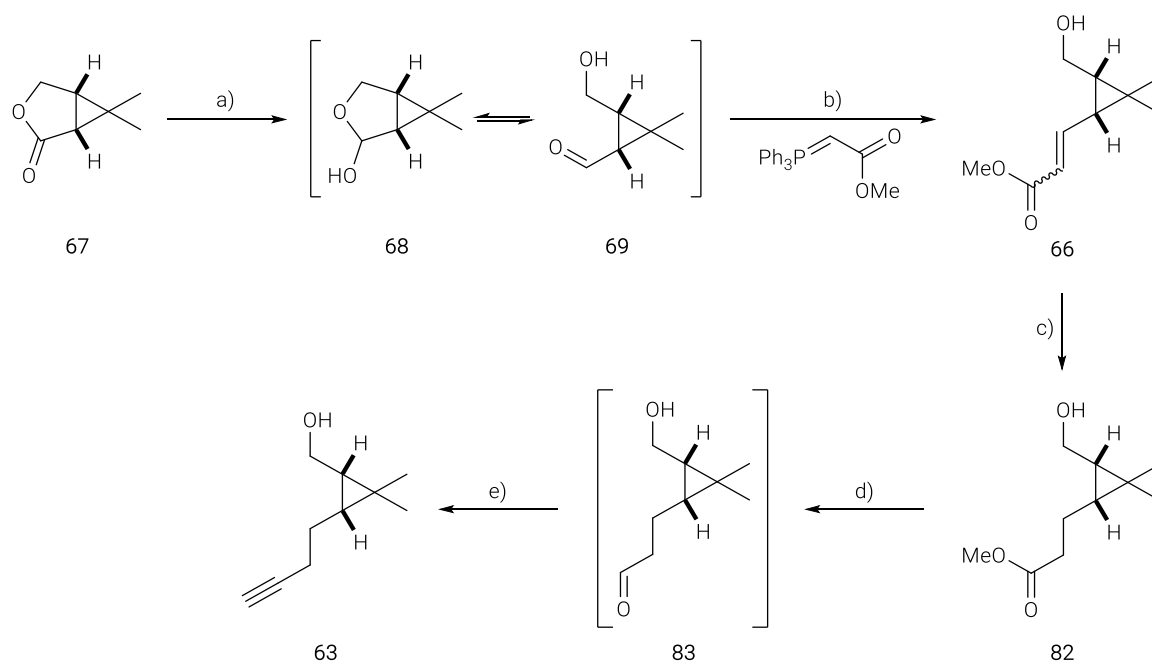
Scheme 16. Synthesis of the cyclopropyl fragment **63**. Conditions: a) DIBAL-H (1.02 equiv, CH$_2$Cl$_2$), CH$_2$Cl$_2$, −78 °C; b) phosphoranylide (2.0 equiv), THF, 60 °C, 81% over 2 steps (E:Z ≥ 20:1); c) E-ester **66** (1.0 equiv), CoCl$_2$·H$_2$O (20 mol%), NaBH$_4$ (5.0 equiv), MeOH, DMF, RT, 94%; d) i) DIBAL-H (2.4 equiv, in CH$_2$Cl$_2$), CH$_2$Cl$_2$, −78 °C, ii) Bestmann-Ohira reagent (1.5 equiv), K$_2$CO$_3$ (2.0 equiv), MeOH, RT, 68% over 2 steps.

The resulting terminal alkyne **63** was subjected to carbometalation with Cp$_2$ZrCl$_2$ and Me$_3$Al in CH$_2$Cl$_2$ at room temperature. The resulting alkenylalumination species were quenched with iodine at −78 °C to obtain the corresponding E-alkenyl iodide **84** in only 13% yield (Scheme 18). Due to this low yielding reaction sequence, the O-silylated alcohol derivative **85** was envisaged to be more suitable for the carbometalation/iodination sequence (Scheme 16).

Therefore, the primary alcohol **82** was TBS-protected and the resulting ester **86** was reduced with DIBAL-H to aldehyde **87**. Bestmann-Ohira homologation afforded terminal alkyne **85** in 82% yield over two steps. In conclusion, the O-silylated cyclopropyl fragment **85** was prepared in nine steps and 26% overall yield (Scheme 16, Scheme 17).
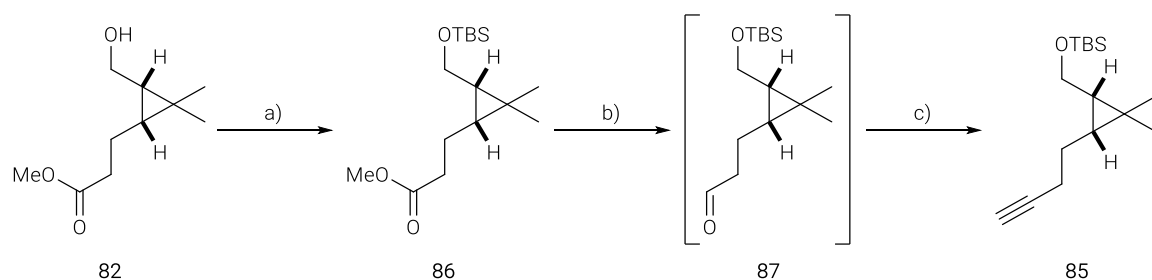
Scheme 17. Synthesis of the TBS-protected cyclopropyl fragment **85**. Conditions: a) TBSCl (1.2 equiv), imidazole (1.5 equiv), DMF, CH$_2$Cl$_2$, RT, 98%; b) DIBAL-H (1.02 equiv, in CH$_2$Cl$_2$), CH$_2$Cl$_2$, −78 °C; c) Bestmann-Ohira reagent (1.5 equiv), K$_2$CO$_3$ (2.0 equiv), MeOH, RT, 82% over 2 steps.

The cyclopropyl fragment **85** were subjected to a carbometalation/iodination sequence to obtain the corresponding E-alkenyl iodide **88** in 39% yield. (Scheme 18, right).
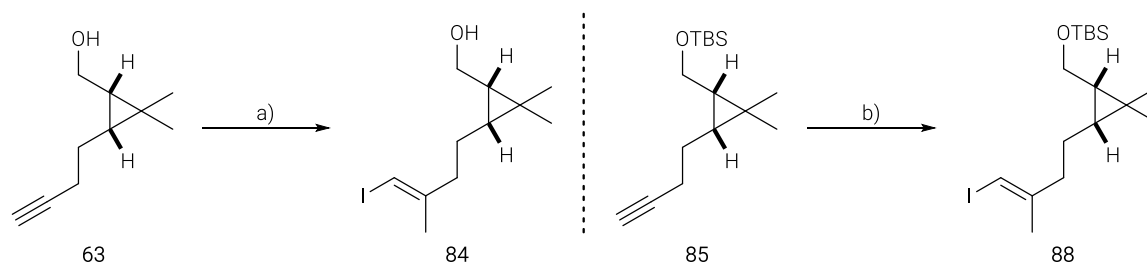
Scheme 18. Carbometalation of the cyclopropyl fragments **84** and **88**. Conditions: a) *i*) Cp_2ZrCl_2 (20 mol%), Me_3Al (3.0 equiv), CH_2Cl_2, RT; *ii*) I_2, THF, −78 °C, 13% over 2 steps (*E:Z* ≥ 20:1); b) *i*) Cp_2ZrCl_2 (20 mol%), Me_3Al (2.0 equiv), H_2O (1.0 equiv), CH_2Cl_2, −7 °C; *ii*) I_2, THF, −78 °C, 39% over 2 steps (*E:Z* ≥ 20:1).

This approach towards the elongated cyclopropyl fragment **62** included many steps with a low yielding carbometalation/iodination sequence. The disillusioning situation caused the termination of this approach and let us develop a significantly distinct synthetic strategy.

2 SECOND APPROACH WITH NEW TARGET –

ENT-DEPRESSIN

Initially, *ent*-depressin (**89**, Scheme 19) was chosen as the prevailing target to develop a synthetic route. The lactone **67** containing the cyclopropane unit was readily available and was used as an intermediate in this approach. The lack of the C10−OH group, in comparison to the previous target sinularcasbane A (**3**), reduced the synthetic effort throughout the development of a viable route.

2.1 ISOLATION AND STRUCTURAL ELUCIDATION

Depressin

Depressin (**9**) was first isolated with eight other casbane analogues from the South China Sea soft coral *Sinularia depressa*, which was collected at a depth of 20 m in the Lingshui Bay, Hainan Province, China (Figure 15).[6] Extraction of the natural material (510 g) and chromatographic purification of the dark brown residue gave depressin (**9**) as a colourless oil (5.6 mg). The casbane diterpene framework was elucidated by 2D-NMR analysis.[6] The *cis* configuration of the cyclopropane was assigned by nOe experiments in combination with the characteristic ^{13}C NMR chemical shifts. The absolute configuration was determined as 1*S*,2*R* by CD analysis.[6]

2.2 RETROSYNTHETIC ANALYSIS

In analogy to the previous retrosynthetic analysis, this approach included the same four final steps, RCAM, *trans*-hydrostannation, *C*-methylation, and oxidation. In this approach, a disconnection was envisaged between C12 and C13, which would lead to the cyclopropyl fragment **90** and the western fragment **91**.

The major challenges regarding the RCAM of diyne **92** to macrocycle **93** would be the terminal alkyne in conjugation to the cyclopropane as well as the C5−OH group (see chapter 3). The concise profile of this approach is based on combining advanced fragments (**90** & **91**), followed by only five steps to complete the total synthesis of *ent*-depressin (**89**).

The corresponding *C-/O*-silylated RCAM precursor would be obtained by chemo- and regioselective hydroboration of the terminal alkene **90** over the alkyne functionality and subsequent sp^2-sp^3 Suzuki cross coupling with the western fragment **91**. The sterically demanding TIPS group of the cyclopropyl fragment **90** was introduced to shield the alkyne and to obtain the desired chemoselectivity during the hydroboration (Scheme 19). A global deprotection would give access to the RCAM-required alkyne functionality (**92**).
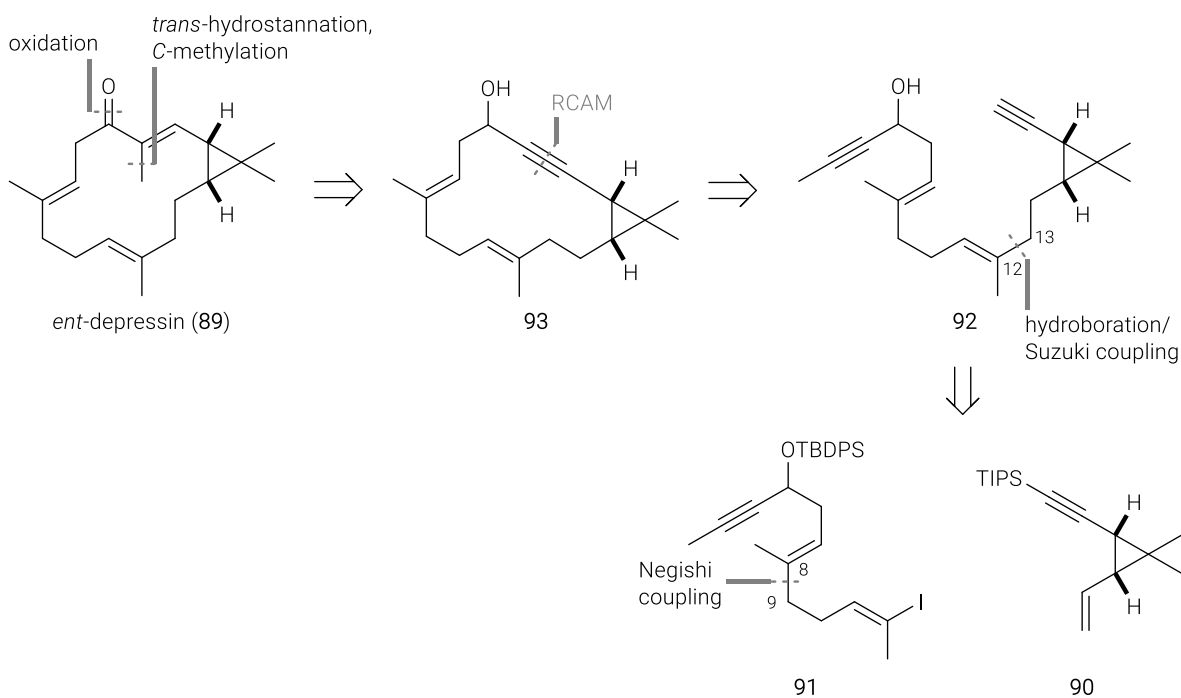
Scheme 19. Retrosynthetic analysis of *ent*-depressin (**89**) – second approach.

The *C*-silyl protected alkyne group of the cyclopropyl fragment **90** would be introduced by oxidation of alcohol **94** and Corey/Fuchs homologation. The previously described synthesis of lactone **67**, followed by reduction and Wittig homologation of the resulting aldehyde would provide terminal alkene **90** (Scheme 20).
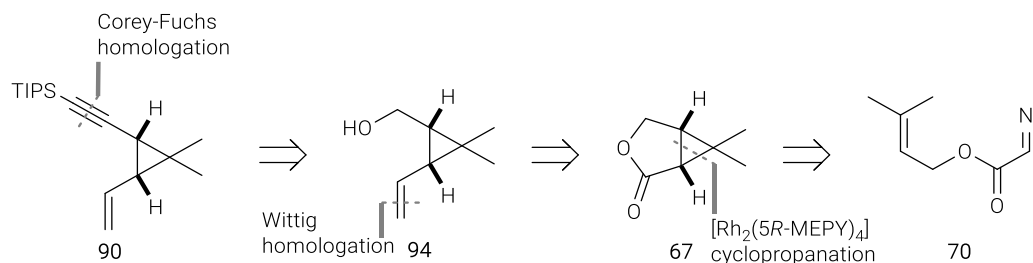
Scheme 20. Retrosynthetic analysis of the cyclopropyl fragment **90** – second approach.

The Suzuki cross coupling partner **91** would be completed by stereoselective iododesilylation of the corresponding alkenyl silane (Scheme 21). The silyl group was envisaged as a masked iodide, allowing the sp^2-sp^3 Negishi cross coupling between C8 and C9 (**95** & **96**) to proceed without any reactivity at the C12 position (Scheme 21). Alkenyl halide **95** would be synthesised by a (formal) hydroboration of **64**, transformation of the resulting boronic ester into alkenyl halide **97**, and introduction of the methyl-capped alkyne unit. The organozinc compound **96** would derive from the corresponding alkyl iodide, which in turn would be obtained by an Appel iodination. A sequence of lithiation/silylation starting from 2,3-dihydrogen furan **98** followed by a nickel(0) catalysed opening of **99** with methyl magnesium bromide would lead to the desired alcohol readily for iodination.[154,155]
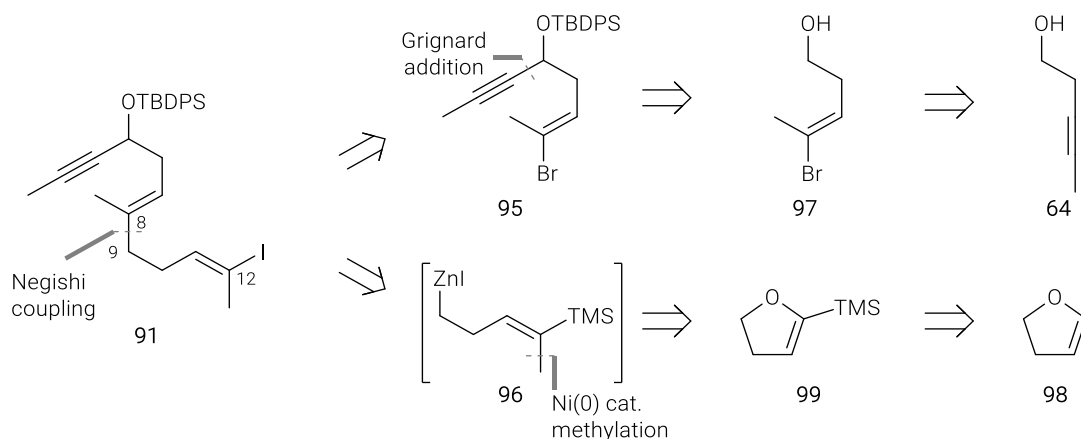
Scheme 21. Retrosynthetic analysis of the western fragment **91** – second approach.

2.3 SYNTHESIS OF THE CYCLOPROPYL FRAGMENT

As in the previous approach, the synthesis of the cyclopropyl fragment **90** commenced with the preparation of β-ketoester **81** from prenyl alcohol **71** and diketene **72** under basic conditions. Introduction of the diazo group to β-ketoester **81** by Regitz diazo transfer and subsequent hydrolysis gave diazoester **70** in three steps and 53% yield (see chapter 1.4.2, Scheme 14).[138] The enantioselective *gem*-dimethyl cyclopropanation led to *cis*-cyclopropyl lactone **67** in 89% yield with 94% *ee* on treatment with [Rh$_2$(5*R*-MEPY)$_4$] (**78**). The selective DIBAL-H reduction of lactone **67** at −78 °C in CH$_2$Cl$_2$ provided lactol **68**, which was in equilibrium with the monocyclic aldehyde **69**. This in turn was used in a Wittig homologation and terminal alkene **94** was isolated in 66% yield, according to a literature known protocol.[156] Dess-Martin oxidation of alcohol **94** gave aldehyde **100**, which was converted into dibromide **101** upon treatment with the *in situ* generated phosphorus ylide in CH$_2$Cl$_2$ at 0 °C. Unfortunately, 8.0 equivalents of triphenylphosphine and 4.0 equivalents of carbon tetrabromide were necessary to consume aldehyde **100** completely. These quantities of triphenylphosphine and carbon tetrabromide were twice as in ordinary procedures.[157] Any further attempts to improve the yield by increasing the temperature or by purifying the aldehyde **100** and bromide **101** intermediates led to decomposition. The dibromination reaction was quenched with pentane at 0 °C, the precipitated triphenylphosphine was filtered off, and crude dibromide **101** was subjected to the Fritsch-Buttenberg-Wiechell rearrangement. Treatment of dibromide **101** with *n*-BuLi at −78 °C and subsequent quenching of the resulting organolithium species with TIPSCl provided the cyclopropyl fragment **90** in 46% yield over the final three steps. Overall, the synthesis of the cyclopropyl fragment **90** was achieved in eight steps and 14% overall yield.
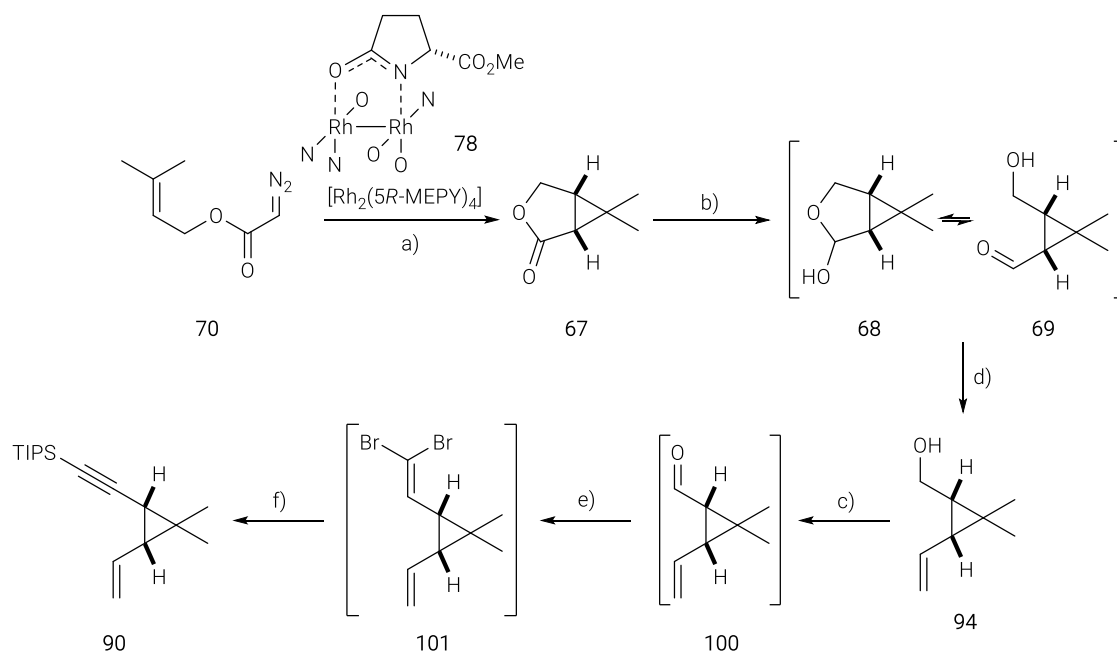
Scheme 22. Synthesis of the cyclopropyl fragment **90**. Conditions: a) [Rh$_2$(5R-MEPY)$_4$]·2MeCN (0.5 mol%), CH$_2$Cl$_2$, reflux, 89% (94% ee); b) DIBAL-H (1.02 equiv in CH$_2$Cl$_2$), CH$_2$Cl$_2$, −78 °C; c) Ph$_3$PCH$_2$ (1.5 equiv), THF, RT, 66% over 2 steps; d) DMP (1.5 equiv), CH$_2$Cl$_2$, RT; e) PPh$_3$ (8.0 equiv), CBr$_4$ (4.0 equiv), CH$_2$Cl$_2$, 0 °C; f) *i*) *n*-BuLi (2.0 equiv), THF, −78 °C; *ii*) TIPSCl (2.0 equiv), −78 °C, 46% over 3 steps.

2.4 SELECTIVE HYDROBORATION OF THE CYCLOPROPYL FRAGMENT

Initially, the feasibility of the chemo- and regioselective hydroboration of the terminal alkene **90** in combination with the subsequent Suzuki cross coupling of the resulting alkyl borane **104** was investigated with alkenyl bromide **102**, instead of the western fragment **91**. The selective hydroboration with the 9-H-9-BBN dimer was carried out in toluene at 100 °C followed by the sp^2-sp^3 Suzuki cross coupling (Scheme 23).[158−162] This sequence yielded the desired isomer **103** in 56% yield and demonstrated the chemo- and regioselective hydroboration of terminal alkene **90** over the sterically shielded alkyne, the integrity of the cyclopropane, and the suitability of borane **104** for Suzuki cross coupling.
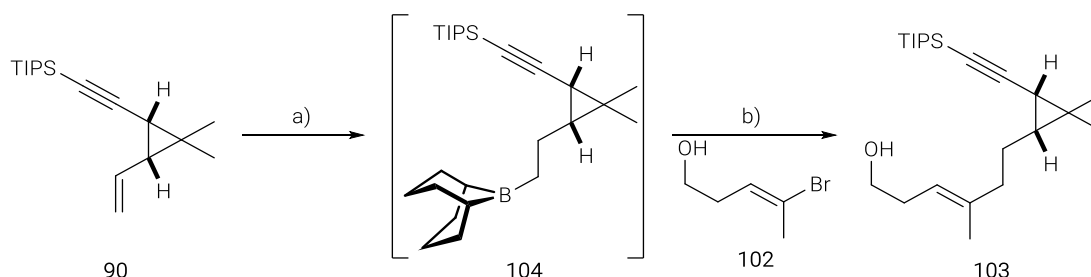
Scheme 23. Selective hydroboration and Suzuki cross coupling. Conditions: a) *i*) 9-H-9-BBN dimer (0.6 equiv), toluene, 100 °C; *ii*) **102** (1.0 equiv), [(dppf)PdCl$_2$] (5 mol%), NaOH (2.6 equiv), H$_2$O, THF, 55 to 75 °C, 56% over 2 steps.

2.5 SYNTHESIS OF THE WESTERN FRAGMENT

The first attempts towards the synthesis of the western fragment **91** intended to use alkenyl bromide **97** (Scheme 21, Scheme 24). Pentynol **64** was transformed into the corresponding *Z*-alkenyl boronic ester **105** via a copper catalysed formal hydroboration in 75% yield.[163] The following bromination gave the desired alkenyl bromide **97** in 81% yield. Unfortunately, the

subsequent Dess-Martin oxidation resulted in a mixture of the desired *E*-alkenyl bromide *E*-**106**, the undesired *Z*-isomer *Z*-**106**, and unknown side-products. Buffering of the reaction mixture on treatment with sodium bicarbonate or accelerating the depletion of acetate of the Dess-Martin periodinane with *t*BuOH led to inconsistent results, especially regarding the *E*-**106**/*Z*-**106** ratio.[164] Hence, alkenyl bromide **97** was replaced by alkenyl iodide **107**. In this case, it was envisaged that the formation of the undesired *Z*-**106** isomer would be suppressed by enhanced hyperconjugation (Scheme 24).
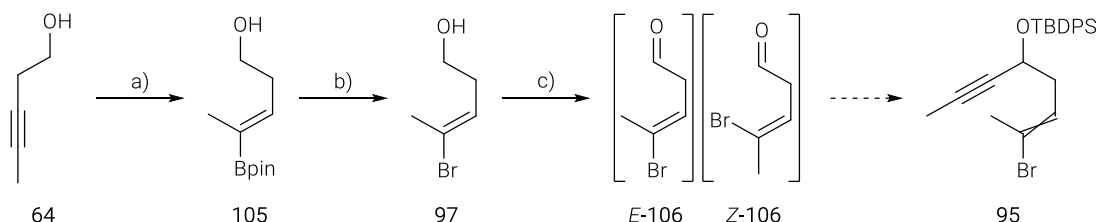
Scheme 24. Synthesis of alkenyl bromide **106**. Conditions: a) CuCl (5 mol%), PPh$_3$ (6 mol%), *t*-BuOK (20 mol%), B$_2$pin$_2$ (1.1 equiv), MeOH (2.0 equiv), THF, RT, 75%; b) CuBr$_2$ (5.0 equiv), EtOH/H$_2$O (1:1), 80 °C, 81%; c) DMP (1.5-2.0 equiv), NaHCO$_3$ (0-10 equiv), *t*-BuOH (0-1.5 equiv), CH$_2$Cl$_2$, 0 °C.

However, direct iodination of boronic ester **105** gave alkenyl iodide **107** in only 10% yield under aqueous basic conditions (Scheme 25). This insufficient result prompted us to explore an unconventional alkenyl halide exchange under Finkelstein conditions.[165] Treatment of alkenyl bromide **97** with sodium iodide and catalytic amounts of copper(I) iodide afforded the desired alkenyl iodide **107** in 82% yield.[165] Subsequent Dess-Martin oxidation at 0 °C, followed by rapid addition of propynyl magnesium bromide to a solution of the corresponding aldehyde in THF at 0 °C gave propargylic alcohol **109** in 62% yield; no isomerisation of the alkene geometry was detected (*E:Z* ≥ 20:1, ^{1}H NMR) (Scheme 25). *O*-silylation of **109** with quantitative yield enabled the Negishi cross coupling with organozinc reagent **96**.
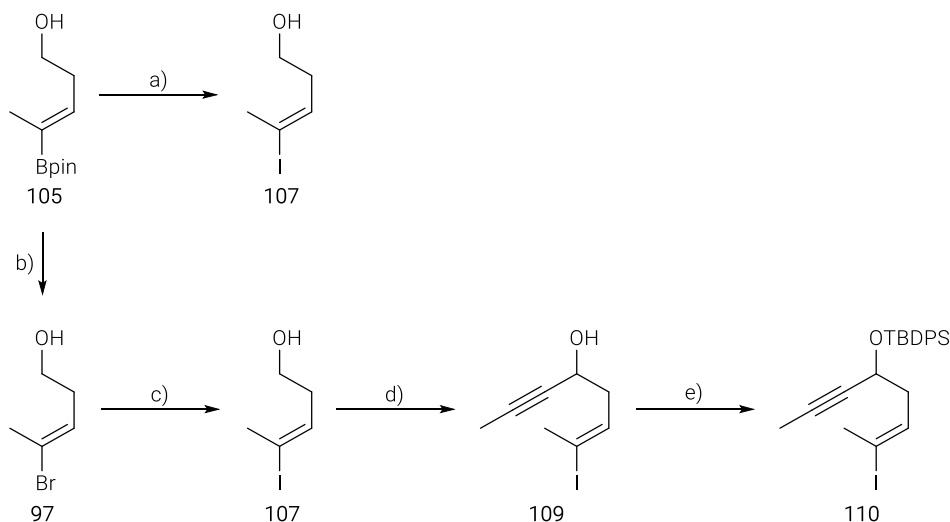
Scheme 25. Synthesis of alkenyl iodide **110**. Conditions: a) NaOH (3.0 equiv), I$_2$ (2.0 equiv), H$_2$O/THF, RT, 10%; b) CuBr$_2$ (5.0 equiv), EtOH/H$_2$O (1:1), 80 °C, 81%; c) CuI (5 mol%), NaI (1.5 equiv), DMEDA (10 mol%), MeOH, 120 °C, 82%; d) *i*) DMP (1.5 equiv), CH$_2$Cl$_2$, 0 °C to RT, *ii*) Propynyl MgBr (3.0 equiv), THF, 0 °C, 62% over 2 steps; e) TBDPSCl (1.5 equiv), imidazole (2.0 equiv), DMF, CH$_2$Cl$_2$, RT, quant.

The synthesis of alkylzinc iodide **96** was accomplished in four steps starting from 4,5-dihydrofuran **98**. This furan was selectively lithiated of the C2 position and the resulting organolithium intermediate was quenched with TMSCl. The obtained 2-silyl dihydrofuran **99** was

converted into **111** in 86% yield with high levels of stereoselectivity by a nickel(0) catalysed opening of the furan ring with methyl magnesium bromide.[154,155] Alcohol **111** was subjected to Appel reaction, providing alkyl iodide **112** in 72% yield. Following the protocol for zinc insertion of Huo and co-worker,[166] **112** was added to a mixture of preactivated zinc in DMF at 50 °C. After 1 hour the resulting organozinc reagent **96** was separated from the remaining zinc to avoid any activation of alkenyl iodide **110** during the following Negishi coupling.[167–169] Next, alkenyl iodide **110** and Pd(PPh$_3$)$_4$ were added to the solution of *in situ* prepared organozinc reagent **96** in DMF. This zinc-insertion/cross coupling sequence provided TMS masked western fragment **113** in 69% yield, in readiness for the stereoselective iododesilylation (Scheme 26).
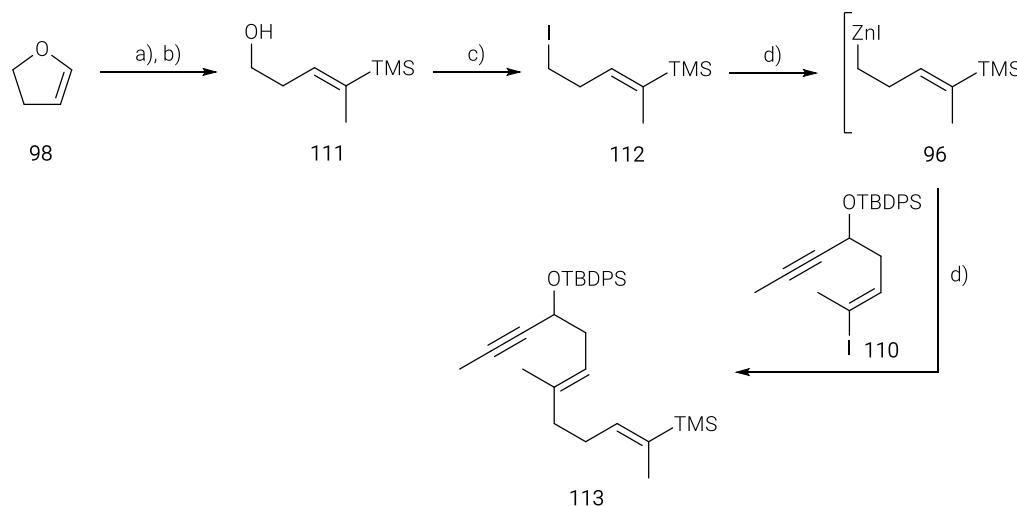
Scheme 26. Synthesis of the TMS masked western fragment **113**. Conditions: a) **98** (1.2 equiv), *t*-BuLi (1.5 equiv), THF, −40 to 0 °C, *ii*) TMSCl (1.0 equiv), THF, −78 °C to RT; b) Ni(dppe)Cl$_2$ (10 mol%), MeMgBr (2.8 equiv), toluene, reflux, 86% over 2 steps; c) NIS (1.3 equiv), PPh$_3$ (1.3 equiv), CH$_2$Cl$_2$, 0 °C to RT, 72%; d) *i*) Zn (2.5 equiv), I$_2$ (6 mol%), DMF, RT, *ii*) **112** (1.3 equiv), 50 °C, *iii*) **110** (1.0 equiv), Pd(PPh$_3$)$_4$ (6 mol%), DMF, RT, 69%.

To the best of my knowledge, the first stereoselective halodesilylation of alkenyl TMS compounds was reported in 1974 by R. B. Miller and T. Reichenbach.[170] Since then, various halodesilylation conditions have been published.[171–174] To date, iododesilylation of various alkenyl silanes (TMS, TIPS, SiMe$_2$Ph, etc.) have be performed under customised conditions with high efficiency and excellent stereoselectivity.[175,176] However, iododesilylation of α- and β-substituted alkenyl silanes, as in this total synthesis, has only little precedent in the literature.[174] The stereoselective iododesilylation of alkenyl silane **113** was investigated and optimised in terms of yield and stereoselectivity, based on conditions reported by Fleming, Kishi, Vilarrasa, Zakarian, and co-workers.[171,174–177] Thereby, a high stereoselectivity was mandatory, since separation of the *E*- and *Z*-isomers was considered as challenging.

Initially, iododesilylation conditions developed by Zakarian and co-workers were applied. *N*-iodosuccinimide (NIS) was added to a mixture of alkenyl silane **113**, 2,6-lutidine, and hexafluoro-*iso*-propanol (HFIP). However, the nonpolar alkenyl silane **113** was insoluble in the polar HFIP, leading to no conversion.[178] The addition of CH$_2$Cl$_2$ to a mixture of **113**, 2,6-lutidine, and HFIP gave a clear solution. Addition of NIS to the resulting solution led to a complex mixture of products, including the desired *E*-isomer **91** and the corresponding *Z*-isomer (Entry 2, Table 2). Vilarrasa and co-workers considered that iodine and HI reduce the stereoselectivity and efficiency during iododesilylation. Therefore, they reported a protocol, where 2,6-lutidine was replaced with by silver(I) carbonate, which acts as a base as well as an iodine and HI scavenger.[175] However, addition of NIS to a mixture of **113**, silver(I) carbonate, HFIP in CH$_2$Cl$_2$,

resulted in decomposition of the starting material (Entry 3, Table 2). In conclusion, the "Zakarian conditions" and "Vilarrasa modification" were not suitable for iododesilylation of alkenyl silane **113**.

Alternatively, a protocol reported by Kishi and co-workers was applied.[177] NIS was added to a solution of **113** in acetonitrile (MeCN) and chloroacetonitrile (ClCH$_2$CN) (vol. 4:1), affording alkenyl iodide **91** in 74% yield with a diastereoselectivity of *E:Z* = 2.6:1 (Entry 4, Table 2). Kishi and co-workers considered a solvent participation of acetonitrile with sterically tolerant allylic carbons under their iododesilylation conditions to occur, which would lower the stereoselectivity. The acetonitrile could open the cyclic iodonium ion **N** (Scheme 27), leading to motif **Q**. A subsequent *anti*-elimination would give the *Z*-alkenyl iodide **R**. By using the less nucleophilic chloroacetonitrile, the cyclic iodonium ion **N** would be opened without direct solvent participation to give motif **O**. In this case, elimination would form *E*-alkenyl iodide **P** with retention of the alkene geometry (Scheme 27). Due to these considerations, NIS was added to a solution of **113** in pure chloroacetonitrile. The starting material was consumed within 30 min and alkenyl iodide **91** was obtained in 69% yield with an increased diastereoselectivity of *E:Z* = 6.1:1 (Entry 5, Table 2).
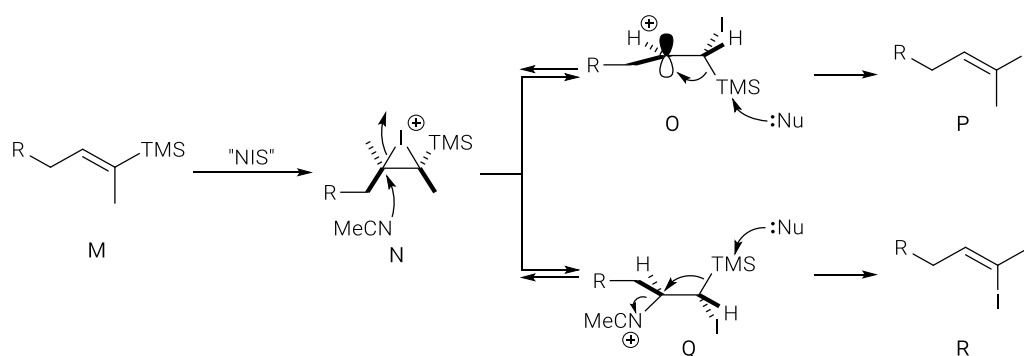
Scheme 27. Mechanism of stereoselective iododesilylation under Kishi reaction conditions.[177]

Regarding the unsatisfying stereoselectivity, the effect of silver(I) carbonate, as described by Vilarrasa and co-workers,[175] under the conditions of Kishi and co-workers was investigated. This novel iododesilylation modification, addition of NIS to a mixture of **113** and silver(I) carbonate in chloroacetonitrile, provided the desired *E*-alkenyl iodide **91** in 76% yield with full retention of the double bond geometry (*E:Z* ≥ 20:1, ^{1}H NMR) (Entry 6, Table 2). In conclusion, the western fragment **91** was obtained in 16% yield comprising eight steps along the longest linear sequence (LLS).

Table 2. Iododesilylation of alkenyl silane **113** – optimisation.
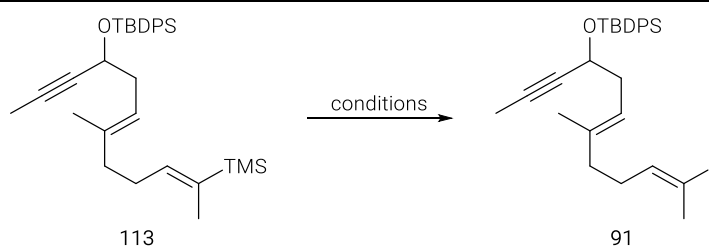
Entry	Reagents	Solvent	Temperature, Time	Results
1	NIS (1.5 equiv), 2,6-lutidine (1.5 equiv)	HFIP	0 °C, 30 min	no reaction, **113** insoluble in HFIP
2	NIS (1.5 equiv), 2,6-lutidine (1.5 equiv)	CH$_2$Cl$_2$/HFIP (25:1)	0 °C, 10 min	full conversion, complex crude NMR spectrum
3	NIS (1.2 equiv), Ag$_2$CO$_3$ (0.3 equiv)	CH$_2$Cl$_2$/HFIP (25:1)	0 °C, 30 min	decomposition
4	NIS (4 × 2.0 equiv)	MeCN/ClCH$_2$CN (4:1)	RT, 5 h	74% (*E:Z* = 2.6:1)
5	NIS (2.0 equiv)	ClCH$_2$CN	RT, 30 min	69% (*E:Z* = 6.1:1)
6	NIS (2.0 equiv), Ag$_2$CO$_3$ (0.75 equiv)	ClCH$_2$CN	RT, 3 h	76% (*E:Z* ≥ 20:1)

E:Z ratios were determined by ^{1}H NMR.

2.6 COUPLING AND MACROCYCLISATION

2.6.1 COUPLING OF THE CYCLOPROPYL AND THE WESTERN FRAGMENT

In analogy to the model system **103**, the cyclopropyl fragment **90** was united with the western fragment **91** by chemoselective hydroboration and sp^2-sp^3 Suzuki cross coupling protocol (Scheme 23). The hydroboration of terminal alkene **90** with the 9-H-9-BBN dimer was carried out at 100 °C in toluene and gave alkyl borane **104**, which was directly coupled with *E*-alkenyl iodide **91** (*E:Z* ≥ 20:1) under Suzuki conditions, using an aqueous sodium hydroxide solution as the base. This attempt led to an inseparable mixture of the desired product **114** and its regioisomer **115** in 49% yield (**114**:**115** = 1.2:1, Entry 1, Table 3). No such isomerisation was detected during the feasibility investigations (Scheme 23). Running the reaction at 70 °C increased the regioselectivity slightly towards the desired product **114** (**114**:**115** = 3.3:1, Entry 2, Table 3). Mechanistic investigations of Suzuki couplings by Kishi and co-workers revealed that the rate-determining step, which would be the problematic step in terms of regioselectivity, occurs after the oxidative addition of the palladium(0) species.[179] Further, they reported a dramatic rate acceleration by application of thallium(I) salts or silver oxide, both acting as a weak base and halide scavanger.[179] In this project, the addition of silver oxide resulted either in a mixture of regioisomers or no conversion of the starting material (Entry 3-5, Table 3). Whereas the employment of thallium(I) ethoxide as additive at room temperature provided the desired coupling product **114** in 93% yield with no regioisomer at the limit of detection (**114**:**115** ≥ 20:1, ^{1}H NMR) (Entry 6, Table 3). Additional literature research revealed the opportunity to use the less toxic barium(II) hydroxide, instead of thallium(I) ethoxide.[180] Thus, barium(II) hydroxide was applied to the Suzuki cross coupling of borane **104** and western fragment **91**. The desired coupling product **114** was obtained in 81% yield with regioselectivity of **114**:**115** ≥ 20:1 (Entry 7, Table 3). These conditions were used in the following approaches as the optimised conditions.

Table 3. Suzuki cross coupling of borane **104** and western fragment **91** – optimisation of regioselectivity.
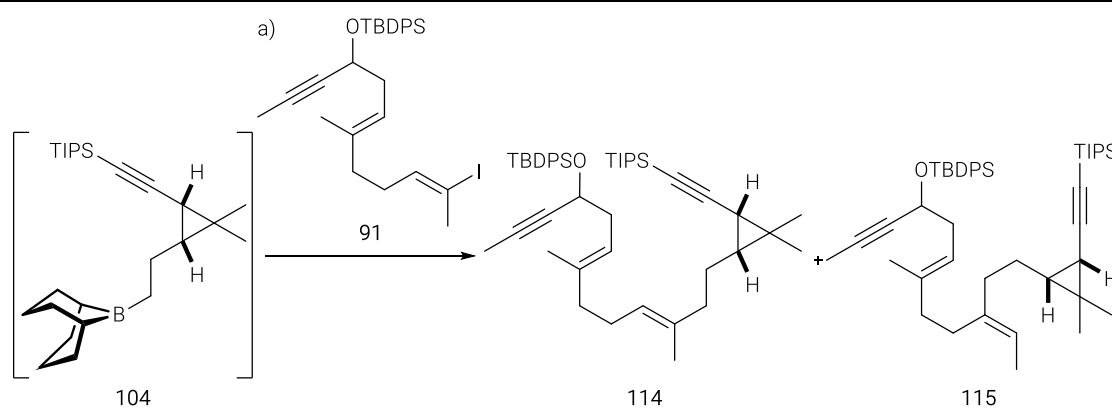
Entry	Base	Temperature	Yield	Regioselectivity 114:115
1	NaOH, H_2O, 3 h	RT	49%	56:44
2	NaOH, H_2O, 3 h	70 °C	47%	77:23
3	Ag_2O, KOH, H_2O, 20 min	RT	51%	58:42
4	Ag_2O, 20 min	RT	no reaction	-
5	Ag_2O, K_2CO_3, H_2O, 20 min	RT	46%	50:50
6	TlOEt, H_2O, 20 min	RT	93%	≥ 20:1
7	$Ba(OH)_2$, H_2O, 20 min	RT	81%	≥ 20:1

Conditions: a) **104** (1.3 equiv), **91** (1.0 equiv), [(dppf)PdCl₂] (10 mol%), toluene, THF, conditions see table; regioisomer ratios were determined by ¹H NMR.

2.6.2 RING-CLOSING ALKYNE METATHESIS

The cleavage of both silyl-protecting groups of **114** upon treatment with TBAF provided **92** in 96% yield (Scheme 28). This RCAM precursor **92** included a terminal and a methyl-capped alkyne as well as an unprotected propargylic alcohol.
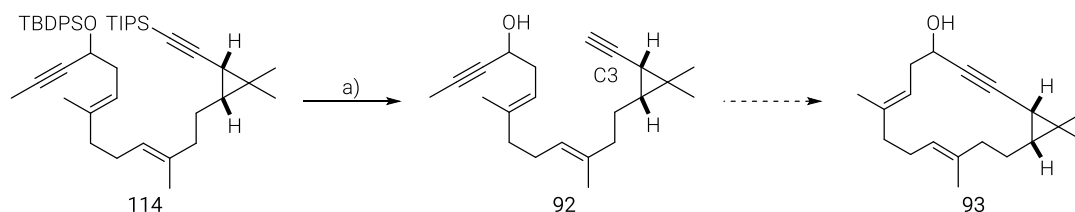
Scheme 28. Global deprotection of coupling product **114** and RCAM idea. Conditions: a) TBAF (6.0 equiv), THF, 0 °C to RT, 96%.

The first RCAM attempts towards the 14-membered macrocycle **93** were catalysed by the molybdenum alkyne metathesis catalyst (systems) **Cat. 1** and **Cat. 2**. Based on literature precedent, the integrity of alkene functionalities was assured.[88,106] In the case of **Cat. 1**, also protic functional groups were tolerated and strained macrocycles have been cyclised under forcing conditions.[106] To the best of my knowledge, RCAM of a methyl-capped and a terminal alkyne, catalysed by a silanolate ligand sphere complex, has only been reported on 21-membered macrocyclisation at room temperature.[124] However, terminal alkynes conjugated

to a cyclopropane motif have not been investigated in RCAM, yet (Scheme 28). In this regard, it remained unclear whether RCAM of terminal alkynes could be performed at elevated temperature, which would be required to overcome the expected ring strain energy and to out-compete side-reactions. The catalytic system's lifetime could be shortened at elevated temperature due to the instability of the intermediate methylidyne complex (see chapter 3).

On the other hand, the strained cyclopropane could open under forcing conditions due to the electronic properties of the corresponding Schrock alkylidyne complex intermediate, which might form at the α position (C3) to the cyclopropane.

When applying the two-component alkyne metathesis catalyst system (**Cat. 1**), a mixture of the silane tethered ligand **52b** and the trisamido alkylidyne complex **49** in toluene was stirred for three minutes, before this catalytic system (**Cat. 1**) was added to the (preheated) mixture of the corresponding RCAM precursor and grounded 4 & 5 Å molecular sieves (MS) in toluene (1 & 2 mм).[106] While the high dilution of the mixture prevented the formation of dimers, the MS 4 & 5 Å sequestered the by-products propyne and butyne, respectively, to shift the equilibrium towards the macrocycle.

In the first attempt, RCAM of diyne **92** was initiated by the addition of **Cat. 1** (10 mol%) at 60 °C. After 4 hours, no conversion was observed. Unfortunately, only minor amounts of the starting material **92** were recovered (Entry 1, Scheme 29, Table 4). Applying 50 mol% of **Cat. 1** under the same conditions afforded 6% of the desired macrocycle **93** (Entry 2, Scheme 29, Table 4). In both attempts, various side-products, which could not be identified, were obtained. Next, the corresponding silyl protected alcohol **116** was utilised. According to a successful formation of a 21-membered macrocycle from a diyne with a terminal and a methyl-capped alkyne in the total synthesis of mandelalide A,[124] the monodentate triphenylsilanolate complex **Cat. 2** (40 mol%) was applied to diyne **116**. This attempt resulted in a complex mixture, which included only 9% of desired product **117** and 34% of the anisole-capped alkyne as the major side-product (Entry 3, Scheme 29, Table 4).[88] The anisole derivative, generated by cross metathesis with the *p*-methoxybenzylidyne ligand of **Cat. 2** and compound **116**, could not re-enter the catalytic cycle. Therefore, **Cat. 2** and other benzylidyne-bearing metathesis catalysts were not considered further. Instead, the two-component alkyne metathesis catalyst system **Cat. 1**, containing a propylidyne ligand, was utilised in the following attempts. **116** was cyclised at room temperature on treatment with 30 mol% of **Cat. 1** to the desired macrocycle **117** in 35% yield, aside cross metathesis products and unidentified side-products (Entry 4, Scheme 29, Table 4). To convert cross metathesis products into the desired macrocycle, the RCAM was performed at elevated temperature. **Cat. 1** (30 mol%) was added to **116** at 50 °C. After 2 hours the starting material was converted into a mixture of the desired macrocycle **117**, cross metathesis products, and unidentified side-products. Since the cross metathesis products were still present, the mixture was stirred for 2.5 hours at 80 °C. This RCAM procedure gave the desired macrocycle **117** in 37% yield, in addition to unidentified side-products (Entry 5, Scheme 29, Table 4). Due to the presence of these side-products in all RCAM attempts, the terminal alkyne motif was considered as problematic. Therefore, the terminal alkyne **116** was methylated on treatment with *n*-BuLi and methyl iodide to provide the bis(methyl-capped alkyne) **118**. The product was successfully cyclised to the desired macrocycle **117** in 70% yield with additional 5% of the closed dimer by applying **Cat. 1** (20 mol%) at 65 °C (Entry 6, Scheme 29, Table 4). The consecutive methylation of terminal alkyne **116** and the successful cyclisation demonstrated that only methyl-capped alkynes should be used in RCAM under forcing conditions. Furthermore, these results also demonstrated the integrity of the cyclopropane and the unsaturated scaffold under these RCAM conditions.
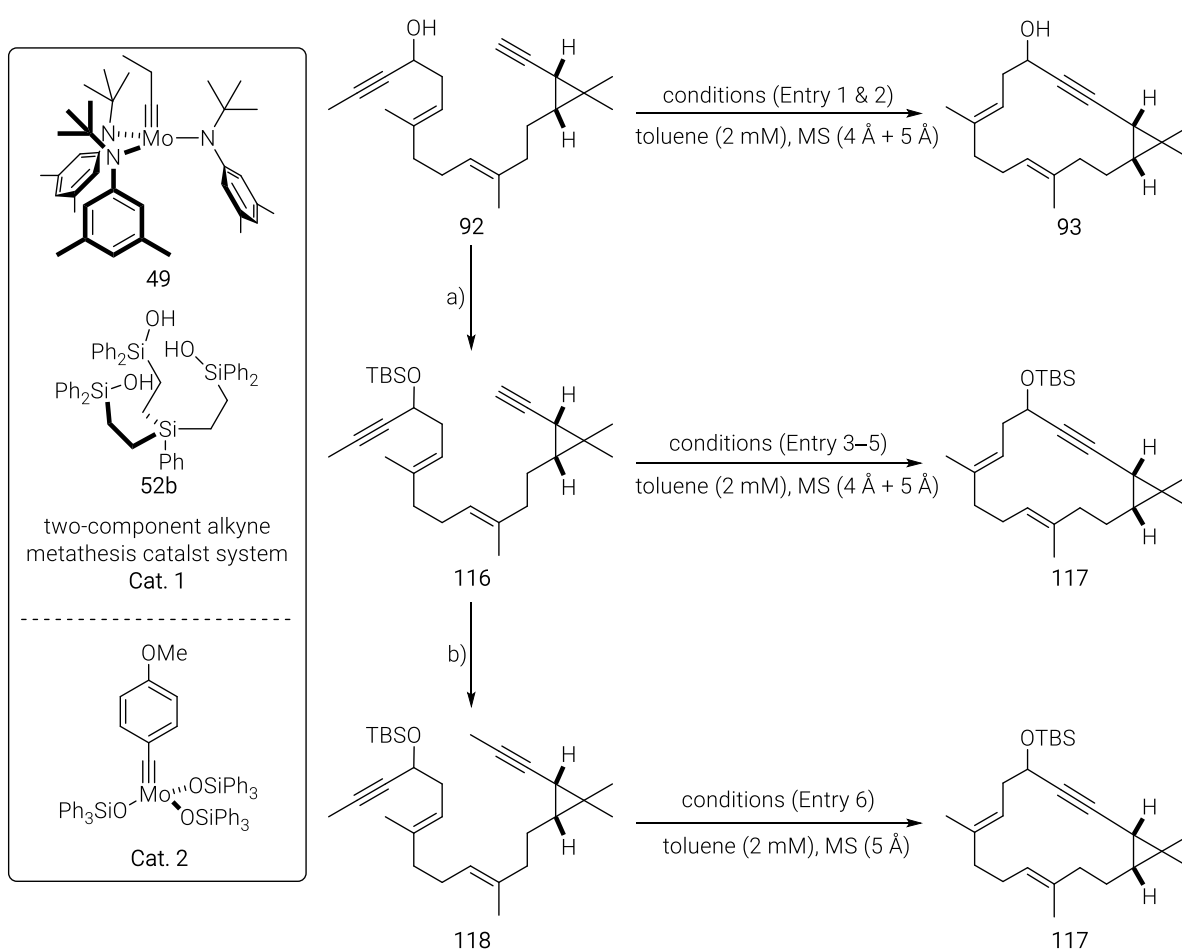
Scheme 29. RCAM investigations. Conditions: a) TBSCl (1.5 equiv), imidazole (2.0 equiv), DMF, CH₂Cl₂, RT, 83%; b) *n*-BuLi (2.0 equiv), MeI (5.0 equiv), THF, −78 °C to RT, 73%.

Table 4. Ring-closing alkyne metathesis investigations.

Entry	Starting Material	Temperature	Catalyst	Results
1	**92**	60 °C	**Cat. 1** (10 mol%), 4 h	recovered SM (**92**), unidentified side-product
2	**92**	60 °C	**Cat. 1** (50 mol%), 4 h	6% (**93**), unidentified side-product
3	**116**	RT to 50 °C	**Cat. 2** (30 mol%), RT, 4 h + **Cat. 2** (10 mol%), 50 °C, 3 h	complex crude NMR; 9% (**117**), 20% Me-capped, 34% anisole-capped, 11% closed dimer
4	**116**	RT	**Cat. 1** (30 mol%), 4 h	35% (**117**), cross metathesis products, unidentified side-products
5	**116**	50 to 80 °C	**Cat. 1** (30 mol%), 4.5 h	37% (**117**), unidentified side-products
6	**118**	65 °C	**Cat. 1** (10 mol%), 2 h + **Cat. 1** (10 mol%) 2 h	70% (**117**), 5% closed dimer

2.6.3 LATE-STAGE DIVERSIFICATION – TOTAL SYNTHESIS OF *ENT*-DEPRESSIN

The *O*-silyl group of **117** was cleaved on treatment with pyridinium *p*-toluenesulfonate (PPTS) and alcohol **93** was obtained in 80% yield (Scheme 30). The unprotected alcohol was required as the directing group in the subsequent *trans*-hydrostannation. Treatment of propargylic alcohol **93** with tributyltin hydride and catalytic amounts of [Cp*RuCl]$_4$ gave the desired alkenyl stannane **119** in 80% yield and excellent regio- and stereoselectivity.[181–184] This transformation introduced the desired alkene geometry and enabled the substitution of the tin group with various functional groups in the following step, bringing some casbane derivatives into reach.
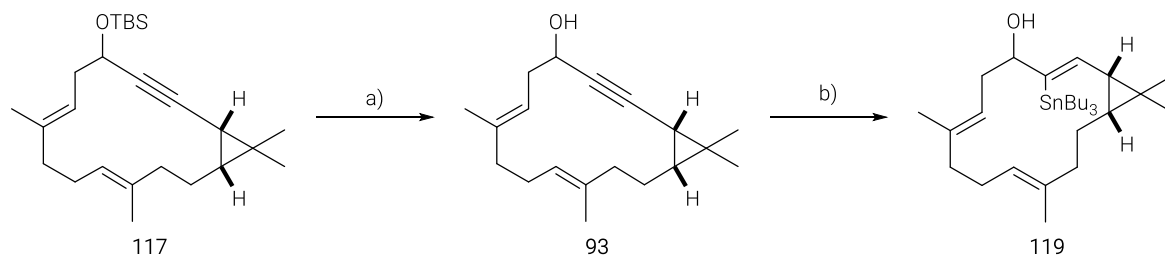
Scheme 30. Deprotection and *trans*-hydrostannation. Conditions: a) PPTS (6.0 equiv), MeOH, RT, 80%, (95% brsm); b) [Cp*RuCl]$_4$ (2.5 mol%), Bu$_3$SnH (1.5 equiv), CH$_2$Cl$_2$, RT, 80%.

C-Methylation of stannane **119** was carried out according to an in-house developed protocol, which relies on the combination of methyl iodide, copper thiophene-2-carboxylate (CuTC) as promotor, and tetra-*n*-butyl ammonium diphenyl phosphinate ([Ph$_2$PO$_2$][Bu$_4$N]) as tin scavenger.[185] In some cases it is beneficial to add catalytic amounts of Pd(PPh$_3$)$_4$ and to run the reaction in DMF instead of DMSO.[185] The high concentration (0.2 M), the order of addition, and

the immediate addition of CuTC after the addition of methyl iodide (10 sec) are essential to obtain high yields.

The protocol with DMSO as solvent gave a 1:1 mixture of the desired methylated product **120** and the protodestannylated alkene **121** (Entry 1, Table 5). Applying the protocol with DMF as solvent and Pd(PPh$_3$)$_4$ as additive led to the methylated product **120** in 62% yield, whereas only 5% of the protodestannylated product **121** was isolated (Entry 2, Table 5).

Table 5. *C*-Methylation of alkenyl stannane **119**.
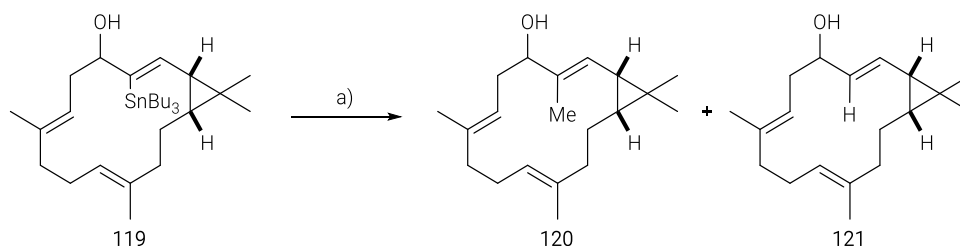
Entry	Specific Conditions	Ratio 119:120:121	Yield		
1	DMSO (0.2 M)	0:48:51	**120**	Me-	39%
			121	H-	41%
2	Pd(PPh$_3$)$_4$ (5 mol%), DMF (0.2 M)	11:73:16	**119**	Bu$_3$Sn-	15%
			120	Me-	62%
			121	H-	5%

General conditions: a) CuTC (1.05 equiv), [Ph$_2$PO$_2$][Bu$_4$N] (1.1 equiv), MeI (3.0 equiv), RT. Specific conditions see table; ratios were determined by ^{1}H NMR.

The oxidation of the alcohol **120** to the corresponding ketone **89** was investigated under three different reaction conditions using either Dess-Martin periodinane, pyridinium chlorochromate, or manganese(II) oxide. The buffered Dess-Martin oxidation generated only traces of *ent*-depressin (**89**) in combination with an inseparable mixture of side-products (Entry 1, Table 6). Treatment of **120** with pyridinium chlorochromate (PCC) and sodium acetate gave *ent*-depressin (**89**) in 25% yield (Entry 2, Table 6). The best result was achieved when using freshly prepared manganese(II) oxide (MnO$_2$)[186] in CH$_2$Cl$_2$ to afford *ent*-depressin (**89**) in 82% yield (Entry 3, Table 6).

Table 6. Oxidation of alcohol **120** to *ent*-depressin (**89**).

Entry	Conditions	Results
1	DMP (2.0 equiv), NaHCO$_3$ (10.0 equiv), CH$_2$Cl$_2$, RT	traces of product
2	PCC (1.5 equiv), NaOAc (20 mol%), CH$_2$Cl$_2$, RT	25%
3	MnO$_2$ (2 × 25.0 equiv), CH$_2$Cl$_2$, RT	82%

Comparison of the spectral data of *ent*-depressin (**89**) with that of the isolated natural product depressin (**9**) showed very good agreement with a maximum deviation of 0.06 ppm in the ^{1}H NMR data and 0.1 ppm in the ^{13}C NMR data (Figure 14). Specific rotation of *ent*-depressin (**89**) supported the assigned absolute stereochemistry of depressin (**9**) (*ent*-depressin (**89**) $[\alpha]_D^{20}$ = +72.0; depressin (**9**)[6] $[\alpha]_D^{20}$ = −80.0).
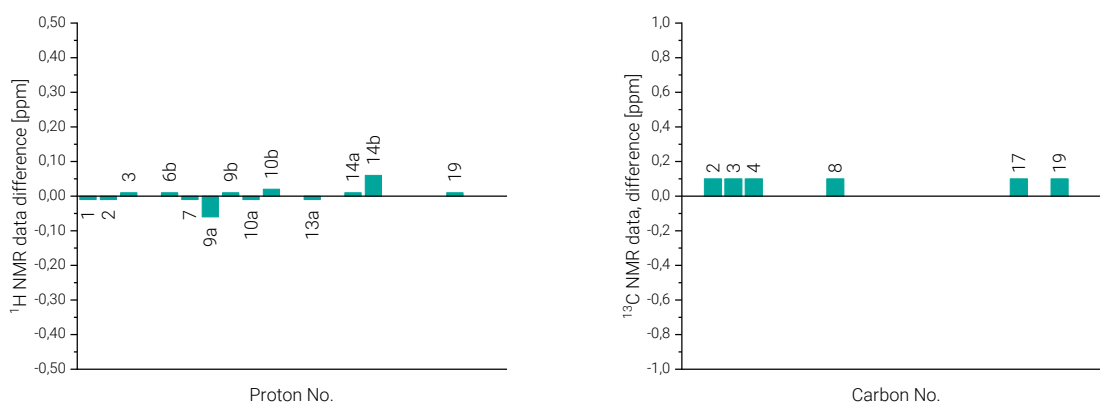
Figure 14. Differences in ^{1}H NMR shifts (left) and ^{13}C NMR shifts (right) between *ent*-depressin (**89**) and natural product depressin (**9**), numbering see Table 6.

2.7 CONCLUSION

The first total synthesis of *ent*-depressin (**89**) demonstrated the feasibility of this blueprint. This accomplishment might bring many casbane diterpenes into reach.

The palladium catalysed Negishi coupling of alkenyl iodide **110** and organozinc compound **96** gave alkenyl silane **113**, which was subjected to a novel iododesilylation procedure, providing the western fragment **91**. Overall, this fragment was synthesised in 16% yield comprising eight steps along the LLS. The synthesis of the cyclopropyl fragment **90** was accomplished in 14% yield and eight steps. Thereby, the enantioselective rhodium-catalysed cyclopropanation represented the key step.

The chemoselective hydroboration of the cyclopropyl fragment **90** with the 9-H-9-BBN dimer and the subsequent Suzuki cross coupling with the western fragment **91** enabled the RCAM investigations towards the three fold unsaturated 14-membered macrocycle **117**. It turned out,

that the RCAM of diyne **118** performed best at elevated temperature and that both alkyne units of the RCAM precursor had to be methyl-capped to obtain macrocyclic alkyne **117** in acceptable yield. A *trans*-hydrostannation and *C*-methylation sequence starting from macrocyclic alkyne **93** gave alcohol **120** with the desired *trans*-alkene geometry. **120** was then oxidised to *ent*-depressin (**89**). The total synthesis of *ent*-depressin (**89**) was achieved in 3% yield comprising 16 steps along the LLS (27 total steps). This accomplishment demonstrates the feasibility of this synthetic blueprint, including RCAM and late-stage diversification of alkenyl stannane **119**, which also might be seen as platform to introduce various functional groups in the future.
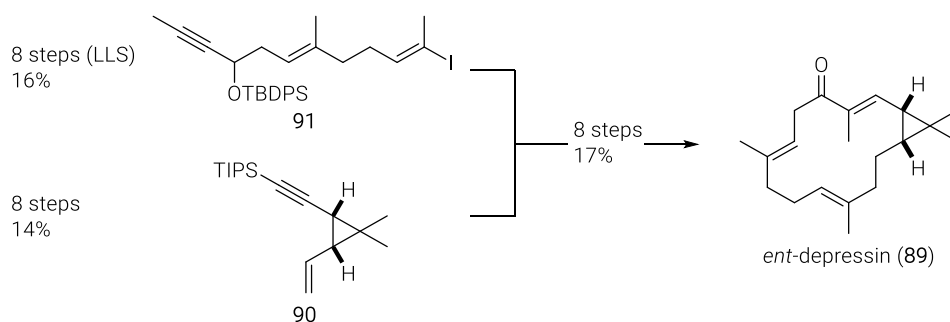
Scheme 31. Summary – total synthesis of *ent*-depressin (**89**).

3 FINAL APPROACH – TOTAL SYNTHESIS OF DEPRESSIN, EUPHORHYLONAL A AND YUEXIANDAJISU A

This approach would combine the general strategy of the previous one with a more concise and elegant synthesis of the casbane framework. The late-stage diversification towards depressin (**9**), euphorhylonal A (**15**), and yuexiandajisu A (**17**) would demonstrate the broadness of this blueprint.

3.1 ISOLATION AND STRUCTURE ELUCIDATION

Euphorhylonal A

Euphorhylonal A (**15**) (Figure 15) was first isolated from the plants *Euphorbia hylonoma* Hand-Mazz and *E. wangii* Oudejans, which were collected at Gansu Province, China.[26] Extraction of the natural materials (*E. hylonoma* Hand-Mazz: 3.0 kg) and chromatographic purification of the residue gave euphorhylonal A (**15**) as a colourless gum (9 mg). The structure was elucidated NMR analysis as well as by comparison to crotonitenone.[187,188] The geometry of the alkenes were assigned by their NMR shifts and the characteristic large coupling constants. The configuration of the C5–OH stereocentre is not discussed by the isolation team, whereas the relative configuration of the cyclopropane is shown to be *cis*.

nominal
euphorhylonal A (**15**)
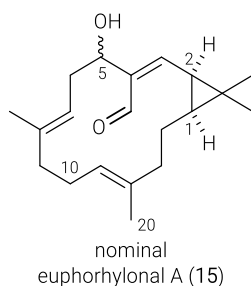
Figure 15. Structure nominal euphorhylonal A (**15**).[26]

3.2 OBJECTIVES

The casbane diterpenes are extremely rare in nature.[4] Their impressive diversity is an excellent opportunity to design a diversity-oriented synthetic route to access many derivatives at once. In particular, depressin (**9**) and euphorhylonal A (**15**) represented the perfect choice to expand the range of the previous described blueprint. In addition, the preparation of each would depict its first total synthesis while confirming the reported stereochemical assignment of depressin (**9**) and clarifying that of euphorhylonal A (**15**). Later, the total synthesis of yuexiandajisu A (**17**), bearing a *trans*-cyclopropane, should be investigated to prove the strategy's versatility. The resulting synthetic plan should be concise, efficient and flexible in order to address many casbane diterpenes at once.

3.3 RETROSYNTHETIC ANALYSIS

This retrosynthetic analysis was based on the concepts of atom economy and diversity-oriented synthesis. Further, it included the in-house developed methodologies of ring-closing alkyne metathesis (RCAM), *trans*-hydrostannation, and *C*-methylation of alkenyl stannanes.

The late-stage diversification would be initiated by a C5−OH directed *trans*-hydrostannation of macrocyclic alkyne **122** to introduce the required alkene geometry. *C*-Methylation of the resulting alkenyl stannane and oxidation of the C5−OH would complete the total synthesis of depressin (**9**). In case of euphorhylonal A (**15**), the C5−OH directed *trans*-hydrostannation would enable the formylation at the C18 position of the resulting alkenyl stannane.

The macrocycle **122** was envisaged to be achieved by RCAM, considering the investigations in chapter 2, precursor **123** containing two methyl-capped alkynes was targeted. The disconnection of **123** at C12 and C13 would allow a segmentation into the cyclopropyl fragment **124** and the western fragment **125**. Subjection of the cyclopropyl fragment **124** to a chemoselective hydroboration of the terminal alkene over the methyl alkyne and subsequent sp^2-sp^3 Suzuki cross coupling of the resulting borane with the western fragment **125** would provide the RCAM precursor **123** in a concise and elegant fashion.
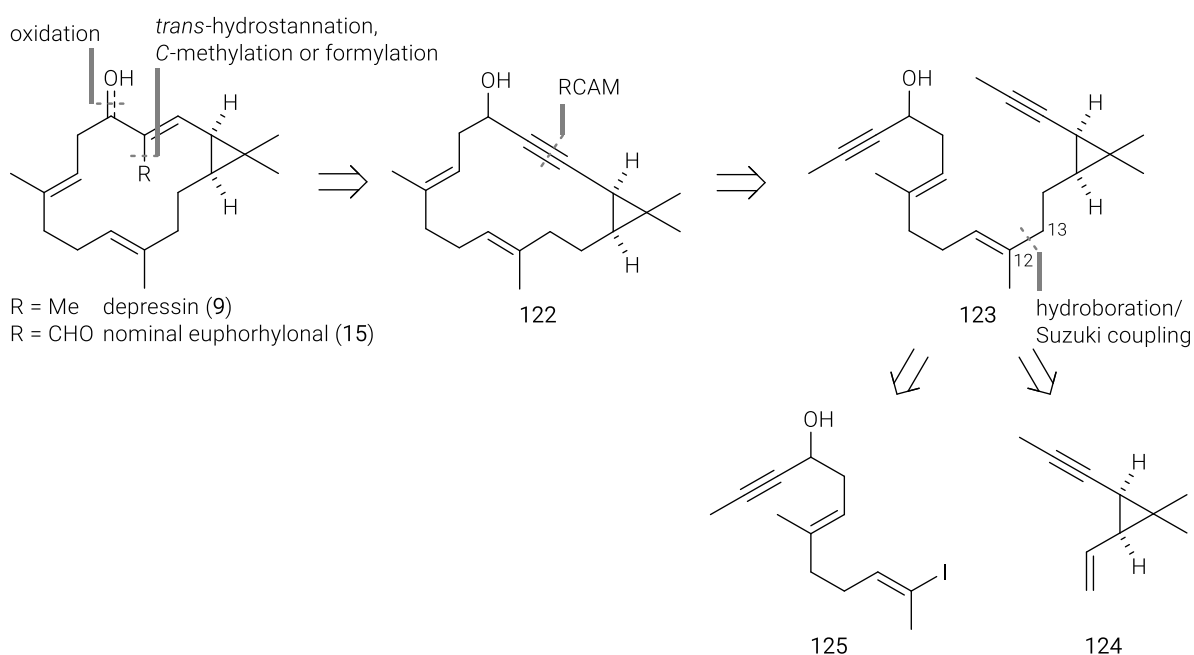
Scheme 32. Retrosynthetic analysis − final approach.

The cyclopropyl fragment **124** would be finalised by oxidation of alcohol **126** and subsequent Corey/Fuchs homologation. Selective reduction of lactone **80** would give access to the corresponding lactol, which would be in an equilibrium with the monocyclic aldehyde. A Wittig homologation would convert the latter into **126**. The reduction of lactone **80** would require low temperature to prevent over-reduction. The enantioselective cyclopropanation of diazoester **70** with [Rh$_2$(5*S*-MEPY)$_4$] would afford lactone **80**, which would be seen as a common intermediate (Scheme 33).[69]
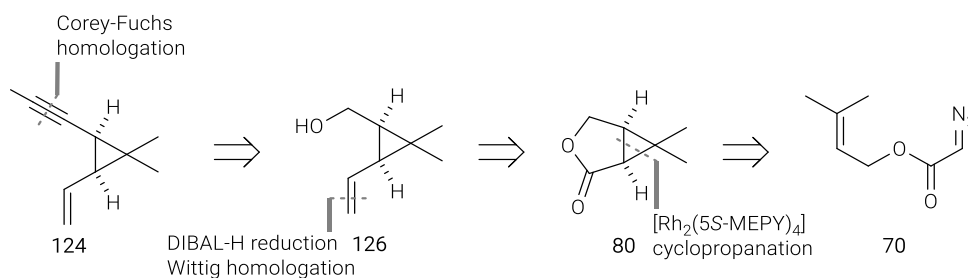
Scheme 33. Retrosynthetic analysis of the cyclopropyl fragment **124**.

The synthesis of the western fragment **125** would be completed by a stereoselective iododesilylation of the corresponding alkenyl silane **127**. In this respect, the silane group would be seen as a masked halide, which would allow the chemoselective Negishi cross coupling between C8 and C9 to proceed. This disconnection would divide the western fragment **125** into alkenyl iodide **128** and organozinc compound **129**. The corresponding alkenyl iodide **128** would derive from alcohol **130**, which was envisaged to be used twice. Oxidation of alcohol **130** and subsequent Grignard addition would result in the formation of propargylic alcohol **131**, which subsequently would be O-silylated with TBDPSCl. The sterically demanding TBDPS group was chosen to prevent any reactivity of the hydroxy and alkyne functionality under Negishi coupling conditions. A stereoselective iododesilylation of the corresponding alkenyl silane would provide alkenyl iodide **128** for Negishi coupling. The corresponding organozinc compound **129** would be prepared by an Appel halogenation of alcohol **130** with subsequent zinc insertion. The common intermediate **130** would be synthesised by a copper mediated hydrosilylation of the pentynol **64** (Scheme 34).[189,190]
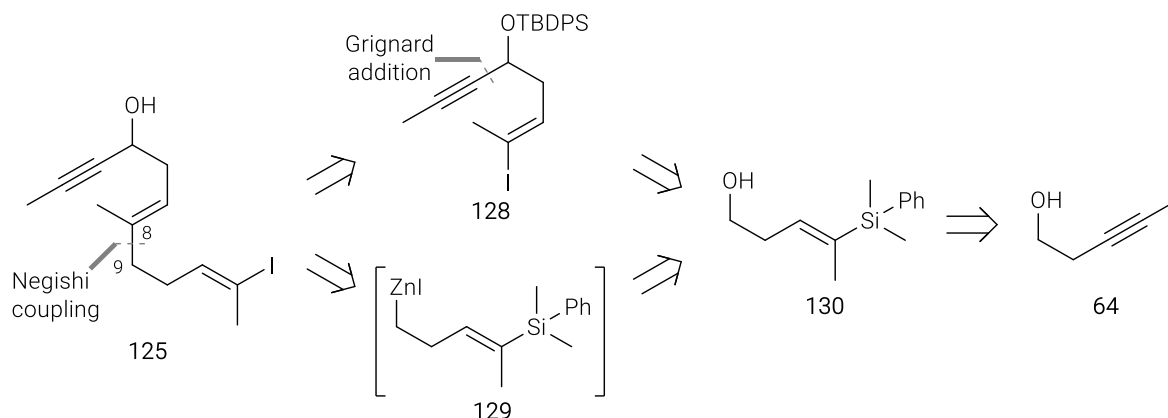
Scheme 34. Retrosynthetic analysis of the western fragment **91**.

3.4 SYNTHESIS OF THE CYCLOPROPYL FRAGMENT

Diazoester **70** was synthesised as described previously (see chapter 1.4.2) from prenyl alcohol **71** and diketene **72** in 53% yield over two steps. The product was converted into lactone **80** with [Rh$_2$(5S-MEPY)$_4$] catalyst (0.6 mol%) in 87% yield with an enantioselectivity of 93% ee.[69,137,143] To preserve the chirality, the selective reduction of lactone **80** to lactol **133** was conducted at low temperature (−78 °C) on treatment with DIBAL-H in CH$_2$Cl$_2$. The resulting bicyclic lactol **133** was in an equilibrium with monocyclic aldehyde **132**, which was transformed into terminal alkene **126** in 55% yield by a Wittig homologation. The methyl-capped alkyne moiety was introduced by a Corey/Fuchs homologation. To ensure the separation of the highly volatile hydrocarbon **124**

($C_{10}H_{14}$) from the mixture, the homologation was carried out in diethyl ether instead of THF. Therefore, alcohol **126** was oxidised with Dess-Martin periodinane to the corresponding aldehyde **134**. The subsequent dibromination was conducted with twice the amount of the phosphorus ylide as ordinary to complete the conversion. Treatment of the resulting crude dibromide **135** with *n*-BuLi at −78 °C in diethyl ether resulted in the formation of organolithium species *via* the Fritsch-Buttenberg-Wiechell rearrangement. The addition of methyl iodide to the resulting mixture led to no reaction. Therefore, DMPU was added to the organolithium species, prior to the addition of methyl iodide to give the volatile cyclopropyl fragment **124** in 51% yield over three steps. Overall, the synthesis, starting from 3-methyl-2-butenol **71** and diketene **72**, was accomplished in 13% yield and eight steps.
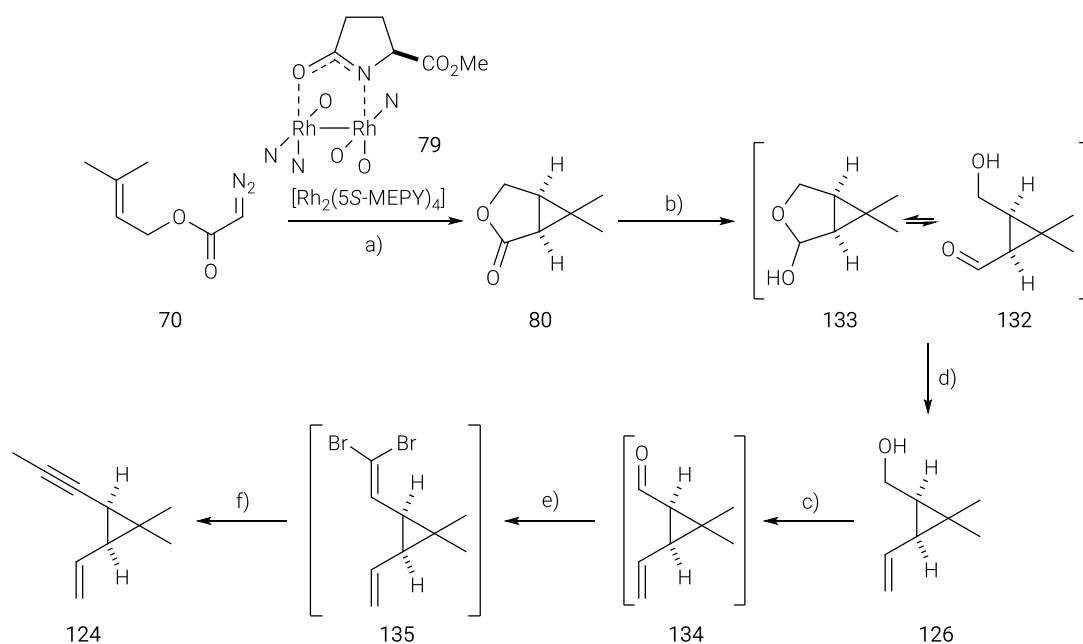
Scheme 35. Synthesis of the cyclopropyl fragment **124**. Conditions: a) [Rh$_2$(5*S*-MEPY)$_4$]·2MeCN (0.6 mol%), CH$_2$Cl$_2$, reflux, 87% (93% *ee*); b) DIBAL-H (1.02 equiv in CH$_2$Cl$_2$), CH$_2$Cl$_2$, −78 °C; c) Ph$_3$PCH$_2$ (3.0 equiv), THF, RT, 55% over 2 steps; d) DMP (1.5 equiv), CH$_2$Cl$_2$, RT; e) PPh$_3$ (8.0 equiv), CBr$_4$ (4.0 equiv), CH$_2$Cl$_2$, 0 °C; f) *i*) *n*-BuLi (5.2 equiv), Et$_2$O, −78 °C, *ii*) DMPU (6.1 equiv), Et$_2$O, −78 °C, *iii*) MeI (15.2 equiv), −78 °C to RT, 51% over 3 steps.

3.5 CHEMOSELECTIVE HYDROBORATION OF THE CYCLOPROPYL FRAGMENT

In the previous approach, the chemoselective hydroboration of the cyclopropyl fragment **90** was based on the sterical shielding of the alkyne by a TIPS group (Scheme 23).

In this approach, the chemoselective hydroboration of the alkene over the methyl-capped alkyne was envisaged following a procedure of Brown and Coleman.[191] Treatment of the cyclopropyl fragment **124** with the 9-H-9-BBN dimer in THF at room temperature resulted in chemoselective formation of borane **136**, which was subjected to Suzuki cross coupling. The choice of THF as the solvent seemed to be decisive. This test reaction sequence, utilising alkenyl iodide **137** instead of the western fragment **91**, gave exclusively isomer **138** in 72% yield (Scheme 36). The application of this reaction sequence to the coupling of cyclopropyl fragment **124** and the western fragment **91** would led to an improvement of the synthetic route in terms of the step

count and efficiency compared to the total synthesis of *ent*-depressin (**89**) in chapter 2, since the methyl-capped alkyne motif could be directly introduced.
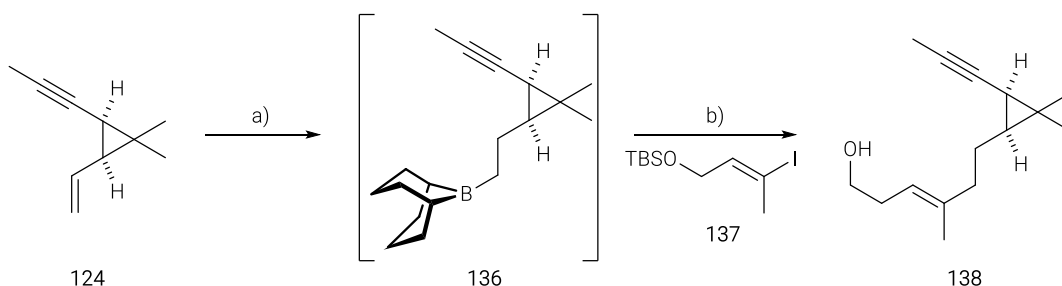
Scheme 36. Proof of concept: Chemoselective hydroboration of cyclopropyl fragment **124**. Conditions: a) **124** (1.2 equiv), 9-H-9-BBN dimer (0.75 equiv), THF, RT; b) *i*) Ba(OH)$_2$·(H$_2$O)$_8$ (5.9 equiv), H$_2$O (5.9 equiv), DMF, *ii*) **137** (1.0 equiv), *iii*) [(dppf)PdCl$_2$] (12 mol%), RT, 72%.

3.6 SYNTHESIS OF THE WESTERN FRAGMENT

The copper-mediated hydrosilylation of internal alkynes was first reported by Fleming and co-workers and later adapted for pentynol **64** by Zakarian and co-workers.[190,192,193] Although the "Fleming hydrosilylation protocol" counted formally as one step, it included several steps: preparation of the corresponding cuprate at −78 °C, deprotonation of pentynol **64** at −30 °C, and cautious treatment of the lithium salt of pentynol **64** with the resulting cuprate at low temperature (−78 °C). However, this procedure provided alkenyl silane **130** in 90% yield with excellent regio- and stereoselectivity (Scheme 37). This procedure limited the scale to three gram. Therefore, a more scalable approach was perused.[i] 4,5-Dihydrofuran **98** was selectively silylated in the C2 position. The subsequent nickel catalysed opening of the resulting silyl dihydrofuran with methyl magnesium bromide, according to a protocol of Kocieński and co-workers, gave **130** in 91% yield over two steps on a 15 gram scale (Scheme 37).[154,155]

The propargylic alcohol **131** was synthesised in 78% yield over two steps by a Dess-Martin oxidation of **130** to the β,γ-unsaturated aldehyde **139** (without any isomerisation, ^{1}H NMR) followed by a Grignard reaction with propynyl magnesium bromide. The resulting C5−OH group was subsequently *O*-silylated in 84% yield (Scheme 37). The sterically demanding TBDPS-group did not only hinder any deactivation of the organozinc species, but also protect the alkyne during the following Negishi coupling.

Alkyl iodide **141** was prepared by Appel iodination of the common intermediate **130** in 93% yield (Scheme 37).

---

[i] This approach was developed in cooperation with Dr. K. Yahata.
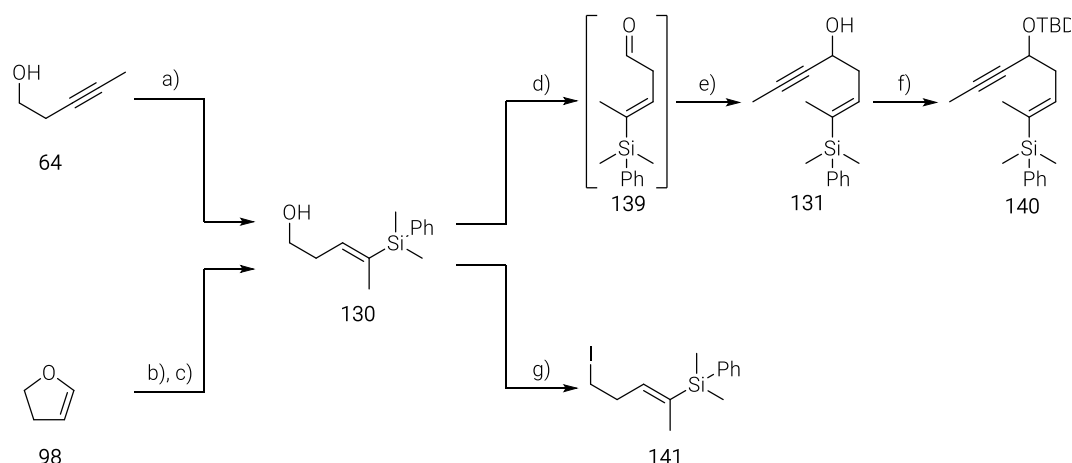
Scheme 37. Synthesis of alkenyl iodide **140** and alkyl iodide **141**. Conditions: a) *i*) **64** (1.0 equiv), *n*-BuLi (1.0 equiv), THF, −78 °C to −30 °C to −78 °C, *ii*) (PhMe$_2$Si)$_2$Cu(CN)Li$_2$ (1.1 equiv), −78 °C, 90%; b) **98** (1.4 equiv), *n*-BuLi (1.3 equiv), PhMe$_2$SiCl (1.0 equiv), THF, −30 °C to RT, quant.; c) Ni(PPh$_3$)$_2$Cl$_2$ (8 mol%), MeMgBr (3.2 equiv), toluene, 105 °C, 91%; d) DMP (1.5 equiv), CH$_2$Cl$_2$, 0 °C to RT; e) Propynyl MgBr (3.3 equiv), THF, 0 °C, 78% over 2 steps; f) TBDPSCl (1.5 equiv), imidazole (2.0 equiv), DMF, CH$_2$Cl$_2$, 84%; g) I$_2$ (1.5 equiv), PPh$_3$ (1.5 equiv), imidazole (1.5 equiv), CH$_2$Cl$_2$, 0 °C to RT, 93%.

In the first attempt, the previous optimised iododesilylation conditions (see chapter 2.3) were applied to alkenyl iodide **140**. NIS was added to a mixture of **140** and silver(I) carbonate in chloroacetonitrile at room temperature. The resulting alkenyl iodide **128** was obtained in 68% yield with a selectivity of *E:Z* = 10:1 (Entry 1, Table 7). Using 2,6-lutidine, instead of silver(I) carbonate, decreased the yield of **128** to 25% with a selectivity of *E:Z* = 13:1 (Entry 2, Table 7). Applying no additive to this iododesilylation gave **128** in 59% yield with a selectivity to *E:Z* = 17:1 (Entry 3, Table 7). Due to this promising result, these reaction conditions were carried out at different temperatures. While at −10 °C only decomposition was observed, 47% yield of **128** with no sign of double bond isomerisation (*E:Z* ≥ 20:1, ^{1}H NMR) was obtained at 40 °C (Entry 4-5, Table 7). Due to these unsatisfying results, HFIP mediated iododesilylation conditions reported by Zakarian and co-workers were applied.[176] 1.5 equivalents of NIS were added to a mixture of **140**, HFIP, and 2,6-lutidine in CH$_2$Cl$_2$ (0.07 M) at −78 °C. Warming the mixture to −10 °C gave **128** in 74% yield with integrity of the double bond (*E:Z* ≥ 20:1, ^{1}H NMR) (Entry 6, Table 7). Dilution with CH$_2$Cl$_2$ allowed the reaction to be carried out at low temperature, since pure HFIP freezes at −4 °C.[194] To further optimise the iododesilylation conditions and to develop a reliable protocol this transformation was conducted at −50 °C and −20 °C. Carrying out this reaction at −50 °C for several hours gave the desired *E*-alkenyl iodide **128** in 65% yield and 15% of the starting material **140** (Entry 7, Table 7). The best result was achieved, when NIS was added to a solution of alkenyl silane **140**, 2,6-lutidine, and HFIP in CH$_2$Cl$_2$ (0.02 M) at −20 °C. After 4 hours, the reaction was quenched at −20 °C and the desired *E*-alkenyl iodide **128** was isolated in 89% yield without any detectable double bond isomerisation (*E:Z* ≥ 20:1, ^{1}H NMR) (Entry 8, Table 7).

Table 7. Iododesilylation of alkenyl silane **140** – optimisation.
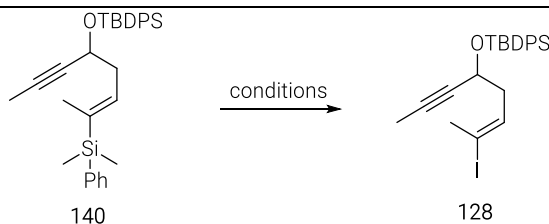
Entry	NIS	Additive/Base	Solvent	Temperature, Time	Results
1	2.0 equiv	Ag$_2$CO$_3$ (0.75 equiv)	ClH$_2$CCN	RT, 4 h	68% (*E:Z* = 10:1)
2	2.0 equiv	2,6-lutidine (2.2 equiv)	ClH$_2$CCN	RT, 10 h	25% (58% brsm)* (*E:Z* = 13:1)
3	2.0 equiv	-	ClH$_2$CCN	RT, 2 h	59%* (*E:Z* = 17:1)
4	2.0 equiv	-	ClH$_2$CCN	−10 °C, 20 h	decomposition
5	2.0 equiv	-	ClH$_2$CCN	40 °C, 4 h	47% (60% brsm)* (*E:Z* ≥ 20:1)
6	1.5 equiv	2,6-lutidine (1.7 equiv), HFIP (133 equiv)	CH$_2$Cl$_2$ (0.07 M)	−78 to −10 °C, 10 min	74%* (*E:Z* ≥ 20:1)
7	1.5 equiv	2,6-lutidine (5.0 equiv), HFIP (24.0 equiv)	CH$_2$Cl$_2$ (0.02 M)	−50 °C, 5 h	65% (80% brsm)* (*E:Z* ≥ 20:1)
8	1.5 equiv	2,6-lutidine (5.0 equiv), HFIP (36.0 equiv)	CH$_2$Cl$_2$ (0.02 M)	−20 °C, 4 h	89% (*E:Z* ≥ 20:1)

E:Z ratios were determined by ^{1}H NMR; * = ^{1}H NMR yield.

With alkenyl iodide **128** in hand, the final steps towards the synthesis of western fragment **125**, including Negishi cross coupling with organozinc compound **129** and subsequent iododesilylation, were investigated.

Alkyl iodide **141** was converted into the corresponding organozinc compound **129** by a zinc-insertion protocol of Knochel and co-workers.[166,195] The *in situ* generated organozinc compound **129** was separated from the unreacted zinc and directly used in the palladium catalysed Negishi cross coupling with alkenyl iodide **128**. This sequence led to the formation of compound **142** in 82% yield (Scheme 38).
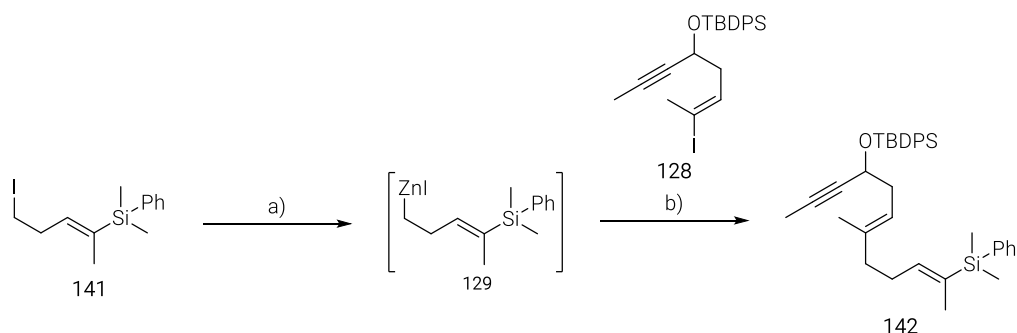
Scheme 38. Synthesis of the silyl masked western fragment **142**. Conditions: a) *i*) Zn (2.6 equiv), LiCl (1.4 equiv), $I_2C_2H_4$ (6 mol%), TMSCl (12 mol%), THF, 65 °C/RT, *ii*) **140** (1.3 equiv), THF, RT; b) **126** (1.0 equiv), Pd(PPh$_3$)$_4$ (6 mol%), THF, RT, 82%.

First, iododesilylation conditions with NIS in chloroacetonitrile were applied, as used in the preparation of western fragment during the total synthesis of *ent*-depressin (**89**) (see chapter 2.5). Unfortunately, alkenyl iodide **143** was obtained in only moderate yields (40-55%) with selectivity of *E:Z* = 10:1 to 15:1 (Entry 1-7, Table 8). Next, "Zakarian iododesilylation conditions" were used. NIS was added to a mixture of **142** and 2,6-lutidine in pure HFIP at 0 °C (Entry 8, Table 8). This attempt led to no reaction, due to poor solubility of the nonpolar alkenyl silane **142** in the polar HFIP.[178] The application of a solvent mixture of CH_2Cl_2 and HFIP dissolved the alkenyl silane **142**, resulting in a clear solution. NIS was added at −10 °C, resulting in decomposition of the starting material. Further iododesilylation attempts were conducted at −20 °C and −50 °C as well as with reduced equivalents of NIS and HFIP in CH_2Cl_2. Unfortunately, these attempts only led to decomposition (Entry 9-11, Table 8). Due to no observable trend during the optimisation, the attempt with 55% yield of alkenyl iodide **143** and a stereoselectivity of *E:Z* = 10:1 was considered as the preliminary best result (Entry 1, Table 8).

Table 8. Iododesilylation of TBDPS-protected propargylic alcohol **141** – optimisation.
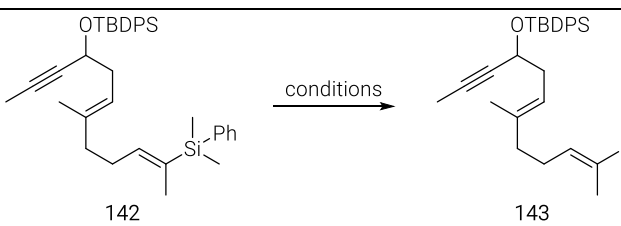
Entry	NIS	Additive/Base	Solvent	Temperature, Time	Yield
1	2.0 equiv	Ag_2CO_3 (0.75 equiv)	ClH_2CCN	RT, 5 h	55% (*E:Z* = 10:1)
2	2.0 equiv	Ag_2CO_3 (0.2 equiv)	ClH_2CCN	RT, 5 h	40% (63% brsm) (*E:Z* = 15:1)
3	2.0 equiv	Ag_2CO_3 (0.75 equiv)	ClH_2CCN	0 °C, 4 h	46% (51% brsm) (*E:Z* = 14:1)
4	2.0 equiv	Ag_2CO_3 (0.75 equiv)	ClH_2CCN	−12 °C, 8 h	48% (64% brsm)* (*E:Z* = 10:1)
5	2.0 equiv	-	ClH_2CCN	RT, 2 h	47% (*E:Z* = 11:1)
6	2.0 equiv	-	ClH_2CCN	40 °C, 4 h	25% (*E:Z* = 10:1)
7	2.0 equiv	-	ClH_2CCN	0 °C, 20 h	25% (30% brsm) (*E:Z* = 10:1)
8	1.5 equiv	2,6-lutidine (2.0 equiv)	HFIP	0 °C, 5 min	no reaction (SM **142** insoluble)
9	3.0 equiv	2,6-lutidine (5.4 equiv), HFIP (100 equiv)	CH_2Cl_2 (0.02 M)	−10 °C, 4 h	decomposition
10	1.9 equiv	2,6-lutidine (5.0 equiv), HFIP (35.0 equiv)	CH_2Cl_2 (0.02 M)	−20 °C, 4.5 h	decomposition
11	1.9 equiv	2,6-lutidine (5.0 equiv), HFIP (35.0 equiv)	CH_2Cl_2 (0.01 M)	−50 °C, 2.5 h	decomposition

E:Z ratios were determined by ^{1}H NMR; * = ^{1}H NMR yield.

O-Silyl cleavage of the TBDPS-protected alcohol **142** (*E:Z* = 10:1) on treatment with TBAF at 0 °C and subsequent separation of the isomers by flash chromatography provided exclusively *E*-alkenyl iodide **125** in 80% yield. Overall, iododesilylation of alkenyl silane **142** with subsequent deprotection gave the *E*-alkenyl iodide synthesis (**125**) in 44% over two steps (Scheme 39).
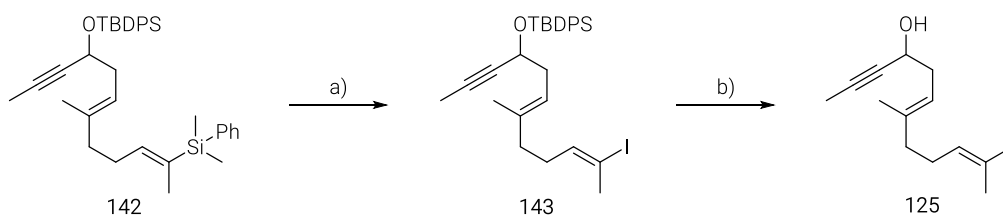
Scheme 39. Synthesis of the western fragment **125**. Conditions: a) NIS (2.0 equiv), Ag_2CO_3 (0.75 equiv), $ClCH_2CN$, RT, 55% (*E:Z* = 10:1); b) TBAF (3.5 equiv), THF, 0 °C, 80% (after flash chromatography: *E:Z* ≥ 20:1).

The unsatisfying 44% yield caused a turnaround of the two last transformations. In this case, the *O*-silyl cleavage would make the resulting alkenyl silane **144** soluble in HFIP, so that the following stereoselective iododesilylation could be investigated under additional conditions. Therefore, the TBDPS-group was cleaved on treatment of **142** with TBAF and the corresponding propargylic alcohol **144** was obtained in 84% yield (Scheme 40).
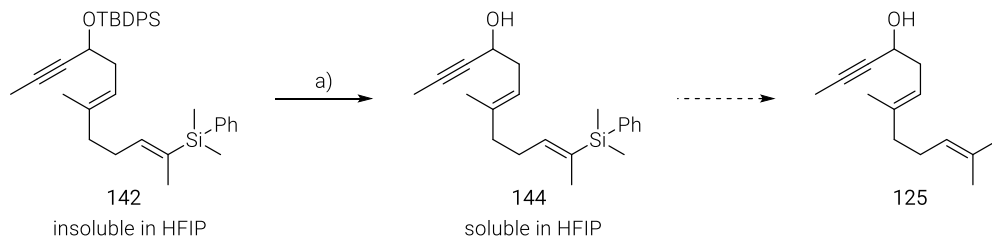
Scheme 40. Synthesis of the silyl masked western fragment **125**. Conditions: a) TBAF (2.0 equiv), THF, 0 °C to RT, 84%.

The subsequent iododesilylation of the resulting propargylic alcohol **144**, which was soluble in HFIP, required modified conditions to prevent any intramolecular nucleophilic attack of the propargylic alcohol towards the HFIP/NIS activated alkene (C7=C8). This kind of HFIP/NIS promoted nucleophilic reactivity of *N*-tosyl amines and carboxylic acids towards alkenes was reported by Gandon and co-workers.[196]

When, NIS was added to a solution of alkenyl silane **144** in HFIP at 0 °C, the iodoetherification product **145** was formed in 73% as a mixture of two diastereomers (Entry 1, Table 9). Reducing the equivalents of NIS led to a mixture of **144** and the desired alkenyl iodide **125** (*E:Z* ≥ 20:1, ^{1}H NMR), and minor amounts of **145** (Entry 2, Table 9). To prevent any iodoetherification from occurring, the nucleophilicity of the C5−OH was envisaged to be decreased by an "*in situ* deactivation strategy" applying acidic conditions. Such acidified iododesilylation conditions were reported by Vanderwal and co-workers, who used acetic acid to prevent any interaction with a tertiary amine.[197] Therefore, 1.1 equivalents of NIS were added to a mixture **144** and 2.2 equivalents of acidic acid in HFIP at 0 °C. The desired alkenyl iodide **125** was obtained in 65% yield with no observable double bond isomerisation (*E:Z* ≥ 20:1, ^{1}H NMR), aside minor iodoetherification product **145** (Entry 3, Table 9). To assure the integrity of the alkene (C7=C8), 10 equivalents, instead of 2.2 equivalents, of acetic acid were applied. After 2 min, this attempt afforded exclusively *E*-alkenyl iodide **125** (*E:Z* ≥ 20:1, ^{1}H NMR) in 67% yield, with additional 5% of the starting material **144**, and no iodoetherification product **145** (Entry 4, Table 9). Prolonging the reaction time to 5 min provided *E*-alkenyl iodide **125** in 82% yield with no observable alkene isomerisation (*E:Z* ≥ 20:1, ^{1}H NMR) on a 1.9 mmol scale (Entry 5, Table 9).

Table 9. Iododesilylation of the silyl masked western fragment **144** – optimisation.
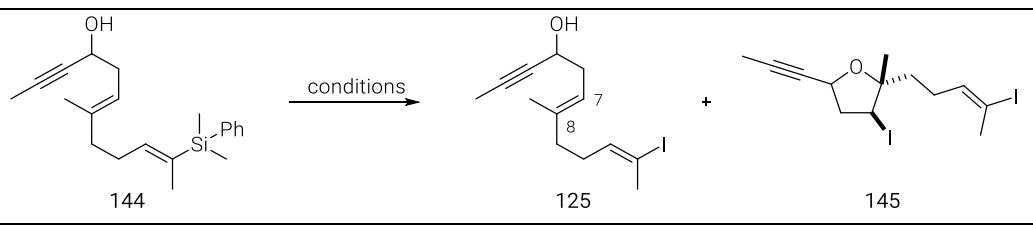
Entry	NIS	AcOH	Solvent	Temperature Time	Yield
1	2.0 equiv	-	HFIP	0 °C, 2 min	73% (**145**, *cis/trans* 42:58)
2	1.0 equiv	-	HFIP	0 °C, 2 min	46% (**125**)*, 45% SM (**144**)*, 8% (**145**)*
3	1.1 equiv	2.2 equiv	HFIP	0 °C, 2 min	65% (**125**)*, 5% (**145**)*
4	1.1 equiv	10.0 equiv	HFIP	0 °C, 2 min	67% (**125**)*, 5% SM (**144**)*
5	1.1 equiv	10.0 equiv	HFIP	0 °C, 5 min	82% (**125**)

All iododesilylations were performed with integrity of the alkene geometry (*E:Z* ≥ 20:1, ^{1}H NMR); * = ^{1}H NMR yield.

The revised order of transformations, first deprotection then iododesilylation, provided the western fragment **125** in 69% yield over the final two steps. This is an increase of 25% yield to the previous approach, in which iododesilylation was performed prior to deprotection (Scheme 39). Overall, the western fragment **125** was synthesised in 30% yield (8 steps, LLS). The modified Zakarian iododesilylation conditions might increase the scope of this methodology and serve as a protecting group free modification in the future.

3.7 COUPLING AND MACROCYCLISATION

The coupling of the fragments **124** and **125** commenced by a chemoselective hydroboration of the terminal alkene **124** in the presence of the methyl-capped alkyne on treatment with the 9-H-9-BBN dimer in THF at room temperature. The resulting borane **136** was subjected to Suzuki coupling with the western fragment **125**. This sequence gave RCAM precursor **123** in 69% yield (Scheme 41).
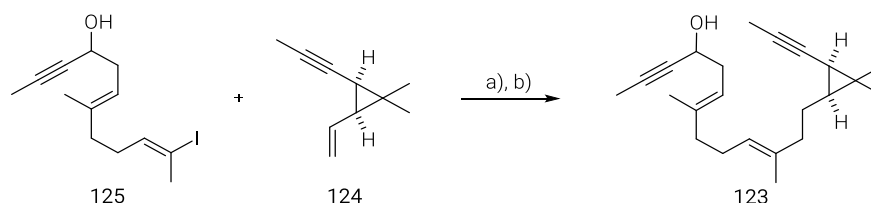
Scheme 41. Coupling of the cyclopropyl fragment **124** and the western fragment **125**. Conditions: a) *i*) **124** (1.3 equiv), 9-H-9-BBN dimer (0.95 equiv), THF, 0 °C to RT, *ii*) **125** (1.0 equiv), [(dppf)PdCl$_2$] (10 mol%), Ba(OH)$_2$·(H$_2$O)$_8$ (1.9 equiv), H$_2$O, THF, RT, 69%.

The RCAM of compound **123**, bearing two methyl-capped alkyne groups, was investigated based on the results of the previous approach. In all RCAM attempts in this paragraph, the catalyst was added to a suspension of the RCAM precursor **123** and 5 Å MS in toluene at the stated temperature. The canopy ligand sphere molybdenum catalyst **Cat. 3** was employed initially, but no reaction was observed at room temperature or at reflux (Entry 1, Table 10).[115] Next, the two-component alkyne metathesis catalyst system **Cat. 1** (10 mol%) was applied at room temperature. After 6 hours, macrocycle **122** was obtained in 46% yield (Entry 2, Table 10).

Running the reaction at 45 °C and utilising 10 mol% of **Cat. 1** cyclised **123** to **122** in 42% yield after 4.5 hours (Entry 3, Table **10**). Applying 20 mol% of **Cat. 1** to **123** at 45 °C afforded 59% yield of macrocycle **122** (Entry 4, Table 10). In each attempt, undefined side-products were observed. To prevent their formation, the temperature was further elevated and the dilution was increased to 1 mM. Thus, the addition of a solution of catalyst system **Cat. 1** in toluene to a refluxing mixture of RCAM precursor **123** and 5 Å MS in toluene led to macrocycle **122** in 81% yield on a 25 μmol scale (Entry 5, Table 10). On a 140 μmol scale, the application of these conditions gave 60% yield of macrocycle **122** (Entry 6, Table 10). The diastereomeric alcohols (5R-**146** & 5S-**147**) of the resulting mixture were separated by flash chromatography.

Table 10. Ring-closing alkyne metathesis of diyne **123** – optimisation.

Entry	Catalyst	Concentration	Temperature	Time	Yield
1	**Cat. 3** (10 mol%)	2 mM	RT to 100 °C	16 h	no reaction
2	**Cat. 1** (10 mol%)	2 mM	RT	6 h	45%
3	**Cat. 1** (10 mol% + 10 mol%)	2 mM	45 °C	4.5 h	42%
4	**Cat. 1** (20 mol%)	2 mM	45 °C	2 h	59%
5	**Cat. 1** (20 mol%)	1 mM	reflux	25 min	81%*
6	**Cat. 1** (20 mol%)	1 mM	reflux	25 min	60%

* = ^{1}H NMR yield, 25 μmol scale.

3.8 TOTAL SYNTHESIS OF DEPRESSIN

The late-stage diversification towards the total synthesis of depressin (**9**) was performed according to the best conditions in the previous total synthesis of *ent*-depressin (**89**) (see chapter 2.6.3).

The C5−OH directed *trans*-hydrostannation of the RCAM product 5S-**147** gave the alkenyl stannane **148** in 88% yield with the desired alkene geometry in excellent regio- und stereoselectivity.[181−184] The following *C*-methylation of alkenyl stannane **148** afforded alcohol **149** in 66% yield. The final oxidation of the allylic alcohol **149** with freshly prepared manganese oxide[186] gave depressin (**9**) in 73% yield (Scheme 42).

Comparison of the spectral data of depressin (**9**) with those of the isolated natural product depressin (**9**) showed very good agreement with a maximum deviation of 0.06 ppm in the ^{1}H NMR data and 0.1 ppm in the ^{13}C NMR data (Figure 16). The specific rotation confirmed the

absolute stereochemistry of depressin (**9**) (synthetic depressin $[\alpha]_D^{20}$ = −85.0); depressin[6] $[\alpha]_D^{20}$ = −80.0).
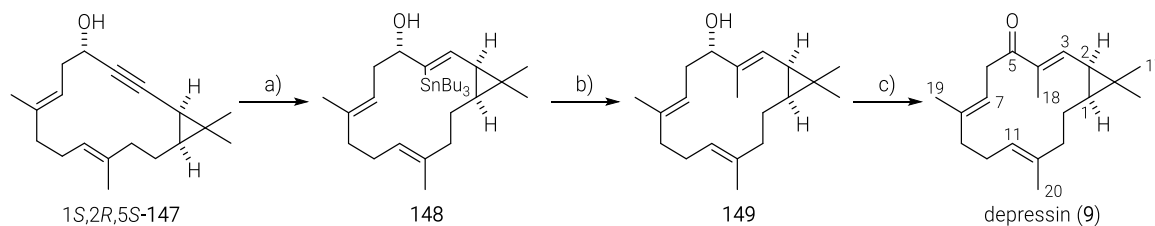
Scheme 42. Total synthesis of depressin (**9**). Conditions: a) [Cp*RuCl]$_4$ (2.5 mol%), Bu$_3$SnH (3.0 equiv), CH$_2$Cl$_2$, RT, 88%; b) MeI (1.5 equiv), CuTC (1.05 equiv), [Ph$_2$PO$_2$][Bu$_4$N] (1.1 equiv), Pd(PPh$_3$)$_4$ (5 mol%), DMF, RT, 66%; c) MnO$_2$ (30.1 equiv), CH$_2$Cl$_2$, RT, 73%.
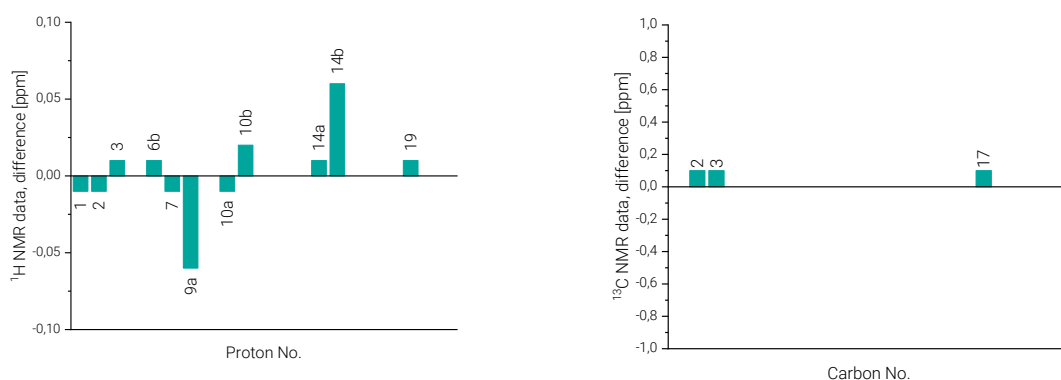
Figure 16. Differences in ^{1}H NMR shifts (left) and ^{13}C NMR shifts (right) between natural product depressin (**9**) and synthetic depressin.

3.9 CONCLUSION

The first total synthesis of depressin (**9**) was achieved in 7% overall yield comprising 13 steps along the LLS (21 total steps). Comparison of the total synthesis of *ent*-depressin (**89**) (see chapter 2) and that of depressin (**9**) revealed that the revised approach led to a reduction of three steps along the LLS and of six steps in the total step count. This improvement was based on a more concise blueprint, using the methyl-capped alkyne **124**, instead of the TIPS-capped alkyne **90**, as the cyclopropyl fragment.

Synthesis of the western fragment **125** commenced by a selective hydrosilylation of pentynol **64** to obtain alkenyl silane **130**, which is used twice in the synthesis and hence reduced the step count and the synthetic effort. The sp^2-sp^3 Negishi cross coupling of building blocks alkenyl iodide **128** and organozinc reagent **129**, which both derived from compound **130**, in combination with the modified stereoselective iododesilylation of the resulting coupling product **144** completed the synthesis of the western fragment **125** in 30% overall yield (8 steps, LLS). The synthesis of the cyclopropyl fragment **124** included an enantioselective rhodium catalysed cyclopropanation as the key step and was accomplished in 13% overall yield and eight steps. The exquisitely chemoselective hydroboration of the cyclopropyl fragment **124** on treatment with the 9-H-9-BBN dimer in THF provided borane **136**, which was merged with the western fragment **124** under Suzuki coupling conditions. The resulting RCAM precursor **123** was cyclised on treatment with the two-component alkyne metathesis catalyst system (**Cat. 1**) at elevated temperature. Employing a *trans*-hydrostannation and *C*-methylation sequence to the

resulting macrocycle **122** followed by C5−OH oxidation completed the total synthesis. Overall, depressin (**9**) was synthesised in 5% overall yield and 13 steps along the LLS (Scheme 43).
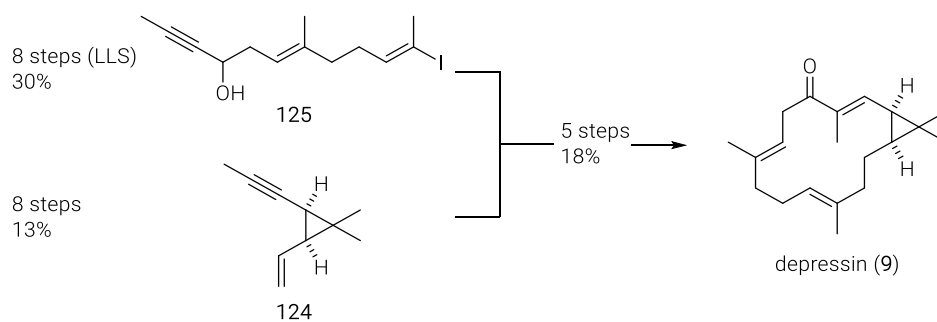
Scheme 43. Summary – total synthesis of depressin (**9**).

3.10 TOTAL SYNTHESIS OF EUPHORHYLONAL A
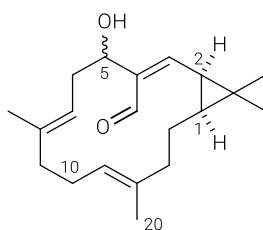
nominal euphorhylonal A (15)

Figure 17. Structure of nominal euphorhylonal A (**15**).[26]

The configurational assignment of the C5–OH group as well as the absolute configuration were not discussed by the isolation team.[26] Therefore, the total synthesis of euphorhylonal A (**15**) would not only demonstrate the versatility of the herein developed synthetic strategy, but also clarify the both uncertainties (Figure 17).

To determine the configuration at C5, the two macrocyclic diastereomeric alcohols (5*R*-**146** & 5*S*-**147**) were separated by flash chromatography (Scheme 44) followed by Mosher ester analysis (see Experimental Part).[198,199]
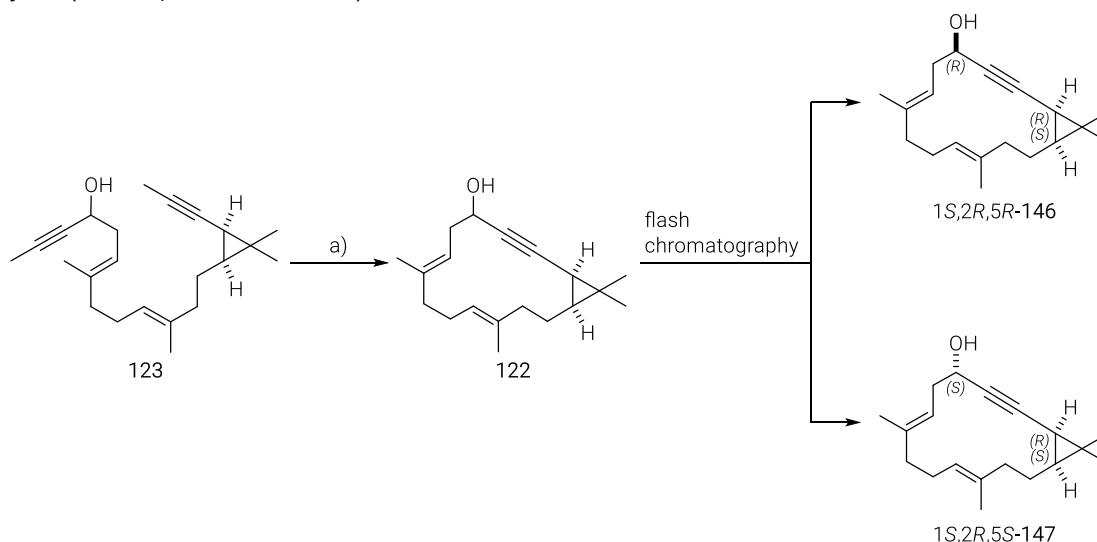
Scheme 44. Separation of macrocyclic diastereomer 1*S*,2*R*,5*R*-**146** and 1*S*,2*R*,5*S*-**147**.

The structure of diastereomer **146** in the solid state (Figure 18, relative configuration) in combination with the corresponding Mosher ester analysis not only revealed the configuration at C5, but also confirmed the absolute configuration of the cyclopropane (Scheme 44, Figure 18).
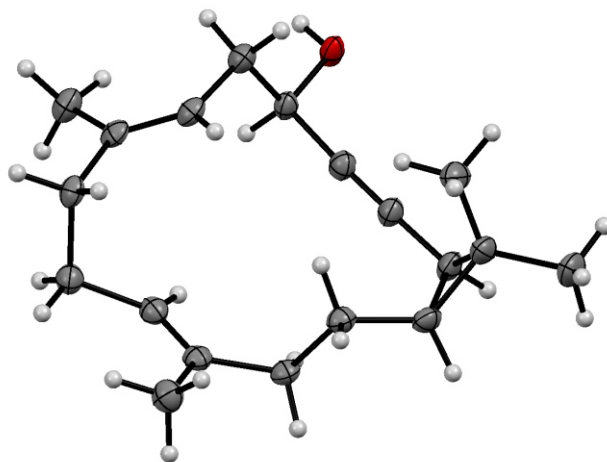
Figure 18. Single crystal X-ray structure of 1*S*,2*R*,5*R*-diastereomer **146** with the relative stereochemical configuration.

3.10.1   LATE-STAGE DIVERSIFICATION – THE ESTER APPROACH

This approach towards the total synthesis of euphorhylonal A (**15**) was inspired by the in-house developed methodologies of hydroxy-directed *trans*-hydrostannation and hydroxy-assisted methoxycarbonylation.[200] In case of the 1*S*,2*R*,5*S*-configured cycloalkyne **147**, the ruthenium catalysed *trans*-hydrostannation gave the desired *E*-alkenyl stannane **148**, as the only observable isomer in 88% yield (Scheme 45).[181–184] The resulting alkenyl stannane **148** was subjected to the palladium catalysed methoxycarbonylation under CO atmosphere in methanol to give methyl ester **150** in 81% yield.[200] The following reduction of ester **150** to 1*S*,2*R*,5*S*-aldehyde **151** was not feasible on treatment with DIBAL-H in different solvents (THF, CH_2Cl_2, toluene) and at various temperatures (−78 °C to −10 °C). The 1*S*,2*R*,5*R*-isomer **146** gave the desired *E*-alkenyl stannane **152** in 79% yield and the subsequent hydroxy-assisted methoxycarbonylation resulted in 77% yield of the corresponding methyl ester **153**. The selective DIBAL-H reduction to 1*S*,2*R*,5*R*-aldehyde **154** was not observed in CH_2Cl_2 at −78 °C. However, using toluene, instead of CH_2Cl_2, as solvent at −78 °C led to the formation of the desired aldehyde **154** in 11% yield (Scheme 45). Comparison of the spectral data of 1*S*,2*R*,5*R*-aldehyde **154** with those of the isolated natural product euphorhylonal A showed no accordance. In conclusion, this synthetic strategy, employing methoxycarbonylation and selective reduction, was not feasible for the total synthesis of euphorhylonal A.
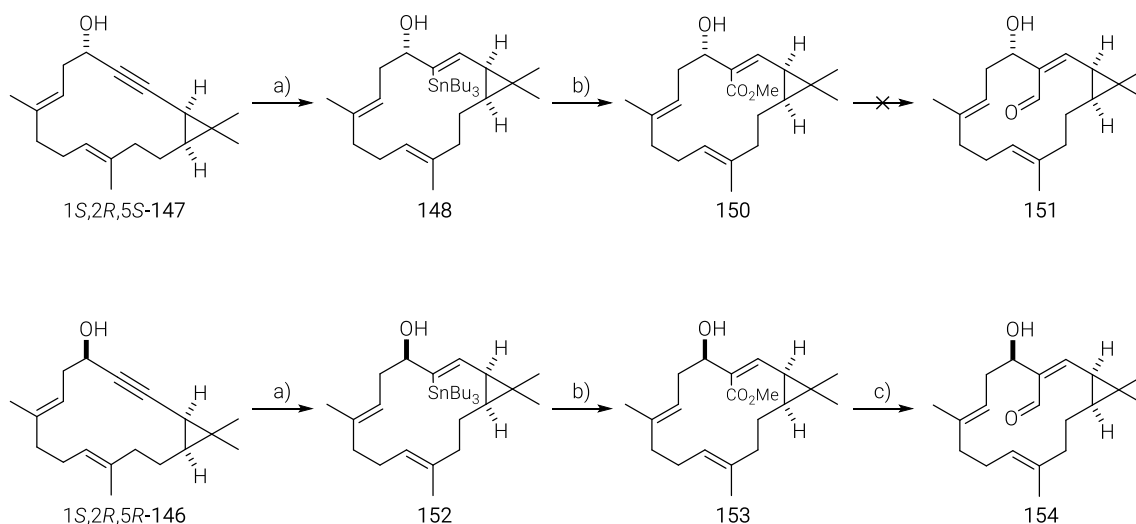
Scheme 45. Late-stage diversification – synthesis of ester **150** and aldehyde **154**. Conditions: a) [Cp*RuCl]$_4$ (2.5 mol%), Bu$_3$SnH (3.0 equiv), CH$_2$Cl$_2$, RT, 88% (1*S*,2*R*,5*S*-**148**), 79% (1*S*,2*R*,5*R*-**152**); b) Pd(OAc)$_2$ (20 mol%), Ph$_3$As (40 mol%), BQ (1.5 equiv), TFA (40 mol%), CO, MeOH, RT, 81% (1*S*,2*R*,5*S*-**150**), 77% (1*S*,2*R*,5*R*-**153**); c) DIBAL-H (2.05 equiv), toluene, −78 °C, 11%.

3.10.2 LATE-STAGE DIVERSIFICATION – THE FORMYLATION APPROACH

This strategy compromised a tin/lithium exchange of stannanes **148** and **152**, followed by formylation of the resulting organolithium species with DMF. According to a procedure of Studer and co-workers.[201] Methyllithium was added to a mixture of the corresponding alkenyl stannane in THF at −78 °C and the resulting mixture was allowed to warm to room temperature. After full conversion of the corresponding stannane, the mixture was cooled to −78 °C and DMF was added. Subsequent warming to room temperature afforded 1*S*,2*R*,5*S*-aldehyde **151** and 1*S*,2*R*,5*R*-aldehyde **154** in 68% and 53% yield, respectively (Scheme 46).
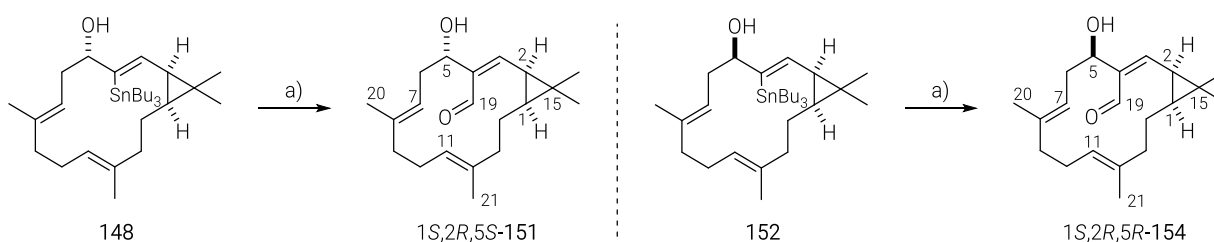
Scheme 46. Synthesis of 1*S*,2*R*,5*S*-aldehyde **151** and 1*S*,2*R*,5*R*-aldehyde **154**. Conditions: a) *i*) MeLi (2.0 equiv in Et$_2$O), THF, −78 °C to RT; *ii*) DMF (8.9 equiv), −78 °C to RT, 68% (1*S*,2*R*,5*S*-**151**), 53% (1*S*,2*R*,5*R*-**154**).

Unfortunately, comparison of the spectral data of 1*S*,2*R*,5*S*-aldehyde **151** and 1*S*,2*R*,5*R*-aldehyde **154** with those of the natural product euphorhylonal A showed no accordance (Figure 19). Hence, the proposed structure of euphorhylonal A must be misassigned at one of the cyclopropyl stereocentres.
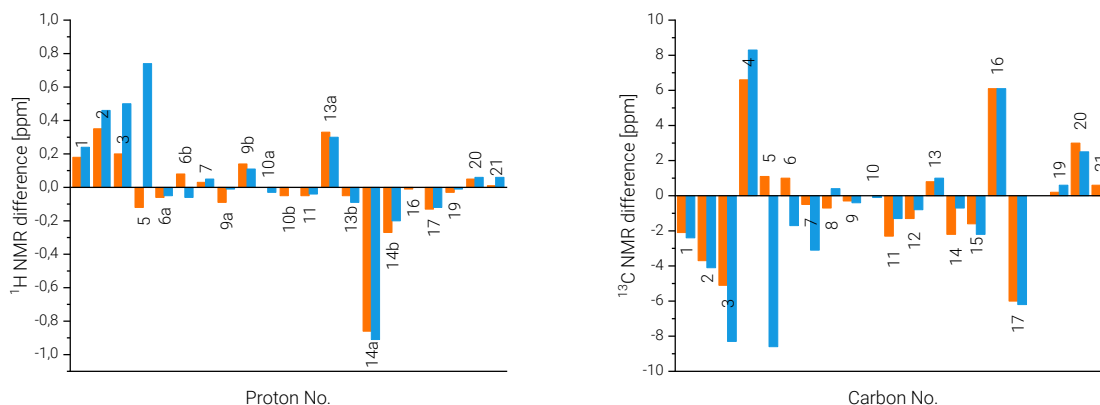
Figure 19. Differences in ^{1}H NMR shifts and ^{13}C NMR shifts between either 1*S*,2*R*,5*S*-**151** (orange) or 1*S*,2*R*,5*R*-**154** (blue) and euphorhylonal A.

3.10.3 STRUCTURE ELUCIDATION OF EUPHORHYLONAL A

Elucidation of the actual configuration of euphorhylonal A was conducted by comparing the analytical data of euphorhylonal A with these of a closely related casbane diterpene, by computational simulation of chemical shielding tensors with subsequent probability calculation, and, finally, by total synthesis.

3.10.4 STRUCTURE ELUCIDATION – COMPARISON

Literature research revealed that pekinenin C (**16**) has a closely related structure. Therefore, its spectral data were compared with those of euphorhylonal A.[16,26] The ^{1}H NMR data sets were in good agreement, except the ^{1}H shift of H-14a. The ^{13}C NMR data showed deviations in shifts of the alkenyl quaternary carbons (C4 (Δ = 4.7 ppm), C8 (Δ = 1.7 ppm), C12 (Δ = 3.1 ppm)) (Figure 20).
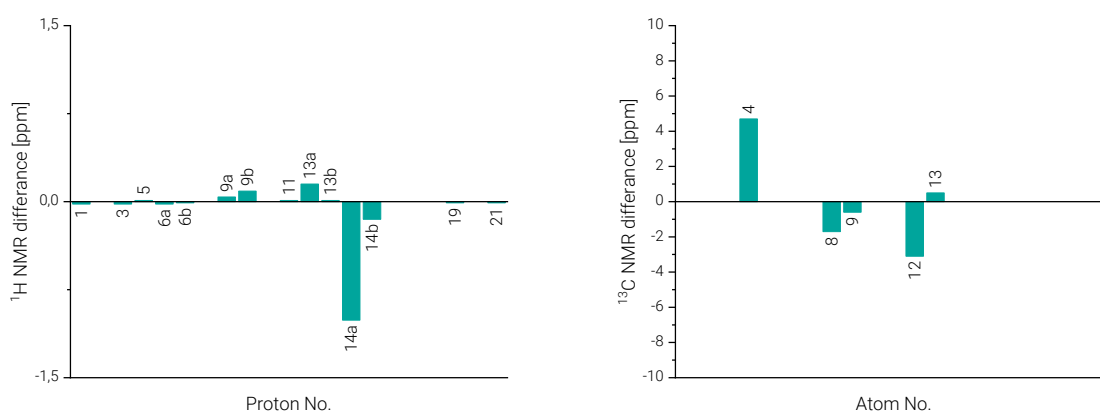
Figure 20. Differences in ^{1}H NMR shifts and ^{13}C NMR shifts of pekinenin C (**16**) with natural product euphorhylonal A, numbering see **Figure 21**.

The similarity of those datasets, especially the cyclopropane related chemical shifts of C1, C3, and C15, suggested a *trans*-cyclopropane motif for euphorhylonal A, instead of a *cis*-cyclopropane. The comparison further indicated, that the C5−OH group were in a *cis* configuration with the C2−H and in *trans* to the C1−H (Figure 21). In combination with the

specific rotation, although these values can only be seen as a hint for a certain configuration at this point, it could be notionally assumed that euphorhylonal A and pekinenin C (**16**) have the same relative configuration but the opposing absolute configuration (pekinenin C (**16**)[16] $[\alpha]_D^{25}$ = −19; euphorhylonal A[26] $[\alpha]_D^{25}$ = +90.5), as illustrated by structure **155** (Figure 21).

1*R*,2*R*,5*S*-**16**
pekinenin C

nominal
euphorhylonal A (**15**)

1*R*,2*R*,5*S*-**155**
tentative reassignment
euphorhylonal A
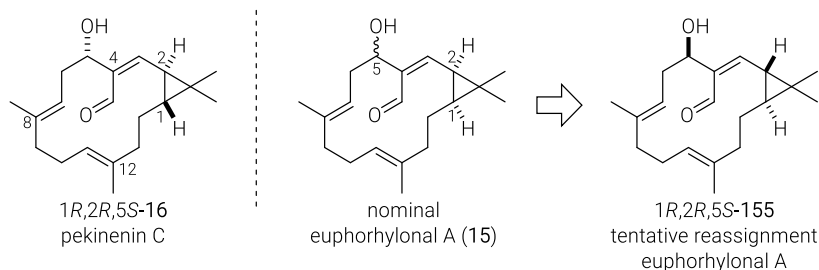
Figure 21. Tentative structure elucidation of euphorhylonal A (**155**).[26]

3.10.5 STRUCTURE ELUCIDATION − COMPUTATIONAL APPROACH

The application of computational spectroscopy to study the congruence of the proposed stereochemical assignment of an organic compound with its experimental data has become quite common.[202−204] This approach, in combination with the application of powerful and freely available statistical analysis tools as, for example, developed by Goodman and co-workers (CP3, DP4, DP4-AI)[205−208] or by Sarotti and co-workers (DP4+, *J*-DP4, DIP, ANN),[209−214] allows a stereochemical assignment with high confidence.[125,204,215−219]

The herein employed DP4+ probability calculation uses the computed chemical shielding tensors of all relevant diastereomers in combination with the experimental NMR data (^{1}H and ^{13}C) of an organic compound with an unknown configuration. The DP4+ program calculates the statistical congruence of each computed data set to the subjected experimental NMR data.

The computational stereochemical assignment approach to clarify the actual configuration of euphorhylonal A commenced by determining all possible diastereomers of euphorhylonal A (**15**) (Figure 22).

151

154

155

156
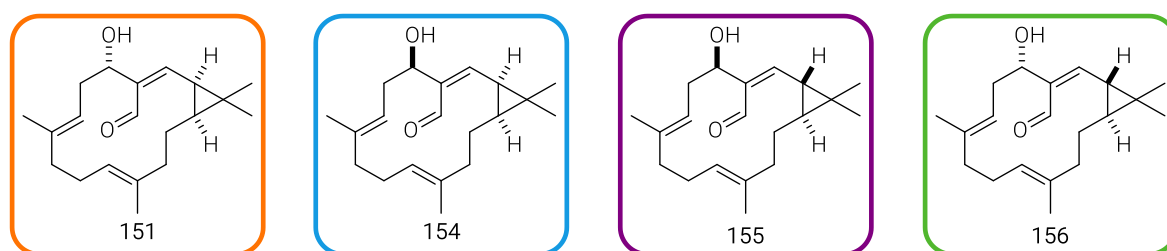
Figure 22. The possible diastereomers of euphorhylonal A (**15**).

Each of these four diastereomers was subjected to conformational sampling using the Conformer-Rotamer Ensemble Sampling Tool (CREST),[220,221] which simulates the molecule movement in solution and generates the most represented conformations. Due to the low level of theory, the conformational sampling was conducted with a 6 kcal/mol threshold. This gave 174 conformers of aldehyde **151**, 146 conformers of aldehyde **154**, 274 conformers of aldehyde **156**, and 155 conformers of aldehyde **155**. The resulting geometries of the conformers were then optimised at the B3LYP-D3BJ-(CPCM)/def2-TZVP level of theory, using the ORCA 4.2 program package.[222,223]

| 1*S*,2*R*,5*S*-**151** | 1*S*,2*R*,5*R*-**154** | 1*S*,2*S*,5*R*-**155** | 1*S*,2*S*,5*S*-**156** |
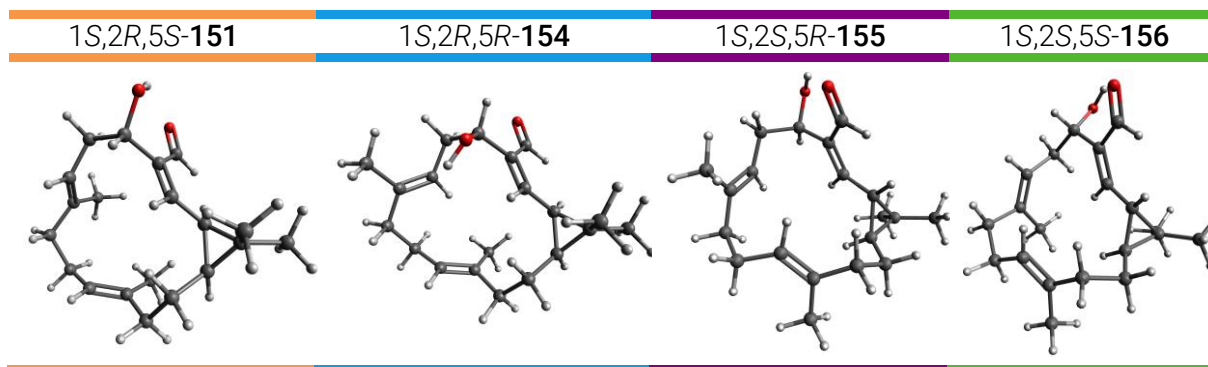
Figure 23. Optimised geometries of the lowest energy conformers of the four possible diastereomers.

Only structures with significant conformational distinctions and a relevant Boltzmann population were used for chemical shielding calculation. Therefore, similar conformers were sorted out, based on the root-mean-square deviations (RMSD) of atomic positions. The remaining conformers (25 conformers of aldehyde **151**, 28 conformers of aldehyde **154**, 31 conformers of aldehyde **156**, 17 conformers of aldehyde **155**) were subjected to numerical frequency calculations on the B3LYP-D3BJ-(CPCM)/def2-TZVP level of theory. The obtained Gibbs free energies (G) of each conformer were used to calculate the Boltzmann distribution for each diastereomer. Thereby, only conformers with a relevant Boltzmann population ($p_i > 4\%$) were considered.

The chemical shielding calculations were performed according to the DP4+ protocol of Sarotti and co-workers.[209] Regarding the solvent modelling, the DP4+ protocol prefers the dielectric polarisable continuum model (PCM) over the gas phase approximation. Since the ORCA 4.2 program package does not include the dielectric PCM, the shielding calculations were conducted in the gas phase. The isotropic shielding tensors of all carbon and hydrogen atoms (σ_i^x) were computed for all relevant conformers at the density functional theory (DFT) level. Gauge-independent atomic orbitals (GIAO)[224–227] were used to avoid the gauge origin problem, in combination with the mPW1PW functional[228] and the split-valence double-zeta Pople basis set (6-31G**)[229] as implemented in the ORCA 4.2 program package.[222,223]

The calculated shielding tensors (σ_i^x) were averaged by the Boltzmann distribution probability (p_i) for each significantly populated conformer i (threshold: $p_i > 4\%$). The Boltzmann averaged shielding tensors were used in the DP4+ calculation. First the congruence probability of the ^{1}H and ^{13}C data are calculated individually. This is followed by a probability calculation combining both datasets, giving the "all data" probability. As depicted in Figure 24, the DP4+ probability regarding the ^{1}H data showed a high congruence with the 1*S*,2*S*,5*S*-diastereomer **156** (green), whereas the probability using the ^{13}C data suggested a high similarity to the 1*S*,2*S*,5*R*-diastereomer **155** (purple). The DP4+ probability calculation using "all data" led to the conclusion that euphorhylonal A likely has the same relative configuration as 1*S*,2*S*,5*R*-aldehyde **155**. The prediction can be made with high confidence (100%).
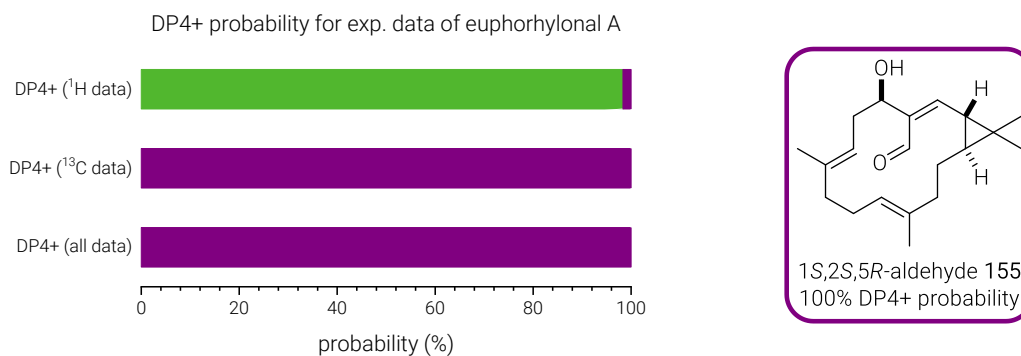
Figure 24. Graph of [1]H-DP4+, ^{13}C-DP4+, and DP4+ probabilities for the congruence of the experimental NMR data of euphorhylonal A[26] with the calculated chemical shielding data of **155** (purple), and **156** (green).

Both approaches, the comparison with pekinenin C (**16**) and the computational studies, suggested that 1*S*,2*S*,5*R*-aldehyde **155**, including a *trans*-cyclopropane motif and a *cis*-relationship between the C5−OH and C2−H, represents the actual structure of euphorhylonal A.

3.10.6 STRUCTURE ELUCIDATION − SYNTHETIC APPROACH

The synthesis of 1*S*,2*S*,5*R*-aldehyde **155** requires the *trans*-cyclopropyl fragment **157**, instead of the *cis*-cyclopropyl fragment **124**. Thereby, the *trans*-cyclopropyl fragment synthesis (**157**) would only differ by an additional epimerisation at the C2 position of *cis*-aldehyde **134** to form the corresponding *trans*-aldehyde **158**. The methyl alkyne unit would be introduced by a Corey/Fuchs homologation.
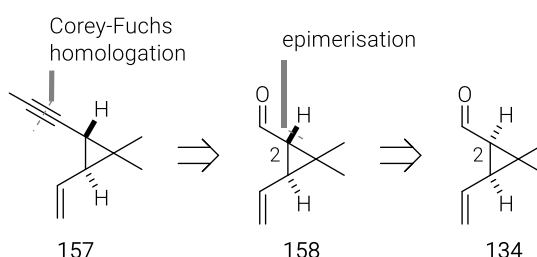
Scheme 47. Retrosynthetic analysis of the *trans*-cyclopropyl fragment **157**.

The aldehyde **134** was synthesised as described in chapter 3.4 and was subjected to epimerisation of the C2 stereocentre under basic conditions. Therefore, potassium carbonate was added to a solution of *cis*-aldehyde **134** in methanol at 50 °C. The desired *trans*-cyclopropane **158** was obtained as a mixture of diastereomers (*trans*/*cis* = 9:1). Attempts to increase the *trans*/*cis* ratio at higher temperatures were unsuccessful. The Corey/Fuchs homologation of the resulting *trans*-cyclopropyl aldehyde **158**, using diethyl ether as solvent and DMPU as promotor, completed the synthesis of *trans*-cyclopropyl fragment **157** in 63% yield over the final four steps (*trans*/*cis* = 9:1) (Scheme 35).
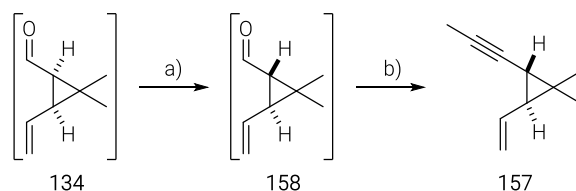
Scheme 48. Synthesis of the *trans*-cyclopropyl fragment **157**. Conditions: a) K_2CO_3 (4.6 equiv), MeOH, 50 °C; b) *i)* PPh$_3$ (8.0 equiv), CBr$_4$ (4.0 equiv), CH$_2$Cl$_2$, 0 °C; *ii)* *n*-BuLi (4.6 equiv), Et$_2$O, −78 °C; *iii)* DMPU (5.5 equiv), Et$_2$O, −78 °C; *iv)* MeI (13.9 equiv), −78 °C to RT, 63% over 4 steps (*trans/cis* = 9:1).

The *trans*-cyclopropyl fragment **157** was subjected to a chemo- and regioselective hydroboration on treatment with the 9-H-9-BBN dimer followed by a Suzuki cross coupling of the resulting borane and the western fragment **125**. The RCAM precursor **159** was obtained in 82% yield (Scheme 49).
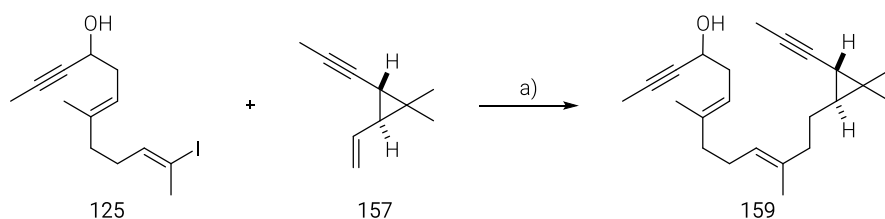
Scheme 49. Coupling of the *trans*-cyclopropyl fragment **157** and the western fragment **125**. Conditions: a) *i)* **157** (1.3 equiv), 9-H-9-BBN dimer (0.95 equiv), THF, 0 °C to RT; *ii)* **125** (1.0 equiv), [(dppf)PdCl$_2$] (5 mol%), Ba(OH)$_2$·(H$_2$O)$_8$ (1.9 equiv), H$_2$O, THF, RT, 82%.

Based on the previous results (see chapter 3.7), the RCAM of diyne **159** was investigated at different temperatures and dilutions, while employing the two-component catalyst system (**Cat. 1**) (Table 11).

A solution of the two-component alkyne metathesis catalyst system (**Cat. 1**, 20 mol%) in toluene was added to a suspension of **159** and 5 Å MS in toluene at room temperature. Under these conditions 47% yield of the desired macrocycle **160** was obtained, aside undefined side-products (Entry 1, Table 11). Performing RCAM at elevated temperature could be beneficial to overcome side-product formation and to improve the yield. In this regard, two attempts under reflux conditions were investigated with concentrations of 1 and 2 mM in toluene, which led to 59% and 57% yield of macrocycle **160**, respectively (Entry 2-3, Table 11). While refluxing in toluene gave slightly higher yields than at room temperature, a minor decrease to 70 °C was found ideal for this particular RCAM of **159**. This optimised conditions generated macrocycle **160** in 76% yield (Entry 4, Table 11).

Table 11. Ring-closing alkyne metathesis of diyne **159** – optimisation.
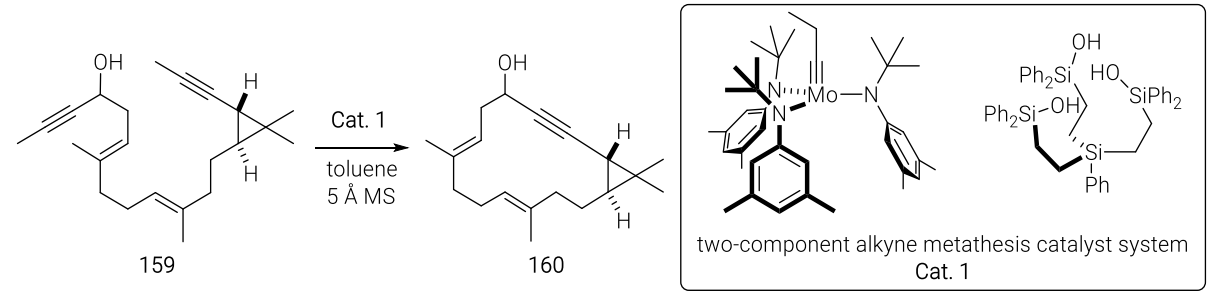
Entry	Catalyst System	Concentration	Temperature	Time	Yield (160)
1	**Cat. 1** (20 mol%)	1 mM	RT	4 h	47%
2	**Cat. 1** (20 mol%)	1 mM	reflux	25 min	59%
3	**Cat. 1** (20 mol%)	2 mM	reflux	30 min	57%
5	**Cat. 1** (20 mol%)	2 mM	70 °C	10 min	76%

At this stage, the diastereomeric alcohols 1*S*,2*S*,5*S*-**161** and 1*S*,2*S*,5*R*-**162** were separated by flash chromatography and the configuration of the C5–OH group of each diastereomer was determined by Mosher ester analysis (see Experimental Part). Both diastereomers were used separately towards the total synthesis and structure elucidation of euphorhylonal A.

1*S*,2*S*,5*S*-**161** was subjected to *trans*-hydrostannation, affording alkenyl stannane **163** in 74% yield with excellent regio- and stereoselectivity. Subsequent treatment of **163** with *n*-BuLi and quenching of the resulting organolithium species with DMF gave 1*S*,2*S*,5*S*-aldehyde **156** in 69% yield (Scheme 50). Unfortunately, the spectral datasets of 1*S*,2*S*,5*S*-aldehyde **156** neither matched with those of pekinenin C (**16**) nor euphorhylonal A.

The same *trans*-hydrostannation and formylation sequence was applied to 1*S*,2*S*,5*R*-**162**. While an excellent regio- and stereoselective *trans*-hydrostannation of propargylic alcohol **162** was expected, next to 65% yield of the desired alkenyl stannane **164** a noticeable amount of the corresponding *a,cis*-alkene side-product **EP-3** was isolated. The reason for the formation of **EP-3** remained unclear.
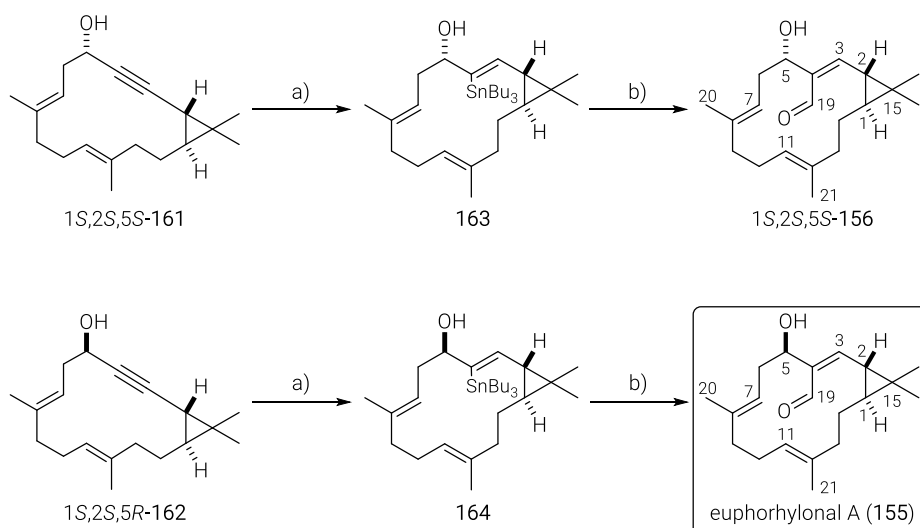
Scheme 50. Late-stage diversification − total synthesis of natural product euphorhylonal A (**155**). Conditions: a) [Cp*RuCl]$_4$ (2.5 mol%), Bu$_3$SnH (3.0 equiv), CH$_2$Cl$_2$, RT, 74% (1*S*,2*S*,5*S*-**163**), 65% (1*S*,2*S*,5*R*-**164**) + 12% **EP-3** (see the Experimental Part); b) *i*) MeLi (2.0 equiv in Et$_2$O), THF, −78 °C to RT; *ii*) DMF (8.9 equiv), −78 °C to RT, 69% (1*S*,2*S*,5*S*-**156**), 51% (1*S*,2*S*,5*R*-**155** or euphorhylonal A (**155**)).

The comparison of the analytical data of 1*S*,2*S*,5*S*-aldehyde **156** (green, Figure 25 & Figure 26) with those of euphorhylonal A and pekinenin C (**16**) showed no accordance in either case. In the case of 1*S*,2*S*,5*R*-aldehyde **155**, the experimental NMR data matched with those of pekinenin C (**16**) but did not match with those of euphorhylonal A in the first place. It turned out, that the isolation team highly likely misassigned the alkenyl quaternary carbon NMR signals (C4, C8, C12) of euphorhylonal A. After revising those assignment, the analytical data of euphorhylonal A were in good agreement with those of 1*S*,2*S*,5*R*-aldehyde **155** (purple) (Figure 25 & Figure 26). The only significant deviation of the ^{1}H NMR data sets was the H-14a ^{1}H NMR signal. This dissonance might be explained by a misassignment in the isolation paper due to the lack of 2D-NMR data. (1*S*,2*S*,5*R*-aldehyde **155** $[\alpha]_D^{25}$ = +74.5, natural product euphorhylonal A[26] $[\alpha]_D^{25}$ = +90.5).
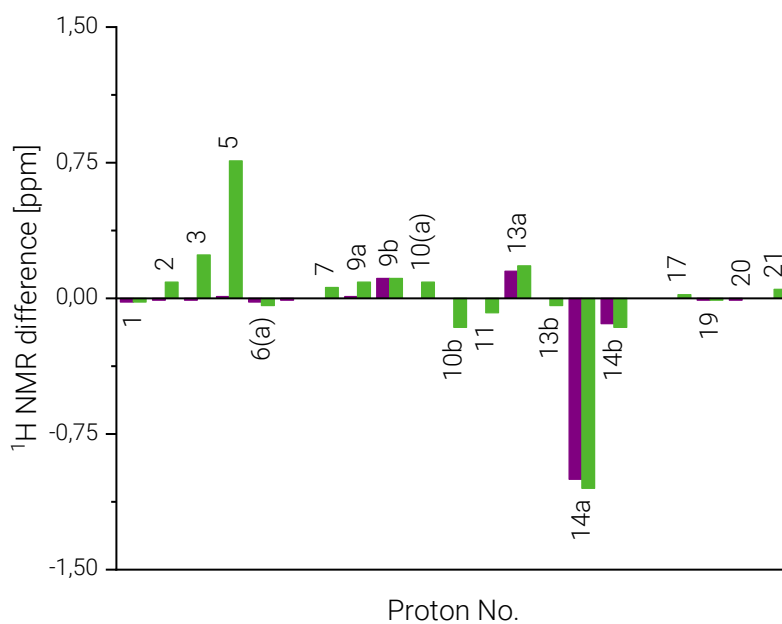
Figure 25. Differences in ¹H NMR shifts between either 1*S*,2*S*,5*R*-**155** (purple) 1*S*,2*S*,5*S*-**156** (green) or and the reassigned NMR data of euphorhylonal A; numbering see Scheme 50.
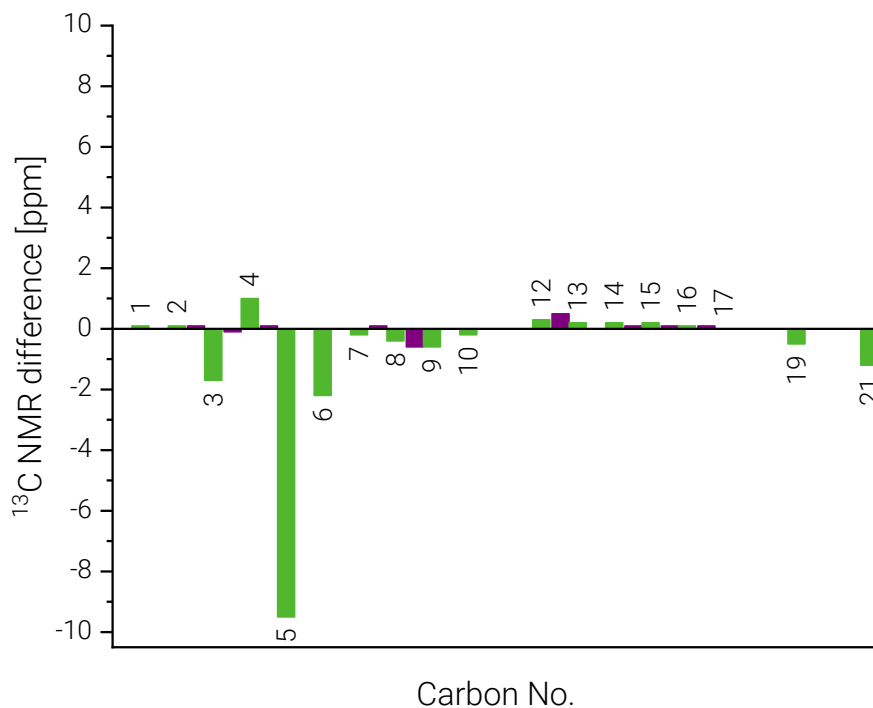
Figure 26. Differences in ¹³C NMR shifts between either 1*S*,2*S*,5*R*-**155** (purple) or 1*S*,2*S*,5*S*-**156** (green) or and the reassigned NMR data of euphorhylonal A; numbering see Scheme 50.

In the case of pekinenin C (**16**), it turned out that the NMR data are identical to those of 1*S*,2*S*,5*R*-aldehyde **155**, whereas the sign of the specific rotation is dextrorotatory (pekinenin C (**16**)[16] $[\alpha]_D^{25}$ = −19). These data analysis revealed an enantiomeric relationship between euphorhylonal A and pekinenin C rather than a diastereomeric.

3.10.7 CONCLUSION

The herein presented total synthesis of euphorhylonal A clarified the structure as 1*S*,2*S*,5*R*-**155** and revealed the highly likely enantiomeric relationship with pekinenin C (**16**). In this case, it also demonstrated that phylogenetically related *Euphorbia* plants can generate *antipodal* casbane diterpenes.[38]

Both diastereomeric alcohols of nominal euphorhylonal A (1*S*,2*R*,5*S*-**151** and 1*S*,2*R*,5*R*-**154**) were prepared along a concise and elegant route. The synthesis of the *cis*-cyclopropyl fragment **124** included an enantioselective rhodium catalysed cyclopropanation to generate the *gem*-dimethyl cyclopropane, followed by a reduction and homologation sequence to afford the cyclopropyl fragment **124** in eight steps and 13% overall yield. The western fragment **125** was prepared as in the total synthesis of depressin (**9**) in 30% yield and eight steps along the LLS, including two individually tuned iododesilylation steps and a sp²-sp³ Negishi cross coupling as key design elements. Due to the uncertainty of the configuration assignment at C5, the western fragment **125** was prepared as a racemate. The coupling of fragments **124** and **125** commenced by chemoselective hydroboration of the terminal alkene in presence of a methyl-capped alkyne on treatment with the 9-H-9-BBN dimer in THF. The resulting borane was subjected to a Suzuki cross coupling with western fragment **125**. The coupling product **123** was cyclised in the subsequent RCAM under optimised conditions. The resulting cyclic diastereomeric alcohols **146** and **147** were separated by flash chromatography and the absolute configuration of each was determined. Both macrocyclic alkynes **146** and **147** were separately subjected to the late-stage diversification *via* a regio- and stereoselective *trans*-hydrostannation and formylation sequence. The resulting *cis*-cyclopropyl aldehydes 1*S*,2*R*,5*S*-**151** and 1*S*,2*R*,5*R*-**154** were prepared in 7% or 5% overall yield, respectively, and twelve steps along the LLS (21 total steps).

Unfortunately, the analytical data of both diastereomers (**151** & **154**) of the nominal structures of euphorhylonal A were not in accordance with those of natural product. Comparison of the analytical datasets of euphorhylonal A with those of pekinenin C (**16**) and computational chemistry-based structure elucidation suggested 1*S*,2*S*,5*R*-aldehyde **155** as the most likely configuration of euphorhylonal A. Therefore, the *trans*-cyclopropyl fragment **157**, instead of its *cis*-analogue **124**, was synthesised in nine steps and 16% overall yield. Their syntheses only differed in an additional epimerisation at C2 position of the *cis*-aldehyde intermediate **134** to afford the thermodynamically favoured *trans*-cyclopropyl aldehyde, which was then converted into the cyclopropyl fragment **157** by a Corey/Fuchs homologation. A chemoselective hydroboration of **157** followed by a Suzuki cross coupling with compound **125** afforded the RCAM precursor **159**. The subsequent RCAM and separation of the resulting diastereomeric alcohols enabled the late-stage diversification. Both macrocyclic alkynes **161** and **162** were subjected to a *trans*-hydrostannation and formylation sequence, affording the *trans*-cyclopropyl aldehydes 1*S*,2*S*,5*R*-**155** and 1*S*,2*S*,5*S*-**156** in 3% or 5% overall yield, respectively, and 13 steps along the LLS (21 total steps).

This collective total synthesis of two natural occurring casbane diterpenes and three derivatives, confirms the versatility of the synthetic strategy and should bring many casbane diterpenes into

reach. The application of the ligand-controlled *gem*-dimethyl cyclopropanation, with or without subsequent epimerisation, enables the preparation of all permutations of the cyclopropyl fragment. Further, the alkenyl stannane motif can be seen as a platform to access all oxygenation patterns of the casbane diterpene family in the "northern" sector.

The analytical data of 1*S*,2*S*,5*R*-**155** were in accordance to those of euphorhylonal A. This synthesis led to the reassignment of euphorhylonal A structure and verified the theoretically proposed configuration. Furthermore, the data analysis suggest rather an enantiomeric relationship between pekinenin C (**16**) and euphorhylonal A, than a diastereomeric, as expected from the originally proposed structures.
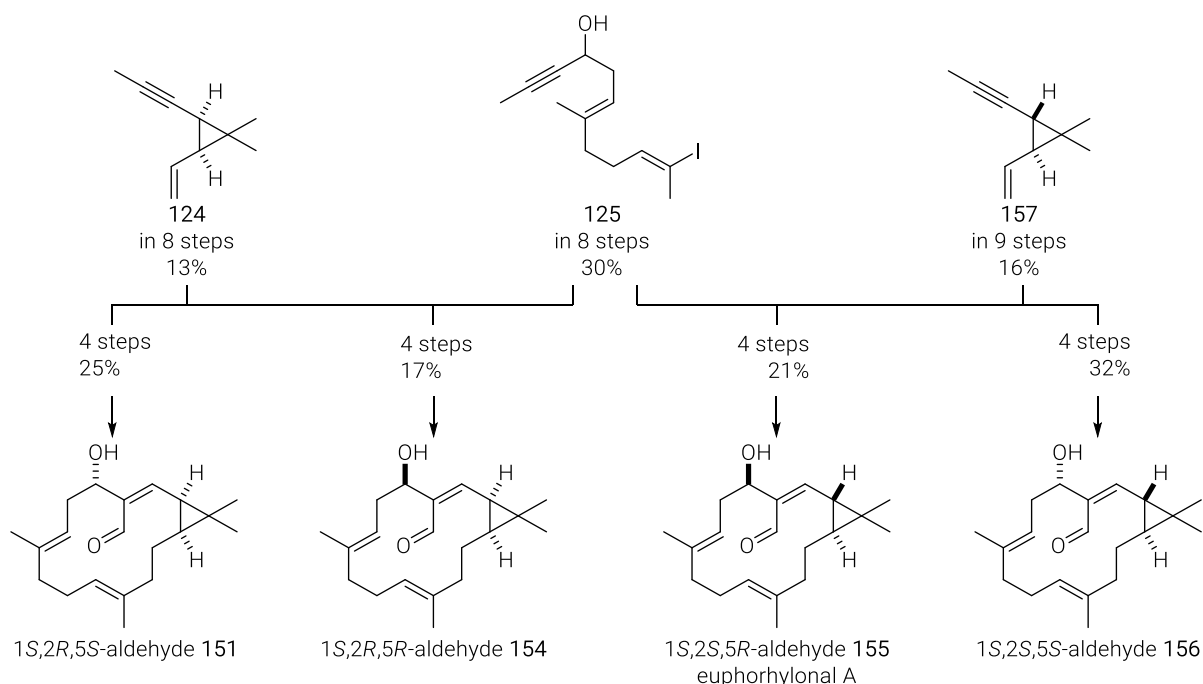
Scheme 51. Summary – total synthesis and structure elucidation of euphorhylonal A (**155**) and its diastereomers.

3.10.8   COMPUTATIONAL STRUCTURE ELUCIDATION – CONTROL EXPERIMENTS

During the total synthesis and clarification of the configurational assignment of euphorhylonal A, all four possible diastereomers were synthesised and their NMR data were recorded (1*S*,2*R*,5*S*-**151**, 1*S*,2*R*,5*R*-**154**, 1*S*,2*S*,5*R*-**155**, and 1*S*,2*S*,5*S*-**156**). In the additional computational assignment of the relative stereochemistry, all chemical shielding tensors for each diastereomer (**151**, **154**, **155**, **156**) were calculated. These experimental and *in silico* data were used to verify the stereochemical assignment of euphorhylonal A by the DP4+ program (chapter 3.10.5) and to confirm the high confidence of those assignments for macrocyclic diterpenes. The experimental NMR data (including ^{1}H and ^{13}C NMR) of each diastereomer were separately subjected to the DP4+ probability calculation sheet, which contained the calculated chemical shielding data of all four diastereomers (**151**, **154**, **155**, **156**).

The experimental NMR data of 1*S*,2*R*,5*S*-**151** were subjected to the DP4+ probability calculation sheet, containing the calculated chemical shielding data for all four diastereomers, led to a congruence between the experimental NMR data and calculated chemical shielding data of aldehyde **151** in high confidence (Figure 27). Using the experimental NMR data of 1*S*,2*R*,5*R*-**154**, led to an accordance with the calculated data of **154** in high confidence (Figure 28). This performance of the DP4+ stereochemical assignment program was further demonstrated by

the congruence between the experimental NMR data of 1*S*,2*S*,5*S*-**156** and 1*S*,2*S*,5*R*-**155** and the corresponding calculated data in high confidence (Figure 30, Figure 29).
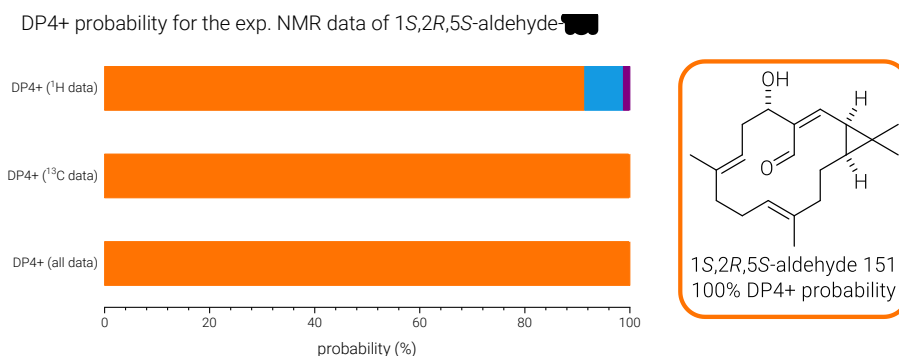
Figure 27. Graph of [1]H-DP4+, ^{13}C-DP4+, and "all data" DP4+ probabilities for the congruence of the experimental NMR data of 1*S*,2*R*,5*S*-**151** with the calculated chemical shielding data of **151** (orange), **154** (blue), and **155** (purple).
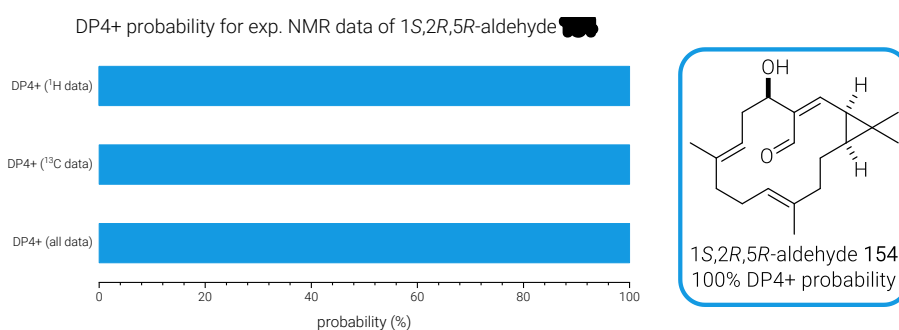
Figure 28. Graph of [1]H-DP4+, ^{13}C-DP4+, and DP4+ probabilities for the congruence of the experimental NMR data of 1*S*,2*R*,5*R*-**154** with the calculated chemical shielding data of **154** (blue).
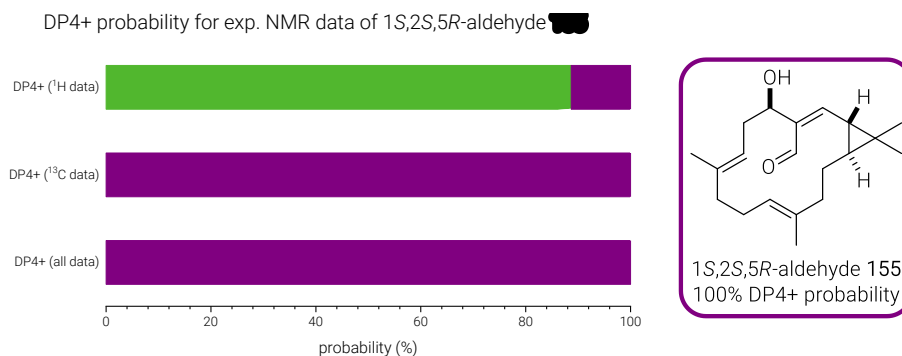
Figure 29. Graph of [1]H-DP4+, ^{13}C-DP4+, and DP4+ probabilities for the congruence of the experimental NMR data of 1*S*,2*S*,5*R*-**155** with the calculated chemical shielding data of **155** (purple) and **156** (green).
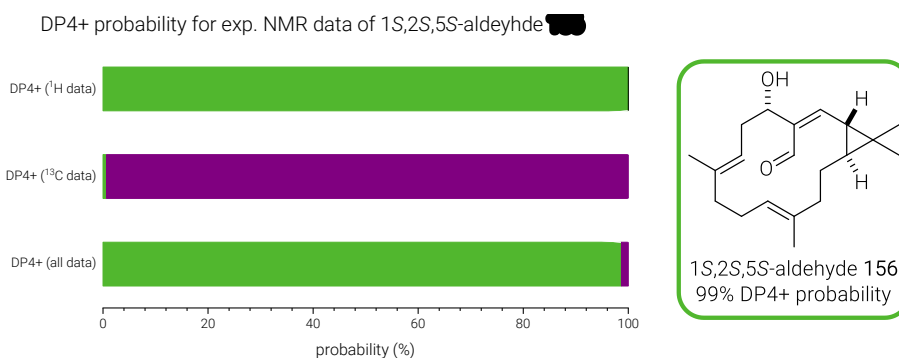
Figure 30. Graph of [1]H-DP4+, ^{13}C-DP4+, and DP4+ probabilities for the congruence of the experimental NMR data of 1*S*,2*S*,5*S*-**156** with the calculated chemical shielding data of **155** (purple) and **156** (green).

3.11 TOTAL SYNTHESIS OF YUEXIANDAJISU A

3.11.1 ISOLATION AND STRUCTURE ELUCIDATION

Yuexiandajisu A

Yuexiandajisu A (**17**) (Figure 31) was first isolated from roots of *Euphorbia ebracteolata* Hayata, which is part of the traditional Chinese medicine "Lang Du".[12] Extraction of the natural material (5 kg) and extensive chromatographic purification of the residue gave yuexiandajisu A (**17**) as orthorhombic crystals (21 mg), next to yuexiandajisu B (**29**). The structure and the relative configuration were elucidated by 2D-NMR analysis and single crystal X-ray analysis.[12] It bears a *trans*-cyclopropane motif and a carboxylic acid functionality at the C18 position beside the casbane diterpene macrocyclic framework. A preliminary bioassay showed antibacterial activities of yuexiandajisu A (**17**).
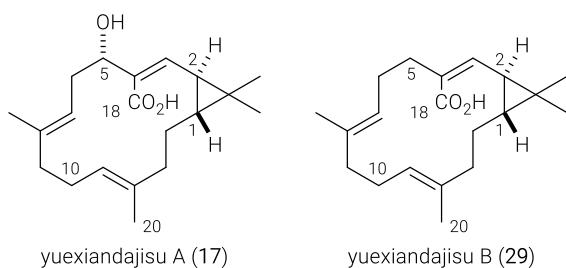
Figure 31. Relative structure of yuexiandajisu A (**17**) and yuexiandajisu B (**29**).[12]

3.11.2 SYNTHESIS

As the bicyclic core structure of yuexiandajisu A (**17**) possesses the same relative configuration as euphorhylonal A (**155**), alkenyl stannane **164** was used as the starting point. **164** was treated with methyllithium at low temperature and the resulting organolithium species was trapped with carbon dioxide (bubbled through the mixture). The sequence completed the total synthesis of (+)-1*S*,2*S*,5*R*-acid *ent*-**17** in 51% yield.
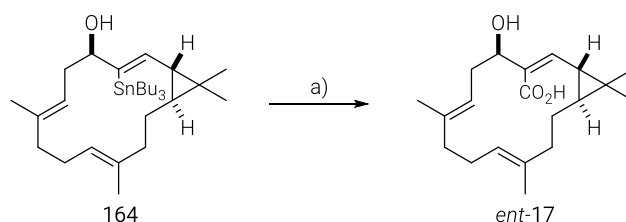
Scheme 52. Late-stage diversification – total synthesis of (+)-yuexiandajisu A (*ent*-**17**); Conditions: a) *i*) MeLi (2.2 equiv in Et$_2$O), THF, −78 °C to RT; *ii*) CO$_2$, −78 °C to RT, 51%.

The NMR data as well as the specific rotation of (+)-1*S*,2*S*,5*R*-acid *ent*-**17** and of the isolated natural product showed good agreement, except of the C-21 ^{13}C NMR signal with a deviation of 1.4 ppm (Figure 32). This confirmed the relative configuration and determined the absolute as 1*S*,2*S*,5*R* (*ent*-**17**) (synthetic (+)-yuexiandajisu A (*ent*-**17**) $[\alpha]_D^{30} = +171.3$); yuexiandajisu A (**17**) $[\alpha]_D^{30} = +172$).
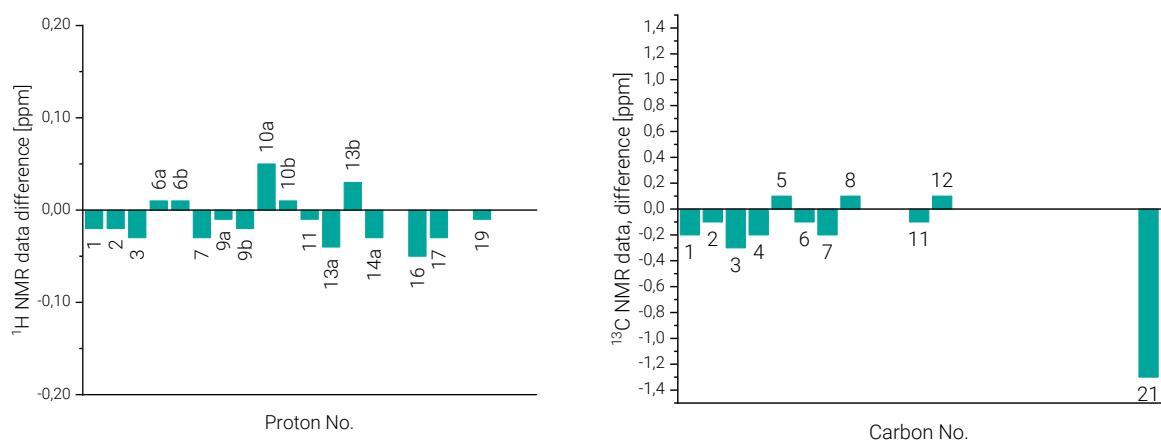
Figure 32. Differences in 1H NMR and 13C NMR shifts between (+)-1*S*,2*S*,5*R*-acid (*ent*-**17**) and yuexiandajisu A.[12]

3.11.3 CONCLUSION

The total synthesis of (+)-yuexiandajisu A (*ent*-**17**) was accomplished in 3% overall yield comprising 13 steps along the LLS (21 total steps). The comparison of the analytical data revealed the absolute configuration of yuexiandajisu A as 1*S*,2*S*,5*R*. This late-stage diversification of alkenyl stannane **164** introduced the carboxylic acid group at the C18 position and represents another example for the manifoldness of this synthetic strategy.
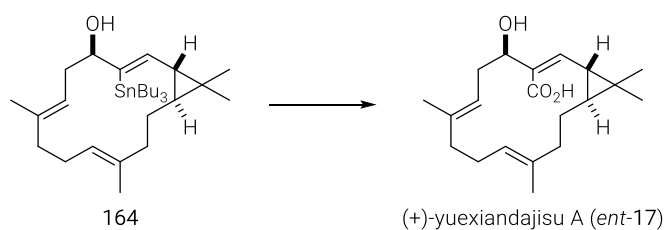
Scheme 53. Summary – total synthesis of (+)-yuexiandajisu A (*ent*-**17**).

3.12 TOTAL SYNTHESIS OF 2-*EPI*-DEPRESSIN

3.12.1 ISOLATION AND STRUCTURE ELUCIDATION

1-*epi*-Depressin

1-*epi*-Depressin (**165**) (Figure 33) was first isolated with eight other casbane analogues from the South China Sea soft coral *Sinularia depressa*, which was collected at a depth of 20 m in the Lingshui Bay, Hainan Province, China. Extraction on the natural materials (510 g) and chromatographic purification of the residue gave 1-*epi*-depressin (**165**) as a colourless oil (6.2 mg). The casbane framework was elucidated by 2D-NMR analysis.[6] The *trans* configuration of the cyclopropane was established by nOe experiments in combination with the ^{13}C NMR chemical shifts and were in accordance to the *trans*-fused yuexiandajisu A (**17**). The absolute configuration was determined by CD as 1*R*,2*R*.[6]
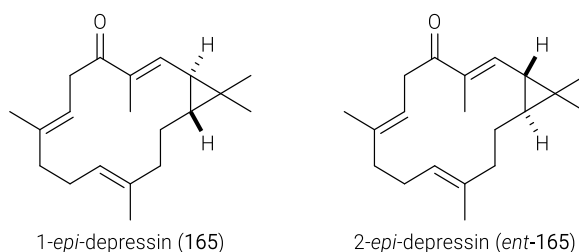
Figure 33. Structure of the natural product 1-*epi*-depressin (**165**) and its enantiomer 2-*epi*-depressin (*ent*-**165**).

3.12.2 SYNTHESIS

The 1*S*,2*S*,5*S*-macrocyclic alkyne **161**, which was used in the synthesis of 1*S*,2*S*,5*S*-**156** (Scheme 50), was employed to synthesise the enantiomer of the natural product 1-*epi*-depressin (**165**) by a convenient *trans*-hydrostannation/*C*-methylation sequence.[6]

1*S*,2*S*,5*S*-**161** was subjected to *trans*-hydrostannation and *C*-methylation. Each step was carried out as described in the total synthesis of *ent*-depressin (**89**) (see chapter 2.6.3), without the intermediate purification. After the *trans*-hydrostannation was completed, the solvent (CH$_2$Cl$_2$) was removed. The resulting crude stannane was dissolved in DMF and the *C*-methylation was conducted as described before (Scheme 54). Alcohol **166** was obtained in 67% yield over both steps. The following C5−OH oxidation with freshly prepared manganese oxide[186] gave 2-*epi*-depressin (*ent*-**165**) in 88% yield.
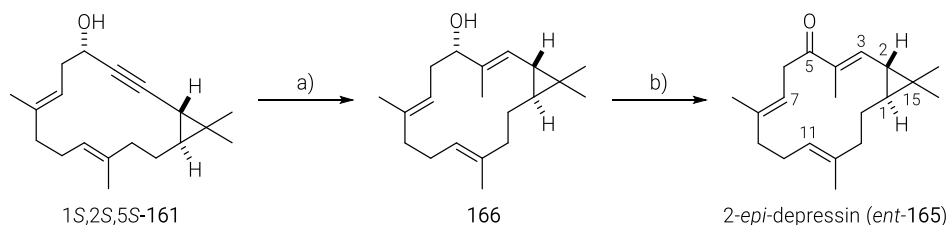
Scheme 54. Late-stage diversification − total synthesis of 2-*epi*-depressin (*ent*-**165**). Conditions: a) *i*) [Cp*RuCl]$_4$ (1.3 mol%), Bu$_3$SnH (1.05 equiv), CH$_2$Cl$_2$, RT; *ii*) [Ph$_2$PO$_2$][Bu$_4$N] (1.1 equiv), Pd(PPh$_3$)$_4$ (5 mol%), MeI (1.5 equiv), CuTC (1.05 equiv), DMF, RT, 67%; b) MnO$_2$ (10.0 equiv), CH$_2$Cl$_2$, 88%.

The NMR data of 2-*epi*-depressin (*ent*-**165**) were in good agreement with those reported for natural occurring 1-*epi*-depressin (**165**), whereas the sign of the specific rotation value was

dextrorotatory (2-*epi*-depressin (*ent*-**165**) $[\alpha]_D^{25}$ = −82.4); natural product 1-*epi*-depressin (**165**)[6] $[\alpha]_D^{25}$ = +34.0). The data analysis showed that 2-*epi*-depressin (*ent*-**165**) is highly likely the enantiomer of 1-*epi*-depressin (**165**)[6].
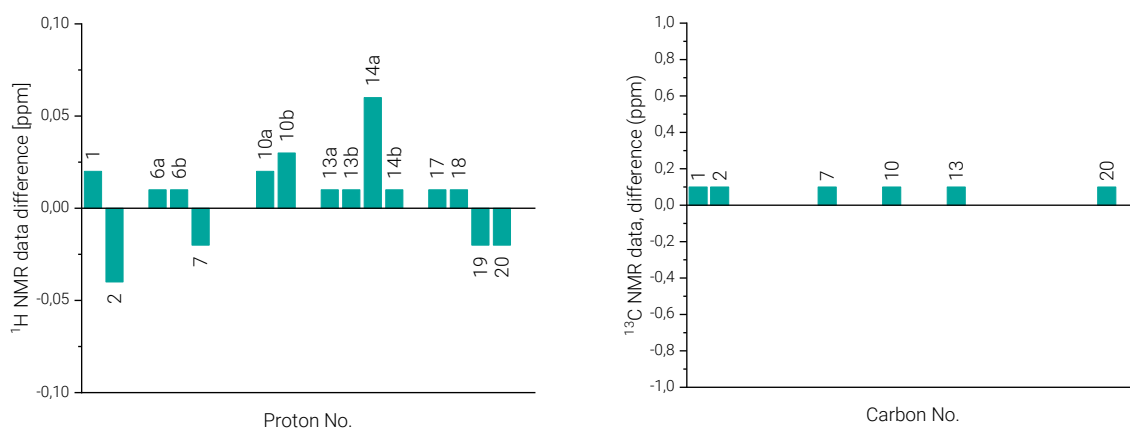
Figure 34. Differences in ¹H NMR and ¹³C NMR shifts between synthetic 2-*epi*-depressin (*ent*-**165**) and 1-*epi*-depressin (**165**), numbering see Scheme 54.

3.12.3 CONCLUSION

The enantiomer 2-*epi*-depressin (*ent*-**165**) of the naturally occurring 1-*epi*-depressin (**165**) was synthesised in 6% overall yield along 14 steps (LLS). Thereby, the proposed absolute configuration of 1-*epi*-depressin (**165**) was confirmed. The direct use of the crude *trans*-hydrostannation product for the *C*-methylation decreased the purification effort and increased the overall yield.
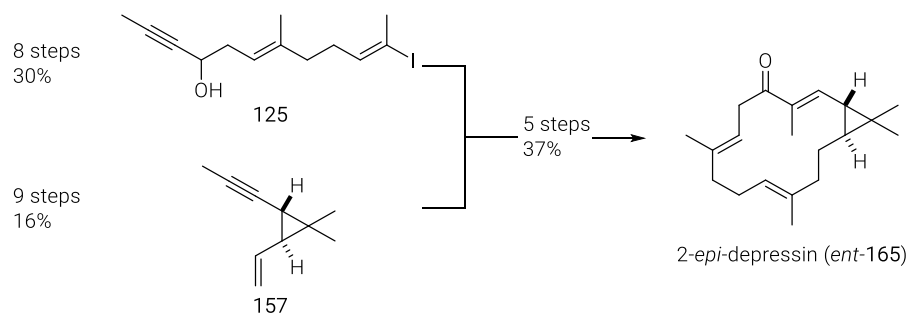
Scheme 55. Summary – total synthesis of 2-*epi*-depressin (*ent*-**165**).

4 STUDIES TOWARDS THE TOTAL SYNTHESIS OF 2-*EPI*-10-HYDROXYDEPRESSIN AND SINULARCASBANE C

4.1 INTRODUCTION

Expanding the strategy to the total synthesis of casbane diterpenes containing an additional hydroxy or ketone group at the C10 position would demonstrate the versatility of the blueprint. The functionalities at the C5 and C10 position exist as a hydroxy or ketone group in different combinations of the oxidation levels (Figure 35). This diversity is extended by combinations with the four possible permutations of the *gem*-dimethyl cyclopropane unit (Figure 35).
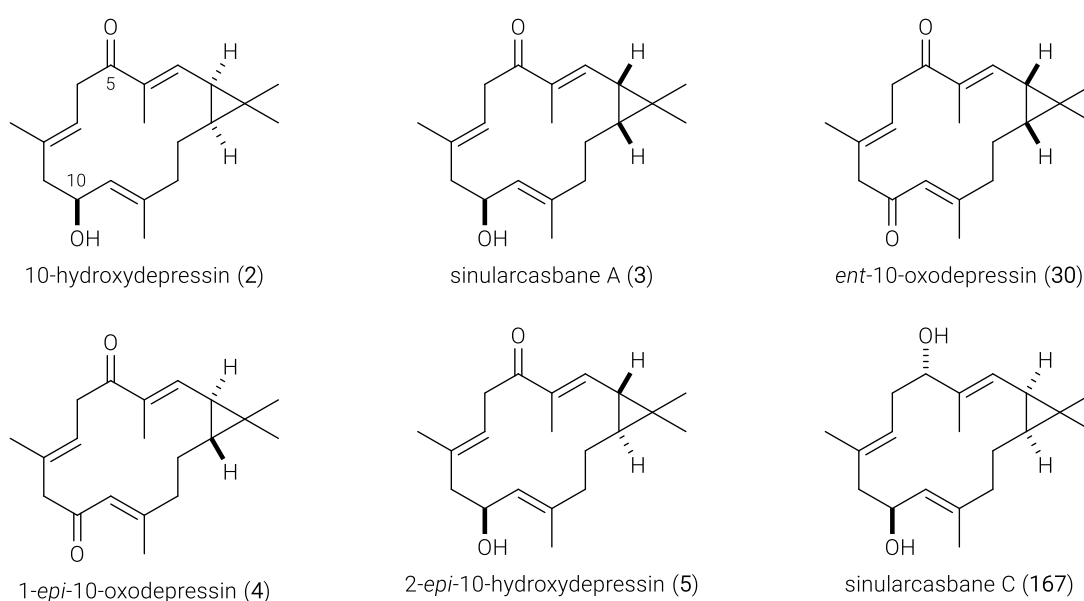
Figure 35. Selection of naturally occurring casbane diterpenes containing two oxygen-based functional groups; 10-hydroxydepressin (**2**)[6], sinularcasbane A (**3**)[7], *ent*-10-oxodepressin (**30**)[28], 1-*epi*-10-oxodepressin (**4**)[6], 2-*epi*-10-hydroxydepressin (**5**)[4], sinularcasbane C (**167**)[7].

4.2 ISOLATION AND STRUCTURE ELUCIDATION

2-*epi*-10-Hydroxydepressin

2-*epi*-10-Hydroxydepressin (**5**) (Figure 35) was first isolated from the South China Sea soft coral *Sinularia depressa*, which was collected at a depth of 20 m in the Lingshui Bay, Hainan Province, China.[4] Extraction of the natural materials (510 g) and chromatographic purification of the residue gave 2-*epi*-10-hydroxydepressin (**5**) as a colourless oil (1.9 mg). The casbane framework was elucidated by 2D-NMR analysis. The analysis of the ROESY and ^{13}C NMR data revealed the presence of a *trans*-configured cyclopropane unit.[4] The absolute configuration of the cyclopropane was determined as 1S,2R by CD. The configuration of the C10−OH centre could not be determined by distance dependent NMR experiments, since the macrocycle was too flexible. Comparison of the C10 ^{13}C NMR chemical shift of 2-*epi*-10-hydroxydepressin (**5**) (δ_C = 65.1 ppm) with that of sinularcasbane A (**3**) (δ_C = 66.2 ppm), showed high similarity. Based on biogenetic considerations in combination with the elucidated absolute configuration of the cyclopropane, the configuration at C10 was tentatively proposed as S.

Sinularcasbane A

Sinularcasbane A (**3**) (Figure 35) was first isolated from the South China Sea soft coral *Sinularia* sp., which was collected off the coast of Ximao Island, Hainan Province, China.[7] Extraction of the natural material (2.7 kg) and chromatographic purification of the residue gave sinularcasbane A (**3**) as a colourless oil (2.1 mg). The casbane framework was elucidated by 2D-NMR analysis, which revealed the same gross structure as 10-hydroxydepressin (**2**).[6,7] Comparison of their ^{13}C NMR data showed a significant distinction between the C20 signals. This suggested a diastereomeric relationship, whereas both natural products contained a *cis*-cyclopropane motif. The configuration at C10 was assigned by biogenetic considerations as *S*. Consequently, the configuration of the cyclopropane of sinularcasbane A (**3**) was assigned opposite to that of 10-hydroxydepressin (**2**).

4.3 RETROSYNTHETIC ANALYSIS

The late-stage diversification towards the desired casbane diterpene would be realised *via* a C5−OH directed *trans*-hydrostannation of macrocyclic alkyne **168**, *C*-methylation of the resulting alkenyl stannane, and in case of a ketone group at C5, oxidation of the hydroxy group. Finally, the *O*-silyl group (C10−OSiR₃) would be cleaved. RCAM of diyne **169**, which would be provided by a hydroboration and Suzuki cross coupling sequence of the cyclopropyl fragment **157** and the western fragment **170**, would form macrocyclic alkyne **168**. Regarding the western fragment **170**, iododesilylation of compound **171** would complete the fragment synthesis (Scheme 56).
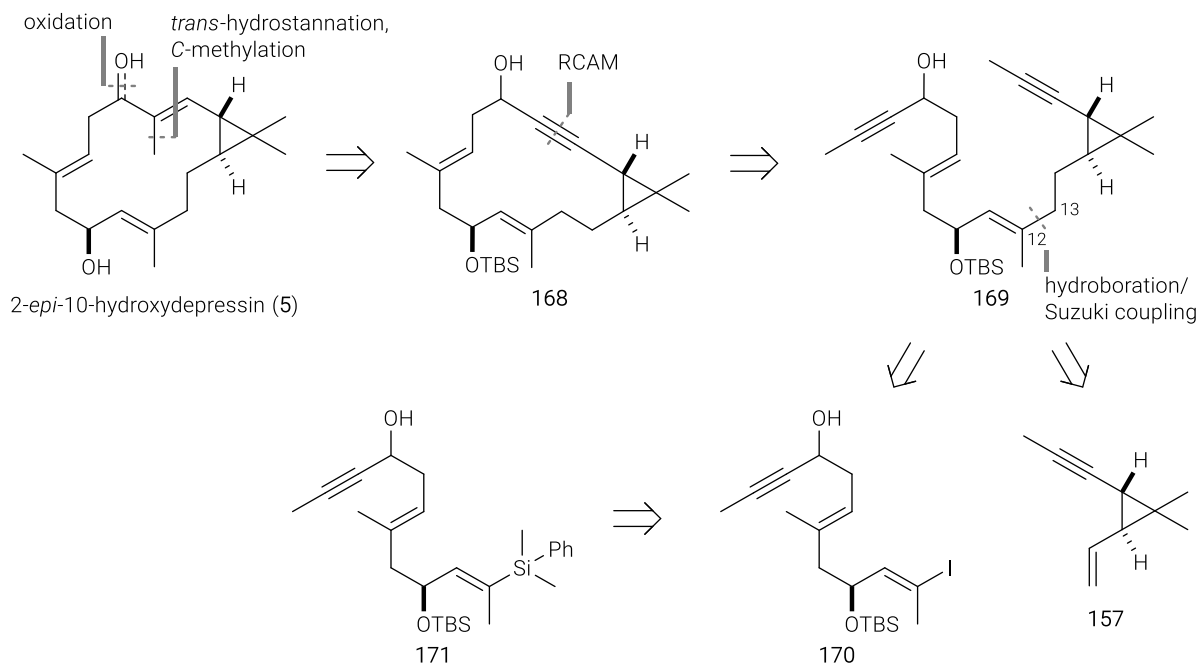
Scheme 56. Retrosynthetic analysis of casbane diterpenes containing functional groups at the C5 and C10 position.

The corresponding alkenyl silane **171** would be divided into alkenyl iodide **172** and boronic ester **173** by a disconnection between C8 and C9 (Scheme 57). The alkenyl silane group could be seen as a masked alkenyl halide and would enable the coupling of C8 and C9 under Suzuki cross coupling[230] or Zweifel olefination[231,232] conditions to occur without any reactivity at C12.

Alkenyl iodide **172** would be synthesised by Dess-Martin oxidation of the common alcohol **130**, Grignard addition to introduce the methyl-capped alkyne unit, trityl-protection of resulting alcohol, and stereoselective iododesilylation. Utilising the sterically demanding trityl group, instead of the TBDPS-group, would establish an orthogonal protecting group strategy, considering an *O*-silyl protection of the C10−OH group. The corresponding boronic ester **173** would be prepared via a stereoselective bisborylation of diene **174**, which was developed by Morken and co-workers[233,234] followed by a site-selective mono-oxidation of the secondary boronic ester group[235] and TBS-protection of the resulting C10−OH group. This sequence would enable the stereoselective introduction of the hydroxy group at C10 position and would provide the boronic ester functionality for the Suzuki cross coupling or Zweifel olefination of **172** and **173**. The corresponding diene **174** would be obtained after tosylation of compound **130** and subsequent elimination. The common alcohol would be prepared by regio- and stereoselective hydroboration of pentynol **64** (Scheme 57).
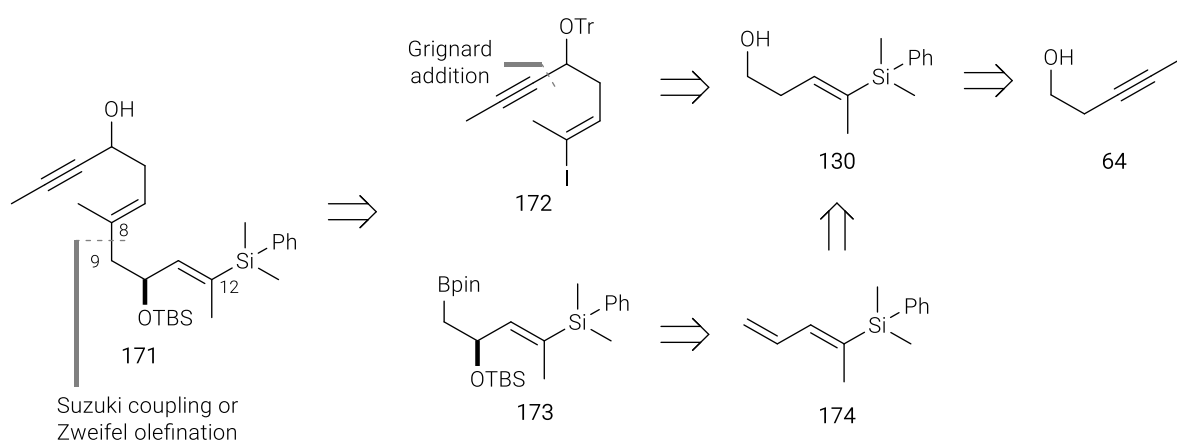
Scheme 57. Retrosynthetic analysis of the western fragment **172**.

The retrosynthetic analysis as well as the forward synthesis of cyclopropyl fragments **157** are discussed in the previous chapters.

4.4 STUDIES TOWARDS THE SYNTHESIS OF THE WESTERN FRAGMENT

The synthesis of bis(pinacolboronate) **175** commenced from the commercially available pentynol **64** by a regio- and stereoselective hydrosilylation.[154,155,192] The resulting alcohol **130** was tosylated in 90% yield (**176**) and subsequent treatment with *t*-BuOK gave *E*-diene **174** in 90% yield (Scheme 58). Subjecting diene **174** to the platinum catalysed bisborylation with the TADDOL ligand **177** provided bis boronic ester **175** in 86% yield with high optical purity (99% *ee*).[233]
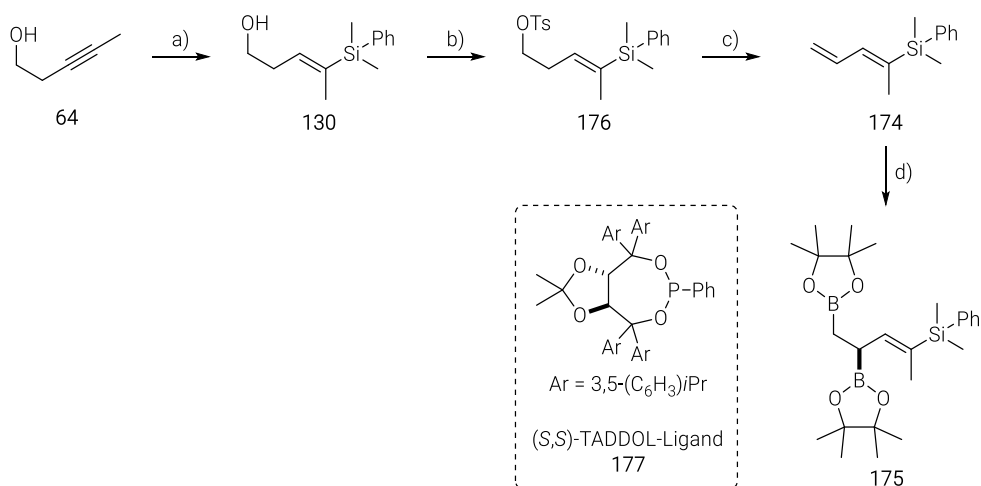
Scheme 58. Synthesis of 1,2-bis(pinacolboronate) **175**. Conditions: a) *i*) **64** (1.0 equiv), *n*-BuLi (1.0 equiv), THF, −78 °C to −30 °C to −78 °C, *ii*) (PhMe$_2$Si)$_2$Cu(CN)Li$_2$ (1.1 equiv), −78 °C, 90%; b) TsCl (1.5 equiv), DMAP (0.2 equiv), Et$_3$N (2.0 equiv), CH$_2$Cl$_2$, RT, 90%; c) *t*-BuOK (1.5 equiv), THF, RT, 80%; d) Pt(dba)$_3$ (3 mol%), (*S*,*S*)-TADDOL-Ligand **177** (4 mol%), B$_2$(pin)$_2$ (1.05 equiv), THF, reflux, 86%, 99% *ee*;

The secondary boronic ester group (**175**) was site-selectively mono-oxidised to the corresponding alcohol **178**. Initially, the best literature conditions were employed.[235] Two equivalents of *N*-methyl morpholine *N*-oxide (NMO) were added to a solution of compound **175** in *n*-butanol or DMSO and secondary alcohol **178** was obtained in only 9% and 28% yield, respectively. Using 10 equivalents of NMO in technical grade acetone reduced significantly the reaction time, which prevented decomposition during the reaction. These conditions led to 72% yield of secondary alcohol **178**. The product was *O*-silylated on treatment with TBSCl in DMF and the resulting boronic ester **173** was isolated in 86% (Scheme 59, left). The absolute configuration of boronic ester **173** was confirmed by the structure of **173** in the solid state (Scheme 59, right).
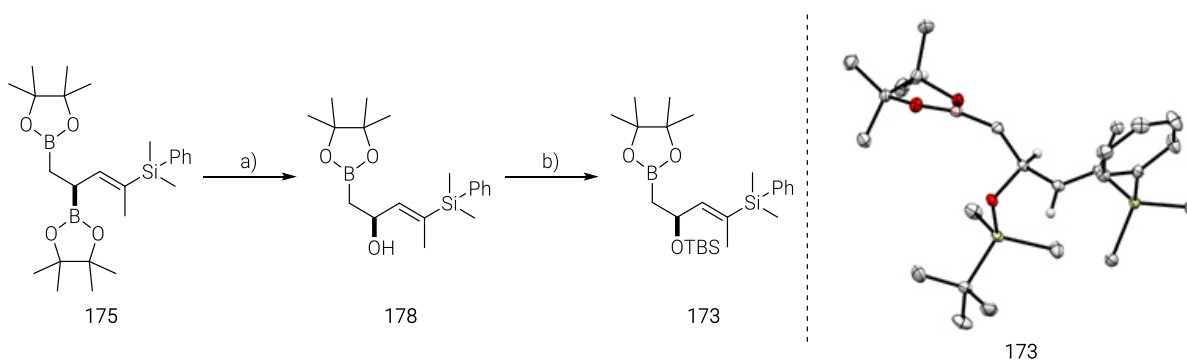
Scheme 59. Synthesis of boronic ester **174**. Conditions: a) NMO (10 equiv), acetone, RT, 72%; b) TBSCl (2.0 equiv), imidazole (1.5 equiv), DMF, 86%; Structure of boronic ester **174** in the solid state; H-atoms are omitted for clarity.

The protecting group strategy for the total synthesis of 2-*epi*-10-hydroxydepressin (**5**) compromised an orthogonal cleavage of protection groups of C5−OH and C10−OH. Therefore, the C5−OH was protected with a trityl group in 83% yield of **179** followed by stereoselective iododesilylation to afford alkenyl iodide **172** in 95% yield with no detected double bond isomerisation (*E:Z* ≥ 20:1, ^{1}H NMR) (Scheme 60).
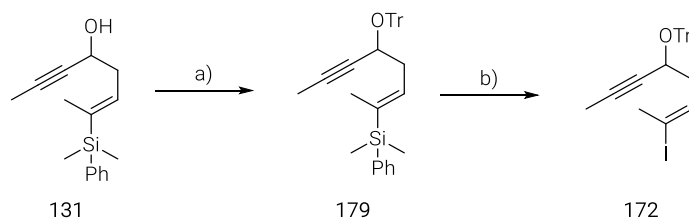
Scheme 60. Synthesis of alkenyl iodide **172**. Conditions: a) TrCl (1.2 equiv), DBU (1.4 equiv), CH$_2$Cl$_2$, RT, 83%; b) NIS (1.9 equiv), 2,6-lutidine (5.0 equiv), HFIP (38.0 equiv), CH$_2$Cl$_2$, −20 °C, 95% (*E*:*Z* ≥ 20:1).

The coupling of alkenyl iodide **172** with boronic ester **173** or **168** was first investigated under Suzuki cross coupling conditions, utilising various palladium catalysts and additives/bases.[161,230,244–246,236–243] Unfortunately, in all attempts, no cross coupling product could be detected. Alternatively, a stereodivergent Zweifel olefination of alkenyl iodide **172** and boronic ester **173** developed by Aggarwal and co-workers was employed.[231,232] The electrophilic selenation of an alkenyl boronate complex followed a *meta*-chloroperoxybenzoic acid (*m*CPBA) promoted *syn* elimination led to the formation of *E*-alkene **180** in 63% yield with a moderate stereoselectivity of approximately *E*:*Z* = 2:1.
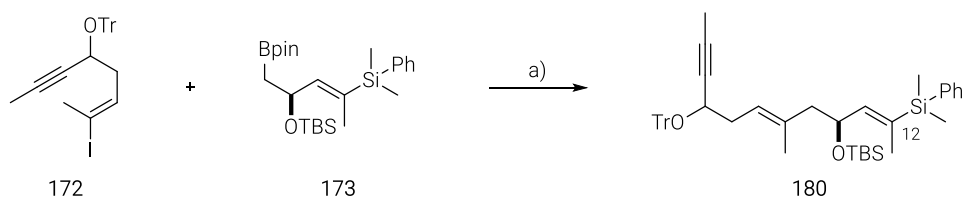
Scheme 61. Zweifel olefination, Conditions: a) *i*) **173** (2.0 equiv), *t*-BuLi (4.1 equiv), THF, −78 °C; *ii*) **174** (1.0 equiv), −78 °C; *iii*) PhSeCl (2.4 equiv) in THF/HFIP, −78 °C to RT; *iv*) *m*CPBA (4.0 equiv), THF, −78 °C to −45 °C, *v*) DMS (20 equiv), −45 °C, 63%.

The alkenyl iodide functionality at C12, required for the Suzuki cross coupling of the western fragment **170** and the cyclopropyl fragment **157**, was envisioned to be installed by a stereoselective iododesilylation after cleavage of the trityl protection group. Therefore, the Zweifel olefination product **180** was treated with lithium chloride in *n*-butanol at 120 °C, which provided propargylic alcohol **181** in 78% yield.[247] The following HFIP mediated iododesilylation was carried out according to the previously developed acidic conditions on treatment with NIS. Unfortunately, this attempt led to decomposition. Therefore, the iododesilylation step was envisaged to be performed prior to the cleavage of the trityl group. Another approach would be the substitution of the corresponding dimethyl phenyl silane group with a trimethyl silane group. In the future, these strategies should be investigated towards the synthesis of the western fragment **170**.
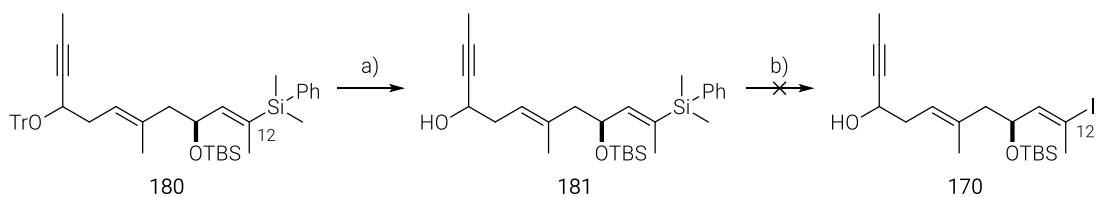
Scheme 62. Synthesis towards the western fragment **170**. Conditions: a) LiCl (10.0 equiv), *n*-BuOH, 120 °C, b) NIS (1.1 equiv), AcOH (10.0 equiv), HFIP, 0 °C, decomposition.

Regarding the total synthesis of sinularcasbane C (**167**), a stereoselective introduction of the C5 stereocentre was required. This additional diversity is feasible by oxidation of propargylic alcohol **131** and subsequent stereoselective Noyori hydrogenation.[248–250]

Dess-Martin oxidation of propargylic alcohol **131** gave ketone **182** in 66% yield. Enantioselective hydrogenation with *S,S*-Noyori catalyst **183** in *iso*-propanol led to the formation of (*S*)-propargylic alcohol **184** in 42% yield with a stereoselectivity of 94% *ee* (Scheme 63). The configuration at C5 was confirmed by Mosher ester analysis. CBS reduction and Midland Alpine borane reduction did not result in any observable reaction. The enantioselective hydrogenation investigations were conducted in collaboration with Philipp Schlathölter.
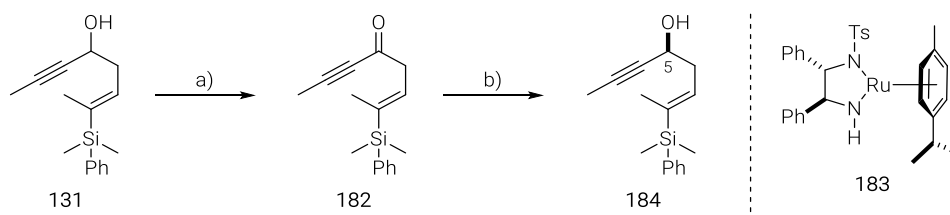
Scheme 63. Synthesis of chiral propargylic alcohol **184**. Conditions: a) DMP (2.0 equiv), CH$_2$Cl$_2$, RT, 66%; b) *S,S*-Noyori catalyst **183** (10 mol%), *i*PrOH, RT, 42% (94% *ee*).

B.2 [RH₂(5S-MEPY)₄] AND [BIRH(5S-MEPY)₄]: CONVENIENT SYNTHESIS AND COMPUTATIONAL ANALYSIS

Remark: The investigations of [Rh₂(MEPY)₄] complexes were initiated by the postdoctoral researcher Dr. Lee R. Collins. This chapter also includes independent research results of Michael Buchsteiner and Dr. Lee R. Collins.

1 INTRODUCTION

In 1990, Doyle and co-workers presented [Rh₂(5S-MEPY)₄] (**79**) as a novel rhodium-rhodium carboxamidate catalyst for enantioselective cyclopropanation of diazoacetate compounds and styrene.[140] One year later, **79** and its enantiomer were employed in an intramolecular cyclopropanation of diazoester **70** resulting in *gem*-dimethyl cyclopropanes **67** and **80** in 83-89% yield with an enantioselectivity of 98% *ee* (Scheme 65, left).[69,137,138,143] Nucleophilic attack of the diazoalkane compound onto the metal centre via alkyl transition state **S**, followed by nitrogen gas release forms a metal carbene **T**. Next, the electron rich alkene abstracts the carbene in a concerted fashion to give the cyclopropane motif (Scheme 64, right). Additional computational studies clarified the enantioselectivity of the intramolecular cyclopropanation with [Rh₂(5S-MEPY)₄] (**79**).[137,251]
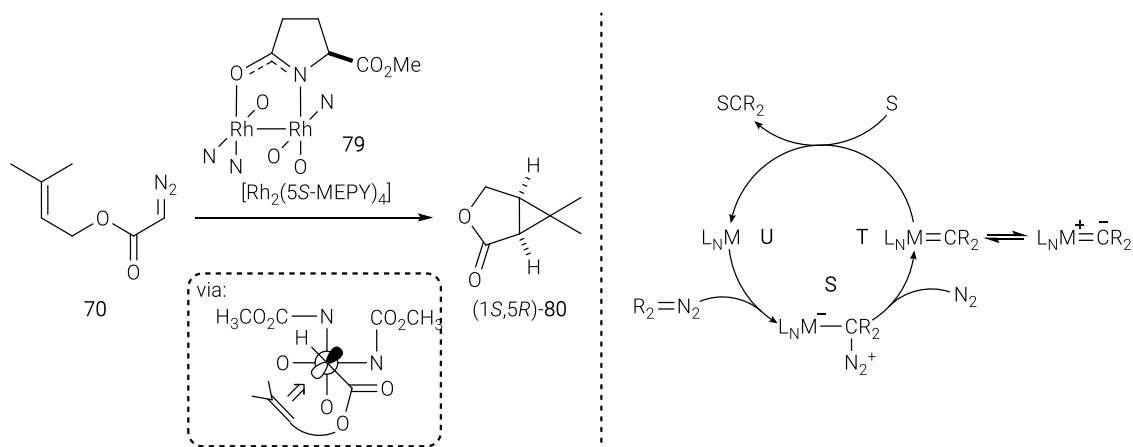
Scheme 64. Dirhodium catalysis, S: substrate.

To date, the [Rh₂(MEPY)₄] complexes are a widely applied as catalysts for cyclopropanations (**80**, **185**, **186**),[69,137,143] cyclopropenations (**187**),[252] hetero-Diels-Alder reactions,[253] and intramolecular C−H insertion reactions (**188**-**190**) (Scheme 65).[254−256]
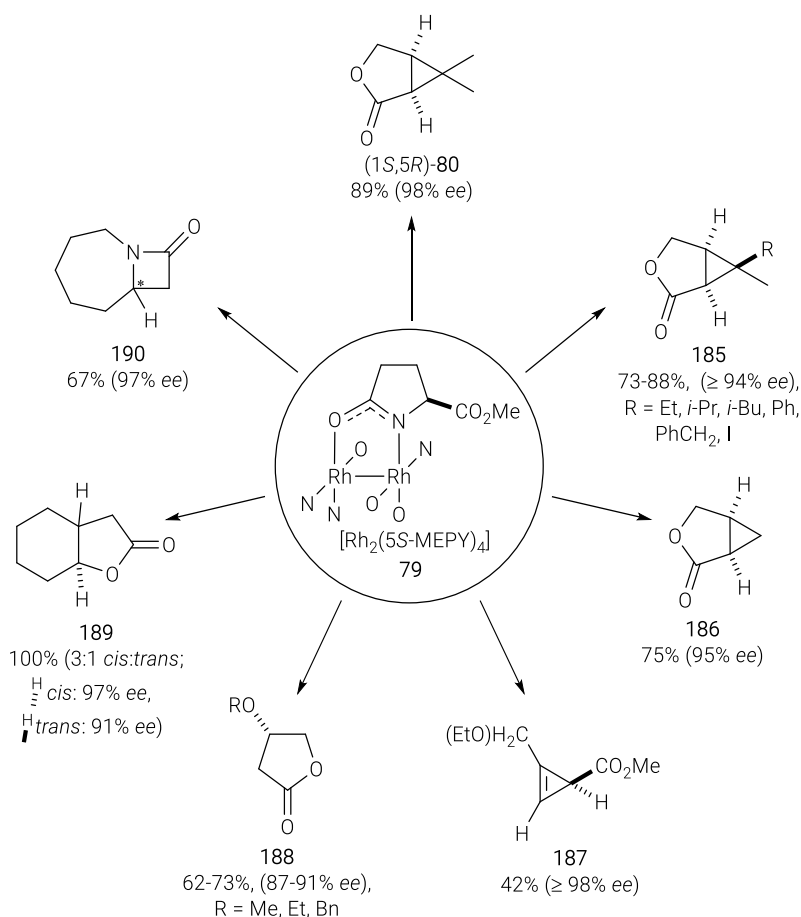
Scheme 65. Applications of Doyle [Rh$_2$(5S-MEPY)$_4$] catalyst (**79**) in enantioselective synthesis.

1.1 SYNTHESIS OF [Rh$_2$(5S-MEPY)$_4$] CATALYST

During the collective total synthesis of casbane diterpenes, the [Rh$_2$(5S-MEPY)$_4$] catalyst **79** was required in certain amounts to provide sufficient amounts of lactone **80**. The known preparation protocol of Doyle and co-workers included purification by reverse phase chromatography (J.T. Baker BAKERBOND Cyano 40 μm prep LC packing, MeOH/MeCN) to separate the desired complex from the remaining methyl pyroglutamate ligand (**191**, MEPY-H). Their procedure led to 58% yield of the desired complex.[137,138]

In a different project, Dr. Lee R. Collins optimised the reaction conditions and developed a convenient work-up procedure in our group. His protocol was optimised in terms of reliability and user-friendliness (Scheme 66):
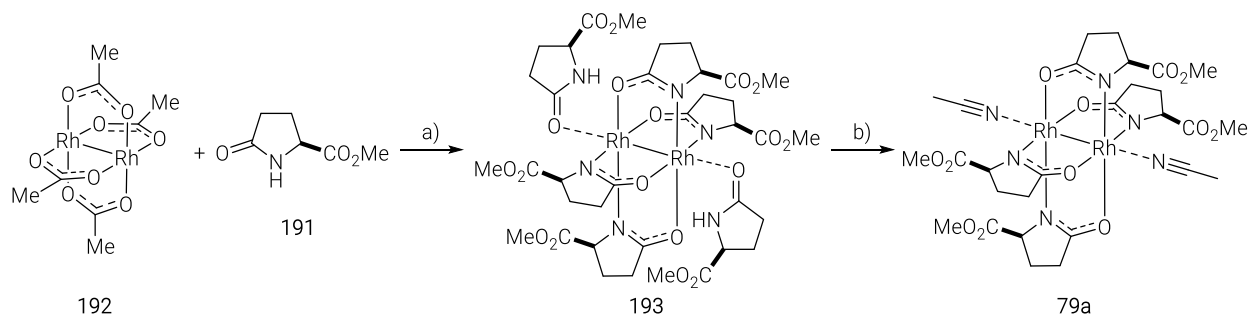
Scheme 66. Convenient synthesis of [Rh$_2$(5S-MEPY)$_4$]·2MeCN complex (**79a**) by a simple purification method. Conditions: a) **192** (1.0 equiv), **191** (6.7 equiv), C$_6$H$_5$Cl, reflux, side-armed frit (K$_2$CO$_3$); b) Simple purification procedure: *i*) dissolve in MeCN, *ii*) adsorb on SiO$_2$, *iii*) rinse with MeCN, *iv*) elute with MeOH, *v*) evaporate and dry in vacuum at 100 °C, *vi*) dry MeCN/evaporation, 81%.

[Rh$_2$(5S-MEPY)$_4$]·2MeCN complex (**79a**) was prepared from commercially available [Rh$_2$(OAc)$_4$] (**192**) by treatment with excess methyl pyroglutamate (**191**, 6.7 equiv, MEPY-H) in refluxing HPLC-grade chlorobenzene for 13 hours (Scheme 66).

To prevent formation of rhodium oxide side-products, the chlorobenzene was degassed by bubbling argon for 20 min, whereas drying of the solvent was not necessary as water is most likely already coordinated to [Rh$_2$(OAc)$_4$] (**192**). The addition of the [Rh$_2$(OAc)$_4$] complex to chlorobenzene coloured the solution deep green. Refluxing overnight turned the solution into a dark red colour. During the reaction, the liberated HOAc coevaporated with chlorobenzene and was removed from the equilibrium by passing the condensed vapour through a side-armed frit filled with K$_2$CO$_3$.[138,257] When the ligand exchange was completed, the mixture was allowed to cool to room temperature and the volatile components were removed under high vacuum. The major product of the resulting blue/violet residue was investigated by Dr. Lee R. Collins. An analytically pure sample of [Rh$_2$(5S-MEPY)$_4$]·2(5S-MEPY-H) **193** was obtained by sublimation (Scheme 66). This complex explained the need of 6.7 equivalents of the MEPY-H ligand to complete the ligand exchange.

The axially bound MEPY-H ligands were substituted with acetonitrile by following steps. Addition of acetonitrile to the blue/violet crude product, causing a colour change to a red solution. Absorption of the dirhodium complex on silica gel decolourised the solution and turned the white silica gel into a red solid. The liberated excess MEPY-H ligand, which were formerly axially bound, was removed by rinsing with acetonitrile. The dirhodium complex was desorbed by washing the reddish silica gel with methanol. The resulting methanol solution, which contained the [Rh$_2$(MEPY)$_4$] complex, was concentrated. This purification protocol was repeated three times, before the solid residue was dried in high vacuum at 100 °C to afford the dirhodium complex, free of any axial ligands, as a turquoise powder. For storage purpose, the turquoise powder was triturated with dry acetonitrile under argon. The red solution was concentrated under high vacuum to give the [Rh$_2$(5S-MEPY)$_4$]·2MeCN complex (**79a**) in 81% yield (Scheme 66, more details and pictures in the Experimental Part).

Gratifyingly, Dr. L. R. Collins obtained a single crystal of the [Rh$_2$(5S-MEPY)$_4$]·2MeCN complex (**79a**) suitable for X-ray diffraction (Figure 36, left).
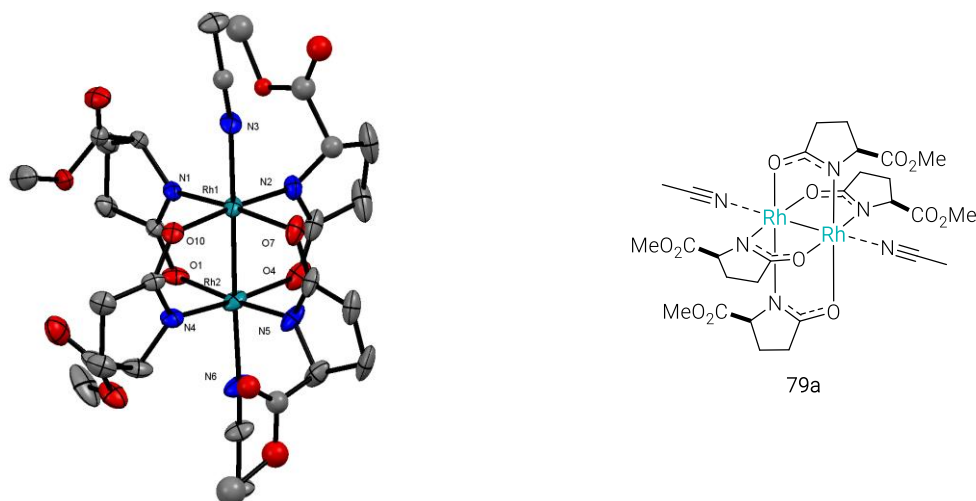
Figure 36. Structure of [Rh$_2$(5S-MEPY)$_4$]·2MeCN (**79a**) in the solid state; H-atoms are omitted for clarity.[ii]

In our hands, these dirhodium carboxamidate catalysts (**78** & **79**) performed the cyclopropanation of diazoester **70** with excellent results in the total synthesis of casbane diterpenes (Scheme 13).
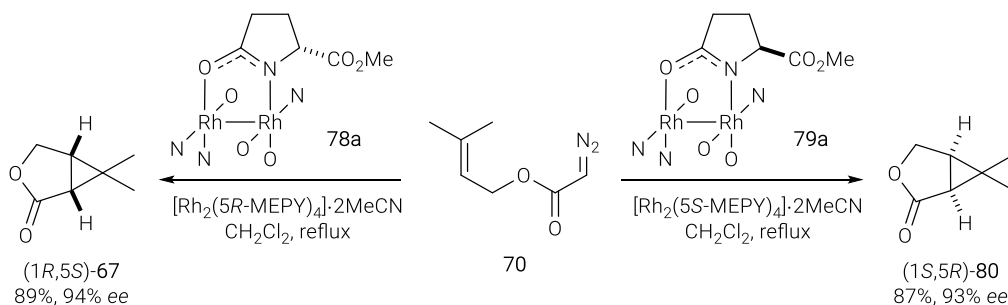
Scheme 67. Enantioselective cyclopropanation of diazoester **70** with [Rh$_2$(5S-MEPY)$_4$] and [Rh$_2$(5R-MEPY)$_4$] catalysts prepared without reverse phase chromatography.[38]

Due to the excellent reactivity profile of the [Rh$_2$(5S-MEPY)$_4$] complex (**79**) and of certain bismuth-rhodium carboxylate paddlewheel complexes,[258–260] the group's attention was driven to the unknown heterobimetallic derivative [BiRh(5S-MEPY)$_4$] complex (**194**). It was expected to show an even better reactivity profile as in the case of the [BiRh(S-PTTL)$_4$] catalyst, which gave a higher enantioselectivity in an intermolecular cyclopropanation of methyl 2-diazo-2-(4-methoxypheny)acetate and styrene compared to its dirhodium analog.[259] Furthermore, it would shine light on these rarely discussed bismuth-rhodium carboxamidate complexes. Therefore, Michael Buchsteiner synthesised the [BiRh(5S-MEPY)$_4$] complex (**194**) by an improved procedure, which was based on previous literature reports of Dikarev and co-workers and Collins *et al.*[257,259,261–264] The commercially available [Rh$_2$(TFA)$_4$]·2MeCN was converted into the heterobimetallic analogue [BiRh(TFA)$_4$] in 82% yield. Then, the trifluoroacetate ligands were replaced by acetate ligands in refluxing toluene, affording [BiRh(OAc)$_4$] complex in 94% yield. Substitution of the acetate ligands with carboxamidate ligands gave the desired [BiRh(5S-MEPY)] complex (**194**) in 51% yield.[257] The detour over the [BiRh(OAc)$_4$] complex was necessary,

---

[ii] [Rh$_2$(5S-MEPY)$_4$]·2MeCN: H-atoms and disorder of two of the −CO$_2$Me groups are omitted for clarity. Single crystals for X-ray diffraction were obtained by Dr. L. R. Collins.[257]

since the direct replacement of the trifluoroacetate ligands with the carboxamidate ligands could not be achieved. This could be attributed to the mismatching pKa values of trifluoroaceatete and methyl pyrogluatamate (**191**, MEPY-H). In addition, M. Buchsteiner was able to obtain a single crystal suitable for X-ray diffraction analysis of the [BiRh(5*S*-MEPY)$_4$]·MeCN complex (**194a**) (Figure 37).
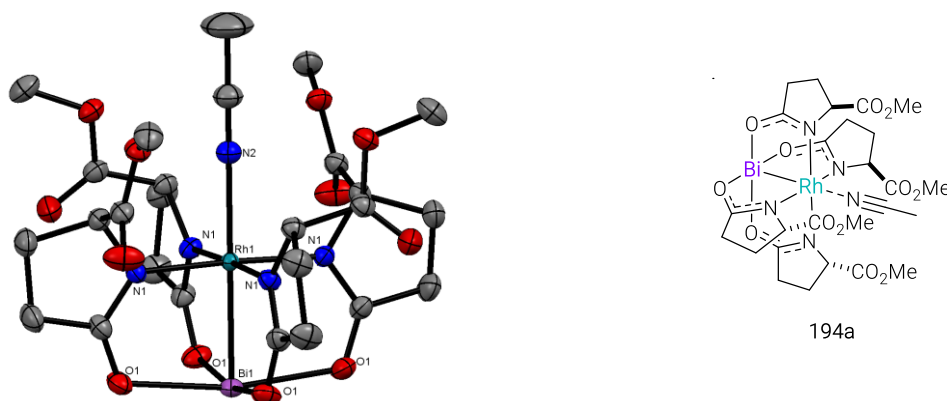
Figure 37. Structure of the [BiRh(5*S*-MEPY)$_4$]·MeCN complex (**194a**) in the solid state; H-atoms are omitted for clarity.[iii]

The X-ray structures of both carboxamidate paddlewheel complexes (**79a** & **194a**) showed significantly different geometries. The dirhodium complex (**79a**) formed in a C$_2$-symmetric arrangement with two equivalent rhodium centres, bearing a mixed coordination sphere of two *cis*-configured *N*- and two *O*-donor atoms at each centre (Figure 36). In contrast, the bismuth-rhodium complex (**194a**) showed a C$_4$-symmetric geometry. This binding motif, where all four oxygen atoms coordinated to the bismuth atom, was attributed to the higher oxophilicity of bismuth compared to rhodium. Hence, the rhodium atom was coordinated by four nitrogen atoms, forming a very tight binding environment (Figure 37). This ligand orientation might have extreme impact on the reactivity profiles. Surprisingly, the [BiRh(5*S*-MEPY)$_4$] complex (**194**) did not show any reactivity towards the intermolecular cyclopropanation of methyl 2-diazo-2-(4-methoxypheny)acetate and styrene, nor towards the intramolecular cyclopropanation of diazoester **70** to the corresponding lactone **80**.

1.2 THEORETICAL INVESTIGATIONS

This striking difference initiated the computational studies to gain a deeper understanding. While dirhodium and bismuth-rhodium carboxylate paddlewheel complexes received attention of the research community in terms of mechanistic studies,[258,265–267] such research reports in the field of bismuth-rhodium carboxamidate complexes, to the best of my knowledge, are rare.[137,268]

Therefore, quantum chemical investigations based on density functional theory (DFT) were conducted, according to previous computational investigations into [RhRh] and [BiRh] carboxylate complexes in our group.[264] The PB86[269] functional and the valence triple-ζ basis set of the Karlsruhe group[270] together with the scalar relativistic zeroth-order regular approximation

---

[iii] Structure of the [BiRh(5*S*-MEPY)$_4$]·MeCN complex (**195a**) in the solid state: One of the independent molecules of in the unit cell is displayed; differing only in minor conformational details from each other; H-atoms are omitted for clarity. Single crystals for X-ray diffraction were obtained by M. Buchsteiner.[257]

(ZORA Hamiltonian)[271,272] were utilised and showed a good balance between accuracy and performance.

The structures obtained by single crystal X-ray analysis (**79a** & **194a**) were geometrically optimised at the DFT level of theory by using the generalised gradient approximation (GGA) functional PB86[269] and the ZORA-def2-TZVP basis set,[270] as implemented in the ORCA 4.2 program package.[222,223] The calculations made use of the D3-dispersion correction of Grimme including Becke–Johnson damping (D3(BJ))[273,274] together with the scalar relativistic zeroth-order regular approximation (ZORA Hamiltonian).[271,272] The resolution of identity approximation (RI) was applied with the corresponding SARC/J auxiliary basis set[275,276] to speed up the calculation of the two-electron integrals.[277–279] The calculations included the implicit solvent effects by employing the conductor–like polarizable continuum model (CPCM) using CH_2Cl_2 as solvent (Figure 38).[280–283] This level of theory is noted as ZORA-BP86-D3BJ-(CPCM)/def2-TZVP. The geometrically optimised structures, using an implicit solvent model, were in good agreement with the solved X-ray structures, concerning bond length and conformational details. This also demonstrated the good performance of the ZORA-BP86-D3BJ-(CPCM)/def2-TZVP level of theory for these complexes.

DFT-optimised structure of [RhRh(5S-MEPY)₄]·2MeCN (79a)	DFT-optimised structure of [BiRh(5S-MEPY)₄]·MeCN (194a)
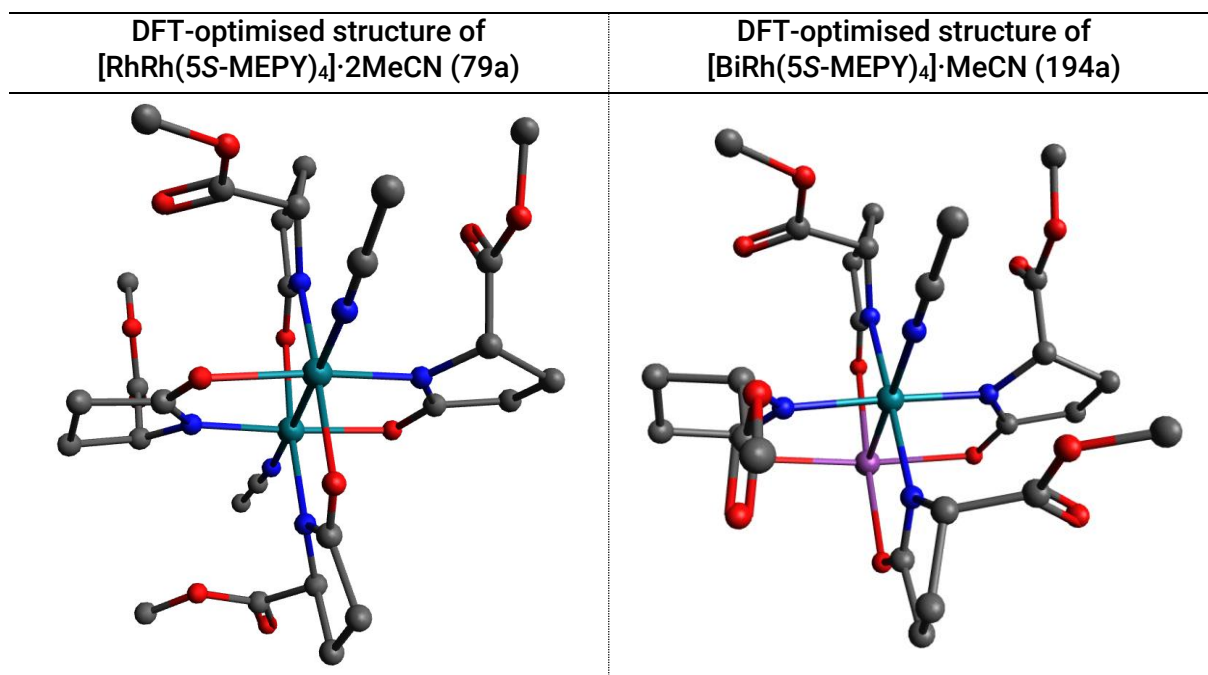
Figure 38. DFT-optimised structures of [RhRh(5*S*-MEPY)₄]·2MeCN (**79a**) and [BiRh(5*S*-MEPY)₄]·MeCN (**194a**).

The axial bound acetonitrile ligands were removed for the electronic structure analysis, since these are unequally distributed at both complexes and thus would influence the electronic structure of each complex differently. Furthermore, these ligands would block the active sites at the rhodium. First, the "bare" structures were optimised in the gas phase using the same level of theory as before (ZORA-BP86-D3BJ-(CPCM)/def2-TZVP). These attempts showed axial coordination between the rhodium and one bridging oxygen atom of the ester groups, which influenced the electronic structure dissimilarly. Applying the conductor–like polarizable continuum model (CPCM) using CH_2Cl_2 as solvent for the geometry optimisation of both complexes ([RhRh(MEPY)₄] (**79**) and [BiRh(MEPY)₄] (**194**)) released these coordination. The visualisation of their molecular orbitals and the corresponding energies showed the strikingly different nature of their electronic structures. In both cases the LUMOs were metal-centred, but

in case of the heterobimetallic analogue the LUMO was significantly higher in energy (−2.55 eV (**79**) versus −3.71 eV (**194**)). This would make the nucleophilic attack of the diazo compound onto the catalyst unfavourable. The HOMO also showed significant differences: in the case of the dirhodium complex (**79**), it was equally populated at both metal centres, whereas in the case of the bismuth-rhodium complex (**194**) it was mainly centred at the rhodium metal. Moreover, the HOMO of the heterobimetallic complex (**194**) lay energetically lower (−4.65 eV (**194**) versus −4.21 eV (**79**)), although the rhodium was coordinated to four nitrogen atoms, which were assumed as stronger donors of the MEPY ligand. Furthermore, the visualised HOMO of the heterobimetallic complex were missing an interaction between the 4d orbital of the rhodium and the 6p orbitals of the bismuth, which could not be compensated by the donor ligands. Consequently, the back-donation from the filled rhodium HOMO to the diazo compound would be weakened, which would disfavour the extrusion of dinitrogen and thereby the carbene formation.
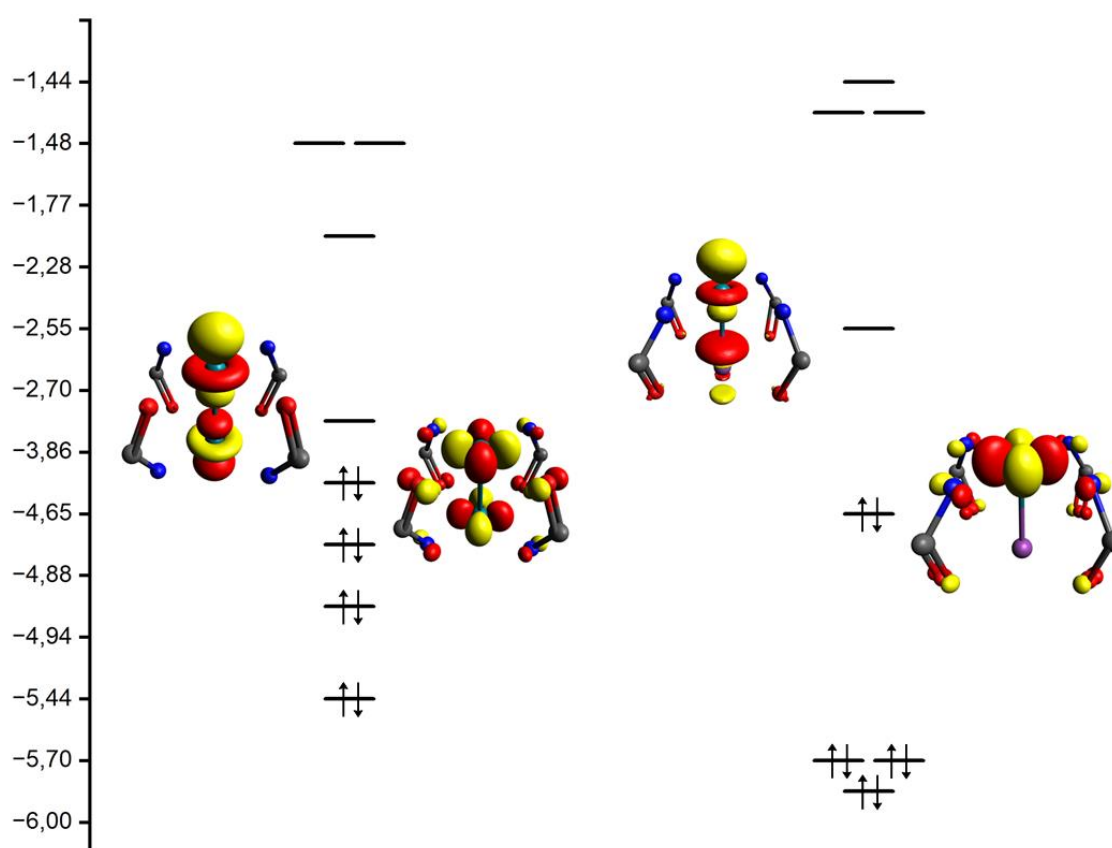
Figure 39. Molecular orbital scheme for „bare" [Rh_2(5*S*-MEPY)$_4$] (**79**, left) and [BiRh(5*S*-MEPY)$_4$] (**194**, right); the structures were truncated for sake of clarity; energy in eV (further illustrations and details in the Experimental Section)

In addition to these unfavourable electronic features, the considerably narrower environment at the active rhodium metal centre (**194**) might additionally hinder the axial binding and formation of a carbene. In case of the C_2-symmetric [Rh_2(5*S*-MEPY)$_4$] complex (**79**), this steric hindrance is absent.

85

1.3 CONCLUSION

The convenient synthesis of the [Rh$_2$(5S-MEPY)$_4$] complex (**79**) provided sufficient catalyst for the collective total synthesis of casbane diterpenes. While the dirhodium carboxamidate and carboxylate complexes as well as bismuth-rhodium carboxylate complexes have great reactivity profiles, the bismuth-rhodium carboxamidate derivative [BiRh(MEPY)$_4$] **194** proved to be unreactive towards diazo decompositions. Computational studies of the electronic structure of the dissimilar analogues [Rh$_2$(5S-MEPY)$_4$] and [BiRh(5S-MEPY)$_4$], revealed significant deviations in the energetic distribution of the molecular orbitals, combined with game-changing structural differences.

C SUMMARY

1 COLLECTIVE TOTAL SYNTHESIS OF CASBANE DITERPENES: ONE STRATEGY – MULTIPLE TARGETS

The family of casbane natural products belongs to a group of diterpenes, which is characterised by an unsaturated 14-membered macrocycle with a fused *gem*-dimethyl cyclopropane and is rarely found in nature. Some casbane diterpene-producing plants are used in traditional Chinese medicine.

The aim of this PhD project was to develop one synthetic strategy to access a series of casbane diterpenes. This strategy, based on adaptably designed building blocks, resulted in the total synthesis of three naturally occurring casbane diterpenes (depressin (**9**), euphorhylonal A (**155**), & yuexiandajisu A (**17**), Figure 40). Thereby, the configuration of euphorhylonal A was clarified in combination with computational chemistry.

depressin (**9**) euphorhylonal A (**155**) (+)-yuexiandajisu A (*ent*-17)
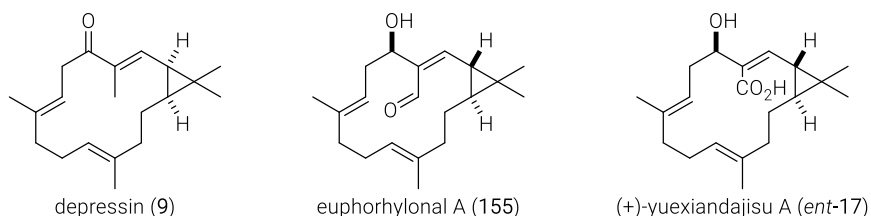
Figure 40. Structure of depressin (**9**), euphorhylonal A (**155**), and yuexiandajisu A (*ent*-**17**).

The total synthesis comprised an enantioselective dirhodium catalysed *gem*-dimethyl cyclopropanation, with or without subsequent equilibration, a sp²-sp³ Negishi cross coupling, a chemoselective hydroboration in combination with a Suzuki cross coupling, a ring-closing alkyne metathesis, a *trans*-hydrostannation, and a late-stage diversification of the scaffold.
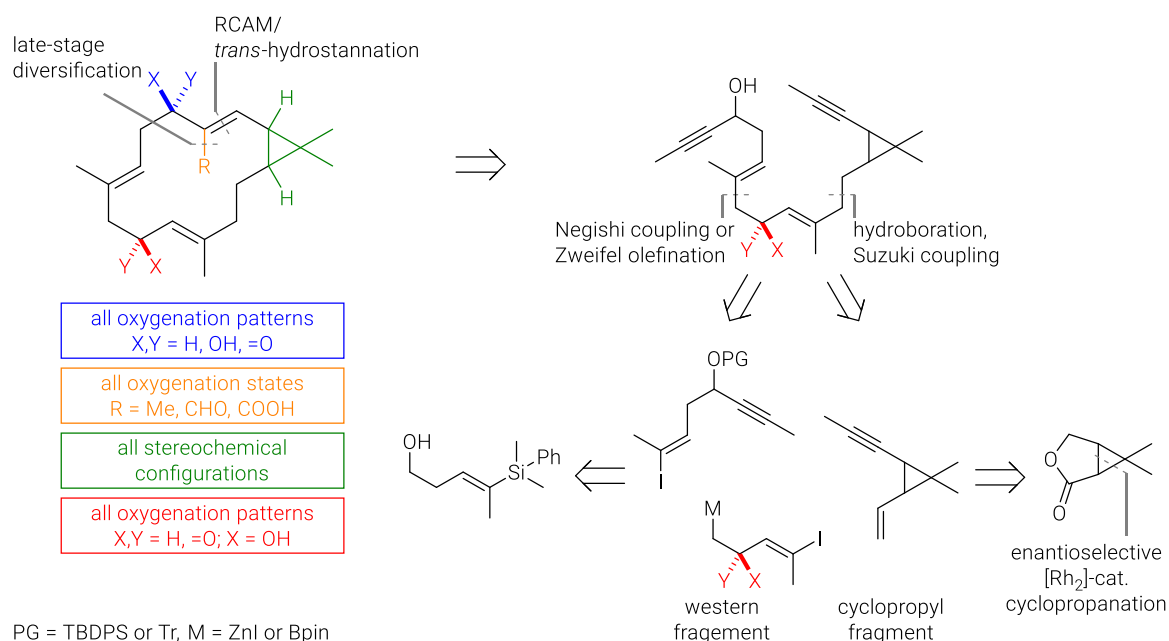
Scheme 68. General retrosynthetic analysis of casbane diterpene natural products.

The synthesis of the western fragment **125** commenced with a regio- and stereoselective hydrosilylation of pentynol **64** to afford alkenyl silane **130**, which is used twice (Scheme 69). This convenience reduced the step count and the practical effort as well as improved the atom economy. Oxidation of alcohol **130** to the corresponding aldehyde, followed by addition of propynyl Grignard reagent and *O*-silylation of the resulting propargylic alcohol provided compound **140**. No efforts towards an asymmetric alkynylation were undertaken, since in the case of depressin (**9**) the corresponding alcohol was oxidised. In addition, the configuration of the corresponding C5–OH group of euphorhylonal A (**17**) has not been assigned in the literature. Therefore, access to both isomer was required anyway. The subsequent iododesilylation under optimised conditions generated alkenyl iodide **128**, which was used in the sp^2-sp^3 Negishi cross coupling with organozinc reagent **129**. Its preparation from the alkenyl silane **130** was achieved by an Appel iodination and *in situ* zinc insertion. The *O*-silyl deprotection of the Negishi cross coupling product **142** enabled the second stereoselective iododesilylation with NIS under acidic conditions in pure HFIP and provided the western fragment **125** with no detected double bond isomerisation. This novel iododesilylation modification prevented an intramolecular iodoetherification from occurring. Overall, the western fragment **125** was prepared in 30% yield comprising eight steps along the LLS (Scheme 69).
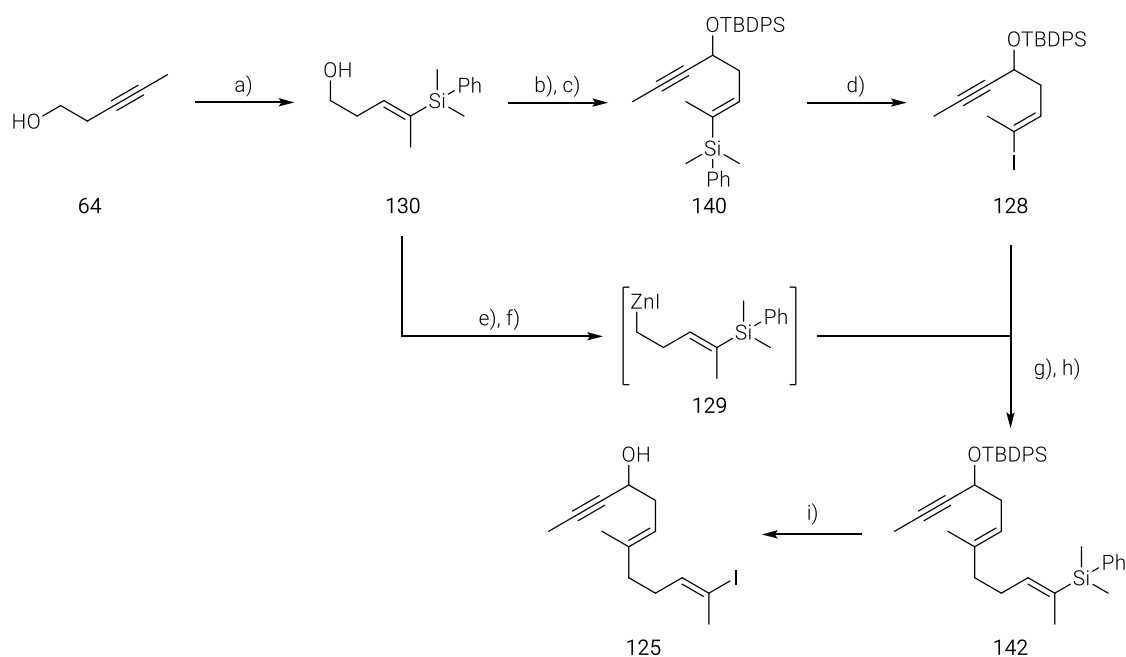
Scheme 69. Synthesis of the western fragment **125**. Conditions: a) *i*) **64**, *n*-BuLi, THF, −78 to −30 to −78 °C; *ii*) (PhMe$_2$Si)$_2$Cu(CN)Li$_2$, −78 °C, 90%; b) *i*) DMP, CH$_2$Cl$_2$, 0 °C to RT; *ii*) Propynyl MgBr, THF, 0 °C, 78% over 2 steps; c) TBDPSCl, DMF, CH$_2$Cl$_2$, RT, 84% d) NIS, 2,6-lutidine, HFIP, CH$_2$Cl$_2$, −20 °C, 89% (*E:Z* ≥ 20:1, ^{1}H NMR); e) I$_2$, PPh$_3$, imidazole, CH$_2$Cl$_2$, 0 °C to RT, 93%; f) *i*) Zn, LiCl, I$_2$C$_2$H$_4$, TMSCl, THF, 65 °C/RT; *ii*) **141**, THF, RT; g) Pd(PPh$_3$)$_4$, THF, RT, 82% (*E:Z* ≥ 20:1, ^{1}H NMR); h) TBAF, THF, 0 °C to RT, 84%; i) NIS, AcOH, HFIP, 0 °C, 82% (*E:Z* ≥ 20:1, ^{1}H NMR).

The cyclopropyl fragment's synthesis (**124**) was initiated by preparing diazoester **70** according to a literature procedure from prenyl alcohol and diketene followed by Regitz diazo transfer. Subsequent treatment with the [Rh$_2$(5*S*-MEPY)$_4$] catalyst (**79**) led to the formation of lactone **80** with high optical purity (Scheme 70). The subsequent reduction at low temperature gave crude lactol **133**, which was directly subjected to a Wittig homologation to give alcohol **126**. At this point, the route was diverged: crude aldehyde **134** was subjected to a Corey/Fuchs homologation and *C*-methylation, affording the *cis*-cyclopropyl fragment **124**. When subjecting

crude aldehyde **134** to basic reaction conditions at elevated temperature, the thermodynamically favoured *trans*-isomer was formed. The subsequent Corey/Fuchs homologation provided the *trans*-cyclopropyl fragment **157**. Overall, the *cis*-cyclopropyl fragment **124** was synthesised in 13% yield and eight steps, whereas the *trans*-cyclopropyl fragment **157** was accomplished in 16% yield and nine steps.
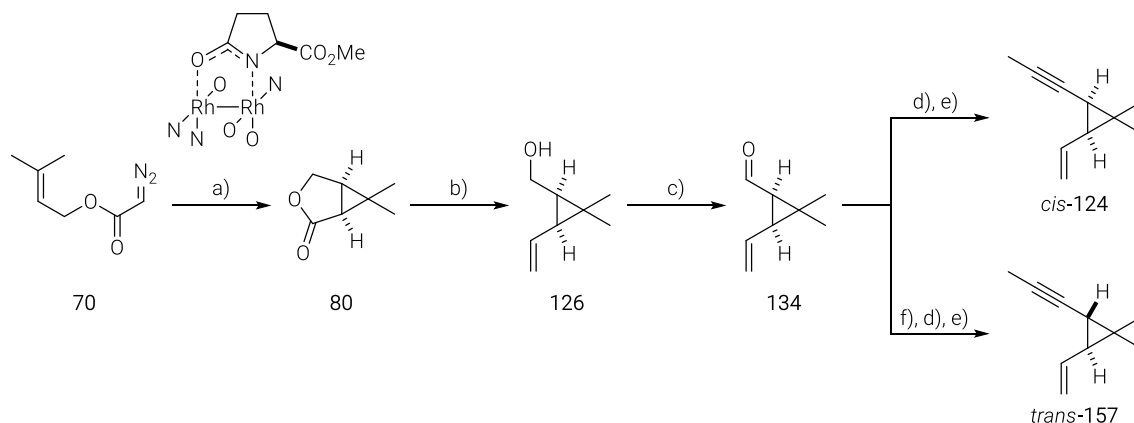
Scheme 70. Synthesis of the cyclopropyl fragments, *cis*-**124** and *trans*-**157**. Conditions: a) [Rh$_2$(5*S*-MEPY)$_4$]·2MeCN (0.6 mol%), CH$_2$Cl$_2$, reflux, 87% (93% *ee*); b) *i*) DIBAL-H, CH$_2$Cl$_2$, −78 °C; *ii*) Ph$_3$PCH$_2$, THF, RT, 55% over 2 steps; c) DMP, CH$_2$Cl$_2$, RT; d) PPh$_3$, CBr$_4$, CH$_2$Cl$_2$, 0 °C; e) *i*) *n*-BuLi, Et$_2$O, −78 °C; *ii*) DMPU, Et$_2$O, −78 °C; *iii*) MeI, −78 °C to RT, 51% over 3 steps (*cis*-**124**), 63% over 4 steps (*trans*-**157**, *trans*/*cis* = 9:1, ^{1}H NMR); f) K$_2$CO$_3$, MeOH, 50 °C.

The chemoselective hydroboration of the terminal alkene in presence of the methyl-capped alkyne of each cyclopropyl fragment (*cis*-**124** & *trans*-**157**) on treatment with the 9-H-9-BBN dimer in THF at room temperature, generated the corresponding borane intermediates, which were merged with the western fragment **125** under Suzuki cross coupling conditions. The resulting RCAM precursors *cis*-**123** and *trans*-**159** were cyclised at elevated temperature to overcome kinetically favoured side-reactions. The diastereomeric alcohols **146**/**147** and **161**/**162** were separated by flash chromatography and the configuration assignment at C5 of each was determined (Scheme 71).
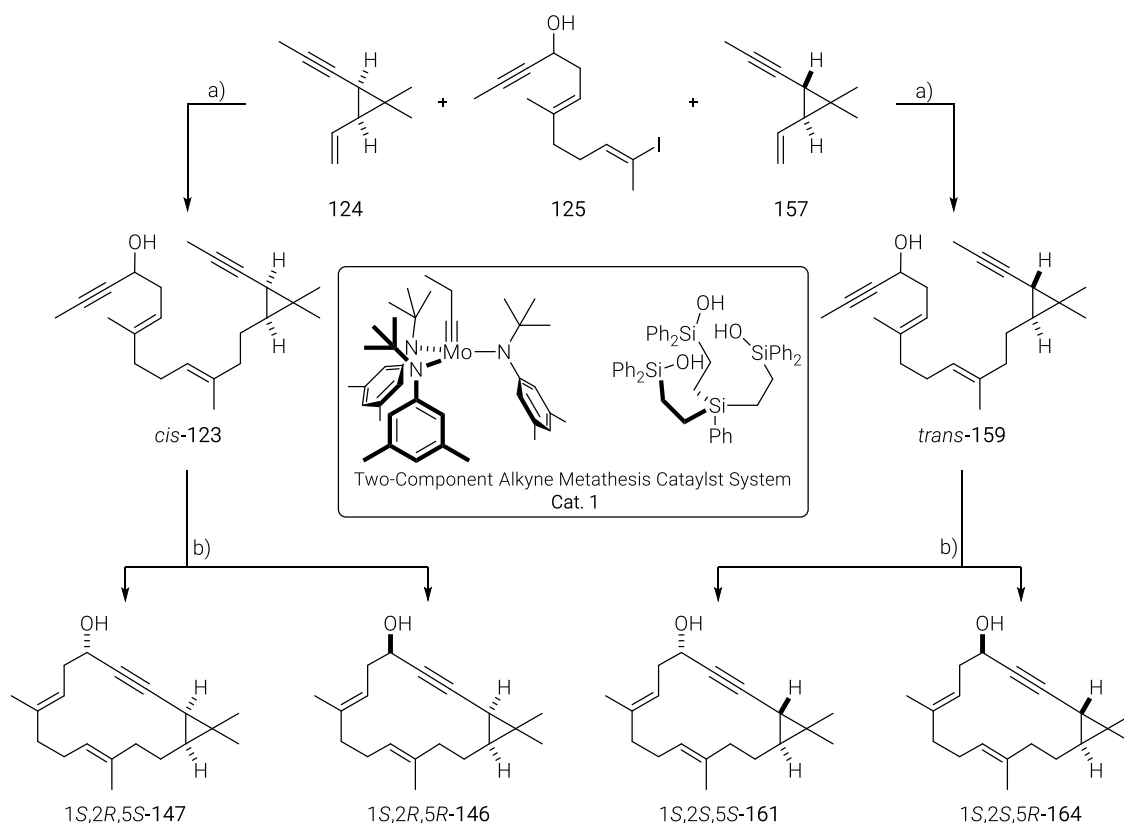
Scheme 71. Conditions: a) *i)* *cis*-**124** or *trans*-**157**, 9-H-9-BBN dimer, THF, 0 °C to RT; *ii)* **125**, [(dppf)PdCl$_2$], Ba(OH)$_2$·(H$_2$O)$_8$, H$_2$O, THF, RT, 69% (*cis*-**123**), 82% (*trans*-**157**); b) **Cat. 1**, 5 Å MS, toluene, 60% (*cis*-**122**, 60%, reflux), 76% (*trans*-**160**, 70 °C), separation of diastereomers by flash chromatography.

The regio- and stereoselective ruthenium catalysed *trans*-hydrostannation of the two *cis*-configured cyclopropyl macrocycles **146** and **147** commenced the late-stage diversification (Scheme 72). The *C*-methylation of stannane **148** and subsequent alcohol oxidation completed the total synthesis of depressin (**9**), which was accomplished in 3% yield along 13 steps (LLS).

To determine the configurational assignment at C5 of euphorhylonal A (**15**), both diastereomeric stannanes **148** and **152**, bearing a *cis*-cyclopropane, were applied to a formylation sequence to afford the corresponding aldehydes **151** and **154** (Scheme 72). Unfortunately, the analytical datasets of either isomer were not in agreement with that of natural product euphorhylonal A.
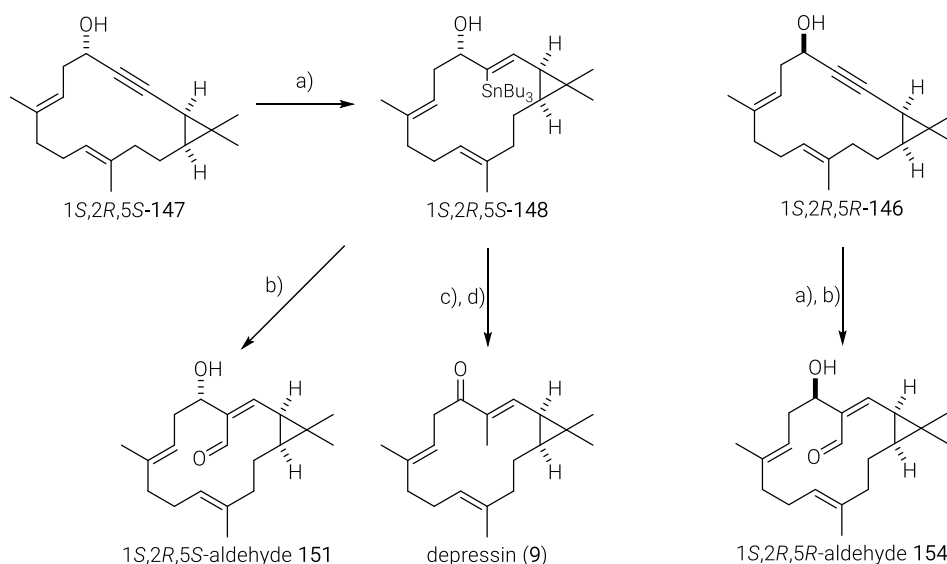
Scheme 72. Synthesis of 1*S*,2*R*,5*S*-aldehyde **151**, 1*S*,2*R*,5*R*-aldehyde **154**, and depressin (**9**). Conditions: a) [Cp*RuCl]₄ (2.5 mol%), Bu₃SnH, CH₂Cl₂, RT, 88% (1*S*,2*R*,5*S*-**148**), 79% (1*S*,2*R*,5*R*-**152**); b) *i*) MeLi, THF, −78 °C to RT; *ii*) DMF, −78 °C to RT, 68% (1*S*,2*R*,5*S*-**151**), 53% (1*S*,2*R*,5*R*-**154**); c) MeI, CuTC, [Ph₂PO₂][Bu₄N], Pd(PPh₃)₄, DMF, RT, 66%; d) MnO₂, CH₂Cl₂, RT, 73%.

Therefore, the misassigned structure of euphorhylonal A was revisited by three different approaches: comparison of its analytical data with that of similar casbane diterpenes, probability calculation for the stereochemical assignment based on GIAO NMR chemical shifts, and total synthesis.

Initially, each of the four possible diastereomers of the nominal euphorhylonal A structure (**15**) was considered as the potentially actual structure of the natural product. However, both structures containing a *cis*-configured cyclopropyl motif were disregarded, due to the previous findings. The analytical data of euphorhylonal A were compared to those of the structurally similar pekinenin C (**16**). In addition, the experimental NMR data were employed to the DP4+ probability analysis program, which used the calculated chemical shielding tensors of all four diastereomers. Both approaches suggested that 1*S**,2*S**,5*R**-**155** represents the most likely configuration for euphorhylonal A.

In terms of the synthetic approach, the *trans*-cyclopropyl macrocycles **161** and **162** were subjected to *trans*-hydrostannation followed by formylation to obtain the corresponding aldehydes **155** and **156** (Scheme 73). Comparison of their analytical data with those of euphorhylonal A showed that the data of 1*S*,2*S*,5*R*-**155** were in very good accordance to those of euphorhylonal A. This result confirmed the predicted configuration. In conclusion, euphorhylonal A (**155**) was synthesised in 3% overall yield comprising 13 steps along the LLS (21 total steps).

The total synthesis of yuexiandajisu A (**17**) utilised the previously generated 1*S*,2*S*,5*R*-stannane **164** in a carboxylation sequence, which completed the total synthesis of (+)-yuexiandajisu A (*ent*-**17**) in 3% overall yield along 13 steps (LLS) (21 total steps). This accomplishment demonstrated the versatility of this synthetic blueprint and determined the previously unknown absolute configuration of yuexiandajisu A.

In an additional approach, the previously used 1*S*,2*S*,5*S*-macrocyclic alkyne **161** was utilised in the synthesis of 2-*epi*-depressin (*ent*-**165**), which is the enantiomer of the natural product 1-*epi*-depressin (**165**). A more convenient *trans*-hydrostannation/*C*-methylation sequence with direct application of crude stannane to the *C*-methylation was investigated. The subsequent

oxidation of the hydroxy functionality gave 2-*epi*-depressin (*ent*-**165**) in 6% overall yield and 14 steps along LLS.
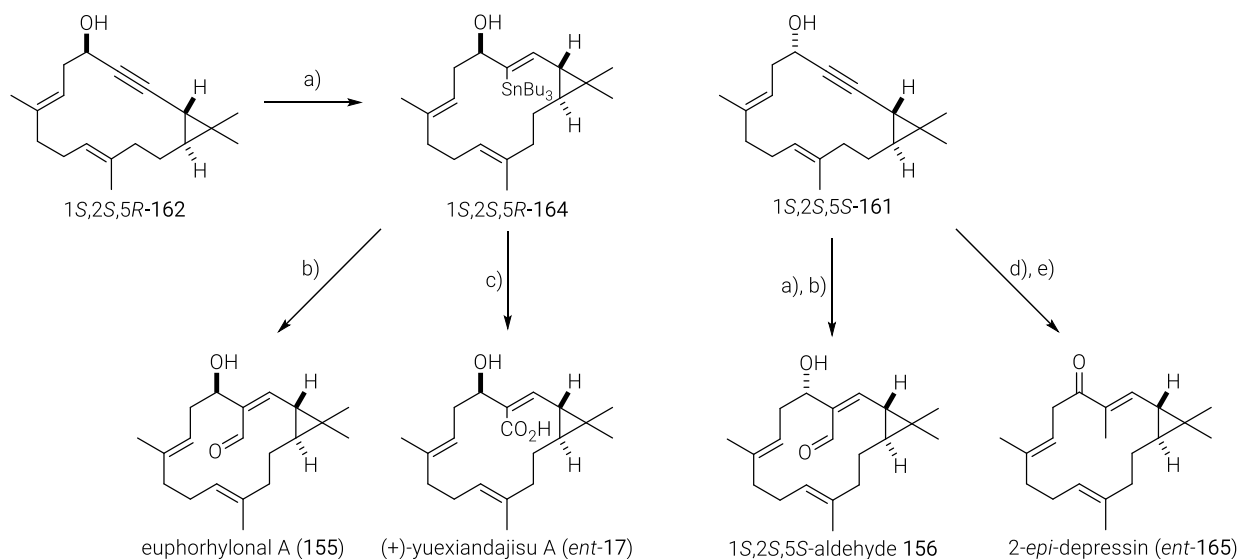
Scheme 73. Synthesis of euphorhylonal A (**155**), (+)-yuexiandajisu A (*ent*-**17**), 1*S*,2*S*,5*S*-aldehyde **156**, and 2-*epi*-depressin (*ent*-**165**). Conditions: a) [Cp*RuCl]$_4$ (2.5 mol%), Bu$_3$SnH, CH$_2$Cl$_2$, RT, 65% (1*S*,2*S*,5*R*-**164**) + 12% (isomer **EP-3**), 74% (1*S*,2*S*,5*S*-**163**); b) *i*) MeLi, THF, −78 °C to RT; *ii*) DMF, −78 °C to RT, 51% (euphorhylonal A (**155**)), 69% (1*S*,2*S*,5*S*-**156**); c) *i*) MeLi, THF, −78 °C to RT; *ii*) CO$_2$, −78 °C to RT, 51%; d) *i*) [Cp*RuCl]$_4$ (1.3 mol%), Bu$_3$SnH, CH$_2$Cl$_2$, RT; *ii*) [Ph$_2$PO$_2$][Bu$_4$N], Ph(PPh$_3$)$_4$, MeI, CuTC, DMF, RT, 67%; e) MnO$_2$, CH$_2$Cl$_2$, RT, 88%.

The first collective total synthesis of three naturally occurring casbane diterpenes (depressin (**9**), euphorhylonal A (**155**), & (+)-yuexiandajisu A (*ent*-**17**)) clarified the configuration of euphorhylonal A (**15**) as 1*S*,2*S*,5*R* (**155**) and determined the absolute configuration of yuexiandajisu A (**17**) as 1*S*,2*S*,5*R* (*ent*-**17**) (Scheme 72 & Scheme 73). Furthermore, these achievements demonstrate the versatility of the chosen synthetic strategy and potentially brings many casbane diterpenes into reach. Thereby, the application of the ligand-controlled *gem*-dimethyl cyclopropanation, with or without subsequent epimerisation, enables the preparation of all permutations of the cyclopropyl fragment. In terms of the late-stage diversification, the alkenyl stannane motif can be seen as a platform to access all oxygenation patterns of the casbane diterpene family in the "northern" sector.

Studies towards the total synthesis of 2-*epi*-10-hydroxydepressin (**5**) and sinularcasbane A (**3**) were initiated by modifications of the western fragment synthesis (Scheme 74). The enantioselective introduction of the hydroxy functionality at C10 was achieved *via* bisborylation of diene **174** and subsequent site-selective mono-oxidation of the resulting bis boronic ester **175**. *O*-Silylation of the product afforded primary boronic ester **173**. Besides, alkenyl iodide **172** was obtained by an adjusted protecting group strategy. A stereodivergent Zweifel olefination *via* β-selenoboronic ester intermediate of alkenyl iodide **172** and primary boronic ester **174** afforded the *E,E*-alkene **180** in moderate selectivity. The first iododesilylation attempts of the unprotected propargylic alcohol, as in the previous total synthesis, led to a complex mixture of compounds. Therefore, iododesilylation of the trityl protected compound needs to be investigated in the future (Scheme 74).
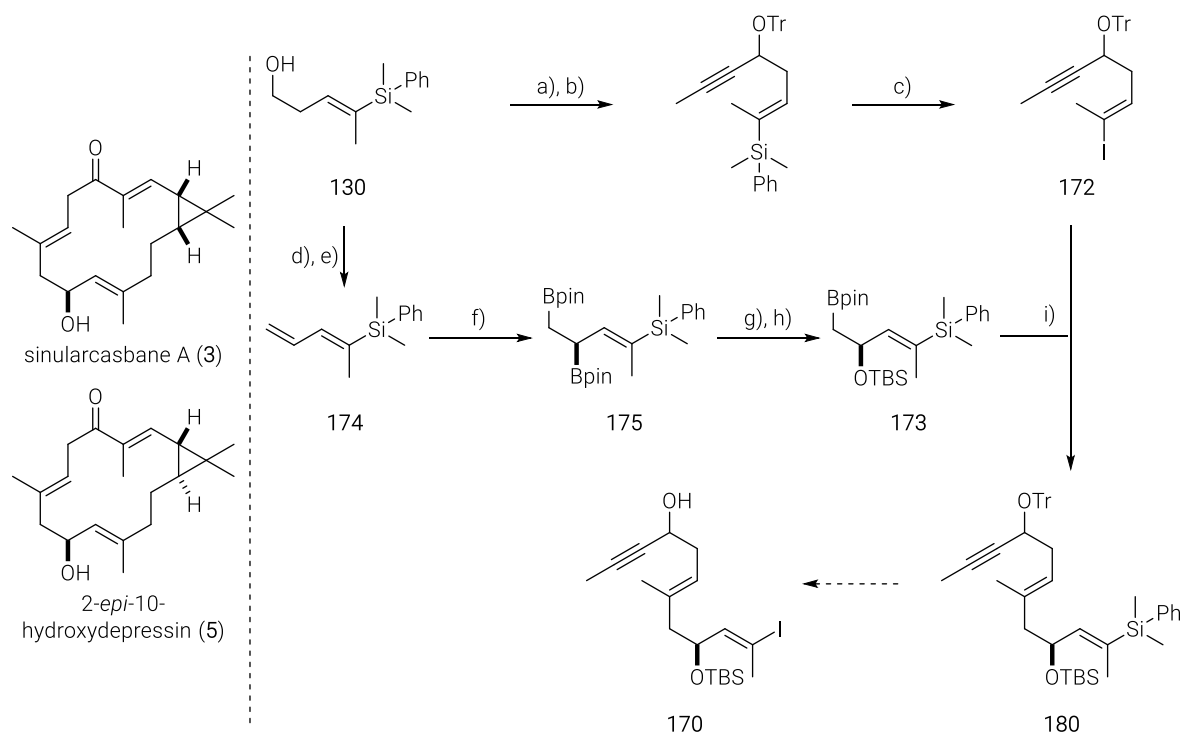
Scheme 74. Towards the total synthesis of sinularcasbane A (**3**) and 2-*epi*-10-hydroxydepressin (**5**). Conditions: a) *i*) DMP, CH$_2$Cl$_2$, 0 °C to RT; *ii*) Propynyl MgBr, THF, 0 °C, 78% over 2 steps; b) TrCl, DBU, CH$_2$Cl$_2$, RT, 83%; c) NIS, 2,6-lutidine, HFIP, CH$_2$Cl$_2$, −20 °C, 95% (*E:Z* ≥ 20:1); d) TsCl, DMAP, Et$_3$N, CH$_2$Cl$_2$, RT, 90%; e) *t*-BuOK, THF, RT, 80%; f) Pt(dba)$_3$ (3 mol%), (*S,S*)-TADDOL-Ligand (4 mol%), B$_2$(pin)$_2$, THF, reflux, 86% (99% *ee*); g) NMO, acetone, RT, 72%; h) TBSCl, imidazole, DMF, 86%; i) *i*) **172** (2.0 equiv), *t*-BuLi (4.1 equiv), THF, −78 °C; *ii*) **175** (1.0 equiv), −78 °C; *iii*) PhSeCl (2.4 equiv) in THF/HFIP, −78 °C to RT; *iv*) *m*CPBA (4.0 equiv), THF, −78 to −45 °C, 63%.

2 [Rh$_2$(5*S*-MEPY)$_4$] AND [BiRh(5*S*-MEPY)$_4$]: CONVENIENT SYNTHESIS AND COMPUTATIONAL ANALYSIS

The [Rh$_2$(MEPY)$_4$] catalysts (**78** & **79**) were applied in the casbane diterpene total synthesis project to enantioselectively introduce the *gem*-dimethyl cyclopropane motif. Furthermore, these catalysts show an impressive versatility in terms of diazo transformations throughout the literature.

In contrast, the heterobimetallic [BiRh(5*S*-MEPY)$_4$] complex (**194**) did not perform any intra- nor intermolecular cyclopropanation. This surprising observation led to the investigations of their electronic and geometric structures based on a computational approach in combination with X-ray structures of both complexes. The structure of the [BiRh(5*S*-MEPY)$_4$] complex (**194**) in the solid state showed a serious steric impediment at the active centre, due to a change of the ligand orientation.

The computed molecular orbitals and the corresponding energy levels showed varied energetic distribution as well as a significant increase of the HOMO/LUMO gap. Furthermore, the frontier orbitals exhibit a dissimilar population at the metal centres (Figure 4). These electronic attributes disfavour the diazo decomposition and carbene formation at the [BiRh(5*S*-MEPY)$_4$] complex (**194**) (Figure 41). In conclusion, the narrow binding environment in combination with the adverse electronic constitution likely cause the poor reactivity of [BiRh(5*S*-MEPY)$_4$] complex (**194**).

[RhRh(5*S*-MEPY)$_4$]	[BiRh(5*S*-MEPY)$_4$]	MO Diagram [RhRh(5*S*-MEPY)$_4$] - [BiRh(5*S*-MEPY)$_4$]
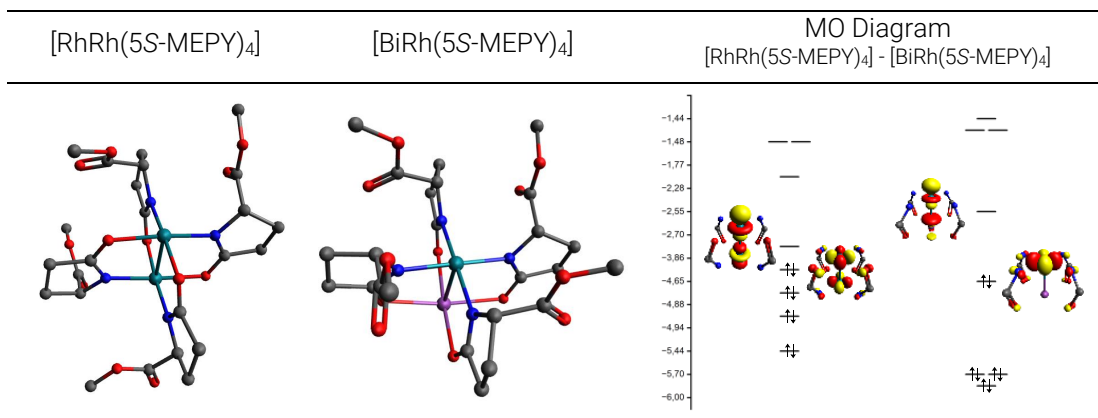
Figure 41. DFT-based geometric optimised structures und MO diagram of [RhRh(5*S*-MEPY)$_4$] (**79**) und [BiRh(5*S*-MEPY)$_4$] (**194**) complexes.

D EXPERIMENTAL PART

1 GENERAL INFORMATION

Unless stated otherwise, all reactions were carried out in flame-dried glassware using anhydrous solvents under argon. The following solvents and reagents were purified by distillation over the drying agents as indicated and were transferred under argon: THF, Et_2O (Mg/anthracene), toluene (Na/K alloy), MeOH (Mg, stored over MS 3 Å); 2,6-lutidine, MeCN, DMF, Et_3N, CH_2Cl_2, DMPU (CaH_2).

All commercially available compounds (Alfa Aesar, Aldrich, TCI Chemicals, Strem Chemicals, ChemPUR, Fluorochem) were used as received, unless stated otherwise. The following compounds were prepared according to the cited literature by myself or within the department of Prof. Dr. Fürstner: Dess-Martin periodinane,[4] active MnO_2,[5] [Cp*RuCl]$_4$,[6] Mo complexes **49**,[7] **Cat. 2**[8] and **Cat. 3**[9], ligand **52a**,[10] Bestmann-Ohira reagent,[11] Pd(PPh$_3$)$_4$[12]. Compounds [Rh$_2$(5R-MEPY)$_4$] (**78**) and [Rh$_2$(5S-MEPY)$_4$] (**79**) were originally prepared by Dr. L. R. Collins and his protocol was optimised.

Hexafluoro-iso-propanol (HFIP) was stored over molecular sieves at RT for 2 d prior to use. CuCN was dried for 14 h at 120 °C (oil bath) under vacuum prior to use, storage and transfer were conducted under argon atmosphere. N-Iodosuccinimide was recrystallised form pentane and stored under Argon in the dark. Diiodoethane was purified by washing a solution in Et_2O with saturated aqueous $Na_2S_2O_3$ solution; the ether phase was dried over $MgSO_4$ and concentrated, and the resulting product stored under argon atmosphere. The molecular sieves were dried at 140°C (oil bath) under vacuum overnight prior to use; they were stored and transferred under argon atmosphere.

Thin layer chromatography (TLC): Macherey-Nagel precoated plates (POLYGRAM®SIL/UV254). Detection was achieved under UV light (254 nm) and by staining with either acidic p-anisaldehyde, cerium ammonium molybdenate, or basic $KMnO_4$ solution. Flash chromatography: Merck silica gel 40-63 µm with predistilled or HPLC grade solvents. Preparative HPLC separations were carried out on an Agilent 1260 Infinity II Preparative LC System.

IR: Spectra were recorded on an Alpha Platinum ATR instrument (Bruker) at ambient temperature, wavenumbers ($\tilde{v}$) in cm^{-1}. MS: ESI-MS: ESQ3000 (Bruker), accurate mass determinations: Bruker APEX III FT-MS (7 T magnet) or Mat 95 (Finnigan). Optical rotations

4   M. Frigerio, M. Santagostino, S. Sputore, *J. Org. Chem.* **1999**, *64*, 4537–4538.

5   J. Attenburrow, A. F. B. Cameron, J. H. Chapman, R. M. Evans, B. A. Hems, A. B. A. Jansen, T. Walker, *J. Chem. Soc.* **1952**, 1094–1111.

6   a) P. J. Fagan, W. S. Mahoney, J. C. Calabrese, I. D. Williams, *Organometallics* **1990**, *9*, 1843–1852; b) P. J. Fagan, M. D. Ward, J. C. Calabrese, *J. Am. Chem. Soc.* **1989**, *111*, 1698–1719.

7   W. Zhang, Y. Lu, J. S. Moore, *Org. Synth.* **2007**, *84*, 163–176.

8   J. Heppekausen, R. Stade, R. Goddard, A. Fürstner, *J. Am. Chem. Soc.* **2010**, *132*, 11045–11057.

9   J. Hillenbrand, M. Leutzsch, E. Yiannakas, C. P. Gordon, C. Wille, N. Nöthling, C. Copéret, A. Fürstner, *J. Am. Chem. Soc.* **2020**, *142*, 11279–11294.

10   S. Schaubach, K. Gebauer, F. Ungeheuer, L. Hoffmeister, M. K. Ilg, C. Wirtz, A. Fürstner, *Chem. Eur. J.* **2016**, *22*, 8494–9507.

11   J. Pietruszka, A. Witt, *Synthesis* **2006**, *24*, 4266–4268.

12   D. R. Coulson, L. C. Satek, S. O. Grim, *Inorg. Synth.* **1972**, *13*, 121.

($[\alpha]_D$) were measured with an A-Krüss Otronic Model P8000-t polarimeter at a wavelength of 589 nm. NMR: Spectra were recorded on a Bruker AVIII 400 or AVIII 600 or AV600neo (the latter two both equipped with cryoprobes) spectrometer in the solvents indicated; chemical shifts (δ) are given in ppm relative to TMS, coupling constants (J) in Hz. The solvent signals were used as references and the chemical shifts converted to the TMS scale (CDCl$_3$: $\delta_C \equiv 77.0$ ppm; residual CHCl$_3$ in CDCl$_3$: $\delta_H \equiv 7.26$ ppm; CD$_2$Cl$_2$: $\delta_C \equiv 53.8$ ppm; residual CDHCl$_2$: $\delta_H \equiv 5.32$ ppm; all spectra were recorded at 25 °C. Multiplets are indicated by the following abbreviations: s: singlet, d: doublet, t: triplet, q: quartet, p: pentet, h: hextet, hept: heptet, m: multiplet, br: broad. ^{13}C spectra were recorded in {^{1}H}-decoupled manner and the values of the chemical shifts are rounded to one decimal point. Signal assignments were established using HSQC, HMBC, COSY, NOESY and other 2D experiments; numbering schemes as shown in the inserts. GC analyses were conducted on an Agilent technologies 7890B instrument with a FID detector.

2 SUPPORTING CRYSTALLOGRAPHIC INFORMATION
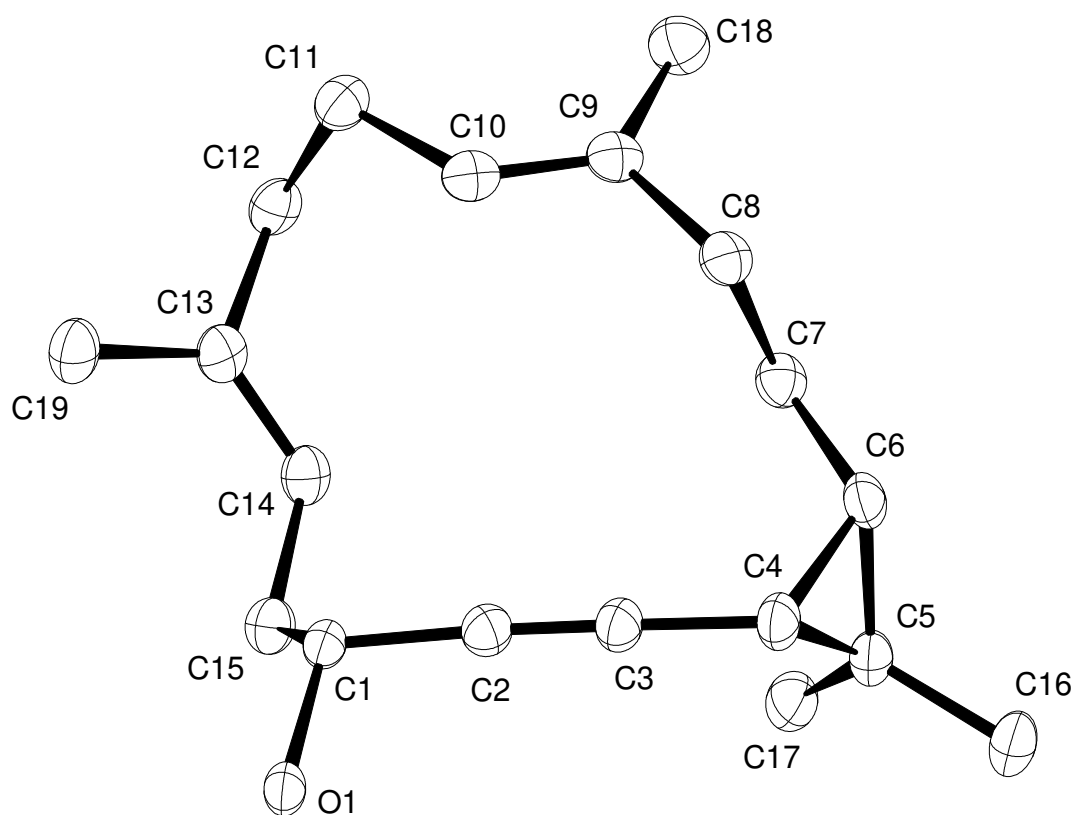
Figure 42. Structure of cycloalkyne **146** in the solid state; arbitrary numbering system.

X-ray crystal structure analysis of macrocycle 146: $C_{19}H_{28}O$, M_r = 272.41 g mol^{-1}, colourless plate, crystal size 0.141 × 0.062 × 0.043 mm^3, tetragonal, space group $P4_3$[78], a = 13.9323(3) Å, b = 13.9323(3) Å, c = 8.8998(3) Å, V = 1727.53(9) Å^3, T = 100(2) K, Z = 4, D_{calc} = 1.047 g cm^{-3}, λ = 1.54178 Å, $\mu(Cu\text{-}K_\alpha)$ = 0.470 mm^{-1}, analytical absorption correction (T_{min} = 0.95, T_{max} = 0.98), Bruker AXS Enraf-Nonius KappaCCD diffractometer with a FR591 rotating Mo-anode X-ray source, 3.172 < θ < 71.125°, 46603 measured reflections, 3122 independent reflections, 2837 reflections with $I > 2\sigma(I)$, R_{int} = 0.0626. S = 1.051, 190 parameters, absolute structure parameter = 0.0(4), residual electron density +0.2 (1.77 Å from H1) / −0.2 (1.02 Å from C6) e Å^{-3}. The hydrogen at O1 was found and refined, all other hydrogens were placed in calculated positions.

The structure was solved by *SHELXT* and refined by full-matrix least-squares (*SHELXL*) against F^2 to R_1 = 0.033 [$I > 2\sigma(I)$], wR_2 = 0.084. **CCDC-2041047.**
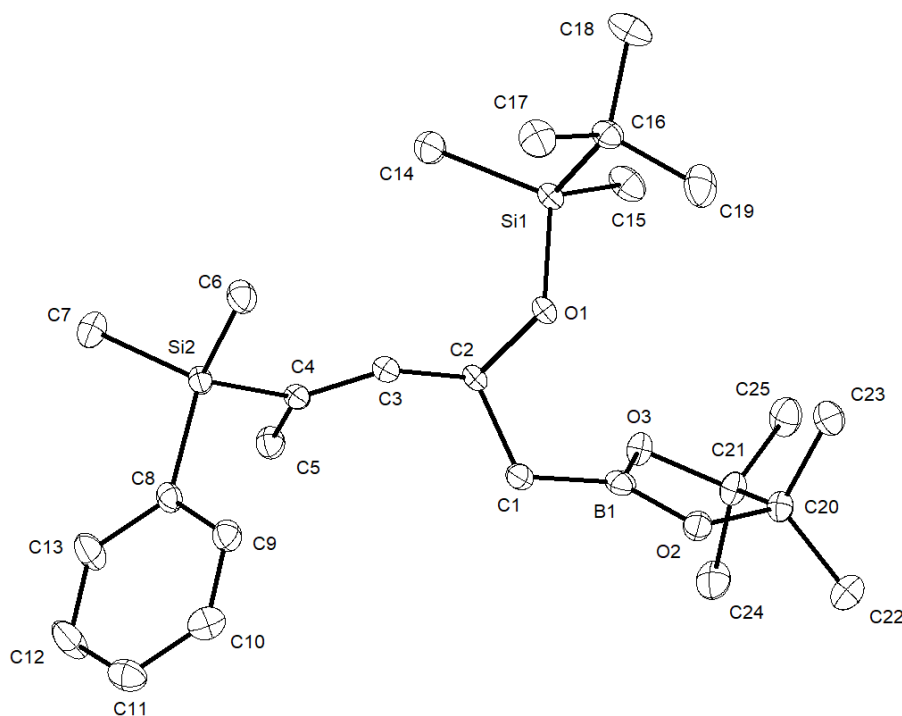
Figure 43. Structure of boronic ester **174** in the solid state; arbitrary numbering system.

X-ray crystal structure analysis 174: $C_{25}H_{45}BO_3Si_2$, M_r = 460.60 g mol^{-1}, colourless, crystal size 0.081 × 0.054 × 0.022 mm^3, orthorhombic, space group P $2_12_12_1$ [19], a = 7.8183(4) Å, b = 11.8370(7) Å, c = 30.6741(17) Å, V = 2838.7(3) Å^3, T = 100(2) K, Z = 4, D_{calc} = 1.078 mg m^{-3}, λ = 0.71073 Å, μ(Mo-$K\alpha$) = 0.147 mm^{-1}, Gaussian absorption correction (T_{min} = 0.99077, T_{max} = 0.99750), Bruker-AXS Mach3 diffractometer with APEX-II detector with IμS microfocus Mo-anode X-ray source and focusing multilayer optics, 1.328 < θ < 31.707°, 99585 measured reflections, 9579 independent reflections, 8910 reflections with I > 2σ(I), R_{int} = 0.0417. The structure was solved by *SHELXT* and refined by full-matrix least-squares (*SHELXL*) against F^2 to R_1 = 0.0290 [I > 2σ(I)], wR_2 = 0.0699, 292 parameters, absolute structure parameter Flack (x) = −0.012(18).

3 CASBANE DITERPENE SYNTHESIS

3.1 FIRST APPROACH

3.1.1 THE CYCLOPROPYL FRAGMENTS – SIMMONS-SMITH CYCLOPROPANATION

Ethyl (*E*)-hept-2-en-6-ynoate (EP-1). DMSO (4.05 mL, 4.46 g, 57.06 mmol) was added to a solution of oxalyl chloride (4.05 g, 2.74 mL, 31.96 mmol) in CH_2Cl_2 (150 mL) at −78 °C and the resulting mixture stirred for 20 min, followed by slow addition of pent-1-yn-5-ol (1.92 g, 2.11 mL, 22.83 mmol) in CH_2Cl_2 (20 mL). After 20 min, Et_3N (11.55 g, 15.91 mL) was added, the mixture was stirred at −78 °C for 30 min, and for 2 h at RT. The mixture was diluted with CH_2Cl_2 (100 mL) and the reaction was quenched with water (20 mL). The aqueous layer was acidified with aqueous 2 M HCl solution and extracted with CH_2Cl_2 (2 x 50 mL). The combined organic phases were washed with 1% aqueous HCl solution, brine and 5% aqueous saturated $NaHCO_3$ solution, dried over $MgSO_4$ and concentrated.
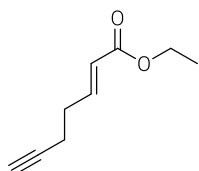
The crude aldehyde was directly added to a solution of LiCl (1.74 g, 41.09 mmol,) in THF (150 mL), followed by DBU (6.14 mL, 6.25 g, 41.09 mmol) and triethyl phosphonoacetate (8.15 mL, 9.21 g, 41.09 mmol) at RT. The resulting mixture was stirred overnight. The reaction was quenched with aqueous saturated NH_4Cl solution, the aqueous layer was separated and extracted with CH_2Cl_2 (3 × 40 mL). The combined organic phases were dried over $MgSO_4$ and concentrated. The residue was purified by flash chromatography (hexane/EtOAc, 20:1) to yield the title compound as a colourless oil. (2.10 g, 13.81 mmol, 61%). ^{1}H NMR (400 MHz, $CDCl_3$) δ = 6.97 (dtd, *J* = 14.8, 6.6, 1.5 Hz, 1H), 5.89 (dq, *J* = 15.6, 1.5 Hz, 1H), 4.19 (qd, *J* = 7.1, 1.6 Hz, 2H), 2.39 (m, 4H), 2.00 (t, *J* = 2.6 Hz, 1H), 1.29 ppm (td, *J* = 7.1, 1.6 Hz, 3H); ^{13}C NMR (101 MHz, $CDCl_3$) δ = 166.5, 146.4, 122.7, 82.8, 69.5, 60.5, 31.2, 17.6, 14.4 ppm; IR (film) $\tilde{v}$ = 3298, 2982, 1715, 1656, 1368, 1314, 1266, 1202, 1155, 1037, 971, 633 cm^{-1}; HRMS (ESI): *m/z* calcd. for $C_9H_{12}O_2$ [*M*[+]+Na]: 175.07295; found: 175.07304.

(*E*)-Hept-2-en-6-yn-1-ol (73a). DIBAL-H (27.13 mL, 27.13 mmol,1.0 M in THF) was added dropwise to a solution of ester **EP-1** (1.88 g, 12.33 mmol) in Et_2O (150 mL) at −78 °C. The resulting mixture was stirred at −78 °C for 3 h and warmed to RT overnight. The reaction was quenched with water at 0 °C. The mixture was filtered through a plug of Celite® and rinsed with Et_2O (3 x 50 mL). The filtrate was dried over $MgSO_4$ and concentrated. The residue was purified by flash chromatography (pentane/Et_2O, 4:1 → 2:1) to yield the title compound as a colourless oil (1.09 g, 9.95 mmol, 81%). ^{1}H NMR (400 MHz, $CDCl_3$): δ = 5.73 (m, 2H), 4.11 (m, 2H), 2.27 (m, 4H), 1.96 (m, 1H), 1.46 ppm (m, 1H); ^{13}C NMR (101 MHz, $CDCl_3$): δ = 130.8, 130.6, 83.9, 68.9, 63.7, 31.3, 18.6 ppm; IR (film) $\tilde{v}$ = 3294, 2918, 1433, 1084, 997, 967, 629 cm^{-1}; HRMS (ESI): *m/z* calcd. for $C_7H_{10}O$ [*M*[+]+Na]: 133.06238; found: 133.06241.
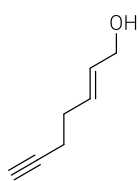
(*trans*-3-(But-3-yn-1-yl)-2,2-dimethylcyclopropyl)methanol (76a). Et_2Zn (2.04 mL, 2.23 mmol, 15% in toluene) was added to a solution of allylic alcohol **73a** (50.0 mg, 0.45 mmol) and cyclohexane disulfonamide **75** (122.7 mg, 0.454 mmol) in CH_2Cl_2 (16 mL) at −10 °C. The resulting mixture was stirred for 10 min at this temperature before 2,2-diiodopropane **74** (268.6 mg, 0.908 mmol) was added dropwise. Stirring was continued at RT for 2 h. The reaction was quenched with 2 M HCl solution and the aqueous layer was extracted with CH_2Cl_2 (3 × 8 mL). The combined organic phases were washed with aqueous saturated $NaSO_3$ solution, dried over $MgSO_4$ and concentrated. The residue was purified by flash chromatography (hexane/EtOAc, 10:1) to yield the title compound as a colourless oil (14.0 mg, 0.9 mmol, 20%, 1% *ee*). ^1H NMR (400 MHz, $CDCl_3$): δ = 3.63 (m, 2H), 2.26 (td, J = 7.0, 2.7 Hz, 2H), 1.97 (t, J = 2.7 Hz, 1H), 1.69 (dq, J = 13.5, 6.7 Hz, 1H), 1.42 (m, 2H), 1.10 (s, 3H), 1.07 (s, 3H), 0.65 (td, J = 7.5, 5.2 Hz, 1H), 0.51 ppm (ddd, J = 8.0, 6.2, 5.3 Hz, 1H); ^{13}C NMR (101 MHz, $CDCl_3$): δ = 84.8, 68.7, 63.9, 33.1, 29.1, 27.7, 21.9, 21.9, 20.3, 19.1 ppm; IR (film) $\tilde{v}$ = 3310, 2971, 2927, 2869, 1455, 1431, 1377, 1261, 1128, 1017, 800, 628 cm^{-1}; HRMS (ESI): m/z calcd. for $C_{10}H_{16}O$ [M^++Na]: 175.10933; found: 175.10939.
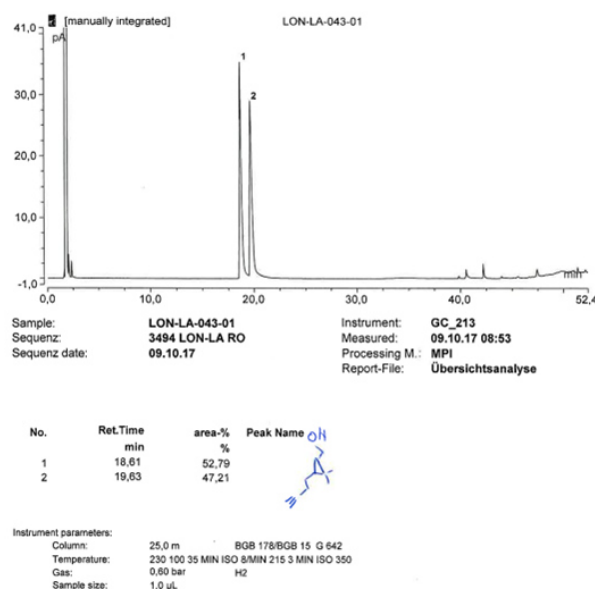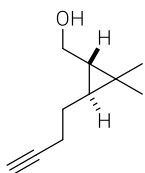
(*E*)-7-(Trimethylsilyl)hept-2-en-6-yn-1-ol (73b). *n*-BuLi (3.94 mL, 5.72 mmol, 1.45 M in hexane) was added dropwise to a solution of (*E*)-hept-2-en-6-yn-1-ol **73a** (300 mg, 2.72 mmol) in THF (4 mL) at −78 °C and the mixture was stirred for 30 min. TMSCl (651 mg, 0.760 mL) was added dropwise at −78 °C, afterwards the mixture was stirred at RT for 2 h. Stirring was continued for 1.5 h after addition of aqueous HCl (1 M, 20 mL). The mixture was diluted with EtOAc (50 mL) and the aqueous layer extracted with EtOAc (3 × 30 mL). The combined organic phases were washed with water (2 × 30 mL), aqueous saturated $NaHCO_3$ solution (30 mL), and brine (50 mL), dried over $MgSO_4$ and concentrated to afford the title compound as a colourless oil. (435 mg, 2.72 mmol, 88%). ^1H NMR (400 MHz, $CDCl_3$): δ = 5.72 (m, 2H), 4.11 (m, 2H), 2.29 (m, 4H), 0.15 ppm (s, 9H); ^{13}C NMR (101 MHz, $CDCl_3$): δ = 131.0, 130.5, 106.7, 85.2, 63.8, 31.5, 20.1, 0.3 ppm; IR (film) $\tilde{v}$ = 3329, 2958, 2174, 1248, 1039, 1000, 967, 836, 758, 697, 638 cm^{-1}; HRMS (ESI): m/z calcd. for $C_{10}H_{18}OSi$ [M^++Na]: 205.10191; found: 205.10202.
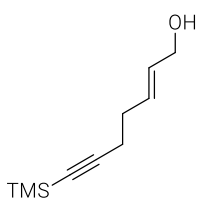
(*trans*-2,2-Dimethyl-3-(4-(trimethylsilyl)but-3-yn-1-yl)cyclopropyl)methanol (76b). Et$_2$Zn (716.0 µL, 795.0 µmol, 15% in toluene) was added to a solution of allylic alcohol **73b** (29.0 mg, 159.0 µmol) and cyclohexane disulfonamide **75** (43.0 mg, 159.0 mmol) in CH$_2$Cl$_2$ (6 mL) at −78 °C. The resulting mixture was stirred for 10 min at this temperature before 2,2-diiodopropane **74** (188.2 mg, 636.0 µmol) was added dropwise and the mixture was stirred at RT for 1 h. The reaction was quenched with 2 M HCl solution and the aqueous layer was extracted with CH$_2$Cl$_2$ (3 × 10 mL). The combined organic phases were washed with aqueous saturated NaSO$_3$ solution, dried over MgSO$_4$ and concentrated. The residue was purified by flash chromatography (hexane/EtOAc, 10:1) to yield the title compound as a colourless oil (21.0 mg, 936.0 µmol, 59%, 0 %ee). ^{1}H NMR (400 MHz, CDCl$_3$): δ = 3.62 (m, 2H), 2.31 (t, J = 7.1 Hz, 2H), 1.69 (dq, J = 13.4, 6.7 Hz, 1H), 1.41 (m, 2H), 1.10 (s, 3H), 1.07 (s, 3H), 0.66 (td, J = 7.5, 5.3 Hz, 1H), 0.48 (m, 1H), 0.15 ppm (s, 9H); ^{13}C NMR (101 MHz, CDCl$_3$): δ = 107.7, 85.1, 63.9, 33.1, 29.3, 27.6, 22.0, 21.9, 20.5, 20.3, 0.3 ppm; IR (film) $\tilde{v}$ = 2956, 2925, 2867, 2173, 1717, 1697, 1275, 1249, 1199, 997, 838, 758, 745, 639 cm^{-1}; HRMS (ESI): m/z calcd. for C$_{13}$H$_{24}$OSi [M^++Na]: 247.14886; found: 247.14898.
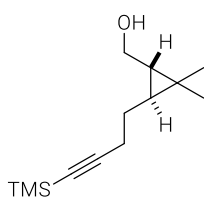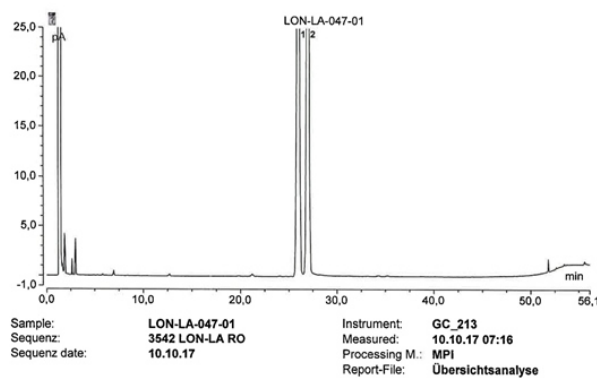
2,2-Diiodopropane (74). The title compound was prepared according to a literature protocol.[284] Acetone (7.56 mL, 5.98 g, 102.96 mmol) was added dropwise to hydrazine monohydrate (10.00 mL, 10.32 g, 206.15 mmol) at RT and the mixture was stirred at 100 °C for 30 min. The resulting mixture was extracted with Et$_2$O (3 × 25 mL) and the combined organic phases were dried over MgSO$_4$. This solution was used without further purification or concentration (concentration would form acetone azine). Et$_3$N (21.53 mL, 15.63 g, 154.44 mmol) was added, followed by a solution of iodine (26.13 g, 102.96 mmol) in Et$_2$O (120 mL) until the brown colour persisted. The mixture was washed with aqueous HCl solution (2 M), aqueous saturated Na$_2$S$_2$O$_3$ solution, water, brine, and was dried over MgSO$_4$ and concentrated. The title compound was obtained as orange oil (6.38 g, 20%). ^{1}H NMR (400 MHz, CDCl$_3$): δ = 3.00 ppm (s, 6H); ^{13}C NMR (101 MHz, CDCl$_3$): δ = 51.0, −10.3 ppm. IR (film) $\tilde{v}$ = 2947, 1439, 1365, 1142, 1078, 889, 543, 524, 441 cm^{-1}; HRMS (ESI): m/z calcd. for C$_3$H$_6$I$_2$ [M^+]: 295.85535; found: 295.85485.

3.1.2 The cyclopropyl fragments – [Rh₂(MEPY)₄] catalysed cyclopropanation

3-Methylbut-2-en-1-yl 3-oxobutanoate (81). The title compound was prepared according to a literature protocol.[138] A solution of freshly distilled diketene **72** (15.70 g, 84.07 mmol) in THF (19 mL) was added to 3-methyl-2-buten-1-ol **71** (16.94 mL, 14.36 g, 166.73 mmol) and sodium acetate (766 mg, 9.34 mmol) in refluxing THF (47 mL) over the course of 1 h. Stirring was continued for 30 min at reflux temperature before the mixture was cooled to RT and concentrated. The residue was purified by distillation to yield the title compound as a colourless liquid (19.76 g, 70%). B.p. 85-88 °C (10 mbar); ^{1}H NMR (400 MHz, CDCl₃): δ = 12.08 (s, enol form), 5.34 (ddt, J = 7.3, 4.2, 1.4 Hz, 1H), 4.98 (m, enol form), 4.64 (d, J = 7.3 Hz, 2H), 3.44 (s, 2H), 2.26 (s, 3H), 1.94 (s, enol form), 1.76 (s, 3H), 1.71 ppm (s, 3H); ^{13}C NMR (101 MHz, CDCl₃): δ = 200.6, 167.1, 139.9, 117.9, 62.2, 50.1, 30.1, 25.7, 18.0 ppm (minor signals of the enol tautomer are visible); IR (film) $\tilde{v}$ = 2973, 2935, 1736, 1714, 1646, 1411, 1360, 1311, 1232, 1147, 953, 542 cm^{-1}; HRMS (ESI): m/z calcd. for C₉H₁₄O₃ [M^++Na]: 193.08351; found: 193.08372.
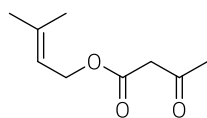
3-Methylbut-2-en-1-yl 2-diazoacetate (70). The title compound was prepared according to a literature protocol.[138] A solution of p-acetamidobenzenesulfonyl azide (18.44 g, 76.76 mmol) in MeCN (50 mL) was added to a solution of 3-methyl-2-buten-1-yl acetoacetate **81** (10.05 g, 59.05 mmol) and Et₃N (10.70 mL, 7.77 g, 76.76 mmol) in MeCN (50 mL) over 30 min. A white precipitate of p-acetamidobenzenesulfonamide was observed after ≈30 min; at this point, additional MeCN (30 mL) was added and stirring continued for additional 4 h. A solution of LiOH (4.67 g, 194.85 mmol) in water (20 mL) was added and the mixture was stirred at RT for 12 h. The aqueous layer was separated and extracted with Et₂O/EtOAc (2:1, 3 × 70 mL). The combined organic phases were dried over MgSO₄ and concentrated. The residue was purified by flash chromatography (hexane/EtOAc, 15:1) to yield the title compound as a yellow oil (9.10 g, 75%). ^{1}H NMR (400 MHz, CDCl₃): δ = 5.34 (ddq, J = 8.6, 5.7, 1.4 Hz, 1H), 4.74 (s, 1H), 4.66 (d, J = 7.2 Hz, 2H), 1.76 (s, 3H), 1.72 ppm (s, 3H); ^{13}C NMR (101 MHz, CDCl₃): δ = 166.9, 139.3, 118.5, 61.7, 46.2, 25.8, 18.0 ppm; IR (film) $\tilde{v}$ = 3113, 2973, 2935, 2103, 1684, 1444, 1386, 1356, 1342, 1234, 1172, 995, 462, 433 cm^{-1}; HRMS (ESI): m/z calcd. for C₇H₁₀N₂O₂ [M^++Na]: 177.06345; found: 177.06346.
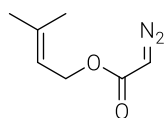
(1*R*,5*S*)-6,6-Dimethyl-3-oxabicyclo[3.1.0]hexan-2-one (67). The title compound was prepared according to a literature protocol.[138] A solution of diazo ester **70** (5.05 g, 32.76 mmol) in CH₂Cl₂ (18 mL) was added to a clear violet solution of [Rh₂(5*R*-MEPY)₄]·2MeCN (**78a**) (138.9 mg, 162.2 μmol, 0.5 mol%) in CH₂Cl₂ (110 mL) at reflux temperature via syringe pump over the course of 30 h. Once the addition was complete, stirring was continued for an additional 30 min before the mixture was cooled to RT and concentrated. The residue was purified by flash chromatography (hexane/EtOAc, 10:1 → 3:1) to give the title compound as a colourless oil (3.68 g, 89%, 94% *ee*). $[\alpha]_D^{20}$ = −87.8 (1.22 g/100mL, CHCl₃); ^{1}H NMR (400 MHz, CDCl₃): δ = 4.36 (dd, J = 9.9, 5.5 Hz, 1H), 4.15 (dt, J = 9.9, 1.0 Hz, 1H), 2.04 (m, 1H), 1.95 (dd, J = 6.3, 1.0 Hz, 1H), 1.18 (s, 3H), 1.17 ppm (s, 3H); ^{13}C NMR (101 MHz, CDCl₃): δ = 175.1, 66.7, 30.7, 30.2, 25.4, 23.2, 14.7 ppm; IR (film) $\tilde{v}$ = 2959, 2908, 1761, 1744, 1381, 1360, 1216, 1175, 1092, 1047, 1021, 973, 957, 891, 855, 655, 634, 490 cm^{-1}; HRMS (ESI): m/z calcd. for C₇H₁₀O₂ [M^+]: 127.07536; found: 127.07538.
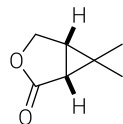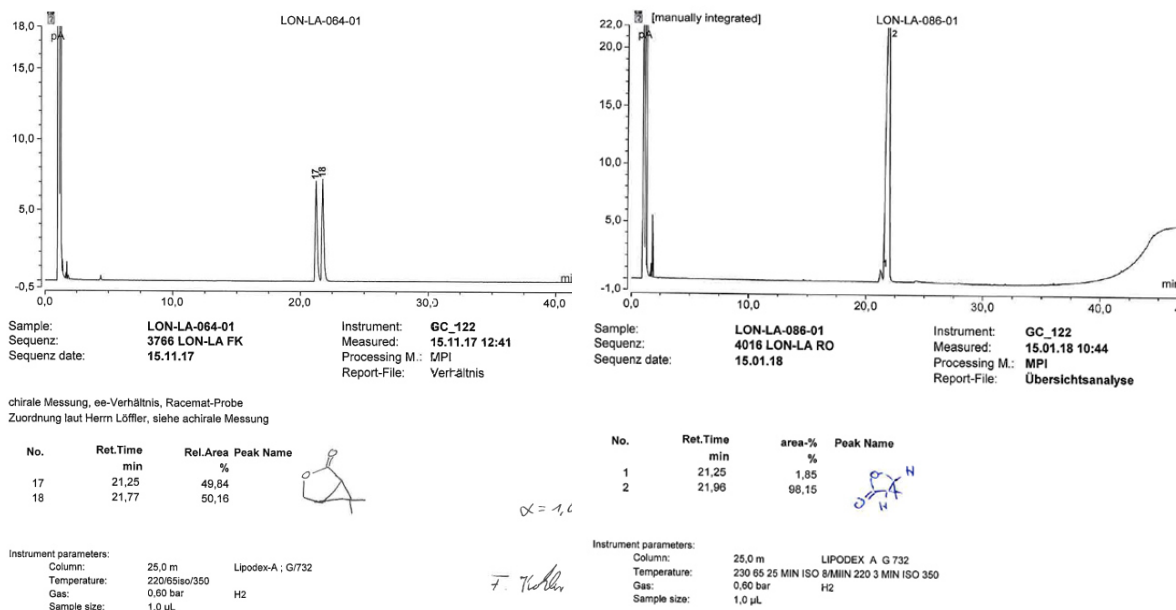
Methyl (*E*)-3-((1*R*,3*S*)-3-(hydroxymethyl)-2,2-dimethylcyclopropyl)acrylate (*E*-66) and Methyl (*Z*)-3-((1*R*,3*S*)-3-(hydroxymethyl)-2,2-dimethylcyclopropyl)acrylate (*Z*-66). DIBAL-H (16.17 mL, 16.17 mmol, 1 M in CH_2Cl_2) was added dropwise over 25 min to a solution of lactone **67** (2.00 g, 15.85 mmol) in CH_2Cl_2 (153 mL) at −77 °C and the resulting mixture was stirred at −78 °C for 1 h. The reaction was quenched with MeOH (45 mL). Aqueous saturated Rochelle solution (50 mL) was added and the mixture was warmed to RT. EtOAc (150 mL) and water (50 mL) was added and the mixture was vigorously stirred for 1 h until the two phases were clear. The aqueous layer was extracted with EtOAc (3 × 50 mL). The combined organic phases were dried over $MgSO_4$ and concentrated.
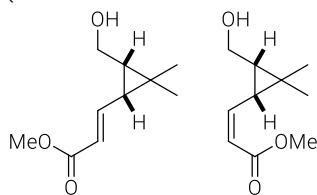
Methyl (triphenylphosphoranylidene)acetate (10.60 g, 31.71 mmol) was added to a solution of crude lactol **68** in THF (90 mL) and the mixture was stirred at 60 °C for 2 d. The mixture was cooled to RT and concentrated. The residue was purified by flash chromatography (hexane/EtOAc, 3:1) to obtain the title compound as a colourless oil (2.34 g, 12.84 mmol, 81%). A small amount of the diastereomers **E-66** & **Z-66** were separated by flash chromatography (hexane/EtOAc, 10:1) for analysis.

*Analytical and spectral data of (E)-diastereomer **E-66**:* $[\alpha]_D^{20}$ = −74.3 (0.9 g/100 mL, CHCl₃); ¹H NMR (500 MHz, CDCl₃): δ = 6.78 (dd, *J* = 15.2, 11.0 Hz, 1H), 5.98 (dd, *J* = 15.3, 0.5 Hz, 1H), 3.84 (dd, *J* = 11.7, 7.7 Hz, 1H), 3.76 (dd, *J* = 11.7, 7.8 Hz, 1H), 3.71 (s, 3H), 1.57 (dd, *J* = 11.0, 8.7 Hz, 1H), 1.42 (dt, *J* = 8.8, 7.8 Hz, 1H), 1.19 (s, 3H), 1.18 ppm (s, 3H); ¹³C NMR (126 MHz, CDCl₃): δ = 166.8, 146.9, 121.4, 59.8, 51.4, 35.4, 31.0, 28.7, 25.5, 15.7 ppm; IR (film) $\tilde{v}$ = 3413, 2950, 1714, 1698, 1633, 1436, 1267, 1148, 1020, 980, 857, 742 cm⁻¹; HRMS (ESI): m/z calcd. for $C_{10}H_{16}O_3$ [*M*⁺+Na]: 207.09916; found: 207.09918.

*Analytical and spectral data of (Z)-diastereomer **Z-66**:* $[\alpha]_D^{20}$ = −62.3 (0.8 g/100 mL, CHCl₃); ¹H NMR (400 MHz, CDCl₃): δ = 6.04 (dd, *J* = 11.5, 10.6 Hz, 1H), 5.87 (dd, *J* = 11.5, 1.0 Hz, 1H), 3.80 (dd, *J* = 11.7, 7.4 Hz, 1H), 3.72 (s, 3H), 3.67 (dd, *J* = 11.6, 8.2 Hz, 1H), 2.72 (ddd, *J* = 10.6, 8.9, 1.0 Hz, 1H), 1.45 (ddd, *J* = 8.9, 8.1, 7.4 Hz, 1H), 1.21 (s, 3H), 1.15 ppm (s, 3H); ¹³C NMR (126 MHz, CDCl₃): δ = 167.3, 147.2, 119.9, 59.9, 51.1, 35.5, 28.7, 27.9, 25.3, 15.5 ppm; IR (film) $\tilde{v}$ = 3228,

2950, 1709, 1619, 1444, 1164, 1059, 1014, 815, 714 cm^{-1}; HRMS (ESI): *m/z* calcd. for C$_{10}$H$_{16}$O$_3$ [*M*$^+$+Na]: 207.09916; found: 207.09914.

Methyl 3-((1*R*,3*S*)-3-(hydroxymethyl)-2,2-dimethylcyclopropyl)propanoate (82). CoCl$_2$·(H$_2$O)$_8$ (0.41 g, 1.74 mmol) was added to a solution of unsaturated cyclopropane *E*-66 (1.60 g, 8.68 mmol) in MeOH (70 mL). The resulting mixture was stirred at RT for 30 min. The Argon atmosphere was exchanged to a hydrogen atmosphere, before a solution of NaBH$_4$ (1.64 g, 43.42 mmol) in DMF (34 mL) was added. The temperature was kept constant at RT with a water bath. The mixture was stirred at RT for 1 h. The reaction was quenched with water and the mixture was diluted with EtOAc (40 mL). The aqueous layer was extracted with EtOAc (3 × 10 mL). The combined organic phases were washed with brine, dried over MgSO$_4$ and concentrated. The residue was purified by flash chromatography (hexane/EtOAc, 4:1 → 3:1) to yield the title compound as a colourless oil (1.42 g, 8.14 mmol, 94%). [α]$_D^{20}$ = +18.0 (1.4 g/100 mL, CHCl$_3$); ^{1}H NMR (400 MHz, CDCl$_3$): δ = 3.67 (m, 5H), 2.40 (dd, *J* = 7.8, 6.9 Hz, 2H), 1.66 (m, 3H), 1.06 (s, 3H), 1.00 (s, 3H), 0.87 (td, *J* = 8.6, 7.2 Hz, 1H), 0.57 ppm (dt, *J* = 8.8, 7.0 Hz, 1H); ^{13}C NMR (101 MHz, CDCl$_3$): δ = 174.5, 59.9, 51.8, 34.7, 29.2, 28.9, 26.7, 20.0, 18.2, 14.9 ppm; IR (film) $\tilde{v}$ = 3406, 2983, 2951, 2866, 1736, 1436, 1375, 1255, 1199, 1166, 1136, 1009 cm^{-1}; HRMS (ESI): *m/z* calcd. for C$_{10}$H$_{18}$O$_3$ [*M*$^+$+Na]: 209.11481; found: 209.11478.
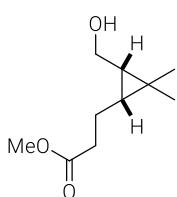
((1*S*,3*R*)-3-(But-3-yn-1-yl)-2,2-dimethylcyclopropyl)methanol (63). DIBAL-H (4.0 mL, 4.0 mmol, 1.0 M in CH$_2$Cl$_2$) was added dropwise to a solution of ester 82 (318.0 mg, 1.7 mmol) in CH$_2$Cl$_2$ (10 mL) −78 °C and the mixture was stirred for 30 min. The reaction was quenched with MeOH (3 mL) and the mixture was stirred for 10 min, aqueous saturated Rochelle solution was added and the mixture warmed to RT. The mixture was diluted with CH$_2$Cl$_2$ (10 mL) and stirred vigorously until both layers were clear. The aqueous layer was extracted with CH$_2$Cl$_2$ (3 × 10 mL). The combined organic phases were washed with brine, dried over MgSO$_4$ and concentrated. The crude aldehyde was used without further purification.
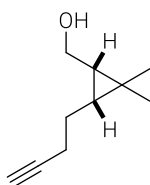
Bestmann-Ohira reagent (492.0 mg, 2.6 mmol) and K$_2$CO$_3$ (471.9 mg, 3.4 mmol) were added to a solution of crude aldehyde 83 in MeOH (24 mL) and the mixture was stirred at RT for 14 h. The mixture was diluted with Et$_2$O (30 mL), washed with aqueous saturated NaHCO$_3$ solution and brine, before it was dried over MgSO$_4$ and concentrated. The residue was purified by flash chromatography (hexane/EtOAc, 10:0 → 5:1) to yield the title compound as a colourless oil (178.0 mg, 1.17 mmol, 68%). [α]$_D^{20}$ = +13.2 (0.87 g/100 mL, CHCl$_3$); ^{1}H NMR (400MHz, CDCl$_3$): δ = 3.66 (m, 2H), 2.26 (tdd, *J* = 7.3, 2.7, 0.8 Hz, 2H), 1.98 (t, *J* = 2.7 Hz, 1H), 1.58 (qd, *J* = 7.1, 5.9 Hz, 2H), 1.42 (br-s, 1H), 1.09 (s, 3H), 1.02 (s, 3H), 0.90 (dt, *J* = 8.9, 7.7 Hz, 1H), 0.71 ppm (dt, *J* = 8.9, 7.1 Hz, 1H); ^{13}C NMR (101 MHz, CDCl$_3$): δ = 84.9, 68.6, 60.1, 29.2, 28.9, 26.8, 23.9, 19.3, 18.3, 15.0 ppm; IR (film) $\tilde{v}$ = 3302, 2982, 2926, 2865, 2116, 1456, 1430, 1376, 1259, 1138, 1023, 1003, 625 cm^{-1}; HRMS (ESI): *m/z* calcd. for C$_{10}$H$_{16}$O [*M*$^+$+Na]: 175.10933; found 175.10941.

((1*S*,3*R*)-3-((*E*)-4-Iodo-3-methylbut-3-en-1-yl)-2,2-dimethylcyclopropyl)methanol (84). AlMe$_3$ (0.32 mL, 630.0 μmol, 2.0 M in toluene) and alkyne 62 (32.0 mg, 210.02 μmol) were added to a pre-stirred (20 min) solution of ZrCp$_2$Cl$_2$ (12.3 mg, 42.0 μmol) in CH$_2$Cl$_2$ (0.8 mL). The resulting mixture was stirred at RT for 15 h. A solution of iodine (106.7 mg, 420.4 μmol) in THF (0.8 mL) was added at −78 °C and the mixture was stirred at −78 °C for 1 h, before it was diluted with CH$_2$Cl$_2$ (2 mL).
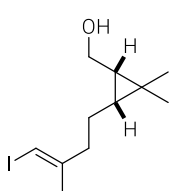
The reaction was quenched with aqueous saturated $Na_2S_2O_3$ solution. The aqueous layer was separated and the organic layer was washed with brine, dried over $MgSO_4$ and concentrated. The residue was purified by flash chromatography (hexane/*tert*-butyl methyl ether, 4:1) to yield the title compound as a colourless oil (8.0 mg, 27.2 µmol, 13%). $[\alpha]_D^{20}$ = +19.4 (0.4 g/100 mL, $CHCl_3$); ^{1}H NMR (400 MHz, $CDCl_3$): δ = 5.88 (q, *J* = 1.2 Hz, 1H), 3.63 (dt, *J* = 7.7, 1.2 Hz, 2H), 2.25 (ddt, *J* = 8.3, 7.0, 1.3 Hz, 2H), 1.83 (s, 3H), 1.47 (m, 2H), 1.07 (s, 3H), 1.01 (s, 3H), 0.84 (m, 1H), 0.57 ppm (m, 1H); ^{13}C NMR (101 MHz, $CDCl_3$): δ = 148.0, 74.9, 60.3, 40.3, 29.4, 28.8, 27.0, 24.1, 23.2, 18.4, 14.9 ppm; IR (film) $\tilde{v}$ = 2958, 2923, 2868, 1705, 1655, 1458, 1377, 1261, 1214, 1090, 1021, 911, 866, 801, 736, 703, 669 cm^{−1}; HRMS (ESI): *m/z* calcd. for $C_{11}H_{19}OI$ [*M*[+]+Na]: 317.03728; found: 317.03723.
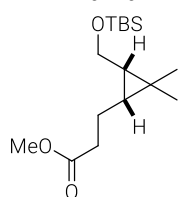
Methyl 3-((1*R*,3*S*)-3-(((*tert*-butyldimethylsilyl)oxy)methyl)-2,2-dimethylcyclopropyl)propanoate (86). TBSCl (291.3 mg, 1.9 mmol) was added to a solution of alcohol **82** (300.0 mg, 1.6 mmol) and imidazole (164.5 mg, 2.4 mmol) in DMF (1 mL) and CH_2Cl_2 (6 mL). The mixture was stirred at RT for 15 min and the reaction was quenched with water. The aqueous layer was separated and the organic layer was washed with brine, dried over $MgSO_4$ and concentrated. The residue was purified by flash chromatography (hexane/EtOAc, 10:1) to yield the title compound as a colourless oil (428.0 mg, 1.4 mmol, 98%). $[\alpha]_D^{20}$ = +7.2 (0.46 g/100 mL, $CHCl_3$); ^{1}H NMR (400 MHz, $CDCl_3$) δ = 3.66 (s, 3H), 3.62 (m, 2H), 2.39 (m, 2H), 1.64 (m, 2H), 1.04 (s, 3H), 0.98 (s, 3H), 0.89 (m, 9H), 0.79 (ddd, *J* = 9.0, 8.1, 7.0 Hz, 1H), 0.57 (dt, *J* = 8.9, 7.4 Hz, 1H), 0.05 (s, 3H), 0.04 ppm (s, 3H). ^{13}C NMR (101 MHz, $CDCl_3$) δ = 174.2, 60.0, 51.4, 34.6, 29.2, 28.5, 26.4, 25.9, 20.3, 18.3, 17.9, 14.8, −5.2 ppm. IR (film) $\tilde{v}$ = 2952, 2929, 2857, 1741, 1472, 1462, 1436, 1361, 1252, 1216, 1193, 1169, 1115, 1070, 1006, 833, 814, 773, 664 cm^{−1}; HRMS (ESI): *m/z* calcd. for $C_{16}H_{32}O_3Si$ [*M*[+]+Na]: 323.20129; found: 323.20123.

((((1*S*,3*R*)-3-(But-3-yn-1-yl)-2,2-dimethylcyclopropyl)methoxy)(*tert*-butyl) dimethyl silane (85). DIBAL-H (2.45 mL, 2.45 mmol, 1.0 M in CH_2Cl_2) was added dropwise to a solution of ester **86** (722.0 mg, 2.40 mmol) in CH_2Cl_2 (14 mL) at −78 °C and the mixture was stirred for 30 min. The reaction was quenched with MeOH (10 mL) and the mixture was stirred for 10 min. An aqueous saturated solution of Rochelle salt was added and the mixture warmed to RT. The mixture was diluted with CH_2Cl_2 (20 mL) and stirred vigorously until both layers were clear. The aqueous layer was extracted with CH_2Cl_2 (3 × 30 mL). The combined organic phases were washed with brine, dried over $MgSO_4$ and concentrated. The crude aldehyde was used without further purification. Bestmann-Ohira reagent (692.3 mg, 3.60 mmol) and K_2CO_3 (664.1 mg, 4.81 mmol) were added to a solution of crude aldehyde **87** in MeOH (34 mL) and the mixture was stirred at RT for 14 h. The mixture was diluted with Et_2O (30 mL), washed with aqueous saturated $NaHCO_3$ solution and brine, before it was dried over $MgSO_4$ and concentrated. The residue was purified by flash chromatography (hexane/*tert*-butyl methyl ether, 1:0 → 10:1) to yield the title compound as a colourless oil (526.0 mg, 1.97 mmol, 82%). $[\alpha]_D^{20}$ = +11.8 (2.06 g/100 mL, $CHCl_3$); ^{1}H NMR (400 MHz, $CDCl_3$): δ = 3.64 (m, 2H), 2.26 (m, 2H), 1.95 (t, *J* = 2.6 Hz, 1H), 1.56 (m, 2H), 1.06 (s, 3H), 0.99 (s, 3H), 0.90 (s, 9H), 0.81 (m, 1H), 0.67 (dt, *J* = 8.9, 7.2 Hz, 1H), 0.05 ppm (s, 6H); ^{13}C NMR (101 MHz, $CDCl_3$): δ = 85.0, 68.2, 60.3, 29.3, 28.7, 26.6, 26.1, 24.3, 19.3, 18.4, 18.2, 15.1, −5.1 ppm; IR (film) $\tilde{v}$ = 3314, 2954, 2929, 2858, 1462, 1252, 1069, 833, 773, 626 cm^{−1}; HRMS (ESI): *m/z* calcd. for $C_{16}H_{30}OSi$ [*M*[+]+Na]: 289.19581; found: 289.19609.

tert-Butyl   (((1S,3R)-3-((E)-4-iodo-3-methylbut-3-en-1-yl)-2,2-dimethylcyclopropyl)methoxy) dimethyl silane (88). AlMe$_3$ (0.19 mL, 375.2 µmol, 2.0 M in toluene) was added to a solution of ZrCp$_2$Cl$_2$ (11.0 mg, 37.5 µmol) in CH$_2$Cl$_2$ (1 mL) and water (3.4 µL, 187.6 µmol). Alkyne **85** (50.0 mg, 187.6 µmol) was added at −7 °C and the mixture was stirred for 1.5 h. A solution of iodine (95.2 mg, 375.2 µmol) in THF (0.5 mL) was added at −78 °C and the resulting mixture was stirred at −78 °C for 2 h, before it was diluted with CH$_2$Cl$_2$ (2 mL). The reaction was quenched with aqueous saturated Na$_2$S$_2$O$_3$ solution. The aqueous layer was separated and the organic layer was washed with brine, dried over MgSO$_4$ and concentrated. The residue was purified by flash chromatography (hexane/tert-butyl methyl ether, 1:0 → 20:1) to yield the title compound as a colourless oil (30.0 mg, 187.6 µmol, 39%). $[\alpha]_D^{20}$ = +20.7 (0.14 g/100 mL, CHCl$_3$); ^{1}H NMR (400 MHz, CDCl$_3$): δ = 5.87 (d, J = 1.1 Hz, 1H), 3.62 (m, 2H), 2.27 (m, 2H), 1.83 (d, J = 1.1 Hz, 3H), 1.44 (m, 2H), 1.04 (s, 3H), 0.96 (s, 3H), 0.89 (s, 9H), 0.77 (ddd, J = 8.9, 8.0, 7.0 Hz, 1H), 0.51 (dt, J = 8.9, 7.2 Hz, 1H), 0.05 ppm (d, J = 1.1 Hz, 6H); ^{13}C NMR (101 MHz, CDCl$_3$): δ = 148.3, 74.7, 60.4, 40.3, 29.4, 28.7, 26.7, 26.1, 24.2, 23.2, 18.4, 18.0, 15.0, −5.0 ppm; IR (film) $\tilde{v}$ = 2928, 2885, 2857, 1978, 1733, 1508, 1472, 1461, 1376, 1361, 1268, 1254, 1228, 1185, 1141, 1078, 1006, 836, 815, 775, 668, 583, 441 cm^{-1}; HRMS (ESI): m/z calcd. for C$_{17}$H$_{33}$IOSi [M$^+$+Na]: 431.12376; found: 431.12426.
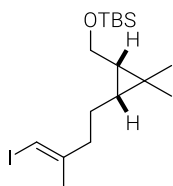
3.2 SECOND APPROACH

3.2.1 FRAGMENT SYNTHESES

((1S,3R)-2,2-Dimethyl-3-vinylcyclopropyl)methanol (94). DIBAL-H (8.2 mL, 6.5 g, 8.2 mmol, 1.0 M in CH$_2$Cl$_2$) was added in dropwise to a solution of the lactone **67** (1.0 g, 8.0 mmol) in CH$_2$Cl$_2$ (21 mL) at −78 °C and the resulting reaction mixture was stirred at −78 °C for 30 min. The reaction mixture was quenched with MeOH (5 mL) at −78 °C, warmed to RT and stirred vigorously with aqueous saturated solution of Rochelle Salt for 1 h. The aqueous layer was extracted with CH$_2$Cl$_2$ (3 × 30 mL). The combined organic phases were dried over MgSO$_4$ and concentrated. The crude was used without further purification.
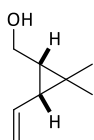
n-BuLi (7.8 mL, 12.0 mmol, 1.6 M in hexane) was added to a solution of methyltriphenylphosphonium bromide (4.3 g, 12.0 mmol) in THF (65 mL) at 0 °C. The mixture was stirred at RT for 30 min. The solution of crude lactol in THF (2 mL) was added to the resulting ylide solution at 0°C and stirred at RT for 20 h. THF (15 mL) was added and the resulting mixture was stirred for additional 5 h. The reaction was quenched with aqueous saturated NH$_4$Cl solution. The aqueous layer was extracted with Et$_2$O (3 × 30 mL). The combined organic phases were dried over MgSO$_4$ and concentrated. The residue was purified by flash chromatography (hexane/Et$_2$O, 3:2) to yield the title compound as a yellow oil (668.0 mg, 5.3 mmol, 66%). $[\alpha]_D^{20}$ = −43.1 (1.17 g/100 mL, CHCl$_3$); ^{1}H NMR (400 MHz, CDCl$_3$) δ = 5.61 (m, 1H), 5.21 (ddd, J = 16.9, 2.1, 0.7 Hz, 1H), 5.06 (ddd, J = 10.3, 2.1, 0.6 Hz, 1H), 3.74 (m, 2H), 1.44 (t, J = 9.3 Hz, 1H), 1.16 (m, 1H), 1.12 (s, 4H), 1.11 ppm (s, 3H); ^{13}C NMR (101 MHz, CDCl$_3$): δ = 134.5, 116.3, 60.4, 32.5, 31.6, 28.9, 22.2, 15.6 ppm; IR (film) $\tilde{v}$ = 3332, 2987, 2945, 2866, 1632, 1454, 1377, 1138, 1016, 988, 895, 725 cm^{-1}; HRMS (ESI): m/z calcd. for C$_8$H$_{14}$O [M$^+$]: 126.10392; found: 126.10402.

(((1S,3R)-2,2-Dimethyl-3-vinylcyclopropyl)ethynyl) triisopropylsilane (90).
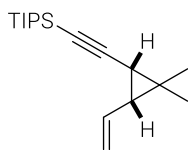
Dess-Martin periodinane (1.98 g, 4.66 mmol) was added to a solution of alcohol **94** (392.0 mg, 3.11 mmol) in CH_2Cl_2 (36 mL) at 0 °C and the resulting mixture was stirred at RT for 3 h. The mixture was diluted with CH_2Cl_2 (50 mL) and stirred rapidly with aqueous saturated solution of $NaHCO_3/Na_2S_2O_3$ (150 mL, vol 1:1) for 30 min. The aqueous layer was extracted with CH_2Cl_2 (3 × 100 mL). The combined organic phases were dried over $MgSO_4$, filtered and concentrated. The crude aldehyde was used without further purification. (Aldehyde **100**: ^{1}H NMR (400 MHz, CDCl$_3$) δ = 9.55 (d, J = 5.7 Hz, 1H), 6.08 (ddd, J = 17.0, 10.4, 9.4 Hz, 1H), 5.20 (m, 2H), 2.10 (ddt, J = 9.3, 8.4, 0.8 Hz, 1H), 1.87 (dd, J = 8.5, 5.7 Hz, 1H), 1.38 (s, 3H), 1.23 ppm (s, 3H).).

The crude aldehyde **100** was added at 0 °C to a mixture of PPh_3 (6.52 g, 24.85 mmol) and CBr_4 (4.12 g, 12.42 mmol) in CH_2Cl_2 (30 mL), which had previously been stirred at RT for 10 min. The resulting mixture was vigorously stirred for 10 min before it was diluted with hexane (30 mL). The suspension was filtered and the filter cake was carefully rinsed with hexane. The combined filtrates were washed with water and brine, dried over $MgSO_4$ and concentrated. The resulting dibromide **101** was used without further purification. (Dibromide **101**: ^{1}H NMR (400 MHz, CD_2Cl_2) δ = 6.30 (d, J = 8.5 Hz, 1H), 5.60 (ddd, J = 16.9, 10.3, 9.2 Hz, 1H), 5.18 (m, 2H), 1.77 (t, J = 9.0 Hz, 1H), 1.70 (t, J = 8.6 Hz, 1H), 1.19 (s, 3H), 1.13 ppm (s, 3H).).

n-BuLi (5.82 mL, 9.32 mmol, 1.6 M in hexane) was added to a solution of the crude dibromide **101** in THF (30 mL) at −78 °C and the mixture was stirred for 1 h. TIPSCl (1.99 mL, 1.80 g, 9.32 mmol) was added at −78 °C and the resulting mixture was warmed overnight to RT. The reaction was quenched with aqueous saturated NH_4Cl solution and MeOH. The aqueous layer was extracted with tert-butyl methyl ether (3 × 20 mL). The combined organic phases were washed with brine, dried over $MgSO_4$ and concentrated. The residue was purified by flash chromatography (hexane) to yield the title compound as a colourless oil (542.0 mg, 1.96 mmol, 63%). $[\alpha]_D^{20}$ = −10.9 (1.17 g/100 mL, CHCl$_3$); ^{1}H NMR (600 MHz, CDCl$_3$): δ = 5.70 (dddd, J = 17.1, 10.4, 8.0, 1.2 Hz, 1H), 5.21 (ddd, J = 17.3, 2.1, 0.5 Hz, 1H), 5.11 (ddd, J = 10.5, 2.1, 0.5 Hz, 1H), 1.53 (m, 2H), 1.17 (s, 3H), 1.12 (s, 3H), 1.06 ppm (m, 21H); ^{13}C NMR (151 MHz, CDCl$_3$): δ = 135.0, 116.2, 106.3, 80.9, 33.9, 27.2, 24.7, 21.8, 18.6, 16.8, 11.3 ppm; IR (film) $\tilde{v}$ = 2942, 2863, 1463, 1437, 1182, 1119, 882, 856, 745, 720, 693, 674, 539, 509 cm^{-1}; HRMS (ESI): m/z calcd. for $C_{18}H_{32}Si$ [M$^+$]: 276.22733; found: 276.22716.

(E)-6-((1R,3S)-2,2-Dimethyl-3-((triisopropylsilyl)ethynyl) cyclopropyl)-4-methyl hex-3-en-1-ol (103).
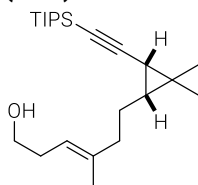
A solution of 9-H-9-BBN (0.45 mL, 0.12 mmol, 0.28 M in toluene) was added to a solution of the terminal alkene **90** (28.5 mg, 0.10 mmol) in toluene (2 mL) in a pressure Schlenk flask. The mixture for stirred at 100 °C for 3 h. The toluene was removed under reduced pressure and the residue was dissolved in THF (2 mL). NaOH (0.31 mL, 0.31 mmol, 1 M in H_2O), alkenyl bromide **102** (17.0 mg, 0.10 mmol) and [(dppf)PdCl$_2$] (3.8 mg, 5.2 mmol, 5 mol%) were added and the mixture was stirred at 75 °C for 3 h. The reaction was quenched with aqueous saturated NH_4Cl solution at RT. The aqueous layer was extracted with Et_2O (3 × 10 mL). The combined organic phases were washed with brine, dried over $MgSO_4$ and concentrated. The residue was purified by flash chromatography (pentane/Et_2O, 10:1) to yield the title compound as a colourless oil (21.0 mg, 58.2 μmol, 56%). $[\alpha]_D^{20}$ = −15.2 (0.04 g/100 mL, CHCl$_3$); ^{1}H NMR (600 MHz, CDCl$_3$): δ = 5.14 (tq, J = 7.3, 1.3 Hz, 1H), 3.62 (t, J = 6.6 Hz, 2H), 2.29 (dddt, J = 7.7, 6.8, 5.9, 0.8 Hz, 2H), 2.15 (m, 1H), 2.05 (m, 1H), 1.65 (m, 3H), 1.55 (m, 2H), 1.23 (d, J = 8.5 Hz, 1H), 1.10 (s, 3H), 1.05 (m, 24H), 0.71 ppm (ddd, J = 8.5, 7.7, 6.4 Hz, 1H); ^{13}C NMR (151 MHz, CDCl$_3$): δ = 139.0, 119.6,

107.3, 79.6, 62.5, 39.1, 31.6, 29.8, 27.6, 24.1, 22.1, 18.8, 18.7, 16.3, 16.2, 11.4 ppm; IR (film) $\tilde{v}$ = 3339, 2942, 2865, 1463, 1382, 1382, 1258, 1048, 882, 824, 673 cm^{-1}; HRMS (ESI): *m/z* calcd. for $C_{23}H_{42}OSi$ [*M*$^+$+Na]: 385.28971; found: 385.29014.

(Z)-4-(4,4,5,5-Tetramethyl-1,3,2-dioxaborolan-2-yl)pent-3-en-1-ol (105). The reaction was carried out according to a literature procedure.[163] CuCl (58.8 mg, 594.4 µmol), PPh$_3$ (187.1 mg, 713.3 µmol) and *t*-BuOK (266.8 mg, 2.4 mmol) were dissolved in THF (5 mL) and the mixture was stirred at RT for 0.5 h. A solution of B$_2$pin$_2$ (3.3 g, 13.1 mmol) in THF (10 mL) was added and the mixture was stirred at RT for 10 min. Subsequently a solution of pentynol **64** (1.0 g, 11.9 mmol) in MeOH (1 mL) and THF (3 mL) was added at 0 °C. The mixture was stirred at RT for 16 h, filtered through a plug of Celite, which was rinsed with Et$_2$O, and the combined filtrates were concentrated. The residue was purified by flash chromatography (hexane/*tert*-butyl methyl ether:CH$_2$Cl$_2$, 7:1:2) to yield the title compound as a colourless oil (2.5 g, 8.9 mmol, 75%). The analytical data match with the reported data.[163] ^{1}H NMR (400 MHz, CDCl$_3$): δ = 6.30 (m, 1H), 3.71 (t, *J* = 6.6 Hz, 2H), 2.43 (qd, *J* = 6.6, 1.0 Hz, 2H), 1.72 (m, 3H), 1.55 (br-s, 1H), 1.26 ppm (s, 12H); ^{13}C NMR (101 MHz, CDCl$_3$): δ = 141.5, 83.4, 62.0, 32.4, 25.0, 14.3 ppm (Signal of alkene $\underline{C}$BO$_2$ is silent); IR (film) $\tilde{v}$ = 3416, 2978, 2930, 2881, 1633, 1368, 1346, 1301, 1146, 1128, 1068, 1047, 858, 666 cm^{-1}; HRMS (ESI): *m/z* calcd. for $C_{11}H_{21}BO_3$ [*M*$^+$+Na]: 235.14759; found: 235.14774.
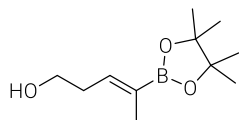
(E)-4-Bromopent-3-en-1-ol (97). A solution of CuBr$_2$ (11.6 g, 51.9 mmol) in water (100 mL) was added to a solution of boronic ester **105** (2.2 g, 10.4 mmol) in EtOH (100 mL) in a pressure Schlenk flask. The resulting mixture was heated to 80 °C immediately and stirred for 14 h. The reaction was quenched with water, followed by dilution with CH$_2$Cl$_2$. The aqueous layer was extracted with CH$_2$Cl$_2$ (3 × 30 mL). The combined organic phases were dried over MgSO$_4$ and concentrated. The residue was purified by flash chromatography (CH$_2$Cl$_2$) to yield the title compound as a colourless oil (1.4 g, 10.4 mmol, 81%). ^{1}H NMR (400 MHz, CDCl$_3$): δ = 5.88 (m, 1H), 3.67 (t, *J* = 6.4 Hz, 2H), 2.30 (tdt, *J* = 7.3, 6.4, 0.9 Hz, 2H), 2.25 ppm (q, *J* = 1.0 Hz, 3H); ^{13}C NMR (101 MHz, CDCl$_3$): δ = 128.3, 122.0, 61.7, 33.2, 23.6 ppm; IR (film) $\tilde{v}$ = 3332, 2951, 2921, 2879, 1651, 1428, 1379, 1186, 1108, 1045, 1011, 844, 636, 504, 421 cm^{-1}; HRMS (ESI): *m/z* calcd. for $C_5H_9OBr^{79}$ [*M*$^+$]: 163.98314; found: 163.98331.
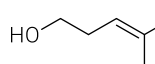
(E)-4-Iodopent-3-en-1-ol (107). *N,N'*-Dimethylethylendiamine (64.8 µL, 602.5 µmol) and alkenyl bromide **97** (1.03 g, 6.21 mmol) were added to a suspension of NaI (7.27 g, 48.48 mmol) and CuI (57.7 mg, 0.30 mmol) in MeOH (10 mL) in a pressure Schlenk flask. The mixture was stirred at 120 °C for 22 h and diluted with CH$_2$Cl$_2$ (5 mL) and water (5 mL). The aqueous layer was extracted with CH$_2$Cl$_2$ (3 × 20 mL). The combined organic phases were dried over MgSO$_4$ and concentrated. The residue was purified by flash chromatography (pentane/Et$_2$O, 1:1) to yield the title compound as a colourless oil (1.07 g, 5.07 mmol, 82%). ^{1}H NMR (400 MHz, CDCl$_3$): δ = 6.20 (td, *J* = 7.6, 1.5 Hz, 1H), 3.66 (t, *J* = 6.4 Hz, 2H), 2.41 (dd, *J* = 1.6, 0.9 Hz, 3H), 2.31 (dtd, *J* = 7.4, 6.5, 1.0 Hz, 2H), 1.43 ppm (br-s, 1H); ^{13}C NMR (101 MHz, CDCl$_3$): δ = 137.2, 96.4, 61.6, 34.1, 27.9 ppm; IR (film) $\tilde{v}$ = 3316, 2948, 2916, 2876, 1637, 1427, 1376, 1184, 1102, 1050, 1011 cm^{-1}; HRMS (ESI): *m/z* calcd. for C_5H_9OI [*M*$^+$]: 211.96926; found: 211.96926.
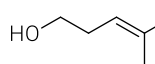
(*E*)-7-Iodooct-6-en-2-yn-4-ol (109). Dess-Martin periodinane (2.08 g, 4.90 mmol) was added to a solution of alcohol **107** (0.69 g, 3.26 mmol) in CH_2Cl_2 (36 mL) at 0 °C and the mixture was stirred at 0 °C for 3 h. The mixture was diluted with CH_2Cl_2 and stirred vigorously with a mixture of aqueous saturated $NaHCO_3$ solution and aqueous saturated $Na_2S_2O_3$ solution (1:1) for 30 min. The aqueous layer was separated and extracted with CH_2Cl_2 (3 × 10 mL). The combined organic phases were dried over $MgSO_4$ and concentrated. The crude aldehyde was used without further purification.
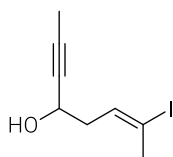
A solution of propynyl magnesium bromide (13.0 mL, 6.5 mmol, 0.5 M in THF) was added rapidly to a solution of crude aldehyde at 0 °C in THF (30 mL) and the mixture was stirred at 0 °C for 3 h. An additional amount of the propynyl magnesium bromide solution (9.8 mL, 4.9 mmol, 0.5 M in THF) was added and the mixture was stirred for 30 min at 0 °C. The reaction was quenched with aqueous saturated NH_4Cl solution. The aqueous layer was extracted with CH_2Cl_2 (3 × 10 mL), and the combined organic layers were dried over $MgSO_4$ and concentrated. The residue was purified by flash chromatography (pentane/Et_2O, 10:1 → 5:1) to yield the title compound as a colourless oil (432.0 mg, 1.7 mmol, 53%). ^{1}H NMR (400 MHz, $CDCl_3$): δ = 6.27 (tq, J = 6.5, 1.3, 0.9 Hz, 1H), 4.36 (tq, J = 6.2, 2.2 Hz, 1H), 2.41 (m, 5H), 1.85 ppm (d, J = 2.1 Hz, 3H); ^{13}C NMR (101 MHz, $CDCl_3$) δ = 135.6, 97.0, 81.9, 79.3, 61.4, 38.9, 28.0, 3.6 ppm; HRMS (ESI): *m/z* calcd. for $C_8H_{11}OI$ [*M*$^+$]: 249.98491; found: 249.98508.

(*E*)-*tert*-Butyl((7-iodooct-6-en-2-yn-4-yl)oxy)diphenylsilane (110). TBDPSCl (677.5 mg, 2.47 mmol) was added to a solution of alcohol **109** (467.0 mg, 1.64 mmol) and imidazole (223.7 mg, 3.29 mmol) in CH_2Cl_2 (13 mL) and DMF (1.3 mL) at RT and the mixture was stirred for 30 min. The mixture was diluted with CH_2Cl_2 and washed with aqueous saturated NH_4Cl solution. The aqueous layer was extracted with CH_2Cl_2 (3 × 10 mL). The combined organic phases were dried over $MgSO_4$ and concentrated. The residue was purified by flash chromatography (pentane/Et_2O, 50:1) to yield the title compound as a colourless oil (835.0 mg, 1.64 mmol, quant.). ^{1}H NMR (400 MHz, $CDCl_3$) δ = 7.71 (ddd, J = 23.3, 7.9, 1.6 Hz, 4H), 7.39 (m, 6H), 6.19 (tq, J = 7.6, 1.6 Hz, 1H), 4.29 (tq, J = 6.2, 2.1 Hz, 1H), 2.33 (m, 2H), 2.27 (dt, J = 1.6, 0.9 Hz, 3H), 1.68 (d, J = 2.1 Hz, 3H), 1.07 (s, 9H); ^{13}C NMR (101 MHz, $CDCl_3$) δ = 136.6, 136.1, 135.9, 133.7, 133.6, 129.7, 129.5, 127.6, 127.3, 96.2, 81.6, 79.8, 62.8, 39.6, 27.8, 26.9, 19.2, 3.5 ppm; IR (film) $\tilde{v}$ = 2957 2930 2856 1472 1427 1360 1105 1071 1052 999 945 821 737 699 610 501 485 422 cm^{-1}; HRMS (ESI): *m/z* calcd. for $C_{24}H_{29}OISi$ [*M*$^+$+Na]: 511.092460; found: 511.09265.
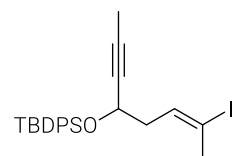
**(*E*)-4-(Trimethylsilyl)pent-3-en-1-ol (111).** *t*-BuLi (33.1 mL, 56.3 mmol, 1.7 M in pentane) was added slowly to a solution of 2,3-dihydronfuran **98** (3.5 mL, 46.4 mmol) in THF (19 mL) at −40 °C and the resulting mixture was stirred at 0 °C for 45 min. A solution of TMSCl (4.9 mL, 38.5 mmol) in THF (5 mL) was added at −78 °C and the mixture was stirred at −78 °C for 10 min, followed by stirring at RT for 45 min. The reaction was quenched with a mixture of aqueous NH_3 solution (25w%) and aqueous saturated NH_4Cl solution (1:1). The aqueous layer was extracted with pentane (2 × 40 mL) and Et_2O (40 mL), the combined organic phases were dried over $MgSO_4$ and concentrated by Kugelrohr distillation (60 °C at atm). The crude product was used as received.
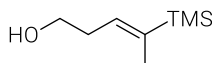
A solution of methyl magnesium bromide (3.2 mL, 9.7 mmol, 3.0 M in Et_2O) was added dropwise to a suspension of [(Ph$_3$P)$_2$NiCl$_2$] (2.5 g, 3.9 mmol, 8 mol%) in toluene (64 mL). The resulting mixture was stirred at RT for 15 min, before additional methyl magnesium bromide solution

(32.3 mL, 97.0 mmol, 3.0 M in Et$_2$O) was added. The mixture was concentrated under reduced pressure. Toluene (85 mL) was added to the residue, followed by a solution of the crude 2-silyldihydrofuran in toluene (9 mL). The resulting mixture was stirred at reflux (110 °C) for 45 min, before the mixture was cooled to 0 °C. The reaction was quenched by pouring the mixture carefully into a vigorously stirred aqueous saturated NH$_4$Cl solution at 0 °C. After stirring the resulting mixture for 20 min, the aqueous layer was extracted with Et$_2$O (4 × 20 mL). The combined organic layers were dried over MgSO$_4$ and concentrated. The residue was purified by flash chromatography (pentane/Et$_2$O, 6:1) to yield the title compound as a colourless oil (5.2 g, 33.0 mmol, 71%). ^{1}H NMR (400 MHz, CDCl$_3$): δ = 5.71 (m, 1H), 3.68 (t, J = 6.6 Hz, 2H), 2.40 (dddd, J = 7.6, 6.7, 5.8, 0.8 Hz, 2H), 1.71 (m, 3H), 0.05 ppm (s, 9H); ^{13}C NMR (101 MHz, CDCl$_3$): δ = 140.3, 134.3, 62.3, 32.1, 14.8, −1.96 ppm; IR (film) $\tilde{v}$ = 3329, 2954, 1619, 1404, 1247, 1046, 832, 748, 689 cm^{-1}; HRMS (ESI): m/z calcd. for C$_8$H$_{18}$OSi [M^+]: 159.11997; found: 159.11980.

(E)-(5-Iodopent-2-en-2-yl) trimethyl silane (112). PPh$_3$ (1.37 g, 5.24 mmol) and N-iodosuccinimide (1.18 g, 5.24 mmol) were added to a solution of trimethylsilyl pentenol **111** (709.0 mg, 4.03 mmol) in CH$_2$Cl$_2$ (13 mL) at 0 °C and the mixture was stirred at 0 °C for 1 h and at RT for 4 h in the dark. The mixture was diluted with pentane (3 mL), filtered through a plug of silica gel, rinsed with pentane (40 mL) and concentrated. The residue was purified by flash chromatography (pentane) to yield the title compound as a yellow oil (781.0 mg, 2.91 mmol, 72%). ^{1}H NMR (400 MHz, CDCl$_3$): δ = 5.62 (m, 1H), 3.15 (t, J = 7.4 Hz, 2H), 2.69 (tdd, J = 7.5, 6.6, 0.9 Hz, 2H), 1.67 (m, 3H), 0.06 ppm (s, 9H); ^{13}C NMR (101 MHz, CDCl$_3$): δ = 141.6, 138.9, 34.7, 16.9, 7.3, 0.0 ppm; IR (film) $\tilde{v}$ = 2955, 1615, 1422, 1246, 1170, 952, 836, 749, 689 cm^{-1}; HRMS (ESI): m/z calcd. for C$_8$H$_{17}$ISi [M^+]: 268.01443; found: 268.01399.

tert-Butyl(((6E,10E)-7-methyl-11-(trimethylsilyl) dodeca-6,10-dien-2-yn-4-yl) oxy) diphenyl silane (113). Iodine (25.4 mg, 0.1 mmol) was added to a suspension of Zn dust (261.4 mg, 4.0 mmol) and DMF (23 mL). The resulting suspension was stirred at RT until it was colourless. Alkyl iodide **112** (536.0 mg, 2.0 mmol) was added and the resulting mixture was stirred at 50 °C for 1 h, before it was filtered through a glasswool frit, rinsing with DMF (2 mL). Alkenyl iodide **110** (781.0 mg, 1.6 mmol) and Pd(PPh$_3$)$_4$ (115.5 mg, 0.1 mmol, 5 mol%) were added and the mixture was stirred at RT for 4 h. The reaction was quenched with aqueous saturated NH$_4$Cl solution. The aqueous layer was extracted with EtOAc (3 × 20 mL). The combined organic phases were dried over MgSO$_4$ and concentrated. The residue was purified by flash chromatography (hexane/toluene, 5:1) to yield the title compound as a colourless oil (554.0 mg, 1.1 mmol, 69%). ^{1}H NMR (400 MHz, CDCl$_3$): δ = 7.72 (ddd, J = 24.8, 7.9, 1.6 Hz, 4H), 7.38 (m, 6H), 5.67 (m, 1H), 5.17 (tt, J = 6.2, 3.5 Hz, 1H), 4.27 (ddt, J = 6.5, 4.4, 2.1 Hz, 1H), 2.34 (td, J = 6.9, 3.7 Hz, 2H), 2.14 (m, 2H), 2.01 (t, J = 7.8 Hz, 2H), 1.67 (d, J = 2.0 Hz, 3H), 1.64 (m, 3H), 1.51 (d, J = 1.3 Hz, 3H), 1.07 (s, 9H), 0.02 ppm (s, 9H); ^{13}C NMR (101 MHz, CDCl$_3$): δ = ^{13}C NMR (101 MHz, CDCl$_3$) δ 138.9, 137.5, 136.1, 136.0, 135.9, 134.0, 134.0, 129.5, 129.4, 127.5, 127.2, 119.6, 80.8, 80.7, 64.1, 39.3, 37.5, 27.0, 26.9, 19.3, 16.3, 14.3, 3.5, −2.08 ppm; IR (film) $\tilde{v}$ = 2955, 2931, 2857, 1428, 1247, 1111, 1073, 835, 740, 701, 613, 504 cm^{-1}; HRMS (ESI): m/z calcd. for C$_{32}$H$_{46}$OSi$_2$ [M^++Na]: 525.29794; found: 525.29801.

tert-Butyl(((6E,10E)-11-iodo-7-methyl dodeca-6,10-dien-2-yn-4-yl) oxy)diphenyl silane (91).
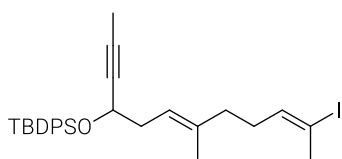
N-Iodosuccinimide (483.2 mg, 2.1 mmol) was added to a suspension of Ag$_2$CO$_3$ (222.0 g, 0.8 mmol) and alkenyl silane **113** (540.0 g, 1.1 mmol) in chloroacetonitrile (18 mL). The reaction mixture was stirred at RT for 3 h in the dark. The reaction was quenched with aqueous saturated Na$_2$S$_2$O$_3$ solution. The aqueous layer was extracted with tert-butyl methyl ether (3 × 50 mL). The combined organic phases were dried over MgSO$_4$ and concentrated. The residue was purified by flash chromatography (hexane/toluene, 10:1) to yield the title compound as a colourless oil (453.0 mg, 0.8 mmol, 76%). ^{1}H NMR (400 MHz, CDCl$_3$) δ = 7.72 (m, 4H), 7.38 (m, 6H), 6.12 (m, 1H), 5.18 (m, 1H), 4.29 (ddt, J = 6.5, 4.3, 2.1 Hz, 1H), 2.35 (m, 5H), 2.04 (ddd, J = 30.7, 8.7, 4.6 Hz, 4H), 1.69 (d, J = 2.1 Hz, 3H), 1.49 (d, J = 1.3 Hz, 3H), 1.07 ppm (s, 9H); ^{13}C NMR (101 MHz, CDCl$_3$): δ = 140.8, 136.4, 136.1, 135.9, 134.0, 133.9, 129.6, 129.4, 127.5, 127.3, 120.4, 93.5, 80.8, 80.7, 64.0, 38.6, 37.5, 29.2, 27.5, 26.9, 19.3, 16.2, 3.5 ppm; IR (film) $\tilde{v}$ = 3071, 3049, 2956, 2929, 2856, 1472, 1427, 1361, 1110, 1073, 940, 822, 739, 701, 613, 505, 487 cm^{-1}; HRMS (ESI): m/z calcd. for C$_{29}$H$_{37}$OSiI [M$^+$+Na]: 579.15506; found: 579.15554.

3.2.2 COMPLETION OF THE TOTAL SYNTHESIS – ENT-DEPRESSIN

tert-Butyl (((6E,10E)-13-((1R,3S)-2,2-dimethyl-3-((triisopropylsilyl) ethynyl) cyclopropyl)-7,11-dimethyltrideca-6,10-dien-2-yn-4-yl)oxy)diphenylsilane (114). A solution of 9-H-9-BBN (5.9 mg, 48.4 μmol) in toluene (1 mL) was added to terminal alkene **90** (10.3 mg, 37.2 μmol) in a pressure Schlenk flask. The reaction mixture for stirred at 100 °C for 2 h. The toluene was removed under reduced pressure and the residue was dissolved in DMF (1 mL). Ba(OH)$_2$·(H$_2$O)$_8$ (14.1 mg, 44.7 mmol), alkenyl iodide **91** (16.4 mg, 29.4 mmol) and [(dppf)PdCl$_2$] (2.7 mg, 3.7 mmol, 10 mol%) were added and the mixture was stirred at RT for 2 h. The reaction was quenched with aqueous saturated NH$_4$Cl solution (2 mL). The aqueous layer was extracted with EtOAc (3 × 10 mL). The combined organic phases were dried over MgSO$_4$ and concentrated. The residue was purified by flash chromatography (hexane/tert-butyl methyl ether, 50:1) to yield the title compound as a colourless oil (17.0 mg, 24.0 μmol, 81%). ^{1}H NMR (400 MHz, CDCl$_3$) δ = 7.72 (ddd, J = 25.3, 7.9, 1.6 Hz, 4H), 7.37 (m, 6H), 5.18 (m, 1H), 5.11 (m, 1H), 4.28 (ddt, J = 6.6, 4.3, 2.1 Hz, 1H), 2.34 (q, J = 6.4 Hz, 2H), 2.03 (m, 6H), 1.67 (d, J = 2.1 Hz, 3H), 1.58 (d, J = 1.3 Hz, 3H), 1.51 (m, 5H), 1.21 (d, J = 8.5 Hz, 1H), 1.07 (m, 36H), 0.71 ppm (dt, J = 8.5, 7.0 Hz, 1H); ^{13}C NMR (101 MHz, CDCl$_3$): δ = 137.9, 136.2, 136.0, 135.1, 134.2, 134.1, 129.7, 129.5, 127.6, 127.4, 124.3, 119.6, 107.6, 81.0, 80.9, 79.7, 64.3, 40.0, 39.2, 37.7, 30.0, 27.8, 27.1, 26.8, 24.3, 22.3, 19.5, 19.0, 18.8, 16.5, 16.4, 16.2, 11.6, 3.62 ppm; IR (film) $\tilde{v}$ = 2941, 2862, 2152, 1462, 1428, 1381, 1363, 1261, 1110, 1072, 997, 940, 883, 822, 739, 701, 677, 612, 505 cm^{-1}; HRMS (ESI): m/z calcd. for C$_{47}$H$_{70}$OSi$_2$ [M$^+$+Na]: 729.48574; found: 729.48627.
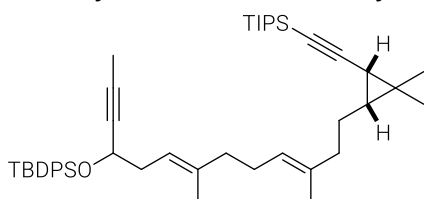
(6E,10E)-13-((1R,3R)-3-Ethynyl-2,2-dimethyl cyclopropyl)-7,11-dimethyltrideca-6,10-dien-2-yn-4-ol (92). TBAF (4.1 mL, 4.1 mmol, 1.0 M in THF) was added to a solution of TMS-protected alkyne **114** (487.0 mg, 0.7 mmol) at 0 °C and the resulting mixture was stirred at 0 °C for 1 h and for 3 h at RT. The reaction was quenched with aqueous saturated NH$_4$Cl solution. The aqueous layer was separated and extracted with tert-butyl
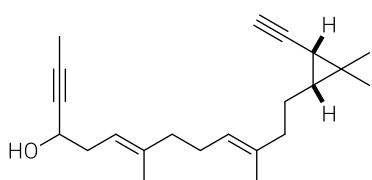
methyl ether (3 × 10 mL). The combined organic phases were dried over MgSO₄ and concentrated. The residue was purified by flash chromatography (hexane/EtOAc, 15:1) to yield the title compound as a colourless oil (206.0 mg, 0.7 mmol, 96%). ^{1}H NMR (400 MHz, CDCl₃): δ = 5.23 (m, 1H), 5.13 (m, 1H), 4.32 (qq, J = 6.1, 2.1 Hz, 1H), 2.41 (m, 2H), 2.06 (m, 6H), 1.89 (d, J = 2.2 Hz, 1H), 1.85 (d, J = 2.1 Hz, 3H), 1.80 (d, J = 5.8 Hz, 1H), 1.65 (s, 3H), 1.61 (s, 3H), 1.49 (dtd, J = 8.7, 7.0, 3.3 Hz, 2H), 1.15 (dd, J = 8.6, 2.2 Hz, 1H), 1.09 (s, 3H), 1.06 (s, 3H), 0.72 ppm (dt, J = 8.6, 7.1 Hz, 1H); ^{13}C NMR (101 MHz, CDCl₃): δ = 139.7, 135.7, 124.2, 118.6, 83.4, 80.8, 80.2, 67.5, 62.3, 39.9, 39.1, 36.8, 29.3, 27.6, 26.5, 24.1, 21.6, 17.2, 16.4, 16.03, 15.98, 3.6 ppm; IR (film) $\tilde{v}$ = 3312, 2983, 2919, 2860, 2109, 1665, 1451, 1378, 1327, 1261, 1122, 986, 882, 808, 688, 636, 551, 456 cm^{-1}; HRMS (ESI): m/z calcd. for C₂₂H₃₂O [M⁺+Na]: 335.23453; found: 335.23427.

tert-Butyl (((6*E*,10*E*)-13-((1*R*,3*R*)-3-ethynyl-2,2-dimethylcyclopropyl)-7,11-dimethyl trideca-6,10-dien-2-yn-4-yl) oxy) dimethyl silane (116).

 Imidazole (88.4 mg, 1.30 mmol) and TBSCl (0.12 mL, 105.9 mg, 0.97 mmol) were added to a solution of propargylic alcohol **92** (203.0 mg, 0.65 mmol) in CH₂Cl₂ (8 mL) and DMF (0.5 mL). The mixture was stirred at RT for 2 h. The reaction was quenched with aqueous saturated NH₄Cl solution. The aqueous layer was extracted with CH₂Cl₂ (3 × 20 mL). The combined organic phases were dried over MgSO₄ and concentrated. The residue was purified by flash chromatography (hexane/toluene, 10:1) to yield the title compound as a colourless oil (206.0 mg, 0.48 mmol, 74%). ^{1}H NMR (400 MHz, CDCl₃): δ = 5.20 (m, 1H), 5.15 (ddt, J = 6.9, 5.6, 1.3 Hz, 1H), 4.26 (tq, J = 6.6, 2.0 Hz, 1H), 2.34 (m, 2H), 2.05 (m, 6H), 1.88 (d, J = 2.3 H, 1H), 1.82 (d, J = 2.1 Hz, 3H), 1.63 (s, 3H), 1.61 (s, 3H), 1.49 (m, 2H), 1.15 (dd, J = 8.6, 2.2 Hz, 1H), 1.09 (s, 3H), 1.06 (s, 3H), 0.90 (s, 9H), 0.72 (dt, J = 8.6, 7.1 Hz, 1H), 0.11 (s, 3H), 0.09 ppm (s, 3H); ^{13}C NMR (101 MHz, CDCl₃): δ = 137.5, 134.9, 124.4, 119.8, 83.4, 81.1, 79.8, 67.5, 63.4, 39.9, 39.2, 37.8, 29.3, 27.6, 26.6, 24.1, 21.6, 18.3, 17.2, 16.4, 15.99, 15.96, 3.6, 1.0, −4.6, −5.0 ppm; IR (film) $\tilde{v}$ = 3315, 2955, 2927, 2856, 2116, 1461, 1378, 1361, 1256, 1078, 1023, 940, 834, 805, 776, 637, 588 cm^{-1}; HRMS (ESI): m/z calcd. for C₂₈H₄₆OSi [M⁺+Na]: 449.32101; found: 449.32096.
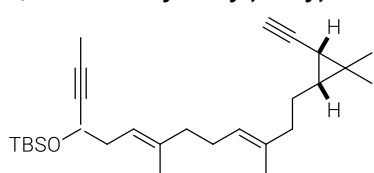
tert-Butyl(((6*E*,10*E*)-13-((1*R*,3*S*)-2,2-dimethyl-3-(prop-1-yn-1-yl)cyclopropyl)-7,11-dimethyl trideca-6,10-dien-2-yn-4-yl)oxy) dimethyl silane (118).

 n-BuLi (0.30 mL, 0.45 mmol, 1.5 M in hexane) was added dropwise to a solution of terminal alkyne **116** (95.0 mg, 0.22 mmol) in THF (4 mL) at −78 °C and the mixture was stirred at −78 °C for 1 h. Methyl iodide (69.3 µL, 1.1 mmol) was added dropwise and the mixture was stirred at RT for 2 h. The reaction was quenched with water at 0 °C, the aqueous layer was extracted with *tert*-butyl methyl ether (3 × 50 mL). The combined organic phases were dried over MgSO₄ and concentrated. The residue was purified by flash chromatography (hexane/toluene, 10:1) to yield the title compound as a colourless oil (72.0 mg, 0.16 mmol, 73%). ^{1}H NMR (400 MHz, CDCl₃): δ = 5.20 (m, 1H), 5.14 (m, 1H), 4.26 (ddt, J = 6.8, 4.6, 2.1 Hz, 1H), 2.34 (m, 2H), 2.04 (m, 6H), 1.82 (t, J = 2.2 Hz, 6H), 1.63 (s, 3H), 1.61 (s, 3H), 1.45 (m, 2H), 1.09 (dq, J = 8.6, 2.2 Hz, 1H), 1.05 (s, 3H), 1.03 (s, 3H), 0.90 (s, 9H), 0.63 (m, 1H), 0.11 (s, 3H), 0.09 ppm (s, 3H); ^{13}C NMR (101 MHz, CDCl₃): δ = 137.6, 135.2, 124.3, 119.8, 81.1, 79.8, 77.6, 74.9, 63.4, 39.9, 39.4, 37.8, 29.0, 27.7, 26.7, 25.8, 24.3, 21.0, 18.3, 17.8, 16.4, 16.1, 15.9, 3.7, 3.6, −4.6, −5.0 ppm; IR (film) $\tilde{v}$ = 2951, 2926, 2856, 1471, 1461, 1451, 1378, 1361, 1341, 1251, 1136, 1078, 1005, 940, 834, 776, 668 cm^{-1}; HRMS (ESI): m/z calcd. for C₂₉H₄₈OSi [M⁺+Na]: 463.33666; found: 463.33669.
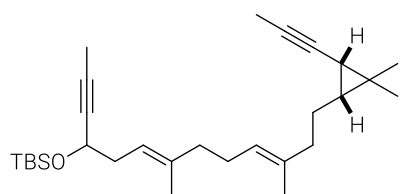
tert-Butyl dimethyl (((1_S_,6_E_,10_E_,14_R_)-7,11,15,15-tetramethyl bicyclo[12.1.0]penta deca-6,10-dien-2-yn-4-yl)oxy) silane (117). MS 5 (100 mg) was added to a solution of diyne **118** (72.0 mg, 0.16 mmol) in toluene (100 mL) and the mixture was stirred at RT for 1 h. In a different Schlenk flask a solution of trisilanol **52b** (12.8 mg, 16.3 µmol) and molybdenum complex **49** (10.8 mg, 16.3 mmol) in toluene (1 mL) was stirred at RT for 3 min and then added to the preheated diyne **118** suspension at 65 °C. The mixture was stirred at 65 °C for 2 h. An additionally freshly prepared solution of trisilanol **52b** (12.8 mg, 16.3 µmol) and molybdenum complex **49** (10.8 mg, 16.3 mmol) in toluene (1 mL) was added to the mixture and stirring continued at 65 °C for 2 h. The mixture was cooled to RT and the reaction was quenched with EtOH. The mixture was filtered through a pad of Celite®, rinsing with toluene, and the combined filtrates were concentrated. The residue was purified by flash chromatography (hexane/toluene 10:1) to yield the title compound as a colourless oil as a mixture of isomers (44.0 mg, 0.13 mmol, 70%). The diastereomers were separated by flash chromatography (hexane/toluene, 20:1) for characterisation purposes.
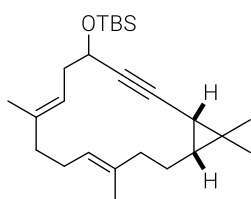
Analytical and spectral data of Fraction A: $[\alpha]_D^{20}$ = −7.6 (0.17 g/100 mL, CHCl$_3$); ^{1}H NMR (500 MHz, CDCl$_3$): δ = 5.06 (m, 2H), 4.36 (ddd, _J_ = 9.9, 4.2, 1.7 Hz, 1H), 2.37 (ddd, _J_ = 13.8, 6.9, 4.4 Hz, 1H), 2.27 (ddd, _J_ = 14.3, 9.8, 6.7 Hz, 1H), 2.26 (m, 1H), 2.10 (t, _J_ = 8.1 Hz, 1H), 2.01 (m, 4H), 1.82 (m, 1H), 1.60 (d, _J_ = 1.4 Hz, 3H), 1.56 (d, _J_ = 1.2 Hz, 3H), 1.16 (dd, _J_ = 8.3, 1.6 Hz, 1H), 1.09 (m, 1H), 1.06 (s, 3H), 1.04 (s, 3H), 0.91 (s, 9H), 0.69 (ddd, _J_ = 11.0, 8.3, 2.6 Hz, 1H), 0.14 (s, 3H), 0.13 ppm (s, 3H); ^{13}C NMR (126 MHz, CDCl$_3$): δ = 135.9, 135.8, 124.0, 121.0, 83.2, 81.7, 63.7, 39.9, 39.6, 37.9, 30.4, 27.5, 26.5, 25.9, 23.9, 21.9, 18.3, 17.8, 16.3, 15.7, 15.4, 1.13, 1.01, −4.45, −4.83 ppm; IR (film) $\tilde{v}$ = 3348, 2954, 2928, 2856, 2218, 1710, 1460, 1378, 1258, 1066, 1047, 861, 836, 801, 778, 740, 669 cm^{-1}; HRMS (ESI): _m/z_ calcd. for C$_{25}$H$_{42}$OSi [_M_$^+$+Na]: 409.28971; found: 409.28979.

Analytical and spectral data of Fraction B: $[\alpha]_D^{20}$ = +29.1 (0.11 g/100 mL, CHCl$_3$); ^{1}H NMR (600 MHz, CDCl$_3$): δ = 5.19 (m, 1H), 5.07 (m, 1H), 4.47 (ddd, _J_ = 8.9, 3.9, 2.0 Hz, 1H), 2.45 (dt, _J_ = 14.0, 8.6 Hz, 1H), 2.24 (m, 1H), 2.13 (m, 4H), 1.99 (m, 2H), 1.74 (m, 1H), 1.62 (d, _J_ = 1.3 Hz, 3H), 1.60 (s, 3H), 1.22 (m, 1H), 1.18 (dd, _J_ = 8.3, 2.0 Hz, 1H), 1.04 (s, 3H), 1.02 (s, 3H), 0.91 (s, 9H), 0.64 (ddd, _J_ = 10.3, 8.3, 2.3 Hz, 1H), 0.14 (s, 3H), 0.11 ppm (s, 3H); ^{13}C NMR (151 MHz, CDCl$_3$): δ = 136.2, 135.1, 123.9, 120.5, 83.4, 81.8, 63.5, 39.6, 39.4, 37.5, 30.4, 27.5, 25.9, 25.0, 24.1, 22.0, 18.4, 18.3, 16.7, 16.5, 16.0, −4.51, −5.01 ppm; IR (film) $\tilde{v}$ = 3354, 2953, 2925, 2854, 2217, 1711, 1461, 1377, 1258, 1079, 1020, 836, 799, 780, 739, 702 cm^{-1}; HRMS (ESI): _m/z_ calcd. for C$_{25}$H$_{42}$OSi [_M_$^+$+Na]: 409.28971; found: 409.28954.

(1_S_,6_E_,10_E_,14_R_)-7,11,15,15-Tetramethylbicyclo[12.1.0]pentadeca-6,10-dien-2-yn-4-ol (93). PPTS (214.5 mg, 0.85 mmol) was added to a solution of TBS-protected macrocycle **117** (55.0 mg, 0.14 mmol) in MeOH (5 mL) and CH$_2$Cl$_2$ (1 mL) and the resulting mixture stirred at RT for 6.5 h. The reaction was quenched with aqueous saturated NaHCO$_3$ solution, the aqueous layer was separated and extracted with _tert_-butyl methyl ether (4 × 5 mL). The combined organic phases were dried over MgSO$_4$ and concentrated. The residue was purified by flash chromatography (hexane/EtOAc 10:1) to yield the title compound as a colourless oil (31.0 mg, 113.8 µmol, 80%) and the starting material as a colourless oil (8.0 mg, 20.7 µmol, 15%). The diastereomers were separated by flash chromatography (hexane/EtOAc, 20:1) for characterisation purposes.
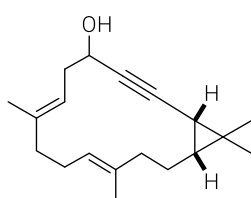
Analytical and spectral data of Fraction A: $[\alpha]_D^{20}$ = +73.3 (0.06 g/100 mL, CHCl$_3$); ^{1}H NMR (600 MHz, CDCl$_3$): δ = 5.11 (m, 2H), 4.52 (tdd, *J* = 7.5, 3.4, 1.8 Hz, 1H), 2.49 (dt, *J* = 14.2, 8.1 Hz, 1H), 2.32 (m, 1H), 2.17 (m, 2H), 2.08 (m, 2H), 2.02 (m, 2H), 1.81 (m, 1H), 1.80 (d, *J* = 7.5 Hz, 1H), 1.63 (s, 3H), 1.63 (s, 3H), 1.20 (dd, *J* = 8.3, 1.9 Hz, 1H), 1.15 (m, 1H), 1.05 (s, 3H), 1.04 (m, 3H), 0.74 ppm (ddd, *J* = 10.7, 8.3, 2.5 Hz, 1H); ^{13}C NMR (151 MHz, CDCl$_3$) δ = 137.7, 135.9, 123.8, 119.8, 84.5, 80.9, 62.6, 39.8, 39.3, 36.1, 30.5, 27.4, 25.7, 24.1, 22.2, 18.0, 16.3, 16.2, 16.1 ppm; IR (film) $\tilde{v}$ = 3397, 2923, 2855, 2230, 2194, 1719, 1666, 1452, 1377, 1260, 1091, 1019, 798, 737, 702, 525 cm^{-1}; HRMS (ESI); *m/z* calcd. for C$_{19}$H$_{28}$O [*M*$^+$]: 272.21347; found: 272.21363.

Analytical and spectral data of Fraction B: $[\alpha]_D^{20}$ = +25.7 (0.14 g/100 mL, CHCl$_3$); ^{1}H NMR (600 MHz, CDCl$_3$): δ = 5.06 (m, 2H), 4.40 (dddd, *J* = 9.7, 5.7, 4.1, 1.7 Hz, 1H), 2.47 (m, 1H), 2.27 (ddd, *J* = 13.9, 9.8, 7.0 Hz, 1H), 2.17 (m, 1H), 2.11 (dd, *J* = 9.5, 7.2 Hz, 1H), 2.01 (m, 4H), 1.84 (dddd, *J* = 13.5, 11.1, 6.8, 2.5 Hz, 1H), 1.78 (d, *J* = 5.5 Hz, 1H), 1.61 (d, *J* = 1.4 Hz, 3H), 1.58 (q, *J* = 0.9 Hz, 3H), 1.18 (dd, *J* = 8.4, 1.7 Hz, 1H), 1.06 (m, 7H), 0.74 ppm (ddd, *J* = 11.0, 8.3, 2.6 Hz, 1H); ^{13}C NMR (151 MHz, CDCl$_3$): δ = 136.7, 135.9, 124.1, 120.0, 84.5, 81.2, 63.0, 39.7, 39.6, 36.8, 30.6, 27.4, 26.4, 23.9, 22.1, 17.7, 16.1, 15.8, 15.6 ppm; IR (film) $\tilde{v}$ = 3263, 2930, 2850, 2231, 1668, 1452, 1378, 1325, 1294, 1261, 1228, 1092, 1015, 853, 832, 802, 525 cm^{-1}; HRMS (ESI): *m/z* calcd. for C$_{19}$H$_{29}$O [*M*$^+$]: 273.22129; found: 273.22092.

(1*R*,2*Z*,6*E*,10*E*,14*R*)-7,11,15,15-Tetramethyl-3-(tributylstannyl)bicyclo[12.1.0]pentadeca-2,6,10-trien-4-ol (119).

A solution of Bu$_3$SnH (0.2 M in CH$_2$Cl$_2$, 0.9 mL, 49.7 µmol) was added dropwise to a solution of [Cp*RuCl]$_4$ (3.1 mg, 11.4 µmol, 2.5 mol%) and alkyne **93** (31.0 mg, 113.8 µmol) in CH$_2$Cl$_2$ (2 mL) at RT. The mixture was stirred for 1.5 h before it was concentrated. The residue was purified by flash chromatography (hexane/EtOAc, 20:1) to yield the title compound as a colourless oil (51.3 mg, 91.0 µmol, 80%). *Analytical and spectral data of both diastereomers:* ^{1}H NMR (400 MHz, CDCl$_3$) δ = 5.96 (dd, *J* = 10.2, 1.7 Hz, 1H, *trans*), 5.81 (d, *J* = 10.3 Hz, 1H, *cis*), 5.97 (m, 3H, *cis, trans*), 4.86 (td, *J* = 6.7, 3.5 Hz, 1H, *cis*), 4.42 (td, *J* = 7.1, 3.6 Hz, 1H, *trans*), 4.11 (dt, *J* = 11.0, 3.2 Hz, 1H, *cis*), 2.58 (dt, *J* = 14.9, 7.6 Hz, 1H, *trans*), 2.39 (m, 1H, *cis*), 2.25 (dd, *J* = 13.8, 7.0 Hz, 3H, *cis, trans*), 2.13 (dd, *J* = 12.9, 6.4 Hz, 7H, *cis, trans*), 2.02 (m, 1H, *trans*), 1.86 (m, 5H, *cis, trans*), 1.65 (s, 3H, *trans*),1.62 (s, 3H, *cis*), 1.60 (s, 3H, *trans*), 1.59 (s, 3H, *cis*), 1.50 (dddd, *J* = 16.7, 7.7, 6.4, 4.6 Hz, 12H, cis, trans), 1.42 (d, *J* = 2.6 Hz, 1H, *cis*), 1.33 (m, 13H, *cis, trans*), 1.19 (m, 2H, cis*, trans*), 1.11 (m, 2H, *cis, trans*), 1.06 (s, 3H, *trans*), 1.06 (s, 3H, *cis*), 1.00 (dd, *J* = 8.3, 4.0 Hz, 6H, *cis*), 0.92 (m, 30H, *cis, trans*), 0.69 ppm (dddd, *J* = 20.3, 10.2, 8.5, 1.5 Hz, 2H, *cis, trans*). ^{13}C NMR (101 MHz, CDCl$_3$) δ = 147.1, 144.2, 139.4, 136.9, 135.4, 134.88, 134.85, 134.3, 125.0, 124.2, 120.4, 117.4, 82.5, 74.5, 40.0, 39.8, 38.7, 38.4, 36.4, 34.2, 32.4, 32.0, 31.7, 30.6, 29.3, 29.3, 28.9 (2 ×), 27.6 (2 ×), 24.3, 24.12, 24.08, 23.2, 22.1, 22.0, 17.4, 17.3, 17.2, 16.9, 15.7, 15.6, 13.7 (2 ×), 11.3, 10.4 ppm. IR (film) $\tilde{v}$ = 2953, 2921, 2870, 2853, 1607, 1455, 1375, 1289, 1192, 1020, 874, 664, 594, 504, 451 cm^{-1}; HRMS (ESI): *m/z* calcd. for C$_{31}$H$_{56}$OSn [*M*$^+$+Na]: 587.32453; found: 587.32451.
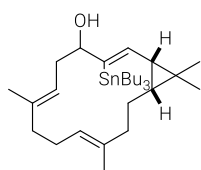
(1*S*,2*E*,6*E*,10*E*,14*R*)-3,7,11,15,15-Pentamethylbicyclo[12.1.0] pentadeca-2,6,10-trien-4-ol (120).
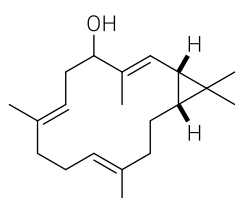
Pd(PPh$_3$)$_4$ (2.1 mg, 1.8 µmol, 5 mol%) was added to a solution of alkenyl stannane **119** (19.8 mg, 35.1 mmol) and [Ph$_2$PO$_2$]$^-$[Bu$_4$N]$^+$ (17.8 mg, 38.7 µmol) in DMF (0.2 mL) and the mixture was stirred for 10 min. Methyl iodide (3.3 µL, 7.5 mg, 52.7 µmol) was added, immediately followed (after 10 sec !) by CuTC (7.0 mg, 36.9 µmol). The resulting mixture was stirred at

RT for 4 h. The reaction was quenched with aqueous Et$_3$N (0.1 ml), the mixture was diluted with *tert*-butyl methyl ether and washed with aqueous NH$_3$ (25%)/NH$_4$Cl solution (1:9). The aqueous layer was extracted with *tert*-butyl methyl ether (3 × 10 mL). The combined organic phases were dried over MgSO$_4$ and concentrated. The residue was purified by flash chromatography (hexane/EtOAc, 10:1) to yield the title compound as a colourless oil (6.3 mg, 62%).

Analytical and spectral data of Fraction A: $[\alpha]_D^{23}$ = +56.7 (0.03 g/100 mL, CHCl$_3$); ^{1}H NMR (600 MHz, CDCl$_3$): δ = 5.20 (dp, J = 8.9, 1.4 Hz, 1H), 4.95 (t, J = 7.0 Hz, 2H), 4.19 (m, 1H), 2.44 (m, 2H), 2.20 (dt, J = 13.7, 6.8 Hz, 1H), 2.10 (m, 2H), 1.95 (m, 1H), 1.86 (dt, J = 13.6, 7.0 Hz, 1H), 1.79 (m, 1H), 1.71 (d, J = 1.1 Hz, 3H), 1.60 (d, J = 1.3 Hz, 3H), 1.59 (d, J = 1.2 Hz, 3H), 1.50 (d, J = 6.3 Hz, 1H), 1.27 (m, 1H), 1.08 (s, 3H), 0.99 (m, 1H), 0.96 (s, 3H), 0.68 ppm (ddd, J = 10.5, 8.8, 1.6 Hz, 1H); ^{13}C NMR (151 MHz, CDCl$_3$): δ = 137.1, 136.3, 135.6, 124.1, 119.8, 118.2, 74.4, 40.3, 39.1, 32.5, 31.2, 28.9, 25.7, 24.3, 24.1, 20.5, 16.7, 16.5, 15.7, 15.6 ppm; IR (film) $\tilde{\nu}$ = 3281, 2956, 2925, 2853, 1455, 1376, 1288, 1260, 1090, 1017, 995, 863, 799, 705, 570, 523 cm^{-1}; HRMS (ESI): m/z calcd. for C$_{20}$H$_{32}$O [M^++Na]: 311.23453; found: 311.23398.

Analytical and spectral data of Fraction C: $[\alpha]_D^{23}$ = +90.0 (0.05 g/100 mL, CHCl$_3$); ^{1}H NMR (600 MHz, CDCl$_3$): δ = 5.10 (dqd, J = 8.9, 1.3, 0.4 Hz, 1H), 4.94 (ddddd, J = 6.6, 5.3, 3.9, 2.4, 1.2 Hz, 1H), 4.77 (m, 1H), 4.08 (ddd, J = 11.2, 4.4, 2.5 Hz, 1H), 2.41 (ddd, J = 14.4, 11.2, 8.5 Hz, 1H), 2.30 (m, 1H), 2.20 (m, 1H), 2.10 (m, 3H), 1.87 (m, 2H), 1.73 (m, 1H), 1.69 (d, J = 1.3 Hz, 3H), 1.60 (m, 3H), 1.58 (m, 3H), 1.42 (d, J = 2.7 Hz, 1H), 1.26 (m, 1H), 1.06 (s, 3H), 0.95 (s, 3H), 0.63 ppm (ddd, J = 10.2, 8.8, 1.4 Hz, 1H); ^{13}C NMR (151 MHz, CDCl$_3$): δ = 137.2, 135.2, 135.0, 125.9, 123.4, 120.5, 79.4, 40.4, 39.3, 33.1, 31.5, 28.8, 25.5, 24.0, 23.6, 20.5, 16.7, 16.1, 15.7, 10.4 ppm; IR (film) $\tilde{\nu}$ = 3357, 2917, 2850, 1727, 1671, 1452, 1377, 1260, 1016, 872, 816, 729, 631, 545, 468 cm^{-1}; HRMS (ESI): m/z calcd. for C$_{20}$H$_{32}$O [M^++Na]: 311.23453; found: 311.23398.

***ent*-Depressin (89).** MnO$_2$ (40.0 mg, 0.46 mmol) was added to a solution of allylic alcohol **120**
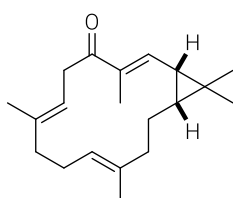
(5.3 mg, 18.4 µmol) in CH$_2$Cl$_2$ (0.5 mL) and the resulting mixture was stirred at RT for 2 h. Additional MnO$_2$ (40.0 mg, 0.46 mmol) was added and the mixture was stirred at RT for 2 h. The mixture was filtered through a plug of silica gel, rinsing with CH$_2$Cl$_2$, and concentrated. The residue was purified by flash chromatography (fine silica, hexane/EtOAc, 10:1) to yield the title compound as a colourless oil (4.3 mg, 15.0 µmol, 82%). $[\alpha]_D^{20}$ = +72.0 (0.05 g/100 mL, CHCl$_3$); ^{1}H NMR (600 MHz, CDCl$_3$): δ = 6.38 (dq, J = 10.2, 1.3 Hz, 1H), 5.07 (ddq, J = 8.2, 5.7, 1.2 Hz, 1H), 4.84 (m, 1H), 3.55 (dd, J = 13.8, 8.6 Hz, 1H), 2.98 (ddm, J = 13.9, 5.6 Hz, 1H), 2.16 (m, 2H), 2.08 (m, 2H), 2.02 (m, 1H), 1.98 (m, 1H), 1.87 (d, J = 1.3 Hz, 3H), 1.75 (ddd, J = 12.8, 9.8, 2.9 Hz, 1H), 1.57 (s, 3H), 1.56 (s, 3H), 1.49 (dd, J = 10.2, 8.5 Hz, 1H), 1.16 (s, 3H), 1.14 (ddd, J = 12.5, 8.5, 2.5 Hz, 1H), 1.09 (s, 3H), 0.86 ppm (m, 1H); ^{13}C NMR (151 MHz, CDCl$_3$) δ = 199.9, 143.2, 137.2, 136.7, 135.9, 124.4, 119.4, 39.9, 39.4, 39.0, 35.2, 29.0, 27.7, 26.3, 25.4, 23.9, 15.9, 15.6, 15.3, 11.7 ppm; IR (film) $\tilde{\nu}$ = 2975, 2925, 2860, 1653, 1625, 1453, 1379, 1318, 1262, 1152, 1110, 1064, 1040, 1021, 918, 870, 827, 801, 733, 595, 523 cm^{-1}; HRMS (ESI): m/z calcd. for C$_{20}$H$_{31}$O [M^+]: 287.23694; found: 287.23676.

Table 12. NMR data of natural product depressin (**9**) and synthetic *ent*-depressin (**89**).

	depressin (**9**)	synthetic **89**		depressin (**9**)	synthetic **89**
$[\alpha]_D$	−80.0°, c = 0.26	+72.0°, c = 0.05			
	¹H NMR δ [ppm] (*J* [Hz])			**¹³C NMR** δ [ppm]	
1	1.15	1.14 (ddd, 12.5, 8.5, 2.5)	1	35.2	35.2
2	1.50 (dd, 10.2, 8.7)	1.49 (dd, 10.2, 8.5)	2	27.6	27.7
3	6.37 (d, 10.2)	6.38 (dq, 10.2, 1.3)	3	143.1	143.2
4	-	-	4	136.6	136.7
5	-	-	5	199.9	199.9
6a	3.55 (dd, 13.8, 5.7)	3.55 (dd, 13.8, 8.6)	6	39.4	39.4
6b	2.97 (dd, 13.8, 5.7)	2.98 (ddm, 13.9, 5.6)	7	119.4	119.4
7	5.08 (t, 6.6)	5.07 (ddq, 8.2, 5.7, 1.2)	8	137.1	137.2
8	-	-	9	39.0	39.0
9a	2.15	2.09	10	23.9	23.9
9b	2.00	2.01	11	124.4	124.4
10a	2.17	2.16	12	135.9	135.9
10b	1.96	1.98	13	39.9	39.9
11	4.84 (t, 5.4)	4.84	14	26.3	26.3
12	-	-	15	25.4	25.4
13a	2.20	2.19	16	29.0	29.0
13b	1.75	1.75 (ddd, 12.8, 9.8, 2.9)	17	15.8	15.9
14a	2.05	2.06	18	11.6	11.7
14b	0.80	0.86	19	15.6	15.6
15	-	-	20	15.3	15.3
16	1.16	1.16			
17	1.09	1.09			
18	1.87	1.87			
19	1.56	1.57			
20	1.56	1.56			

3.3 FINAL APPROACH

3.3.1 FRAGMENT SYNTHESES

(1S,5R)-6,6-Dimethyl-3-oxabicyclo[3.1.0]hexan-2-one (80). A solution of diazo ester **70** (5.15 g, 33.41 mmol) in CH_2Cl_2 (17 mL) was added to a clear violet solution of $[Rh_2(5S\text{-MEPY})_4]\cdot(MeCN)_2$ (168.3 mg, 196.5 µmol, 0.6 mol%) in CH_2Cl_2 (110 mL) at reflux temperature via syringe pump over the course of 18 h. Once the addition was complete, stirring was continued for an additional 30 min before the mixture was cooled to RT and concentrated. The residue was purified by flash chromatography (hexane/EtOAc, 10:1 → 3:1) to give the title compound as a colourless oil (3.68 g, 87%, 93% ee). $[\alpha]_D^{20}$ = +86.9 (1.09 g/100 mL, $CHCl_3$); ^{1}H NMR (400 MHz, $CDCl_3$): δ = 4.36 (dd, J = 9.9, 5.5 Hz, 1H), 4.15 (dt, J = 9.9, 1.1 Hz, 1H), 2.04 (ddd, J = 6.5, 5.5, 1.1 Hz, 1H), 1.95 (dd, J = 6.3, 1.0 Hz, 1H), 1.18 (s, 3H), 1.17 ppm (s, 3H); ^{13}C NMR (101 MHz, $CDCl_3$) δ = 175.0, 66.5, 30.5, 30.0, 25.2, 23.0, 14.4 ppm; IR (film) $\tilde{v}$ = 2961, 2909, 2878, 1766, 1458, 1382, 1361, 1283, 1217, 1178, 1118, 1092, 1049, 1023, 974, 958, 892, 857 cm^{-1}; HRMS (ESI): m/z calcd. for $C_7H_{10}O_2$ [M^++Na]: 149.05730; found: 149.05725.
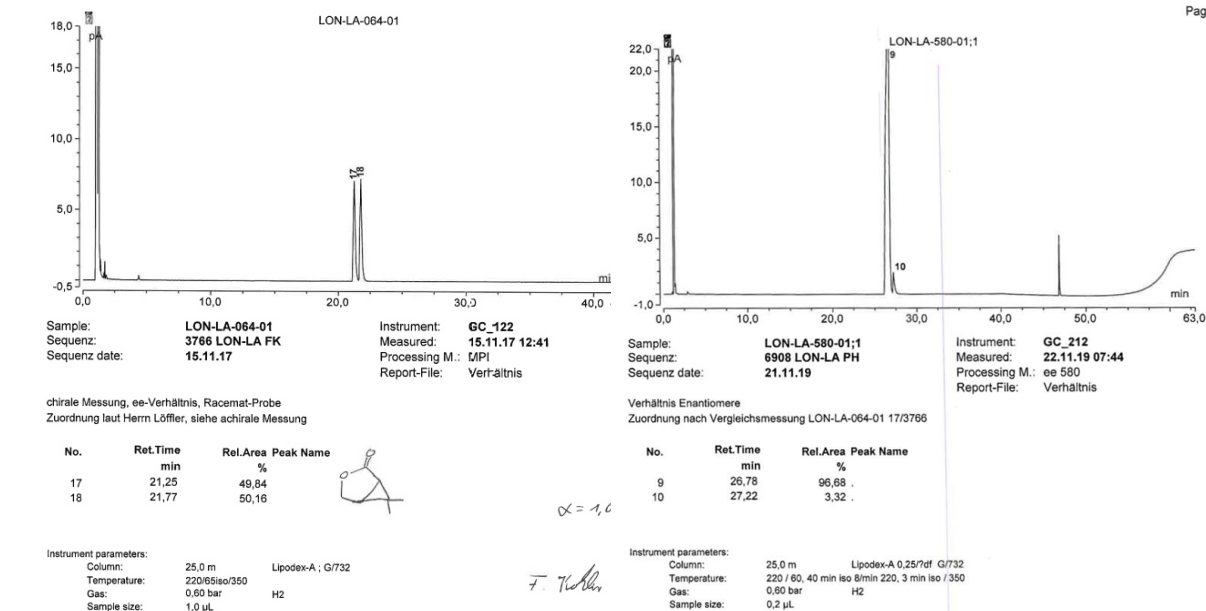
((1R,3S)-2,2-Dimethyl-3-vinylcyclopropyl)methanol (126). DIBAL-H (1.0 M in CH_2Cl_2, 9.06 mL, 9.06 mmol) was added dropwise to a solution of lactone **80** (1.12 g, 8.89 mmol) in CH_2Cl_2 at −78 °C and the resulting mixture was stirred for 30 min at this temperature. The reaction was quenched at −78 °C with MeOH, followed by addition of saturated aqueous Rochelle Salt solution. The resulting mixture was rapidly stirred at RT for 1 h before the aqueous layer was separated and extracted with CH_2Cl_2 (3 × 30 mL). The combined organic phases were dried over $MgSO_4$ and concentrated, and the crude lactol was used without further purification.

n-BuLi (1.6 M in hexane, 16.66 mL, 26.66 mmol) was added to a suspension of methyltriphenylphosphonium bromide (9.52 g, 26.66 mmol) in THF (84 mL) at 0 °C and the resulting suspension was stirred at RT for 1 h. A solution of the lactol in THF (2 mL) was added to the ylide suspension at 0 °C and the resulting mixture was stirred at RT for 3 h. The reaction was quenched with saturated aqueous NH_4Cl solution, and the aqueous layer was separated

and was extracted with Et_2O (3 × 20 mL). The combined organic phases were dried over $MgSO_4$ and concentrated. The residue was purified by flash chromatography (pentane/Et_2O, 10:1) to yield the title compound as a colourless oil (614 mg, 55%). $[\alpha]_D^{20}$ = +44.2 (1.29 g/100 mL, $CHCl_3$); ^{1}H NMR (400 MHz, $CDCl_3$): δ = 5.62 (dt, J = 16.9, 10.1 Hz, 1H), 5.21 (ddd, J = 17.0, 2.1, 0.7 Hz, 1H), 5.06 (ddd, J = 10.3, 2.1, 0.6 Hz, 1H), 3.72 (m, 2H), 1.44 (t, J = 9.3 Hz, 1H), 1.17 (m, 1H), 1.13 (s, 3H), 1.11 ppm (s, 3H); ^{13}C NMR (101 MHz, $CDCl_3$): δ = 134.3, 116.1, 60.3, 32.3, 31.3, 28.7, 22.0, 15.4 ppm; IR (film) $\tilde{v}$ = 3330, 3081, 2986, 2946, 2925, 2866, 1632, 1454, 1377, 1259, 1165, 1017, 988, 896, 801, 725, 661 cm^{-1}; HRMS (ESI): m/z calcd. for $C_8H_{14}O$ [M^++H]: 127.11174; found: 127.11160.

(2R,3S)-1,1-Dimethyl-2-(prop-1-yn-1-yl)-3-vinylcyclopropane (124). Dess-Martin-periodinane (2.6 g, 6.2 mmol) was added to a solution of alcohol **126** (523.0 mg, 4.1 mmol) in CH_2Cl_2 (40 mL) at 0 °C. The resulting mixture was stirred at 0 °C for 10 min, followed by stirring at RT for 4 h. The reaction was quenched with saturated aqueous $NaHCO_3$/$Na_2S_2O_3$ solution (1:1 v/v, 50 mL). The mixture was rapidly stirred for 30 min, the aqueous layer was separated and extracted with CH_2Cl_2 (3 × 30 mL), the organic phases were dried over $MgSO_4$, filtered and concentrated, and the resulting aldehyde **134** was used without further purification.
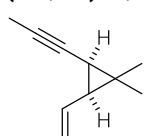
The crude aldehyde **134** was added at 0 °C to a mixture of PPh_3 (8.70 g, 33.15 mmol) and CBr_4 (5.50 g, 16.58 mmol) in CH_2Cl_2 (40 mL), which had previously been stirred at RT for 10 min. The resulting mixture was vigorously stirred for 10 min before it was diluted with pentane (10 mL). The suspension was filtered through a plug of Celite®, which was carefully rinsed with pentane (20 mL). The combined filtrates were washed with water and brine, dried over $MgSO_4$ and concentrated. The resulting dibromide was used without further purification.

n-BuLi (1.6 M in hexane, 12.95 mL, 20.72 mmol) was added to a solution of the dibromide **135** in Et_2O (65 mL) at −78 °C and the mixture was stirred for 1 h at this temperature. DMPU (3.01 mL, 3.19 g, 24.87 mmol) was added at −78 °C, followed, after 10 min, by MeI (3.87 mL, 8.82 g, 62.17 mmol) . The resulting mixture was warmed to RT overnight. The reaction was quenched with saturated aqueous NH_4Cl solution, and the aqueous layer was separated and extracted with pentane (2 × 10 mL) and Et_2O (1 × 10 mL). The combined organic phases were washed with saturated aqueous NaCl solution, dried over $MgSO_4$ and concentrated. The residue was purified by flash chromatography (pentane) to yield the title compound as a colourless oil (262.0 mg, 51%). $[\alpha]_D^{20}$ = +82.6 (0.99 g/100 mL, $CHCl_3$); ^{1}H NMR (600 MHz, CD_2Cl_2): δ = 5.65 (ddd, J = 17.2, 10.4, 9.4 Hz, 1H), 5.18 (ddd, J = 17.1, 2.2, 0.6 Hz, 1H), 5.08 (ddd, J = 10.4, 2.1, 0.6 Hz, 1H), 1.81 (d, J = 2.2 Hz, 3H), 1.44 (dd, J = 9.3, 8.4 Hz, 1H), 1.40 (dq, J = 8.3, 2.2 Hz, 1H), 1.11 (s, 3H), 1.08 ppm (s, 3H); ^{13}C NMR (151 MHz, CD_2Cl_2): δ = 136.0, 115.8, 76.9, 76.5, 33.6, 27.3, 24.1, 21.2, 16.9, 3.7 ppm; HRMS (ESI): m/z calcd. for $C_{10}H_{14}$ [M^+]: 134.10900; found: 134.10911.

(2S,3S)-1,1-Dimethyl-2-(prop-1-yn-1-yl)-3-vinylcyclopropane (157). Dess-Martin-periodinane (10.15 g, 23.93 mmol) was added to a solution of alcohol **126** (1.51 g, 12.96 mmol) in CH_2Cl_2 (115 mL) at 0 °C. The resulting mixture was stirred at 0 °C for 10 min and for another 4 h at RT. The reaction was quenched with saturated aqueous $NaHCO_3$/$Na_2S_2O_3$ solution (200 mL, vol 1:1). The mixture was rapidly stirred for 30 min before the aqueous layer was separated and extracted with CH_2Cl_2 (3 × 40 mL). The combined organic phases were dried over $MgSO_4$, filtered and concentrated, and the resulting crude aldehyde **134** was used without further purification.
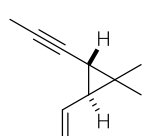
K$_2$CO$_3$ (8.3 g, 59.83 mmol) was added to a solution of the crude aldehyde in MeOH (50 mL). The resulting suspension was stirred at 50 °C for 3 h. The reaction was quenched at RT with saturated aqueous NH$_4$Cl solution. The aqueous layer was separated and extracted with CH$_2$Cl$_2$ (3 × 40 mL), and the combined organic phases were dried over MgSO$_4$ and concentrated. The resulting aldehyde 2-*epi*-**158** was used without further purification.

This crude aldehyde was added to a mixture of PPh$_3$ (25.11 g, 95.72 mmol) and CBr$_4$ (15.87 g, 47.86 mmol) in CH$_2$Cl$_2$ (115 mL) at 0 °C, which had previously been stirred at RT for 10 min. After 10 min, the mixture was diluted with pentane and the suspension filtered through a plug of Celite, which was carefully rinsed with pentane. The combined filtrates were washed with water and brine, dried over MgSO$_4$ and concentrated. The resulting dibromide was used without further purification.

n-BuLi (1.6 M in hexane, 37.4 mL, 59.83 mmol) was added to a solution of the crude dibromide in Et$_2$O (100 mL) at −78 °C and the mixture was stirred for 1 h. DMPU (8.7 mL, 71.79 mmol) was added at −78°C, followed, after 10 min, by MeI (11.17 mL, 179.48 mmol). The resulting mixture was warmed to RT overnight before the reaction was quenched with saturated aqueous NH$_4$Cl solution. The aqueous layer was separated and extracted with pentane (3 × 10 mL), and the combined organic phases were washed with saturated aqueous NaCl solution, dried over MgSO$_4$ and concentrated. The residue was purified by flash chromatography (pentane) to yield the title compound as a colourless oil (1.02 g, 63%, *cis/trans* = 1:9). $[\alpha]_D^{20}$ = −66.9 (2.08 g/100 mL, CHCl$_3$); ^{1}H NMR (600 MHz, CD$_2$Cl$_2$): δ = 5.50 (dddd, *J* = 17.0, 10.3, 8.9, 0.4 Hz, 1H), 5.12 (ddd, *J* = 17.0, 1.9, 0.8 Hz, 1H), 5.01 (ddd, *J* = 10.3, 1.9, 0.6 Hz, 1H), 1.78 (d, *J* = 2.1 Hz, 3H), 1.37 (dd, *J* = 8.8, 5.1 Hz, 1H), 1.19 (s, 3H), 1.14 (dd, *J* = 5.0, 2.3 Hz, 1H), 1.05 ppm (s, 3H); ^{13}C NMR (151 MHz, CD$_2$Cl$_2$): δ = 137.0, 115.3, 78.7, 74.8, 38.2, 25.2, 23.0, 22.2, 20.8, 3.6 ppm; HRMS (ESI): *m/z* calcd. for C$_{10}$H$_{14}$ [*M*$^+$+H]: 135.11683; found: 135.11686.

(*E*)-4-(Dimethyl(phenyl)silyl)pent-3-en-1-ol (130).

PhMe$_2$SiCl (7.39 mL, 7.51 g, 44.00 mmol) was added to a suspension of lithium sand (916 mg, 132.0 mmol) in THF (120 mL) at −10 °C. The resulting mixture was stirred at −10 °C for 36 h. [The titer of the PhMe$_2$SiLi solution was determined by addition of an aliquot of the resulting mixture (2 mL) to water (5 mL) followed by titration with HCl (1 M in water)].
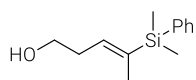
The resulting PhMe$_2$SiLi solution (102.00 mL, 37.74 mmol, 0.37 M in THF) was added dropwise to a suspension of CuCN (1.69 g, 18.87 mmol, dried at 120 °C for 14 h under high vacuum prior to use) in THF (5 mL) at −78 °C. The resulting mixture was stirred at −30 °C for 30 min before it was cooled to −78 °C.

n-BuLi (1.59 M in hexane, 98.7 mL, 16.98 mmol) was added dropwise to a solution of 3-pentyn-1-ol **64** (1.43 g, 16.98 mmol) in Et$_2$O at −78 °C. The mixture was stirred at −30 °C for 20 min before it was cooled to −78 °C. The resulting mixture was added dropwise to the solution of the higher order silyl cuprate at −78 °C. The mixture was stirred at −78 °C for 1 h before the reaction was quenched with saturated aqueous NH$_4$Cl/NH$_3$ solution. The aqueous layer was separated and extracted with ethyl acetate (3 × 200 mL). The combined organic phases were washed with brine, dried over MgSO$_4$ and concentrated. The residue was purified by flash chromatography (hexane/EtOAc, 10:1) to yield the title compound as a colourless oil (3.38 g, 90%). ^{1}H NMR (400 MHz, CDCl$_3$): δ = 7.49 (m, 2H), 7.35 (dd, *J* = 5.0, 1.8 Hz, 3H), 5.82 (ddt, *J* = 6.9, 5.2, 1.8 Hz, 1H), 3.69 (t, *J* = 6.6 Hz, 2H), 2.43 (dddd, *J* = 7.6, 6.7, 5.8, 0.9 Hz, 2H), 1.71 (dd, *J* = 1.7, 0.9 Hz, 3H), 1.46 (s, 1H), 0.34 ppm (s, 6H); ^{13}C NMR (101 MHz, CDCl$_3$): δ = 138.3, 138.1, 136.5, 133.9, 128.9, 127.7, 62.1, 32.1, 15.0, −3.5 ppm; IR (film) $\tilde{\nu}$ = 3337, 3068, 2956, 1618, 1427, 1248,

1110, 1045, 831, 814, 773, 731, 700, 638, 473 cm^{-1}; HRMS (ESI): m/z calcd. for $C_{13}H_{21}OSi$ [M^+]: 221.13562; found: 221.13540.

(4,5-Dihydrofuran-2-yl)dimethyl(phenyl)silane (EP-2). n-BuLi (1.6 M in hexane, 73.0 mL, 116.8 mmol) was added to a solution of 2,3-dihydrofuran **98** (9.5 mL, 8.8 g, 125.6 mmol) in THF (45 mL) at −30 °C. The resulting mixture was stirred for 30 min at this temperature and for another 30 min at RT. The solution was cooled to −30°C before PhMe$_2$SiCl (15.0 mL, 15.3 g, 89.4 mmol) was introduced and stirring was continued for 30 min. The mixture was slowly warmed over 1 h and stirred at RT for 12 h. The reaction was quenched with aqueous saturated NH$_4$Cl solution. The aqueous layer was separated and extracted with pentane (3 × 200 mL). The combined organic phases were washed with aqueous saturated NaCl solution, dried over MgSO$_4$ and concentrated. The residue was filtered through a plug of basic alumina, rinsing with pentane, and the combined filtrates were concentrated. The residue was purified by flash chromatography (hexane/EtOAc, 50:1) to yield the title compound as a colourless oil (18.7 g, quant.). ^{1}H NMR (400 MHz, CDCl$_3$): δ = 7.58 (m, 2H), 7.36 (m, 3H), 5.25 (t, J = 2.6 Hz, 1H), 4.31 (t, J = 9.6 Hz, 2H), 2.60 (td, J = 9.6, 2.6 Hz, 2H), 0.42 ppm (s, 6H); ^{13}C NMR (101 MHz, CDCl$_3$): δ = 160.7, 136.8, 133.9, 129.3, 127.8, 113.1, 70.6, 30.7, −3.5 ppm; IR (film) $\tilde{v}$ = 3393, 3070, 2958, 1768, 1733, 1428, 1406, 1252, 1190, 1152, 1118, 1041, 998, 868, 830, 782, 736, 700, 645, 471, 447 cm^{-1}. HRMS (ESI): m/z calcd. for $C_{12}H_{16}OSi$ [M^++H]: 205.10432; found: 205.10418.

(E)-4-(Dimethyl(phenyl)silyl)pent-3-en-1-ol (130). MeMgBr (3.0 M in Et$_2$O, 77.0 mL, 231.0 mmol) was added to a suspension of [(PPh$_3$)$_2$NiCl$_2$] (3.8 g, 5.8 mmol, 8 mol%) in toluene (50 mL). The resulting mixture was stirred at RT for 20 min before the bulk of the solvent was removed under reduced pressure and the dark residue was suspended in toluene (461 mL). A solution of compound **EP-2** (14.8 g, 72.1 mmol) in toluene (50 mL) was added and the resulting mixture stirred at 105 °C (bath temperature) for 30 h. After cooling to RT, the reaction was quenched with aqueous saturated NH$_4$Cl solution. The aqueous layer was separated and extracted with $tert$-butyl methyl ether (3 × 200 mL). The combined organic phases were washed with aqueous saturated NaCl solution, dried over MgSO$_4$ and concentrated. The residue was purified by flash chromatography (hexane/EtOAc, 10:1) to yield the title compound as a colourless oil (14.5 g, 91%). Spectral data as described above.

(E)-7-(Dimethyl(phenyl)silyl)oct-6-en-2-yn-4-ol (131). Dess-Martin-periodinane (9.53 g, 22.46 mmol) was added to a solution of alcohol **130** (3.30 g, 14.97 mmol) in CH$_2$Cl$_2$ (144 mL) at 0 °C. The resulting mixture was stirred at 0 °C for 15 min, followed by stirring at RT for 4 h. The mixture was diluted with CH$_2$Cl$_2$ (50 mL) and stirred rapidly with saturated aqueous NaHCO$_3$/Na$_2$S$_2$O$_3$ solution (1:1 v/v, 50 mL) for 30 min. The aqueous layer was separated and extracted with CH$_2$Cl$_2$ (3 × 100 mL). The organic phases were dried over MgSO$_4$, filtered and concentrated. The resulting aldehyde **139** was used without further purification.

Propynyl magnesium bromide (0.5 M in THF, 100.0 mL, 50.0 mmol) was rapidly added to a solution of the crude aldehyde **139** in THF (390 mL) at 0 °C and the resulting mixture was stirred at 0 °C for 5 h. The reaction was quenched with saturated aqueous NH$_4$Cl (30 mL). The aqueous layer was separated and extracted with EtOAc (3 × 100 mL). The combined organic phases were washed with saturated aqueous NaCl solution, dried over MgSO$_4$ and concentrated. The residue

was purified by flash chromatography (hexane/EtOAc, 10:1) to yield the title compound as a yellow oil (3.01 g, 78%). ^{1}H NMR (400 MHz, CDCl$_3$): δ = 7.50 (m, 2H), 7.34 (m, 3H), 5.91 (ddt, J = 6.8, 5.1, 1.8 Hz, 1H), 4.40 (tt, J = 6.4, 2.1 Hz, 1H), 2.54 (m, 2H), 1.83 (d, J = 2.1 Hz, 3H), 1.70 (m, 3H), 1.65 (s, 1H), 0.35 ppm (d, J = 0.7 Hz, 6H); ^{13}C NMR (101 MHz, CDCl$_3$): δ = 138.5, 138.4, 135.2, 133.9, 128.9, 127.7, 81.2, 80.0, 62.1, 37.2, 15.2, 3.5, −3.5 ppm; IR (film) $\tilde{v}$ = 3341, 3068, 2956, 2918, 2856, 1619, 1427, 1247, 1147, 1110, 1028, 830, 810, 772, 729, 699, 638, 471 cm^{-1}; HRMS (ESI): m/z calcd. for C$_{16}$H$_{22}$OSi [M^++Na]: 281.13321; found: 281.13354.

(E)-tert-Butyl-((7-(dimethyl(phenyl)silyl)oct-6-en-2-yn-4-yl)oxy)diphenylsilane (140).
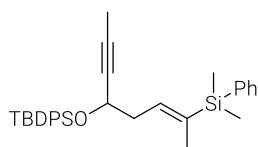
Imidazole (0.48 g, 7.04 mmol) and TBDPSCl (1.37 mL, 1.45 g, 5.28 mmol) were added to a solution of propargylic alcohol **131** (0.91 g, 3.52 mmol) in CH$_2$Cl$_2$ (45 mL) and DMF (3 mL) and the resulting mixture was stirred at RT for 1 h. The reaction was quenched with saturated aqueous NH$_4$Cl solution and the aqueous layer was extracted with CH$_2$Cl$_2$ (3 × 15 mL). The combined organic phases were dried over MgSO$_4$ and concentrated. The residue was purified by flash chromatography (hexane/EtOAc, 10:1) to yield the title compound as a colourless oil (1.75 g, 84%). ^{1}H NMR (400 MHz, CDCl$_3$): δ = 7.73 (ddd, J = 25.2, 8.0, 1.5 Hz, 4H), 7.49 (m, 2H), 7.36 (m, 9H), 5.95 (tt, J = 5.0, 1.8 Hz, 1H), 4.39 (ddt, J = 6.4, 4.3, 2.1 Hz, 1H), 2.50 (m, 2H), 1.63 (d, J = 2.1 Hz, 3H), 1.60 (m, 3H), 1.07 (s, 9H), 0.31 ppm (d, J = 2.4 Hz, 6H); ^{13}C NMR (101 MHz, CDCl$_3$): δ = 138.6, 136.6, 136.5, 136.1, 135.9, 134.0, 133.9, 129.6, 129.4, 128.7, 127.6, 127.5, 127.2, 81.1, 80.5, 63.6, 37.8, 26.9, 19.3, 15.0, 3.4, −3.4 ppm; IR (film) $\tilde{v}$ = 3069, 2957, 2931, 2857, 1472, 1427, 1110, 1079, 819, 773, 736, 700, 612, 505, 486 cm^{-1}; HRMS (ESI): m/z calcd. for C$_{32}$H$_{40}$OSi$_2$ [M^++Na]: 519.25099; found: 519.25144.

(E)-tert-Butyl-((7-iodooct-6-en-2-yn-4-yl)oxy)diphenylsilane (128).
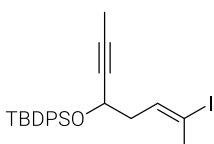
N-Iodosuccinimide (2.35 g, 10.45 mmol) was added to a solution of 2,6-lutidine (3.20 mL, 2.95 g, 27.50 mmol), hexafluoro-iso-propanol (HFIP) (20.85 mL, 33.28 g, 198.0 mmol) and compound **140** (2.73 g, 5.50 mmol) in CH$_2$Cl$_2$ (236 mL) at −20 °C. The mixture was stirred at −20 °C for 4 h before the reaction was quenched with saturated aqueous Na$_2$S$_2$O$_3$ solution and MeOH at this temperature. The aqueous layer was separated and extracted with $tert$-butyl methyl ether (3 × 100 mL). The combined organic phases were dried over MgSO$_4$ and concentrated, and the residue was purified by flash chromatography (hexane/toluene, 10:1) to yield the title compound as a colourless oil (2.40 g, 89%). ^{1}H NMR (400 MHz, CDCl$_3$): δ = 7.72 (m, 4H), 7.39 (m, 6H), 6.19 (ddt, J = 9.2, 7.7, 1.5 Hz, 1H), 4.29 (ddt, J = 6.1, 4.1, 2.1 Hz, 1H), 2.33 (m, 2H), 2.27 (m, 3H), 1.68 (d, J = 2.1 Hz, 3H), 1.07 ppm (s, 9H); ^{13}C NMR (101 MHz, CDCl$_3$): δ = 136.6, 136.1, 135.9, 133.7, 133.6, 129.7, 129.5, 127.6, 127.3, 96.2, 81.6, 79.8, 62.8, 39.6, 27.8, 26.9, 19.2, 3.5 ppm; IR (film) $\tilde{v}$ = 2930, 2856, 1427, 1105, 1071, 1052, 945, 821, 737, 699, 610, 501, 485 cm^{-1}; HRMS (ESI): m/z calcd. for C$_{24}$H$_{29}$OSi [M+Na$^+$]: 511.09246; found: 511.09265.

(E)-(5-Iodopent-2-en-2-yl)dimethyl(phenyl)silane (141).
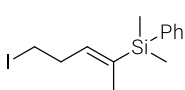
PPh$_3$ (384 mg, 1.46 mmol), imidazole (99.6 mg, 1.46 mmol) and iodine (371 mg, 1.46 mmol) were added to a solution of alcohol **130** (215 mg, 0.976 mmol) in CH$_2$Cl$_2$ (4 mL) at 0 °C. The mixture was warmed to RT over 30 min and the reaction was quenched with water (2 mL). The aqueous layer was separated and extracted with pentane (3 × 10 mL). The combined organic phases were dried over MgSO$_4$ and concentrated, and the residue was purified by flash chromatography (pentane) to yield the title compound as a colourless oil (300 mg, 93%).

^{1}H NMR (400 MHz, CDCl$_3$): δ = 7.51 (m, 2H), 7.35 (dd, *J* = 4.9, 1.9 Hz, 3H), 5.72 (m, 1H), 3.17 (t, *J* = 7.3 Hz, 2H), 2.73 (tdd, *J* = 7.5, 6.6, 0.9 Hz, 2H), 1.67 (m, 3H), 0.35 ppm (s, 6H); ^{13}C NMR (101 MHz, CDCl$_3$): δ = 139.0, 138.1, 137.5, 134.0, 128.9, 127.7, 32.6, 15.0, 4.9, −3.5 ppm; IR (film) $\tilde{v}$ = 3067, 3007, 2956, 1615, 1427, 1245, 1171, 1110, 950, 831, 813, 773, 731, 700, 638, 473 cm^{-1}; HRMS (ESI): *m/z* calcd. for C$_{13}$H$_{19}$ISi [*M*$^+$]: 330.02953; found: 330.02986.

tert-Butyl-(((6*E*,10*E*)-11-(dimethyl(phenyl)silyl)-7-methyldodeca-6,10-dien-2-yn-4-yl)oxy)diphenyl-silane (142).
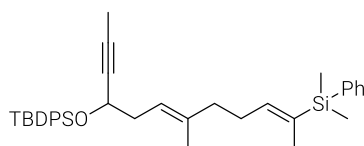
A thoroughly dried Schlenk flask was charged with LiCl (95.3 mg, 2.3 mmol) and Zn dust (267.5 mg, 4.1 mmol) and was then heated under vacuum. After reaching ambient temperature, THF (24 mL) was added, followed by 1,2-diiodoethane (26.0 mg, 92.1 µmol) and TMSCl (23.4 µL, 20.0 mg, 184.2 µmol). The resulting suspension was stirred for 2 min at reflux temperature to ensure activation of the zinc dust.

Alkyl iodide **141** (699.8 mg, 2.1 mmol) was added and the mixture was stirred at RT for 3 h before it was filtered through a glasswool filter that was rinsed with THF (2 mL). Alkenyl iodide **128** (793.1 mg, 1.6 mmol) was added to the solution of the organozinc derivative, followed by Pd(PPh$_3$)$_4$ (106.5 mg, 92.1 µmol, 6 mol%). The resulting mixture was stirred at RT for 3 h before it was diluted with toluene (10 mL) and filtered through a plug of Celite®, which was carefully rinsed with toluene (20 mL). The combined filtrates were concentrated and the residue purified by flash chromatography (hexane/toluene, 10:1) to give the title compounds as a colourless oil (753.2 mg, 82%). ^{1}H NMR (400 MHz, CDCl$_3$): δ = 7.72 (ddd, *J* = 25.1, 7.9, 1.6 Hz, 4H), 7.48 (m, 2H), 7.36 (m, 9H), 5.78 (m, 1H), 5.18 (m, 1H), 4.28 (ddt, *J* = 6.5, 4.3, 2.1 Hz, 1H), 2.35 (td, *J* = 7.0, 3.5 Hz, 2H), 2.18 (m, 2H), 2.02 (t, *J* = 7.8 Hz, 2H), 1.66 (d, *J* = 2.1 Hz, 3H), 1.63 (s, 3H), 1.51 (s, 3H), 1.07 (s, 9H), 0.30 ppm (s, 6H); ^{13}C NMR (101 MHz, CDCl$_3$): δ = 141.3, 138.8, 137.4, 136.1, 135.9, 134.02, 133.95, 133.93, 133.90, 129.5, 129.4, 128.7, 127.6, 127.4, 127.2, 119.7, 80.78, 80.75, 64.1, 39.2, 37.5, 27.1, 26.9, 19.3, 16.2, 14.7, 3.5, −3.4 ppm; IR (film) $\tilde{v}$ = 3069, 2957, 2931, 2857, 1617, 1472, 1428, 1247, 1111, 1074, 940, 815, 773, 737, 701, 613, 505 cm^{-1}; HRMS (ESI): *m/z* calcd. for C$_{37}$H$_{48}$OSi$_2$ [*M*+Na$^+$]: 587.31359; found: 587.31403.

tert-Butyl(((6*E*,10*E*)-11-iodo-7-methyldodeca-6,10-dien-2-yn-4-yl)oxy)diphenylsilane (91).
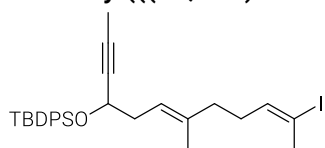
N-Iodosuccinimide (367.2 mg, 1.6 mmol) was added to a suspension of Ag$_2$CO$_3$ (168.8 g, 0.6 mmol) and alkenyl silane **142** (461.0 g, 0.8 mmol) in chloroacetonitrile (13 mL). The reaction mixture was stirred at RT for 5 h in the absence of light. The reaction was quenched with aqueous saturated Na$_2$S$_2$O$_3$ solution. The aqueous layer was separated and extracted with MTBE (3 × 10 mL). The combined organic phases were dried over MgSO$_4$ and concentrated. The residue was purified by flash chromatography (hexane/toluene 20:1) to yield the title compound as a colourless oil (251.0 mg, 55%, *E:Z* = 10:1). ^{1}H NMR (400 MHz, CDCl$_3$) δ = 7.72 (ddd, *J* = 24.9, 7.9, 1.5 Hz, 1H), 7.38 (m, 6H), 6.11 (td, *J* = 7.2, 1.5 Hz, 1H), 5.17 (tt, *J* = 6.0, 1.3 Hz, 1H), 4.29 (tq, *J* = 6.5, 2.2 Hz, 1H), 2.34 (m, 5H), 2.07 (p, *J* = 8.2, 7.4 Hz, 2H), 2.00 (m, 2H), 1.69 (d, *J* = 2.1 Hz, 3H), 1.49 (s, 3H), 1.07 ppm (s, 9H); ^{13}C NMR (101 MHz, CDCl$_3$): δ = 140.8, 136.4, 136.1, 135.9, 134.0, 133.9, 129.6, 129.4, 127.5, 127.3, 120.4, 93.5, 80.8, 80.7, 64.0, 38.6, 37.4, 29.2, 27.5, 26.9, 19.3, 16.2, 3.5 ppm. IR (film) $\tilde{v}$ = 3071, 3049, 2930, 2856, 1472, 1462, 1427, 1390, 1361, 1344, 1110, 1074, 1007, 940, 822, 739, 701, 613, 505, 487 cm^{-1}; HRMS (ESI): *m/z* calcd. for C$_{29}$H$_{37}$OSiI [*M*$^+$+Na]: 579.15506; found: 579.15552.

(6*E*,10*E*)-11-iodo-7-methyldodeca-6,10-dien-2-yn-4-ol (125). TBAF (1 M in THF, 1.7 mL, 1.7 mmol) was added to a solution of compound **143** (265.0 mg, 0.5 mmol) in THF (20 mL) at 0 °C. The mixture was stirred at 0 °C for 8 and for another 2 h at RT. The reaction was quenched with saturated aqueous NH$_4$Cl solution and the aqueous layer was separated and extracted with MTBE (3 × 5 mL). The combined organic phases were dried over MgSO$_4$ and concentrated, and the residue was purified by flash chromatography (hexane/EtOAc, 10:1) to yield the title compound as a colourless oil (153.0 mg, 80%). ^{1}H NMR (400 MHz, CDCl$_3$): δ = 6.13 (m, 1H), 5.25 (m, 1H), 4.34 (m, 1H), 2.41 (m, 2H), 2.37 (m, 3H), 2.16 (m, 2H), 2.09 (m, 2H), 1.86 (d, *J* = 2.1 Hz, 3H), 1.64 ppm (s, 3H); ^{13}C NMR (101 MHz, CDCl$_3$): δ = 140.7, 138.1, 119.6, 93.6, 81.1, 80.1, 62.4, 38.7, 36.8, 29.1, 27.5, 16.3, 3.6 ppm; IR (film) $\tilde{\nu}$ = 3375, 2917, 2854, 2237, 1765, 1716, 1669, 1635, 1430, 1377, 1261, 1176, 1135, 1102, 1037, 881, 838, 802, 702, 620, 562, 534 cm^{-1}; HRMS (ESI): *m/z* calcd. for C$_{13}$H$_{18}$OI [*M*$^+$]: 317.03969; found: 317.03945.
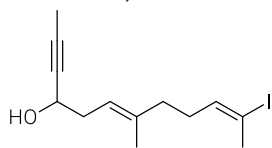
(6*E*,10*E*)-11-(Dimethyl(phenyl)silyl)-7-methyldodeca-6,10-dien-2-yn-4-ol (144). TBAF (1 M in THF, 4.67 mL, 4.67 mmol) was added to a solution of compound **142** (1.32 g, 2.34 mmol) in THF (57 mL) at 0 °C. The mixture was stirred at 0 °C for 10 min and for another 5 h at RT. The reaction was quenched with saturated aqueous NH$_4$Cl solution and the aqueous layer was separated and extracted with EtOAc (3 × 100 mL). The combined organic phases were dried over MgSO$_4$ and concentrated, and the residue was purified by flash chromatography (hexane/EtOAc, 10:1) to yield the title compound as a colourless oil (637.0 mg, 84%). ^{1}H NMR (400 MHz, CDCl$_3$): δ = 7.49 (m, 2H), 7.34 (m, 3H), 5.78 (tq, *J* = 6.7, 1.8 Hz, 1H), 5.24 (q, *J* = 1.3 Hz, 1H), 4.31 (m, 1H), 2.41 (m, 2H), 2.25 (m, 2H), 2.12 (dd, *J* = 8.6, 6.5 Hz, 2H), 1.84 (d, *J* = 2.1 Hz, 3H), 1.76 (d, *J* = 5.7 Hz, 1H), 1.66 (dd, *J* = 1.7, 0.9 Hz, 6H), 0.32 ppm (s, 6H); ^{13}C NMR (101 MHz, CDCl$_3$): δ = 141.0, 139.4, 138.8, 134.3, 133.9, 128.8, 127.6, 118.8, 80.9, 80.2, 62.3, 39.2, 36.8, 27.0, 16.4, 14.8, 3.6, −3.5 ppm; IR (film) $\tilde{\nu}$ = 3365, 2955, 2919, 2855, 1617, 1428, 1247, 1110, 1039, 999, 831, 814, 773, 731, 701 cm^{-1}; HRMS (ESI): *m/z* calcd. for C$_{21}$H$_{30}$OSi [*M*$^+$+Na]: 349.19581; found: 349.19563.
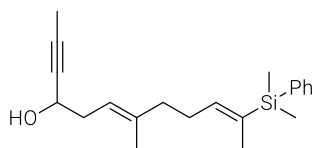
3-Iodo-2-((*E*)-4-iodopent-3-en-1-yl)-2-methyl-5-(prop-1-yn-1-yl)tetrahydrofuran (145).
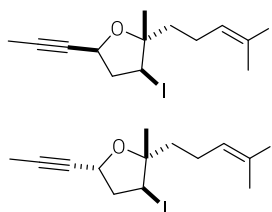
N-Iodosuccinimide (20.1 mg, 89.4 µmol) was added to a solution of compound **144** (14.6 mg, 44.7 µmol) in hexafluoro-*iso*-propanol (HFIP) (1.2 mL). The mixture was stirred at 0 °C for 2 min before the reaction was quenched with saturated aqueous Na$_2$S$_2$O$_3$ solution. The aqueous layer was separated and extracted with *tert*-butyl methyl ether (3 × 5 mL). The combined organic phases were dried over MgSO$_4$ and concentrated, and the residue was purified by flash chromatography (hexane/EtOAc, 20:1) to yield the title compounds as a colourless oil each (14.4 mg, *cis/trans* = 42:58, 73%).

*Analytical and spectral data of **cis-isomer***: ^{1}H NMR (600 MHz, CDCl$_3$): δ = 6.13 (m, 1H), 4.48 (ddq, *J* = 8.8, 6.5, 2.1 Hz, 1H), 3.90 (dd, *J* = 11.8, 7.1 Hz, 1H), 2.75 (dt, *J* = 12.7, 6.9 Hz, 1H), 2.51 (m, 1H), 2.37 (d, *J* = 1.3 Hz, 3H), 2.14 (dd, *J* = 7.1, 4.0 Hz, 2H), 1.84 (d, *J* = 2.2 Hz, 3H), 1.74 (m, 1H), 1.59 (m, 1H), 1.46 ppm (s, 3H); ^{13}C NMR (151 MHz, CDCl$_3$): δ = 140.4, 94.0, 84.3, 81.6, 78.8, 66.9, 44.5, 37.3, 27.5, 26.0, 25.7, 25.2, 3.7 ppm.

*Analytical and spectral data of **trans-isomer***: ^{1}H NMR (600 MHz, CDCl$_3$): δ = 6.17 (tt, *J* = 7.7, 1.6 Hz, 1H), 4.66 (ddq, *J* = 8.5, 4.3, 2.1 Hz, 1H), 4.16 (dd, *J* = 9.4, 7.4 Hz, 1H), 2.60 (m, 2H), 2.39 (d, *J* = 1.3 Hz, 3H), 2.29 (m, 2H), 1.83 (d, *J* = 2.1 Hz, 3H), 1.74 (m, 2H), 1.34 ppm (s, 3H); ^{13}C NMR (151 MHz, CDCl$_3$): δ = 140.6, 93.9, 84.7 81.7, 78.8, 66.7, 44.7, 37.4, 27.9, 27.5, 25.7, 25.5, 3.7 ppm; IR (film) $\tilde{\nu}$ = 2971, 2918, 2851, 2243, 1784, 1716, 1677, 1635, 1592, 156, 1448, 1428, 1356, 1260,

1172, 1155, 1108, 10590, 1015, 952, 917, 804, 737, 701, 664, 618 cm^{-1}; HRMS (ESI): *m/z* calcd. for C$_{13}$H$_{18}$OI$_2$ [*M*$^+$+Na]: 466.93393; found: 466.93403.

(6*E*,10*E*)-11-Iodo-7-methyldodeca-6,10-dien-2-yn-4-ol (125). *N*-Iodosuccinimide (454.9 mg, 2.0 mmol) was added to a solution of compound **144** (617.0 mg, 1.9 mmol) in hexafluoro-*iso*-propanol (HFIP) (50 mL) and HOAc (1.1 mL, 18.9 mmol). The mixture was stirred at 0 °C for 5 min before the reaction was quenched with saturated aqueous Na$_2$S$_2$O$_3$ solution. The aqueous layer was separated and extracted with *tert*-butyl methyl ether (3 × 50 mL). The combined organic phases were dried over MgSO$_4$ and concentrated, and the residue was purified by flash chromatography (hexane/EtOAc, 10:1) to yield the title compound as a colourless oil (423.2 mg, 70%). ^{1}H NMR (400 MHz, CDCl$_3$): δ = 6.13 (tt, *J* = 5.7, 1.6 Hz, 1H), 5.24 (ddt, *J* = 8.6, 7.3, 1.3 Hz, 1H), 4.34 (ddt, *J* = 6.2, 4.2, 2.1 Hz, 1H), 2.41 (ddt, *J* = 7.2, 6.3, 0.8 Hz, 2H), 2.36 (dt, *J* = 1.7, 0.9 Hz, 3H), 2.13 (m, 4H), 1.86 (d, *J* = 2.1 Hz, 3H), 1.64 ppm (m, 3H); ^{13}C NMR (101 MHz, CDCl$_3$): δ = 140.7, 138.1, 119.6, 93.6, 81.0, 80.1, 62.3, 38.7, 36.8, 29.0, 27.5, 16.3, 3.6 ppm; IR (film) $\tilde{v}$ = 3391, 2917, 2854, 1765, 1714, 1634, 1430, 1377, 1256, 1175, 1135, 1104, 1053, 880, 839, 621 cm^{-1}; HRMS (ESI): *m/z* calcd. for C$_{13}$H$_{19}$OI [*M*$^+$+Na]: 341.03728; found: 341.03766.
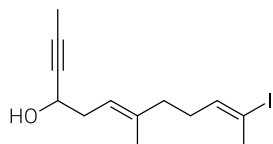
3.3.2 COMPLETION OF THE TOTAL SYNTHESES

Suzuki Coupling Product 123. A solution of 9-H-9-BBN (173.5 mg, 1.4 mol) in THF (4 mL) was added to a solution of compound **124** (530.0 mg, 947.7 µmol, 24% *w/w* in pentane) in THF (15 mL) at 0 °C. The ice bath was removed and the mixture was stirred at RT for 3 h. Water (1.5 mL, 1.5 g, 83.3 mmol) and Ba(OH)$_2$·(H$_2$O)$_8$ (448.5 mg, 1.4 mmol) were sequentially added and the mixture was stirred for 15 min. Alkenyl iodide **125** (232.1 mg, 729.6 µmol) and [(dppf)PdCl$_2$] (69.3 mg, 94.8 µmol, 10 mol%) were introduced and the resulting mixture was stirred at RT for 2 h. The reaction was quenched with saturated aqueous NH$_4$Cl solution. The aqueous layer was separated and extracted with *tert*-butyl methyl ether (3 × 50 mL), the combined organic phases were dried over MgSO$_4$ and concentrated, and the residue was purified by flash chromatography (hexane/EtOAc, 20:1) to yield the title compound as a colourless oil (165.3 mg, 69%). ^{1}H NMR (400 MHz, CDCl$_3$) δ = 5.23 (ddt, *J* = 7.4, 6.1, 1.3 Hz, 1H), 5.13 (ddd, *J* = 6.9, 5.5, 2.7 Hz, 1H), 4.32 (ddt, *J* = 6.1, 4.1, 2.1 Hz, 1H), 2.41 (t, *J* = 6.8 Hz, 2H), 2.07 (m, 6H), 1.85 (d, *J* = 2.1 Hz, 3H), 1.81 (d, *J* = 2.2 Hz, 3H), 1.65 (s, 3H), 1.62 (s, 3H), 1.45 (m, 2H), 1.09 (dq, *J* = 8.5, 2.2 Hz, 1H), 1.05 (s, 3H), 1.03 (s, 3H), 0.63 ppm (dt, *J* = 8.6, 7.1 Hz, 1H); ^{13}C NMR (101 MHz, CDCl$_3$) δ = 139.8, 135.6, 124.1, 118.5, 80.8, 80.2, 77.6, 74.9, 62.3, 39.9, 39.3, 36.8, 29.0, 27.7, 26.5, 24.3, 21.0, 17.8, 16.4, 16.1, 16.0, 3.7, 3.6 ppm; IR (film) $\tilde{v}$ = 3394, 2981, 2918, 2858, 1450, 1378, 1134, 1038, 881, 831 cm^{-1}; HRMS (ESI): *m/z* calcd. for C$_{23}$H$_{34}$O [*M*$^+$+H]: 327.26824; found: 327.26802.
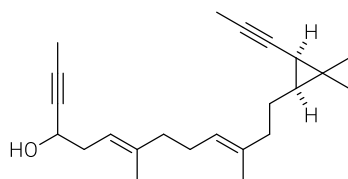
Suzuki Coupling Product 159. Prepared analogously as a colourless oil (222.3 mg, 82%). ^{1}H NMR (600 MHz, CDCl$_3$) δ = 5.23 (m, 1H), 5.11 (tq, *J* = 7.0, 1.5 Hz, 1H), 4.32 (tdq, *J* = 6.0, 4.1, 1.8 Hz, 1H), 2.41 (m, 2H), 2.07 (m, 6H), 1.85 (d, *J* = 2.1 Hz, 3H), 1.80 (d, *J* = 2.1 Hz, 3H), 1.65 (s, 3H), 1.59 (s, 3H), 1.45 (m, 1H), 1.37 (m, 1H), 1.15 (s, 3H), 1.04 (s, 3H), 0.69 (dt, *J* = 4.4, 2.2 Hz, 1H), 0.62 ppm (td, *J* = 7.2, 5.2 Hz, 1H); ^{13}C NMR (151 MHz, CDCl$_3$) δ = 139.7, 135.0, 124.3, 118.6, 80.8, 80.2, 80.1, 73.3, 62.3, 39.8, 39.6, 36.8, 33.7,

27.7, 26.5, 23.5, 22.4, 20.1, 20.0, 16.4, 16.0, 3.7, 3.6 ppm; IR (film) $\tilde{v}$ = 3411, 2970, 2918, 2857, 1667, 1450, 1379, 1333, 1124, 1036, 881, 839 cm^{-1}; HRMS (ESI): *m/z* calcd. for C$_{23}$H$_{34}$O [*M*$^+$+Na]: 349.25018; found: 349.24996.

Cycloalkynes 146 and 147. Powdered MS 5 (100 mg) and MS 4 (100 mg) [pre-activated at

146   147
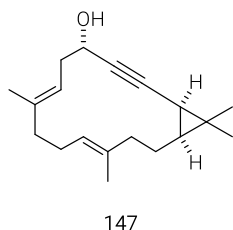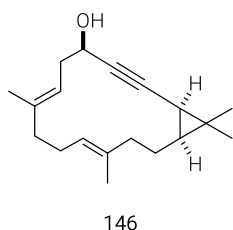
140 °C under vacuum overnight] were added to a solution of diyne **123** (45.7 mg, 140.0 µmol) in toluene (150 mL) and the mixture was stirred at RT for 1 h. In a second Schlenk flask, a solution of trisilanol **52b** (24.2 mg, 30.8 µmol) in toluene (1 mL) was added to the molybdenum complex **49** (18.6 mg, 28.0 µmol) and the mixture was stirred at RT for 5 min. The resulting catalyst solution was added to the preheated solution of the diyne at reflux temperature. After stirring for 25 min, the mixture was cooled to RT before it was filtered through a pad of Celite®, which was rinsed with toluene. The combined filtrates were concentrated and the residue was purified by flash chromatography (hexane/EtOAc, 20:1) to yield the title compounds as a colourless oil (22.6 mg, 83.0 µmol, 60%).

Analytical and spectral data of macrocycle **147**: [α]$_D^{20}$ = −4.2 (0.13 g/100 mL, CHCl$_3$); ^{1}H NMR (600 MHz, CDCl$_3$): δ = 5.06 (m, 2H), 4.40 (ddd, *J* = 9.7, 4.1, 1.7 Hz, 1H), 2.47 (ddd, *J* = 13.9, 6.7, 4.1 Hz, 1H), 2.27 (ddd, *J* = 14.1, 9.9, 7.1 Hz, 1H), 2.17 (m, 1H), 2.11 (m, 1H), 2.01 (m, 4H), 1.84 (dddd, *J* = 13.6, 11.2, 6.8, 2.6 Hz, 1H), 1.61 (d, *J* = 1.3 Hz, 3H), 1.57 (m, 3H), 1.18 (dd, *J* = 8.3, 1.7 Hz, 1H), 1.07 (s, 3H), 1.06 (m, 1H), 1.05 (s, 3H), 0.75 ppm (ddd, *J* = 11.1, 8.4, 2.6 Hz, 1H); ^{13}C NMR (151 MHz, CDCl$_3$): δ = 136.7, 135.9, 124.1, 120.0, 84.5, 81.2, 63.0, 39.7, 39.6, 36.8, 30.6, 27.4, 26.4, 23.9, 22.1, 17.7, 16.1, 15.8, 15.6 ppm. IR (film) $\tilde{v}$ = 3278, 2948, 2929, 2852, 1667, 1452, 1378, 1325, 1294, 1261, 1092, 1016, 853, 832, 537, 525 cm^{-1}. HRMS (ESI): *m/z* calcd. for C$_{19}$H$_{28}$O [*M*$^+$+Na]: 295.20323; found: 295.20323.

Analytical and spectral data of macrocycle **146**: [α]$_D^{20}$ = −80.9 (0.11 g/100 mL, CHCl$_3$); ^{1}H NMR (600 MHz, CDCl$_3$): δ = 5.11 (m, 2H), 4.52 (ddd, *J* = 7.6, 3.4, 1.8 Hz, 1H), 2.49 (dt, *J* = 14.1, 8.1 Hz, 1H), 2.31 (m, 1H), 2.16 (m, 2H), 2.04 (m, 4H), 1.81 (m, 1H), 1.63 (s, 6H), 1.20 (dd, *J* = 8.3, 1.8 Hz, 1H), 1.17 (m, 1H), 1.05 (s, 3H), 1.04 (s, 3H), 0.74 ppm (ddd, *J* = 10.8, 8.3, 2.5 Hz, 1H); ^{13}C NMR (151 MHz, CDCl$_3$): δ = 137.7, 135.9, 123.8, 119.8, 84.4, 80.9, 62.6, 39.8, 39.3, 36.1, 30.5, 27.4, 25.7, 24.1, 22.2, 18.0, 16.3, 16.2, 16.1 ppm; IR (film) $\tilde{v}$ = 3354, 2980, 2918, 2857, 2224, 1667, 1450, 1377, 1261, 1095, 1035, 992, 883, 801, 525 cm^{-1}. HRMS (ESI): *m/z* calcd. for C$_{19}$H$_{28}$O [*M*$^+$+Na]: 295.20323; found: 295.20317.

Cycloalkynes 161 and 162. Prepared analogously as a colourless oil (42.5 mg, 76%). *Analytical*

162   161
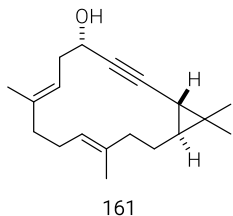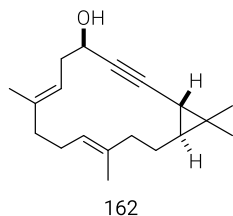
and spectral data of compound **162**: [α]$_D^{20}$ = +47.6 (0.45 g/100 mL); ^{1}H NMR (600 MHz, CDCl$_3$): δ = 5.28 (tq, *J* = 7.3, 1.4 Hz, 1H), 5.22 (m, 1H), 4.49 (t, *J* = 5.2 Hz, 1H), 2.38 (m, 2H), 2.19 (m, 6H), 1.87 (m, 1H), 1.79 (s, 1H), 1.59 (s, 6H), 1.13 (s, 3H), 1.04 (s, 3H), 0.92 (m, 1H), 0.65 (s, 1H), 0.64 ppm (m, 1H) ; ^{13}C NMR (151 MHz, CDCl$_3$): δ = 137.1, 133.1, 126.2, 119.0, 87.8, 78.0, 62.8, 39.0, 38.5, 36.2, 34.0, 24.8, 24.4, 23.5, 23.4, 20.4, 19.2, 15.8, 15.0 ppm. IR (film) $\tilde{v}$ = 3358, 2969, 2923, 2857, 2232, 1437, 1378, 1308, 1256, 1098, 1037, 864, 896, 823 cm^{-1}. HRMS (ESI): *m/z* calcd. for C$_{19}$H$_{28}$O [*M*$^+$]: 272.21347; found: 272.21351.

Analytical and spectral data of compound **161**: $[\alpha]_D^{20}$ = −5.5 (1.50 g/100 mL); ^{1}H NMR (600 MHz, CDCl$_3$): δ = 5.13 (m, 2H), 4.44 (m, 1H), 2.41 (m, 1H), 2.34 (m, 2H), 2.16 (m, 4H), 2.08 (td, *J* = 12.5, 3.3 Hz, 1H), 1.86 (ddt, *J* = 14.0, 12.3, 3.1 Hz, 1H), 1.70 (s, 1H), 1.59 (s, 3H), 1.56 (s, 3H), 1.16 (s, 3H), 1.05 (s, 3H), 0.89 (m, 1H), 0.67 (ddd, *J* = 11.6, 5.2, 3.0 Hz, 1H), 0.63 ppm (dd, *J* = 5.3, 2.5 Hz, 1H); ^{13}C NMR (151 MHz, CDCl$_3$): δ = 136.9, 133.3, 126.3, 120.0, 87.8, 79.1, 63.1, 39.0, 38.6, 37.4, 34.3, 25.0, 24.5, 24.0, 23.6, 20.5, 19.2, 15.4, 15.2 ppm. IR (film) $\tilde{v}$ = 3328, 2969, 2923, 2856, 2226, 1440, 1378, 1306, 1256, 1113, 1029, 965, 867, 825 cm^{−1}. HRMS (ESI): *m/z* calcd. for C$_{19}$H$_{28}$O [*M*+]: 272.21347; found: 272.21331.

Compound 148. A solution of Bu$_3$SnH (0.2 M in CH$_2$Cl$_2$, 0.8 mL, 157.5 µmol) was added dropwise to a solution of [Cp*RuCl]$_4$ (1.4 mg, 1.1 µmol, 2.5 mol%) and alkyne **147** (14.3 mg, 52.5 µmol) in CH$_2$Cl$_2$ (2 mL) at RT. The mixture was stirred for 2 h before it was concentrated. The residue was purified by flash chromatography (hexane/EtOAc, 20:1) to yield the title compound as a colourless oil (26.1 mg, 46.3 µmol, 88%). $[\alpha]_D^{20}$ = −30.0 (0.02 g/100 mL, CHCl$_3$); ^{1}H NMR (600 MHz, CDCl$_3$): δ = 5.81 (dd, *J* = 125.9, 120.5 Hz, 1H), 4.99 (m, 1H), 4.86 (td, *J* = 6.8, 3.6 Hz, 1H), 4.11 (dt, *J* = 11.0, 3.0 Hz, 1H), 2.39 (ddd, *J* = 13.7, 5.7, 3.8 Hz, 1H), 2.26 (dt, *J* = 13.4, 6.1 Hz, 1H), 2.12 (m, 4H), 1.92 (m, 2H), 1.81 (dddd, *J* = 14.1, 7.1, 5.7, 1.5 Hz, 1H), 1.62 (d, *J* = 1.3 Hz, 3H), 1.59 (d, *J* = 1.3 Hz, 3H), 1.51 (m, 6H), 1.43 (d, *J* = 2.6 Hz, 1H), 1.34 (h, *J* = 7.3 Hz, 6H), 1.17 (m, 1H), 1.12 (dd, *J* = 10.4, 8.5 Hz, 1H), 1.06 (s, 3H), 0.99 (m, 6H), 0.95 (s, 3H), 0.90 (t, *J* = 7.3 Hz, 9H), 0.67 ppm (ddd, *J* = 10.3, 8.5, 1.4 Hz, 1H); ^{13}C NMR (151 MHz, CDCl$_3$): δ = 147.1, 139.4, 134.89, 134.86, 124.2, 120.4, 82.5, 39.8, 38.6, 36.4, 32.4, 30.6, 29.3, 28.9, 27.5, 24.1, 23.1, 22.1, 17.3, 16.9, 15.7, 13.7, 11.3 ppm; ^{119}Sn NMR (224 MHz, CDCl$_3$) δ = −57.2 ppm; IR (film) $\tilde{v}$ = 3424, 2954, 2923, 2870, 2854, 1674, 1606, 1456, 1376, 1260, 1081, 1019, 866, 799, 665, 597,504 cm^{−1}; HRMS (ESI): *m/z* calcd. for C$_{31}$H$_{56}$OSn [*M*++Na]: 587.3245; found: 587.32415.
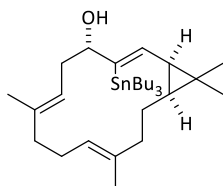
Compound 152. Prepared analogously from **146** as a colourless oil (12.8 mg, 79%). $[\alpha]_D^{20}$ = −16.8 (0.74 g/100 mL, CHCl$_3$); ^{1}H NMR (400 MHz, CDCl$_3$): δ = 5.96 (dddd, *J* = 129.9, 10.4, 3.0, 1.7 Hz, 1H), 4.98 (m, 2H), 4.43 (m, 1H), 2.58 (dt, *J* = 14.9, 7.5 Hz, 1H), 2.26 (m, 2H), 2.13 (m, 3H), 2.00 (m, *J* = 17.0, 10.2, 5.2 Hz, 1H), 1.88 (m, 2H), 1.65 (d, *J* = 1.3 Hz, 3H), 1.60 (s, 3H), 1.50 (m, *J* = 16.5, 9.8, 4.7, 2.6 Hz, 6H), 1.33 (m, 6H), 1.20 (m, 1H), 1.11 (dd, *J* = 10.3, 8.4 Hz, 1H), 1.06 (s, 3H), 0.95 (m, 9H), 0.90 (t, *J* = 7.3 Hz, 9H), 0.72 ppm (ddd, *J* = 10.9, 8.4, 1.4 Hz, 1H) ppm; ^{13}C NMR (101 MHz, CDCl$_3$): δ = 144.2, 136.9, 135.4, 134.3, 125.0, 117.4, 74.5, 40.0, 38.4, 34.2, 32.0, 31.6, 29.3, 28.9, 27.5, 24.3, 24.1, 21.9, 17.3, 17.5, 15.6, 13.7, 10.4 ppm; ^{119}Sn NMR (149 MHz, CDCl$_3$) δ = −54.6 ppm; IR (film) $\tilde{v}$ = 3453, 2953, 2921, 2871, 2853, 1608, 1455, 1376, 1289, 1261, 1058, 1020, 874, 802, 688, 666, 593 cm^{−1}; HRMS (ESI): *m/z* calcd. for C$_{31}$H$_{56}$OSn [*M*++Na]: 587.3245; found: 587.32483.
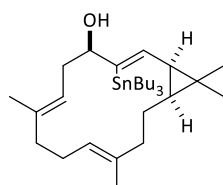
Compound 163. Prepared analogously from **161** as a colourless oil (18.7 mg, 74%). $[\alpha]_D^{20}$ = −22.6 (1.73 g/100 mL); ^{1}H NMR (400 MHz, CDCl$_3$): δ = 5.75 (ddd, *J* = 132.2, 9.8, 1.2 Hz, 1H), 5.00 (dt, *J* = 11.4, 6.1 Hz, 2H), 4.38 (m, 1H), 2.55 (dt, *J* = 15.9, 8.2 Hz, 1H), 2.26 (m, 2H), 2.04 (m, 6H), 1.57 (s, 3H), 1.53 (s, 3H), 1.50 (m, 6H), 1.34 (m, 6H), 1.21 (d, *J* = 6.2 Hz, 1H), 1.05 (s, 3H), 1.04 (s, 3H), 0.96 (m, 7H), 0.90 (t, *J* = 7.3 Hz, 9H), 0.68 (m, 1H), 0.52 ppm (ddd, *J* = 10.9, 4.9, 3.2 Hz, 1H); ^{13}C NMR (101 MHz, CDCl$_3$): δ = 142.8, 140.1, 133.7, 133.0, 126.0, 121.1, 74.4, 38.8,
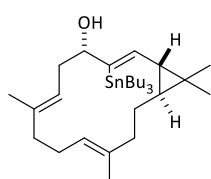
38.4, 34.8, 34.1, 33.8, 29.3, 27.6, 24.4, 24.3, 23.8, 23.0, 21.9, 15.9, 14.8, 13.7, 10.2 ppm; ^{119}Sn NMR (149 MHz, CDCl$_3$): δ = −49.71 ppm; IR (film) $\tilde{v}$ = 3457, 2955, 2923, 2871, 2853, 1612, 1455, 1376, 1118, 1070, 1018, 962, 897, 872, 687, 665, 596 cm^{-1}. HRMS (ESI): m/z calcd. for C$_{31}$H$_{56}$OSn [M$^+$+Na]: 587.3245; found: 587.32455.

Compound 164 and Isomer EP-3. Prepared analogously from **162** as a colourless oil (6.9 mg, 65%). $[\alpha]_D^{20}$ = +7.0 (0.57 g/100 mL, CHCl$_3$); ^{1}H NMR (400 MHz, CDCl$_3$): δ = 5.54 (dd, J = 126.4, 10.0 Hz, 1H), 5.08 (d, J = 5.9 Hz, 1H), 4.89 (m, 1H), 4.20 (m, 1H), 2.44 (m, 1H), 2.05 (m, 7H), 1.58 (m, 3H), 1.56 (s, 3H), 1.50 (m, 7H), 1.34 (dq, J = 14.2, 7.3 Hz, 6H), 1.06 (s, 3H), 1.03 (s, 3H), 0.99 (m, 7H), 0.90 (t, J = 7.3 Hz, 9H), 0.73 (m, 1H), 0.47 (dt, J = 11.0, 4.5 Hz, 1H); ^{13}C NMR (101 MHz, CDCl$_3$): δ = 145.1, 143.7, 134.8, 132.7, 126.3, 120.7, 81.8, 38.9, 38.0, 35.6, 33.8, 33.5, 29.3, 27.6, 24.4, 24.2, 23.9, 22.9, 22.0, 17.1, 14.9, 13.7, 11.1 ppm; ^{119}Sn NMR (149 MHz, CDCl$_3$) : δ = −56.35 ppm; IR (film) $\tilde{v}$ = 3423, 1954, 2923, 2870, 2853, 1608, 1455, 1376, 1259, 1182, 1119, 1020, 964, 897, 877, 691, 669, 593, 541 cm^{-1}. HRMS (ESI): m/z calcd. for C$_{31}$H$_{56}$OSn [M$^+$+Na]: 587.3245; found: 587.32466.
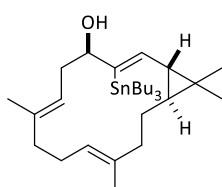
In this case, a second isomer was obtained, which was identified as the corresponding "*alpha,cis*"-adduct (**EP-3**) (1.3 mg, 12%): ^{1}H NMR (600 MHz, CDCl$_3$) δ = 5.22 (dd, J = 75.0, 7.0, 1.5 Hz, 1H), 5.21 (m, 1H), 5.10 (t, J = 6.7 Hz, 1H), 4.70 (s, 1H), 2.55 (ddd, J = 14.0, 8.4, 5.1 Hz, 1H), 2.20 (m, 4H), 2.16 (d, J = 5.9 Hz, 1H), 2.12 (m, 2H), 1.92 (m, 1H), 1.77 (m, 1H), 1.62 (s, 3H), 1.64 (s, 3H), 1.47 (m, 7H), 1.30 (m, 7H), 1.05 (s, 3H), 1.02 (s, 3H), 0.87 (m, 15H), 0.55 ppm (dt, J = 8.2, 5.1 Hz, 1H). ^{13}C NMR (151 MHz, CDCl$_3$) δ = 146.0, 140.1, 137.3, 134.6, 124.4, 118.6, 39.2, 38.3, 35.0, 34.8, 32.7, 29.1, 27.4, 25.8, 24.7, 23.0, 21.8, 21.4, 17.8, 16.7, 13.7, 9.9, 1.0 ppm.
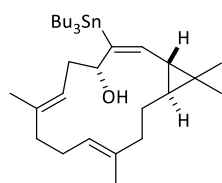
Compound 149. Pd(PPh$_3$)$_4$ (2.7 mg, 2.3 µmol, 5 mol%) was added to a solution of alkenyl stannane **148** (26.1 mg, 46.3 mmol) and [Ph$_2$PO$_2$]$^-$[Bu$_4$N]$^+$ (23.4 mg, 51.0 µmol) in DMF (0.2 mL) and the mixture was stirred for 10 min. Methyl iodide (4.3 µL, 9.9 mg, 69.5 µmol) was added, immediately followed (after 10 sec !) by CuTC (9.3 mg, 48.6 µmol). The resulting mixture was stirred at RT for 4 h. At this point, additional Pd(PPh$_3$)$_4$ (1.4 mg, 1.2 mmol, 2.5 mol%), methyl iodide (2.2 µL, 5.0 mg, 34.8 µmol), and CuTC (4.7 mg, 24.3 µmol) were added sequentially (10 sec time difference between MeI and CuTC) and stirring was continued for another 2 h. The reaction was quenched with aqueous Et$_3$N (0.1 ml), the mixture diluted with *tert*-butyl methyl ether and washed with aqueous NH$_3$ (25%)/NH$_4$Cl solution (1:9). The aqueous layer was separated and extracted with *tert*-butyl methyl ether (3 × 10 mL). The combined organic phases were dried over MgSO$_4$ and concentrated, and the residue was purified by flash chromatography (hexane/EtOAc, 10:1) to yield the title compound as a colourless oil (2.4 mg, 67%). $[\alpha]_D^{20}$ = −77.4 (0.28 g/100 mL, CHCl$_3$); ^{1}H NMR (600 MHz, CDCl$_3$): δ = 5.10 (m, 1H), 4.94 (ddt, J = 6.5, 5.2, 1.3 Hz, 1H), 4.78 (ddq, J = 7.7, 5.2, 1.3 Hz, 1H), 4.08 (m, 1H), 2.41 (ddd, J = 14.4, 11.2, 8.6 Hz, 1H), 2.31 (m, 1H), 2.20 (dt, J = 14.1, 6.9 Hz, 1H), 2.09 (m, 3H), 1.87 (m, 2H), 1.73 (m, 1H), 1.69 (d, J = 1.3 Hz, 3H), 1.60 (s, 3H), 1.58 (s, 3H), 1.42 (d, J = 2.8 Hz, 1H), 1.26 (m, 1H), 1.07 (s, 3H), 0.96 (s, 3H), 0.63 ppm (ddd, J = 10.2, 8.8, 1.4 Hz, 1H); ^{13}C NMR (151 MHz, CDCl$_3$): δ = 137.2, 135.2, 135.0, 125.9, 123.4, 120.5, 79.4, 40.4, 39.3, 33.1, 31.5, 28.8, 25.5, 24.0, 23.6, 20.5, 16.7, 16.1, 15.7, 10.4 ppm; IR (film) $\tilde{v}$ = 3342, 2918, 2858, 1448, 1376, 1013, 871 cm^{-1}; HRMS (ESI): m/z calcd. for C$_{20}$H$_{32}$O [M$^+$+Na]: 311.23453; found: 311.23490.

Depressin (9). MnO$_2$ (43.4 mg, 0.5 mmol) was added to a solution of alcohol **149** (4.8 mg, 16.6 µmol) in CH$_2$Cl$_2$ (2 mL). The suspension was stirred at RT for 4 h before it was filtered through a plug of silica, which was carefully rinsed with *tert*-butyl methyl ether. The combined filtrates were concentrated and the residue was purified by flash chromatography (hexane/EtOAc, 20:1) to yield the title compound as a colourless oil (3.5 mg, 73%). $[\alpha]_D^{20}$ = −85.0 (0.02 g/100 mL, CHCl$_3$); ^{1}H NMR (600 MHz, CDCl$_3$): δ = 6.38 (dq, *J* = 10.2, 1.3 Hz, 1H), 5.07 (ddt, *J* = 8.7, 5.9, 1.4 Hz, 1H), 4.84 (dd, *J* = 9.0, 5.1 Hz, 1H), 3.55 (dd, *J* = 13.9, 8.6 Hz, 1H), 2.98 (dd, *J* = 13.9, 5.7 Hz, 1H), 2.08 (m, 6H), 1.87 (d, *J* = 1.3 Hz, 3H), 1.75 (ddd, *J* = 12.8, 9.9, 2.9 Hz, 1H), 1.57 (t, *J* = 1.2 Hz, 3H), 1.56 (s, 3H), 1.49 (dd, *J* = 10.2, 8.6 Hz, 1H), 1.16 (m, 3H), 1.14 (m, 1H), 1.09 (s, 3H), 0.86 ppm (dddd, *J* = 13.8, 12.6, 9.6, 2.9 Hz, 1H); ^{13}C NMR (151 MHz, CDCl$_3$): δ = 199.9, 143.2, 137.1, 136.6, 135.9, 124.4, 119.4, 39.9, 39.4, 39.0, 35.2, 29.0, 27.7, 26.3, 25.4, 23.9, 15.9, 15.6, 15.3, 11.6 ppm; IR (film) $\tilde{\nu}$ = 2923, 2853 1654, 1626, 1454, 1379, 1318, 1270, 1189, 1152, 1110, 1064, 1041, 1018, 870, 827, 801, 762, 748, 595, 523 cm^{-1}; HRMS (ESI): *m/z* calcd. for C$_{20}$H$_{30}$O [*M*$^+$]: 287.23694; found: 287.23682.
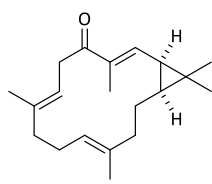
Table 13. Comparison of the analytical and NMR data of natural product depressin (**9**) and synthetic depressin (**9**).

	depressin (**9**)	synthetic **9**		depressin (**9**)	synthetic **9**
$[\alpha]_D$	−80.0°, c = 0.26	−85.0°, c = 0.02			
	^{1}H NMR δ [ppm] (*J* [Hz])			^{13}C NMR δ [ppm]	
1	1.15	1.14 (m)	1	35.2	35.2
2	1.50 (dd, 10.2, 8.7)	1.49 (dd, 10.2, 8.6)	2	27.6	27.7
3	6.37 (d, 10.2)	6.38 (dq, 1.3, 10.2)	3	143.1	143.2
4	-	-	4	136.6	136.6
5	-	-	5	199.9	199.9
6a	3.55 (dd, 13.8, 5.7)	3.55 (dd, 13.9, 8.6)	6	39.4	39.4
6b	2.97 (dd, 13.8, 5.7)	2.98 (dd, 13.9, 5.7)	7	119.4	119.4
7	5.08 (t, 6.6)	5.07 (ddt, 8.7, 5.9, 1.4, 1.4)	8	137.1	137.1
8	-	-	9	39.0	39.0
9a	2.15	2.09 (m)	10	23.9	23.9
9b	2.00	2.00 (m)	11	124.4	124.4
10a	2.17	2.16 (m)	12	135.9	135.9
10b	1.96	1.98 (m)	13	39.9	39.9
11	4.84 (t, 5.4)	4.84 (dd, 9.0, 5.1)	14	26.3	26.3
12	-	-	15	25.4	25.4
13a	2.20	2.20 (d, 12.8)	16	29.0	29.0
13b	1.75	1.75 (ddd, 12.8, 9.9, 2.9)	17	15.8	15.9
14a	2.05	2.06 (m)	18	11.6	11.6
14b	0.80	0.86 (dddd, 13.8, 12.6, 9.6, 2.9)	19	15.6	15.6
15	-	-	20	15.3	15.3
16	1.16	1.16 (s)			
17	1.09	1.09 (s)			
18	1.87	1.87 (d, 1.3)			
19	1.56	1.57 (t, 1.2)			
20	1.56	1.56 (s)			

Methyl (1*R*,2*Z*,4*S*,6*E*,10*E*,14*S*)-4-hydroxy-7,11,15,15-tetramethyl bicyclo[12.1.0]pentadeca-2,6,10-triene-3-carboxylate (150). *p*-Benzoquinone (1.6 mg, 15.2 µmol), Ph$_3$As (1.2 mg, 4.0 µmol, 40 mol%) and Pd(OAc)$_2$ (0.5 mg, 2.0 µmol, 20 mol%) were added to a solution of stannane **148** (5.7 mg, 10.1 µmol) in TFA (0.05 m, 0.08 mL) in MeOH (0.3 mL). The Schlenk flask was flushed for 2 min with CO before the mixture was stirred under CO atmosphere (balloon) at RT for 2 h. The flask was vented, the mixture was diluted with *tert*-butyl methyl ether and filtered through a plug of Celite®. The filtrate was evaporated and the crude material purified by flash chromatography (hexane/EtOAc, 10:1) to yield the title compound as a colourless oil (2.6 mg, 77% yield). $[\alpha]_D^{20}$ = −50.0 (0.11 g/100 mL, CHCl$_3$); ^{1}H NMR (600 MHz, CDCl$_3$): δ = 5.79 (d, J = 10.7 Hz, 1H), 4.93 (tt, J = 6.2, 1.4 Hz, 1H), 4.89 (ddt, J = 9.0, 6.3, 1.4 Hz, 1H), 4.00 (td, J = 11.1, 4.3 Hz, 1H), 3.81 (s, 3H), 3.44 (d, J = 10.6 Hz, 1H), 2.63 (ddd, J = 13.6, 11.4, 9.2 Hz, 1H), 2.43 (m, 1H), 2.28 (dt, J = 15.0, 5.3 Hz, 1H), 2.11 (m, 4H), 1.97 (ddd, J = 13.9, 9.4, 4.9 Hz, 1H), 1.91 (m, 1H), 1.83 (dddd, J = 14.3, 6.4, 5.1, 1.5 Hz, 1H), 1.63 (s, 3H), 1.53 (s, 3H), 1.17 (dtd, J = 14.4, 9.5, 4.7 Hz, 1H), 1.10 (s, 3H), 0.99 (s, 3H), 0.90 ppm (ddd, J = 10.0, 8.6, 1.5 Hz, 1H); ^{13}C NMR (151 MHz, CDCl$_3$): δ = 168.3, 145.1, 136.2, 134.7, 130.7, 123.5, 120.4, 78.6, 51.2, 39.7, 39.1, 35.7, 34.7, 28.9, 28.2, 25.2, 24.1, 22.9, 17.5, 16.0, 15.9 ppm; IR (film) $\tilde{\nu}$ = 3521, 3431, 2976, 2947, 2918, 2861, 1715, 1686, 1627, 1437, 1377, 1351, 1310, 1263, 1222, 1196, 1152, 1139, 1111, 1044, 986, 920, 833, 797, 557, 461 cm^{-1}; HRMS (ESI): *m/z* calcd. for C$_{21}$H$_{32}$O$_3$ [*M*$^+$+Na]: 355.22436; found: 355.22405.
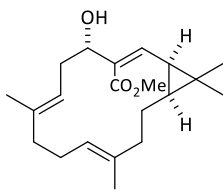
Methyl (1*R*,2*Z*,4*R*,6*E*,10*E*,14*S*)-4-hydroxy-7,11,15,15-tetramethylbicyclo[12.1.0]pentadeca-2,6,10-triene-3-carboxylate (153). *p*-Benzoquinone (1.6 mg, 15.2 µmol), Ph$_3$As (1.2 mg, 4.0 µmol, 40 mol%) and Pd(OAc)$_2$ (0.5 mg, 2.0 µmol, 20 mol%) were added to a solution of stannane **152** (5.7 mg, 10.1 µmol) in TFA (0.05 m, 0.08 mL) in MeOH (0.3 mL). The Schlenk flask was flushed for 2 min with CO before the mixture was stirred under CO atmosphere (balloon) at RT for 2 h. The flask was vented, the mixture was diluted with *tert*-butyl methyl ether and filtered through a plug of Celite®. The filtrate was evaporated and the crude material purified by flash chromatography (hexane/EtOAc, 10:1) to yield the title compound as a colourless oil (2.6 mg, 77% yield). $[\alpha]_D^{20}$ = −64.5 (0.20 g/100 mL, CHCl$_3$); ^{1}H NMR (600 MHz, CDCl$_3$): δ = 5.98 (dd, J = 10.6, 1.2 Hz, 1H), 4.92 (m, 2H), 4.74 (td, J = 6.6, 3.2 Hz, 1H), 3.78 (s, 3H), 2.49 (m, 2H), 2.27 (m, 1H), 2.23 (dd, J = 10.5, 8.4 Hz, 1H), 2.12 (m, 2H), 1.99 (m, 1H), 1.94 (d, J = 6.0 Hz, 1H), 1.91 (m, 2H), 1.64 (d, J = 1.4 Hz, 3H), 1.56 (d, J = 1.4 Hz, 3H), 1.14 (m, 1H), 1.12 (s, 3H), 0.99 (s, 3H), 0.96 ppm (m, 1H); ^{13}C NMR (151 MHz, CDCl$_3$): δ = 168.2, 140.9, 137.7, 135.4, 132.0, 124.6, 117.5, 70.1, 51.2, 39.8, 38.8, 34.3, 33.1, 28.9, 27.9, 24.8, 24.4, 24.0, 17.0, 16.6, 15.7 ppm; IR (film) $\tilde{\nu}$ = 3468, 2977, 2917, 2859, 1697, 1628, 1435, 1375, 1321, 1217, 1194, 1151, 1118, 1098, 1051, 1001, 914, 893, 874, 799, 733, 548, 525, 459 cm^{-1}; HRMS (ESI): *m/z* calcd. for C$_{21}$H$_{32}$O$_3$ [*M*$^+$+Na]: 355.22436; found: 355.22479.
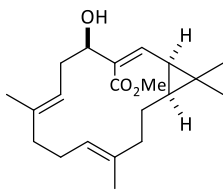
Compound 151 ("Nominal Euphorhylonal A"). MeLi (1.6 M in Et$_2$O, 16.1 µL, 25.8 µmol) was added dropwise to a solution of alkenyl stannane **148** (6.6 mg, 13.1 mmol) in THF (1.5 mL) at −78 °C. The mixture was stirred at −78 °C for 5 min and for additional 30 min at RT before it was cooled again to −78°C. DMF (9.1 µl, 117.1 mmol) was added dropwise at this temperature and stirring was continued for 20 min at −78 °C and for 1 h at RT. The reaction was quenched with a saturated aqueous NH$_4$Cl solution, and the aqueous layer was separated and extracted with *tert*-butyl methyl ether (3 × 5 mL). The combined organic phases were dried over MgSO$_4$ and concentrated, and the residue was purified by flash chromatography (hexane/EtOAc, 20:1) to yield the title compound as a colourless oil (2.4 mg, 68%). $[\alpha]_D^{20}$ = −37.7 (0.11 g/100 mL,
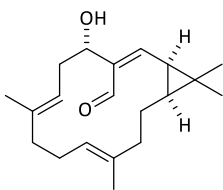
CHCl$_3$); ^{1}H NMR (600 MHz, CDCl$_3$): δ = 10.13 (d, J = 2.0 Hz, 1H), 6.19 (d, J = 11.2 Hz, 1H), 4.90 (m, 2H), 3.95 (tdd, J = 10.9, 4.1, 2.0 Hz, 1H), 3.50 (d, J = 10.7 Hz, 1H), 2.70 (ddd, J = 13.7, 11.3, 9.2 Hz, 1H), 2.45 (dt, J = 12.9, 5.1 Hz, 1H), 2.33 (dt, J = 15.5, 5.6 Hz, 1H), 2.13 (m, 3H), 1.96 (dd, J = 11.2, 8.3 Hz, 1H), 1.91 (m, 2H), 1.87 (dddd, J = 14.5, 6.2, 4.7, 1.5 Hz, 1H), 1.62 (t, J = 0.9 Hz, 3H), 1.51 (d, J = 1.2 Hz, 3H), 1.28 (m, 1H), 1.16 (s, 3H), 1.03 (s, 3H), 1.02 ppm (td, J = 9.7, 8.3 Hz, 1H); ^{13}C NMR (151 MHz, CDCl$_3$): δ = 192.7, 151.3, 139.2, 136.6, 134.3, 123.5, 120.3, 77.5, 39.4, 38.9, 35.7, 35.6, 28.9, 26.8, 25.4, 24.1, 22.0, 17.7, 16.1, 15.9 ppm; IR (film) $\tilde{v}$ = 3436, 2921, 2853, 1734, 1657, 1620, 1452, 1377, 1260, 1091, 1017, 985, 798 cm^{-1}; HRMS (ESI): m/z calcd. for C$_{20}$H$_{30}$O$_2$ [M^++Na]: 325.21380; found: 325.21422.

Compound 154. Prepared analogously from **152** as a colourless oil (2.1 mg, 53%). $[\alpha]_D^{20}$ = −77.4 (0.06 g/100 mL, CHCl$_3$); ^{1}H NMR (600 MHz, CDCl$_3$): δ = 10.18 (s, 1H), 6.49 (dd, J = 11.1, 1.2 Hz, 1H), 4.91 (m, 2H), 4.81 (tt, J = 5.2, 2.8 Hz, 1H), 2.55 (m, 1H), 2.45 (dt, 1H), 2.31 (dt, 1H), 2.12 (m, 3H), 2.07 (dd, J = 11.1, 8.3 Hz, 1H), 1.95 (m, 3H), 1.88 (d, J = 5.4 Hz, 1H), 1.63 (d, J = 1.3 Hz, 3H), 1.53 (d, J = 1.2 Hz, 3H), 1.22 (m, 1H), 1.17 (s, 3H), 1.08 (m, 1H), 1.04 ppm (s, 3H); ^{13}C NMR (151 MHz, CDCl$_3$): δ = 190.9, 148.1, 140.9, 137.7, 134.8, 124.6, 117.7, 67.8, 39.6, 38.8, 35.3, 33.0, 28.9, 26.2, 25.0, 24.0, 23.5, 17.2, 16.5, 15.7 ppm; IR (film) $\tilde{v}$ = 3429, 2919, 2862, 1662, 1654, 1448, 1377, 1377, 1150, 1125, 1097, 1057, 1020, 800, 672 cm^{-1}; HRMS (ESI): m/z calcd. for C$_{20}$H$_{30}$O$_2$ [M^++Na]: 325.21380; found: 325. 21437.
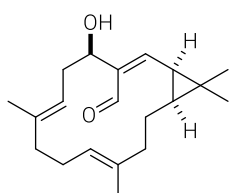
The reaction delivered a side-product (ca. 10%) which was identified as allylic alcohol **EP-4** formed by protodestannation: $[\alpha]_D^{20}$ = −43.8 (0.21 g/100 mL, CHCl$_3$); ^{1}H NMR (400 MHz, CDCl$_3$): δ = 5.62 (ddd, J = 15.6, 3.5, 0.7 Hz, 1H), 5.41 (ddd, J = 15.5, 8.9, 1.8 Hz, 1H), 4.99 (m, 2H), 4.32 (s, 1H), 2.40 (m, 2H), 2.22 (dd, J = 13.7, 6.6 Hz, 1H), 2.13 (m, 3H), 2.00 (m, 1H), 1.91 (dt, J = 14.1, 7.2 Hz, 1H), 1.81 (dtd, J = 13.1, 6.5, 1.8 Hz, 1H), 1.64 (s, 3H), 1.60 (s, 3H), 1.43 (d, J = 7.2 Hz, 1H), 1.23 (m, 1H), 1.05 (s, 3H), 0.98 (s, 3H), 0.65 ppm (ddd, J = 10.4, 8.7, 1.8 Hz, 1H); ^{13}C NMR (101 MHz, CDCl$_3$): δ = 136.9, 135.5, 132.5, 126.5, 124.0, 118.5, 71.0, 40.1, 38.8, 34.9, 30.9, 29.6, 28.8, 24.2, 24.0, 20.8, 17.0, 16.4, 15.8 ppm; IR (film) $\tilde{v}$ = 3367, 2923, 2857, 1719, 1666, 1453, 1376, 1260, 1071, 1019, 968, 872, 801, 735 cm^{-1}; HRMS (ESI): m/z calcd. for C$_{19}$H$_{30}$O [M^++Na]: 297.21888; found: 297.21886.
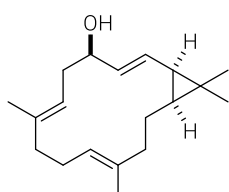
Euphorhylonal A (155). Prepared analogously as a colourless oil (2.7 mg, 61%). $[\alpha]_D^{20}$ = +77.3; $[\alpha]_D^{25}$ = +74.5 (0.11 g/100 mL, CHCl$_3$); ^{1}H NMR (600 MHz, CDCl$_3$): δ = 10.12 (d, J = 1.3 Hz, 1H), 5.98 (d, J = 11.4 Hz, 1H), 4.96 (t, J = 6.0 Hz, 1H), 4.86 (t, J = 6.9 Hz, 1H), 4.08 (td, J = 10.1, 9.6, 4.9 Hz, 1H), 3.55 (d, J = 9.9 Hz, 1H), 2.61 (m, 1H), 2.50 (m, 1H), 2.13 (m, 4H), 2.00 (m, 2H), 1.61 (m, 1H), 1.56 (s, 3H), 1.53 (s, 3H), 1.17 (s, 3H), 1.16 (s, 3H), 0.85 ppm (m, 1H); ^{13}C NMR (151 MHz, CDCl$_3$): δ = 192.1, 156.5, 137.2, 135.7, 132.6, 125.9, 120.8, 76.5, 39.1, 38.6, 37.7, 34.7, 29.1, 28.5, 24.2, 24.1, 22.9, 22.0, 15.9, 14.7 ppm; IR (film) $\tilde{v}$ = 3432, 2924, 2854, 1656, 1620, 1454, 1437, 1378, 1260, 1230, 1113, 1043, 1019, 965, 904 cm^{-1}. HRMS (ESI): m/z calcd. for C$_{20}$H$_{30}$O$_2$ [M^++Na]: 325.21380; found: 325.21378.
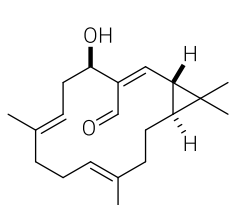
The reaction delivered a side-product (< 10%) which was identified as allylic alcohol **EP-5** formed by protodestannation: $[\alpha]_D^{20}$ = +52.5 (0.84 g/100 mL, CHCl$_3$); ^{1}H NMR (600 MHz, CDCl$_3$): δ = 5.38 (dd, J = 15.2, 8.3 Hz, 1H), 5.20 (dd, J = 15.2, 8.9 Hz, 1H), 5.06 (m, 1H), 5.00 (m, 1H), 4.16 (td, J = 8.9, 4.6 Hz, 1H), 2.45 (m, 1H), 2.13 (m, 7H), 1.92 (ddt, J = 14.6, 10.9, 3.8 Hz, 1H), 1.57 (s, 3H), 1.55 (s, 3H), 1.04 (s, 6H), 1.01 (m, 1H), 0.81 (dd, J = 8.9, 5.2 Hz, 1H), 0.37 ppm (ddd, J = 11.0, 5.1, 3.8 Hz, 1H); ^{13}C NMR (151 MHz, CDCl$_3$): δ = 135.5, 135.2, 133.0, 130.6, 125.7, 120.6, 74.1, 39.3, 38.4, 34.9, 32.7, 32.4, 24.5, 24.3, 22.8, 22.6, 21.7, 16.3, 14.8 ppm. IR (film) $\tilde{\nu}$ = 3370, 2956, 2922, 2871, 2855, 1664, 1455, 1377, 1292, 1252, 1182, 1151, 1075, 1023, 960, 878, 696, 675, 600, 519 cm^{-1}. HRMS (ESI): m/z calcd. for C$_{19}$H$_{30}$O [M^++Na]: 297.21888; found: 297.21873.
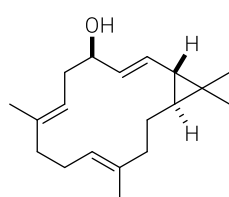
Compound 156. Prepared analogously from **163** as a colourless oil (5.1 mg, 69%). $[\alpha]_D^{20}$ = +63.5; $[\alpha]_D^{25}$ = +98.7 °, (0.55 g/100 mL, CHCl$_3$); ^{1}H NMR (400 MHz, CDCl$_3$): δ = 10.17 (s, 1H), 6.23 (d, J = 11.4 Hz, 1H), 4.91 (td, J = 6.2, 3.2 Hz, 1H), 4.88 (m, 1H), 4.83 (dd, J = 7.5, 5.5 Hz, 1H), 2.47 (t, J = 7.5 Hz, 2H), 2.05 (m, 9H), 1.70 (dd, J = 11.4, 4.9 Hz, 1H), 1.57 (s, 3H), 1.52 (s, 3H), 1.18 (s, 3H), 1.17 (s, 3H), 0.82 ppm (ddd, J = 11.5, 5.0, 2.9 Hz, 1H); ^{13}C NMR (101 MHz, CDCl$_3$): δ = 190.9, 154.7, 138.3, 135.2, 132.9, 125.9, 120.6, 66.9, 38.8, 38.6, 37.8, 32.5, 29.2, 28.6, 24.3, 23.9, 22.9, 21.9, 15.4, 14.7 ppm. IR (film) $\tilde{\nu}$ = 3368, 2922, 2870, 2853, 1660, 1625, 1552, 1440, 1378, 1259, 1227, 1141, 1065, 1031, 999, 963, 805, 688, 668 cm^{-1}. HRMS (ESI): m/z calcd. for C$_{20}$H$_{30}$O$_2$ [M^++Na]: 325.21380; found: 325.21354.
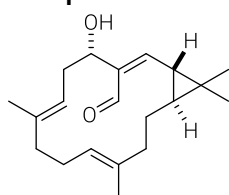
The reaction delivered a side-product (< 10%) which was identified as allylic alcohol **EP-6** formed by protodestannation: $[\alpha]_D^{20}$ = −10.2 (0.42 g/100 mL, CHCl$_3$); ^{1}H NMR (600 MHz, CDCl$_3$): δ = 5.59 (ddd, J = 15.7, 4.7, 0.9 Hz, 1H), 5.48 (ddd, J = 15.7, 7.3, 1.4 Hz, 1H), 5.06 (m, 1H), 4.98 (m, 1H), 4.26 (m, 1H), 2.36 (m, 2H), 2.26 (dt, J = 11.9, 7.4 Hz, 1H), 2.12 (m, 4H), 2.03 (td, J = 12.5, 3.4 Hz, 1H), 1.92 (ddt, J = 15.0, 11.9, 3.2 Hz, 1H), 1.57 (s, 3H), 1.53 (s, 3H), 1.05 (s, 3H), 1.01 (s, 3H), 0.96 (m, 1H), 0.78 (dd, J = 7.3, 5.4 Hz, 1H), 0.41 ppm (ddd, J = 11.4, 5.3, 3.2 Hz, 1H); ^{13}C NMR (151 MHz, CDCl$_3$): δ = 135.4, 133.6, 131.7, 130.4, 125.6, 121.1, 70.6, 39.1, 38.6, 35.2, 33.0, 31.5, 24.8, 24.3, 22.9, 22.4, 21.7, 15.5, 14.8 ppm. IR (film) $\tilde{\nu}$ = 3345, 2919, 2850, 1729, 1668, 1453, 1377, 1287, 1258, 1105, 1083, 1018, 962, 881, 835 cm^{-1}. HRMS (ESI): m/z calcd. for C$_{19}$H$_{30}$O [M^++Na]: 297.21888; found: 297.21893
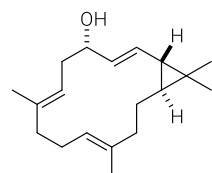
Table 14. Comparison of the analytical and ^{1}H NMR data (δ [ppm] (J [Hz])) of euphorhylonal A and pekinenin C (**16**) with those of various synthetic samples.

	Euphorhylonal A	pekinenin C (**16**)	1S,2R,5S-**151**	1S,2R,5R-**154**	1S,2S,5R-**155**	1S,2S,5S-**156**
$[\alpha]_D$	+90.5°, c = 0.3	−19°, c = 0.04	−37.7°, c = 0.11	−77.4°, c = 0.28	+77.3°, c = 0.11	+98.7°, c = 0.55
1	0.84 (m)	0.82 (m)	1.02 (td, 9.7, 8.3)	1.08 (m)	0.82 (m)	0.82 (m)
2	1.61 (dd, 11.4, 4.9)	1.61 (m)	1.96 (dd, 11.2, 8.3)	2.07 (dd, 11.1, 8.3)	1.60 (dd, 11.4, 5.0)	1.70 (dd, 11.4, 4.9)
3	5.99 (d, 11.4)	5.97 (d, 11.5)	6.19 (d, 11.2)	6.49 (dd, 11.1, 1.2)	5.98 (d, 11.4)	6.23 (d, 11.4)
5	4.07 (dd, 6.5, 1)	4.08 (dd, 10.0, 4.5)	3.95 (tdd, 10.9,	4.81 (m)	4.08 (td)	4.83 (dd, 7.5, 5.5)
6(a)	2.51 (m)	2.49 (m)	2.45 (dt, 13.7)	2.46 (m)	2.49 (dt, 14.4, 5.2)	2.47 (t, 7.5)
6b	2.62 (m)	2.61 (m)	2.70 (ddd, 13.7, 11	2.56 (m)	2.61 (ddd, 14.3,	-
7	4.86 (t, 7.0)	4.86 (t, 7.0)	4.89 (m)	4.91 (m)	4.86 (dd, 7.7, 5.7)	4.92 (m)
9(a)	2.00 (m)	2.04 (m)	1.91 (m)	1.99 (m)	2.01 (m)	2.09 (m)
9b	-	2.09 (m)	2.14 (m)	2.11 (m)	2.11 (m)	2.11 (m)
10(a)	2.14 (m)	2.14 (m)	2.14 (m)	2.11 (m)	2.14 (m)	2.23 (m)
10b	-	-	2.09 (m)	-	-	1.98 (m)
11	4.96 (t, 6.6)	4.97 (t, 6.0)	4.91 (m)	4.92 (m)	4.96 (t, 6.0, 6.0)	4.88 (m)
13(a)	2.00 (m)	2.15 (m)	2.33 (dt, 15.5, 5.6)	2.30 (m)	2.15 (m)	2.18 (m)
13b	-	2.01 (m)	1.95 (m)	1.91 (m)	2.00 (m)	1.96 (m)
14(a)	2.14 (m)	1.13 (m)	1.28 (m)	1.23 (m)	1.14 (m)	1.09 (m)
14b	-	1.99 (m)	1.87 (dddd, 14.5,	1.94 (m)	2.00 (m)	1.98 (m)
16	1.17 (s)	1.17 (s)	1.16 (s)	1.17 (s)	1.17 (s)	1.17 (s)
17	1.16 (s)	1.16 (s)	1.03 (s)	1.04 (s)	1.16 (s)	1.18 (s)
18	-	-	3.50 (d, 10.7)	1.86 (s)	3.55 (d, 9.9)	-
19	1.54 (s)	1.53 (s)	1.51 (d, 1.2)	1.53 (s)	1.53 (s)	1.53 (s)
20	1.57 (s)	1.57 (s)	1.62 (t, 0.9)	1.63 (s)	1.56 (s)	1.57 (s)
21	10.12 (d, 1.4)	10.11 (s)	10.13 (d, 2.0)	10.18 (s)	10.12 (d, 1.4)	10.17 (s)

Table 15. Comparison of the ^{13}C NMR data (δ [ppm]) of euphorhylonal A and pekinenin C (**16**) as reported in the literature with those of various synthetic compounds.

	Euphorhylonal A original	reassigned	pekinenin C (**16**)	1S,2R,5S-**151**	1S,2R,5R-**154**	1S,2S,5R-**155**	1S,2S,5S-**156**
1	37.7	37.7	37.7	35.6	35.3	37.7	37.8
2	29.1	29.1	29.1	25.4	25.0	29.1	29.2
3	156.4	156.4	156.4	151.3	148.1	156.5	154.7
4	132.6	137.3	137.3	139.2	140.9	137.2	138.3
5	76.4	76.4	76.4	77.5	67.8	76.5	66.9
6	34.7	34.7	34.7	35.7	33.0	34.7	32.5
7	120.8	120.8	120.8	120.3	117.7	120.8	120.6
8	137.3	135.6	135.6	136.6	137.7	135.7	135.2
9	39.2	39.2	38.6	38.9	38.8	38.6	38.6
10	24.1	24.1	24.1	24.1	24.0	24.1	23.9
11	125.9	125.9	125.9	123.5	124.6	125.9	125.9
12	135.6	132.6	132.5	134.3	134.8	132.6	132.9
13	38.6	38.6	39.1	39.4	39.6	39.1	38.8
14	24.2	24.2	24.2	22.0	23.5	24.2	24.4
15	28.4	28.4	28.4	26.8	26.2	28.5	28.6
16	22.8	22.8	22.8	28.9	28.9	22.9	22.9
17	21.9	21.9	21.9	15.9	15.7	22.0	21.9
18	-	-	-	-	-	-	-
19	15.9	15.9	15.9	16.1	16.5	15.9	15.4
20	14.7	14.7	14.7	17.7	17.2	14.7	14.7
21	192.1	192.1	192.1	192.7	190.9	192.1	190.9

(+)-Yuexiandajisu A (*ent*-17). MeLi (1.6 M in Et$_2$O, 7.6 µL, 12.1 µmol) was added dropwise to a solution of alkenyl stannane **164** (3.1 mg, 5.5 µmol) in THF (1.6 mL) at −78 °C. The mixture was stirred at −78 °C for 10 min and for additional 15 min at RT before it was cooled again to −78°C. CO$_2$ was bubbled through the mixture for 5 min at −78 °C and for 30 min at RT. The reaction was quenched with a saturated aqueous NH$_4$Cl solution, and the aqueous layer was separated and extracted with *tert*-butyl methyl ether (3 × 5 mL). The combined organic phases were dried over MgSO$_4$ and concentrated, and the residue was purified by flash chromatography (hexane/EtOAc, 10:1 → EtOAc), followed by preparative HPLC (Eclipse Plus C18, 50 mm × 1.8 µm, ⌀ 4.6 mm, methanol / 0.1% TFA in water = 80:20, 1.0 mL/min, 20.1 MPa, 308 K, UV, 254 nm) to yield the title compound as a colourless amorphous solid (0.9 mg, 51%). $[\alpha]_D^{30}$ = +171.3 (0.08 g/100 mL, EtOH); ^{1}H NMR (600 MHz, CDCl$_3$): δ = 5.71 (d, J = 11.0 Hz, 1H), 5.01 (d, J = 6.8 Hz, 1H), 4.87 (m, 1H), 4.16 (dd, J = 11.0, 5.2 Hz, 1H), 2.64 (m, 1H), 2.49 (m, 1H), 2.08 (m, 6H), 2.04 (dd, J = 11.1, 5.1 Hz, 1H), 1.95 (ddt, J = 15.1, 11.5, 3.8 Hz, 1H), 1.58 (s, 3H), 1.56 (s, 3H), 1.16 (m, 1H), 1.14 (s, 3H), 1.12 (s, 3H), 0.73 ppm (dt, J = 11.1, 4.5 Hz, 1H); ^{13}C NMR (151 MHz, CDCl$_3$): δ = 170.5, 153.2, 136.1, 133.0, 126.8, 125.4, 120.4, 78.1, 39.1, 38.6, 37.1, 34.6, 31.8, 27.9, 24.10, 24.12, 22.9, 22.0, 16.2, 14.8 ppm; IR (film) $\tilde{v}$ = 3401, 2923, 2853, 1675, 1437, 1408, 1377, 1263, 1244, 1190, 1142, 1114, 1029, 880, 804, 747, 601, 491 cm^{-1}; HRMS (ESI): *m/z* calcd. for C$_{20}$H$_{30}$O$_3$ [*M*$^+$]: 317.21222; found: 317.21231.
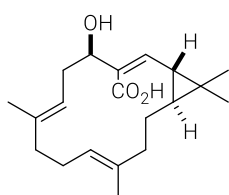
Table 16. Comparison of the analytical and NMR data of yuexiandajisu A (**17**) and synthetic ent-**17**.

	yuexiandajisu A (**17**)		synthetic ent-**17**		yuexiandajisu A (**17**)		synthetic ent-**17**
$[\alpha]_D^{30}$	**+172°,** c = 0.78		**+171.3°,** c = 0.04				
	¹H NMR δ [ppm] (J [Hz])				¹³C NMR δ [ppm]		
	original	*reassigned*			*original*	*reassigned*	
1	0.75 (m)	0.75 (m)	0.73 (m)	1	37.3	37.3	37.1
2	2.06 (m)	2.06 (m)	2.04 (dd, J = 11.1, 5.1)	2	31.9	31.9	31.8
3	5.74 (d, 11.1)	5.74 (d, 11.1)	5.71 (d, 11.0)	3	153.5	153.5	153.2
4	-	-	-	4	127.0	127.0	126.8
5	4.15 (dd, 11.0, 5.3)	4.15 (dd, 11.0, 5.3)	4.16 (dd, 11.0, 5.2)	5	78.0	78.0	78.1
6a	2.48 (m)	2.48 (m)	2.49 (m)	6	34.7	34.7	34.6
6b	2.67 (m)	2.67 (m)	2.64 (m)	7	120.6	120.6	120.4
7	4.88 (dd, 7.2, 5.2)	4.88 (dd, 7.2, 5.2)	4.87 (m, 1H)	8	136.0	136.0	136.1
8	-	-	-	9	38.6	38.6	38.6
9(a)	2.04 (m)	2.04 (m)	2.02 (m)	10	39.1	24.1	24.1
9b	-	-	2.09 (m)	11	125.5	125.5	125.4
10(a)	2.12 (m)	2.12 (m)	2.13 (m)	12	132.9	132.9	133.0
10b	-	-		13	24.1	39.1	39.1
11	5.02 (t, br)	5.02 (t, br)	5.01 (d, 6.8)	14	24.1	24.1	24.1
12	-	-	-	15	27.9	27.9	27.9
13a	2.14 (m)	2.14 (m)	2.10 (m)	16	22.0	22.9	22.9
13b	-	-	2.17 (m)	17	22.9	22.0	22.0
14a	1.19 (m)	1.19 (m)	1.16 (m)	18	-	-	-
14b	1.95 (m)	1.95 (m)	1.95 (ddt, 15.1, 11.5, 3.8)	19	16.2	16.2	16.2
15	-	-	-	20	14.8	14.8	14.8
16	1.15 (s)	1.19 (s)	1.14 (s)	21	171.8	171.8	170.5
17	1.19 (s)	1.15 (s)	1.12 (s)				
18	-	-	-				
19	1.57 (s)	1.58 (s)	1.58 (s)				
20	1.58 (s)	1.57 (s)	1.56 (s)				

(1S,2E,4S,6E,10E,14S)-3,7,11,15,15-Pentamethylbicyclo[12.1.0]pentadeca-2,6,10-trien-4-ol (166). A solution of Bu_3SnH (0.2 M in CH_2Cl_2, 0.13 mL, 25.4 µmol) was added dropwise to a solution of $[Cp^*RuCl]_4$ (0.4 mg, 1.2 µmol, 1.3 mol%) and alkyne **161** (6.6 mg, 24.2 µmol) in CH_2Cl_2 (0.4 mL) at RT. The mixture was stirred for 30 min before it was concentrated. The residue was dissolved in DMF (0.1 mL), then $Pd(PPh_3)_4$ (1.4 mg, 1.2 µmol, 5 mol%) and $[Ph_2PO_2]^-[Bu_4N]^+$ (12.2 mg, 26.6 µmol) were added and the mixture was stirred for 10 min. Methyl iodide (2.3 µL, 5.2 mg, 36.3 µmol) was added, immediately followed (after 10 sec !) by CuTC (4.9 mg, 25.4 µmol). The resulting mixture was stirred at RT for 1 h. The reaction was quenched with aqueous Et_3N (0.1 ml), the mixture diluted with *tert*-butyl methyl ether and washed with aqueous NH_3 (25%)/NH_4Cl solution (1:9). The aqueous layer was separated and extracted with *tert*-butyl methyl ether (3 × 5 mL). The combined organic phases were dried over $MgSO_4$ and concentrated, and the residue was purified by flash chromatography (hexane/EtOAc, 10:1) to yield the title compound as a colourless oil (4.7 mg, 67%). $[\alpha]_D^{20}$ = +47.4 (0.43 g/100 mL, $CHCl_3$); ^1H NMR (400 MHz, $CDCl_3$): δ = 4.99 (m, 3H), 4.16 (t, J = 5.4 Hz, 1H), 2.40 (t, J = 6.2 Hz, 2H), 2.04 (m, 7H), 1.70 (d, J = 1.3 Hz, 3H), 1.56 (s, 3H), 1.54 (s, 3H), 1.07 (s, 3H), 1.07 (s, 3H), 1.00 (m, 1H), 0.87 (dd, J = 9.8, 5.3 Hz, 1H), 0.37 ppm (ddd, J = 11.2, 5.2, 3.4 Hz, 1H); ^{13}C NMR (101 MHz, $CDCl_3$): δ = 134.2, 133.6, 133.0, 125.5, 125.4, 120.3, 74.5, 39.5, 38.6, 33.2, 32.9, 29.2, 24.6, 24.0, 23.2, 22.9, 22.0, 15.9, 15.6, 14.7 ppm; IR (film) $\tilde{v}$ = 3425, 3368, 3284, 2969, 2920, 2861, 1439, 1377, 1058, 1018, 976, 877, 822, 800, 572, 564, 451 cm^{-1}; HRMS (ESI): *m/z* calcd. for $C_{20}H_{32}O$ [*M*+Na]: 311.23453; found: 311.23437.
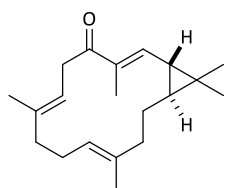
2-*epi*-Depressin (*ent*-165). MnO_2 (11.0 mg, 0.1 mmol) was added to a solution of alcohol **166** (3.1 mg, 10.7 µmol) in CH_2Cl_2 (0.5 mL). The suspension was stirred at RT for 4 h before it was filtered through a plug of silica, which was carefully rinsed with *tert*-butyl methyl ether. The combined filtrates were concentrated and the residue was purified by flash chromatography (hexane/EtOAc, 20:1) to yield the title compound as a colourless oil (2.7 mg, 88%). $[\alpha]_D^{20}$ = −82.4 (0.33 g/100 mL, $CHCl_3$); ^1H NMR (600 MHz, $CDCl_3$): δ = 6.11 (dq, J = 10.2, 1.3 Hz, 1H), 5.19 (dm, J = 11.2 Hz, 1H), 4.88 (d, J = 7.5 Hz, 1H), 3.72 (dd, J = 13.9, 11.3 Hz, 1H), 2.84 (ddt, J = 13.8, 5.1, 1.9 Hz, 1H), 2.30 (m, 1H), 2.18 (m, 2H), 2.10 (m, 2H), 1.94 (m, 2H), 1.81 (d, J = 1.2 Hz, 3H), 1.57 (m, 6H), 1.16 (s, 3H), 1.12 (s, 3H), 1.04 (m, 2H), 0.73 ppm (ddd, J = 11.9, 5.1, 3.0 Hz, 1H); ^{13}C NMR (151 MHz, $CDCl_3$): δ = 201.2, 149.4, 135.1, 133.5, 132.8, 125.4, 121.8, 40.4, 38.9, 38.4, 37.6, 32.0, 28.1, 24.4, 24.1, 23.7, 22.0, 14.8, 14.8, 11.2 ppm; IR (film) $\tilde{v}$ = 2966, 2923, 2855, 1732, 1671, 1653, 1632, 1437, 1381, 1338, 1306, 1275, 1216, 1168, 1152, 1115, 1083, 1063, 1030, 971, 932, 915, 899, 875, 835, 815, 755, 710, 615, 586, 539, 515 cm^{-1}; HRMS (ESI): *m/z* calcd. for $C_{20}H_{30}O$ [*M*+Na]: 309.21888; found: 309.218930.

Table 17. Comparison of the analytical and NMR data of natural occurring 1-*epi*-depressin (**165**) and synthetic 2-*epi*-depressin (*ent*-**165**).

	1-*epi*-depressin (**165**)	2-*epi*-depressin (*ent*-**165**)		1-*epi*-depressin (**165**)	2-*epi*-depressin (*ent*-**165**)
$[\alpha]_D^{20}$	**+34.0°, c = 0.25**	**−82.4°, c = 0.33**			
	¹H NMR δ [ppm] (*J* [Hz])			**¹³C NMR** δ [ppm]	
1	0.71 (m)	0.73 (m)	1	37.5	37.6
2	1.08 (m)	1.04 (m)	2	31.9	32.0
3	6.11 (d, 10.2)	6.11 (dq, 10.2, 1.3)	3	149.4	149.4
4	-	-	4	132.8	132.8
5	-	-	5	201.2	201.2
6a	3.71 (dd, 13.8, 11.1)	3.72 (dd, 13.7, 11.3)	6	40.4	40.4
6b	2.83 (br-d, 13.8)	2.84 (ddt, 13.8, 5.1, 1.9)	7	121.7	121.8
7	5.21 (br-d, 11.1)	5.19 (dm, 11.2)	8	135.1	135.1
8	-	-	9	38.4	38.4
9a	2.18 (m)	2.18 (m)	10	24.0	24.1
9b	2.10 (m)	2.10 (m)	11	125.4	125.4
10a	2.28 (m)	2.30 (m)	12	133.5	133.5
10b	2.07 (m)	2.10 (m)	13	38.8	38.9
11	4.88 (br-d, 8.4)	4.88 (d, 7.5)	14	24.4	24.4
12	-	-	15	28.1	28.1
13a	2.17 (m)	2.18 (m)	16	22.0	22.0
13b	1.93 (m)	1.94 (m)	17	23.7	23.7
14a	1.88 (m)	1.94 (m)	18	11.2	11.2
14b	1.03 (m)	1.04 (m)	19	14.7	14.8
15	-	-	20	14.8	14.8
16	1.16 (s)	1.16 (s)			
17	1.11 (s)	1.12 (s)			
18	1.80 (s)	1.81 (d, 1.2)			
19	1.59 (s)	1.57 (m)			
20	1.59 (s)	1.57 (m)			

3.3.3 MOSHER ESTER ANALYSES

Mosher Ester (ME-1a). (*R*)-(−)-α-Methoxy-α-(trifluormethyl)phenylacetyl chloride (1.0 µL, 4.7 µmol) was added to a solution of DMAP (0.1 mg, 1.0 µmol), Et_3N (2.0 µL, 14.3 µmol) and propargylic alcohol **146** (1.3 mg, 4.7 µmol) in CH_2Cl_2 (0.2 mL). The mixture was stirred at RT for 1 h before it was diluted with Et_2O (1 mL) and washed with aqueous saturated NH_4Cl solution. The aqueous layer was separated and extracted with *tert*-butyl methyl ether (3 × 2 mL). The combined organic phases were dried over $MgSO_4$ and concentrated, and the residue was purified by flash chromatography (hexane/EtOAc, 20:1) to yield the title compound as a colourless oil (2.3 mg, 99%). $[\alpha]_D^{20}$ = +11.1 (0.18 g/100 mL, $CHCl_3$); ^{1}H NMR (600 MHz, $CDCl_3$): δ = 7.56 (m, 2H), 7.39 (m, 3H), 5.59 (ddd, *J* = 9.5, 4.1, 1.8 Hz, 1H), 5.05 (dddt, *J* = 7.9, 6.7, 5.4, 1.2 Hz, 2H), 3.57 (q, *J* = 1.1 Hz, 3H), 2.52 (m, 1H), 2.46 (ddd, *J* = 14.2, 9.5, 6.7 Hz, 1H), 2.15 (m, 2H), 2.01 (m, 4H), 1.81 (dddd, *J* = 13.6, 11.3, 6.6, 2.5 Hz, 1H), 1.59 (d, *J* = 1.4 Hz, 3H), 1.58 (d, *J* = 1.2 Hz, 3H), 1.18 (dd, *J* = 8.3, 1.9 Hz, 1H), 1.05 (m, 4H), 0.94 (s, 3H), 0.74 ppm (ddd, *J* = 10.9, 8.3, 2.5 Hz, 1H); ^{13}C NMR (151 MHz, $CDCl_3$): δ = 165.5, 137.8, 135.8, 132.1, 129.5, 128.3, 127.5, 123.9, 123.2 (q), 118.6, 86.6, 76.0, 67.1, 55.5, 39.6, 39.6, 33.4, 30.9, 27.4, 26.1, 23.8, 22.5, 17.6, 16.0, 15.8, 15.6 ppm ($\underline{C}_{q, sp3}$ signal is missing); IR (film) $\tilde{v}$ = 2946, 2927, 2853, 1750, 1452, 1268, 1251, 1170, 1122, 1081, 1016, 991, 968, 719, 697 cm^{-1}; HRMS (ESI): *m/z* calcd. for $C_{29}H_{35}F_3O_3$ [*M*$^+$+Na]: 511.24305; found: 511.24310.
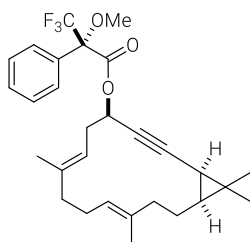
Mosher Ester (ME-1b). Prepared analogously using (*S*)-(+)-α-methoxy-α-(trifluoromethyl)phenylacetyl chloride and compound **146**; colourless oil (2.1 mg, 78%). $[\alpha]_D^{20}$ = +94.1 (0.17 g/100 mL, $CHCl_3$); ^{1}H NMR (600 MHz, $CDCl_3$): δ = 7.57 (m, 2H), 7.40 (m, 3H), 5.59 (ddd, *J* = 9.6, 4.1, 1.8 Hz, 1H), 5.07 (m, 1H), 5.02 (tq, *J* = 6.5, 0.9 Hz, 1H), 3.60 (m, 3H), 2.45 (m, 1H), 2.38 (m, 1H), 2.17 (m, 1H), 2.11 (m, 1H), 2.02 (m, 4H), 1.84 (dddd, *J* = 13.5, 11.1, 6.5, 2.5 Hz, 1H), 1.60 (d, *J* = 1.4 Hz, 3H), 1.57 (q, *J* = 0.9 Hz, 3H), 1.21 (dd, *J* = 8.3, 1.8 Hz, 1H), 1.06 (m, 1H), 1.06 (s, 3H), 1.03 (s, 3H), 0.77 ppm (ddd, *J* = 10.9, 8.3, 2.5 Hz, 1H); ^{13}C NMR (151 MHz, $CDCl_3$): δ = 165.6, 137.9, 135.8, 132.4, 129.5, 128.3, 127.4, 123.9, 123.3 (q), 118.5, 86.6, 84.4 (q), 76.1, 66.9, 55.4, 39.6, 39.6, 33.3, 30.9, 27.4, 26.2, 23.8, 22.5, 17.7, 16.1, 15.8, 15.5 ppm; IR (film) $\tilde{v}$ = 2980, 2945, 2928, 2863, 1750, 1452, 1268, 1248, 1185, 1169, 1122, 1016, 991, 920, 717, 698 cm^{-1}; HRMS (ESI): *m/z* calcd. for $C_{29}H_{35}F_3O_3$ [*M*$^+$+Na]: 511.24305; found: 511.24322.
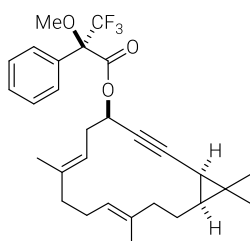
Table 18. Mosher ester analysis of **ME-1a** and **ME-1b**.

	Mosher Ester (ME-1a)	Mosher Ester (ME-1b)	
Position	δ_S (^{1}H, [ppm])	δ_R (^{1}H, [ppm])	$\Delta\delta^{SR} = \delta_S - \delta_R$
14a	1.81	1.84	−0.03
14b	1.03	1.07	−0.04
1	0.74	0.77	−0.03
2	1.18	1.21	−0.03
3	-	-	-
4	-	-	-
5	5.59	5.59	±0.00
6a	2.52	2.45	+0.07
6b	2.46	2.38	+0.08
7	5.04	5.02	+0.02
19	1.58	1.57	+0.01
9a	2.12	2.11	+0.01
9b	2.02	2.00	+0.02

Mosher Ester (ME-2a). Prepared analogously from compound **147** and (*R*)-(−)-α-methoxy-α-(trifluormethyl)phenylacetyl chloride (1.0 μL, 5.5 μmol) as a colourless oil (1.4 mg, 72%). $[\alpha]_D^{20}$ = −172.0 (0.05 g/100 mL, CHCl$_3$); ^{1}H NMR (600 MHz, CDCl$_3$): δ = 7.58 (m, 2H), 7.39 (m, 3H), 5.71 (ddd, *J* = 8.1, 3.8, 1.9 Hz, 1H), 5.14 (ddq, *J* = 8.6, 6.1, 1.3 Hz, 1H), 5.07 (ddq, *J* = 8.5, 5.9, 1.1 Hz, 1H), 3.61 (q, *J* = 1.2 Hz, 3H), 2.52 (dt, *J* = 14.2, 8.3 Hz, 1H), 2.33 (dm, *J* = 14.2 Hz, 1H), 2.11 (m, 3H), 1.98 (m, 3H), 1.81 (dddd, *J* = 13.8, 9.6, 6.0, 2.4 Hz, 1H), 1.62 (d, *J* = 1.2 Hz, 3H), 1.45 (t, *J* = 1.1 Hz, 3H), 1.19 (dd, *J* = 8.2, 1.9 Hz, 1H), 1.18 (m, 1H), 1.05 (s, 3H), 1.02 (s, 3H), 0.74 ppm (ddd, *J* = 10.5, 8.2, 2.4 Hz, 1H); ^{13}C NMR (151 MHz, CDCl$_3$): δ = 165.8, 138.0, 135.3, 132.7, 129.5, 128.3, 127.4, 124.1, 123.3 (q), 118.4, 86.8, 84.3 (q), 76.2, 66.8, 55.5, 39.6, 39.4, 32.9, 30.9, 27.4, 25.6, 24.0, 22.6, 18.0, 16.4, 16.2, 15.7 ppm; IR (film) $\tilde{v}$ = 2982, 2923, 2853, 1750, 1452, 1269, 1237, 1184, 1170, 1123, 1018, 992, 917, 844, 716, 697 cm^{-1}; HRMS (ESI): *m/z* calcd. for C$_{29}$H$_{35}$F$_3$O$_3$ [*M*$^+$+Na]: 511.24305; found: 511.24320.
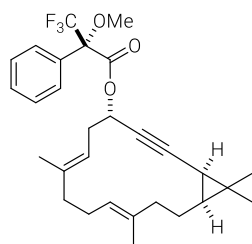
Mosher Ester (ME-2b). Prepared analogously from compound **147** and (*S*)-(+)-α-methoxy-α-(trifluormethyl)phenylacetyl chloride (1.0 μL, 5.5 μmol) as a colourless oil (1.3 mg, 72%). $[\alpha]_D^{20}$ = +15.0 (0.04 g/100 mL, CHCl$_3$); ^{1}H NMR (600 MHz, CDCl$_3$): δ = 7.55 (m, 2H), 7.39 (m, 3H), 5.65 (ddd, *J* = 8.4, 3.9, 1.9 Hz, 1H), 5.08 (m, 1H), 4.96 (t(m), *J* = 7.0 Hz, 1H), 3.57 (m, 3H), 2.61 (dt, *J* = 14.1, 8.4 Hz, 1H), 2.39 (dt, *J* = 14.2, 5.0 Hz, 1H), 2.11 (m, 3H), 2.08 (m, 1H), 1.99 (m, 1H), 1.90 (ddd, *J* = 14.3, 9.3, 5.8 Hz, 1H), 1.77 (dddd, *J* = 13.7, 9.4, 6.0, 2.3 Hz, 1H), 1.59 (d, *J* = 1.3 Hz, 3H), 1.57 (t, *J* = 1.0 Hz, 3H), 1.16 (dd, *J* = 8.3, 1.9 Hz, 1H), 1.15 (m, 1H), 1.05 (s, 3H), 1.02 (s, 3H), 0.71 ppm (ddd, *J* = 10.5, 8.3, 2.3 Hz, 1H); ^{13}C NMR (151 MHz, CDCl$_3$): δ = 165.6, 138.1, 135.2, 132.2, 129.5, 128.3, 127.4, 123.9, 123.3 (q), 118.4, 86.6, 84.6 (q), 76.0, 67.0, 55.5, 39.6, 39.4, 33.0, 30.9, 27.4, 25.4, 24.0, 22.6, 18.1, 16.4, 16.2, 15.9 ppm; IR (film) $\tilde{v}$ = 2981, 2924, 2854, 1749, 1452, 1259, 1185, 1168, 1119, 1101, 1082, 1015, 992, 798, 717, 696 cm^{-1}; HRMS (ESI): *m/z* calcd. for C$_{29}$H$_{35}$F$_3$O$_3$ [*M*$^+$+Na]: 511.24305; found: 511.24328.
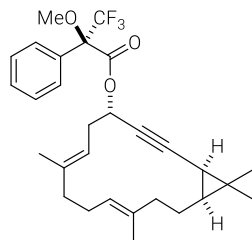
Table 19. Mosher ester analysis of **ME-2a** and **ME-2b**.

	Mosher Ester (ME-2a)	Mosher Ester (ME-2b)

Position	δ_S (^{1}H, [ppm])	δ_R (^{1}H, [ppm])	$\Delta\delta^{SR} = \delta_S - \delta_R$
14a	1.81	1.77	+0.04
14b	1.18	1.15	+0.03
1	0.74	0.71	+0.03
2	1.19	1.16	+0.03
3	-	-	-
4	-	-	-
5	5.71	5.65	+0.06
6a	2.52	2.61	−0.09
6b	2.33	2.39	−0.06
7	5.07	5.08	−0.01
19	1.45	1.57	−0.12
9a	2.09	2.11	−0.02
9b	1.96	1.97	−0.01

Mosher Ester (ME-3a). Prepared analogously from side-product **EP-4** and (*R*)-(−)-α-methoxy-α-(trifluormethyl)phenylacetyl chloride (1.7 μL, 2.4 mg, 8.2 μmol) as a colourless oil (2.4 mg, 4.9 μmol, 90%). $[\alpha]_D^{20}$ = −96.0 (0.05 g/100 mL, CHCl$_3$); ^{1}H NMR (600 MHz, CDCl$_3$): δ = 7.55 (dd, *J* = 7.3, 2.6 Hz, 2H), 7.39 (m, 3H), 5.62 (m, 1H), 5.49 (dd, *J* = 15.7, 4.0 Hz, 1H), 5.38 (ddd, *J* = 15.6, 8.8, 1.5 Hz, 1H), 5.00 (m, 1H), 4.94 (t, *J* = 6.9 Hz, 1H), 3.57 (d, *J* = 1.2 Hz, 3H), 2.50 (m, 2H), 2.18 (m, 3H), 2.06 (m, 1H), 1.96 (t, *J* = 11.5 Hz, 1H), 1.88 (dt, *J* = 14.1, 6.9 Hz, 1H), 1.76 (dtd, *J* = 13.9, 6.9, 1.9 Hz, 1H), 1.59 (s, 3H), 1.58 (s, 3H), 1.19 (t, *J* = 8.9 Hz, 1H), 1.01 (s, 3H), 0.93 (m, 1H), 0.83 (s, 3H), 0.63 ppm (ddd, *J* = 10.5, 8.7, 1.9 Hz, 1H); ^{13}C NMR (151 MHz, CDCl$_3$): δ = 165.6, 137.1, 135.4, 132.5, 129.8, 129.5, 128.3, 127.4, 126.0, 123.4, 118.4, 75.9, 55.4, 39.9, 39.1, 31.7, 31.2, 29.6, 28.7, 24.1, 23.6, 21.2, 16.7, 16.0, 15.6 ppm (CF$_3$ and C$_{q, sp3}$ signals are missing); IR (film) $\tilde{v}$ = 2952, 2918, 2850, 1745, 1452, 1383, 1261, 1185, 1169, 1121, 1106, 1081, 1019, 991, 965, 799, 717, 672 cm^{-1}; HRMS (ESI): *m/z* calcd. for C$_{29}$H$_{37}$F$_3$O$_3$ [*M*$^+$+Na]: 513.25870; found: 513.25861.
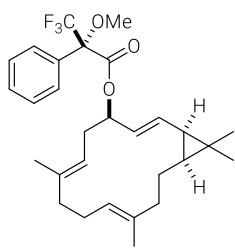
Mosher Ester (ME-3b). Prepared analogously from side-product **EP-4** and (*S*)-(+)-α-methoxy-α-(trifluormethyl)phenylacetyl chloride (1.7 μL, 2.4 mg, 8.2 μmol) as a colourless oil (2.1 mg, 78%) $[\alpha]_D^{20}$ = −18.1 (0.52 g/100 mL, CHCl$_3$); ^{1}H NMR (600 MHz, CDCl$_3$): δ = 7.54 (m, 2H), 7.39 (m, 3H), 5.60 (dd, *J* = 7.7, 3.7 Hz, 1H), 5.56 (dd, *J* = 15.4, 4.0 Hz, 1H), 5.49 (ddd, *J* = 15.4, 8.6, 1.1 Hz, 1H), 4.93 (m, 2H), 3.56 (d, *J* = 1.2 Hz, 3H), 2.47 (q, *J* = 7.3 Hz, 1H), 2.41 (ddd, *J* = 14.8, 7.9, 3.1 Hz, 1H), 2.20 (dd, *J* = 14.2, 6.9 Hz, 1H), 2.12 (m, 2H), 2.06 (m, 1H), 1.93 (t, *J* = 10.4 Hz, 1H), 1.88 (dt, *J* = 14.0, 6.9 Hz, 1H), 1.79 (dtd, *J* = 13.9, 7.0, 2.0 Hz, 1H), 1.59 (s, 3H), 1.57 (s, 3H), 1.23 (t, *J* = 8.7 Hz, 1H), 1.04 (s, 3H), 0.95 (td, *J* = 7.1, 3.4 Hz, 1H), 0.91 (s, 3H), 0.66 ppm (ddd, *J* = 10.7, 8.7, 1.9 Hz, 1H); ^{13}C NMR (151 MHz, CDCl$_3$): δ = 165.7, 137.0, 135.4, 132.4, 130.3, 129.5, 128.4, 127.4, 126.0, 123.4, 118.4, 76.0, 55.3, 39.9, 39.1, 31.4, 31.2, 29.7, 29.6, 28.7, 24.1, 23.8, 16.7, 15.9, 15.8 ppm (CF$_3$ and C$_{q, sp3}$ signals are missing); IR (film) $\tilde{v}$ = 2962, 2916, 2850, 1749, 1446, 1412, 1258, 1078, 1010, 684, 789, 700, 662, 466 cm^{-1}; HRMS (ESI): *m/z* calcd. for C$_{29}$H$_{37}$F$_3$O$_3$ [*M*$^+$+Na]: 513.25870; found: 513.25910.
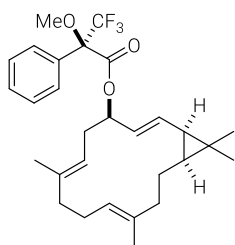
Table 20. Mosher ester analysis of **ME-3a** and **ME-3b**.

	Mosher Ester (ME-3a)	**Mosher Ester (ME-3b)**	

Position	δ_S (^{1}H, [ppm])	δ_R (^{1}H, [ppm])	$\Delta\delta^{SR} = \delta_S - \delta_R$
14a	0.93	0.95	−0.02
14b	1.76	1.79	−0.03
1	0.63	0.66	−0.03
2	1.19	1.23	−0.04
3	5.38	5.49	−0.11
4	5.49	5.56	−0.07
5	5.62	5.60	+0.02
6a	2.51	2.47	+0.04
6b	2.50	2.41	+0.09
7	4.99	4.93	+0.06
19	1.58	1.57	+0.01
9a	1.96	1.93	+0.03
9b	2.13	2.12	+0.01

Mosher Ester (ME-4a). Prepared analogously from compound **162** and (*R*)-(−)-α-methoxy-α-(trifluormethyl)phenylacetyl chloride as a colourless oil (2.6 mg, 97%). $[\alpha]_D^{20}$ = −57.6 (0.25 g/100 mL, CHCl₃); ¹H NMR (600 MHz, CDCl₃): *δ* = 7.56 (m, 2H), 7.40 (m, 3H), 5.59 (ddd, *J* = 6.7, 4.3, 1.2 Hz, 1H), 5.18 (td, *J* = 7.3, 6.9, 1.4 Hz, 1H), 5.11 (m, 1H), 3.57 (d, *J* = 1.1 Hz, 3H), 2.50 (m, 2H), 2.21 (m, 1H), 2.17 (m, 1H), 2.14 (m, 3H), 2.07 (td, *J* = 13.1, 12.1, 3.2 Hz, 1H), 1.85 (ddt, *J* = 14.1, 10.9, 3.1 Hz, 1H), 1.57 (s, 3H), 1.55 (s, 3H), 1.12 (s, 3H), 1.03 (s, 3H), 0.93 (m, 1H), 0.64 (m, 1H), 0.61 ppm (dd, *J* = 5.3, 1.2 Hz, 1H); ¹³C NMR (151 MHz, CDCl₃): *δ* = 165.6, 138.0, 133.1, 132.2, 129.5, 128.3, 127.6, 126.1, 118.1, 89.9, 73.1, 67.2, 55.5, 39.1, 38.7, 34.3, 33.1, 24.7, 24.5, 23.4, 23.4, 20.4, 19.2, 15.7, 15.1 ppm (C̲F₃ and C̲q, sp3 signals are missing); IR (film) $\tilde{v}$ = 2972, 2923, 2852, 2239, 1750, 1497, 1451, 1379, 1270, 1250, 1185, 1169, 1122, 1081, 1017, 991, 965, 920, 882, 831, 764, 718, 696 cm⁻¹; HRMS (ESI): *m/z* calcd. for C₂₉H₃₅F₃O₃ [*M*⁺+Na]: 511.24305; found: 511.24336.
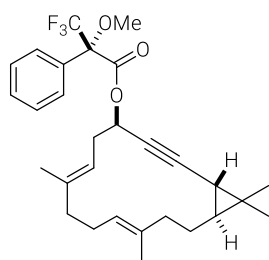
Mosher Ester (ME-4b). Prepared analogously from compound **162** and (*S*)-(+)-α-methoxy-α-(trifluormethyl)phenylacetyl chloride as a colourless oil (2.1 mg, 78%). $[\alpha]_D^{20}$ = −6.1 (0.18 g/100 mL, CHCl₃); ¹H NMR (600 MHz, CDCl₃): *δ* = 7.59 (dd, *J* = 6.8, 3.0 Hz, 2H), 7.40 (m, 3H), 5.61 (ddd, *J* = 5.9, 4.7, 1.1 Hz, 1H), 5.18 (m, 2H), 3.61 (d, *J* = 1.1 Hz, 3H), 2.44 (dd, *J* = 7.7, 5.0 Hz, 2H), 2.25 (dd, *J* = 10.9, 5.1 Hz, 1H), 2.16 (m, 4H), 2.10 (ddd, *J* = 13.1, 10.8, 3.2 Hz, 1H), 1.86 (ddt, *J* = 14.2, 11.1, 3.0 Hz, 1H), 1.59 (s, 3H), 1.52 (s, 3H), 1.12 (s, 3H), 1.04 (s, 3H), 0.93 (dddd, *J* = 14.5, 11.4, 6.1, 3.2 Hz, 1H), 0.67 (m, 1H), 0.64 ppm (dd, *J* = 5.3, 1.1 Hz, 1H); ¹³C NMR (151 MHz, CDCl₃): *δ* = 165.7, 138.0, 133.2, 132.5, 129.5, 128.3, 127.5, 126.1, 118.2, 90.0, 73.2, 67.1, 55.4, 39.1, 38.7, 34.3, 32.9, 24.8, 24.4, 23.6, 23.4, 20.4, 19.2, 15.5, 15.1 ppm (C̲F₃ and C̲q, sp3 signals are missing); IR (film) $\tilde{v}$ = 2971, 2924, 2849, 2236, 1751, 1496, 1452, 1379, 1270, 1250, 1239, 1185, 1169, 1123, 1081, 1018, 992, 964, 717 cm⁻¹; HRMS (ESI): *m/z* calcd. for C₂₉H₃₅F₃O₃ [*M*⁺+Na]: 511.24305; found: 511.24328.
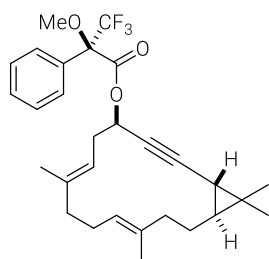
Table 21. Mosher ester analysis of **ME-4a** and **ME-4b**.

	Mosher Ester (ME-4a)	Mosher Ester (ME-4b)
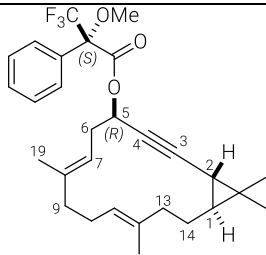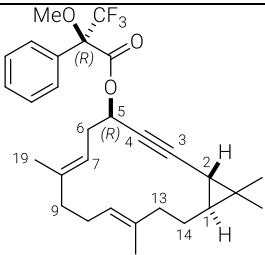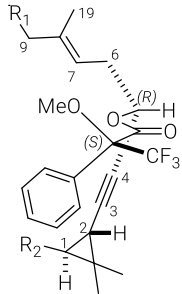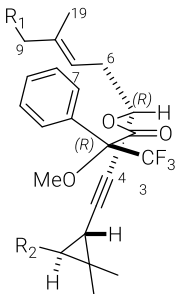
Position	δ_S (^{1}H, [ppm])	δ_R (^{1}H, [ppm])	$\Delta\delta^{SR} = \delta_S - \delta_R$
14a	0.93	0.93	±0.00
14b	1.85	1.86	−0.01
1	0.64	0.67	−0.03
2	0.61	0.64	−0.03
3	-	-	-
4	-	-	-
5	5.59	5.61	−0.02
6	2.50	2.44	+0.06
7	5.18	5.17	+0.01
19	1.55	1.52	+0.03
9	2.14	2.14	±0.00

Mosher Ester (ME-5a). Prepared analogously from compound **161** and (*R*)-(−)-α-methoxy-α-(trifluormethyl)phenylacetyl chloride as a colourless oil (2.2 mg, 62%). $[\alpha]_D^{20}$ = +92.4 (0.17 g/100 mL, CHCl$_3$); ^{1}H NMR (600 MHz, CDCl$_3$): δ = 7.57 (dd, *J* = 7.7, 2.0 Hz, 2H), 7.39 (m, 3H), 5.57 (ddd, *J* = 10.5, 4.9, 2.3 Hz, 1H), 5.14 (d, *J* = 7.6 Hz, 1H), 5.11 (m, 1H), 3.60 (d, *J* = 1.1 Hz, 3H), 2.48 (m, 1H), 2.35 (m, 2H), 2.18 (m, 4H), 2.08 (td, *J* = 12.5, 3.2 Hz, 1H), 1.87 (ddt, *J* = 15.0, 12.1, 2.9 Hz, 1H), 1.59 (s, 3H), 1.55 (s, 3H), 1.13 (s, 3H), 1.05 (s, 3H), 0.90 (m, 1H), 0.68 (m, 1H), 0.67 ppm (m, 1H); ^{13}C NMR (151 MHz, CDCl$_3$): δ = 165.7, 138.2, 133.3, 132.5, 129.5, 128.3, 127.4, 126.0, 118.3, 90.1, 74.0, 66.7, 55.5, 38.8, 38.4, 34.4, 33.4, 24.8, 24.3, 24.2, 23.5, 20.4, 19.1, 15.3, 15.0 ppm (C̲F$_3$ and C̲$_{q, sp3}$ signals are missing); IR (film) $\tilde{v}$ = 2923, 2853, 2243, 1191, 1170, 1122, 1082, 116, 991, 921, 909, 718, 698 cm^{-1}; HRMS (ESI): *m/z* calcd. for C$_{29}$H$_{35}$F$_3$O$_3$ [*M*$^+$+Na]: 511.24305; found: 511.24323.
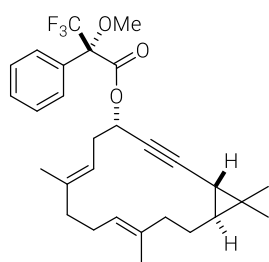
Mosher Ester (ME-5b). Prepared analogously from compound **161** and (*S*)-(+)-α-methoxy-α-(trifluormethyl)phenylacetyl chloride as a colourless oil (5.3 mg, 72%). $[\alpha]_D^{20}$ = −101.7 (0.53 g/100 mL, CHCl$_3$); ^{1}H NMR (600 MHz, CDCl$_3$): δ = 7.56 (dd, *J* = 7.4, 2.2 Hz, 2H), 7.40 (m, 3H), 5.55 (ddd, *J* = 10.4, 5.0, 2.1 Hz, 1H), 5.13 (m, 2H), 3.56 (d, *J* = 1.1 Hz, 3H), 2.54 (m, 1H), 2.46 (m, 1H), 2.33 (dq, *J* = 15.9, 7.5 Hz, 1H), 2.19 (t, *J* = 5.1 Hz, 2H), 2.14 (br-s, 2H), 2.07 (td, *J* = 12.6, 3.3 Hz, 1H), 1.85 (ddd, *J* = 12.2, 10.2, 3.1 Hz, 1H), 1.58 (s, 3H), 1.56 (s, 3H), 1.04 (s, 3H), 1.04 (s, 3H), 0.89 (m, 1H), 0.65 (m, 1H), 0.64 ppm (s, 1H); ^{13}C NMR (151 MHz, CDCl$_3$): δ = 165.6, 138.2, 133.3, 132.2, 129.5, 128.3, 127.6, 125.9, 118.3, 90.0, 73.8, 67.0, 55.5, 38.8, 38.5, 34.4, 33.5, 24.8, 24.3, 24.2, 23.4, 20.4, 19.0, 15.3, 15.0 ppm (C̲F$_3$ and C̲$_{q, sp3}$ signals are missing); IR (film) $\tilde{v}$ = 2924, 2852, 2236, 1749, 1452, 1379, 1352, 1252, 1185, 1168, 1121, 990, 964, 920, 871, 801, 764, 720, 696 cm^{-1}; HRMS (ESI): *m/z* calcd. for C$_{29}$H$_{35}$F$_3$O$_3$ [*M*$^+$+Na]: 511.24305; found: 511.24327.
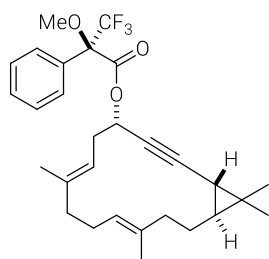
Table 22. Mosher ester analysis of **ME-5a** and **ME-5b**.

	Mosher Ester (ME-5a)	Mosher Ester (ME-5b)
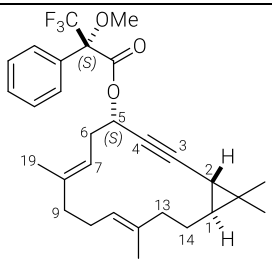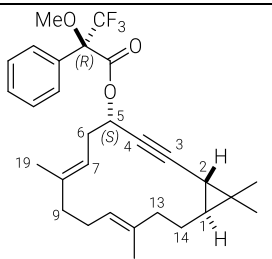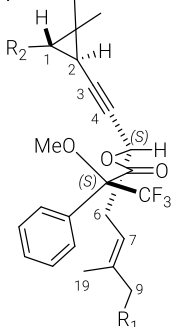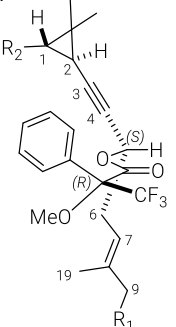
Position	δ_S (¹H, [ppm])	δ_R (¹H, [ppm])	$\Delta\delta^{SR} = \delta_S - \delta_R$
14a	0.91	0.89	+0.02
14b	1.87	1.85	+0.02
1	0.68	0.65	+0.03
2	0.67	0.64	+0.03
3	-	-	-
4	-	-	-
5	5.57	5.55	+0.02
6a	2.36	2.46	−0.10
6b	2.48	2.54	−0.06
7	5.11	5.12	−0.01
19	1.55	1.56	−0.01
9	2.19	2.19	±0.00

Mosher Ester (ME-6a). Prepared analogously from side-product **EP-5** and (*R*)-(−)-α-methoxy-α-(trifluormethyl)phenylacetyl chloride as a colourless oil (2,3 mg, 4.7 μmol, 85%). $[\alpha]_D^{20}$ = +92.5 (0.16 g/100 mL, CHCl₃); ¹H NMR (600 MHz, CDCl₃): δ = 7.52 (m, 2H), 7.39 (m, 3H), 5.48 (ddt, *J* = 12.5, 8.3, 4.1 Hz, 1H), 5.36 (dd, *J* = 15.2, 8.7 Hz, 1H), 5.27 (dd, *J* = 15.3, 8.2 Hz, 1H), 5.00 (m, 2H), 3.58 (d, *J* = 1.2 Hz, 3H), 2.53 (dt, *J* = 11.8, 5.7 Hz, 1H), 2.37 (dt, *J* = 14.0, 8.4 Hz, 1H), 2.14 (m, 1H), 2.09 (t, *J* = 4.8 Hz, 2H), 2.03 (m, 1H), 1.91 (ddt, *J* = 14.5, 11.1, 3.6 Hz, 1H), 1.57 (s, 3H), 1.55 (s, 3H), 1.04 (m, 7H), 0.78 (dd, *J* = 8.6, 5.2 Hz, 1H), 0.40 ppm (m, 1H); ¹³C NMR (151 MHz, CDCl₃): δ = 165.7, 138.7, 137.2, 133.3, 132.5, 129.4, 128.3, 127.5, 125.6, 124.8, 119.1, 78.3, 55.4, 39.2, 38.6, 32.74, 32.69, 31.8, 24.4, 24.3, 23.1, 22.7, 21.7, 16.2, 14.8 ppm ($\underline{C}F_3$ and $\underline{C}_{q, sp3}$ signals are missing); IR (film) $\tilde{\nu}$ = 2924, 2853, 1744, 1663, 1497, 1452, 1378, 1270, 1259, 1290, 1169, 1121, 1081, 1018, 991, 963, 919, 720, 697 cm⁻¹. HRMS (ESI): *m/z* calcd. for C₂₉H₃₇F₃O₃ [*M*⁺+Na]: 513.25870; found: 513.25917.
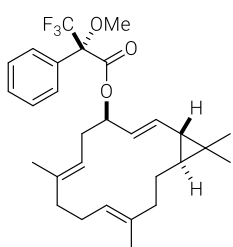
Mosher Ester (ME-6b). Prepared analogously from side-product **EP-5** and (*S*)-(+)-α-methoxy-α-(trifluormethyl)phenylacetyl chloride as a colourless oil (1.9 mg, 3.9 μmol, 71%). $[\alpha]_D^{20}$ = +56.7 (0.03 g/100 mL, CHCl₃); ¹H NMR (600 MHz, CDCl₃): δ = 7.54 (m, 2H), 7.39 (m, 3H), 5.49 (m, 1H), 5.40 (m, 2H), 5.02 (t, *J* = 6.0 Hz, 1H), 4.97 (t, *J* = 7.1 Hz, 1H), 3.57 (d, *J* = 1.2 Hz, 3H), 2.48 (dt, *J* = 12.1, 5.6 Hz, 1H), 2.27 (m, 1H), 2.07 (m, 6H), 1.92 (m, 1H), 1.56 (s, 6H), 1.04 (s, 3H), 1.01 (m, 4H), 0.82 (m, 1H), 0.41 ppm (dt, *J* = 11.2, 4.4 Hz, 1H); ¹³C NMR (151 MHz, CDCl₃): δ = 165.8, 138.7, 137.1, 133.2, 132.7, 129.5, 128.3, 127.4, 125.6, 125.0, 119.1, 78.2, 55.3, 39.2, 38.6, 32.8, 32.6, 31.6, 24.4, 24.3, 23.1, 22.7, 21.7, 16.1, 14.8 ppm ($\underline{C}F_3$ and $\underline{C}_{q, sp3}$ signals are missing); IR (film) $\tilde{\nu}$ = 2923, 2852, 1745, 1452, 1378, 1270, 1259, 1180, 1169, 1122, 1081, 1020, 992, 964, 919, 719 cm⁻¹. HRMS (ESI): *m/z* calcd. for C₂₉H₃₇F₃O₃ [*M*⁺+Na]: 513.25870; found: 513.25897.
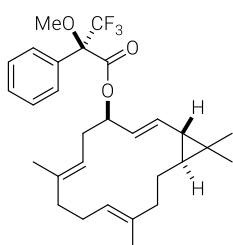
Table 23. Mosher ester analysis of **ME-6a** and **ME-6b**.

	Mosher Ester (ME-6a)	Mosher Ester (ME-6b)	
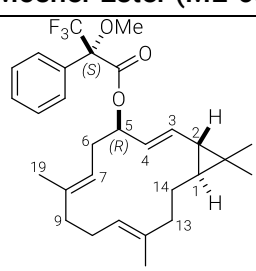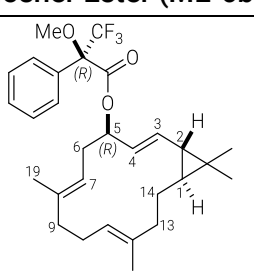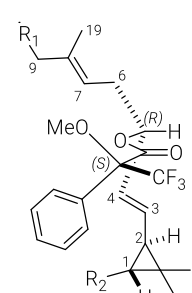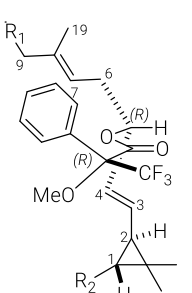
Position	δ_S (^{1}H, [ppm])	δ_R (^{1}H, [ppm])	$\Delta\delta^{SR} = \delta_S - \delta_R$
14a	1.00	1.01	−0.01
14b	1.91	1.92	−0.01
1	0.40	0.41	−0.01
2	0.78	0.81	−0.03
3	5.35	5.40	−0.05
4	5.28	5.39	−0.11
5	5.48	5.49	−0.01
6a	2.38	2.27	+0.11
6b	2.54	2.48	+0.06
7	5.01	4.97	+0.04
19	1.57	1.56	+0.01
9	2.10	2.08	+0.02

Mosher Ester (ME-7a). Prepared analogously from side-product **EP-6** and (*R*)-(−)-α-methoxy-α-(trifluormethyl)phenylacetyl chloride as a colourless oil (2.4 mg, 4.9 µmol, 90%). $[\alpha]_D^{20}$ = −14.6 (0.35 g/100 mL, CHCl$_3$); ^{1}H NMR (600 MHz, CDCl$_3$): δ = 7.53 (m, 2H), 7.38 (m, 3H), 5.62 (dd, *J* = 15.8, 8.2 Hz, 1H), 5.53 (m, 1H), 5.47 (dd, *J* = 15.6, 6.1 Hz, 1H), 4.98 (dd, *J* = 9.6, 5.0 Hz, 1H), 4.94 (m, 1H), 3.55 (d, *J* = 1.2 Hz, 3H), 2.54 (dt, *J* = 14.1, 9.6 Hz, 1H), 2.31 (d, *J* = 15.3 Hz, 1H), 2.25 (m, 1H), 2.10 (m, 4H), 2.00 (td, *J* = 12.4, 3.3 Hz, 1H), 1.92 (m, 1H), 1.55 (s, 3H), 1.51 (s, 3H), 1.06 (s, 3H), 0.97 (m, 4H), 0.79 (dd, *J* = 8.0, 5.4 Hz, 1H), 0.46 ppm (ddd, *J* = 11.4, 5.4, 3.5 Hz, 1H); ^{13}C NMR (151 MHz, CDCl$_3$): δ = 165.9, 137.0, 136.4, 133.6, 132.6, 129.5, 127.4, 125.5, 123.4, 119.7, 75.3, 55.4, 39.0, 38.6, 32.7, 32.0, 31.3, 29.7, 24.6, 24.3, 24.3, 22.3, 21.8, 15.5, 14.8 ppm (CF$_3$ and C$_{q, sp3}$ signals are missing); IR (film) $\tilde{v}$ = 2961, 2923, 2852, 1744, 1662, 1451, 1378, 1258, 1184, 1168, 1081, 1012, 865, 791, 719, 697, 661 cm^{-1}; HRMS (ESI): *m/z* calcd. for C$_{29}$H$_{37}$F$_3$O$_3$ [*M*$^+$+Na]: 513.25870; found: 513.25889.
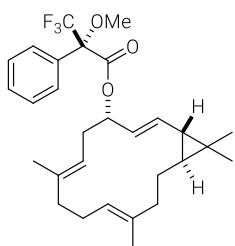
Mosher Ester (ME-7b). Prepared analogously from side-product **EP-6** and (*S*)-(+)-α-methoxy-α-(trifluormethyl)phenylacetyl chloride as a colourless oil (2.2 mg, 4.5 µmol, 82%). $[\alpha]_D^{20}$ = −108.6 (0.14 g/100 mL, CHCl$_3$); ^{1}H NMR (600 MHz, CDCl$_3$): δ = 7.52 (m, 2H), 7.38 (m, 3H), 5.52 (m, 2H), 5.42 (dd, *J* = 15.7, 5.8 Hz, 1H), 5.02 (t, *J* = 7.3 Hz, 1H), 4.93 (m, 1H), 3.56 (d, *J* = 1.2 Hz, 3H), 2.59 (dt, *J* = 14.0, 9.4 Hz, 1H), 2.40 (m, 1H), 2.26 (m, 1H), 2.16 (m, 1H), 2.11 (m, 3H), 2.00 (td, *J* = 12.2, 3.4 Hz, 1H), 1.91 (m, 1H), 1.55 (s, 3H), 1.52 (s, 3H), 1.04 (s, 3H), 0.96 (m, 1H), 0.88 (s, 3H), 0.76 (dd, *J* = 7.9, 5.4 Hz, 1H), 0.41 ppm (ddd, *J* = 11.4, 5.4, 3.5 Hz, 1H); ^{13}C NMR (151 MHz, CDCl$_3$): δ = 165.7, 136.6, 136.4, 133.6, 132.5, 129.4, 128.3, 127.4, 125.4, 123.5, 119.6, 75.3, 55.4, 39.0, 38.6, 32.7, 31.9, 31.6, 24.6, 24.3, 24.1, 22.2, 21.7, 15.5, 14.7 ppm (CF$_3$ and C$_{q, sp3}$ signals are missing); IR (film) $\tilde{v}$ = 2922, 2851, 1744, 1665, 1452, 1378, 1259, 1185, 1168, 1119, 1102, 1082, 1018, 992, 963, 799, 719 cm^{-1}; HRMS (ESI): *m/z* calcd. for C$_{29}$H$_{37}$F$_3$O$_3$ [*M*$^+$+Na]: 513.25870; found: 513.25883.
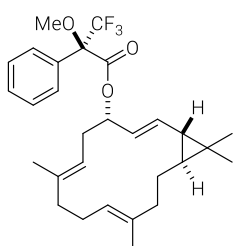
Table 24. Mosher ester analysis of **ME-7a** and **ME-7b**.

	Mosher Ester (ME-7a)	Mosher Ester (ME-7b)	
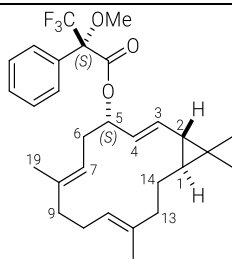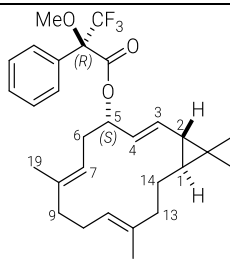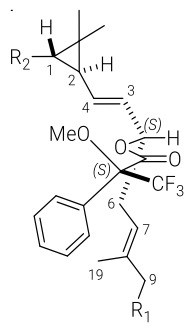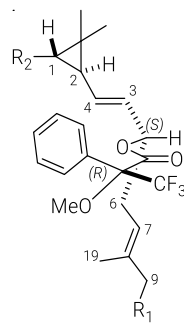
Position	δ_S (^{1}H, [ppm])	δ_R (^{1}H, [ppm])	$\Delta\delta^{SR} = \delta_S - \delta_R$
14a	0.97	0.95	+0.02
14b	1.92	1.91	+0.01
1	0.46	0.41	+0.05
2	0.80	0.76	+0.04
3	5.62	5.52	+0.10
4	5.47	5.43	+0.04
5	5.53	5.53	±0.00
6a	2.32	2.40	−0.08
6b	2.54	2.59	−0.05
7	4.98	5.02	−0.04
19	1.51	1.53	−0.02
9a	2.08	2.11	−0.03
9b	2.15	2.16	−0.01

3.3.4 COMPUTATIONAL DETAILS FOR STRUCTURE ELUCIDATION

Conformational Search

Starting from the initial set of candidate structures for the four diastereomers, a set of conformers was generated using the semiempirical XTB code (version 6.1).[285] The conformational search was performed by means of the conformer–rotamer ensemble sampling (CREST) algorithm[220,221,286] using the semiempirical tight-binding based quantum chemistry method GFN2-xTB.[287] The default settings and thresholds for the meta-dynamic sampling based conformational search were applied, including the implicit solvent model for CH_3Cl.

Geometric Optimisation

All geometry optimisations presented in the chemical shielding calculation project were carried out with the ORCA 4.2 program package.[222,223] The optimisations were conducted at DFT level using the B3LYP functional[288] and the def2-TZVP basis set,[270] in combination with the D3 version of Grimme's dispersion correction including Becke–Johnson damping (D3(BJ)).[273,274] Implicit solvent effects were included by the conductor–like polarizable continuum model (CPCM)[280–283] using the Van-der-Waals Gaussian surface type for $CHCl_3$. In all cases, a fine integration grid (grid7) was used as well as very tight SCF convergence criteria. The RIJCOSX approximation was utilised with the def2/J auxiliary basis set[289] and an increased grid setting (gridx7) for the calculation of the two-electron integrals.[277–279] This level of theory is noted as B3LYP-D3BJ-(CPCM)/def2-TZVP.

Similarity Check

The relevant conformers with significantly conformational distinctions were sorted out, based on the root-mean-square deviations (RMSD) of atomic positions within 3.0 kcal/mol threshold from the lowest conformer in single point energy. The RMSD values were calculated by an automated script[290–292] and pairs with a RMSD value lower than 1.5 Å and a single point energy difference low than 0.5 Kcal/mol underwent a visual similarity check in Chemcraft.[293]

Boltzmann distribution

The Boltzmann distribution (p_i) was calculated based on the Gibbs free energies (ΔG) obtained from the frequency calculation at the B3LYP-D3BJ-(CPCM)/def2-TZVP level of theory.

$$p_i = \frac{N_i}{N} = \frac{e^{\frac{-\Delta G_i}{k_B T}}}{\sum_j^M e^{\frac{-\Delta G_j}{k_B T}}} \text{ (eq. 1)}$$

The Boltzmann distribution was calculated according to eq. 1 and is summarized in Table 25: p_i probability of conformer i, k_B is the Boltzmann constant (1.380649×10^{-23} J/K), T is the temperature (298.15 K), and ΔG is the relative free Gibbs energy of conformer i to the lowest free Gibbs energy conformer, M is the number of all relevant conformers ($p_i > 4\%$).

Table 25. The relevant populated conformers of the four diastereomers 1*S*,2*R*,5*S*-**151**; 1*S*,2*R*,5*R*-**154**, 1*S*,2*S*,5*R*-**155**, and 1*S*,2*S*,5*S*-**156** based on their Boltzmann distribution.

1*S*,2*R*,5*S*-**151**		1*S*,2*R*,5*R*-**154**		1*S*,2*S*,5*R*-**155**		1*S*,2*S*,5*S*-**156**	
Conformer	p_i	Conformer	p_i	Conformer	p_i	Conformer	p_i
010	0.194	003	0.217	002	0.330	013	0.543
001	0.151	053	0.100	001	0.202	017	0.155
007	0.144	024	0.070	006	0.174	092	0.065
034	0.143	079	0.070	020	0.075	055	0.063
011	0.104	012	0.070	004	0.063	039	0.049
020	0.099	090	0.062	009	0.060	001	0.042
017	0.094	063	0.060	013	0.056	042	0.042
014	0.071	020	0.057	003	0.041	019	0.041
		030	0.055				
		119	0.052				
		058	0.052				
		056	0.049				
		013	0.047				
		021	0.042				

Chemical Shielding Calculation:

All chemical shielding calculations were carried out for the relevant conformers (Table 25) by means of the ORCA 4.2 program package[222,223] at the recommended level of theory for the DP4+ probability calculations.[209] The chemical shielding tensors (σ_i^x) were calculated at DFT level using the mPW1PW functional[228] and the 6-31+G** basis sets,[229] together with gauge including atomic orbitals (GIAO).[273,274] Very tight convergence thresholds were used for the SCF (10^{-9}) and CPSCF (10^{-10}) iterations. The RIJCOSX approximation was utilised with the def2/J auxiliary basis set[289] and an increased grid setting (gridx7) for the calculation of the two-electron integrals.[277–279] This level of theory is noted as mPW1PW/6-31G**.

The chemical shielding tensors (σ_i^x) were averaged by the Boltzmann distribution probability (p_i) for each relevant populated conformer i ($p_i > 4\%$) ($\sigma^x = \sum_j^M \sigma_i^x p_i$). The Boltzmann averaged shielding (σ^x) is then used in the DP4+ probability calculation.

The Boltzmann averaged chemical shielding were employed in the DP4+ (128) Excel sheet provided by Sarotti and co-workers.[294]

Table 26. DP4+ (128) Calculation for the exp. NMR data of euphorhylonal A.

Functional mPW1PW91		Solvent Gas Phase	Basis Set 6-31+G(d,p)	Type of Data Shielding Tensor	
		DP4+	0.00%	0.00%	100.00%	0.00%
Nuclei	sp²?	**euphorhylonal A** (natural material)	1*S*,2*R*,5*S*-**151**	1*S*,2*R*,5*R*-**154**	1*S*,2*S*,5*R*-**155**	1*S*,2*S*,5*S*-**156**
		Exp. NMR data δ [ppm]	Calculated chemical shielding σ^x [ppm]			
H		0.84	30.6763	30.5987	30.6403	30.8645
H		1.61	29.8017	29.5805	29.8229	29.8658
H	x	5.99	25.3481	24.9709	25.3474	25.2949
H		4.07	28.0864	26.8123	27.7261	26.9570
H		2.51	28.8829	28.8818	28.9996	29.2696
H		2.62	29.3253	29.3841	28.8224	29.1337
H	x	4.86	26.2342	26.2149	26.2170	26.3329
H		2.00	29.6564	29.5956	29.5181	29.5370
H		2.00	29.6261	29.5915	29.3623	29.4599
H		2.14	29.4048	29.4768	29.3589	29.5321
H		2.14	29.5146	29.4544	29.2200	29.3279
H	x	4.96	26.2969	26.3219	26.0531	26.2835
H		2.00	29.7334	29.7541	29.3550	29.6321
H		2.00	29.4251	29.4340	29.4293	29.5083
H		2.14	30.2309	30.2571	30.4327	30.7018
H		2.14	29.9242	29.8530	29.4538	29.6132
H		1.17	30.5670	30.5553	30.3672	30.5655
H		1.16	30.6941	30.7178	30.3888	30.5907
H		1.54	30.2696	30.2534	29.9108	30.1300
H		1.57	29.9584	29.9229	29.8437	30.0214
H	x	10.12	21.3449	21.2600	21.1506	21.2585
C		37.70	158.6394	158.5659	155.3878	156.4035
C		29.10	168.3814	168.6740	164.5127	165.0972
C	x	156.40	46.1648	49.3041	41.1267	43.0058
C	x	132.60	58.8579	58.8834	60.2837	60.5571
C		76.40	116.8904	126.2698	116.8704	127.0219
C		34.70	158.4013	161.4028	158.7280	162.4680
C	x	120.80	77.7804	80.1806	74.7359	74.9217
C	x	137.30	60.6279	59.3175	61.7764	62.6679
C		39.20	156.5388	156.2727	154.7284	155.5693
C		24.10	169.4500	169.5282	168.2447	169.6852
C	x	125.90	70.6287	70.8479	70.3211	71.3453
C	x	135.60	64.1009	62.9155	64.8161	64.7766
C		38.60	154.2140	154.2907	154.1903	155.9731
C		24.20	172.4855	170.8511	168.9221	169.9936
C		28.40	165.3912	165.7858	162.4579	163.5641
C		22.80	167.5315	167.7086	172.0241	173.8746
C		21.90	179.8399	180.0354	173.1121	174.3148
C		15.90	178.0967	178.4680	178.2749	179.9401
C		14.70	177.8666	178.1363	179.7310	181.0824
C	x	192.10	9.9695	13.0171	11.0983	11.9738

Table 27. DP4+ (128) Probability calculation results based on the exp. NMR data of euphorhylonal A.

Exp. Data of **euphorhylonal A**	1*S*,2*R*,5*S*-**151**	1*S*,2*R*,5*R*-**154**	1*S*,2*S*,5*R*-**155**	1*S*,2*S*,5*S*-**156**
DP4+ (¹H data)	0.00%	0.00%	1.65%	98.35%
DP4+ (¹³C data)	0.00%	0.00%	100.00%	0.00%
DP4+ (all data)	**0.00%**	**0.00%**	**100.00%**	**0.00%**

Table 28. DP4+ (128) Calculation for the exp. NMR data of 1*S*,2*R*,5*S*-aldehyde **151**.

Functional		Solvent	Basis Set		Type of Data	
mPW1PW91		Gas Phase	6-31+G(d,p)		Shielding Tensor	
		DP4+	**100.00%**	**0.00%**	**0.00%**	**0.00%**
Nuclei	sp²?	1*S*,2*R*,5*S*-**151**	1*S*,2*R*,5*S*-**151**	1*S*,2*R*,5*R*-**154**	1*S*,2*S*,5*R*-**155**	1*S*,2*S*,5*S*-**156**
		Exp. NMR data δ [ppm]	Calculated chemical shielding σˣ [ppm]			
H		1.02	30.6763	30.5987	30.6403	30.8645
H		1.96	29.8017	29.5805	29.8229	29.8658
H	x	6.19	25.3481	24.9709	25.3474	25.2949
H		3.95	28.0864	26.8123	27.7261	26.9570
H		2.45	28.8829	28.8818	28.9996	29.2696
H		2.7	29.3253	29.3841	28.8224	29.1337
H	x	4.89	26.2342	26.2149	26.2170	26.3329
H		1.91	29.6564	29.5956	29.5181	29.5370
H		2.14	29.6261	29.5915	29.3623	29.4599
H		2.09	29.4048	29.4768	29.3589	29.5321
H		2.14	29.5146	29.4544	29.2200	29.3279
H	x	4.91	26.2969	26.3219	26.0531	26.2835
H		1.95	29.7334	29.7541	29.3550	29.6321
H		2.33	29.4251	29.4340	29.4293	29.5083
H		1.28	30.2309	30.2571	30.4327	29.6132
H		1.87	29.9242	29.8530	29.4538	30.7018
H		1.16	30.5670	30.5553	30.3672	30.5655
H		1.03	30.6941	30.7178	30.3888	30.5907
H		1.51	30.2696	30.2534	29.9108	30.1300
H		1.62	29.9584	29.9229	29.8437	30.0214
H	x	10.13	21.3449	21.2600	21.1506	21.2585
C		35.6	158.6394	158.5659	155.3878	156.4035
C		25.4	168.3814	168.6740	164.5127	165.0972
C	x	151.3	46.1648	49.3041	41.1267	43.0058
C	x	139.2	58.8579	58.8834	60.2837	60.5571
C		77.5	116.8904	126.2698	116.8704	127.0219
C		35.7	158.4013	161.4028	158.7280	162.4680
C	x	120.3	77.7804	80.1806	74.7359	74.9217
C	x	136.6	60.6279	59.3175	61.7764	62.6679
C		38.9	156.5388	156.2727	154.7284	155.5693
C		24.1	169.4500	169.5282	168.2447	169.6852
C	x	123.6	70.6287	70.8479	70.3211	71.3453
C	x	134.3	64.1009	62.9155	64.8161	64.7766
C		39.4	154.2140	154.2907	154.1903	155.9731
C		22	172.4855	170.8511	168.9221	169.9936
C		26.8	165.3912	165.7858	162.4579	163.5641
C		28.9	167.5315	167.7086	172.0241	173.8746
C		15.9	179.8399	180.0354	173.1121	174.3148
C		16.1	178.0967	178.4680	178.2749	179.9401
C		17.7	177.8666	178.1363	179.7310	181.0824
C	x	192.7	9.9695	13.0171	11.0983	11.9738

Table 29. DP4+ (128) Probability calculation results based on the exp. NMR data of 1*S*,2*R*,5*S*-**151**.

Exp. Data of 1*S*,2*R*,5*S*-aldehyde **151**	1*S*,2*R*,5*S*-**151**	1*S*,2*R*,5*R*-**154**	1*S*,2*S*,5*R*-**155**	1*S*,2*S*,5*S*-**156**
DP4+ (¹H data)	91.40%	7.37%	1.23%	0.00%
DP4+ (¹³C data)	100.00%	0.00%	0.00%	0.00%
DP4+ (all data)	**100.00%**	**0.00%**	**0.00%**	**0.00%**

Table 30. DP4+ (128) Calculation for the exp. NMR data of 1*S*,2*R*,5*R*-aldehyde **154**.

Functional mPW1PW91	Solvent Gas Phase	Basis Set 6-31+G(d,p)		Type of Data Shielding Tensor	
		DP4+	**0.00%**	**100.00%**	**0.00%**	**0.00%**
Nuclei	sp²?	1*S*,2*R*,5*R*-**154**	1*S*,2*R*,5*S*-**151**	1*S*,2*R*,5*S*-**154**	1*S*,2*S*,5*R*-**155**	1*S*,2*S*,5*S*-**156**
		Exp. NMR data δ [ppm]	Calculated chemical shielding σˣ [ppm]			
H		1.08	30.6763	30.5987	30.6403	30.8645
H		2.07	29.8017	29.5805	29.8229	29.8658
H	x	6.49	25.3481	24.9709	25.3474	25.2949
H		4.81	28.0864	26.8123	27.7261	26.9570
H		2.46	28.8829	28.8818	28.9996	29.2696
H		2.56	29.3253	29.3841	28.8224	29.1337
H	x	4.91	26.2342	26.2149	26.2170	26.3329
H		1.99	29.6564	29.5956	29.5181	29.5370
H		2.11	29.6261	29.5915	29.3623	29.4599
H		2.11	29.4048	29.4768	29.3589	29.5321
H		2.11	29.5146	29.4544	29.2200	29.3279
H	x	4.92	26.2969	26.3219	26.0531	26.2835
H		1.91	29.7334	29.7541	29.3550	29.6321
H		2.30	29.4251	29.4340	29.4293	29.5083
H		1.23	30.2309	30.2571	30.4327	30.7018
H		1.94	29.9242	29.8530	29.4538	29.6132
H		1.17	30.5670	30.5553	30.3672	30.5655
H		1.04	30.6941	30.7178	30.3888	30.5907
H		1.53	30.2696	30.2534	29.9108	30.1300
H		1.63	29.9584	29.9229	29.8437	30.0214
H	x	10.18	21.3449	21.2600	21.1506	21.2585
C		35.30	158.6394	158.5659	155.3878	156.4035
C		25.00	168.3814	168.6740	164.5127	165.0972
C	x	148.10	46.1648	49.3041	41.1267	43.0058
C	x	140.90	58.8579	58.8834	60.2837	60.5571
C		67.80	116.8904	126.2698	116.8704	127.0219
C		33.00	158.4013	161.4028	158.7280	162.4680
C	x	117.70	77.7804	80.1806	74.7359	74.9217
C	x	137.70	60.6279	59.3175	61.7764	62.6679
C		38.80	156.5388	156.2727	154.7284	155.5693
C		24.00	169.4500	169.5282	168.2447	169.6852
C	x	124.60	70.6287	70.8479	70.3211	71.3453
C	x	134.80	64.1009	62.9155	64.8161	64.7766
C		39.60	154.2140	154.2907	154.1903	155.9731
C		23.50	172.4855	170.8511	168.9221	169.9936
C		26.20	165.3912	165.7858	162.4579	163.5641
C		28.90	167.5315	167.7086	172.0241	173.8746
C		15.70	179.8399	180.0354	173.1121	174.3148
C		16.50	178.0967	178.4680	178.2749	179.9401
C		17.20	177.8666	178.1363	179.7310	181.0824
C	x	190.90	9.9695	13.0171	11.0983	11.9738

Table 31. DP4+ (128) Probability calculation results based on the exp. NMR data of 1*S*,2*R*,5*R*-**154**.

Exp. NMR data of 1*S*,2*R*,5*R*-**154**	1*S*,2*R*,5*S*-**151**	1*S*,2*R*,5*R*-**154**	1*S*,2*S*,5*R*-**155**	1*S*,2*S*,5*S*-**156**
DP4+ (¹H data)	0.00%	99.98%	0.00%	0.02%
DP4+ (¹³C data)	0.00%	100.00%	0.00%	0.00%
DP4+ (all data)	**0.00%**	**100.00%**	**0.00%**	**0.00%**

Table 32. DP4+ (128) Probability calculation for the exp. NMR data 1*S*,2*S*,5*R*-aldehyde **155**.

Functional mPW1PW91	Solvent Gas Phase	Basis Set 6-31+G(d,p)		Type of Data Shielding Tensor	
	DP4+	0.00%	0.00%	100.00%	0.00%
Nuclei sp²?	1*S*,2*S*,5*R*-**155**	1*S*,2*R*,5*S*-**151**	1*S*,2*R*,5*R*-**154**	1*S*,2*S*,5*R*-**155**	1*S*,2*S*,5*S*-**156**
	Exp. NMR data δ [ppm]	Calculated chemical shielding σ^x [ppm]			
H	0.82	30.6763	30.5987	30.6403	30.8645
H	1.60	29.8017	29.5805	29.8229	29.8658
H x	5.98	25.3481	24.9709	25.3474	25.2949
H	4.08	28.0864	26.8123	27.7261	26.9570
H	2.49	28.8829	28.8818	28.9996	29.2696
H	2.61	29.3253	29.3841	28.8224	29.1337
H x	4.86	26.2342	26.2149	26.2170	26.3329
H	2.01	29.6564	29.5956	29.5181	29.5370
H	2.11	29.6261	29.5915	29.3623	29.4599
H	2.14	29.4048	29.4768	29.3589	29.5321
H	2.14	29.5146	29.4544	29.2200	29.3279
H x	4.96	26.2969	26.3219	26.0531	26.2835
H	2.15	29.7334	29.7541	29.3550	29.6321
H	2.00	29.4251	29.4340	29.4293	29.5083
H	1.14	30.2309	30.2571	30.4327	30.7018
H	2.00	29.9242	29.8530	29.4538	29.6132
H	1.17	30.5670	30.5553	30.3672	30.5655
H	1.16	30.6941	30.7178	30.3888	30.5907
H	1.53	30.2696	30.2534	29.9108	30.1300
H	1.56	29.9584	29.9229	29.8437	30.0214
H x	10.12	21.3449	21.2600	21.1506	21.2585
C	37.70	158.6394	158.5659	155.3878	156.4035
C	29.10	168.3814	168.6740	164.5127	165.0972
C x	156.50	46.1648	49.3041	41.1267	43.0058
C x	137.20	58.8579	58.8834	60.2837	60.5571
C	76.50	116.8904	126.2698	116.8704	127.0219
C	34.70	158.4013	161.4028	158.7280	162.4680
C x	120.80	77.7804	80.1806	74.7359	74.9217
C x	135.70	60.6279	59.3175	61.7764	62.6679
C	38.60	156.5388	156.2727	154.7284	155.5693
C	24.10	169.4500	169.5282	168.2447	169.6852
C x	125.90	70.6287	70.8479	70.3211	71.3453
C x	132.60	64.1009	62.9155	64.8161	64.7766
C	39.10	154.2140	154.2907	154.1903	155.9731
C	24.20	172.4855	170.8511	168.9221	169.9936
C	28.50	165.3912	165.7858	162.4579	163.5641
C	22.90	167.5315	167.7086	172.0241	173.8746
C	22.00	179.8399	180.0354	173.1121	174.3148
C	15.90	178.0967	178.4680	178.2749	179.9401
C	14.70	177.8666	178.1363	179.7310	181.0824
C x	192.30	9.9695	13.0171	11.0983	11.9738

Table 33. DP4+ (128) Probability calculation results based on the exp. NMR data of 1*S*,2*S*,5*R*-**155**.

Exp. Data of 1*S*,2*S*,5*R*-**155**	1*S*,2*R*,5*S*-**151**	1*S*,2*R*,5*R*-**154**	1*S*,2*S*,5*R*-**155**	1*S*,2*S*,5*S*-**156**
DP4+ (¹H data)	0.00%	0.00%	11.31%	88.69%
DP4+ (¹³C data)	0.00%	0.00%	100.00%	0.00%
DP4+ (all data)	**0.00%**	**0.00%**	**100.00%**	**0.00%**

Table 34. DP4+ (128) Calculation for the exp. NMR data of 1*S*,2*S*,5*S*-aldehyde **156**.

Functional	Solvent	Basis Set		Type of Data	
mPW1PW91	Gas Phase	6-31+G(d,p)		Shielding Tensor	
		DP4+	**0.00%**	**0.00%**	**0.00%**	**98.71%**
Nuclei	sp²?	1*S*,2*S*,5*S*-**156**	1*S*,2*R*,5*S*-**151**	1*S*,2*R*,5*R*-**154**	1*S*,2*S*,5*R*-**155**	1*S*,2*S*,5*S*-**156**
		Exp. NMR data δ [ppm]	Calculated chemical shielding σˣ [ppm]			
H		1.04	30.6763	30.5987	30.6403	30.8645
H		2.00	29.8017	29.5805	29.8229	29.8658
H	x	6.76	25.3481	24.9709	25.3474	25.2949
H		4.76	28.0864	26.8123	27.7261	26.9570
H		2.60	28.8829	28.8818	28.9996	29.2696
H		2.45	29.3253	29.3841	28.8224	29.1337
H	x	5.36	26.2342	26.2149	26.2170	26.3329
H		2.19	29.6564	29.5956	29.5181	29.5370
H		2.26	29.6261	29.5915	29.3623	29.4599
H		2.18	29.4048	29.4768	29.3589	29.5321
H		2.47	29.5146	29.4544	29.2200	29.3279
H	x	5.33	26.2969	26.3219	26.0531	26.2835
H		2.21	29.7334	29.7541	29.3550	29.6321
H		2.02	29.4251	29.4340	29.4293	29.5083
H		1.13	30.2309	30.2571	30.4327	30.7018
H		2.12	29.9242	29.8530	29.4538	29.6132
H		1.17	30.5670	30.5553	30.3672	30.5655
H		1.15	30.6941	30.7178	30.3888	30.5907
H		1.63	30.2696	30.2534	29.9108	30.1300
H		1.74	29.9584	29.9229	29.8437	30.0214
H	x	10.37	21.3449	21.2600	21.1506	21.2585
C		42.86	158.6394	158.5659	155.3878	156.4035
C		34.09	168.3814	168.6740	164.5127	165.0972
C	x	161.01	46.1648	49.3041	41.1267	43.0058
C	x	136.40	58.8579	58.8834	60.2837	60.5571
C		71.14	116.8904	126.2698	116.8704	127.0219
C		34.91	158.4013	161.4028	158.7280	162.4680
C	x	121.67	77.7804	80.1806	74.7359	74.9217
C	x	138.32	60.6279	59.3175	61.7764	62.6679
C		42.51	156.5388	156.2727	154.7284	155.5693
C		28.27	169.4500	169.5282	168.2447	169.6852
C	x	125.57	70.6287	70.8479	70.3211	71.3453
C	x	135.92	64.1009	62.9155	64.8161	64.7766
C		42.08	154.2140	154.2907	154.1903	155.9731
C		27.32	172.4855	170.8511	168.9221	169.9936
C		37.01	165.3912	165.7858	162.4579	163.5641
C		23.34	167.5315	167.7086	172.0241	173.8746
C		23.10	179.8399	180.0354	173.1121	174.3148
C		17.90	178.0967	178.4680	178.2749	179.9401
C		16.74	177.8666	178.1363	179.7310	181.0824
C	x	189.48	9.9695	13.0171	11.0983	11.9738

Table 35. DP4+ (128) Probability Calculation results based on the exp. NMR data of 1*S*,2*S*,5*S*-aldehyde **156**.

Exp. Data of 1*S*,2*S*,5*S*-**156**	1*S*,2*R*,5*S*-**151**	1*S*,2*R*,5*R*-**154**	1*S*,2*S*,5*R*-**155**	1*S*,2*S*,5*S*-**156**
DP4+ (¹H data)	0.00%	0.00%	0.01%	99.99%
DP4+ (¹³C data)	0.00%	0.00%	99.34%	0.66%
DP4+ (all data)	**0.00%**	**0.00%**	**1.29%**	**98.71%**

3.4 Synthesis towards 2-*epi*-10-hydroxydepressin

(*E*)-dimethyl(penta-2,4-dien-2-yl)(phenyl)silane (176). Tosyl chloride (106.8 mg, 0.6 mmol) was added to a reaction mixture of DMAP (4.5 mg, 37.3 µmol), Et$_3$N (0.1 mL, 75.6 mg, 746.9 µmol) and alcohol **130** (82.3 mg, 373.4 µmol) in CH$_2$Cl$_2$ at 0 °C. The resulting mixture was stirred for 4 h at RT. The reaction was quenched with aqueous saturated NH$_4$Cl solution. The aqueous layer was separated and extracted with CH$_2$Cl$_2$ (3 × 15 mL). The combined organic phases were dried over MgSO$_4$ and concentrated, and the residue was purified by flash chromatography (hexane/EtOAc, 20:1) to yield the title compound as a colourless oil (126.0 mg, 90%). ^{1}H NMR (400 MHz, CDCl$_3$) δ = 7.78 (d, *J* = 8.3 Hz, 2H), 7.45 (m, 2H), 7.33 (m, 5H), 5.63 (m, 1H), 4.06 (t, *J* = 7.0 Hz, 2H), 2.49 (qd, *J* = 6.9, 1.0 Hz, 1H), 2.44 (s, 3H), 1.62 (m, 3H), 0.30 ppm (s, 6H); ^{13}C NMR (101 MHz, CDCl$_3$) δ = 144.6, 139.0, 137.9, 133.9, 133.8, 133.2, 129.8, 128.9, 127.8, 127.7, 69.4, 28.2, 21.6, 15.0, −3.6 ppm; IR (film) $\tilde{v}$ = 2957, 1598, 1427, 1359, 1248, 1188, 1175, 1109, 1098, 964, 913, 811, 772, 732, 701, 662, 575, 554 cm^{-1}; MS (ESI) calcd for C$_{20}$H$_{26}$O$_3$Si [*M*$^+$+Na] 397.12634, found 397.12642.
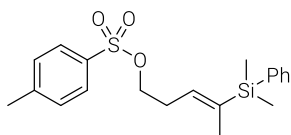
(*E*)-dimethyl(penta-2,4-dien-2-yl)(phenyl)silane (174). Potassium *tert*-butanolate (36.2 mg, 0.3 mmol) was added to a solution of tosyl alcohol **178** (80.5 mg, 0.2 mmol) in THF at 0 °C. The resulting mixture was stirred for 3 h at RT. The reaction was quenched with pentane, filtered and concentrated. The residue was purified by flash chromatography (pentane) to yield the title compound as a colourless oil (35.0 mg, 80%). ^{1}H NMR (400 MHz, CDCl$_3$) δ = 7.50 (m, 2H), 7.35 (dd, *J* = 4.9, 1.9 Hz, 3H), 6.76 (ddd, *J* = 16.8, 10.7, 10.1 Hz, 1H), 6.37 (ddt, *J* = 10.7, 1.7, 0.8 Hz, 1H), 5.20 (m, 1H), 1.81 (d, *J* = 1.7 Hz, 3H), 0.37 ppm (s, 6H); ^{13}C NMR (101 MHz, CDCl$_3$) δ = 139.0, 138.3, 138.0, 134.0, 132.5, 128.9, 127.7, 118.0, 15.4, −3.6 ppm; IR (film) $\tilde{v}$ = 3069, 3013, 2958, 2925, 2855, 1575, 1428, 1248, 1111, 986, 910, 832, 814, 773, 730, 699, 645 cm^{-1}; MS (ESI) calcd for C$_{13}$H$_{18}$Si [*M*$^+$+H] 203.12505, found 203.12490.
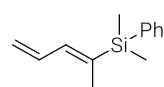
(*S,E*)-(4,5-bis(4,4,5,5-tetramethyl-1,3,2-dioxaborolan-2-yl)pent-2-en-2-yl)dimethyl (phenyl) silane (175). In a pressure Schlenk tube, a solution of Pt(dba)$_3$ (26.6 mg, 29.6 µmol), *S,S*-TADDOL-Ligand **177** (35.9 mg, 39.5 µmol, 4 mol%), and B$_2$pin$_2$ (263.5 mg, 1.0 mmol) in THF (14 mL) was stirred for 20 min at 80 °C. After the reaction mixture was cooled to ambient temperature, diene **176** (200.0 mg, 988.3 µmol) was added and the reaction mixture was stirred at 65° C for 16 h.
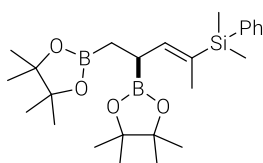
The reaction was quenched with water. The aqueous layer was separated and extracted with Et$_2$O (3 × 15 mL). The combined organic phases were dried over MgSO$_4$ and concentrated, and the residue was purified by flash chromatography (hexane/EtOAc, 100:1) to yield the title compound as a colourless oil (389.0 mg, 86%, 99% ee). $[\alpha]_D^{20}$ = +32.6 (0.58 g/100 mL, CHCl$_3$); ^{1}H NMR (400 MHz, CDCl$_3$) δ = 7.50 (m, 2H), 7.31 (m, 3H), 5.77 (dd, *J* = 9.1, 1.8 Hz, 1H), 2.39 (td, *J* = 9.3, 6.2 Hz, 1H), 1.68 (d, *J* = 1.7 Hz, 3H), 1.21 (m, 24H), 1.06 (dd, *J* = 15.9, 9.4 Hz, 1H), 0.93 (dd, *J* = 15.9, 6.2 Hz, 1H), 0.30 (s, 3H), 0.29 ppm (s, 3H); ^{13}C NMR (101 MHz, CDCl$_3$) δ = 144.8, 139.4, 134.0, 131.6, 128.5, 127.5, 82.9, 82.8, 24.9, 24.7, 24.6, 24.6, 15.2, −3.12, −3.5 ppm; IR (film) $\tilde{v}$ = 2977, 2930, 1606, 1467, 1369, 1313, 1270, 1246, 1213, 1142, 1110, 967, 831, 812, 772, 729, 700 cm^{-1}; MS (ESI) calcd for C$_{25}$H$_{42}$B$_2$O$_4$Si [*M*$^+$+Na] 479.29307, found 479.29370.

LON-LA-622-01-Racemat
150 mm Chiralcel OJ-3R, 3 µm, 4.6 mm i.D.,
MeCN/Wasser = 60:40
0.5 ml/min, 86 bar / 298 K

PDA Ch1 220nm

Peak #	Ret. Time	Area %	Name
1	3,69	0,28	
2	6,02	0,32	
3	6,46	0,17	
4	7,16	0,13	
5	7,75	1,67	
6	7,89	2,18	
7	10,28	0,13	
8	14,65	0,86	
9	15,24	40,26	1. Enantiomer
10	16,27	1,35	
11	16,63	2,56	
12	18,09	6,59	
13	19,50	39,77	2. Enantiomer
14	21,08	0,18	
15	22,43	0,14	
16	25,81	2,02	
17	28,59	1,39	
Total		100,00	

LON-LA-621-01 (0.3 mg/0.15 ml CH3CN/2-Prop.=2:1)
150 mm Chiralcel OJ-3R, 3 µm, 4.6 mm i.D.,
MeCN/Wasser = 60:40
0.5 ml/min, 86 bar / 298 K

PDA Ch1 220nm

Peak #	Ret. Time	Area %	Name
1	4,88	0,31	
2	5,73	0,12	
3	6,02	0,42	
4	6,42	0,38	
5	7,75	2,70	
6	10,29	0,35	
7	11,62	0,45	
8	15,28	0,46	1. Enantiomer
9	16,05	0,17	
10	18,18	0,32	
11	19,67	90,50	2. Enantiomer 99% ee
12	25,92	0,61	
13	27,56	0,15	
14	28,72	3,05	
Total		100,00	

(*S,E*)-4-(dimethyl(phenyl)silyl)-1-(4,4,5,5-tetramethyl-1,3,2-dioxaborolan-2-yl)pent-3-en-2-ol (178).
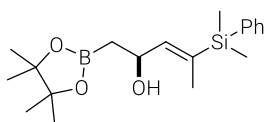
4-Methyl morpholine *N*-oxide (1.3 g, 11.4 mmol) was added to a solution of 1,2-bis(boronate) **175** (520.0 mg, 1.1 mmol) in acetone (52 mL, technical grade). The resulting mixture was stirred for 2 h at RT, concentrated and the residue was purified by flash chromatography (hexane/EtOAc, 4:1) to yield the title compound as a colourless oil (285.0 mg, 72%).

$[\alpha]_D^{20}$ = −10.4 (0.80 g/100 mL, CHCl$_3$); ^{1}H NMR (400 MHz, CDCl$_3$) δ = 7.48 (m, 2H), 7.33 (dd, *J* = 5.1, 1.9 Hz, 3H), 5.84 (dd, *J* = 7.9, 1.7 Hz, 1H), 4.79 (dt, *J* = 7.9, 6.4 Hz, 1H), 1.71 (d, *J* = 1.7 Hz, 3H), 1.23 (s, 12H), 1.19 (dd, *J* = 6.4, 1.9 Hz, 2H), 0.34 (s, 3H), 0.33 ppm (s, 3H); ^{13}C NMR (101 MHz, CDCl$_3$) δ = 144.8, 134.9, 134.0, 128.9, 127.7, 83.4, 65.5, 24.9, 24.7, 15.0, −3.56, −3.7 ppm; IR (film) $\tilde{v}$ = 3395, 2976, 2958, 2927, 2856, 1719, 1472, 1441, 1429, 1370, 1324, 1249, 1216, 1145, 1110, 1010, 983, 965, 912, 886, 831, 813, 773, 730, 699, 673, 645, 578, 542, 520, 475, 451 cm^{-1}; MS (ESI) calcd for C$_{19}$H$_{31}$BO$_3$Si [*M*$^+$+Na] 369.20277, found 369.20294.

(*S,E*)-tert-butyl((4-(dimethyl(phenyl)silyl)-1-(4,4,5,5-tetramethyl-1,3,2-dioxaborolan-2-yl) pent-3-en-2-yl)oxy)dimethylsilane (173).
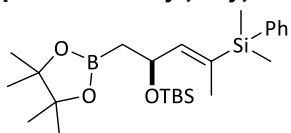
TBSCl (65.3 mg, 433.1 µmol) was added to a solution of allylic alcohol **178** (75.0 mg, 216.5 µmol) and imidazole (22.1 mg, 324.8 µmol) in DMF (5 mL) and the resulting reaction mixture was stirred at RT for 14 h. The reaction was quenched with aqueous saturated NH$_4$Cl solution. The aqueous layer was separated and extracted with *tert*-butyl methyl ether (3 × 15 mL). The combined organic phases were dried over MgSO$_4$ and concentrated, and the residue was purified by flash chromatography (hexane/EtOAc, 20:1) to yield the title compound as a colourless oil (85.7 mg, 86%).

$[\alpha]_D^{20}$ = −14.8 (2.06 g/100 mL, CHCl$_3$); ^{1}H NMR (400 MHz, CDCl$_3$) δ = 7.48 (m, 2H), 7.32 (m, 3H), 5.81 (dq, *J* = 8.4, 1.7 Hz, 1H), 4.81 (ddd, *J* = 8.3, 7.4, 6.3 Hz, 1H), 1.68 (d, *J* = 1.7 Hz, 3H), 1.20 (s, 6H), 1.19 (s, 6H), 1.13 (dd, *J* = 13.8, 6.8 Hz, 2H), 0.86 (s, 9H), 0.32 (s, 6H), 0.03 (s, 3H), 0.01 ppm

(s, 3H); ^{13}C NMR (101 MHz, CDCl$_3$) δ = 146.6, 138.3, 134.0, 131.2, 128.8, 127.6, 82.9, 66.4, 25.9, 25.0, 24.8, 18.2, 15.0, −3.65, −3.67, −4.3, −4.6 ppm; IR (film) $\tilde{v}$ = 3423, 3048, 3070, 2999, 2927, 2957, 2856, 1719, 1683, 1636, 1428, 1411, 1362, 1251, 1158, 1112, 1071, 1028, 815, 833, 777, 733, 701, 472 cm^{-1}; MS (ESI) calcd for C$_{25}$H$_{45}$BO$_3$Si$_2$ [M^++Na] 483.28925, found 483.28979.

(E)-Dimethyl(phenyl)(5-(trityloxy)oct-2-en-6-yn-2-yl)silane (179).
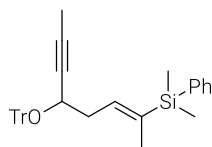
Trityl chloride (694.0 mg, 2.5 mmol) was added to a solution of propargylic alcohol **131** (536.0 mg, 2.1 mmol) in CH$_2$Cl$_2$ (10 mL). The resulting mixture was stirred for 14 h at RT and the reaction was quenched with saturated aqueous NH$_4$Cl solution. The aqueous layer was separated and extracted with *tert*-butyl methyl ether (3 × 10 mL). The organic phases were dried over MgSO$_4$, filtered and concentrated. The residue was purified by flash chromatography (hexane/EtOAc, 20:1) to yield the title compound as a colourless oil (862.1 mg, 83%).^{1}H NMR (400 MHz, CDCl$_3$) δ = 7.53 (m, 6H), 7.47 (m, 2H), 7.26 (m, 12H), 5.86 (m, 1H), 3.97 (m, 1H), 2.32 (dp, J = 14.6, 7.8, 7.1 Hz, 2H), 1.57 (dd, J = 1.7, 0.8 Hz, 3H), 1.54 (s, 3H), 0.31 (s, 3H), 0.30 ppm (s, 3H); ^{13}C NMR (101 MHz, CDCl$_3$): δ = 144.6, 138.6, 136.8, 136.1, 134.0, 129.1, 128.7, 127.6, 127.5, 126.9, 87.4, 81.6, 79.6, 64.2, 36.0, 15.0, 3.5, −3.5 ppm; IR (film) $\tilde{v}$ = 3064, 3022, 2957, 2916, 2853, 1620, 1597, 1490, 1448, 1427, 1340, 1247, 1224, 1185, 1153, 1110, 1041, 1029, 1001, 929, 898, 831, 813, 772, 745, 732, 702, 666, 633, 477, 423 cm^{-1}; HRMS (ESI): m/z calcd. for C$_{35}$H$_{36}$OSi [M^++Na]: 523.24276; found: 523.24298.

(E)-(((7-Iodooct-6-en-2-yn-4-yl)oxy)methanetriyl)tribenzene (172).
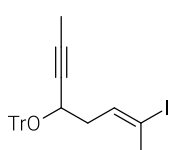
N-Iodosuccinimide (319.3 mg, 1.4 mmol) was added to a solution of 2,6-lutidine (0.4 mL, 400.0 mg, 3.7 mmol), hexafluoro-*iso*-propanol (HFIP) (3.0 mL, 4.8 g, 28.4 mmol) and compound **181** (374.0 mg, 746.9 µmol) in CH$_2$Cl$_2$ (34 mL) at −20 °C. The mixture was stirred at −20 °C for 1 h before the reaction was quenched with saturated aqueous Na$_2$S$_2$O$_3$ solution and MeOH at this temperature. The aqueous layer was separated and extracted with *tert*-butyl methyl ether (3 × 20 mL). The combined organic phases were dried over MgSO$_4$ and concentrated, and the residue was purified by flash chromatography (hexane/toluene, 10:1) to yield the title compound as a colourless oil (351.0 mg, 95%, *E/Z* ≥ 95:5). ^{1}H NMR (400 MHz, CDCl$_3$) δ = 7.52 (m, 6H), 7.28 (m, 9H), 6.15 (td, J = 7.8, 1.5 Hz, 1H), 4.00 (tt, J = 5.1, 2.1 Hz, 1H), 2.25 (d, J = 1.3 Hz, 3H), 2.09 (m, 2H), 1.61 ppm (d, J = 2.1 Hz, 3H); ^{13}C NMR (101 MHz, CDCl$_3$): δ = 144.3, 136.5, 129.0, 127.7, 127.1, 95.9, 87.8, 82.0, 78.9, 63.6, 37.8, 27.9, 3.6 ppm; IR (film) $\tilde{v}$ = 3057, 3031, 2954, 2916, 2851, 2239, 1638, 1597, 1490, 1448, 1376, 1349, 1262, 1220, 1184, 1152, 1088, 1039, 1028, 1001, 944, 928, 899, 877, 843, 759, 746, 704, 645, 632, 535, 504, 475 cm^{-1}; HRMS (ESI): m/z calcd. for C$_{27}$H$_{25}$OI [M^++Na]: 515.08423; found: 515.08476.

Compound (180).

t-BuLi (73.5 µL, 1.7 M in hexane, 124.9 µmol) was added dropwise to a solution of alkenyl iodide **172** (30.0 mg, 60.9 µmol) in THF (2 mL) at −78 °C and the resulting mixture was stirred for 10 min. Next, a solution of boronic ester **173** (14.0 mg, 30.5 µmol) in THF (0.5 mL) was added dropwise. The resulting solution was stirred at −78 °C for 30 min and a solution of PhSeCl (14.0 mg, 73.1 µmol, in 0.5 mL THF/HFIP, 1:1 *v/v*) was added dropwise. The resulting solution was stirred at −78 °C for 30 min, warmed to RT and stirred for additional 30 min. The resulting mixture was filtered through a short plug of silica gel, followed by rinsing with diethyl ether. The filtrate was concentrated and the residue was dissolved in THF (3 mL). *m*CPBA (27.3 mg, 121.9 µmol, ≤77%, in 0.5 mL THF) was added dropwise at −78 °C, the
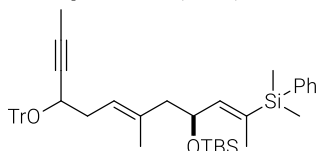
resulting solution was warmed to −45 °C and stirred for 30 min. Then the reaction was quenched with dimethylsulfide (45 μL, 0.6 mmol) at −45 °C. The mixture was allowed to warm to RT and was filtered through a short plug of silica gel, rinsing with diethyl ether, and the filtrate was concentrated. The residue was purified by flash chromatography (hexane/EtOAc, 20:1) to yield the title compound separately. (13.5 mg, 63%, *E*-**180**; 6.1 mg, 28% *Z*-isomer).

Analytical and spectral data of E-isomers: ^{1}H NMR (600 MHz, CDCl$_3$) δ = 7.53 (m, 6H), 7.46 (dq, *J* = 6.3, 1.7 Hz, 2H), 7.33 (m, 3H), 7.21 (m, 6H), 5.73 (dp, *J* = 6.2, 1.4 Hz, 3H), 5.16 (m, 1H), 4.55 (td, *J* = 7.8, 5.2 Hz, 1H), 3.94 (m, 1H), 2.19 (m, 3H), 2.02 (dt, *J* = 13.2, 4.9 Hz, 1H), 1.59 (dd, *J* = 3.7, 1.7 Hz, 3H), 1.54 (dd, *J* = 7.0, 2.0 Hz, 3H), 1.52 (dd, *J* = 3.4, 1.3 Hz, 3H), 0.83 (d, *J* = 6.4 Hz, 9H), 0.30 (m, 6H), −0.03 (d, *J* = 3.8 Hz, 3H), −0.04 ppm (d, *J* = 1.7 Hz, 3H); ^{13}C NMR (151 MHz, CDCl$_3$): δ = 145.4, 144.6, 138.17, 138.15, 133.94, 133.86, 133.78, 132.60, 132.55, 129.10, 129.09, 128.85, 128.85, 127.68, 127.67, 127.6, 126.9, 122.6, 87.60, 87.58, 81.18, 81.15, 79.8, 79.7, 68.7, 68.5, 64.8, 48.1, 48.0, 35.89, 35.86, 25.87, 25.85, 25.8, 18.22, 18.21, 17.3, 17.1, 15.0, 3.64, 3.62, −3.58, −3.60, −3.64, −3.65, −4.52, −4.84 ppm (2 diastereomers); IR (film) $\tilde{v}$ = 3058, 2954, 2926, 2854, 1491, 1462, 1448, 1428, 1408, 1361, 1249, 1218, 1185, 1153 ,1109, 1045, 1028, 1004, 942, 898 833, 812, 774, 745, 732, 701, 671, 666, 634, 477, 427 cm^{-1}; HRMS (ESI): *m/z* calcd. for C$_{46}$H$_{58}$O$_2$Si$_2$ [*M*$^+$+Na]: 721.38676; found: 721.38714.

Analytical and spectral data of Z-isomers: ^{1}H NMR (600 MHz, CDCl$_3$) δ = 7.52 (m, 6H), 7.48 (m, 2H), 7.33 (m, 3H), 7.25 (d, *J* = 7.3 Hz, 6H), 7.20 (m, 3H), 5.74 (ddd, *J* = 18.9, 8.0, 1.7 Hz, 1H), 5.22 (m, 1H), 4.58 (m, 1H), 3.91 (dtt, *J* = 7.0, 4.4, 2.2 Hz, 1H), 2.23 (m, 3H), 1.97 (ddd, *J* = 18.4, 13.3, 5.5 Hz, 1H), 1.71 (m, 3H), 1.62 (dd, *J* = 5.4, 1.7 Hz, 3H), 1.53 (m, 3H), 0.85 (d, *J* = 1.6 Hz, 9H), 0.33 (m, 6H), −0.02 ppm (t, *J* = 2.1 Hz, 6H); ^{13}C NMR (151 MHz, CDCl$_3$): δ = 145.5, 145.4, 144.6, 138.1, 138.1, 134.1, 134.1, 134.0, 132.7, 132.6, 129.1, 128.9, 128.9, 127.70, 127.70, 127.5, 126.9, 122.4, 122.3, 87.49, 87.46, 81.21, 81.19, 79.7, 68.17, 68.16, 64.74, 64.73, 40.4, 40.3, 35.88, 35.86, 25.9, 25.84, 25.81, 24.8, 24.7, 18.2, 15.03, 15.00, 3.6, −3.6, −4.52, −4.54, −4.78, −4.79 ppm (2 diastereomers); IR (film) $\tilde{v}$ = 3064, 3023, 2955, 2926, 2855, 1598, 1491, 1462, 1448, 1428, 1376, 1360, 1250, 1221, 1183, 1153, 1109, 1046, 1028, 940, 899, 833, 812, 774, 745, 702, 666, 634, 561, 473, 438, 417 cm^{-1}; HRMS (ESI): *m/z* calcd. for C$_{46}$H$_{58}$O$_2$Si$_2$ [*M*$^+$+Na]: 721.38676; found: 721.38689.

Compound (181). LiCl (2.7 mg, 64.4 μmol) was added a solution of trityl protected **180** (4.5 mg, 6.4 μmol) in *n*-BuOH (0.5 mL). The resulting mixture was stirred at 120 °C for 6 h. The mixture was allowed to cool to RT and concentrated. The residue was purified by flash chromatography (hexane/MTBE 10:1) to yield the title compound (2.3 mg, 78%). ^{1}H NMR (400 MHz, CDCl$_3$) δ = 7.47 (m, 2H), 7.34 (dd, *J* = 5.1, 1.8 Hz, 3H), 5.75 (dt, *J* = 8.0, 1.8 Hz, 1H), 5.25 (q, *J* = 7.2 Hz, 1H), 4.63 (td, *J* = 7.7, 5.6 Hz, 1H), 4.29 (m, 1H), 2.38 (t, *J* = 6.7 Hz, 2H), 2.25 (dd, *J* = 11.9, 7.5 Hz, 1H), 2.11 (dd, *J* = 13.2, 5.3 Hz, 1H), 1.84 (dd, *J* = 2.2, 0.9 Hz, 3H), 1.68 (s, 3H), 1.64 (d, *J* = 1.6 Hz, 3H), 0.86 (s, 9H), 0.33 (s, 6H), 0.01 (s, 3H), −0.01 ppm (s, 3H); ^{13}C NMR (101 MHz, CDCl$_3$): δ = 145.2, 138.1, 136.2, 133.9, 133.0, 128.9, 127.7, 121.8, 121.6, 80.9, 80.2, 68.3, 62.2, 48.10 37.1, 37.0, 25.8, 18.2, 17.3, 17.2, 15.0, 3.6, −3.6, −3.7, −4.4, −4.8 ppm (2 diastereomers); IR (film) $\tilde{v}$ = 2955, 2926, 2855, 1462, 1428, 1408, 1378, 1361, 1249, 1109, 1062, 950, 940, 832, 811, 774, 731, 700, 671, 665, 638, 545, 517, 476, 435 cm^{-1}; HRMS (ESI): *m/z* calcd. for C$_{27}$H$_{44}$O$_2$Si$_2$ [*M*$^+$+Na]: 479.27721; found: 479.27721.
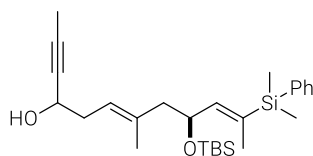
(*E*)-7-(Dimethyl(phenyl)silyl)oct-6-en-2-yn-4-one (182). Dess-Martin periodinane (1.6 g, 3.8 mmol) was added to a solution of propargylic alcohol **131** (485.4 mg, 1.8 mmol) in CH$_2$Cl$_2$

(12 mL) at 0 °C. The resulting mixture was stirred for 4 h at RT. Then, the mixture was stirred rapidly with saturated aqueous NaHCO₃/Na₂S₂O₃ solution (1:1 *v/v*, 30 mL) for 30 min. The aqueous layer was separated and extracted with CH₂Cl₂ (3 × 20 mL). The organic phases were dried over MgSO₄, filtered and concentrated. The residue was purified by flash chromatography (hexane/EtOAc, 20:1) to yield the title compound as a colourless oil (317 mg, 66%). ¹H NMR (400 MHz, CDCl₃) δ = 7.50 (m, 2H), 7.35 (m, 3H), 6.02 (tq, *J* = 6.9, 1.8 Hz, 1H), 3.38 (m, 2H), 2.00 (s, 3H), 1.69 (dt, *J* = 1.7, 0.9 Hz, 3H), 0.36 ppm (s, 6H); ¹³C NMR (101 MHz, CDCl₃): δ = 185.5, 139.8, 137.9, 133.9, 130.6, 129.0, 127.7, 90.7, 80.3, 45.1, 15.3, 4.0, −3.6 ppm; IR (film) $\tilde{v}$ = 2957, 2217, 1671, 1614, 1427, 1409, 1303, 1247, 1165, 1111, 998, 950, 812, 830, 773, 731, 699, 636, 471 cm⁻¹; HRMS (ESI): *m/z* calcd. for C₁₆H₂₀OSi [*M*⁺+H]: 257.13562; found: 257.13569.
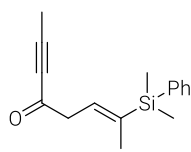
(*S,E*)-7-(Dimethyl(phenyl)silyl)oct-6-en-2-yn-4-ol (184). RuCl(*p*-cymne)[(*S,S*)-Ts-DPEN] (**183**) (12. mg, 19.5 mmol) was added to a solution of propargylic ketone **182** (50.0 mg, 195.0 µmol) in *iso*-propanol (0.5 mL) at 0 °C. The mixture was stirred for 4 h at RT and the reaction was quenched with aqueous saturated NH₄Cl solution. The aqueous layer was separated and extracted with CH₂Cl₂ (3 × 5 mL). The organic phases were dried over MgSO₄, filtered and concentrated. The residue was purified by flash chromatography (hexane/EtOAc, 10:1) to yield the title compound as a colourless oil (21.4 mg, 42%, 94% *ee*). $[\alpha]_D^{20}$ = −3.5 (0.83 g/100 mL, CHCl₃); analytical data see racemic compound **131**.
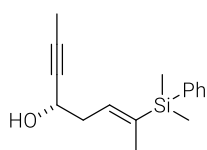
Mosher Ester (ME-8a). (*R*)-(−)-α-Methoxy-α-(trifluormethyl)phenylacetyl chloride (4.0 µL, 2.3 µmol) was added to a solution of DMAP (0.4 mg, 3.3 µmol), Et₃N (6.0 µL, 46.1 µmol) and propargylic alcohol **184** (4.0 mg, 15.5 µmol) in CH₂Cl₂ (0.5 mL). The mixture was stirred at RT for 1 h before the reaction mixture was concentrated, and the residue was purified by flash chromatography (hexane/EtOAc, 20:1) to yield the title compound as a colourless oil (5.9 mg, 80%). $[\alpha]_D^{20}$= −37.9 (0.42 g/100 mL, CHCl₃); ¹H NMR (400 MHz, CDCl₃) δ = 7.49 (m, 4H), 7.35 (m, 6H), 5.77 (m, 1H),
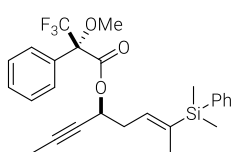
5.55 (ddt, *J* = 6.5, 4.3, 2.1 Hz, 1H), 3.56 (d, *J* = 1.2 Hz, 3H), 2.63 (dd, *J* = 7.2, 6.1 Hz, 2H), 1.84 (d, *J* = 2.1 Hz, 3H), 1.63 (m, 3H), 0.29 (s, 3H), 0.29 ppm (s, 3H); ^{13}C NMR (101 MHz, CDCl$_3$): δ = 165.8, 138.9, 138.1, 133.9, 133.7, 132.3, 129.6, 128.9, 128.4, 127.7, 127.4, 83.3, 75.5, 66.2, 55.4, 33.8, 15.0, 3.5, −3.6, −3.7 ppm (<u>C</u>F$_3$ and <u>C</u>$_{q,\,sp3}$ signals are missing); IR (film) $\tilde{v}$ = 3069, 2955, 2922, 2850, 1750, 1621, 1494, 1451, 1428, 1325, 1247, 1168, 1109, 1081, 1015, 991, 918, 831, 813, 773, 730, 717, 699, 641 cm^{-1}; HRMS (ESI): *m/z* calcd. for C$_{26}$H$_{29}$F$_3$O$_3$Si [*M*$^+$+Na]: 497.17303; found: 497.17314.

Mosher Ester (ME-8b). Prepared analogously from compound **184** and (*S*)-(−)-α-methoxy-α-(trifluormethyl)phenylacetyl chloride as a colourless oil (5.9 mg, 80%). [α]$_D^{20}$= 22.1 (0.19 g/100 mL, CHCl$_3$); ^{1}H NMR (400 MHz, CDCl$_3$) δ = 7.48 (m, 4H), 7.37 (m, 6H), 5.82 (ddq, *J* = 6.7, 5.2, 1.7 Hz, 1H), 5.54 (tdd, *J* = 8.1, 4.2, 2.1 Hz, 1H), 3.49 (d, *J* = 1.2 Hz, 3H), 2.67 (d, *J* = 5.3 Hz, 2H), 1.80 (d, *J* = 2.1 Hz, 3H), 1.68 (m, 3H), 0.31 ppm (s, 6H); ^{13}C NMR (101 MHz, CDCl$_3$): δ = 165.8, 139.1, 138.0, 134.0, 133.95, 133.92, 132.1, 129.6, 129.0, 128.3, 127.7, 127.5, 83.1, 75.3, 66.5, 33.9, 15.1, 3.5, −3.6, −3.7 ppm (<u>C</u>F$_3$ and <u>C</u>$_{q,\,sp3}$ signals are missing); IR (film) $\tilde{v}$ = 3069, 2923, 2851, 1749, 1621, 1428, 1326, 1247, 1184, 1167, 1109, 1081, 1015, 990, 917, 831, 812, 773, 731, 718, 699, 642, 537, 473 cm^{-1}; HRMS (ESI): *m/z* calcd. for C$_{26}$H$_{29}$F$_3$O$_3$Si [*M*$^+$+Na]: 497.17303; found: 497.17323.

Table 36. Mosher ester analysis **ME-8a** and **ME-8b**.
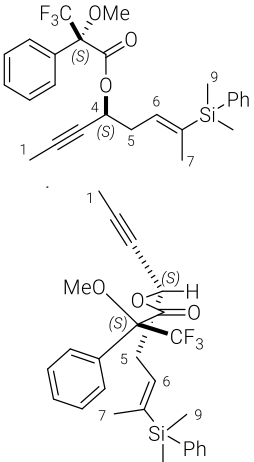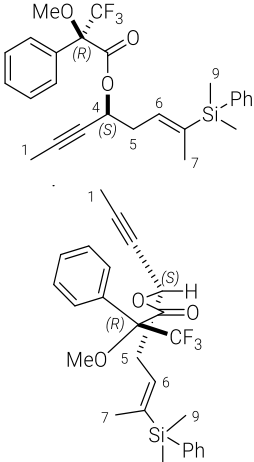
Position	δ_S (^{1}H, [ppm])	δ_R (^{1}H, [ppm])	$\Delta\delta^{SR} = \delta_S - \delta_R$
1	1.84	1.80	−0.04
4	5.55	5.63	+0.08
5	2.63	2.67	+0.04
6	5.77	5.89	+0.12
7	1.63	1.68	+0.05
9	0.29	0.31	+0.02

4 [Rh₂(5S-MEPY)₄] AND [BiRh(5S-MEPY)₄]: CONVENIENT SYNTHESIS AND COMPUTATIONAL ANALYSIS

4.1 SYNTHESIS OF [Rh₂(5S-MEPY)₄]·2MeCN

[Rh₂(5S-MEPY)₄]·2MeCN (79a). A 50-mL, two-necked, round-bottom flask equipped with magnetic stir bar, an inert gas adapter on the side neck, a frit with a bridging side arm with a reflux condenser on top, followed by an inert gas adapter, was evacuated, flame-dried, and allowed to cool to RT under vacuum, before it was refilled with an argon (Figure 44a). The frit with a bridging side arm was filled with a layer of dry sand (3 g) followed by a layer of dry K₂CO₃ (4.4 g). The inert gas adapter on the side neck was replaced by a glass stopper (Figure 44b). The flask was charged with chlorobenzene (22.5 mL), which had been degassed by bubbling argon through for 20 min. Afterwards, [Rh₂(OAc)₄] (300.0 mg, 678.8 μmol) was added, resulting in a dark green reaction mixture (Figure 44c), followed by methyl 2-pyrrolidone-5S-carboxylate (S-**191**) (5S-MEPY–H, 651.0 mg, 4.5 mmol). The mixture was stirred at 145 °C for 13 h, causing a colour change to dark red (Figure 44d). The mixture was allowed to cool to RT and the solvent was evaporated under high vacuum (1 × 10⁻³ mbar) to obtain a violet/deep blue residue.
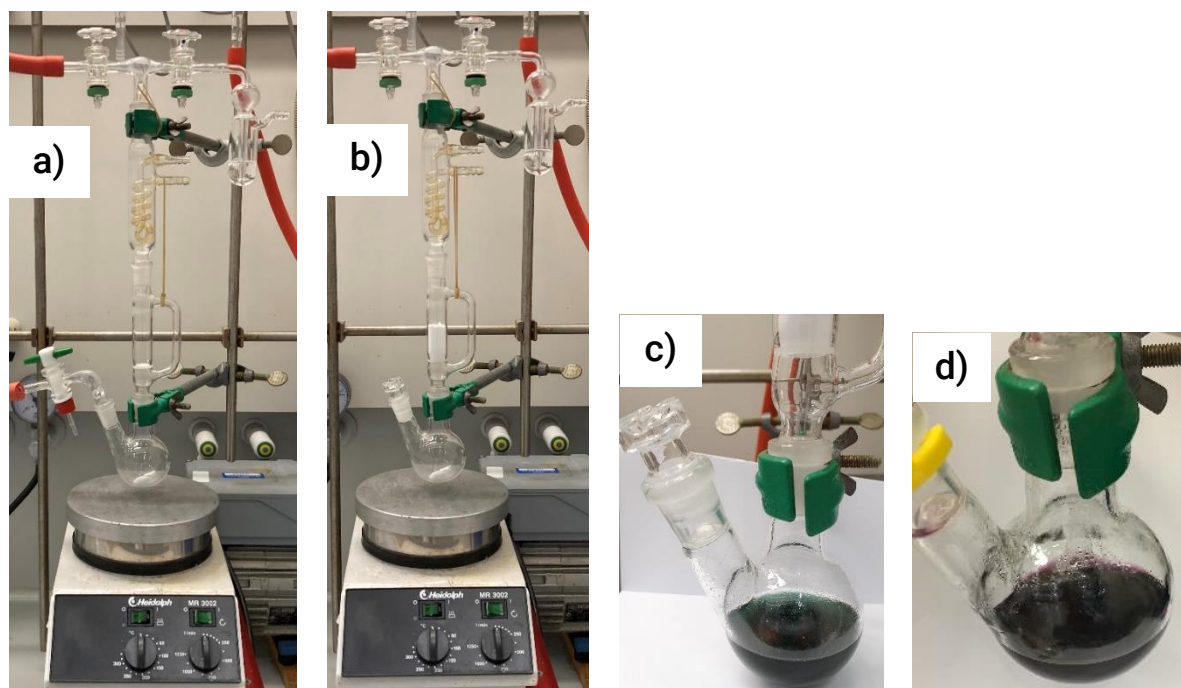
Figure 44. a) Apparatus with argon atmosphere; b) Frit filled with sand and K₂CO₃; c) Reaction mixture prior to reaction; d) Reaction mixture after reaction (145 °C, 13 h).

The crude material was dissolved in MeCN (20 mL, technical grade) under air forming a red solution (Figure 45a). Silica gel (8.0 g) was added to the red solution and the suspension was stirred for 5 min at RT, causing a decolourisation of the solution (Figure 45b and c). The reddish silica gel was filtered off and rinsed with MeCN (3 × 50 mL) (Figure 45d); the combined MeCN

filtrates were discarded. The red silica gel residue was washed with MeOH (3 × 50 mL), first forming a violet solid, until it was colourless (Figure 46a). The red MeOH filtrate was concentrated to yield a violet solid (Figure 46b). This purification procedure was repeated three times.

A flame-dried Schlenk tube with a magnetic stir bar was charged with the violet solid and was heated in high vacuum (1×10^{-3} bar) at 100 °C for 14 h with gentle stirring, causing a colour change to turquoise (Figure 46c). The flask was refilled with argon, followed by addition of dry MeCN (1 mL) at RT. After stirring for 5 min, the remaining solvent was removed and the material was dried under high vacuum (1×10^{-3} mbar) for 12 h to obtain the title compound as a red/violet solid (Figure 46d). $[\alpha]_D^{20}$ = −335.7 (0.014 g/100 mL, CHCl$_3$); ^{1}H NMR (600 MHz, CDCl$_3$) δ = 4.32 − 4.27 (m, 2H), 3.95 (d, J = 8.7 Hz, 2H), 3.71 (s, 6H), 3.68 (s, 6H), 2.61 (m, 8H), 2.40 (m, 4H), 2.24 (m, 4H), 2.15 (m, 4H), 1.87 ppm (m, 4H); ^{13}C NMR (151 MHz, CDCl$_3$) δ = 188.6, 188.3, 175.5, 175.2, 115.4, 66.8, 66.7, 52.1, 51.9, 31.8, 31.6, 26.1, 25.4, 3.07 ppm; IR (film) $\tilde{v}$ = 2950, 1729, 1608, 1428, 1279, 1193, 1168, 1117, 1043, 987, 686, 595 cm^{-1}; HRMS (ESI$^+$): m/z calcd. for C$_{28}$H$_{38}$N$_6$O$_{12}$Rh$_2$ [M+Na−(2×MeCN)]$^+$: 797.00190; found: 797.00231.
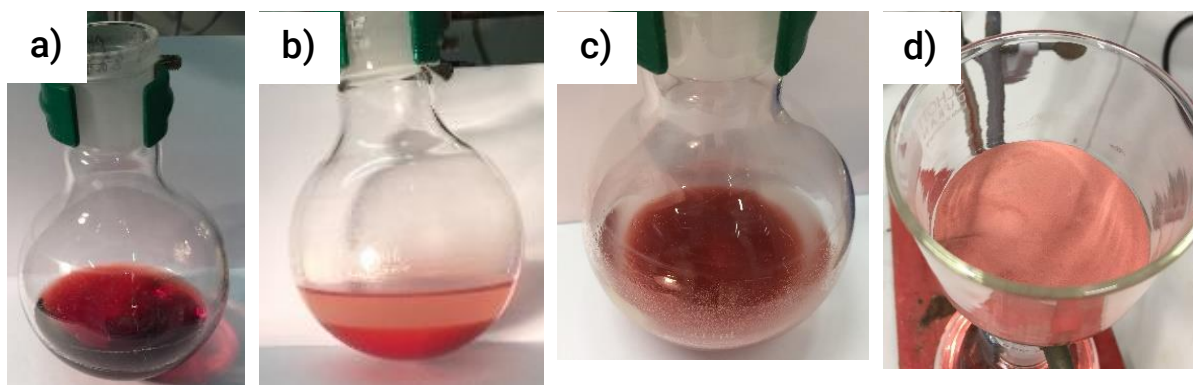
Figure 45. a) Crude of the reaction mixture dissolved in MeCN; b) and c) Dirhodium Complex adsorbed on the silica gel during purification procedure; d) Dry residue of filtration and washing with MeCN.
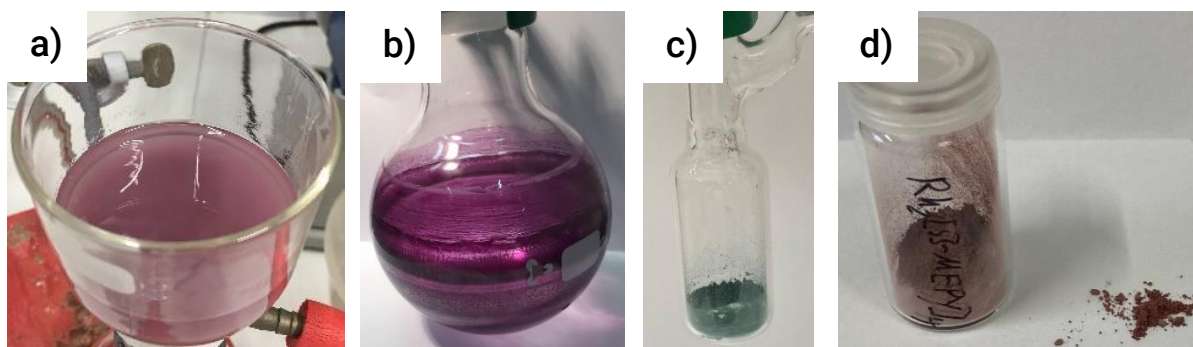
Figure 46. a) MeOH wash of the silica gel residue; b) Concentrated MeOH filtrate, Violet solid material; c) [Rh$_2$(5S-MEPY)$_4$] complex, after stirring at 100 °C for 14 h.

4.2 COMPUTATIONAL DETAILS

All calculations of the [BiRh(5*S*-MEPY)$_4$] and [BiRh(5*S*-MEPY)$_4$] complexes were carried out with the ORCA 4.2 program package.[222,223] All geometries were optimised at DFT level using the BP86[269] functional and the ZORA-def2-TZVP basis set.[270] The D3 version of Grimme's dispersion correction including Becke–Johnson damping (D3BJ)[273,274] was applied together with the scalar relativistic zeroth-order regular approximation (ZORA Hamiltonian).[271,272] The resolution-of-identity (RI) approximation was utilized with the corresponding SARC/J auxiliary basis set[275,276] to speed up the calculation of the two-electron integrals.[277–279] The calculations include the implicit solvent effects by employing the conductor–like polarizable continuum model (CPCM)[280–283] using the Van-der-Waals Gaussian surface type for CH_2Cl_2 solvent. In all cases, a fine integration grid (grid7, nofinalgrid) was used as well as very tight SCF convergence criteria. Stationary points were characterised by the numeric calculation of the Hessian. This level of theory is noted as ZORA-BP86-D3BJ-(CPCM)/def2-TZVP. The molecular orbitals were visualized by Avogadro, using an isosurface value of 0.08.

4.2.1 GEOMETRY OPTIMISED STRUCTURES

[BiRh(5*S*-MEPY)$_4$]·MeCN (194a)

X-Ray Structure	DFT-optimised structure
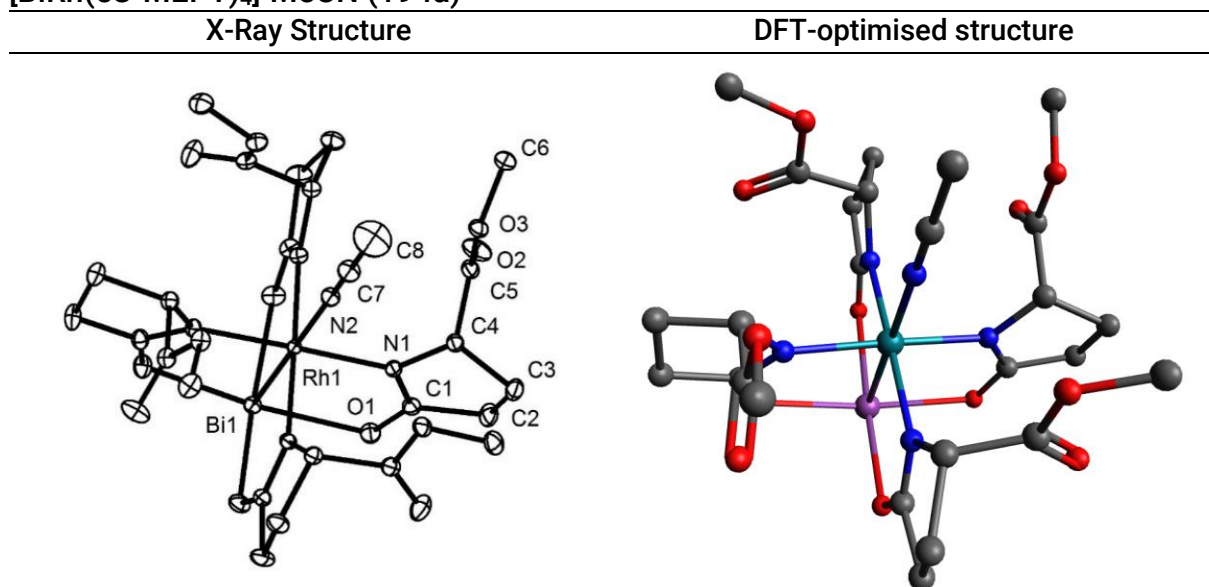
Figure 47. Structure of [BiRh(5*S*-MEPY)$_4$]·MeCN (**194a**) in the solid state (left); DFT-optimised structure (right).

Table 37. Selected Bond Lengths [Å] of [BiRh(5*S*-MEPY)$_4$]·MeCN (**194a**); the crystallographic data refer to the two independent molecules in the unit cell.

	X-Ray	DFT
Bi–Rh	2.573(2) / 2.577(2)	2.61
Bi–O (average)	2.37	2.40 – 2.41
Rh–N (average)	2.06	2.07
Rh–NCCH$_3$	2.231(3) / 2.240(3)	2.18

[RhRh(5*S*-MEPY)₄]·2MeCN (79a)

X-Ray structure	DFT-optimised structure
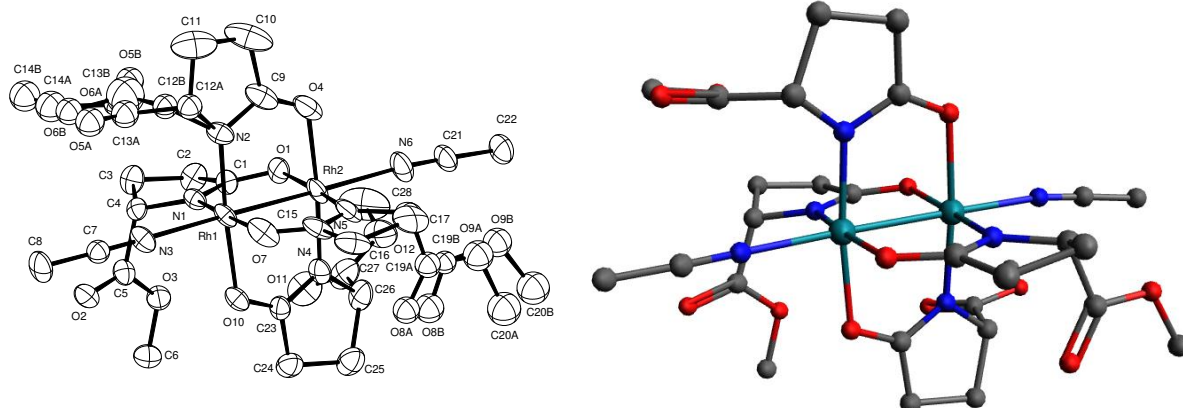
Figure 48. Structure of [RhRh(5*S*-MEPY)₄]·2MeCN (**79a**) in the solid state (left); DFT-optimised structure (right).

Table 38. Selected Bond Lengths [Å] of [RhRh(5*S*-MEPY)₄]·2MeCN (**79a**).

	X-Ray	DFT
Rh–Rh	2.455(1)	2.50
Rh–O (average)	2.08	2.11
Rh–N	2.01	2.02 – 2.04
Rh–NCMe	2.211(6) / 2.229(6)	2.15 / 2.14

[RhRh(5*S*-MEPY)₄] (79) and [BiRh(5*S*-MEPY)₄] (194)

[RhRh(5*S*-MEPY)₄]	[BiRh(5*S*-MEPY)₄]
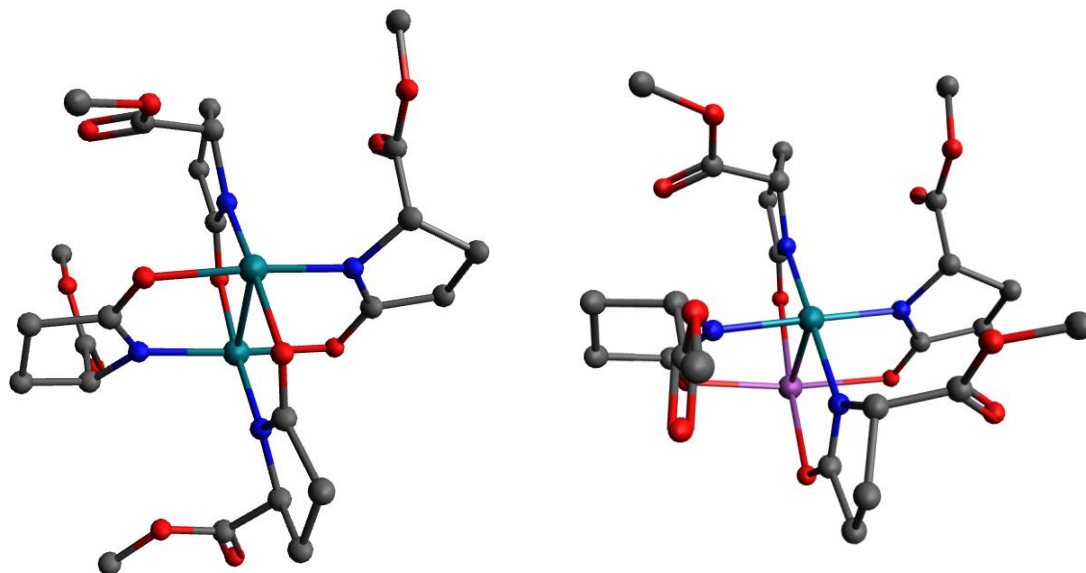
Figure 49. Structures of [RhRh(5*S*-MEPY)₄] (**79**, left) and [BiRh(5*S*-MEPY)₄] (**194**, right) as optimised by DFT.

Table 39. Selected Bond Lengths [Å] of [BiRh(5*S*-MEPY)₄] (**79**) and [RhRh(5S-MEPY)₄] (**194**) as optimised by DFT.

	[BiRh(5*S*-MEPY)₄]	[RhRh(5*S*-MEPY)₄]
M–Rh	2.59	2.44
M–O	2.40	2.10
Rh–N	2.05	2.01 – 2.02

4.2.2 ELECTRONIC STRUCTURES

Table 40. Energies of molecular orbitals (eV) without axial ligands.

MO	[RhRh(5*S*-MEPY)$_4$]	[BiRh(5*S*-MEPY)$_4$]
LUMO+3	−1.48 eV	−1.44 eV
LUMO+2	−1.48 eV	−1.46 eV
LUMO+1	−1.81 eV	−1.46 eV
LUMO	−3.71 eV	−2.55 eV
	Δ 0.50 eV	Δ 2.10 eV
HOMO	−4.21 eV	−4.65 eV
HOMO−1	−4.86 eV	−5.70 eV
HOMO−2	−4.90 eV	−5.70 eV
HOMO−3	−5.44 eV	−5.73 eV
HOMO−4	−5.75 eV	−6.07 eV
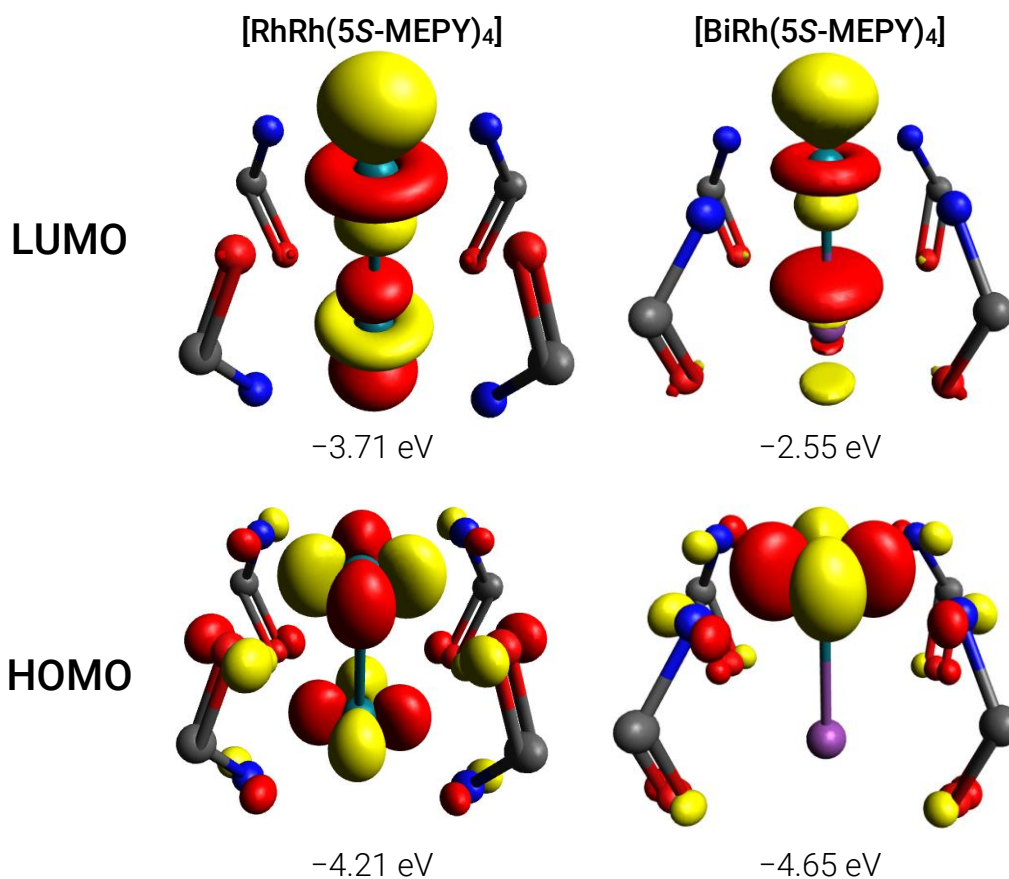
Figure 50. Molecular Orbitals Scheme: HOMO and LUMO.

Molecular Orbital Energy Diagrams
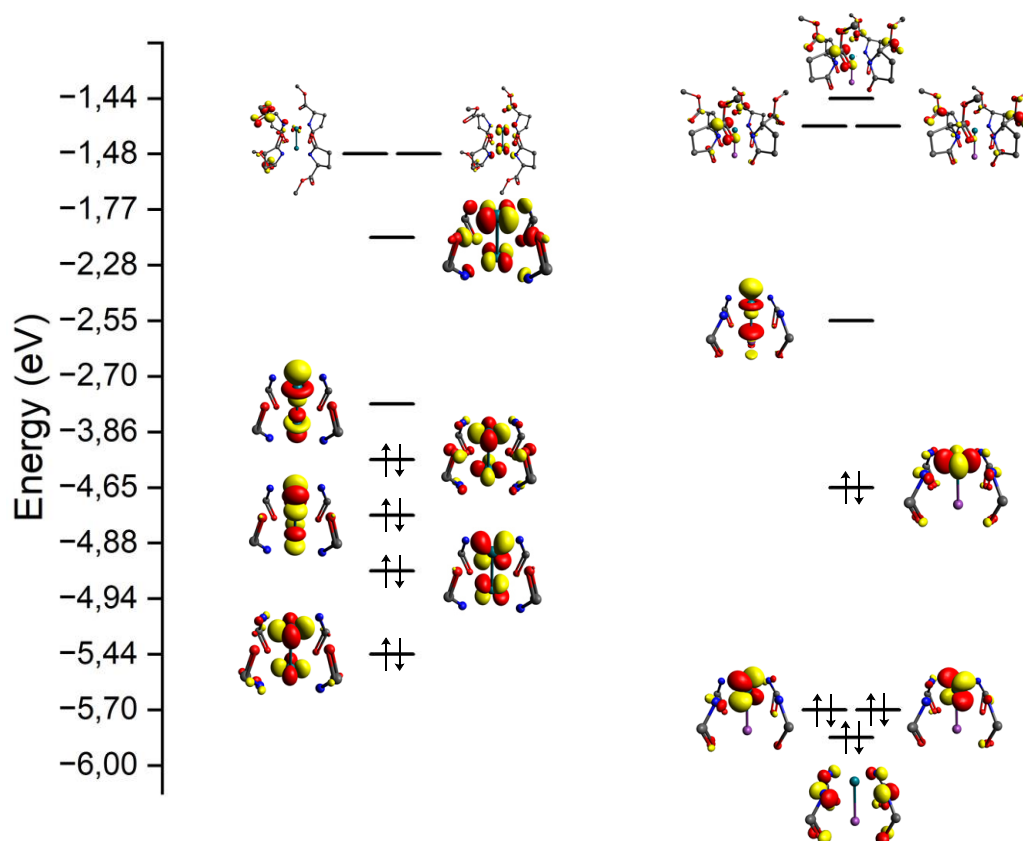
Figure 51. Molecular Orbital Scheme for [RhRh(5*S*-MEPY))₄] (left, **79**) and [BiRh(5*S*-MEPY)₄] (right, **194**). The structures are truncated for sake of clarity.

Molecular Orbital Scheme of [RhRh(5*S*-MEPY)₄]

−1.48 eV
LUMO+2, LUMO+3

−1.81 eV
LUMO+1

−3.71 eV
LUMO

−4.21 eV
HOMO

−4.86 eV
HOMO−1

−4.90 eV
HOMO−2

−5.44 eV
HOMO−3

−5.75 eV
HOMO−4

−6.03 eV
HOMO−5

−6.24 eV
HOMO−6
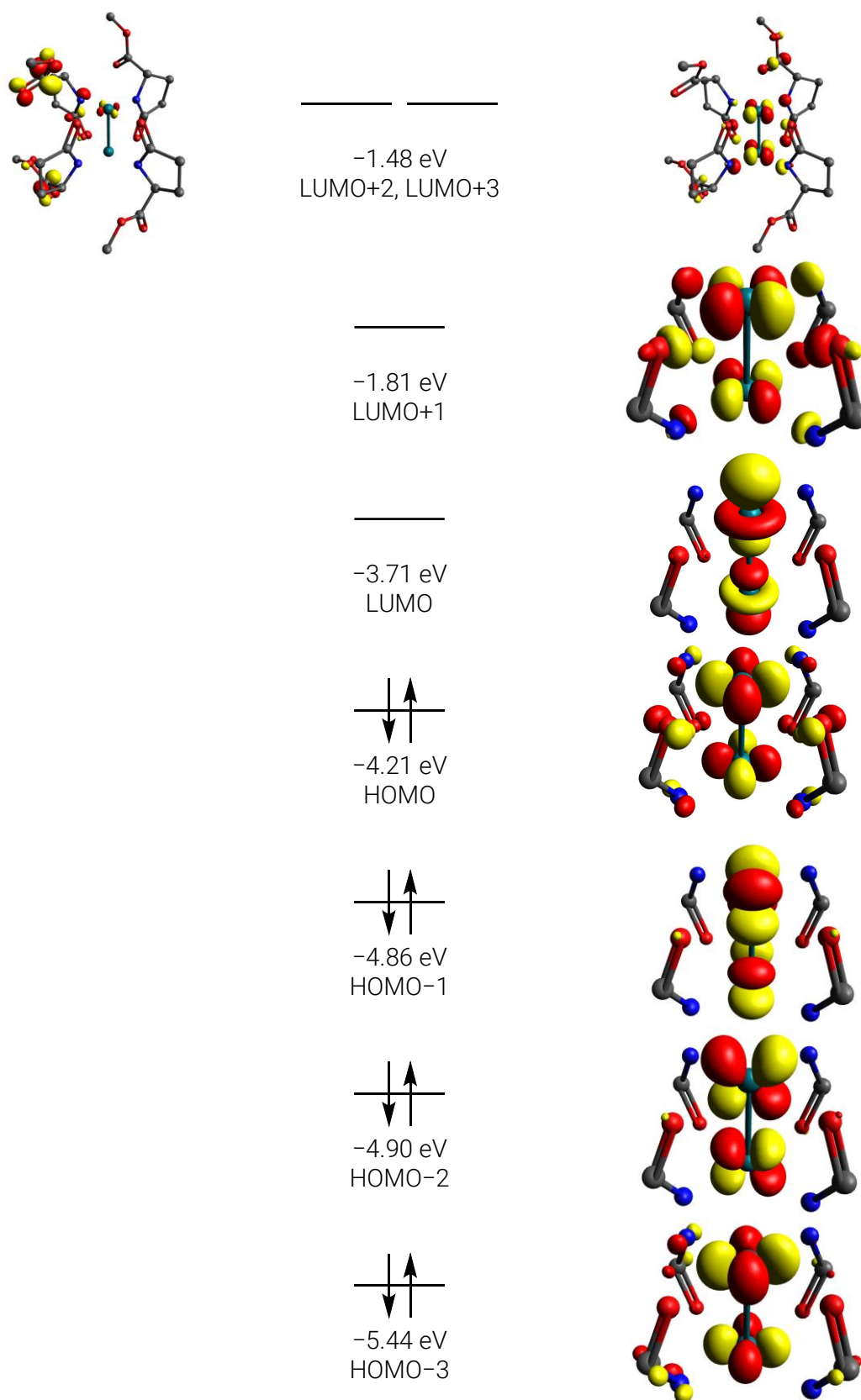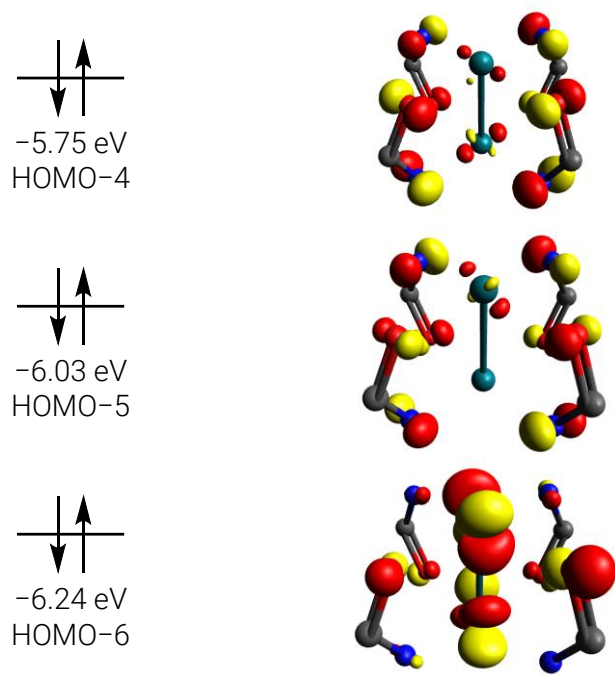
Figure 52. Molecular Orbital Scheme of [RhRh(5S-MEPY)$_4$] (**79**)

Molecular Orbital Scheme of [BiRh(5*S*-MEPY)₄]
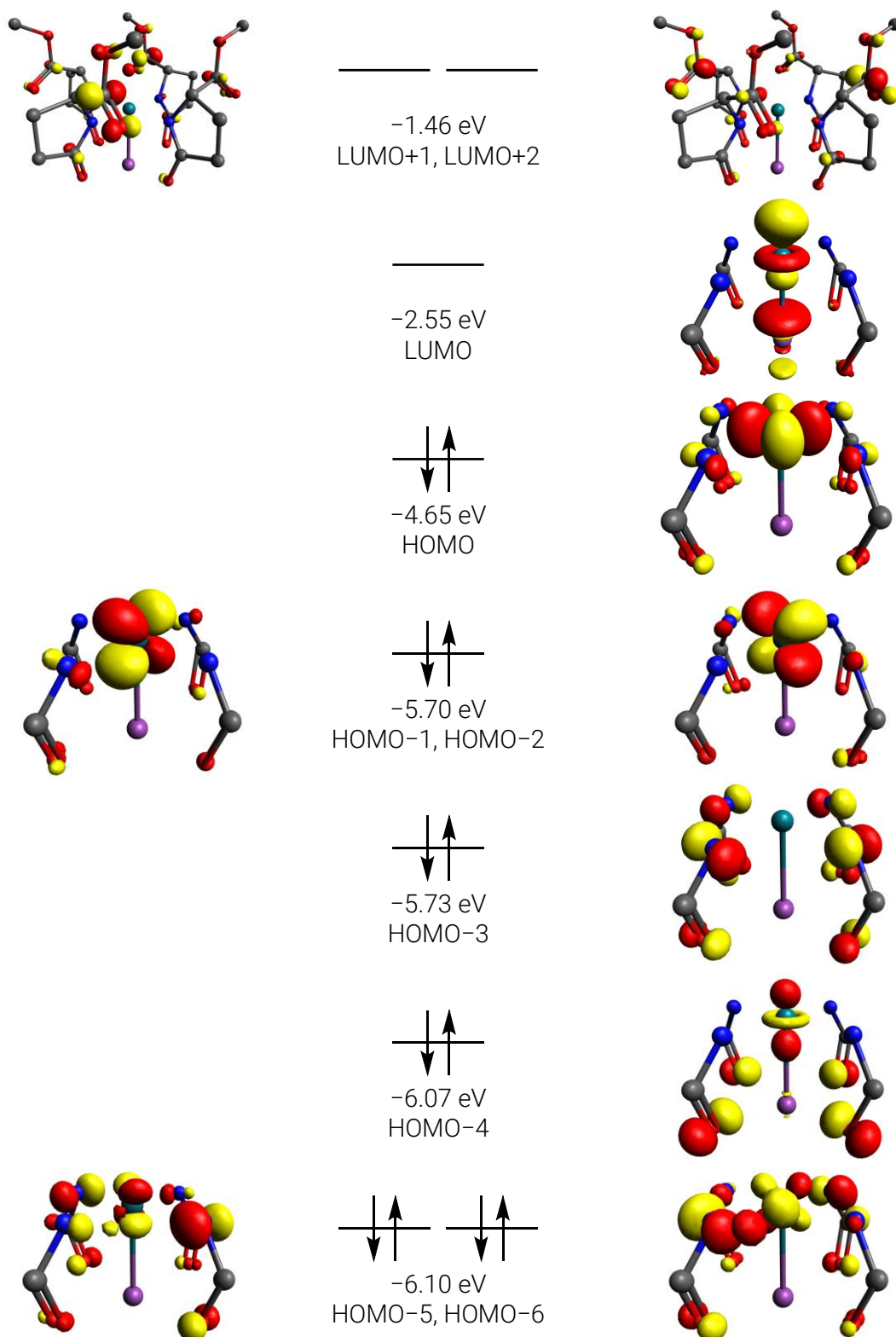
Figure 53. Molecular Orbital Scheme of [BiRh(5S-MEPY)4] (**194**).

E BIBLIOGRAPHY

(1)   Wöhler, F. *Ann. Phys.* **1828**, *88*, 253–256.
(2)   Nicolaou, K. C.; Vourloumis, D.; Winssinger, N.; Baran, P. S. *Angew. Chem. Int. Ed.* **2000**, *39*, 44–122.
(3)   Gershenzon, J.; Dudareva, N. *Nat. Chem. Biol.* **2007**, *3*, 408–414.
(4)   Jiang, C.-S.; Li, Y.; Han, G.-Y.; Guo, Y.-W. *Chin. J. Nat. Med.* **2014**, *12*, 853–856.
(5)   Yang, B.; Huang, J.; Lin, X.; Liao, S.; Zhou, X.; Liu, J.; Wang, J.; Wang, L.; Liu, Y. *Helv. Chim. Acta* **2015**, *98*, 834–841.
(6)   Li, Y.; Carbone, M.; Vitale, R. M.; Amodeo, P.; Castelluccio, F.; Sicilia, G.; Mollo, E.; Nappo, M.; Cimino, G.; Guo, Y. W.; Gavagnin, M. *J. Nat. Prod.* **2010**, *73*, 133–138.
(7)   Yin, J.; Zhao, M.; Ma, M.; Xu, Y.; Xiang, Z.; Cai, Y.; Dong, J.; Lei, X.; Huang, K.; Yan, P. *Mar. Drugs* **2013**, *11*, 455–465.
(8)   Liu, J.; Li, H.; Wu, M. J.; Tang, W.; Wang, J. R.; Gu, Y. C.; Wang, H.; Li, X. W.; Guo, Y. W. *J. Org. Chem.* **2020**, DOI: 10.1021/acs.joc.0c02397.
(9)   Hegazy, M. E. F.; Mohamed, T. A.; Elshamy, A. I.; Al-Hammady, M. A.; Ohta, S.; Paré, P. W. *Molecules* **2016**, *21*, 308.
(10) Roy, P. K.; Ashimine, R.; Miyazato, H.; Taira, J.; Ueda, K. *Molecules* **2016**, *21*, 1–9.
(11) Fan, L.; Xiao, Q.; Chen, Y.; Chen, G.; Duan, J.; Tao, W. *Front. Pharmacol.* **2017**, *8*, 1–9.
(12) Xu, Z. H.; Sun, J.; Xu, R. S.; Qin, G. W. *Phytochemistry* **1998**, *49*, 149–151.
(13) Shao, F. G.; Bu, R.; Zhang, C.; Chen, C. J.; Huang, J.; Wang, J. H. *J. Asian Nat. Prod. Res.* **2011**, *13*, 805–810.
(14) Cao, Y.; Cheng, F.; Yao, W.; Bao, B.; Zhang, K.; Zhang, L.; Ding, A. *Int. J. Mol. Sci.* **2016**, *17*, 850–812.
(15) Liang, Q.-L. L.; Dai, C.-C. C.; Jiang, J.-H. H.; Tang, Y.-P. P.; Duan, J.-A. A. *Fitoterapia* **2009**, *80*, 514–516.
(16) Tao, W. W.; Duan, J. A.; Tang, Y. P.; Yang, N. Y.; Li, J. P.; Qian, Y. F. *Phytochemistry* **2013**, *94*, 249–253.
(17) Wang, K.; Yu, H.; Wu, H.; Wang, X.; Pan, Y.; Chen, Y.; Liu, L.; Jin, Y.; Zhang, C. *Nat. Prod. Res.* **2015**, *29*, 1456–1460.
(18) Wang, K.; Liu, L. L.; Huang, J.; Yu, H.; Wu, H.; Duan, Y.; Cui, X.; Zhang, X.; Liu, L. L.; Wang, W. *Molecules* **2017**, *22*, 465.
(19) Huang, C.-S.; Luo, S.-H.; Li, Y.-L.; Li, C.-H.; Hua, J.; Liu, Y.; Jing, S.; Wang, Y.; Yang, M.-J.; Li, S.-H. *Nat. Products Bioprospect.* **2014**, *4*, 91–100.
(20) Maslovskaya, L. A.; Savchenko, A. I.; Krenske, E. H.; Gordon, V. A.; Reddell, P. W.; Pierce, C. J.; Parsons, P. G.; Williams, C. M. *Chem. Commun.* **2014**, *50*, 12315–12317.
(21) Maslovskaya, L. A.; Savchenko, A. I.; Krenske, E. H.; Pierce, C. J.; Gordon, V. A.; Reddell, P. W.; Parsons, P. G.; Williams, C. M. *Angew. Chem. Int. Ed.* **2014**, *53*, 7006–7009.
(22) Maslovskaya, L. A.; Savchenko, A. I.; Gordon, V. A.; Reddell, P. W.; Pierce, C. J.; Parsons, P. G.; Williams, C. M. *Chem. - Eur. J.* **2017**, *23*, 537–540.
(23) Maslovskaya, L. A.; Savchenko, A. I.; Pierce, C. J.; Boyle, G. M.; Gordon, V. A.; Reddell, P. W.; Parsons, P. G.; Williams, C. M. *Chem. - Eur. J.* **2019**, *25*, 1525–1534.
(24) Maslovskaya, L. A.; Savchenko, A. I.; Krenske, E. H.; Chow, S.; Gordon, V. A.; Reddell, P. W.; Pierce, C. J.; Parsons, P. G.; Boyle, G. M.; Williams, C. M. *European J. Org. Chem.* **2020**, *2020*, 1042–1045.
(25) Vasas, A.; Hohmann, J. *Chem. Rev.* **2014**, *114*, 8579–8612.
(26) Chen, H.; Jia, Z. J. *Indian J. Chem. - Sect. B Org. Med. Chem.* **1996**, *35*, 1308–1310.
(27) Horie, K.; Sakai, K.; Okugi, M.; Toshima, H.; Hasegawa, M. *Phytochem. Lett.* **2016**, *15*, 57–62.
(28) Inoue, Y.; Sakai, M.; Yao, Q.; Tanimoto, Y.; Toshima, H.; Hasegawa, M. *Biosci. Biotechnol. Biochem.* **2013**, *77*, 760–765.
(29) Robinson, D. R.; West, C. A. *Biochemistry* **1970**, *9*, 70–79.

(30)   Robinson, D. R.; West, C. A. *Biochemistry* **1970**, *9*, 80–89.

(31)   Sitton, D.; West, C. A. *Phytochemistry* **1975**, *14*, 1921–1925.

(32)   Liu, H.-B.; Zhang, H.; Yu, J.-H.; Yue, J.-M. *J. Asian Nat. Prod. Res.* **2015**, *17*, 1117–1128.

(33)   Bai, Y.; Yang, Y. ping; Ye, Y. *Tetrahedron Lett.* **2006**, *47*, 6637–6640.

(34)   Kong, L. Y.; Li, Y.; Wu, X. L.; Min, Z. Da. *Planta Med.* **2002**, *68*, 249–252.

(35)   Choi, Y. H.; Kim, J.; Pezzuto, J. M.; Kinghorn, A. D.; Farnsworth, N. R.; Letter, H.; Wagner, H. *Tetrahedron Lett.* **1986**, *27*, 5795–5798.

(36)   Kashman, Y.; Bernart, M. W.; TischLer, M.; Cardellina, J. H.; Boyd, M. R. *J. Nat. Prod.* **1994**, *57*, 426–430.

(37)   Choi, Y. H.; Pezzuto, J.; Kinghorn, A. D.; Farnsworth, N. R. *J. Nat. Prod.* **1988**, *51*, 110–116.

(38)   Löffler, L. E.; Wirtz, C.; Fürstner, A. *Angew. Chem. Int. Ed.* **2021**, *60*, 5316–5322.

(39)   Dueber, M. T.; Adolf, W.; West, C. A. *Plant Physiol.* **1978**, *62*, 598–603.

(40)   Crombie, L.; Kneen, G.; Pattenden, G. *J. Chem. Soc. Chem. Commun.* **1976**, 66–68.

(41)   Guilford, W. J.; Coates, R. M. *J. Am. Chem. Soc.* **1982**, *104*, 3506–3508.

(42)   Durán-Peña, M. J.; Botubol Ares, J. M.; Collado, I. G.; Hernández-Galán, R. *Nat. Prod. Rep.* **2014**, *31*, 940–952.

(43)   Thibodeaux, C. J.; Chang, W. C.; Liu, H. W. *Chem. Rev.* **2012**, *112*, 1681–1709.

(44)   Mau, C. J. D.; West, C. A. *Proc. Natl. Acad. Sci. U. S. A.* **1994**, *91*, 8497–8501.

(45)   Huang, Q.; Huang, K.; Scott, A. I. *Tetrahedron Lett.* **1998**, *39*, 2033–2036.

(46)   Kirby, J.; Nishimoto, M.; Park, J. G.; Withers, S. T.; Nowroozi, F.; Behrendt, D.; Rutledge, E. J. G.; Fortman, J. L.; Johnson, H. E.; Anderson, J. V.; Keasling, J. D. *Phytochemistry* **2010**, *71*, 1466–1473.

(47)   Callari, R.; Meier, Y.; Ravasio, D.; Heider, H. *Front. Bioeng. Biotechnol.* **2018**, *6*, 1–11.

(48)   Luo, D.; Callari, R.; Hamberger, B.; Wubshet, S. G.; Nielsen, M. T.; Andersen-Ranberg, J.; Hallström, B. M.; Cozzi, F.; Heider, H.; Møller, B. L.; Staerk, D.; Hamberger, B. *Proc. Natl. Acad. Sci. U. S. A.* **2016**, *113*, E5082–E5089.

(49)   Adolf, W.; Hecker, E.; Santhanakrishnan, T. S.; Matyukhina, L. G.; Saltikova, I. A. *Tetrahedron Lett.* **1970**, *26*, 2241–2244.

(50)   Stockwell, B. R. *Nature* **2004**, *432*, 846–854.

(51)   Jassbi, A. R. *Phytochemistry* **2006**, *67*, 1977–1984.

(52)   Ma, Q. G.; Liu, W. Z.; Wu, X. Y.; Zhou, T. X.; Qin, G. W. *Phytochemistry* **1997**, *44*, 663–666.

(53)   Wang, L.; Duan, H.; Wang, Y.; Liu, K.; Jiang, P.; Qu, Z.; Yagasaki, K.; Zhang, G. *Cytotechnology* **2010**, *62*, 357–366.

(54)   Liu, W. Z.; Wu, X. Y.; Yang, G. J.; Ma, Q. G.; Zhou, T. X.; Tang, X. C.; Qin, G. W. *Chinese Chem. Lett.* **1996**, *7*, 917–918.

(55)   Wenzi, L.; Fenglei, H.; Xiaoyun, W.; Guowei, Q. *J. Chinese Med. Mater.* **1997**, *20*, 351–353.

(56)   Carneiro, V. A.; Dos Santos, H. S.; Arruda, F. V. S.; Bandeira, P. N.; Albuquerque, M. R. J. R.; Pereira, M. O.; Henriques, M.; Cavada, B. S.; Teixeira, E. H. *Molecules* **2011**, *16*, 190–201.

(57)   Sá, N. C.; Cavalcante, T. T. A.; Araújo, A. X.; Santos, H. S. Dos; Albuquerque, M. R. J. R.; Bandeira, P. N.; Cunha, R. M. S. Da; Cavada, B. S.; Teixeira, E. H. *Arch. Oral Biol.* **2012**, *57*, 550–555.

(58)   Vasconcelos, M. A.; Arruda, F. V. S.; Santos, H. S.; Rodrigues, A. S.; Bandeira, P. N.; Albuquerque, M. R. J. R.; Cavada, B. S.; Teixeira, E. H.; Henriques, M.; Pereira, M. O. *Ind. Crops Prod.* **2014**, *61*, 499–509.

(59)   Zhang, C. X.; Yan, S. J.; Zhang, G. W.; Lu, W. G.; Su, J. Y.; Zeng, L. M.; Gu, L. Q.; Yang, X. P.; Lian, Y. J. *J. Nat. Prod.* **2005**, *68*, 1087–1089.

(60)   Zhan, C.; Lei, L.; Liu, Z.; Zhou, S.; Yang, C.; Zhu, X.; Guo, H.; Zhang, F.; Peng, M.; Zhang, M.; Li, Y.; Yang, Z.; Sun, Y.; Shi, Y.; Li, K.; Liu, L.; Shen, S.; Wang, X.; Shao, J.; Jing, X.; Wang, Z.; Li, Y.; Czechowski, T.; Hasegawa, M.; Graham, I.; Tohge, T.; Qu, L.; Liu, X.; Fernie, A. R.; Chen, L. L.; Yuan, M.; Luo, J. *Nat. Plants* **2020**, *6*, 1447–1454.

(61)   Stekoll, M.; West, C. A. *Plant Physiol.* **1978**, *61*, 38–45.

(62)   West, C. A. *Naturwissenschaften* **1981**, *68*, 447–457.

(63)   Vickers, C. E.; Williams, T. C.; Peng, B.; Cherry, J. *Curr. Opin. Chem. Biol.* **2017**, *40*, 47–56.

(64)   Shao, J.; Sun, Y.; Liu, H.; Wang, Y. *Curr. Opin. Biotechnol.* **2021**, *69*, 10–16.

(65)   Toma, K.; Miyazaki, E.; Murae, T.; Takahashi, T. *Chem. Lett.* **1982**, *11*, 863–864.

(66)   Pattenden, G.; Smithies, A. J. *J. Chem. Soc., Perkin Trans. 1* **1996**, 57–61.

(67)   McMurry, J. E.; Bosch, G. K. *J. Org. Chem.* **1987**, *52*, 4885–4893.

(68)   Motherwell, W. B.; Roberts, L. R. *Tetrahedron Lett.* **1995**, *36*, 1121–1124.

(69)   Doyle, M. P.; Pieters, R. J.; Martin, S. F.; Austin, R. E.; Oalmann, C. J.; Müller, P. *J. Am. Chem. Soc.* **1991**, *113*, 1423–1424.

(70)   Doyle, M. P.; Yan, M. *Arkivoc* **2002**, 180–185.

(71)   Driggers, E. M.; Hale, S. P.; Lee, J.; Terrett, N. K. *Nat. Rev. Drug Discov.* **2008**, *7*, 608–624.

(72)   Mortensen, K. T.; Osberger, T. J.; King, T. A.; Sore, H. F.; Spring, D. R. *Chem. Rev.* **2019**, *119*, 10288–10317.

(73)   Yu, X.; Sun, D. *Molecules* **2013**, *18*, 6230–6268.

(74)   Fürstner, A. *Acc. Chem. Res.* **2021**, *54*, 861–874.

(75)   Saridakis, I.; Kaiser, D.; Maulide, N. *ACS Cent. Sci.* **2020**, *6*, 1869–1889.

(76)   Schrock, R. R. *Angew. Chem. Int. Ed.* **2006**, *45*, 3748–3759.

(77)   Chauvin, Y. *Angew. Chem. Int. Ed.* **2006**, *45*, 3740–3747.

(78)   Grubbs, R. H. *Angew. Chem. Int. Ed.* **2006**, *45*, 3760–3765.

(79)   Fürstner, A. *Angew. Chem. Int. Ed.* **2000**, *39*, 3012–3043.

(80)   Ogba, O. M.; Warner, N. C.; O'Leary, D. J.; Grubbs, R. H. *Chem. Soc. Rev.* **2018**, *47*, 4510–4544.

(81)   Fürstner, A. *Science* **2013**, *341*, 1229713.

(82)   Nicolaou, K. C.; Bulger, P. G.; Sarlah, D. *Angew. Chem. Int. Ed.* **2005**, *44*, 4490–4527.

(83)   Pennella, F.; Banks, R. L.; Bailey, G. C. *Commun. Chem.* **1968**, 1967–1968.

(84)   Mortreux, A.; Blanchard, M. *J. Chem. Soc. Chem. Commun.* **1974**, *2*, 786–787.

(85)   Katz, T. J.; McGinnis, J. *J. Am. Chem. Soc.* **1975**, *97*, 1592–1594.

(86)   Fischer, E. O.; Kreis, G.; Kreiter, C. G.; Müller, J.; Huttner, G.; Lorenz, H. *Angew. Chem. Int. Ed.* **1973**, *12*, 564–565.

(87)   Huttner, G.; Lorenz, H.; Gartzke, W. *Angew. Chem. Int. Ed.* **1974**, *13*, 609–611.

(88)   Heppekausen, J.; Stade, R.; Goddard, R.; Fürstner, A. *J. Am. Chem. Soc.* **2010**, *132*, 11045–11057.

(89)   Wengrovius, J. H.; Sancho, J.; Schrock, R. R. *J. Am. Chem. Soc.* **1981**, *103*, 3932–3934.

(90)   Weinstock, I. A.; Schrock, R. R.; Davis, W. M. *J. Am. Chem. Soc.* **1991**, *113*, 135–144.

(91)   Pedersen, S. F.; Schrock, R. R.; Churchill, M. R.; Wasserman, H. J. *J. Am. Chem. Soc.* **1982**, *104*, 6808–6809.

(92)   Freudenberger, J. H.; Schrock, R. R.; Churchill, M. R.; Rheingold, A. L.; Ziller, J. W. *Organometallics* **1984**, *3*, 1563–1573.

(93)   Churchill, M. R.; Ziller, J. W.; Freudenberger, J. H.; Schrock, R. R. *Organometallics* **1984**, *3*, 1554–1562.

(94)   Laplaza, C. E.; Cummins, C. C. *Science* **1995**, *268*, 861–863.

(95)   Laplaza, C. E.; Odom, A. L.; Davis, W. M.; Cummins, C. C.; Protasiewicz, J. D. *J. Am. Chem. Soc.* **1995**, *117*, 4999–5000.

(96)   Cummins, C. C. *Chem. Commun.* **1998**, *7*, 1777–1786.

(97)   Fürstner, A.; Mathes, C.; Lehmann, C. W. *J. Am. Chem. Soc.* **1999**, *121*, 9453–9454.

(98)   Fürstner, A.; Davies, P. W. *Chem. Commun.* **2005**, 2307–2320.

(99)   Fürstner, A.; Mathes, C.; Lehmann, C. W. *Chem. - Eur. J.* **2001**, *7*, 5299–5317.

(100)   Zhang, W.; Kraft, S.; Moore, J. S. *Chem. Commun.* **2003**, *3*, 832–833.

(101)   Zhang, W.; Kraft, S.; Moore, J. S. *J. Am. Chem. Soc.* **2004**, *126*, 329–335.

(102)   Zhang, W.; Lu, Y.; Moore, J. S. *Org. Synth.* **2007**, *84*, 163–176.

(103)   Fürstner, A. *Angew. Chem. Int. Ed.* **2013**, *52*, 2794–2819.

(104)   Heppekausen, J.; Stade, R.; Kondoh, A.; Seidel, G.; Goddard, R.; Fürstner, A. *Chem. - Eur. J.* **2012**, *18*, 10281–10299.

(105)   Haack, A.; Hillenbrand, J.; van Gastel, M.; Fürstner, A.; Neese, F. *ACS Catal.* **2021**, *11*, 9086–9101.

(106)   Schaubach, S.; Gebauer, K.; Ungeheuer, F.; Hoffmeister, L.; Ilg, M. K.; Wirtz, C.; Fürstner, A. *Chem. - Eur. J.* **2016**, *22*, 8494–8507.

(107) Schrock, R. R. *Acc. Chem. Res.* **1986**, *19*, 342–348.

(108) Schrock, R. R. *J. Chem. Soc., Dalt. Trans.* **2001**, 2541–2550.

(109) Schrock, R. R. *Chem. Rev.* **2002**, *102*, 145–179.

(110) Jyothish, K.; Zhang, W. *Angew. Chem. Int. Ed.* **2011**, *50*, 3435–3438.

(111) Yang, H.; Liu, Z.; Zhang, W. *Adv. Synth. Catal.* **2013**, *355*, 885–890.

(112) Jyothish, K.; Wang, Q.; Zhang, W. *Adv. Synth. Catal.* **2012**, *354*, 2073–2078.

(113) Du, Y.; Yang, H.; Zhu, C.; Ortiz, M.; Okochi, K. D.; Shoemaker, R.; Jin, Y.; Zhang, W. *Chem. - Eur. J.* **2016**, *22*, 7959–7963.

(114) Hillenbrand, J.; Leutzsch, M.; Fürstner, A. *Angew. Chem. Int. Ed.* **2019**, *58*, 15690–15696.

(115) Hillenbrand, J.; Leutzsch, M.; Yiannakas, E.; Gordon, C. P.; Wille, C.; Nöthling, N.; Copéret, C.; Fürstner, A. *J. Am. Chem. Soc.* **2020**, *142*, 11279–11294.

(116) Freudenberger, J. H.; Schrock, R. R. *Organometallics* **1986**, *5*, 1411–1417.

(117) McCullough, L. G.; Listemann, M. L.; Schrock, R. R.; Churchill, M. R.; Ziller, J. W. *J. Am. Chem. Soc.* **1983**, *105*, 6729–6730.

(118) Churchill, M. R.; Ziller, J. W. *J. Organomet. Chem.* **1985**, *281*, 237–248.

(119) Lhermet, R.; Fürstner, A. *Chem. - Eur. J.* **2014**, *20*, 13188–13193.

(120) Listemann, M. L.; Schrock, R. R. *Organometallics* **1985**, *4*, 74–83.

(121) Chisholm, M. H.; Folting, K.; Huffman, J. C.; Rothwell, I. P. *J. Am. Chem. Soc.* **1982**, *104*, 4389–4399.

(122) Chisholm, M. H.; Folting, K.; Hoffman, D. M.; Huffman, J. C. *J. Am. Chem. Soc.* **1984**, *106*, 6794–6805.

(123) Chisholm, M. H. *Acc. Chem. Res.* **1990**, *23*, 419–425.

(124) Willwacher, J.; Fürstner, A. *Angew. Chem. Int. Ed.* **2014**, *53*, 4217–4221.

(125) Willwacher, J.; Heggen, B.; Wirtz, C.; Thiel, W.; Fürstner, A. *Chem. - Eur. J.* **2015**, *21*, 10416–10430.

(126) Haberlag, B.; Freytag, M.; Jones, P. G.; Tamm, M. *Adv. Synth. Catal.* **2014**, *356*, 1255–1265.

(127) Ehrhorn, H.; Bockfeld, D.; Freytag, M.; Bannenberg, T.; Kefalidis, C. E.; Maron, L.; Tamm, M. *Organometallics* **2019**, *38*, 1627–1639.

(128) Haberlag, B.; Freytag, M.; Daniliuc, C. G.; Jones, P. G.; Tamm, M. *Angew. Chem. Int. Ed.* **2012**, *51*, 13019–13022.

(129) Hötling, S.; Bittner, C.; Tamm, M.; Dähn, S.; Collatz, J.; Steidle, J. L. M.; Schulz, S. *Org. Lett.* **2015**, *17*, 5004–5007.

(130) Thombal, R. S.; Jadhav, V. H. *Org. Biomol. Chem.* **2015**, *13*, 9485–9491.

(131) Gao, J.; Sun, D.; Yu, K.; Xie, H.; Ding, H. *Org. Lett.* **2019**, *21*, 9603–9607.

(132) Rummelt, S. M.; Preindl, J.; Sommer, H.; Fürstner, A. *Angew. Chem. Int. Ed.* **2015**, *54*, 6241–6245.

(133) Meng, Z.; Souillart, L.; Monks, B.; Huwyler, N.; Herrmann, J.; Müller, R.; Fürstner, A. *J. Org. Chem.* **2018**, *83*, 6977–6994.

(134) Kwon, Y.; Schulthoff, S.; Dao, Q. M.; Wirtz, C.; Fürstner, A. *Chem. - Eur. J.* **2018**, *24*, 109–114.

(135) Coombs, J. R.; Zhang, L.; Morken, J. P. *J. Am. Chem. Soc.* **2014**, *136*, 16140–16143.

(136) Doyle, M. P.; Bagheri, V.; Pearson, M. M.; Edwards, J. D. *Tetrahedron Lett.* **1989**, *30*, 7001–7004.

(137) Doyle, M. P.; Winchester, W. R.; Hoorn, J. A. A.; Lynch, V.; Simonsen, S. H.; Ghosh, R. *J. Am. Chem. Soc.* **1993**, *115*, 9968–9978.

(138) Doyle, M. P.; Winchester, W. R.; Protopopova, M. N.; Kazala, A. P.; Westrum, L. J. *Org. Synth.* **1996**, *73*, 13–24.

(139) Doyle, M. P.; Bagheri, V.; Wandless, T. J.; Ham, N. K.; Brinker, D. A.; Eagle, C. T.; Loh, K. L. *J. Am. Chem. Soc.* **1990**, *112*, 1906–1912.

(140) Doyle, M. P.; Brandes, B. D.; Kazala, A. P.; Pieters, R. J.; Jarstfer, M. B.; Watkins, L. M.; Eagle, C. T. *Tetrahedron Lett.* **1990**, *31*, 6613–6616.

(141) Colacot, T. J. *Proc. Indian Acad. Sci. Chem. Sci.* **2000**, *112*, 197–207.

(142) Doyle, M. P. *J. Org. Chem.* **2006**, *71*, 9253–9260.

(143) Doyle, M. P.; Bailey, A. S.; Dyatkin, A. B.; Kalinin, A. V.; Kwan, M. M. Y.; Pieters, R. J.;

Protopopova, M. N.; Raab, C. E.; Roos, G. H. P.; Zhou, Q. L.; Austin, R. E.; Dwyer, M. P.; Liras, S.; Oalmann, C. J.; Martin, S. F. *J. Am. Chem. Soc.* **1995**, *117*, 5763–5775.

(144) Doyle, M. P.; Peterson, C. S.; Zhou, Q. L.; Nishiyama, H. *Chem. Commun.* **1997**, *21*, 211–212.

(145) Martin, S. F.; Dorsey, G. O.; Gane, T.; Hillier, M. C.; Kessler, H.; Baur, M.; Mathä, B.; Erickson, J. W.; Bhat, T. N.; Munshi, S.; Gulnik, S. V.; Topol, I. A. *J. Med. Chem.* **1998**, *41*, 1581–1597.

(146) Martin, S. F.; Hillier, M. C. *Tetrahedron Lett.* **1998**, *39*, 2929–2932.

(147) Podlech, J. *J. prakt. Chem.* **1998**, *340*, 479–482.

(148) Inoue, S.; Nagatani, K.; Tezuka, H.; Hoshino, Y.; Nakada, M. *Synlett* **2017**, *28*, 1065–1070.

(149) Danheiser, R. L.; Miller, R. F.; Brisbois, R. G.; Park, S. Z. *J. Org. Chem.* **1990**, *55*, 1959–1964.

(150) Danheiser, R. L.; Brisbois, R. G.; Kowalczyk, J. J.; Miller, R. F. *J. Am. Chem. Soc.* **1990**, *112*, 3093–3100.

(151) Watson, W. *Org. Process Res. Dev.* **2012**, *16*, 1877.

(152) Minuth, T.; Boysen, M. M. K. *Synthesis (Stuttg).* **2010**, 2799–2803.

(153) He, R.; Deng, M. Z. *Tetrahedron* **2002**, *58*, 7613–7617.

(154) Kocieński, P. J.; Pritchard, M.; Wadman, S. N.; Whitby, R. J.; Yeates, C. L. *J. Chem. Soc. Perkin Trans. 1* **1992**, *130*, 3419–3429.

(155) Ashworth, P. A.; Dixon, N. J.; Kocieński, P. J.; Wadman, S. N. *J. Chem. Soc. Perkin Trans. 1* **1992**, 3431–3438.

(156) MacKlin, T. K.; Micalizio, G. C. *Nat. Chem.* **2010**, *2*, 638–643.

(157) Corey, E. J.; Fuchs, P. L. *Tetrahedron Lett.* **1972**, *13*, 3769–3772.

(158) Miyaura, N.; Suzuki, A. *J. Chem. Soc. Chem. Commun.* **1979**, 866–867.

(159) Miyaura, N.; Yamada, K.; Suzuki, A. *Tetrahedron Lett.* **1979**, *20*, 3437–3440.

(160) Woodward, R. B.; Logusch, E.; Nambiar, K. P.; Sakan, K.; Ward, D. E.; Au-Yeung, B. W.; Balaram, P.; Browne, L. J.; Card, P. J.; Chen, C. H.; Chenevert, R. B.; Fliri, A.; Frobel, K.; Gais, H. J.; Garratt, D. G.; Hayakawa, K.; Heggie, W.; Hesson, D. P.; Hoppe, D.; Hoppe, I.; Hyatt, J. A.; Ikeda, D.; Jacobi, P. A.; Kim, K. S.; Kobuke, Y.; Kojima, K.; Krowicki, K.; Lee, V. J.; Leutert, T.; Malchenko, S.; Martens, J.; Matthews, R. S.; Ong, B. S.; Press, J. B.; Rajan Babu, T. V.; Rousseau, G.; Sauter, H. M.; Suzuki, M.; Tatsuta, K.; Tolbert, L. M.; Truesdale, E. A.; Uchida, I.; Ueda, Y.; Uyehara, T.; Vasella, A. T.; Vladuchick, W. C.; Wade, P. A.; Williams, R. M.; Wong, H. N. C. *J. Am. Chem. Soc.* **1981**, *103*, 3213–3215.

(161) Chemler, S. R.; Trauner, D.; Danishefsky, S. J. *Angew. Chem. Int. Ed.* **2001**, *40*, 4544–4568.

(162) Predeus, A. V.; Gopalsamuthiram, V.; Staples, R. J.; Wulff, W. D. *Angew. Chem. Int. Ed.* **2013**, *52*, 911–915.

(163) Hesse, M. J.; Butts, C. P.; Willis, C. L.; Aggarwal, V. K. *Angew. Chem. Int. Ed.* **2012**, *51*, 12444–12448.

(164) Linderman, R. J.; Graves, D. M. *J. Org. Chem* **1989**, *54*, 661–668.

(165) Klapars, A.; Buchwald, S. L. *J. Am. Chem. Soc.* **2002**, *124*, 14844–14845.

(166) Huo, S. *Org. Lett.* **2003**, *5*, 423–425.

(167) Baba, S.; Negishi, E. ichi. *J. Am. Chem. Soc.* 1976, pp 6729–6731.

(168) Negishi, E.; King, A. O.; Okukado, N. *J. Org. Chem.* **1977**, *42*, 1821–1823.

(169) King, A. O.; Okukado, N.; Negishi, E. I. *J. Chem. Soc. Chem. Commun.* **1977**, 683–684.

(170) Miller, R. B.; Reichenbach, T. *Tetrahedron Lett.* **1974**, *15*, 543–546.

(171) Chan, T. H.; Fleming, I. *Synthesis (Stuttg).* **1979**, *10*, 761–786.

(172) Miller, R. B.; McGarvey, R. *Synth. Commun.* **1978**, *8*, 291–299.

(173) Chan, T. H.; Lau, P. W. K.; Mychajlowskij, W. *Tetrahedron Lett.* **1977**, *38*, 3317–3320.

(174) Fleming, I.; Barbero, A.; Walter, D. *Chem. Rev.* **1997**, *97*, 2063–2192.

(175) Sidera, M.; Costa, A. M.; Vilarrasa, J. *Org. Lett.* **2011**, *13*, 4934–4937.

(176) Ilardi, E. A.; Stivala, C. E.; Zakarian, A. *Org. Lett.* **2008**, *10*, 1727–1730.

(177) Stamos, D. P.; Taylor, A. G.; Kishi, Y. *Tetrahedron Lett.* **1996**, *37*, 8647–8650.

(178) Colomer, I.; Chamberlain, A. E. R.; Haughey, M. B.; Donohoe, T. J. *Nat. Rev. Chem.* **2017**, *1*.

(179) Uenishi, J. ichi; Beau, J. M.; Armstrong, R. W.; Kishi, Y. *J. Am. Chem. Soc.* **1987**, *109*, 4756–4758.

(180) Fürstner, A.; Nevado, C.; Waser, M.; Tremblay, M.; Chevrier, C.; Teplý, F.; Aïssa, C.; Moulin,

E.; Müller, O. *J. Am. Chem. Soc.* **2007**, *129*, 9150–9161.

(181) Rummelt, S. M.; Fürstner, A. *Angew. Chem. Int. Ed.* **2014**, *53*, 3626–3630.

(182) Rummelt, S. M.; Radkowski, K.; Roşca, D. A.; Fürstner, A. *J. Am. Chem. Soc.* **2015**, *137*, 5506–5519.

(183) Roşca, D. A.; Radkowski, K.; Wolf, L. M.; Wagh, M.; Goddard, R.; Thiel, W.; Fürstner, A. *J. Am. Chem. Soc.* **2017**, *139*, 2443–2455.

(184) Fürstner, A. *J. Am. Chem. Soc.* **2019**, *141*, 11–24.

(185) Huwyler, N.; Radkowski, K.; Rummelt, S. M.; Fürstner, A. *Chem. - Eur. J.* **2017**, *23*, 12412–12419.

(186) Attenburrow, J.; Cameron, A. F. B.; Chapman, J. H.; Evans, R. M.; Hems, B. A.; Jansen, A. B. A.; Walker, T. *J. Chem. Soc.* **1952**, 1094–1111.

(187) Burke, B. A.; Chan, W. R.; Pascoe, K. O.; Blount, J. F.; Manchand, P. S. *J. Chem. Soc. Trans. 1* **1981**, 2666–2669.

(188) Commissiong, M. A.; Pascoe, K. O. *Tetrahedron Lett.* **1984**, *25*, 711–712.

(189) Araoz, R.; Servent, D.; Molgoí, J.; Iorga, B. I.; Fruchart-Gaillard, C.; Benoit, E.; Gu, Z.; Stivala, C.; Zakarian, A. *J. Am. Chem. Soc.* **2011**, *133*, 10499–10511.

(190) Herrmann, A. T.; Martinez, S. R.; Zakarian, A. *Org. Lett.* **2011**, *13*, 3636–3639.

(191) Brown, C. A.; Coleman, R. A. *J. Org. Chem.* **1979**, *44*, 2328–2329.

(192) Fleming, I.; Newton, T. W.; Roessler, F. *J. Chem. Soc. Perkin Trans. 1* **1981**, 2527–2532.

(193) Bertz, S. H.; Fairchild, E.; Dieter, K. *Encycl. Reagents Org. Synth.* **2006**, 1–7.

(194) Safety Data Sheet: 1,1,1,3,3,3-Hexafluoro-2-propanol. Version 7.1 Sigma Aldrich, 20. July 2021, downloaded 10. August 2021. https://www.sigmaaldrich.com/DE/de/product/ALDRICH/105228.

(195) Krasovskiy, A.; Malakhov, V.; Gavryushin, A.; Knochel, P. *Angew. Chem. Int. Ed.* **2006**, *45*, 6040–6044.

(196) Qi, C.; Force, G.; Gandon, V.; Lebœuf, D. *Angew. Chem. Int. Ed.* **2021**, *60*, 946–953.

(197) Martin, D. B. C.; Vanderwal, C. D. *J. Am. Chem. Soc.* **2009**, *131*, 3472–3473.

(198) Dale, J. A.; Mosher, H. S. *J. Am. Chem. Soc.* **1973**, *95*, 512–519.

(199) Hoye, T. R.; Jeffrey, C. S.; Shao, F. *Nat. Protoc.* **2007**, *2*, 2451–2458.

(200) Sommer, H.; Fürstner, A. *Org. Lett.* **2016**, *18*, 3210–3213.

(201) Li, Y.; Chakrabarty, S.; Mück-Lichtenfeld, C.; Studer, A. *Angew. Chem. Int. Ed.* **2016**, *55*, 802–806.

(202) Tantillo, D. J. *Nat. Prod. Rep.* **2013**, *30*, 1079–1086.

(203) Lodewyk, M. W.; Siebert, M. R.; Tantillo, D. J. *Chem. Rev.* **2012**, *112*, 1839–1862.

(204) Willoughby, P. H.; Jansma, M. J.; Hoye, T. R. *Nat. Protoc.* **2014**, *9*, 643–660.

(205) Smith, S. G.; Goodman, J. M. *J. Org. Chem.* **2009**, *74*, 4597–4607.

(206) Smith, S. G.; Goodman, J. M. *J. Am. Chem. Soc.* **2010**, *132*, 12946–12959.

(207) Ermanis, K.; Parkes, K. E. B.; Agback, T.; Goodman, J. M. *Org. Biomol. Chem.* **2019**, *17*, 5886–5890.

(208) Howarth, A.; Ermanis, K.; Goodman, J. M. *Chem. Sci.* **2020**, *11*, 4351–4359.

(209) Grimblat, N.; Zanardi, M. M.; Sarotti, A. M. *J. Org. Chem.* **2015**, *80*, 12526–12534.

(210) Zanardi, M. M.; Suárez, A. G.; Sarotti, A. M. *J. Org. Chem.* **2017**, *82*, 1873–1879.

(211) Zanardi, M. M.; Marcarino, M. O.; Sarotti, A. M. *Org. Lett.* **2020**, *22*, 52–56.

(212) Grimblat, N.; Gavín, J. A.; Hernández Daranas, A.; Sarotti, A. M. *Org. Lett.* **2019**, *21*, 4003–4007.

(213) Sarotti, A. M. *Org. Biomol. Chem.* **2013**, *11*, 4847–4859.

(214) Zanardi, M. M.; Biglione, F. A.; Sortino, M. A.; Sarotti, A. M. *J. Org. Chem.* **2018**, *83*, 11839–11849.

(215) Della-Felice, F.; Pilli, R. A.; Sarotti, A. M. *J. Braz. Chem. Soc.* **2018**, *29*, 1041–1075.

(216) Ndukwe, I. E.; Wang, X.; Lam, N. Y. S.; Ermanis, K.; Alexander, K. L.; Bertin, M. J.; Martin, G. E.; Muir, G.; Paterson, I.; Britton, R.; Goodman, J. M.; Helfrich, E. J. N.; Piel, J.; Gerwick, W. H.; Williamson, R. T. *Chem. Commun.* **2020**, *56*, 7565–7568.

(217) Li, S. W.; Cuadrado, C.; Yao, L. G.; Daranas, A. H.; Guo, Y. W. *Org. Lett.* **2020**, *22*, 4093–4096.

(218) Sarotti, A. M. *Org. Biomol. Chem.* **2018**, *16*, 944–950.

(219) Sarotti, A. M. *J. Org. Chem.* **2020**, *85*, 11566–11570.

(220) Grimme, S. *J. Chem. Theory Comput.* **2019**, *15*, 2847–2862.

(221) Pracht, P.; Bohle, F.; Grimme, S. *Phys. Chem. Chem. Phys.* **2020**, *22*, 7169–7192.

(222) Neese, F. *Wiley Interdiscip. Rev. Comput. Mol. Sci.* **2012**, *2*, 73–78.

(223) Neese, F. *Wiley Interdiscip. Rev. Comput. Mol. Sci.* **2018**, *8*, 4–9.

(224) Ditchfield, R. *J. Chem. Phys.* **1972**, *56*, 5688–5691.

(225) Ditchfield, R. *Mol. Phys.* **1974**, *27*, 789–807.

(226) McMichael Rohlfing, C.; Allen, L. C.; Ditchfield, R. *Chem. Phys.* **1984**, *87*, 9–15.

(227) Wolinski, K.; Hinton, J. F.; Pulay, P. *J. Am. Chem. Soc.* **1990**, *112*, 8251–8260.

(228) Adamo, C.; Barone, V. *J. Chem. Phys.* **1998**, *108*, 664–675.

(229) Hehre, W. J.; Ditchfield, R.; Pople, J. A. *J. Chem. Phys.* **1972**, *56*, 2257–2261.

(230) Mlynarski, S. N.; Schuster, C. H.; Morken, J. P. *Nature* **2014**, *505*, 386–390.

(231) Armstrong, R. J.; Aggarwal, V. K. *Synth.* **2017**, *49*, 3323–3336.

(232) Armstrong, R. J.; García-Ruiz, C.; Myers, E. L.; Aggarwal, V. K. *Angew. Chem. Int. Ed.* **2017**, *56*, 786–790.

(233) Coombs, J. R.; Haeffner, F.; Kliman, L. T.; Morken, J. P. *J. Am. Chem. Soc.* **2013**, *135*, 11222–11231.

(234) Fyfe, J. W. B.; Watson, A. J. B. *Chem* **2017**, *3*, 31–55.

(235) Yan, L.; Morken, J. P. *Org. Lett.* **2019**, *21*, 3760–3763.

(236) Liu, X.; Sun, C.; Mlynarski, S.; Morken, J. P. *Org. Lett.* **2018**, *20*, 1898–1901.

(237) Potter, B.; Szymaniak, A. A.; Edelstein, E. K.; Morken, J. P. *J. Am. Chem. Soc.* **2014**, *136*, 17918–17921.

(238) Lennox, A. J. J.; Lloyd-Jones, G. C. *Chem. Soc. Rev.* **2014**, *43*, 412–443.

(239) Thomas, A. A.; Zahrt, A. F.; Delaney, C. P.; Denmark, S. E. *J. Am. Chem. Soc.* **2018**, *140*, 4401–4416.

(240) Ahmed, E. A. M. A.; Lu, X.; Gong, T. J.; Zhang, Z. Q.; Xiao, B.; Fu, Y. *Chem. Commun.* **2017**, *53*, 909–912.

(241) Ding, J.; Rybak, T.; Hall, D. G. *Nat. Commun.* **2014**, *5*, 1–9.

(242) Wang, X.; Zhang, S.; Cui, P.; Li, S. *Org. Lett.* **2020**, *22*, 8702–8707.

(243) Endo, K.; Ohkubo, T.; Shibata, T. *Org. Lett.* **2011**, *13*, 3368–3371.

(244) Li, J. H.; Li, J. L.; Wang, D. P.; Pi, S. F.; Xie, Y. X.; Zhang, M. B.; Hu, X. C. *J. Org. Chem.* **2007**, *72*, 2053–2057.

(245) Sun, C.; Potter, B.; Morken, J. P. *J. Am. Chem. Soc.* **2014**, *136*, 6534–6537.

(246) Yu, Z.; Ely, R. J.; Morken, J. P. *Angew. Chem. Int. Ed.* **2014**, *53*, 9632–9636.

(247) Behloul, C.; Chouti, A.; Chabour, I.; Bey, H. B.; Guijarro, D.; Foubelo, F.; Nájera, C.; Yus, M. *Tetrahedron Lett.* **2016**, *57*, 3526–3528.

(248) Noyori, R.; Ohta, M.; Hsiao, Y.; Kitamura, M. *J. Am. Chem. Soc.* **1986**, *108*, 7117–7119.

(249) M. Kitamura; Ohkuma, T.; Inoue, S.; Sayo, N.; Kumobayashi, H.; Akutagawa, S.; Ohta, T.; Takaya, H.; Noyori*, R. *J. Am. Chem. Soc.* **1988**, *110*, 629–631.

(250) Arai, N.; Satoh, H.; Utsumi, N.; Murata, K.; Tsutsumi, K.; Ohkuma, T. *Org. Lett.* **2013**, *15*, 3030–3033.

(251) Doyle, M. P. *Aldrichimica Acta* **1996**, *29*, 3–11.

(252) Doyle, M. P.; Protopopova, M.; Müller, P.; Ene, D.; Shapiro, E. A. *J. Am. Chem. Soc.* **1994**, *116*, 8492–8498.

(253) Doyle, M. P.; Phillips, I. M.; Wenhao Hu. *J. Am. Chem. Soc.* 2001, pp 5366–5367.

(254) Doyle, M. P.; van Oeveren, A.; Westrum, L. J.; Clayton, T. W.; Protopopova, M. N. *J. Am. Chem. Soc.* **1991**, *113*, 8982–8984.

(255) Doyle, M. P.; Dyatkin, A. B.; Cañas, F.; Pierson, D. A.; van Basten, A.; Roos, G. H. P.; Müller, P.; Polleux, P. *J. Am. Chem. Soc.* **1994**, *116*, 4507–4508.

(256) Doyle, M. P.; Kalinin, A. V. *Synlett* **1995**, 1075–1076.

(257) Löffler, L. E.; Buchsteiner, M.; Lee, R.; Caló, F. P.; Singha, S.; Fürstner, A. *Helv. Chim. Acta* **2021**, *104*, e2100042.

(258) Ren, Z.; Sunderland, T. L.; Tortoreto, C.; Yang, T.; Berry, J. F.; Musaev, D. G.; Davies, H. M.

L. *ACS Catal.* **2018**, *8*, 10676−10682.

(259) Collins, L. R.; Auris, S.; Goddard, R.; Fürstner, A. *Angew. Chem. Int. Ed.* **2019**, *58*, 3557−3561.

(260) Singha, S.; Buchsteiner, M.; Bistoni, G.; Goddard, R.; Fürstner, A. *J. Am. Chem. Soc.* **2021**, *143*, 5666−5673.

(261) Dikarev, E. V.; Gray, T. G.; Li, B. *Angew. Chem. Int. Ed.* **2005**, *44*, 1721−1724.

(262) Dikarev, E. V.; Li, B.; Zhang, H. *J. Am. Chem. Soc.* **2006**, *128*, 2814−2815.

(263) Filatov, A. S.; Napier, M.; Vreshch, V. D.; Sumner, N. J.; Dikarev, E. V.; Petrukhina, M. A. *Inorg. Chem.* **2012**, *51*, 566−571.

(264) Collins, L. R.; Van Gastel, M.; Neese, F.; Fürstner, A. *J. Am. Chem. Soc.* **2018**, *140*, 13042−13055.

(265) Hansen, J.; Autschbach, J.; Davies, H. M. L. *J. Org. Chem.* **2009**, *74*, 6555−6563.

(266) Hansen, J.; Li, B.; Dikarev, E.; Autschbach, J.; Davies, H. M. L. *J. Org. Chem.* **2009**, *74*, 6564−6571.

(267) Berry, J. F. *Dalt. Trans.* **2012**, *41*, 700−713.

(268) Sunderland, T. L.; Berry, J. F. *J. Coord. Chem.* **2016**, *69*, 1949−1956.

(269) Becke, A. D. *Phys. Rev. A* **1988**, *38*, 3098−3100.

(270) Weigend, F.; Ahlrichs, R. *Phys. Chem. Chem. Phys.* **2005**, *7*, 3297−3305.

(271) Van Lenthe, E.; Snijders, J. G.; Baerends, E. J. *J. Chem. Phys.* **1996**, *105*, 6505−6516.

(272) Van Lenthe, E.; Wormer, P. E. S.; Van Der Avoird, A. *J. Chem. Phys.* **1998**, *108*, 4783−4796.

(273) Grimme, S.; Ehrlich, S.; Goerigk, L. *J. Comput. Chem.* **2011**, *32*, 1456−1465.

(274) Grimme, S.; Antony, J.; Ehrlich, S.; Krieg, H. *J. Chem. Phys.* **2010**, *132*, 154104−154119.

(275) Pantazis, D. A.; Neese, F. *Theor. Chem. Acc.* **2012**, *131*, 1−7.

(276) Rolfes, J. D.; Neese, F.; Pantazis, D. A. *J. Comput. Chem.* **2020**, *41*, 1842−1849.

(277) Vahtras, O.; Almlöf, J.; Feyereisen, M. W. *Chem. Phys. Lett.* **1993**, *213*, 514−518.

(278) Eichkorn, K.; Treutler, O.; Öhm, H.; Häser, M.; Ahlrichs, R. *Chem. Phys. Lett.* **1995**, *240*, 283−290.

(279) Ahlrichs, R. *Phys. Chem. Chem. Phys.* **2004**, *6*, 5119−5121.

(280) Klamt, A.; Schüürmann, G. *J. Chem. Soc. Perkin Trans. 2* **1993**, 799−805.

(281) Andzelm, J.; Kölmel, C.; Klamt, A. *J. Chem. Phys.* **1995**, *103*, 9312−9320.

(282) Barone, V.; Cossi, M. *J. Phys. Chem. A* **1998**, *102*, 1995−2001.

(283) Cossi, M.; Rega, N.; Scalmani, G.; Barone, V. *J. Comput. Chem.* **2003**, *24*, 669−681.

(284) Redies, K. M.; Fallon, T.; Oestreich, M. *Organometallics* **2014**, *33*, 3235−3238.

(285) Xtb Version 6.1; please contact xtb(at)thch.uni-bonn.de for access. University Bonn 2019.

(286) Grimme, S.; Bannwarth, C.; Dohm, S.; Hansen, A.; Pisarek, J.; Pracht, P.; Seibert, J.; Neese, F. *Angew. Chem. Int. Ed.* **2017**, *56*, 14763−14769.

(287) Bannwarth, C.; Ehlert, S.; Grimme, S. *J. Chem. Theory Comput.* **2019**, *15*, 1652−1671.

(288) Lee, C.; Yang, W.; Parr, R. G. *Phys. Rev. B* **1988**, *37*, 785−789.

(289) Weigend, F. *Phys. Chem. Chem. Phys.* **2006**, *8*, 1057−1065.

(290) Walker, M. W.; Shao, L.; Volz, R. A. *CVGIP IMAGE Underst.* **1991**, *54*, 358−367.

(291) Kabsch, W. *Acta Crystallogr. Sect. A* **1976**, *A32*, 922−923.

(292) Calculate root-mean-square deviation (RMSD) of two molecules using rotation, http://github.com/charnley/rmsd.

(293) Chemcraft - graphical software for visualization of quantum chemistry computations, https://chemcraftprog.com/.

(294) DP4+(128) Excel sheet, https://sarotti-nmr.weebly.com.

(295) Moura, V. L. A.; Monte, F. J. O.; Filho, R. B. *J. Nat. Prod.* **1990**, *53*, 1566−1571.

(296) E Silva Filho, F. A.; Nunes Da Silva Junior, J.; Braz-Filho, R.; De Simone, C. A.; Silveira, E. R.; Lima, M. A. S. *Helv. Chim. Acta* **2013**, *96*, 1146−1154.

(297) Silva-Filho, F. A. E.; Braz-Filho, R.; Silveira, E. R.; Lima, M. A. S. *Magn. Reson. Chem.* **2011**, *49*, 370−373.

(298) Liu, X. X.; Ma, H.; He, W.; Sun, Y.; Lan, W. *Chem. Nat. Compd.* **2018**, *54*, 910−912.

(299) Görner, C.; Schrepfer, P.; Redai, V.; Wallrapp, F.; Loll, B.; Eisenreich, W.; Haslbeck, M.; Brück, T. *Microb. Cell Fact.* **2016**, *15*, 86.

F ABBREVIATIONS

Ac	acetyl
Ar	aryl
9-H-9-BBN	9-borobicyclo[3.3.1]nonane
BC − AD	before Christ − anno Domini
Bn	benzyl
BQ	1,4-benzoquinone
brsm	based on recovered starting material
Bu	butyl
°C	degree Celsius
CD	circular dichroism
$CHCl_3$	chloroform
CH_2Cl_2	dichloromethane
$ClCH_2CN$	chloroacetonitrile
$Cl_2CHCH_3CH_3$	1,1-dichloropropane
COSY	Correlation Spectroscopy
Cp*	pentamethylcyclopentadiene
CPCM	conductor-like polarizable continuum model
deg.	degassed
D	Deuterium
2D	two-dimensional
DBU	1,8-diazabicyclo[5.4.0]undec-7-ene
DFT	density functional theory
DIBAL-H	diisobutylaluminium hydride
dist.	distilled
DMAP	4-dimethylaminopyridine
DMF	*N,N*-dimethylformamide
DMP	Dess-Martin periodinane
DMPU	*N,N'*-dimethylpropyleneurea
DMSO	dimethyl sulfoxide
dppf	1,1'-bis(diphenylphosphino)ferrocene
dr	diastereomeric ratio
E	entgegen, German word for "opposite"
E.	*Euphorbia*
ee	enantiomeric excess
ESI	electron spray ionisation
equiv	equivalents
Et	ethyl
Et_2O	diethyl ether
GC	gas chromatography
gem	geminal
GIAO	Gauge-independent atomic orbitals
GGPP	geranylgeranyl pyrophosphate
h	hours
HFIP	hexafluoro-2-propanol

HMBC	Heteronuclear Multiple Bond Correlation
HMG-CoA	β-Hydroxy β-methylglutaryl-CoA
HMQC	Heteronuclear Multiple Quantum Coherence
HPLC	High Performance Liquid Chromatography
HSQC	Heteronuclear single quantum coherence spectroscopy
Hz	hertz
IR	infrared
J	NMR coupling constant
L	neutral ligand
LC	liquid chromatography
lit.	literature
LLS	longest linear sequence
M	metal
M	molar/moles
Me	methyl
MeCN	acetonitrile
MeOH	methanol
MEPY	methyl 2-pyrrolidone-5-carboxylate
mp	melting point
MS	mass spectroscopy or molecular sieves
m/z	mass to charge ratio
n	normal-form (unbranched chain)
NBS	*N*-bromosuccinimide
NIS	*N*-iodosuccinimide
nm	nanometre
NMO	4-methylmorpholine 4-oxide
NMR	nuclear magnetic resonance
nOe	Nuclear Overhauser Exchange
NOESY	Nuclear Overhauser Exchange Spectroscopy
Nu	nucleophile
OPP	pyrophosphate
p	*para*
PCC	pyridinium chlorochromate
PCM	dielectric polarisable continuum model
PG	protecting group
Ph	phenyl
Pin	pinacolato
pKa	acid dissociation constant
PKC	protein kinase C
ppm	parts per million
PPTS	pyridinium *p*-toluenesulfonate
*i*Pr	*iso*-propyl
R	any group
RCAM	ring-closing alkyne metathesis
RCM	ring-closing alkene metathesis
RMSD	root-mean-square deviation of atomic positions
RT	room temperature

S	substrate
SM	starting material
sp.	specie
t or *tert*	tertiary
T	tritium
TADDOL	α,α,α',α'-tetraaryl-2,2-disubstituted 1,3-dioxolane-4,5-dimethanol
TBDPS	*tert*-butyldiphenylsilyl
TBAF	tetra-*n*-butylammonium fluoride
TBS	*tert*-butyldimethylsilyl
TC	thiophene-2-carboxylate
TFA	trifluoroacetic acid
THF	tetrahydrofuran
TIPS	triisopropylsilyl
TLC	thin layer chromatography
TMS	trimethylsilyl
t_R	retention time
Tr or Trityl	triphenylmethyl
Ts	tosyl
X-ray	X-radiation
Z	zusammen, German word for "together"

G APPENDIX

1 NATURAL OCCURRING CASBANE DITERPENES

Table 41. Casbane diterpenes

Name (*Isolation Organism*)	Structure	Citation of first isolation
(−)-casbene[29–31] (seedlings of castor bean, *Ricinus communis* L.)		D. R. Robinson *et al. Biochemistry* **1970**, *9*, 70−79. D. R. Robinson *et al. Biochemistry* **1970**, *9*, 80−89. D. Sitton *et al. Phytochemistry* **1975**, *14*, 1921−1925.
2-*epi*-10-hydroxydepressin[4] (*Sinularia depressa*)		C.-S. S. Jiang *et al. Chin. J. Nat. Med.* **2014**, *12*, 853−856.
sinularcasbane A[7] (*Sinularia* sp.)		J. Yin *et al. Mar. Drugs* **2013**, *11*, 455−465.
sinularcasbane B[7] (*Sinularia* sp.)		J. Yin *et al. Mar. Drugs* **2013**, *11*, 455−465.
sinularcasbane C[7] (*Sinularia* sp.)		J. Yin *et al. Mar. Drugs* **2013**, *11*, 455−465.
sinularcasbane D[7] (*Sinularia* sp.)		J. Yin *et al. Mar. Drugs* **2013**, *11*, 455−465.
sinularcasbane E[7] (*Sinularia* sp.)		J. Yin *et al. Mar. Drugs* **2013**, *11*, 455−465.
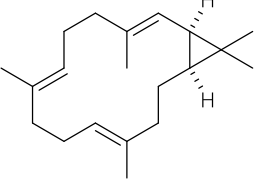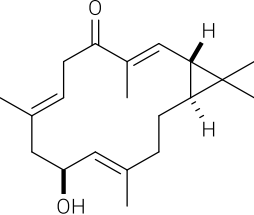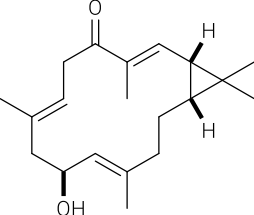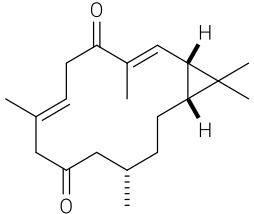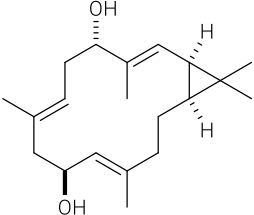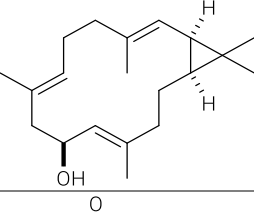
sinularcasbane F[7] (*Sinularia* sp.)		J. Yin *et al. Mar. Drugs* **2013**, *11*, 455–465.
sinularcasbane G[5] (*Sinularia* sp.)		B. Yang *et al. Helv. Chim. Acta* **2015**, *98*, 834–841.
sinularcasbane H[5] (*Sinularia* sp.)		B. Yang *et al. Helv. Chim. Acta* **2015**, *98*, 834–841.
sinularcasbane I[5] (*Sinularia* sp.)		B. Yang *et al. Helv. Chim. Acta* **2015**, *98*, 834–841.
sinularcasbane J[5] (*Sinularia* sp.)		B. Yang, J. Huang, X. Lin, S. Liao, X. Zhou, J. Liu, J. Wang, L. Wang, Y. Liu, *Helv. Chim. Acta* **2015**, *98*, 834–841.
sinularcasbane K[5] (*Sinularia* sp.)		B. Yang *et al. Helv. Chim. Acta* **2015**, *98*, 834–841.
sinularcasbane L[5] (*Sinularia* sp.)		B. Yang *et al. Helv. Chim. Acta* **2015**, *98*, 834–841.
sinularcasbane M[9] (*Sinularia polydactyla*)		M. E. F. Hegazy *et al. Molecules* **2016**, *21*, 308.
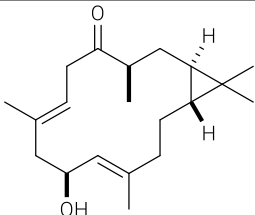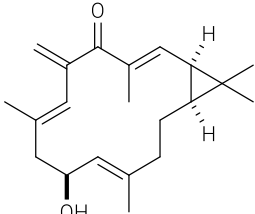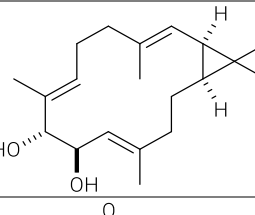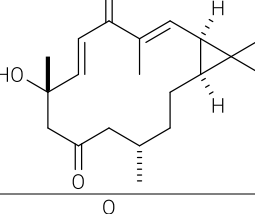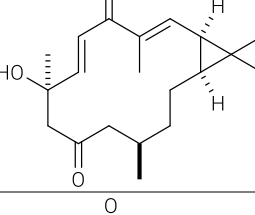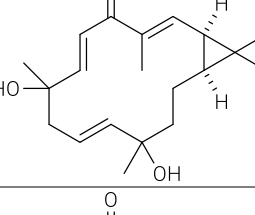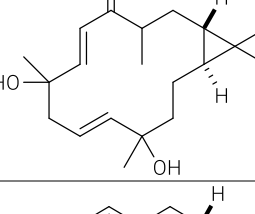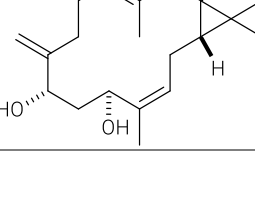
sinularcasbane N[9] (*Sinularia polydactyla*)		M. E. F. Hegazy *et al. Molecules* **2016**, *21*, 308.
depressin[6] (*Sinularia depressa*)		Y. Li *et al. J. Nat. Prod.* **2010**, *73*, 133−138.
1-*epi*-depressin[6] (*Sinularia depressa*)		Y. Li *et al. J. Nat. Prod.* **2010**, *73*, 133−138.
10-hydroxydepressin[6] (*Sinularia depressa*)		Y. Li *et al. J. Nat. Prod.* **2010**, *73*, 133−138.
1-*epi*-10-hydroxydepressin[6] (*Sinularia depressa*)		Y. Li *et al. J. Nat. Prod.* **2010**, *73*, 133−138.
1-*epi*-10-oxodepressin[6] (*Sinularia depressa*)		Y. Li *et al. J. Nat. Prod.* **2010**, *73*, 133−138.
10-oxo-11,12-dihydrodepressin[6] (*Sinularia depressa*)		Y. Li *et al. J. Nat. Prod.* **2010**, *73*, 133−138.
1-*epi*-10-oxo-11,12-dihydrodepressin[6] (*Sinularia depressa*)		Y. Li *et al. J. Nat. Prod.* **2010**, *73*, 133−138.
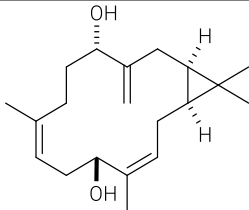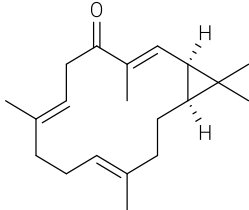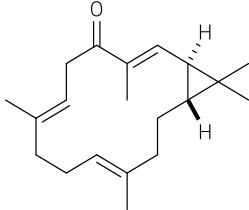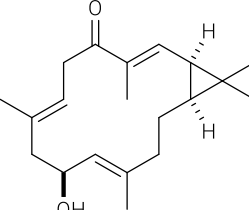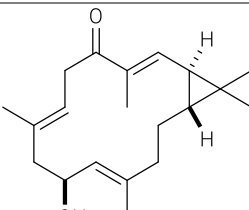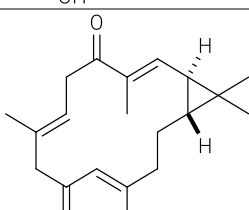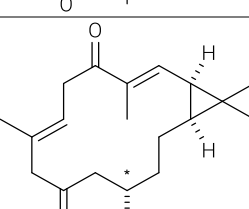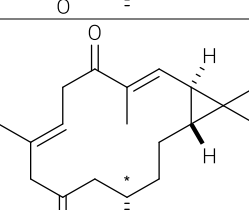
2-*epi*-10-oxo-11,12-dihydrodepressin[6] (*Sinularia depressa*)		Y. Li *et al. J. Nat. Prod.* **2010**, *73*, 133–138.
8,10-dihydroxy-*iso*-depressin[6] (*Sinularia depressa*)		Y. Li *et al. J. Nat. Prod.* **2010**, *73*, 133–138.
10-oxodepressin[6] (DMP-Oxidation product of 10-hydroxydepressin)		Y. Li *et al. J. Nat. Prod.* **2010**, *73*, 133–138.
Sinuereperoxide A[8] (*Sinularia erecta*)		J. Liu *et al. J. Org. Chem.* **2020**, DOI 10.1021/acs.joc.0c02397.
10-oxo-3,4,11,12-Tetrahydrodepressin[8] (*Sinularia erecta*)		J. Liu *et al. J. Org. Chem.* **2020**, DOI 10.1021/acs.joc.0c02397.
10-oxo-11,12-dihydrodepressin[8] (*Sinularia erecta*)		J. Liu *et al. J. Org. Chem.* **2020**, DOI 10.1021/acs.joc.0c02397.
microclavatin[59] (*Sinularia microclavata*)		C. X. Zhang *et al. J. Nat. Prod.* **2005**, *68*, 1087–1089.
yuexiandajisu A[12] (*Euphorbia ebracteolata*)		Z. H. Xu *et al. Phytochemistry* **1998**, *49*, 149–151. Biological acitivity: K. Wang *et al. Molecules* **2017**, *22*, 465.

(+)-yuexiandajisu A[38] (determined absolute structure by total synthesis)		L. E. Löffler *et al. Angew. Chem. Int. Ed.* **2021**, *60*, 5316–5322.
yuexiandajisu B[12] (*Euphorbia ebracteolata*)		Z. H. Xu *et al. Phytochemistry* **1998**, *49*, 149–151.
pekinenin A[13] (*Euphorbia pekinensis*)		F. G. Shao *et al. J. Asian Nat. Prod. Res.* **2011**, *13*, 805–810.
pekinenin B[13] (*Euphorbia pekinensis*)		F. G. Shao *et al. J. Asian Nat. Prod. Res.* **2011**, *13*, 805–810.
pekinenin C[16] (*Euphorbia pekinensis*)		W. W. Tao *et al. Phytochemistry* **2013**, *94*, 249–253. Biological acitivity: K. Wang *et al. Molecules* **2017**, *22*, 465. Y. Cao *et al. Int. J. Mol. Sci.* **2016**, *17*, 850–812.
pekinenin D[16] (*Euphorbia pekinensis*)		W. W. Tao *et al. Phytochemistry* **2013**, *94*, 249–253.
pekinenin E[16] (*Euphorbia pekinensis*)		W. W. Tao *et al. Phytochemistry* **2013**, *94*, 249–253. Biological Activity: L. Fan *et al. Front. Pharmacol.* **2017**, *8*:424.
pekinenin F[16] (*Euphorbia pekinensis*)		W. W. Tao *et al. Phytochemistry* **2013**, *94*, 249–253.

pekinenin G[17] (*Euphorbia pekinensis*)		K. Wang *et al. Nat. Prod. Res.* **2015**, *29*, 1456−1460.
euphpekinensin[34] or **pekinenal (euphpekinin)**[15] (*Euphorbia pekinensis*)		L. Y. Kong *et al. Planta Med.* **2002**, *68*, 249−252. Q.-L. L. Liang *et al. Fitoterapia* **2009**, *80*, 514−516.
euphorhylonal A[26] (*Euphorbia hylonoma* Hand-Mazz and *E. wangii* Oudejans)		H. Chen *et al. Indian J. Chem. - Sect. B Org. Med. Chem.* **1996**, *35*, 1308−1310.
euphorhylonal A[38] (revised absolute structure by total synthesis)		L. E. Löffler *et al. Angew. Chem. Int. Ed.* **2021**, *60*, 5316−5322.
***ent*-10-oxodepressin**[28] (*Oryza sativa* cv. Koshihikari)		Y. Inoue *et al. Biosci. Biotechnol. Biochem.* **2013**, *77*, 760−765.
5-dihydro-ent-10-oxodepresssin[27] (*Oryza sativa* cv. Koshihikari)		K. Horie *et al. Phytochem. Lett.* **2016**, *15*, 57−62.
5-deoxo-ent-10-oxodepressin[27] (*Oryza sativa* cv. Koshihikari)		K. Horie *et al. Phytochem. Lett.* **2016**, *15*, 57−62.
casbene diterpenoid[295] (*Croton nepetaefolius* Baill)		V. L. A. Moura *et al. J. Nat. Prod.* **1990**, *53*, 1566−1571. Biological Activity: N. C. Sá *et al. Arch. Oral Biol.* **2012**, *57*, 550−555. M. A. Vasconcelos *et al. Ind. Crops Prod.* **2014**, *61*, 499−509. V. A. Carneiro *et al. Molecules* **2011**, *16*, 190−201.
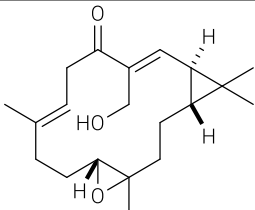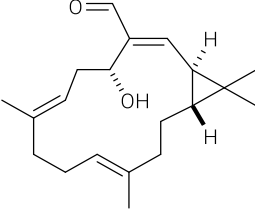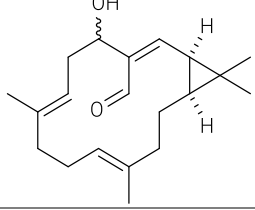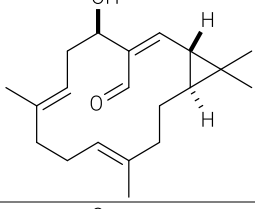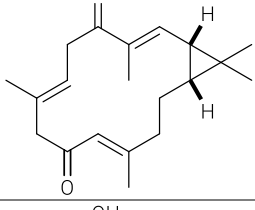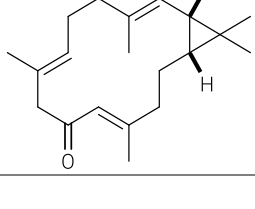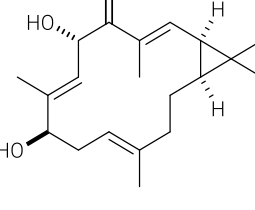
casbene diterpenoid acetate[295] (synthesised for characterisation of casbene diterpenoid)		V. L. A. Moura *et al. J. Nat. Prod.* **1990**, *53*, 1566–1571.
(2*E*,5β,6*E*,12*E*)-5-hydroxycasba-2,6,12-trien-4-one[296] (*Croton argyrophyllus*)		F. A. E Silva Filho *et al. Helv. Chim. Acta* **2013**, *96*, 1146–1154.
1-hydroxy-(2*E*,6*Z*,12*E*)-casba-2,6,12-triene-4,5-dione[297] (*Croton argyrophyllus* Muell.)		F. A. E. Silva-Filho *et al. Magn. Reson. Chem.* **2011**, *49*, 370–373.
6*E*,12*E*-casba-1,3,6,12-tetraen-1,4-epoxy-5-one[297] (*Croton argyrophyllus* Muell.)		F. A. E. Silva-Filho *et al. Magn. Reson. Chem.* **2011**, *49*, 370–373.
crotonitenone[187] (*Croton nitens* Sw.)		B. A. Burke *et al. J. Chem. Soc. Trans. 1* **1981**, 2666–2669.
crotonitenone acetate[187] (synthesised for characterization of crotonitenone)		B. A. Burke *et al. J. Chem. Soc. Trans. 1* **1981**, 2666–2669.
6-oxo-crotonitenone[187] (synthesised for characterisation of crotonitenone)		B. A. Burke *et al. J. Chem. Soc. Trans. 1* **1981**, 2666–2669.
EBC-131[21] (*Croton insularis*)		L. A. Maslovskaya *et al. Angew. Chem. Int. Ed.* **2014**, *53*, 7006–7009. L. A. Maslovskaya *et al. Chem. Eur. J.* **2019**, *25*, 1525–1534.
EBC-180[21] (*Croton insularis* Baill)		L. A. Maslovskaya *et al. Angew. Chem. Int. Ed.* **2014**, *53*, 7006–7009. L. A. Maslovskaya *et al. Chem. Eur. J.* **2019**, *25*, 1525–1534.
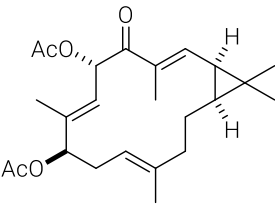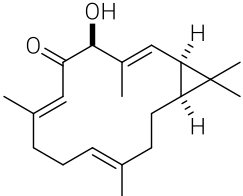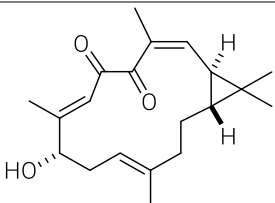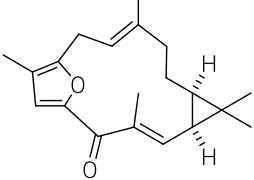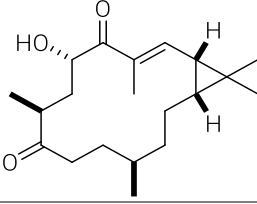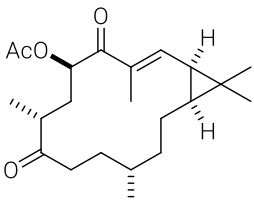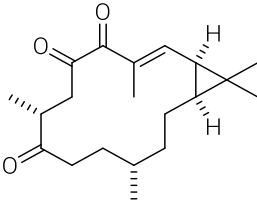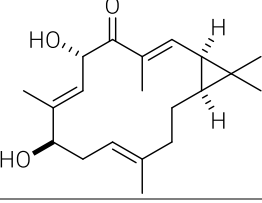
EBC-181[21] (*Croton insularis* Baill)		L. A. Maslovskaya *et al Angew. Chem. Int. Ed.* **2014**, *53*, 7006–7009. L. A. Maslovskaya *et al Chem. Eur. J.* **2019**, *25*, 1525–1534.
EBC-182[23] (*Croton insularis*)		L. A. Maslovskaya *et al. Chem. Eur. J.* **2019**, *25*, 1525–1534.
EBC-217[23] (*Croton insularis*)		L. A. Maslovskaya *et al. Chem. Eur. J.* **2019**, *25*, 1525–1534.
EBC-218[23] (*Croton insularis*)		L. A. Maslovskaya *et al. Chem. Eur. J.* **2019**, *25*, 1525–1534.
EBC-220[23] (*Croton insularis*)		L. A. Maslovskaya *et al. Chem. Eur. J.* **2019**, *25*, 1525–1534.
EBC-304[22] (*Croton insularis*)		L. A. Maslovskaya *et al. Chem. Eur. J.* **2017**, *23*, 537–540.
EBC-320[22] (*Croton insularis*)		L. A. Maslovskaya *et al. Chem. Eur. J.* **2017**, *23*, 537–540.
EBC-324[20] (*Croton insularis*)		L. A. Maslovskaya *et al. Chem. Commun.* **2014**, *50*, 12315–12317.
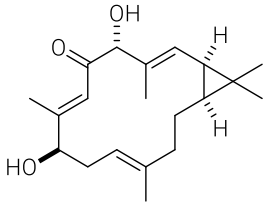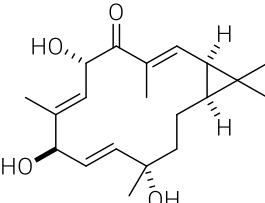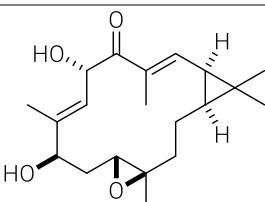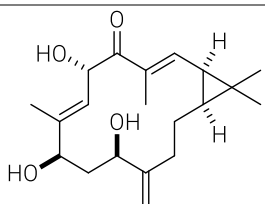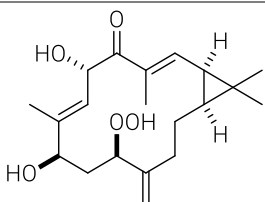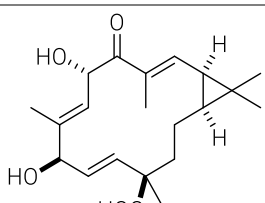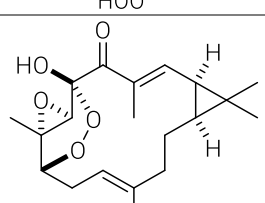
Compound	Structure	Reference
EBC-342[24] (*Croton insularis*)		L. A. Maslovskaya *et al. Eur. J. Org. Chem.* **2020**, *2020*, 1042–1045.
EBC-343[23] (*Croton insularis*)		L. A. Maslovskaya *et al. Chem. Eur. J.* **2019**, *25*, 1525–1534.
EBC-357[23] (*Croton insularis*)		L. A. Maslovskaya *et al. Chem. Eur. J.* **2019**, *25*, 1525–1534.
EBC-361[23] (*Croton insularis*)		L. A. Maslovskaya *et al. Chem. Eur. J.* **2019**, *25*, 1525–1534.
EBC-365[23] (*Croton insularis*)		L. A. Maslovskaya *et al. Chem. Eur. J.* **2019**, *25*, 1525–1534.
EBC-373[23] (*Croton insularis*)		L. A. Maslovskaya *et al. Chem. Eur. J.* **2019**, *25*, 1525–1534.
koumbalones A[36] (*Maprounea africana* Muell. Arg.)		Y. Kashman *et al. J. Nat. Prod.* **1994**, *57*, 426–430.
koumbalones B[36] (*Maprounea africana* Muell. Arg.)		Y. Kashman *et al. J. Nat. Prod.* **1994**, *57*, 426–430.
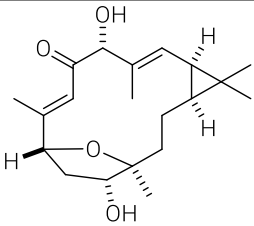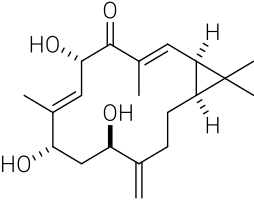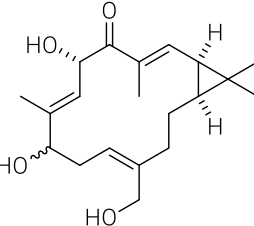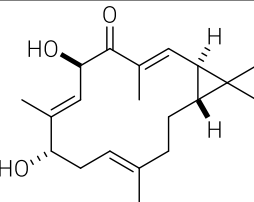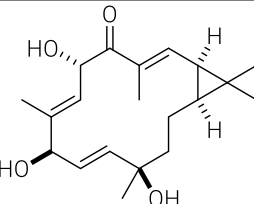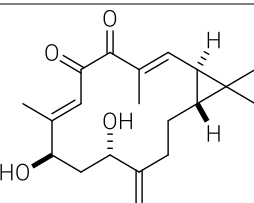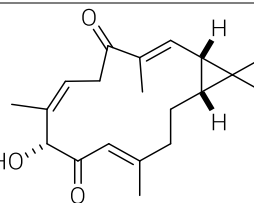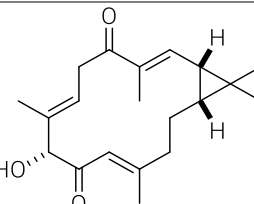
hookerianolide A[33] (*Mallotus Hookerianus*)		Y. Bai *et al. Tetrahedron Lett.* **2006**, *47*, 6637–6640.
hookerianolide B[33] (*Mallotus Hookerianus*)		Y. Bai *et al. Tetrahedron Lett.* **2006**, *47*, 6637–6640.
hookerianolide C[33] (*Mallotus Hookerianus*)		Y. Bai *et al. Tetrahedron Lett.* **2006**, *47*, 6637–6640.
agrostistachin[35] (*Agrostistachys hookeri* Benth. & Hook. f.)		Y. H. Choi *et al. Tetrahedron Lett.* **1986**, *27*, 5795–5798. Biological activity: Y. H. Choi *et al. J. Nat. Prod.* **1988**, *51*, 110–116.
agrostistachin[35] (*Agrostistachys hookeri* Benth. & Hook. f.)		Y. H. Choi *et al. Tetrahedron Lett.* **1986**, *27*, 5795–5798.
agrostistachin diacetate[35] (synthesised for characterisation of agrostistachin)		Y. H. Choi *et al. Tetrahedron Lett.* **1986**, *27*, 5795–5798.
14-dehydroxy- **agrostistachin**[37] (*Agrostistachys hookeri* Benth. & Hook. f.)		Y. H. Choi *et al. J. Nat. Prod.* **1988**, *51*, 110–116.
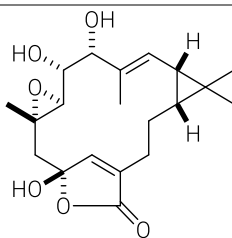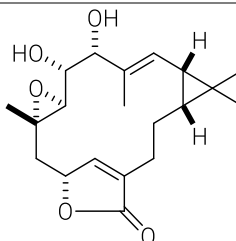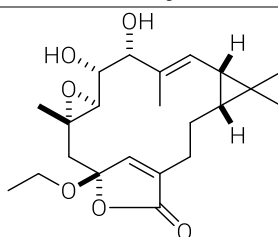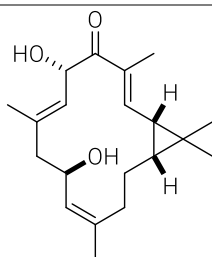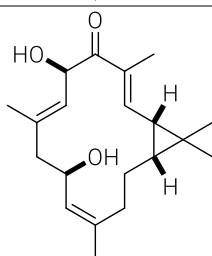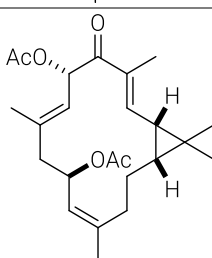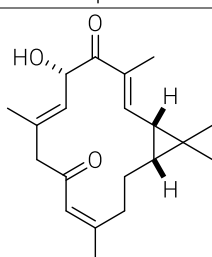
14-dehydroxy-agrostistachin acetate[37] (synthesised for characterisation of 14-dehydro-agrostistachin)		Y. H. Choi *et al. J. Nat. Prod.* **1988**, *51*, 110−116.
17-hydroxy-agrostistachin[37] (*Agrostistachys hookeri* Benth. & Hook. f.)		Y. H. Choi *et al. J. Nat. Prod.* **1988**, *51*, 110−116.
17-hydroxy-agrostistachin triacetate[37] (synthesised for characterisation of 17-dehydro-agrostistachin)		Y. H. Choi *et al. J. Nat. Prod.* **1988**, *51*, 110−116.
agroskerin[37] (*Agrostistachys hookeri* Benth. & Hook. f.)		Y. H. Choi *et al. J. Nat. Prod.* **1988**, *51*, 110−116.
agroskerin acetate[37] (synthesised for characterization of agroskerin)		Y. H. Choi *et al. J. Nat. Prod.* **1988**, *51*, 110−116.
sapidisin A[32] (*Sapium discolor*)		H.-B. Liu *et al. J. Asian Nat. Prod. Res.* **2015**, *17*, 1117−1128.
sapidisin B[32] (*Sapium discolor*)		H.-B. Liu *et al. J. Asian Nat. Prod. Res.* **2015**, *17*, 1117−1128.
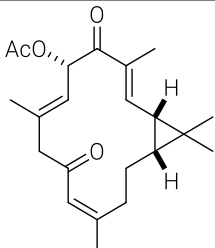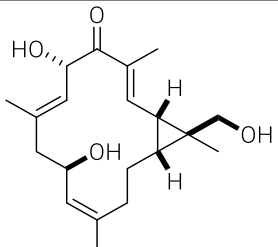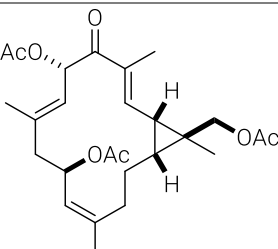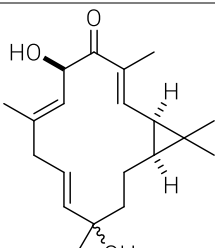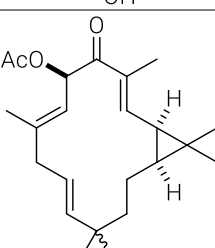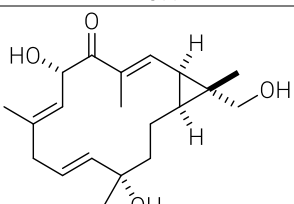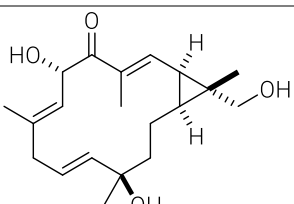
sapidisin C[32] (*Sapium discolor*)		H.-B. Liu *et al. J. Asian Nat. Prod. Res.* **2015**, *17*, 1117−1128.
No name[10] (*Lobophytum* sp.)		P. K. Roy *et al. Molecules* **2016**, *21*, 1−9.
8,12-dihydroxy-1βH,2αH-casba-3*E*,7*E*,11*E*-trien-5-one[298] (*Euphorbia rapulum*)		X. X. Liu *et al. Chem. Nat. Compd.* **2018**, *54*, 910−912
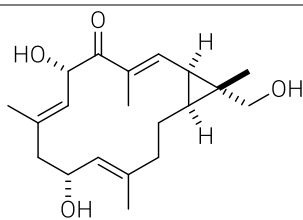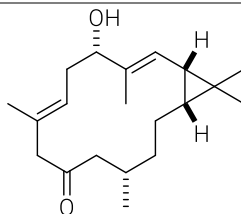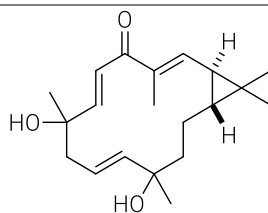
* tentatively assigned

2 ENZYMATIC SYNTHESISED CASBANE DITERPENES

Table 42. Enzymatic synthesized casbane diterpenes.

Name	Structure	Citation
9-ketocasbene[48]		D. Luo *et al. Proc. Natl. Acad. Sci.* **2016**, *113*, E5082−E5089.
5-hydroxy-casbene[48]		D. Luo *et al. Proc. Natl. Acad. Sci.* **2016**, *113*, E5082−E5089.
5-hydroxy-9-ketocasbene[48]		D. Luo *et al. Proc. Natl. Acad. Sci.* **2016**, *113*, E5082−E5089.
9-hydroxy-casbene[48]		D. Luo *et al. Proc. Natl. Acad. Sci.* **2016**, *113*, E5082−E5089.
5-keto-6,9-casbene diol[48]		D. Luo *et al. Proc. Natl. Acad. Sci.* **2016**, *113*, E5082−E5089.
6-keto-5,9-casbene diol[48]		D. Luo *et al. Proc. Natl. Acad. Sci.* **2016**, *113*, E5082−E5089.
5,9-diketo-casbene[48]		D. Luo *et al. Proc. Natl. Acad. Sci.* **2016**, *113*, E5082−E5089.
sinularcasbane D[299]		C. Görner *et al. Microb. Cell Fact.* **2016**, *15*, 86.
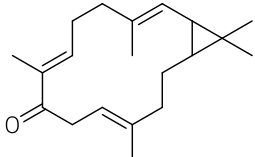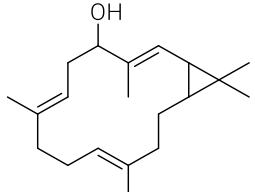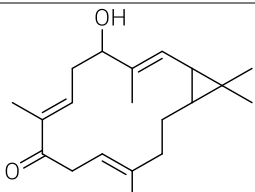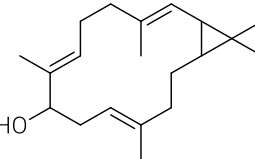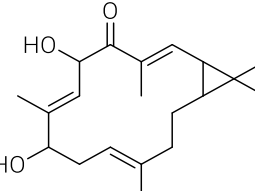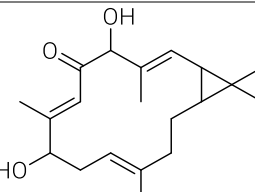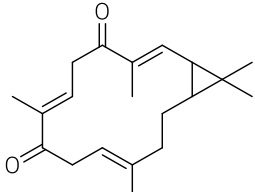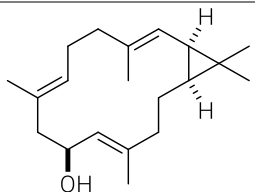
3 SYNTHESISED CASBANE DITERPENES

Table 43. Casbane diterpenes by classic total synthesis.

Name	Structure	Citation
(−)-casbene		See chapter 2.3
ent-depressin		See chapter 2.6.3
1*S*,2*R*,5*S*-aldeyhde		L. E. Löffler *et al. Angew. Chem. Int. Ed.* **2021**, *60*, 5316−5322. (see chapter 3.10)
1*S*,2*R*,5*R*-aldeyhde		L. E. Löffler *et al. Angew. Chem. Int. Ed.* **2021**, *60*, 5316−5322. (see chapter 3.10)
1*S*,2*S*,5*S*-aldeyhde		L. E. Löffler *et al. Angew. Chem. Int. Ed.* **2021**, *60*, 5316−5322. (see chapter 3.10)
2-*epi*-depressin (enantiomer of the natural product 1-*epi*-depressin)		See chapter 3.12
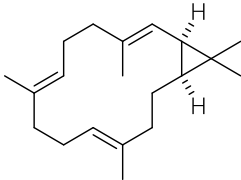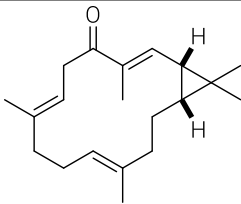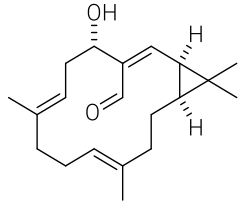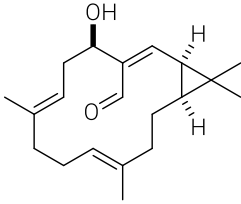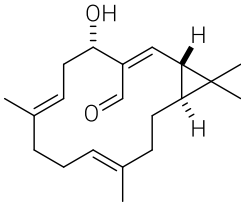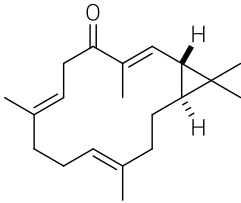
4 LOCALITY AND ORGANISM OF CASBANE DITERPENES

Table 44. Locality of casbane diterpenes producing organisms.

Source	Locality	Casbane diterpene
Soft coral		
Alcyoniidae		
Kingdom: Animalia; Phylum: Cnidaria; Class: Anthozoa; Order: Alcyonacea; Family: Alcyoniidae		
Sinularia sp.	Soft coral, coast of Ximao island, Hainan province, China, South China Sea	sinularcasbanes A−F[7]
Sinularia sp.	Soft coral, coast of Dongluo Island, Hainan Province, China, South China Sea	sinularcasbanes G-L[5]
Sinularia polydactyla	Soft coral, coast of Hurghada, Egypt, Red Sea	sinularcasbane M, N, O[9]
Sinularia microclavata	Soft coral, Bay of Sanya, Hainan Island, China, South China Sea	microclavatin[59]
Sinularia erecta	Soft coral, coast of Ximao Island, Hainan province, China, South China Sea	sinuereperoxide A[8], 10-oxo-3,4,11,12-Tetrahydrodepressin[8], 10-oxo-11,12-dihydrodepressin[8]
Sinularia depressa	Soft coral, Specimens of *S. depressa*, Lingshui Bay, Hainan Province, China, South China Sea	depressin[6], 1-*epi*-depressin[6], 10-hydroxydepressin[6], 1-*epi*-10-hydroxydepressin[6], 10-oxo-11,12-dihydroxydepressin[6], 1-*epi*-10-oxo-11,12-dihydrodepressin[6], 1-*epi*-10-oxodepressin[6], 2-*epi*-10-oxo-11,12-dihydrodepressin[6], 8,10-dihydroxy-iso-depressin[6], 2-*epi*-10-hydroxydepressin[4]

Lobophytum sp.	Soft coral, coast of Irabu Island, Okinawa, Japan, East China Sea	No name[10]	

Plants

Euphorbiaceae

Kingdom: *Plantae*; Clade: *Tracheophytes*; Clade: *Angiosperms*; Clade: *Eudicots*; Clade: *Rosids*; Order: *Malpighiales*; Family: *Euphorbiaceae*;

Agrostistachys hookeri Benth. & Hook. f.	Plant, Twigs of *A. Hookeri*, Sri Lanka.	agrostistachin[35], 14-dehydroagrostistachin[37], 17-hydroxyagrostistachin[37], agroskerin[37]	
S*apium discolor*, Also named as *Triadica cochinchinensis*	Plant, Twigs and leaves of *S. discolor*, Jianfengling, Hainan Island, China	sapidisin A[32], sapidisin B[32], sapidisin C[32]	
Ricinus communis L.	seedlings of castor bean	(−)-casbene[30,31]	Subfamily: *Acalyphoideae*; Tribe: *Acalypheae*; Subtribe: *Ricininae*; Genus: *Ricinus* L.

Euphorbioideae

Kingdom: *Plantae*; Clade: *Tracheophytes*; Clade: *Angiosperms*; Clade: *Eudicots*; Clade: *Rosids*; Order: *Malpighiales*; Family: *Euphorbiaceae*; Subfamily: *Euphorbioideae*; Tribe: *Euphorbieae*

Euphorbia ebracteolata Hayata	Plant, roots of *E. ebracteolata*, Hayata, Anhui Province, China	yuexiandajisu A[12], yuexiandajisu B[12]	
Euphorbia jolkinii	Plant, roots of *E. jolkinii* (or *E. nematocypha*), Zhongdian county, Yunnan province, China	pikenal[19], pekinenin A[19], pekinenin D[19]	
Euphorbia pekinensis	Plant, Roots of *E. pekinensis*, Yulin City, Guangxi Province, China	pekinenin A-B[16]	
Euphorbia pekinensis	Plant, Roots of *E. pekinensis*, Nanning City,	pekinenin C-F[16]	

	Guangxi Province, China		
Euphorbia pekinensis	Plant, Roots of *E. pekinensis*, Anguo, China (Anguo Chinese Herbal Medicine Factory)	pekinenin G[17]	
	Plant, Roots of E. *pekinensis*, suburbs of Nanjing, Jiangsu, China	euphpekinensin[34] pekinenal[15]	
Euphorbia rapulum	Whole plant, *Euphorbia rapulum*, Ili Kazakh, Xinjiang, China	8,12-dihydroxy-1βH,2αH-casba-3*E*,7*E*,11*E*-trien-5-one[298]	
Maprounea africana Muell. Arg.	Plant, roots of *M. africana* Muell. Arg., near Camp Koumbala, Central African Republic	koumbalones A[36], koumbalones B[36]	Tribe: *Hippomaneae*; Subtribe: *Hippomaninae*; Genus: *Maprounea*

Crotonoideae

Kingdom: *Plantae*; Clade: *Tracheophytes*; Clade: *Angiosperms*; Clade: *Eudicots*; Clade: *Rosids*; Order: *Malpighiales*; Family: *Euphorbiaceae*; Genus: *Croton*			
Croton nepetaefolius, Also known as *Croton nepetifolius*	Plant, *C. nepetaefolius* Baill, Cocalzinho-Viçosa- Ceará, Brazil	casbene diterpenoid[295],	
Croton nepetaefolius	Plant, *C. nepetaefolius*, Caucaia, Ceará, Brazil	CD[57], CD1CN[58]	
Croton argyrophyllus	Plant, stems and roots of *C. argyrophyllus* Mull., Jacobina County, Bahia State, Northeast of Brazil	(2*E*,5b,6*E*,12*E*)-5-hydroxycasba-2,6,12-trien-4-one[296]	
Croton argyrophyllus	Plant, the aerial parts of *C. argyrophyllus* Muell. Jacobina	1-hydroxy-(2*E*,6*Z*,12*E*)-casba-2,6,12-triene-4,5-dione[297],	

	County, Bahia State, Northeast of Brazil	6*E*,12*E*-casba-1,3,6,12-tetraen-1,4- epoxy-5-one[297]	
Croton nitens	Plant, milled leaves and twigs of *C. nitens* Sw. (*C. nitens* is the Jamaican variety of *C. eluteria* L.)	crotonitenone[187]	
Croton insularis	Plant, stems of *C. insularis* Baill., Yungaburra, north Queensland. Natural population of the species: semi-deciduous vine forest at Iron Range, Queensland.	EBC-131[21,23], EBC-180[21,23], EBC-181[21,23], EBC-182[23], EBC-217[23], EBC-218[23], EBC-220[23], EBC-304[22], EBC-320[22], EBC-324[20], EBC-342[24], EBC-343[23], EBC-357[23], EBC-361[23], EBC-365[23], EBC-373[23]	EBC = EcoBiotics Compound (EcoBiotics Ltd., Yungaburra, Australia, www.ecobiotics.com.au)

Acalyphoideae

Kingdom: *Plantae*; Clade: *Tracheophytes*; Clade: *Angiosperms*; Clade: *Eudicots*; Clade: *Rosids*; Order: Malpighiales; Family: *Euphorbiaceae*; Subfamily: *Acalyphoideae;* Tribe: *Acalypheae*; Subtribe: *Rottlerinae*; Genus: *Mallotus*

Mallotus Hookerianus Muell. Arg.	Plant powder, Hainan Province, China	hookerianolide A[33], hookerianolide B[33], hookerianolide C[33]

Asian Rice Plant

Kingdom: *Plantae*; Clade: *Tracheophytes*; Clade: *Angiosperms*; Clade: *Monocots*; Clade: *Commelinids*; Order: *Poales*; Family: *Poaceae*; Genus: *Oryza*

Oryza sativa	*ent*-10-oxodepressin[28], 5-dihydro-ent-10-oxodepresssin[27], 5-deoxo-ent-10-oxodepressin[27]

5 CARTESIAN COORDINATES AND ELECTRONIC ENERGIES

5.1 GEOMETRICALLY OPTIMISED STRUCTURES FOR THE STRUCTURE ELUCIDATION

Cartesian coordinates (in Å), electronic energies (in a.u.), and the Gibbs free energies for the structure elucidation of euphorhylonal A. Calculations reported at the B3LYP-D3BJ-(CPCM)/def2-TZVP level.

Optimised geometries of 1*S*,2*R*,5*S*-151 conformers

52
Coordinates from ORCA-job conformer 010
Single point energy: -930.428372603381
Gibbs free energy: -930.01903839

C	-3.01468535	-0.91087902	0.57671206
C	-1.96481813	-1.91839471	0.9350997
C	-1.26853565	-2.70230188	0.10660308
C	-1.38755111	-2.65269128	-1.39182242
H	-1.4500605	-3.66228099	-1.80781632
H	-0.50383372	-2.18440363	-1.83332082
H	-2.25560159	-2.08982402	-1.72735403
C	-0.34018609	-3.75983728	0.6508182
C	1.10627331	-3.72091526	0.11829907
C	1.92246378	-2.58662388	0.65808152
C	2.49496396	-1.57657368	-0.00409213
C	2.38653174	-1.37902647	-1.49234651
H	1.93183807	-2.22904273	-1.99643181
H	3.37688877	-1.21601129	-1.92680589
H	1.79103863	-0.49514147	-1.72896855
C	3.36058734	-0.5854049	0.74536585
H	4.26418691	-0.39228185	0.15598909
H	3.68846284	-1.04461609	1.68040629
C	2.72041999	0.76792163	1.09789407
C	2.33318046	1.60415669	-0.10148486
C	1.71187424	2.95520131	0.00223677
C	2.12523546	4.00101077	-1.0094881
H	1.32604744	4.73092169	-1.16352192

204

52
Coordinates from ORCA-job conformer 001
Single point energy: -930.4278610745
Gibbs free energy: -930.01880363

H	3.0090006	4.54069662	-0.65711206
H	2.36614196	3.54961039	-1.97319805
C	1.36296686	3.53743225	1.3544787
H	1.1281384	2.78293922	2.10202498
H	0.50671323	4.21132172	1.2732946
H	2.20928129	4.11904038	1.72893584
C	0.88509061	1.78384287	-0.57355672
C	-0.24158506	1.26974433	0.18400268
C	-1.48782879	0.96744364	-0.24720062
C	-1.86177453	1.08381717	-1.64727243
O	-3.00719343	0.95140204	-2.06644134
H	-1.05352941	1.30510116	-2.36125425
C	-2.56278958	0.55155577	0.73704097
H	-2.16727786	0.68138395	1.74632536
O	-3.68920978	1.43496861	0.65618723
H	-4.00492387	1.3826381	-0.25874278
H	-0.08084008	1.15830561	1.25049333
H	0.76407413	1.83053716	-1.64613831
H	3.02444364	1.49965496	-0.93151451
H	1.8681366	0.59120701	1.7546736
H	3.44869033	1.33148282	1.69055606
H	2.08198699	-2.62523916	1.73471325
H	1.58606106	-4.65812954	0.42194721
H	1.09554588	-3.72390863	-0.97111569
H	-0.75950879	-4.73874061	0.38765009
H	-0.32461979	-3.70674888	1.74236562
H	-1.77794026	-2.02870648	2.0010535
H	-3.38162419	-1.05329147	-0.43899519
H	-3.87058727	-1.03606277	1.24694553

52
Coordinates from ORCA-job conformer 001
Single point energy: -930.4278610745
Gibbs free energy: -930.01880363

C	3.07322642	0.93656764	1.09171916
C	1.92363972	1.898887	1.09195891
C	1.36455605	2.49278231	0.03318252
C	1.80771036	2.26297905	-1.38544612
H	1.09989803	1.61341029	-1.90992831
H	2.78754278	1.79598465	-1.45185917
H	1.83734161	3.2061273	-1.93785308
C	0.22951476	3.47249501	0.20277294
C	-1.05518239	3.11902801	-0.57371971
C	-1.71717043	1.87198923	-0.06681909
C	-3.01897341	1.6714263	0.15385611
C	-4.08900006	2.69879297	-0.10314729
H	-4.77185004	2.34615032	-0.88304579
H	-3.69540893	3.66301729	-0.41604264
H	-4.69620643	2.85167853	0.79460143

C	-3.57564364	0.37552814	0.69571775
H	-4.36970624	0.03501828	0.01848192
H	-4.09013358	0.60450556	1.63706457
C	-2.61247724	-0.78518623	0.94083741
C	-2.07496404	-1.40465419	-0.33884532
C	-1.50522678	-2.78364064	-0.39138213
C	-1.81416619	-3.63687764	-1.601006
H	-1.92458498	-3.02763371	-2.49942926
H	-1.0190346	-4.36623956	-1.77742902
H	-2.74667001	-4.18792194	-1.44787909
C	-1.33913369	-3.58040027	0.88334552
H	-0.51504162	-4.29094129	0.7845217
H	-2.24947724	-4.15191572	1.0828901
H	-1.14253268	-2.95808919	1.75423202
C	-0.58230913	-1.57920033	-0.65415489
C	0.44232175	-1.21370653	0.30873493
C	1.76197129	-1.0009349	0.10431366
C	2.37530258	-1.20473716	-1.19705087
O	3.5798197	-1.10960895	-1.41157734
H	1.70362849	-1.47948022	-2.02499241
C	2.64626358	-0.53951757	1.24326112
H	2.08242569	-0.64100716	2.17281651
O	3.79416783	-1.37914293	1.40005453
H	4.2486036	-1.37351662	0.54355908
H	0.10754898	-1.09765588	1.33439785
H	-0.32713686	-1.44947028	-1.69611404
H	-2.64328537	-1.12199572	-1.21876911
H	-1.8088235	-0.45563936	1.60195073
H	-3.15991299	-1.54992244	1.49800955
H	-1.03272965	1.05639748	0.13445893
H	-1.73157613	3.97195255	-0.52319263
H	-0.8015376	2.99777048	-1.63289123
H	0.56938289	4.4534213	-0.15023678
H	-0.00893909	3.57844255	1.26387825
H	1.50111273	2.11870046	2.06965316
H	3.6723021	1.0261056	0.1854652
H	3.73303651	1.15334476	1.93638332

52

Coordinates from ORCA-job conformer 007

Single point energy: -930.428338220852

Gibbs free energy: -930.01875519

C	-3.1272258	-0.38023169	-0.75002196
C	-2.5600625	0.9730749	-1.05475575
C	-2.25664292	1.944035	-0.18826777
C	-2.38190254	1.80340612	1.30375935
H	-2.85468649	2.68941686	1.73701582
H	-1.39538705	1.71433421	1.76639499
H	-2.9586435	0.92929371	1.59745385

C	-1.81717398	3.30077655	-0.68057152
C	-0.4946274	3.83234878	-0.09355361
C	0.72547818	3.12913663	-0.60463626
C	1.63970459	2.43501635	0.08003319
C	1.57905233	2.204158	1.56636827
H	2.53602068	2.46083451	2.02948798
H	1.39286578	1.15261553	1.79318713
H	0.80120344	2.79017372	2.05081518
C	2.85437443	1.88346547	-0.63694331
H	3.73941067	2.06185457	-0.01576001
H	3.00118616	2.44661274	-1.56110227
C	2.82173899	0.39129859	-1.00835648
C	2.74816876	-0.54265317	0.17901731
C	2.71989262	-2.0281293	0.05926367
C	3.47217942	-2.83318919	1.09580494
H	4.51128399	-2.97440232	0.78464423
H	3.47413417	-2.33224521	2.06508384
H	3.02279157	-3.82173485	1.22233424
C	2.68750631	-2.68836766	-1.30161784
H	3.71015354	-2.86994053	-1.64225359
H	2.19056426	-2.08839482	-2.06079635
H	2.17868907	-3.65378729	-1.24733656
C	1.47195848	-1.28676865	0.58983108
C	0.26845076	-1.25751394	-0.22186976
C	-1.01066325	-1.50033626	0.14605669
C	-1.3663059	-1.7940596	1.52466959
O	-2.48504746	-2.14361704	1.88707007
H	-0.568364	-1.69181024	2.27628818
C	-2.11620598	-1.53243369	-0.89036734
H	-1.65661278	-1.46924011	-1.87869257
O	-2.79220543	-2.79656837	-0.8687196
H	-3.14389971	-2.89679606	0.02895655
H	0.41772988	-1.06414748	-1.27825306
H	1.3325826	-1.38841048	1.6563322
H	3.30592741	-0.18124573	1.03686039
H	1.9978291	0.22205778	-1.7022454
H	3.73834943	0.1703823	-1.56531768
H	0.88560206	3.2350798	-1.67665629
H	-0.42029743	4.88864286	-0.37576102
H	-0.54230212	3.81092953	0.99461514
H	-2.60270152	4.02047653	-0.41905147
H	-1.74997437	3.28967312	-1.77137753
H	-2.4062767	1.18081056	-2.11134507
H	-3.56393654	-0.4193236	0.24718717
H	-3.93087776	-0.59664087	-1.460268

52

Coordinates from ORCA-job conformer 034

Single point energy: -930.427394770448

Gibbs free energy: -930.01874642

C	2.63633033	0.99416847	-1.27924299
C	2.59742801	-0.32806737	-0.57466556
C	2.73085809	-0.54843235	0.73491517
C	2.97043295	0.53545229	1.74976154
H	3.79015424	0.25675871	2.41876203
H	2.08254167	0.65841422	2.37949905
H	3.20267038	1.50174909	1.30948619
C	2.68308226	-1.93048579	1.35092892
C	1.98448691	-3.04609514	0.5631622
C	0.48681389	-2.98096029	0.63767254
C	-0.4099963	-2.95749499	-0.35167902
C	-0.0598052	-2.94485744	-1.81406704
H	-0.41661861	-3.86090362	-2.29613358
H	1.00922366	-2.86300124	-1.99453193
H	-0.54808261	-2.11459767	-2.33131992
C	-1.88887211	-3.04090558	-0.04897366
H	-2.03027847	-3.29020855	1.00565534
H	-2.29819329	-3.87804506	-0.62606979
C	-2.72906704	-1.79379472	-0.37700826
C	-2.6450662	-0.7067108	0.66920494
C	-3.16363337	0.67718856	0.44154812
C	-3.86839108	1.36725104	1.58801821
H	-3.46902692	1.04712822	2.55166088
H	-3.75949919	2.45283924	1.51601962
H	-4.93761075	1.13649407	1.57047126
C	-3.68044327	1.09554332	-0.91727386
H	-3.5791644	2.17658202	-1.04161314
H	-4.74167337	0.84841141	-1.00592129
H	-3.15537416	0.61767982	-1.74167755
C	-1.6527836	0.45299602	0.63333432
C	-0.72077664	0.62666463	-0.47407954
C	0.26492609	1.54235175	-0.59378796
C	0.42802257	2.60848471	0.37997288
O	1.25230979	3.51160681	0.27927534
H	-0.26078524	2.60260853	1.23944422
C	1.24234867	1.46967545	-1.74538599
H	0.85623461	0.75138172	-2.47164036
O	1.34456704	2.70995346	-2.45052968
H	1.59400892	3.37362559	-1.78939221
H	-0.82062295	-0.06871331	-1.30028575
H	-1.29220585	0.77603815	1.60018427
H	-2.80812583	-1.08595725	1.67359281
H	-2.47377028	-1.42075428	-1.36894603

H	-3.77804892	-2.09950214	-0.44253111
H	0.09739864	-3.00263741	1.6543835
H	2.34052833	-3.07302482	-0.46587154
H	2.29560463	-3.99743946	1.01055824
H	2.20169751	-1.84922704	2.33208325
H	3.71511233	-2.23424213	1.56538346
H	2.40214118	-1.17622621	-1.22132626
H	3.06729993	1.7745652	-0.65352543
H	3.25693648	0.92057553	-2.17707679

52

Coordinates from ORCA-job conformer 011

Single point energy: -930.427434083114

Gibbs free energy: -930.01845008

C	2.95152335	0.15128555	-0.83543611
C	2.37995282	-1.12088222	-0.28657119
C	2.29525782	-1.48095201	0.99582189
C	2.79667961	-0.64316886	2.13991411
H	1.95021232	-0.26111491	2.72096759
H	3.39687995	0.20747923	1.82722774
H	3.39441645	-1.25188613	2.82502849
C	1.7020591	-2.79817649	1.44755648
C	0.75200154	-3.52699826	0.48895331
C	-0.62823972	-2.9384402	0.45281431
C	-1.34809806	-2.53227174	-0.59637878
C	-0.85796516	-2.54589905	-2.01801752
H	-0.97172155	-1.56399579	-2.4851297
H	-1.4536224	-3.24294072	-2.6165082
H	0.18677672	-2.83395952	-2.1050709
C	-2.78908009	-2.10949132	-0.42124992
H	-3.1218031	-2.36288997	0.58842797
H	-3.39517937	-2.70916289	-1.11000918
C	-3.1110099	-0.62799682	-0.68822436
C	-2.78555555	0.28790075	0.46862266
C	-2.77028379	1.77770272	0.34299814
C	-3.3301184	2.59019555	1.48909587
H	-2.85263494	3.57246987	1.54132046
H	-4.40426268	2.74732101	1.35357012
H	-3.18013705	2.08625539	2.44517219
C	-2.94689322	2.44217282	-1.00461795
H	-2.52445804	1.86631877	-1.82539115
H	-2.46591874	3.42355821	-1.00613941
H	-4.00981097	2.59242097	-1.21137695
C	-1.46020049	1.02615437	0.64278595
C	-0.40062613	0.93826307	-0.35452049
C	0.84948081	1.44527297	-0.28591716
C	1.25999606	2.30117899	0.81430816

O	2.35245634	2.85515734	0.8834637
H	0.51870771	2.47250018	1.61075611
C	1.86724563	1.11986358	-1.3560705
H	1.34368707	0.63966278	-2.18535428
O	2.46533152	2.29492987	-1.91081143
H	2.85493123	2.77533727	-1.16448892
H	-0.63752684	0.39097691	-1.26036122
H	-1.12977128	1.13531948	1.66650984
H	-3.18662311	-0.07665116	1.40959814
H	-2.63178652	-0.30027769	-1.61083381
H	-4.18648818	-0.54399716	-0.87378673
H	-1.11019879	-2.88962629	1.4280838
H	1.18961178	-3.60197036	-0.50567655
H	0.6611599	-4.5578152	0.85134549
H	1.17305981	-2.62731107	2.39216752
H	2.53393232	-3.46507552	1.70562697
H	1.96519328	-1.78637066	-1.03541912
H	3.55043783	0.67954923	-0.09500357
H	3.60656574	-0.06863312	-1.68364557

52

Coordinates from ORCA-job conformer 020

Single point energy: -930.427377443487

Gibbs free energy: -930.01840508

C	-2.42892759	-1.39842105	-1.36570411
C	-2.59264652	-0.05955693	-0.71253612
C	-2.89453578	0.18583813	0.56425401
C	-3.1463291	-0.8841194	1.59125082
H	-2.33577282	-0.8930138	2.32792473
H	-3.22375438	-1.8829054	1.16954807
H	-4.06679847	-0.67268784	2.14389785
C	-3.04351296	1.58305965	1.12530698
C	-2.4275445	2.74632455	0.3383805
C	-0.94079073	2.86552561	0.50762237
C	0.01387572	2.93005203	-0.4242597
C	-0.23724664	2.83271261	-1.90376686
H	-1.27914047	2.63929871	-2.14648758
H	0.36129147	2.03684425	-2.3550939
H	0.06003834	3.76222276	-2.40006554
C	1.44752183	3.21356337	-0.03692575
H	1.49108332	3.48984628	1.01954081
H	1.7735343	4.09325691	-0.6038071
C	2.46725315	2.08992203	-0.2960387
C	2.48947563	1.02579111	0.77657264
C	3.20574957	-0.27613674	0.61499937
C	3.94628253	-0.82988348	1.81182907
H	4.97153372	-0.44876971	1.83342114

H	3.46034256	-0.54687135	2.74687773
H	3.99618056	-1.92132478	1.76885879
C	3.83932195	-0.65177501	-0.70656165
H	4.86266048	-0.26981206	-0.75148727
H	3.30004418	-0.26320562	-1.56777011
H	3.88582615	-1.73909487	-0.80652893
C	1.67063786	-0.26340252	0.73801786
C	0.82383102	-0.59749421	-0.39911171
C	-0.05752534	-1.61549263	-0.50964144
C	-0.17404114	-2.63340129	0.52105149
O	-0.88673782	-3.6275124	0.427156
H	0.44549441	-2.49965511	1.42190009
C	-0.96012131	-1.71821101	-1.71880836
H	-0.61574132	-0.99324947	-2.45923614
O	-0.86394463	-2.9940521	-2.35897443
H	-1.08317701	-3.65082515	-1.6807558
H	0.90106497	0.05363355	-1.26302403
H	1.31694212	-0.60640213	1.7002215
H	2.55186872	1.44836322	1.77495702
H	2.30973532	1.6640782	-1.28692548
H	3.46546064	2.53786416	-0.32661961
H	-0.62326231	2.96245869	1.54471123
H	-2.71594755	2.69647306	-0.71087802
H	-2.8773572	3.66783464	0.72629194
H	-2.62310616	1.59026081	2.13776113
H	-4.11541867	1.77111948	1.263721
H	-2.40521118	0.7844833	-1.36669181
H	-2.80965559	-2.20398719	-0.73990206
H	-2.98895498	-1.42726583	-2.3052741

52

Coordinates from ORCA-job conformer 017

Single point energy: -930.427432052119

Gibbs free energy: -930.01835551

C	2.86080418	0.39174683	-1.13980801
C	2.45685544	-0.93113548	-0.56174257
C	2.48762973	-1.29267619	0.72292092
C	2.96606574	-0.39980533	1.83463586
H	2.11905944	-0.10014608	2.46158107
H	3.45883572	0.50424277	1.48610633
H	3.65962871	-0.9395412	2.48638922
C	2.06814063	-2.66472469	1.20647733
C	1.09752388	-3.46868643	0.33219554
C	-0.32503179	-3.00230105	0.43802577
C	-1.17399108	-2.65142319	-0.53144192
C	-0.82358751	-2.61502478	-1.9934043
H	0.22977765	-2.8057474	-2.18321681

H	-1.07029892	-1.646195	-2.43576077
H	-1.40847609	-3.36141698	-2.5408945
C	-2.62038206	-2.3473648	-0.21347694
H	-2.83575114	-2.6401172	0.81724464
H	-3.24181655	-2.98212282	-0.85545702
C	-3.07602109	-0.89116876	-0.41684862
C	-2.70359058	0.03099064	0.72073892
C	-2.8153892	1.51938284	0.62522555
C	-3.30952614	2.27176013	1.84039517
H	-4.40071135	2.34823042	1.8220255
H	-3.02141903	1.76853186	2.76471093
H	-2.90386652	3.28696291	1.86261321
C	-3.1835381	2.18461176	-0.68256471
H	-2.8123357	1.65030321	-1.55464658
H	-2.77711079	3.19860515	-0.71689574
H	-4.27059726	2.259091	-0.77158777
C	-1.42840776	0.86730302	0.77014298
C	-0.47538687	0.87307496	-0.33425643
C	0.71673489	1.50460828	-0.39574979
C	1.14088284	2.41714887	0.65239728
O	2.17512449	3.07607587	0.61443271
H	0.46127897	2.53132531	1.51166636
C	1.65422755	1.26165424	-1.55700452
H	1.09987449	0.73349234	-2.33558487
O	2.09692996	2.47995856	-2.16152398
H	2.50261883	2.99942295	-1.45050114
H	-0.74738106	0.29150975	-1.20827512
H	-0.99925947	0.99024052	1.75509083
H	-2.97573619	-0.37663605	1.68974043
H	-2.71458341	-0.51630958	-1.3745705
H	-4.16778284	-0.88533821	-0.49482831
H	-0.71257807	-3.00086675	1.45570276
H	1.44117746	-3.49707377	-0.70091139
H	1.13247651	-4.50616219	0.6853422
H	1.62289726	-2.55467896	2.20160593
H	2.97956834	-3.25366563	1.36695806
H	2.07020636	-1.63964903	-1.28596383
H	3.46981047	0.96876444	-0.4451016
H	3.45946997	0.23701892	-2.04219595

52

Coordinates from ORCA-job conformer 014
Single point energy: -930.426973458514
Gibbs free energy: -930.01808235

C	-2.79876573	-0.89749503	0.18022717
C	-2.45921905	0.5637428	0.20613708
C	-2.94829939	1.51491671	-0.59410606

C	-3.92071505	1.25680494	-1.71347029
H	-4.83757139	1.83669156	-1.56591966
H	-4.1934298	0.20924194	-1.81638516
H	-3.49271924	1.58892328	-2.66438257
C	-2.62030172	2.98169233	-0.43316607
C	-1.50931271	3.3758393	0.54638926
C	-0.12793599	3.15618996	0.00378794
C	0.92731378	2.57308965	0.57904486
C	0.91256704	1.97016557	1.95649458
H	1.65337804	2.46678398	2.59112041
H	1.18532638	0.91421857	1.92657954
H	-0.05670047	2.05426007	2.44353539
C	2.25328854	2.55627936	-0.15198137
H	3.05661451	2.79327157	0.55504084
H	2.24669126	3.35533738	-0.89632486
C	2.6215611	1.25281711	-0.88274
C	2.98630247	0.10083041	0.02491667
C	3.27669795	-1.274685	-0.47298888
C	4.38964027	-2.04793344	0.19955837
H	4.21702732	-3.12471017	0.1233454
H	5.34736868	-1.82679685	-0.28033265
H	4.47279726	-1.78889676	1.25617513
C	3.12108567	-1.60967277	-1.940415
H	4.06045785	-1.41088482	-2.46272722
H	2.3419303	-1.0340715	-2.43492599
H	2.88849903	-2.66982835	-2.06630276
C	2.027442	-1.03719181	0.39986028
C	0.69852063	-1.14128699	-0.1749092
C	-0.39741816	-1.74458838	0.34083355
C	-0.36858458	-2.40490666	1.6369134
O	-1.30032406	-3.0572046	2.09698473
H	0.55669518	-2.30967236	2.22532758
C	-1.69810021	-1.7810704	-0.43584408
H	-1.50304988	-1.42162871	-1.4479327
O	-2.16343967	-3.12680317	-0.592668
H	-2.26063743	-3.48221372	0.30420346
H	0.5697336	-0.69839302	-1.15643992
H	2.14106454	-1.39523091	1.4126114
H	3.6004413	0.4081653	0.86600353
H	1.81195973	0.99007808	-1.56409829
H	3.49127092	1.46536168	-1.51365142
H	0.02323141	3.57935481	-0.98852757
H	-1.62433363	4.44883576	0.74151818
H	-1.65532023	2.88086116	1.5062149
H	-3.54833786	3.48685873	-0.13790367
H	-2.37902673	3.39333046	-1.42076716
H	-1.74348576	0.85164009	0.966805

| H | -2.98299946 | -1.24521142 | 1.20042911 |
| H | -3.70768741 | -1.08888557 | -0.38906777 |

Optimised geometries of the 1*S*,2*R*,5*R*-154 conformers

52

Coordinates from ORCA-job conformer 003

Single point energy: -930.427533580154

Gibbs free energy: -930.01848461

C	-2.2501591	-1.98955498	0.33276712
C	-2.49216609	-0.50948136	0.36613527
C	-3.37274682	0.18164904	-0.36601459
C	-4.29701009	-0.4332959	-1.38319987
H	-4.16765262	-1.50711111	-1.4917013
H	-5.34007182	-0.23757607	-1.11547479
H	-4.13623706	0.02644824	-2.36305107
C	-3.58675344	1.66902132	-0.20641773
C	-2.6489832	2.44412523	0.72552504
C	-1.30819247	2.74975621	0.12420382
C	-0.08999277	2.61123116	0.65539261
C	0.17546633	2.04546011	2.02313514
H	0.69511074	2.78443882	2.64112177
H	0.8279617	1.17273835	1.96629062
H	-0.73418749	1.75334744	2.54362009
C	1.11749232	3.10387364	-0.11430947
H	1.78953696	3.62833661	0.57460224
H	0.78248665	3.84228221	-0.84594248
C	1.9353666	2.04529326	-0.87502724
C	2.72936835	1.10281056	0.00045908
C	3.50010918	-0.05641088	-0.5392863
C	4.83985492	-0.36554052	0.09218765
H	5.63227409	0.20705892	-0.39854961
H	4.84786352	-0.11260929	1.15362294
H	5.08226029	-1.42691934	-0.00818649
C	3.44284383	-0.39946204	-2.01184615
H	3.63548941	-1.4646869	-2.16120743
H	4.215243	0.15653935	-2.54971166
H	2.48619926	-0.16560525	-2.47326013
C	2.27787717	-0.31887285	0.35926514
C	1.05959723	-0.88469006	-0.19655318
C	0.29294482	-1.88223299	0.2943048
C	0.65119499	-2.59303005	1.51331275
O	0.02862905	-3.54395981	1.96629803
H	1.55599588	-2.24371754	2.03647158

C	-0.95736297	-2.35587793	-0.42705203
H	-0.90909871	-3.44425072	-0.49706516
O	-1.02614099	-1.88362306	-1.76908405
H	-1.41284285	-0.99561606	-1.74534377
H	0.73129495	-0.46952772	-1.14060831
H	2.53993175	-0.62844373	1.36056375
H	3.20692544	1.60784219	0.83475646
H	1.26942263	1.5054666	-1.54874121
H	2.64468916	2.57921726	-1.51649279
H	-1.36602871	3.19831905	-0.86679112
H	-3.13988319	3.40050915	0.94215346
H	-2.56060875	1.9316911	1.68331663
H	-3.55978605	2.13048455	-1.20105165
H	-4.61893359	1.80646908	0.13819088
H	-1.86300967	0.03788022	1.05712249
H	-2.16260468	-2.37407584	1.35026721
H	-3.07293731	-2.52193845	-0.14308272

52

Coordinates from ORCA-job conformer 053

Single point energy: -930.426533596240

Gibbs free energy: -930.01774911

C	-2.63607538	-1.83169921	-0.69851505
C	-2.72085662	-0.3674126	-1.00834442
C	-2.91872382	0.63288576	-0.14433202
C	-3.00570256	0.45237218	1.34625802
H	-2.10767287	0.83960388	1.83450019
H	-3.85197763	1.01274273	1.75424261
H	-3.1105871	-0.58943694	1.64058324
C	-3.14029878	2.04073746	-0.64074639
C	-2.21955987	3.1198741	-0.03619341
C	-0.80787303	3.05884066	-0.53323528
C	0.3139029	2.83384497	0.15730645
C	0.34882941	2.5633659	1.63786929
H	1.10369187	3.18990357	2.12115632
H	0.62420603	1.52653924	1.84081408
H	-0.60733799	2.75296544	2.1209521
C	1.65200745	2.89621753	-0.54834801
H	2.36038955	3.44104695	0.08603973
H	1.53739953	3.47977885	-1.46434605
C	2.28974533	1.5514238	-0.93585041
C	2.65155488	0.67366927	0.24156298
C	3.29691942	-0.66372999	0.10122282
C	4.34408207	-1.05210648	1.12152505
H	5.33116962	-0.70275151	0.80475644
H	4.12886976	-0.61682655	2.09862418
H	4.3940052	-2.13850969	1.23482037

C	3.55158118	-1.25122853	-1.26959799
H	2.83200529	-0.92682876	-2.01825681
H	3.52881577	-2.34319676	-1.22919595
H	4.5445609	-0.95316178	-1.61610243
C	1.85516162	-0.57117468	0.64555097
C	0.760275	-1.08136786	-0.16333939
C	-0.2480535	-1.90457712	0.20010618
C	-0.41184706	-2.35539416	1.57409391
O	-1.27920679	-3.13316099	1.94814983
H	0.30530865	-1.95491634	2.30863167
C	-1.23494055	-2.44789314	-0.81700892
H	-1.34221723	-3.51991306	-0.61928733
O	-0.79880175	-2.2566066	-2.16416237
H	0.00353297	-2.77532134	-2.30152689
H	0.77893717	-0.81602513	-1.21272784
H	1.7883626	-0.7343503	1.71140452
H	2.99492031	1.2403828	1.10104483
H	1.62422478	1.0365289	-1.62936472
H	3.20429733	1.77026983	-1.49715274
H	-0.70232217	3.24846411	-1.6004153
H	-2.63729121	4.09315838	-0.31708162
H	-2.2636047	3.07152687	1.05135384
H	-3.05454587	2.06199322	-1.7300343
H	-4.17339399	2.31974674	-0.39900417
H	-2.65367958	-0.11127432	-2.06160387
H	-3.00098501	-2.05174977	0.30285993
H	-3.27516904	-2.37808358	-1.39905673

52

Coordinates from ORCA-job conformer 024
Single point energy: -930.426102008073
Gibbs free energy: -930.01741955

C	-2.56556523	-1.91337089	-0.70789655
C	-2.70023667	-0.45276143	-1.01348643
C	-2.96448128	0.53474775	-0.1525813
C	-3.0977487	0.34253562	1.33313169
H	-3.97982182	0.86719463	1.71169498
H	-3.17171143	-0.70403868	1.61953004
H	-2.23436221	0.7624643	1.85556905
C	-3.21654564	1.93721206	-0.64937046
C	-2.33503897	3.03897862	-0.02590191
C	-0.91973173	3.03126114	-0.51662264
C	0.20408228	2.80944095	0.17181424
C	0.2360677	2.48425984	1.64151544
H	0.99203919	3.08918794	2.14957625
H	0.50646119	1.43947555	1.80625134
H	-0.7206671	2.65957071	2.12910531

C	1.54322221	2.93302138	-0.5232511
H	2.22465391	3.49768562	0.12348317
H	1.41088427	3.52389475	-1.43214733
C	2.23838942	1.6207604	-0.92405208
C	2.64368515	0.7502965	0.24488816
C	3.35089933	-0.55418954	0.09435107
C	4.41371833	-0.89990764	1.11412419
H	4.17506768	-0.48502043	2.09470498
H	4.5165962	-1.98355688	1.21737853
H	5.383153	-0.49935958	0.80350681
C	3.638005	-1.11635663	-1.28070091
H	4.61548139	-0.76468785	-1.62116028
H	2.90506008	-0.82366892	-2.02927416
H	3.6700991	-2.20821741	-1.24966788
C	1.90669616	-0.53577143	0.63717537
C	0.83474402	-1.08205621	-0.17775562
C	-0.17805016	-1.89718132	0.19382561
C	-0.36902112	-2.30007163	1.57788526
O	-1.22690903	-3.08396352	1.96215761
H	0.31857182	-1.85244683	2.31294061
C	-1.1362816	-2.47977459	-0.81797195
H	-1.20383352	-3.55486665	-0.61403704
O	-0.59934359	-2.28114506	-2.12813743
H	-1.22762651	-2.64751842	-2.76162246
H	0.87793376	-0.85666882	-1.23432403
H	1.84585653	-0.70817852	1.70176044
H	2.9574097	1.32462903	1.11065691
H	1.59356187	1.08272044	-1.61946279
H	3.14007973	1.88533601	-1.48644473
H	-0.81387545	3.26116517	-1.57576612
H	-2.78317706	4.0014383	-0.29644431
H	-2.38271649	2.97466733	1.060701
H	-3.11214008	1.96472932	-1.73687906
H	-4.26086121	2.18683991	-0.42481584
H	-2.60533652	-0.18602959	-2.06220522
H	-2.93626404	-2.1552711	0.28643696
H	-3.18162064	-2.48080522	-1.41594496

52

Coordinates from ORCA-job conformer 079
Single point energy: -930.425591546629
Gibbs free energy: -930.01740687

C	2.64068881	1.28428194	-1.20358514
C	2.64621353	-0.07592551	-0.57171109
C	2.75320996	-0.35157036	0.73020175
C	2.89249474	0.69358988	1.8022757
H	1.97836853	0.73089875	2.40493507

H	3.70514859	0.43221855	2.48684807
H	3.0778065	1.69320823	1.41762711
C	2.78113806	-1.76447541	1.27599158
C	2.09015672	-2.86287844	0.45795832
C	0.59536608	-2.84108277	0.58629249
C	-0.33217899	-2.81648532	-0.37374717
C	-0.02764391	-2.76882607	-1.84568741
H	1.0215764	-2.57843987	-2.05753969
H	-0.61215131	-1.99243595	-2.34546458
H	-0.30415611	-3.7171862	-2.31862788
C	-1.79971951	-2.92367436	-0.02903772
H	-1.9084175	-3.22671204	1.01542658
H	-2.22893927	-3.72907766	-0.63588394
C	-2.64453142	-1.65860186	-0.26549359
C	-2.51725359	-0.62419346	0.82848471
C	-3.0359596	0.77362689	0.68242845
C	-3.70181097	1.41123558	1.8809701
H	-3.59217737	2.49905741	1.85590459
H	-4.77190137	1.18355933	1.88909911
H	-3.27159376	1.04703579	2.81529605
C	-3.59078193	1.25577781	-0.63936857
H	-3.48405324	2.34088416	-0.71847221
H	-4.65613833	1.02059011	-0.70987851
H	-3.09149817	0.81226874	-1.4986081
C	-1.52415636	0.53061447	0.80868641
C	-0.62524684	0.74808256	-0.32510406
C	0.27156271	1.7433547	-0.47907619
C	0.36372755	2.82914969	0.48628401
O	1.15766685	3.75679133	0.41375503
H	-0.36160394	2.79852269	1.3164542
C	1.24290755	1.76346502	-1.63913962
H	1.34334924	2.79468867	-1.99141492
O	0.82580315	0.92868662	-2.72169452
H	-0.00357011	1.27663725	-3.07208548
H	-0.66925036	0.0253208	-1.12979495
H	-1.12507945	0.80813288	1.77513046
H	-2.65386961	-1.04937986	1.81835996
H	-2.41687913	-1.23710919	-1.24486371
H	-3.69676416	-1.95669334	-0.31278981
H	0.24030984	-2.89323224	1.61443899
H	2.40888508	-2.829687	-0.58292202
H	2.44479094	-3.82478402	0.84705701
H	3.83109576	-2.03963309	1.43474209
H	2.33597175	-1.75325384	2.27692093
H	2.52418044	-0.89994489	-1.2643171
H	3.0463534	2.04114234	-0.53473357
H	3.26479789	1.27980091	-2.10178604

52

Coordinates from ORCA-job conformer 012

Single point energy: -930.425680770735

Gibbs free energy: -930.01740679

C	-3.24460878	-0.66364999	0.91265801
C	-2.17348231	-1.71222464	0.9347433
C	-1.63702925	-2.33704726	-0.11801534
C	-2.02394688	-2.06049025	-1.5449407
H	-2.96211556	-1.51745171	-1.63128585
H	-1.25503046	-1.46322643	-2.04446775
H	-2.11227708	-2.99387451	-2.10769788
C	-0.58584845	-3.40353381	0.06773666
C	0.74452053	-3.13807486	-0.6655663
C	1.4848255	-1.95259518	-0.11971202
C	2.79486659	-1.85092467	0.11894091
C	3.79134731	-2.94587485	-0.15459543
H	4.49637428	-2.63015453	-0.9305895
H	3.33147748	-3.87587048	-0.48079359
H	4.38686707	-3.15356267	0.73996953
C	3.43605095	-0.61323124	0.70162071
H	4.27328052	-0.32427631	0.05305112
H	3.90408086	-0.89993588	1.65152942
C	2.56093186	0.61569952	0.94457734
C	2.10637709	1.29543627	-0.33637333
C	1.64172876	2.71462936	-0.3758037
C	2.04996969	3.56421032	-1.55836656
H	1.31865084	4.35631399	-1.74107366
H	3.01754021	4.03864308	-1.36954469
H	2.13835574	2.96525264	-2.46614857
C	1.50224875	3.49754214	0.91061767
H	2.45027129	3.98589532	1.15190986
H	1.2235688	2.87695061	1.75992103
H	0.74450005	4.27733405	0.80187294
C	0.64063111	1.58843883	-0.6855667
C	-0.43042365	1.27893379	0.24862867
C	-1.75538579	1.17285972	0.00642066
C	-2.3166111	1.43547253	-1.3090879
O	-3.5104558	1.39405624	-1.57523911
H	-1.59622976	1.70286661	-2.09863216
C	-2.72763502	0.78190324	1.09186508
H	-3.59544588	1.44715728	1.02493791
O	-2.09483016	0.95243954	2.36229332
H	-2.71641473	0.66366374	3.04074125
H	-0.13714488	1.12133185	1.27823375
H	0.40605562	1.49657861	-1.73623203
H	2.67813951	0.98845158	-1.20594592

H	1.71721302	0.34169313	1.58046569
H	3.1535096	1.325677	1.52773525
H	0.85685388	-1.09581163	0.09473507
H	1.35233641	-4.04085781	-0.60778729
H	0.53322273	-2.98479373	-1.72987829
H	-0.38768327	-3.54230253	1.13333085
H	-0.98851466	-4.35039684	-0.31138658
H	-1.79391032	-1.9753583	1.91778378
H	-3.81597107	-0.69100251	-0.01427485
H	-3.9562515	-0.84922104	1.72489615

52

Coordinates from ORCA-job conformer 090

Single point energy: -930.425581790538

Gibbs free energy: -930.01729569

C	2.29084314	1.6519596	-1.4903774
C	2.59048483	0.37679192	-0.75995172
C	2.85372132	0.24275512	0.54190324
C	2.8931829	1.38773287	1.51672741
H	2.85715817	2.36613146	1.04450595
H	2.04505729	1.3178471	2.20640092
H	3.79803993	1.3358171	2.12992375
C	3.17614259	-1.08834972	1.18796291
C	2.69669507	-2.36443726	0.48508544
C	1.23325102	-2.63333612	0.68082068
C	0.28934254	-2.87537463	-0.23217587
C	0.52705874	-2.88456615	-1.71688925
H	-0.16718298	-2.21626124	-2.23264481
H	0.35066432	-3.8869838	-2.12066278
H	1.53547457	-2.58271136	-1.98837699
C	-1.1110931	-3.25495439	0.19213261
H	-1.12285501	-3.46506433	1.26457013
H	-1.36920392	-4.19234421	-0.31384594
C	-2.219807	-2.23392012	-0.12310082
C	-2.31543417	-1.10548716	0.87770132
C	-3.137803	0.12192957	0.63635308
C	-3.91240571	0.69545821	1.80174635
H	-3.39600842	0.52052548	2.74690291
H	-4.05360699	1.77346441	1.68400537
H	-4.9022283	0.23375824	1.86588142
C	-3.80816557	0.35187581	-0.70002405
H	-3.94824203	1.4225011	-0.87080648
H	-4.79499173	-0.11850135	-0.71222028
H	-3.2378565	-0.04408148	-1.53790103
C	-1.60804749	0.23797125	0.73313621
C	-0.79864671	0.55177198	-0.44246133
C	-0.09551849	1.67794362	-0.68125239

C	-0.16090397	2.81413053	0.2267152
O	0.43618015	3.86890979	0.06168551
H	-0.81983595	2.69467977	1.10258722
C	0.81076926	1.80711847	-1.8872613
H	0.68622663	2.80859004	-2.3109056
O	0.53550212	0.82824183	-2.89161042
H	-0.35426177	0.98114306	-3.23274265
H	-0.74255058	-0.20846489	-1.21114157
H	-1.27151905	0.67859434	1.66163396
H	-2.33701847	-1.46235098	1.90307294
H	-2.10319451	-1.86084851	-1.14069864
H	-3.17967206	-2.75994538	-0.11259192
H	0.9291709	-2.67337759	1.72571733
H	2.97126376	-2.35119787	-0.56883326
H	3.25067498	-3.20147585	0.92647193
H	4.26410184	-1.13694964	1.32031665
H	2.76731956	-1.08217854	2.20467367
H	2.5591052	-0.51525273	-1.37335523
H	2.56007896	2.5263309	-0.901674
H	2.87054387	1.6958464	-2.41712652

52

Coordinates from ORCA-job conformer 063

Single point energy: -930.426572960458

Gibbs free energy: -930.01726395

C	-2.20610326	-2.32639671	-0.84633896
C	-2.61112954	-0.90199327	-1.08033597
C	-2.98860213	-0.00532021	-0.16384384
C	-2.9890856	-0.26571666	1.31717789
H	-2.85378726	-1.31688084	1.56140287
H	-2.183799	0.2886423	1.80597302
H	-3.92505061	0.07567182	1.76922466
C	-3.51960775	1.34250103	-0.58745745
C	-2.84535048	2.56736187	0.06162208
C	-1.45487166	2.82667662	-0.43115828
C	-0.31047779	2.84008052	0.25876565
C	-0.21396115	2.55604857	1.73388538
H	-1.18806709	2.49424586	2.21414047
H	0.36232758	3.33942117	2.23429774
H	0.30856758	1.61533769	1.91891391
C	0.981124	3.2112408	-0.43957549
H	1.5597132	3.87056233	0.21716572
H	0.74198319	3.79038661	-1.33412622
C	1.88808616	2.04748682	-0.87351866
C	2.41781836	1.21251705	0.27099882
C	3.33175052	0.04840265	0.08433545
C	4.42852543	-0.15743581	1.105542

H	5.32250472	0.40580655	0.82207885
H	4.1177749	0.17756625	2.09635043
H	4.70544615	-1.21307775	1.1730419
C	3.71481756	-0.41051784	-1.3053888
H	3.9252069	-1.483023	-1.31064034
H	4.62345412	0.10691386	-1.62415914
H	2.94678586	-0.21478375	-2.05048595
C	1.89850487	-0.18908765	0.60678407
C	0.94227848	-0.88056022	-0.24293599
C	0.14532905	-1.92913643	0.06025186
C	0.09700487	-2.49233511	1.40154766
O	-0.57072159	-3.4672598	1.71893233
H	0.71127191	-1.98897844	2.16546635
C	-0.70465125	-2.61232664	-0.9950302
H	-0.57225027	-3.69185357	-0.8652759
O	-0.33358253	-2.24575527	-2.32513661
H	0.56475111	-2.55821277	-2.48869781
H	0.89611805	-0.55332698	-1.2739685
H	1.86008742	-0.41307351	1.6629956
H	2.62878557	1.79851031	1.15970908
H	1.34868658	1.43677614	-1.59809717
H	2.73985654	2.47651727	-1.41183744
H	-1.39432772	3.05739706	-1.49382979
H	-3.46121886	3.44003661	-0.18364493
H	-2.87447053	2.46980982	1.14629161
H	-3.46079912	1.43209009	-1.67507427
H	-4.58406458	1.37857712	-0.32410103
H	-2.63192099	-0.59059092	-2.12050702
H	-2.50448625	-2.67208336	0.14160371
H	-2.71713557	-2.96263582	-1.57537432

52
Coordinates from ORCA-job conformer 020
Single point energy: -930.425539910005
Gibbs free energy: -930.01721382

C	-0.97620745	-2.29998541	-1.01339978
C	-2.05414216	-1.54836793	-0.28417366
C	-2.80311229	-0.53832176	-0.73294422
C	-2.64186619	0.09002167	-2.08769052
H	-2.3687446	1.14456838	-1.99320083
H	-1.88338676	-0.40285693	-2.69253374
H	-3.5876895	0.05873316	-2.63775804
C	-3.89832421	0.03722974	0.13285646
C	-3.73523857	1.54365626	0.43700812
C	-2.35619794	1.82770045	0.94535646
C	-1.48730663	2.74711391	0.51979288
C	-1.79176265	3.80173898	-0.50729096

H	-2.83206193	3.79472255	-0.8255238
H	-1.16436124	3.6816638	-1.3952221
H	-1.56903676	4.79404841	-0.10198801
C	-0.06719937	2.71733949	1.02118449
H	0.01616071	1.95628272	1.7999142
H	0.21027758	3.67525306	1.47514542
C	0.93364393	2.38747327	-0.10652725
C	2.18152035	1.73211383	0.42660968
C	3.13922826	0.95777101	-0.41372484
C	4.61076208	1.05371232	-0.07741765
H	5.13782305	0.1419087	-0.37063093
H	5.06720793	1.8913309	-0.61289772
H	4.76621477	1.20982399	0.99114721
C	2.88016221	0.7365465	-1.88810785
H	3.32235078	1.55326031	-2.46455561
H	1.82342738	0.68785179	-2.14060998
H	3.34619368	-0.19463932	-2.2193103
C	2.27538857	0.21840268	0.63770195
C	1.23778804	-0.70151227	0.19241916
C	1.05605833	-1.98940256	0.56548271
C	1.90602941	-2.61555869	1.57052116
O	1.88414995	-3.81446607	1.8256726
H	2.59838546	-1.96326682	2.1237604
C	0.04725817	-2.92669565	-0.0762152
H	-0.49953641	-3.4278205	0.73125008
O	0.75192065	-3.931089	-0.83045594
H	1.28983455	-4.41786418	-0.18993025
H	0.56390552	-0.32102007	-0.56440184
H	2.84011561	-0.08152633	1.50800204
H	2.64355743	2.2909069	1.23528222
H	0.44084715	1.74513803	-0.83619181
H	1.20969716	3.29750929	-0.64599581
H	-2.00460445	1.1288427	1.7014753
H	-3.95352967	2.128979	-0.45621949
H	-4.4911761	1.81796459	1.18117762
H	-4.86747492	-0.11208698	-0.35680021
H	-3.92875017	-0.51336723	1.07597453
H	-2.2704481	-1.92174322	0.71429715
H	-1.42368142	-3.13965683	-1.55662809
H	-0.47818324	-1.68721546	-1.76674774

52
Coordinates from ORCA-job conformer 030
Single point energy: -930.426133676596
Gibbs free energy: -930.01718881

C	-2.19977505	-2.31996881	-0.90019546
C	-2.61268153	-0.89506527	-1.1117132

C	-3.01037877	-0.01966984	-0.18344883
C	-3.0384633	-0.3135068	1.29093147
H	-3.97938529	0.02530797	1.73426786
H	-2.91494335	-1.3708795	1.51366752
H	-2.23748871	0.22329501	1.80585182
C	-3.53268118	1.33772538	-0.58639057
C	-2.8557021	2.54659501	0.09000808
C	-1.46573549	2.81582179	-0.39936552
C	-0.31899933	2.80241813	0.28686759
C	-0.22091651	2.46765592	1.75133017
H	0.27571893	1.50708251	1.90205583
H	-1.19379157	2.41711841	2.23553963
H	0.3797707	3.21758148	2.27351681
C	0.97110915	3.1942906	-0.40246591
H	1.54049752	3.8509193	0.26516534
H	0.72844661	3.78324854	-1.28967041
C	1.89316869	2.0473004	-0.84946427
C	2.4299406	1.20381257	0.28547647
C	3.35718125	0.0523066	0.08867756
C	4.44920195	-0.15377155	1.11523073
H	4.12638786	0.16109862	2.10882666
H	4.74067744	-1.20629305	1.16828333
H	5.3371068	0.42651499	0.84746694
C	3.75738034	-0.38191212	-1.30413458
H	2.9957016	-0.1811867	-2.05419718
H	3.97621435	-1.45235847	-1.32455661
H	4.66481744	0.14836152	-1.6049293
C	1.92413626	-0.2091144	0.59918944
C	0.97737512	-0.89230227	-0.26642335
C	0.14045569	-1.91120803	0.03287251
C	0.0325512	-2.44384081	1.38155031
O	-0.65440223	-3.40648395	1.69691228
H	0.61917086	-1.92522853	2.15642672
C	-0.68800134	-2.59313334	-1.03027718
H	-0.54794031	-3.67296707	-0.90267087
O	-0.19971721	-2.20302604	-2.31631932
H	-0.76118927	-2.61845459	-2.98135149
H	0.97685918	-0.58872745	-1.30415747
H	1.88082986	-0.44590149	1.65229612
H	2.62863321	1.77994541	1.18345224
H	1.36423244	1.43925546	-1.58389589
H	2.74089892	2.49493652	-1.37900226
H	-1.40791255	3.08062245	-1.45416221
H	-3.47090565	3.42560182	-0.13292201
H	-2.88292174	2.42294792	1.172091
H	-3.46553056	1.44744111	-1.67169569
H	-4.59861446	1.37404554	-0.32951002

H	-2.61431189	-0.558633	-2.14454504
H	-2.51606959	-2.69398021	0.07209112
H	-2.69613429	-2.94671072	-1.65067184

52

Coordinates from ORCA-job conformer 119
Single point energy: -930.425351547617
Gibbs free energy: -930.01713759

C	-2.40777692	-1.52151165	-1.29096919
C	-2.58595162	-0.22390904	-0.56337652
C	-2.8601956	-0.05954078	0.73257990
C	-3.05929957	-1.18996551	1.70523734
H	-3.97544812	-1.03700981	2.28390405
H	-3.11246558	-2.16766607	1.23342829
H	-2.23537797	-1.21116627	2.42637619
C	-3.02997236	1.29951325	1.3758163
C	-2.48980898	2.52626494	0.63122111
C	-1.00223306	2.69330784	0.74442087
C	-0.09591812	2.86775559	-0.22091514
C	-0.41281921	2.87400452	-1.69089479
H	-1.45952551	2.66791011	-1.90065944
H	0.18365627	2.13169221	-2.22707478
H	-0.16429998	3.84738472	-2.12633364
C	1.3434911	3.17691174	0.12264388
H	1.4269931	3.37773893	1.19372224
H	1.61124713	4.10723985	-0.39152209
C	2.38856597	2.11442492	-0.26381229
C	2.51272097	0.98752391	0.73524103
C	3.27297135	-0.26866439	0.45219216
C	4.10479392	-0.85835767	1.56937205
H	5.1117723	-0.43060497	1.56064812
H	3.66047826	-0.65701241	2.54542604
H	4.20090574	-1.94157411	1.45453622
C	3.84739901	-0.53077367	-0.92280139
H	3.94365347	-1.60641305	-1.09148802
H	4.84563001	-0.09173858	-1.00122292
H	3.23868585	-0.12366292	-1.72727042
C	1.74931144	-0.333855	0.656074
C	0.85492408	-0.62889468	-0.45708099
C	0.00717492	-1.67228976	-0.58207592
C	-0.029378	-2.74142367	0.40323113
O	-0.74139198	-3.73378696	0.32765853
H	0.66137208	-2.63544531	1.25528449
C	-0.95148987	-1.78052596	-1.74130862
H	-0.90545258	-2.80103969	-2.13706983
O	-0.5494437	-0.85938652	-2.75795683
H	-1.18906447	-0.91862213	-3.47720579

H	0.86272756	0.06821806	-1.28364162
H	1.46492705	-0.74802956	1.61312953
H	2.61363131	1.34950913	1.75416419
H	2.18949414	1.74388986	-1.2691592
H	3.36562228	2.60467763	-0.32082598
H	-0.64049392	2.72397543	1.77110841
H	-2.82160497	2.52266632	-0.40636511
H	-2.95558588	3.40722965	1.08872924
H	-4.10065775	1.44052892	1.56930155
H	-2.56641408	1.26618326	2.36883508
H	-2.43609549	0.65887617	-1.17246204
H	-2.71929232	-2.37180919	-0.68818707
H	-3.02677378	-1.53222735	-2.19594906

52

Coordinates from ORCA-job conformer 058

Single point energy: -930.425381477570

Gibbs free energy: -930.01713143

C	-2.31092966	-1.60440868	-1.48120211
C	-2.58701129	-0.33429849	-0.7351933
C	-2.89630019	-0.21288194	0.55765554
C	-3.03560892	-1.37291837	1.50530231
H	-3.01757341	-2.34242632	1.01434151
H	-2.22233162	-1.35397872	2.2386283
H	-3.96786103	-1.29164026	2.07257359
C	-3.17310514	1.11969213	1.21977156
C	-2.6607192	2.38971105	0.52960687
C	-1.19019356	2.6228906	0.72049071
C	-0.24732297	2.86287927	-0.19426866
C	-0.49282639	2.89550529	-1.67758168
H	0.17665792	2.21092968	-2.20426433
H	-0.28766387	3.89642028	-2.07135438
H	-1.51237314	2.62963079	-1.94549678
C	1.15956673	3.22155709	0.22696085
H	1.18088343	3.40878466	1.30351656
H	1.41851038	4.16844798	-0.26066294
C	2.26200062	2.20367001	-0.11899428
C	2.36999139	1.06115123	0.86423199
C	3.19084928	-0.16113272	0.60009128
C	3.97805863	-0.74654588	1.75117488
H	3.47133363	-0.58309263	2.70362911
H	4.11978585	-1.82284311	1.61969151
H	4.96768407	-0.28372249	1.81007557
C	3.84977823	-0.37359824	-0.74509651
H	3.99136636	-1.44159705	-0.92976211
H	4.83528088	0.09959698	-0.75894606
H	3.2720116	0.03054608	-1.57362593

C	1.66161032	-0.28309754	0.71278965
C	0.8433926	-0.58117676	-0.45796006
C	0.07408179	-1.66962448	-0.67145284
C	0.06797176	-2.78621051	0.26027986
O	-0.57471728	-3.81653138	0.10873841
H	0.71813244	-2.6789942	1.14366867
C	-0.82616447	-1.77972014	-1.87599384
H	-0.71486905	-2.78201534	-2.30375556
O	-0.42482961	-0.80424917	-2.84078006
H	-1.03354015	-0.86003367	-3.58663805
H	0.84272309	0.1546898	-1.2503072
H	1.33614944	-0.73112456	1.64134686
H	2.40039719	1.40482966	1.89396311
H	2.13244312	1.84676083	-1.14066414
H	3.22249697	2.72865881	-0.11186194
H	-0.88039653	2.64256141	1.76429391
H	-2.94090335	2.39524444	-0.5230452
H	-3.19124084	3.23562366	0.98272332
H	-4.25840743	1.19991756	1.35878623
H	-2.76002851	1.08845206	2.2346236
H	-2.48512444	0.56767554	-1.32591359
H	-2.60227082	-2.48339835	-0.90987645
H	-2.89211779	-1.62574389	-2.41061086

52

Coordinates from ORCA-job conformer 056

Single point energy: -930.425612726082

Gibbs free energy: -930.01707164

C	-2.58784017	-1.55731858	-0.85723948
C	-2.65285333	-0.1923452	-0.23914022
C	-2.66823826	0.09464706	1.06460014
C	-2.62212454	-0.94014525	2.15509225
H	-2.75377863	-1.95833873	1.79801996
H	-1.65856494	-0.88956632	2.67384957
H	-3.39098457	-0.73728935	2.90676415
C	-2.76814274	1.50845892	1.59876248
C	-2.2787982	2.6516648	0.70075458
C	-0.7836297	2.77307959	0.66202842
C	0.03213944	2.81443056	-0.39431809
C	-0.42384061	2.70385958	-1.82292479
H	-0.2375619	3.64438949	-2.35197184
H	-1.48072026	2.46664341	-1.91501009
H	0.135213	1.93199532	-2.35777722
C	1.51106845	3.06988588	-0.21430688
H	1.70371911	3.38841806	0.813252
H	1.78534153	3.91178606	-0.86025559
C	2.44999426	1.89717312	-0.55151796

C	2.56545492	0.86923852	0.55004867
C	3.20686535	-0.46827795	0.34442772
C	4.07390654	-1.01590207	1.45581897
H	5.10693174	-0.67588945	1.33643125
H	3.72070016	-0.68713436	2.43449289
H	4.07886049	-2.10944878	1.44441375
C	3.64936811	-0.90907624	-1.03311807
H	3.01562675	-0.52354992	-1.82931856
H	3.63919603	-2.00016726	-1.10023475
H	4.67218356	-0.5739983	-1.22500491
C	1.70352242	-0.38357847	0.65293547
C	0.70424464	-0.70908778	-0.36370766
C	-0.12068896	-1.77570677	-0.39168638
C	-0.01904904	-2.83370813	0.60295547
O	-0.73131007	-3.82754929	0.63276269
H	0.77956472	-2.71496841	1.35402876
C	-1.20608341	-1.91329335	-1.43750581
H	-1.24521216	-2.9575252	-1.76294378
O	-0.99047454	-1.06905847	-2.57029231
H	-0.17177529	-1.34196525	-3.00256603
H	0.60144043	-0.01249456	-1.18608225
H	1.45620043	-0.6872218	1.66114892
H	2.77384171	1.31989692	1.51587759
H	2.1525516	1.44215213	-1.4965334
H	3.45173561	2.30301135	-0.72484812
H	-0.3247458	2.88122941	1.64367406
H	-2.70598027	2.56909138	-0.29763601
H	-2.67828367	3.58296018	1.11961427
H	-3.81557251	1.68730611	1.87133398
H	-2.21660191	1.55634484	2.54424742
H	-2.6633484	0.62759164	-0.94693229
H	-2.8469054	-2.33600535	-0.1425436
H	-3.3018521	-1.62646303	-1.68304911

52
Coordinates from ORCA-job conformer 013
Single point energy: -930.426035083288
Gibbs free energy: -930.01704491

C	-1.12720798	-1.89162056	-1.52690881
C	-1.77234155	-0.53591077	-1.41410857
C	-2.97533486	-0.27265096	-0.89607338
C	-3.89234553	-1.32452255	-0.33682181
H	-4.90162667	-1.2030555	-0.74076191
H	-3.55538346	-2.33669234	-0.55305729
H	-3.97666491	-1.22850472	0.75019236
C	-3.46909759	1.14763675	-0.78335251
C	-3.35338349	1.72044798	0.65268297

C	-1.93234285	1.68604261	1.12914831
C	-1.00795222	2.64003507	0.99133708
C	-1.27298369	4.00265774	0.41486375
H	-0.87887856	4.77966997	1.07730746
H	-2.33220624	4.1942991	0.25419
H	-0.76261877	4.12431442	-0.54548544
C	0.42829769	2.34202871	1.33298695
H	0.4783434	1.37391951	1.83502653
H	0.82731381	3.08822682	2.02913019
C	1.32830689	2.29363237	0.07873334
C	2.56265843	1.46216038	0.3212725
C	3.3457412	0.76110051	-0.73641499
C	4.84275543	0.65626334	-0.53689536
H	5.24330879	-0.2171974	-1.05807507
H	5.34293721	1.54382981	-0.93427236
H	5.09792179	0.56912176	0.52048209
C	2.94982231	0.86697689	-2.19302376
H	3.4448143	1.7313988	-2.64261727
H	1.87999842	0.98916126	-2.34676988
H	3.2695681	-0.02289964	-2.7406407
C	2.50137603	-0.07604595	0.23778446
C	1.28460109	-0.74424029	-0.20654069
C	0.64412542	-1.78633841	0.36918243
C	1.10154876	-2.33726817	1.63891553
O	0.59893911	-3.31703327	2.17848131
H	1.93715719	-1.82241172	2.13640417
C	-0.58634399	-2.45856895	-0.21380604
H	-1.3817492	-2.38937624	0.53700321
O	-0.30718106	-3.84952265	-0.45339848
H	-0.07501802	-4.22520848	0.40870461
H	0.84974535	-0.35822788	-1.11789414
H	3.07702771	-0.58201361	0.99864525
H	3.14836006	1.80317481	1.1698063
H	0.74792035	1.8900749	-0.75067708
H	1.62357733	3.30436425	-0.21551846
H	-1.60166079	0.73293127	1.53132863
H	-3.75197951	2.73617813	0.64826007
H	-3.98560551	1.13703114	1.32704303
H	-2.89148347	1.79014173	-1.45122635
H	-4.51678738	1.20046841	-1.09760325
H	-1.19215727	0.30843469	-1.7731714
H	-1.8502438	-2.62777042	-1.88469435
H	-0.32278051	-1.8674438	-2.26583731

52

Coordinates from ORCA-job conformer 021

Single point energy: -930.426461968024

Gibbs free energy: -930.01694422

C	-2.99198932	-1.31713586	-0.60536295
C	-2.83627957	0.1305582	-0.96860005
C	-2.70884292	1.1671254	-0.13368314
C	-2.65623409	1.03345764	1.36237351
H	-2.98445779	0.05608091	1.70845885
H	-1.63695755	1.18418183	1.7264537
H	-3.27823641	1.79598873	1.8392776
C	-2.67989414	2.57854346	-0.66620502
C	-1.52832144	3.46364133	-0.1513101
C	-0.17567818	3.0750487	-0.66576628
C	0.9071822	2.70991329	0.02782966
C	0.94386113	2.58814829	1.52781647
H	1.07496255	1.54817201	1.83334027
H	0.04002708	2.96188856	2.00372772
H	1.7950087	3.14373034	1.93164383
C	2.21404122	2.45516831	-0.69464574
H	3.02800033	2.89815403	-0.10992661
H	2.19417631	2.98034769	-1.65211159
C	2.57405777	0.98782039	-0.98266953
C	2.73521047	0.13056718	0.25309168
C	3.0946937	-1.31646338	0.20929187
C	4.02479036	-1.84239117	1.28020325
H	5.06711684	-1.71945529	0.97171357
H	3.88635494	-1.31202347	2.22366183
H	3.85156681	-2.90716965	1.45802994
C	3.24671971	-2.02962009	-1.11636142
H	2.61436739	-1.62062868	-1.90129906
H	3.00785612	-3.09065373	-1.0106339
H	4.28356837	-1.95442691	-1.45445823
C	1.69413078	-0.89999187	0.70619533
C	0.53256172	-1.21892779	-0.10841048
C	-0.63468571	-1.79091612	0.25900453
C	-0.89764545	-2.16294307	1.64097746
O	-1.9016324	-2.74997032	2.02127199
H	-0.12104473	-1.89353505	2.37491049
C	-1.70300773	-2.14912919	-0.76012999
H	-1.96790268	-3.19574984	-0.595452
O	-1.22232504	-2.09615364	-2.1023997
H	-1.18484801	-1.17108721	-2.3775068
H	0.63989811	-1.02599344	-1.16750827
H	1.57483649	-0.97925748	1.77697398
H	3.1753624	0.66801207	1.08669604
H	1.8288518	0.57255602	-1.6615097
H	3.52042813	0.98349302	-1.53367986
H	-0.07266963	3.13789517	-1.74821019
H	-1.7384503	4.48651702	-0.48379069
H	-1.54741316	3.48824923	0.93756429
H	-2.66230115	2.55662428	-1.75876372
H	-3.61894072	3.06498205	-0.37445349
H	-2.86451055	0.35621185	-2.03236043
H	-3.34658881	-1.43978643	0.41623562
H	-3.73893291	-1.77107717	-1.26270394

Optimised geometries of 1*S*,2*S*,5*R*-155 conformers

52

Coordinates from ORCA-job conformer 002

Single point energy: -930.431565879773

Gibbs free energy: -930.02270476

C	-3.16471645	-0.29861503	0.71832882
C	-2.29970091	0.8496852	1.14328675
C	-2.21923664	2.06769366	0.6036491
C	-3.0534616	2.53079243	-0.55832832
H	-2.43256685	2.73839142	-1.43440776
H	-3.80952845	1.80471554	-0.84833506
H	-3.56100746	3.46776529	-0.30830796
C	-1.25324004	3.08276538	1.16410567
H	-0.69885045	2.63131214	1.99003443
H	-1.81580486	3.92954106	1.57537271
C	-0.24980543	3.64494392	0.13323916
C	0.51398739	2.585211	-0.60084885
C	1.83133595	2.36300693	-0.61691351
C	2.84082348	3.15413491	0.16753509
H	3.35515574	2.51751534	0.89333967
H	3.613381	3.5540254	-0.49701095
H	2.39717378	3.98480494	0.7119665
C	2.40230991	1.27822066	-1.49881154
H	3.05487729	1.74395323	-2.24725091
H	1.58788777	0.79542141	-2.04414514
C	3.22049319	0.19774513	-0.77495304
C	2.43102376	-0.54644508	0.27316662
C	1.35202114	-1.54629299	-0.16584357
C	0.04912371	-1.53619012	0.47234292
C	-1.18014696	-1.68039083	-0.07607584
C	-1.36547249	-1.82770566	-1.50790728
O	-2.45781935	-1.97356186	-2.0499741
H	-0.45913511	-1.79879972	-2.13260265
C	-2.41710991	-1.64074467	0.80174064

H	-2.09747343	-1.78503911	1.83607175
O	-3.29618763	-2.73287546	0.52228929
H	-3.49148862	-2.6816675	-0.42646924
H	0.06871175	-1.39302296	1.54832611
H	1.38147143	-1.78358968	-1.22033113
C	2.61113003	-1.99089564	0.59976026
C	3.58678346	-2.8438408	-0.18234334
H	4.60057551	-2.721434	0.20901005
H	3.60113355	-2.59730106	-1.24288647
H	3.31743276	-3.8986904	-0.08860711
C	2.49830906	-2.41059666	2.04998521
H	2.09849431	-3.42419374	2.13679879
H	3.49087204	-2.40243594	2.50776339
H	1.86574708	-1.74120673	2.63174782
H	2.13125974	0.06790177	1.11563669
H	3.59978913	-0.49650314	-1.52555898
H	4.09887523	0.64559536	-0.30094924
H	-0.09936447	1.92454296	-1.2085803
H	0.41869571	4.33396892	0.64931612
H	-0.80187245	4.24502072	-0.59829856
H	-1.65512068	0.64316995	1.99542465
H	-4.03615855	-0.38868555	1.37709481
H	-3.54286168	-0.16651224	-0.29534259

52

Coordinates from ORCA-job conformer 001
Single point energy: -930.430134643610
Gibbs free energy: -930.02224046

C	3.36115158	0.23944884	0.22199577
C	2.49865437	1.43134365	0.53596388
C	2.0667563	2.35751828	-0.32437197
C	2.38949361	2.33813429	-1.79295314
H	3.13138397	1.58399224	-2.04960513
H	1.49237408	2.13662347	-2.3866155
H	2.76480794	3.31381423	-2.11517869
C	1.18727751	3.49533031	0.13236074
H	1.55961489	4.42796189	-0.3031169
H	1.25194325	3.5982246	1.21829913
C	-0.29471519	3.33072864	-0.25965095
C	-0.97219847	2.24188397	0.52661992
C	-2.283635	2.04252699	0.67462689
C	-3.33599317	2.89692584	0.02560227
H	-4.06041468	3.24736966	0.76740352
H	-2.91655137	3.7638248	-0.48208459
H	-3.90235148	2.32118169	-0.713574
C	-2.79109312	0.87386805	1.48208742
H	-3.56572014	1.2136203	2.17795425

H	-1.97278561	0.46878675	2.08167781
C	-3.3720398	-0.2659383	0.62328485
C	-2.37085766	-0.77502639	-0.38293376
C	-1.15690175	-1.57340033	0.09579911
C	0.16453997	-1.21655724	-0.38733795
C	1.36909976	-1.37863634	0.20856637
C	1.50240733	-2.03361609	1.49761518
O	2.57819513	-2.310516	2.01862863
H	0.5697189	-2.30225041	2.01867835
C	2.6332087	-0.92030671	-0.48837744
H	2.35531051	-0.58834927	-1.4893091
O	3.53777875	-2.01345957	-0.69315735
H	3.74574256	-2.3594775	0.18751233
H	0.18174739	-0.74965187	-1.36792704
H	-1.22894155	-1.93019398	1.11404254
C	-2.22502527	-2.18801637	-0.83343976
C	-3.0683285	-3.28378357	-0.21920051
H	-3.24634938	-3.12584254	0.84359058
H	-2.57235318	-4.25046003	-0.33618341
H	-4.0383178	-3.34321158	-0.72098929
C	-1.88793112	-2.44504127	-2.28654982
H	-2.81009144	-2.58038668	-2.85795049
H	-1.33795968	-1.6205285	-2.73850966
H	-1.29135412	-3.35447265	-2.39507287
H	-2.11665551	-0.04453036	-1.14298743
H	-3.69547612	-1.06876019	1.28725491
H	-4.26535063	0.07897196	0.09402324
H	-0.30362583	1.53727149	1.01198256
H	-0.36050231	3.12542948	-1.33415714
H	-0.80627247	4.28466274	-0.10824714
H	2.19069147	1.53093518	1.57271548
H	4.19813254	0.51931542	-0.42283114
H	3.78940831	-0.14860014	1.14698033

52

Coordinates from ORCA-job conformer 006
Single point energy: -930.431511341530
Gibbs free energy: -930.02209819

C	-3.24722332	-0.69276955	-0.56364811
C	-2.22718574	-1.69667989	-1.00941482
C	-1.48699952	-2.4987055	-0.23793808
C	-1.52944835	-2.48758629	1.26511615
H	-2.38617282	-1.94693678	1.65993498
H	-1.55472884	-3.50738331	1.65919039
H	-0.62955367	-2.01591824	1.6702382
C	-0.58849063	-3.54334296	-0.85483958
H	-0.5463785	-3.39822559	-1.9374228

H	-1.05747312	-4.52114632	-0.687268
C	0.84118241	-3.62698485	-0.28920925
C	1.74815889	-2.50054433	-0.68538639
C	2.48932346	-1.71090213	0.09857799
C	2.45932309	-1.73807121	1.60197598
H	1.82111168	-2.52381192	1.99891781
H	3.46759998	-1.88141487	2.00318578
H	2.09844403	-0.78578246	1.99987531
C	3.51404021	-0.78028231	-0.50842113
H	3.46521432	-0.85192995	-1.59811192
H	4.50601691	-1.14595631	-0.21524034
C	3.42948882	0.69752209	-0.10247419
C	2.20462773	1.38888597	-0.64737789
C	0.93331646	1.53949463	0.18117215
C	-0.35950451	1.28621602	-0.43230089
C	-1.55424178	1.05894687	0.15754404
C	-1.71005498	1.10209714	1.60097461
O	-2.78812915	1.00508586	2.17923145
H	-0.79458427	1.2496979	2.19508186
C	-2.77943428	0.77087782	-0.68319195
H	-2.52803988	0.96950714	-1.72701633
O	-3.85342644	1.66618367	-0.3740252
H	-4.02160967	1.56433325	0.57530199
H	-0.36010363	1.29064456	-1.5188163
H	1.03610718	1.29932128	1.23016001
C	1.77521403	2.75988208	-0.24657031
C	2.4954391	3.48321284	0.8702741
H	2.82365206	2.80814051	1.65937904
H	1.83893989	4.23282601	1.31915155
H	3.37584141	4.00220124	0.48052351
C	1.23907896	3.69437045	-1.30938485
H	0.49676558	4.37830525	-0.88955718
H	2.05626988	4.29696929	-1.71484211
H	0.77776478	3.15971521	-2.13870306
H	2.0093167	1.15298596	-1.68999299
H	3.474977	0.79237362	0.98328394
H	4.31850312	1.20534533	-0.49073118
H	1.86073227	-2.37516412	-1.7611462
H	1.28047928	-4.55442489	-0.6757448
H	0.80068722	-3.74442278	0.79282228
H	-2.09570312	-1.77701482	-2.08626377
H	-4.14072968	-0.78132224	-1.18876888
H	-3.55880196	-0.86718999	0.46576567

52

Coordinates from ORCA-job conformer 020

Single point energy: -930.430525194417

Gibbs free energy: -930.02130580

C	-2.50015355	-1.51593474	-1.04160546
C	-1.49857246	-2.31396506	-0.25914475
C	-0.2798128	-2.71860412	-0.62695071
C	0.36539037	-2.39515875	-1.94521413
H	1.25259204	-1.77229955	-1.79716917
H	0.70489183	-3.30992035	-2.44087852
H	-0.30173999	-1.87162492	-2.62728187
C	0.53648801	-3.5858867	0.3028583
H	0.6388609	-4.5831177	-0.14178164
H	-0.01071286	-3.71270798	1.24009529
C	1.9511439	-3.06311709	0.61025508
C	1.94577463	-1.67745671	1.19072476
C	2.87368932	-0.72886518	1.04195017
C	4.1392869	-0.91197126	0.24972854
H	4.15991994	-0.25123938	-0.62225071
H	5.00864602	-0.64713981	0.85965781
H	4.27274182	-1.9331378	-0.10035544
C	2.69215586	0.63173284	1.66962595
H	3.52349237	0.83369623	2.3546358
H	1.77560572	0.63349395	2.26426502
C	2.62251576	1.78100991	0.64631709
C	1.54457375	1.54859464	-0.3805187
C	0.08723473	1.86168414	-0.04502964
C	-0.9335557	0.87389962	-0.34855773
C	-2.16771768	0.72757524	0.1894606
C	-2.67260151	1.70187042	1.14185399
O	-3.79898088	1.67832231	1.63312137
H	-1.99415435	2.52431413	1.41299125
C	-3.1293822	-0.36904729	-0.24696934
H	-3.8894595	0.09897062	-0.88781026
O	-3.78774099	-0.95478372	0.88327652
H	-4.16995343	-0.21273472	1.37901678
H	-0.64613434	0.16236878	-1.11065952
H	-0.05015089	2.46421491	0.84184375
C	0.84803761	2.6041536	-1.1659533
C	1.12875689	4.06774875	-0.90586619
H	2.00528475	4.39195775	-1.47413029
H	1.31351942	4.27482899	0.14724994
H	0.28026554	4.67806597	-1.22501469
C	0.50408264	2.31156197	-2.61075914
H	0.36304397	1.24745565	-2.79645634
H	-0.40803663	2.83487343	-2.90939248
H	1.3141216	2.65703558	-3.25862384

H	1.6593676	0.61185462	-0.91505367
H	2.45105935	2.71529607	1.18271032
H	3.58547707	1.888167	0.13815301
H	1.07317276	-1.43359418	1.79268955
H	2.56060707	-3.10146339	-0.2935408
H	2.4141632	-3.76381546	1.31536911
H	-1.8446675	-2.61013962	0.72594435
H	-2.0887055	-1.12798551	-1.97277239
H	-3.33300995	-2.16876498	-1.3250455

52

Coordinates from ORCA-job conformer 004
Single point energy: -930.429033357734
Gibbs free energy: -930.02113835

C	-3.03175074	-0.78458699	0.69621036
C	-2.47590905	0.61027082	0.74792751
C	-2.91928277	1.68108705	0.0873241
C	-4.11484059	1.66016758	-0.82424408
H	-4.62090101	0.69732748	-0.84471615
H	-4.84183424	2.41649318	-0.5107742
H	-3.82054109	1.91792718	-1.84680673
C	-2.26744943	3.04345827	0.20077612
H	-2.89936763	3.67950672	0.83220054
H	-2.29171118	3.50951372	-0.79139869
C	-0.82630631	3.08204323	0.71526593
C	0.12983508	2.41277302	-0.23479315
C	1.44141515	2.62349692	-0.36419355
C	2.22326954	3.59121787	0.47917278
H	2.85914005	4.22433131	-0.14700769
H	1.5821012	4.23369894	1.08043662
H	2.8918441	3.05927453	1.16386059
C	2.23745513	1.83865388	-1.37672706
H	2.77081098	2.52991412	-2.03925708
H	1.55046949	1.26138891	-1.99965861
C	3.26866793	0.87497608	-0.76118506
C	2.65460873	-0.07254318	0.23969482
C	1.68592965	-1.1632995	-0.22797195
C	0.43492415	-1.34947845	0.48393339
C	-0.77126005	-1.75138794	0.01933327
C	-0.9767246	-2.10021396	-1.37489579
O	-2.02764329	-2.54878163	-1.82266144
H	-0.12345817	-1.95385874	-2.05580859
C	-1.95902347	-1.85439337	0.95674064
H	-1.58956152	-1.72736576	1.97661102
O	-2.53817971	-3.16349681	0.92530883
H	-2.79930135	-3.31832538	0.00489135
H	0.47925154	-1.12627679	1.54602449

H	1.67602071	-1.32539468	-1.29700392
C	3.04075581	-1.50062936	0.42670225
C	4.06048472	-2.14643543	-0.48617825
H	5.07466124	-1.9251005	-0.14190425
H	3.97116331	-1.80709557	-1.51719192
H	3.93491439	-3.23192894	-0.47926223
C	3.07439118	-2.05755521	1.83403126
H	2.81052186	-3.11824366	1.84232599
H	4.08493482	-1.96168639	2.23988721
H	2.39903831	-1.53227911	2.50820233
H	2.32508766	0.41638551	1.15025132
H	3.74666506	0.32303916	-1.5714846
H	4.06133752	1.44227789	-0.26440708
H	-0.31696892	1.66104456	-0.87855289
H	-0.77467626	2.61363549	1.70468822
H	-0.54182579	4.12501207	0.87210397
H	-1.61162194	0.7305034	1.39293923
H	-3.80604199	-0.92616394	1.4588358
H	-3.49880412	-0.98885975	-0.26745456

52

Coordinates from ORCA-job conformer 009
Single point energy: -930.430301551874
Gibbs free energy: -930.02109690

C	-3.10809219	-0.94998119	0.17312695
C	-1.89342202	-1.837758	0.18403508
C	-1.30603718	-2.39808739	-0.87502116
C	-1.82863616	-2.25150821	-2.27853045
H	-1.16640871	-1.60787827	-2.86731188
H	-1.85199558	-3.22185635	-2.78299855
H	-2.82930006	-1.82418081	-2.31440065
C	-0.0434579	-3.22063839	-0.78568022
H	0.68486668	-2.79895002	-1.48946845
H	-0.26733428	-4.22282394	-1.17239458
C	0.6328489	-3.36346755	0.58669641
C	1.22472494	-2.09307107	1.13390853
C	2.44954041	-1.61028661	0.90786841
C	3.47034698	-2.27961014	0.0300506
H	3.1668402	-3.27844664	-0.27835908
H	3.64929799	-1.69447525	-0.87716807
H	4.43181225	-2.3546291	0.54732183
C	2.87999814	-0.31162773	1.54326165
H	3.76061098	-0.49170057	2.17111406
H	2.08376535	0.04296351	2.20179372
C	3.23020961	0.80669711	0.5465439
C	2.11601933	1.09912137	-0.4279462
C	0.81996619	1.75777696	0.05925474

C	-0.45386878	1.20921547	-0.36642496
C	-1.63050679	1.13204328	0.29841421
C	-1.78121876	1.63611345	1.6493375
O	-2.83208067	1.60261381	2.28438426
H	-0.88691193	2.07642311	2.11782445
C	-2.82597271	0.47181562	-0.36021956
H	-2.61224914	0.39477888	-1.42667009
O	-3.99958206	1.2839077	-0.2691203
H	-4.13103795	1.45871863	0.67571279
H	-0.45529289	0.79159136	-1.36856933
H	0.87523585	2.16866281	1.0579401
C	1.76167427	2.45256739	-0.94374965
C	2.47083514	3.68465721	-0.42427994
H	2.69295037	3.62158953	0.63997537
H	1.84860515	4.56867184	-0.5839752
H	3.4121694	3.83724484	-0.95976989
C	1.3495392	2.58098772	-2.39499698
H	2.22816685	2.81096457	-3.00343786
H	0.90946355	1.6654132	-2.7878011
H	0.62922805	3.39230224	-2.52799621
H	1.93842623	0.2968081	-1.1362619
H	3.48731137	1.70082663	1.11555806
H	4.12539502	0.53519576	-0.02092583
H	0.57743857	-1.49989554	1.77149379
H	1.41007141	-4.12402763	0.48720188
H	-0.0916458	-3.76070577	1.30285031
H	-1.43781356	-1.97581021	1.15557423
H	-3.90872971	-1.36501836	-0.44416449
H	-3.50101144	-0.8595194	1.18723211

52
Coordinates from ORCA-job conformer 013
Single point energy: -930.429498603893
Gibbs free energy: -930.02103131

C	-2.98136489	-0.72726922	-0.39436873
C	-2.44235174	0.67092112	-0.28425625
C	-2.7217107	1.56240207	0.66915706
C	-3.6206258	1.27233473	1.84050122
H	-4.44028455	1.99648289	1.88625841
H	-4.04859873	0.27255274	1.81441461
H	-3.06231777	1.37533674	2.77632415
C	-2.21191384	2.98539796	0.65503499
H	-1.81296788	3.22273667	1.64877266
H	-3.09185007	3.63140483	0.54628794
C	-1.17373232	3.38601632	-0.40174693
C	0.24485696	3.07412775	-0.02135774
C	1.21870893	2.51754195	-0.74761873

C	1.03629439	1.96858283	-2.13426886
H	1.24591477	0.8958889	-2.15717594
H	0.029351	2.11850759	-2.51760417
H	1.7389564	2.43955254	-2.82908607
C	2.63065328	2.48331342	-0.20709493
H	2.6341921	2.92177311	0.79402474
H	3.25554409	3.13019859	-0.83484947
C	3.30398165	1.10404907	-0.14068183
C	2.51486578	0.12179179	0.69262777
C	1.72206611	-0.99671931	0.01257958
C	0.34952537	-1.24255794	0.41035647
C	-0.66533851	-1.75051886	-0.32606759
C	-0.45813601	-2.23449102	-1.67936356
O	-1.33367047	-2.75360851	-2.36579028
H	0.55786944	-2.13915681	-2.09260873
C	-2.06892506	-1.79809949	0.23696115
H	-2.01228956	-1.60426473	1.30973077
O	-2.65415109	-3.09724413	0.11202375
H	-2.61169823	-3.31973328	-0.83089728
H	0.10212053	-0.95053718	1.42688712
H	1.95639969	-1.12689753	-1.03454893
C	2.91577221	-1.29316908	0.93573528
C	4.14702693	-1.85042783	0.2553917
H	4.28829753	-1.43904278	-0.7434425
H	4.07395013	-2.93718975	0.16707542
H	5.04025728	-1.62294222	0.84407585
C	2.66439406	-1.8891745	2.30373435
H	1.80964159	-1.43467354	2.80336962
H	2.48667626	-2.96549964	2.23400949
H	3.54064174	-1.73555277	2.93914563
H	1.98699468	0.58142939	1.52268907
H	3.45880794	0.70995089	-1.14686414
H	4.30057081	1.23697524	0.29247873
H	0.51680896	3.42992853	0.97137306
H	-1.24364395	4.47471211	-0.5141195
H	-1.43812847	2.97225169	-1.37441329
H	-1.75612082	0.95943846	-1.07102124
H	-3.95819589	-0.82149578	0.08121661
H	-3.11397745	-0.9790276	-1.44930624

52
Coordinates from ORCA-job conformer 003
Single point energy: -930.429150429653
Gibbs free energy: -930.02072358

C	-3.31151551	-0.24441335	-0.64127036
C	-2.4704211	-1.45362773	-0.90811096
C	-2.03746526	-2.36427833	-0.03379647

C	-2.35442168	-2.35270471	1.43427847
H	-2.97258531	-1.51055091	1.73704776
H	-2.8690914	-3.27619544	1.7184629
H	-1.42936202	-2.3244905	2.01879694
C	-1.12368986	-3.48929243	-0.49195688
H	-1.59337101	-4.04321239	-1.30899218
H	-0.98438797	-4.19797485	0.32809896
C	0.25677164	-2.99393196	-0.96540766
C	0.95650316	-2.15853687	0.06372235
C	2.26208706	-2.07152267	0.32636083
C	3.3317138	-2.8496457	-0.38621262
H	3.97605662	-3.3652659	0.33256439
H	2.92748184	-3.58780101	-1.07647028
H	3.98053965	-2.17902361	-0.95906635
C	2.74729525	-1.07098776	1.34633376
H	3.49573381	-1.53157153	1.99969357
H	1.90924339	-0.76868968	1.97824127
C	3.36195839	0.19576858	0.71908871
C	2.43170973	0.87164205	-0.26026479
C	1.14436247	1.53297816	0.23593142
C	-0.10971443	1.29478489	-0.45719344
C	-1.37281348	1.29082316	0.03033742
C	-1.64579388	1.53606155	1.43594586
O	-2.77206379	1.66425989	1.90621449
H	-0.7752981	1.61222486	2.10613814
C	-2.55868167	1.07728866	-0.89094046
H	-2.18921569	1.07258151	-1.91850295
O	-3.46314385	2.18702918	-0.81957744
H	-3.74635371	2.24118077	0.10569845
H	-0.01486262	1.10998817	-1.52332524
H	1.09571824	1.66888012	1.3073636
C	2.27844167	2.34593885	-0.4242815
C	3.0080985	3.3052177	0.49021976
H	4.02472477	3.47979687	0.12657176
H	3.0728344	2.93856548	1.51362154
H	2.49147894	4.26792689	0.51188484
C	2.08750341	2.89509107	-1.82185111
H	3.05938145	3.16412103	-2.24399157
H	1.62570995	2.17340379	-2.49432057
H	1.46838104	3.79579509	-1.80818033
H	2.28900935	0.30955405	-1.17637922
H	3.63615376	0.87802881	1.52476139
H	4.29056945	-0.05707824	0.19874277
H	0.30366308	-1.50028835	0.6276547
H	0.10428736	-2.39176742	-1.86924677
H	0.86414294	-3.84944733	-1.26699252
H	-2.15902004	-1.56821844	-1.94529446

| H | -4.17147228 | -0.23490021 | -1.31880351 |
| H | -3.70416195 | -0.23814853 | 0.37413339 |

Optimised geometries of 1*S*,2*S*,5*S*-156 conformers

52

Coordinates from ORCA-job conformer 013

Single point energy: -930.431398773673

Gibbs free energy: -930.0227583

C	-2.23473691	-2.01588196	-0.64369368
C	-1.03839129	-2.61669059	0.03339621
C	0.19444004	-2.80341154	-0.4447719
C	0.64282713	-2.40172622	-1.82144914
H	1.4055174	-1.61949585	-1.76555677
H	1.10270875	-3.25084709	-2.33619624
H	-0.17207702	-2.03418739	-2.44168992
C	1.23963895	-3.48014431	0.41043543
C	2.553351	-2.69446199	0.57300787
C	2.34204894	-1.31394897	1.12792596
C	3.06838934	-0.22057154	0.88287875
C	4.27692143	-0.20323603	-0.01308358
H	4.08943742	0.38184936	-0.91876424
H	4.58949488	-1.19966663	-0.31723509
H	5.11886629	0.27538112	0.49631957
C	2.696021	1.10787458	1.49473956
C	2.34989694	2.19093371	0.4552582
C	1.24805748	1.7405663	-0.46861772
C	0.31130777	2.62742854	-1.2124571
C	-0.20817826	1.81073317	-0.01006388
C	-1.05536375	0.64472279	-0.18495809
C	-2.1621976	0.28806157	0.50510474
C	-2.73327045	1.15351339	1.52478744
O	-3.80927941	0.93742085	2.07187251
H	-2.16508379	2.05758979	1.79440326
C	-2.93676185	-0.9874997	0.23694712
O	-4.20288539	-0.68581756	-0.3763963
H	-4.69265132	-0.15009347	0.26284012
H	-3.13090037	-1.45709281	1.20863944
H	-0.73353317	-0.02572569	-0.97094121
H	-0.37460462	2.41661125	0.8698152
C	-0.09682289	2.22178789	-2.61253646
H	-1.11001932	2.56361897	-2.83917312
H	0.58020017	2.67853068	-3.33942859
H	-0.06028374	1.14292679	-2.75935034
C	0.35149571	4.12667994	-1.01468316

H	1.10647342	4.57500127	-1.66679218
H	0.58443669	4.4042425	0.01240497
H	-0.61491881	4.56775485	-1.2711475
H	1.47956425	0.81774021	-0.98934301
H	3.23692513	2.43880151	-0.1354222
H	2.06536045	3.10261506	0.98243056
H	1.83964134	0.97047305	2.15923717
H	3.52727372	1.47481125	2.10753874
H	1.49090177	-1.21008729	1.79715721
H	3.20204257	-3.27349052	1.24108349
H	3.07351142	-2.6497314	-0.38465632
H	0.81584003	-3.67925755	1.39773458
H	1.48510489	-4.45295597	-0.03192192
H	-1.22875765	-2.95220869	1.0509182
H	-1.99462978	-1.57998435	-1.61383719
H	-2.97549399	-2.80007703	-0.83350568

52

Coordinates from ORCA-job conformer 017

Single point energy: -930.429899451491

Gibbs free energy: -930.02157607

C	-2.98852923	-0.11312131	0.84491561
C	-2.55381018	1.18629331	0.23844232
C	-1.72064491	2.10464075	0.73411828
C	-1.0215002	1.99296978	2.05956081
H	0.06096617	1.92547136	1.91813141
H	-1.20382444	2.8870382	2.66379419
H	-1.34042211	1.12682151	2.63536239
C	-1.44646261	3.371023	-0.04225536
C	0.04518403	3.68884997	-0.25450164
C	0.79369197	2.561771	-0.90604656
C	2.0534543	2.18076648	-0.67978407
C	2.97507051	2.86264167	0.29454912
H	3.23095507	2.20131528	1.12771646
H	2.5505777	3.77407385	0.70916989
H	3.91836929	3.1219431	-0.19622944
C	2.64700127	1.00621987	-1.41924529
C	3.1562945	-0.12195497	-0.5042905
C	2.0807378	-0.63976491	0.4161611
C	2.01134888	-2.01880641	0.97652216
C	1.02205999	-1.6037604	-0.12859058
C	-0.37822711	-1.35278882	0.15653722
C	-1.46203167	-1.5729579	-0.62212238
C	-1.33144997	-2.12951702	-1.964708
O	-2.26327958	-2.31902207	-2.7317548
H	-0.30893356	-2.38062176	-2.29092709
C	-2.86706148	-1.28189799	-0.13881054

O	-3.46699268	-2.47169243	0.40738982
H	-2.89129296	-2.79459893	1.11234379
H	-3.47568579	-1.05760104	-1.01536292
H	-0.56280897	-0.9149284	1.13034263
H	1.26427074	-2.0207426	-1.0958331
C	1.51536751	-2.18479143	2.3973459
H	0.83744326	-1.38700545	2.69868879
H	0.999084	-3.14003783	2.52379963
H	2.36514459	-2.17126483	3.08491033
C	3.03408074	-3.06214832	0.58224257
H	2.62749594	-4.06457873	0.73743097
H	3.93216879	-2.9667155	1.19899532
H	3.33093091	-2.98009043	-0.46236139
H	1.66683647	0.12153908	1.06852199
H	3.99849376	0.23563787	0.09552477
H	3.54476311	-0.92584186	-1.13088724
H	1.89938555	0.59741138	-2.10316408
H	3.4891275	1.35141962	-2.03047811
H	0.22501964	1.99697188	-1.64173179
H	0.10323199	4.58760136	-0.88007591
H	0.50109298	3.95625326	0.69912816
H	-1.94313878	3.30640354	-1.01335386
H	-1.89585114	4.21903304	0.48828132
H	-2.99086582	1.38968638	-0.73731774
H	-2.44811742	-0.33994475	1.76529818
H	-4.048143	-0.05832682	1.11682794

52

Coordinates from ORCA-job conformer 092

Single point energy: -930.429576748674

Gibbs free energy: -930.02076067

C	-3.37417951	-0.32650924	-0.34189748
C	-2.46906604	-1.4006646	-0.86634535
C	-1.7791586	-2.29250892	-0.14846117
C	-1.75711562	-2.32389311	1.35479968
H	-1.86941321	-3.34776034	1.72257494
H	-0.79797943	-1.95767428	1.73162343
H	-2.53596185	-1.71175034	1.80299487
C	-1.01489116	-3.40147537	-0.83144829
C	0.41791463	-3.6513416	-0.32525212
C	1.42382703	-2.61477393	-0.7271696
C	2.26732081	-1.92475494	0.04713266
C	2.28514343	-1.98540926	1.54964939
H	2.02590865	-1.01417927	1.9798693
H	3.28915364	-2.2284313	1.91160293
H	1.59204626	-2.71993345	1.95272883
C	3.35707469	-1.08275034	-0.57522559

C	3.41752886	0.38899464	-0.14352379
C	2.23726335	1.19136707	-0.63201475
C	1.9545302	2.59483468	-0.20991855
C	1.02476748	1.45497714	0.25217009
C	-0.31328697	1.32857862	-0.3066157
C	-1.49742649	1.23686501	0.33532043
C	-1.58054348	1.27785173	1.78687968
O	-2.62451753	1.22662419	2.42295912
H	-0.62363181	1.37301793	2.3258281
C	-2.80122832	1.09722603	-0.42551049
O	-2.6682709	1.41960289	-1.81152954
H	-2.44104059	2.3545791	-1.88744625
H	-3.53324328	1.76849678	0.0353881
H	-0.36363091	1.32253947	-1.38994414
H	1.15280673	1.19860182	1.2946031
C	1.4589989	3.57909699	-1.2472291
H	0.80355871	4.32785384	-0.79396628
H	2.30802138	4.10551964	-1.69160781
H	0.91151903	3.09198952	-2.05327817
C	2.79283485	3.24222273	0.87060314
H	2.23310595	4.0482819	1.35190215
H	3.69870175	3.67804267	0.43928978
H	3.0935704	2.53506781	1.64246974
H	1.97551916	0.98030192	-1.66534439
H	4.3339399	0.82434982	-0.55544944
H	3.50821545	0.45920716	0.94136098
H	4.31925073	-1.54296595	-0.3182435
H	3.27014592	-1.12873131	-1.66393227
H	1.51277931	-2.47249468	-1.80301972
H	0.40496183	-3.79703696	0.75403059
H	0.74191903	-4.60742831	-0.75361501
H	-1.57605632	-4.33158086	-0.67546525
H	-0.99703251	-3.22450012	-1.90990999
H	-2.3916792	-1.46062739	-1.94821791
H	-4.30491437	-0.32234523	-0.91698222
H	-3.64135799	-0.50378276	0.69810939

52

Coordinates from ORCA-job conformer 055

Single point energy: -930.429803713468

Gibbs free energy: -930.02071807

C	2.29002059	1.80887369	-0.74503293
C	0.94147297	2.33140251	-0.3390675
C	-0.13647962	2.50441762	-1.1050705
C	-0.1694138	2.23022914	-2.58341644
H	-0.55446167	3.10204622	-3.12148885
H	0.80503928	1.98387661	-2.9994476

H	-0.85536787	1.40437592	-2.80018763
C	-1.46104079	2.98934771	-0.55729344
C	-1.69736909	2.84409805	0.95458612
C	-1.67820818	1.41299645	1.42373957
C	-2.67886536	0.53232508	1.33593472
C	-4.03185109	0.8579918	0.76506798
H	-4.17655899	1.92639466	0.61439167
H	-4.82432711	0.49188674	1.42465523
H	-4.17802933	0.36564631	-0.20142872
C	-2.4833629	-0.89885424	1.77230008
C	-2.48514775	-1.91018074	0.60791352
C	-1.42431009	-1.58738281	-0.41279099
C	-0.66943072	-2.56254318	-1.24860149
C	0.04972922	-1.86866238	-0.08075592
C	0.99043773	-0.78077025	-0.26438398
C	2.04688961	-0.43005432	0.50576004
C	2.48838648	-1.25819271	1.6138778
O	3.49845819	-1.02860554	2.27230662
H	1.88490505	-2.14868526	1.84989266
C	2.85574168	0.83377033	0.28245995
O	4.2004567	0.52098874	-0.11588703
H	4.58393589	0.01175097	0.6120084
H	2.895819	1.3544681	1.24782787
H	0.7673425	-0.13801235	-1.10434338
H	0.19179298	-2.5107906	0.77720201
C	-0.33289804	-2.16786007	-2.67090036
H	-0.22812471	-1.09034259	-2.78977649
H	0.59706137	-2.64051629	-2.99729469
H	-1.13001137	-2.49842361	-3.34206622
C	-0.89425484	-4.04997491	-1.08272928
H	-1.75467975	-4.37244203	-1.67565052
H	-1.07452121	-4.32966485	-0.04561365
H	-0.02000447	-4.60428954	-1.43281501
H	-1.56739174	-0.62323553	-0.88762756
H	-3.46406842	-1.9168097	0.1189959
H	-2.33580785	-2.91000349	1.01790903
H	-1.53390117	-0.98655976	2.30544113
H	-3.27723184	-1.18065839	2.47275205
H	-0.7364615	1.05424864	1.82618728
H	-0.94891223	3.41916912	1.50449556
H	-2.66067127	3.30693021	1.18175595
H	-1.59744213	4.03902153	-0.84715799
H	-2.25427498	2.44124016	-1.07668424
H	0.85772954	2.55998229	0.71870774
H	2.27070752	1.3343392	-1.72695304
H	3.01132354	2.63033097	-0.81210142

52

Coordinates from ORCA-job conformer 039

Single point energy: -930.429149404836

Gibbs free energy: -930.02049284

C	-3.20147168	-1.14119649	0.37424945
C	-2.80355369	0.17610143	0.96710757
C	-2.59089548	1.32252082	0.31385766
C	-2.67659903	1.46606863	-1.18057263
H	-1.67749828	1.56255657	-1.61478506
H	-3.15800378	0.61775343	-1.66103373
H	-3.22553596	2.37264804	-1.45075924
C	-2.30974443	2.59748351	1.07208043
C	-1.12463877	3.44039657	0.56477925
C	0.23203598	2.88667007	0.88249692
C	1.25002689	2.640818	0.05158374
C	1.17671988	2.7768142	-1.44410524
H	1.31733863	1.80687177	-1.92883905
H	1.9775851	3.42713996	-1.80986312
H	0.22724815	3.18134659	-1.78658202
C	2.61490429	2.29544454	0.60152263
C	3.27024934	1.01369884	0.06866634
C	2.55610299	-0.24006161	0.50898719
C	2.86321201	-1.60163283	-0.02005077
C	1.52468875	-0.92710351	-0.37853579
C	0.28009968	-1.40568079	0.20382425
C	-0.87182879	-1.739646	-0.41761098
C	-0.9994459	-1.68183359	-1.8643045
O	-1.99951278	-2.01022603	-2.48907439
H	-0.11336393	-1.32525621	-2.41349698
C	-2.08132713	-2.20248279	0.35592806
O	-1.67532832	-2.55096009	1.68198382
H	-2.46137548	-2.83501946	2.16335578
H	-2.48256904	-3.09010563	-0.14594761
H	0.28629005	-1.52452779	1.28051032
H	1.48935586	-0.56852491	-1.39775378
C	2.87036984	-2.76894087	0.9432864
H	2.56985788	-3.69208345	0.44044793
H	3.88037567	-2.91664018	1.33530397
H	2.20448368	-2.61283079	1.79091518
C	3.84435035	-1.76759051	-1.15986752
H	4.86842032	-1.81069695	-0.77778719
H	3.78703068	-0.95224602	-1.87971575
H	3.64911704	-2.70148466	-1.69310367
H	2.27812592	-0.22643899	1.55938692
H	4.29895166	0.98136076	0.44270493
H	3.34400017	1.05381531	-1.01908891
H	3.286225	3.13078112	0.36621684

H	2.55917829	2.23803502	1.69172917
H	0.41656633	2.74082543	1.9456864
H	-1.2387537	3.62826269	-0.50194182
H	-1.20154995	4.4196676	1.05230335
H	-3.2053117	3.22747303	0.99952888
H	-2.17102604	2.37126164	2.13240927
H	-2.68942333	0.18732202	2.04745632
H	-4.03045904	-1.56558028	0.95277301
H	-3.55973714	-1.03052497	-0.64772349

52

Coordinates from ORCA-job conformer 001

Single point energy: -930.428183188577

Gibbs free energy: -930.02034726

C	-2.90082703	-1.19621618	0.58305727
C	-2.89648003	0.20562421	0.05237154
C	-2.4605722	1.32370898	0.63805223
C	-1.84828399	1.38341146	2.00892794
H	-2.35852946	2.13158568	2.62325344
H	-1.88979898	0.43156989	2.53419245
H	-0.80018095	1.69003049	1.94752935
C	-2.58799043	2.64799157	-0.07762182
C	-1.28437284	3.46190958	-0.17024857
C	-0.15962739	2.69041612	-0.79958159
C	1.14182201	2.76567414	-0.50978615
C	1.71830556	3.69377533	0.52455004
H	0.98068866	4.38118491	0.9323879
H	2.52880838	4.28674582	0.08938634
H	2.1557215	3.13585265	1.35786449
C	2.14279966	1.89298355	-1.2267753
C	2.94398191	0.96564347	-0.29535698
C	2.04771099	0.08326085	0.53482361
C	2.410639	-1.25100602	1.07932827
C	1.4202322	-1.16220906	-0.10497726
C	0.00552339	-1.40371003	0.07107177
C	-0.86073795	-2.00810595	-0.77473434
C	-0.48604022	-2.56888631	-2.07508465
O	0.62690373	-2.61260286	-2.57569112
H	-1.34427854	-2.98746345	-2.63709169
C	-2.32051798	-2.19865641	-0.41921747
O	-2.55131378	-3.55260683	0.01908004
H	-1.92246052	-3.74114928	0.7278598
H	-2.90602849	-2.12093833	-1.3396703
H	-0.40728455	-1.02881205	0.99979448
H	1.84143713	-1.45828699	-1.0521348
C	1.89630527	-1.62402214	2.45325271
H	0.96593379	-1.11472598	2.70192475

H	1.72947934	-2.7015894	2.53028864
H	2.63631711	-1.34623892	3.20867369
C	3.75059902	-1.87589857	0.75823173
H	4.51678217	-1.50339491	1.44441072
H	4.07444869	-1.66373421	-0.25944301
H	3.69777428	-2.96121573	0.87373838
H	1.35214556	0.63704226	1.15618713
H	3.57615347	1.5608526	0.37066126
H	3.61876882	0.36281171	-0.90410688
H	1.6226518	1.28325161	-1.96921841
H	2.85466389	2.5263711	-1.76879456
H	-0.45967063	1.98779268	-1.57396321
H	-1.5004206	4.36065447	-0.76026242
H	-1.00271661	3.8153038	0.82217115
H	-2.97422591	2.47123695	-1.08440713
H	-3.33030897	3.26445187	0.44330153
H	-3.31434674	0.3021825	-0.94795026
H	-2.38193691	-1.28014207	1.53893105
H	-3.93178354	-1.51802057	0.76506664

52

Coordinates from ORCA-job conformer 042

Single point energy: -930.429151453692

Gibbs free energy: -930.02033265

C	-3.3591269	-0.66512435	0.30215166
C	-2.82601006	0.62086139	0.86229778
C	-2.36177995	1.67058202	0.17623186
C	-2.27280797	1.71693567	-1.32311808
H	-1.23229486	1.63132088	-1.64813388
H	-2.83153657	0.91835346	-1.80439129
H	-2.64277725	2.6739214	-1.70164035
C	-1.96041191	2.93764887	0.8926082
C	-0.64152061	3.58584955	0.43365922
C	0.60416699	2.84416703	0.81762141
C	1.61784452	2.45988198	0.03487763
C	1.63875522	2.60978624	-1.46160167
H	0.77551282	3.1470954	-1.84679476
H	1.66448459	1.63129878	-1.94884334
H	2.54123128	3.14055481	-1.78056573
C	2.8931854	1.92392982	0.64360202
C	3.3822412	0.56144931	0.13180551
C	2.49549633	-0.58017276	0.56147835
C	2.61204101	-1.97244984	0.03547548
C	1.38348154	-1.11790624	-0.33141595
C	0.08135202	-1.40984886	0.25124569
C	-1.102159	-1.60536543	-0.36664888
C	-1.19845101	-1.62742758	-1.81794783
O	-2.22482094	-1.85960355	-2.44216887
H	-0.26189119	-1.44168752	-2.36870431
C	-2.37920462	-1.85174751	0.41419101
O	-2.13502944	-2.18898839	1.77882618
H	-1.90284058	-1.38521534	2.26062948
H	-2.87195203	-2.72849989	-0.01028072
H	0.07615278	-1.4965022	1.33205736
H	1.40072433	-0.76072398	-1.351726
C	2.44804285	-3.12818902	0.99877311
H	1.80767279	-2.87726972	1.84349372
H	2.0200594	-3.99895938	0.49494411
H	3.42457977	-3.41903051	1.39537522
C	3.56597193	-2.27585487	-1.09916442
H	3.62618091	-1.46159845	-1.8200111
H	3.24455522	-3.1742456	-1.63226328
H	4.57221562	-2.46091722	-0.7121184
H	2.21330303	-0.52765775	1.60966971
H	4.38788418	0.39246439	0.53074023
H	3.48602614	0.58267165	-0.95388734
H	3.68581284	2.65529581	0.44233039
H	2.78222074	1.87570796	1.73004279
H	0.71271934	2.67355684	1.88756469
H	-0.67938724	3.76952091	-0.63916189
H	-0.59577879	4.57471172	0.90549662
H	-2.75440163	3.67652818	0.72606118
H	-1.92533595	2.75440683	1.96962177
H	-2.84208384	0.70865436	1.94668258
H	-4.26425483	-0.95238291	0.84509491
H	-3.6318659	-0.56205705	-0.74642015

52

Coordinates from ORCA-job conformer 019

Single point energy: -930.428264599861

Gibbs free energy: -930.02032472

C	-2.90065524	-1.53745382	0.46495453
C	-2.52739715	-0.18871317	1.00329513
C	-2.89177008	1.00946036	0.5417671
C	-3.81557663	1.21770307	-0.62591755
H	-4.61855872	1.90882463	-0.35206443
H	-3.28850983	1.6714098	-1.47000145
H	-4.26986671	0.29283319	-0.97397181
C	-2.37617733	2.26477969	1.20162387
C	-1.6272643	3.22269956	0.24931753
C	-0.50658393	2.56981887	-0.50142001
C	0.80244969	2.83108501	-0.44097015
C	1.42722627	3.85405694	0.46661537
H	2.09161631	3.3757018	1.19213906

H	0.69210925	4.43202052	1.02230206
H	2.04558169	4.54997817	-0.10916529
C	1.75979608	2.10800072	-1.35825298
C	2.90583062	1.35428519	-0.66588792
C	2.43118152	0.2809586	0.28228231
C	3.1246483	-1.02499744	0.49621516
C	1.80181869	-0.99875308	-0.28328761
C	0.57386924	-1.52032326	0.29490776
C	-0.52834828	-1.99726962	-0.32380859
C	-0.6474378	-1.99915499	-1.77265308
O	-1.63270381	-2.39067376	-2.38446806
H	0.218007	-1.61220126	-2.33477424
C	-1.71954135	-2.52655455	0.4571429
O	-1.3719487	-2.93476629	1.78144003
H	-1.31799177	-2.16088855	2.35422646
H	-2.05831635	-3.43934862	-0.03539526
H	0.55351602	-1.53338922	1.37844476
H	1.9265865	-1.10508952	-1.35215665
C	3.15644427	-1.5888193	1.90101895
H	3.14959828	-2.68182155	1.88709619
H	4.07318832	-1.26642334	2.4015084
H	2.31761604	-1.24976771	2.5077344
C	4.35762578	-1.38380314	-0.30540451
H	4.49886667	-2.46746011	-0.3059903
H	5.24883962	-0.93082373	0.13795687
H	4.29173869	-1.05718216	-1.34215841
H	1.91910445	0.66333544	1.15911226
H	3.538362	2.0566854	-0.11508436
H	3.53741063	0.91934588	-1.44126049
H	1.19866237	1.40391482	-1.97720421
H	2.20894342	2.84180977	-2.03871392
H	-0.81750488	1.79143	-1.19402696
H	-2.3438892	3.62430206	-0.47509261
H	-1.27416001	4.07331271	0.83215841
H	-3.21851211	2.817665	1.63435066
H	-1.71125777	1.99142652	2.02420967
H	-1.87002405	-0.18737093	1.87090141
H	-3.68905985	-1.99579472	1.07288015
H	-3.28186922	-1.46408768	-0.55188832

5.2 OPTIMISED GEOMETRIES OF THE RHODIUM AND BISMUTH COMPLEXES

Cartesian coordinates (in Å), electronic energies (in a.u.). Calculations reported at the BP86-D3BJ-(CPCM)/ZORA-def2-TZVP level.

86

Coordinates from ORCA-job [RhRh(MEPY)₄]·2MeCN

Single point energy: -12000.058831422017

Rh	3.75859638	9.72477119	12.2378933
Rh	6.12772809	9.37083194	12.953055
O	6.58966986	8.61152475	11.0443895
O	1.36281544	7.17006434	9.65384348
O	3.31067738	6.20380347	10.2936691
O	6.60349303	11.3045646	12.2644988
O	1.43550422	12.9118032	10.0377323
O	3.12903177	11.7168313	9.12097382
O	3.32981781	10.6061455	14.1088115
O	7.89177273	8.88221856	16.9526465
O	3.2483289	7.85670908	13.0655578
O	6.5656021	5.37279918	11.8698987
O	8.42458496	5.7507306	13.1135114
N	4.34359957	8.82718833	10.5217211
N	4.39050349	11.554513	11.6113671
N	1.7186047	9.96743741	11.6288818
N	5.48974713	7.54677402	13.5507685
N	5.53468071	10.2089017	14.6969345
N	8.15823874	9.04409452	13.5731799
C	5.58803843	8.46067208	10.2627647
C	5.71956091	7.80355529	8.90444706
H	5.88790145	6.72544981	9.04733664
H	6.57933829	8.20630265	8.35314238
C	4.3664584	8.1102337	8.24619046
H	4.43969146	9.0097975	7.62106847
H	3.98471868	7.29213268	7.62309334
C	3.43476494	8.42887801	9.45086975
H	2.73454622	9.23949233	9.22755398
C	2.57206142	7.2256195	9.8204597
C	2.57850565	5.0027675	10.634236
H	2.04412986	4.61949184	9.75562995
H	1.86365103	5.21425211	11.4393479
H	3.33608993	4.28806023	10.9683544

C	0.63034194	10.0188183	11.2255799
C	-0.707957	10.098757	10.6836222
H	-0.8356257	11.061564	10.1688003
H	-1.4517772	10.0186831	11.4882283
H	-0.8638129	9.28125349	9.96617283
C	5.61534426	12.0013988	11.8464312
C	5.73916331	13.4952155	11.6342269
C	4.41103751	13.8710579	10.9679256
C	3.48399481	12.6549211	11.2890772
C	2.553145	12.4230232	10.1132064
C	2.32396304	11.5565023	7.9263986
C	4.30909663	10.6491913	14.9311177
C	4.16780962	11.2294385	16.3242329
H	3.58988696	10.5290044	16.9463119
H	3.62359599	12.1825662	16.3012149
C	5.62652695	11.364666	16.7856869
C	6.39465608	10.3715083	15.8632994
C	6.60107799	9.03909404	16.5781375
C	8.18544675	7.66909194	17.6912759
H	7.57654989	7.6209575	18.6025793
C	9.20438958	8.74168703	13.9780123
C	10.4862676	8.32693902	14.5053633
H	11.2860974	8.55046101	13.7862125
H	10.467906	7.24485342	14.6964398
H	10.6914087	8.85468274	15.4469879
C	4.22579284	7.16053231	13.5091393
C	4.03532018	5.76435146	14.0657186
H	3.80272355	5.0735799	13.2429592
H	3.19337498	5.73853349	14.7702465
C	5.39339211	5.46870602	14.7196962
H	5.71925632	4.42824077	14.5992219
H	5.36477636	5.70311869	15.7909144
C	6.35733253	6.47791729	14.036072
C	7.09517422	5.81904954	12.8732884
C	9.21647245	5.12365061	12.0729645
H	9.11622574	5.68577266	11.1361332
H	8.89103085	4.08710596	11.9189669
H	10.2482796	5.1559436	12.4348408
O	5.72096369	8.23390236	16.8294923
H	4.5427692	13.9576632	9.88109014
H	6.62324759	13.7442396	11.0328087
H	5.86459841	13.9695728	12.620625
H	3.9789988	14.8078606	11.3364936
H	5.77177804	11.1477546	17.8511685
H	6.00102052	12.3774341	16.5886043
H	7.37574481	10.7615383	15.5668147
H	7.98371625	6.79018303	17.0657059

H	9.24942125	7.72999596	17.9374379
H	7.09939565	6.87436461	14.7374405
H	2.83411863	12.8677532	12.1525657
H	1.40333987	11.0073236	8.16149947
H	2.94692658	10.984404	7.23285952
H	2.07132203	12.53693	7.50386156

74

Coordinates from ORCA-job [RhRh(MEPY)$_4$]

Single point energy: -11734.155165757438

Rh	3.82766857	9.70837392	12.2797167
Rh	6.12320156	9.29069341	12.9976987
O	6.59257097	8.46956735	11.1374902
O	1.30295244	7.28708365	10.0118913
O	3.2226967	6.11883181	10.3206645
O	6.71354992	11.1635346	12.2870833
O	1.49691694	12.6224761	10.1485751
O	3.27597501	11.7020383	9.08421199
O	3.38744583	10.6430076	14.0952187
O	7.75334928	8.60667319	16.9607887
O	3.21977692	7.88623618	13.1026278
O	6.57008806	5.13730263	11.9929796
O	8.28000674	6.4115022	12.7760209
N	4.36417246	8.75886101	10.5877623
N	4.51851259	11.4879046	11.6167241
N	5.44152858	7.50908479	13.6215324
N	5.56406131	10.164369	14.7251081
C	5.59235222	8.33248396	10.3453905
C	5.70090974	7.6305704	9.01122026
H	5.83930798	6.5535946	9.18874346
H	6.57041133	7.99163881	8.44675884
C	4.35398806	7.95552218	8.34518226
H	4.45450968	8.82298983	7.68037636
H	3.94264577	7.12269532	7.76289672
C	3.4341298	8.35722604	9.53250878
H	2.76817732	9.18921516	9.27864371
C	2.52120829	7.21929208	9.98696787
C	2.43360133	4.97179408	10.7229366
H	1.79356403	4.64526229	9.89337169
H	1.81260354	5.22678593	11.5904504
H	3.16130801	4.19629023	10.9786057
C	5.7618475	11.8916572	11.8293763
C	5.94523319	13.3636531	11.5389716
C	4.62759301	13.7568354	10.8567767
C	3.64988843	12.6095124	11.2571528
C	2.67467645	12.3032552	10.130751
C	2.43465233	11.4845351	7.92207011

C	4.35389271	10.6553724	14.9391086
C	4.21780031	11.2494933	16.3237993
H	3.58628966	10.5883925	16.936029
H	3.73222164	12.2331115	16.2830293
C	5.67323279	11.301803	16.8154947
C	6.40265828	10.2594773	15.9163309
C	6.47977735	8.90844895	16.6265928
C	7.92780572	7.37866659	17.716789
H	7.36870722	7.43399232	18.6590697
C	4.17073256	7.14877741	13.5501249
C	3.94544501	5.74505373	14.0624791
H	3.66394853	5.09583547	13.2222584
H	3.12097045	5.725448	14.7874971
C	5.30920444	5.36943218	14.66726
H	5.60842917	4.33926579	14.4432395
H	5.29716528	5.50109702	15.7560085
C	6.29356303	6.39818988	14.0652271
C	7.04037213	5.8843111	12.8348539
C	9.02592127	6.12300964	11.5648149
H	8.49876746	6.55178695	10.7039944
H	9.1398961	5.03942649	11.4379239
H	9.99901225	6.60281343	11.7031623
O	5.51944247	8.20768021	16.8952399
H	4.75260893	13.7679093	9.76663386
H	6.83474887	13.5424987	10.9211153
H	6.09586178	13.8850605	12.4975213
H	4.24278049	14.7327888	11.1721254
H	5.78205195	11.0806943	17.8840403
H	6.11076503	12.289339	16.6215942
H	7.4185373	10.5799988	15.6520164
H	7.57823179	6.52048107	17.1292174
H	9.00254304	7.30574174	17.9051907
H	7.03079745	6.75613434	14.7953818
H	3.06929535	10.9613068	7.20119423
H	2.09854986	12.4473958	7.51729847
H	1.5638672	10.8732703	8.19002057
H	3.03318325	12.8928956	12.1246071

80
Coordinates from ORCA-job [BiRh(MEPY)₄]·MeCN
Single point energy: -29420.354933194278

C	4.40802365	3.125648	7.52233652
C	3.78115225	1.78240242	7.84373905
C	3.57614176	1.84981217	9.36084691
H	3.74441477	0.89423919	9.87276425
H	2.56513987	2.20133831	9.59866917

C	4.58212084	2.95042216	9.80473341
H	4.17945887	3.56450673	10.6165459
C	5.86374623	2.29190979	10.2996272
C	7.07526848	1.66207069	12.2431515
H	6.94391488	1.76712264	13.3238759
H	8.01360351	2.13135425	11.9219148
H	7.07178705	0.6049413	11.9501108
C	5.64819509	5.66188627	12.0153927
C	5.64353119	5.66835741	13.4588903
Bi	5.64657765	5.65597785	6.06260177
N	4.81418582	3.76140061	8.61071919
N	5.65087122	5.65748507	10.8561372
O	4.51147085	3.5510745	6.32027075
O	6.68291293	1.72761896	9.59556325
O	5.94431807	2.35104259	11.6502309
Rh	5.65120333	5.65609762	8.67517964
C	6.88685948	8.18831476	7.51821115
C	7.5114142	9.53326874	7.83751545
H	6.81044873	10.3285823	7.54117906
H	8.43736016	9.6751003	7.26529572
C	7.72755483	9.46266877	9.35281105
H	7.56505382	10.4170123	9.86885522
H	8.74002934	9.10886058	9.58110869
C	6.72463738	8.36142432	9.80155954
H	7.13120627	7.74735376	10.6115214
C	5.44468616	9.01856399	10.3029951
C	4.24398474	9.64854286	12.2532318
H	4.37889055	9.5392383	13.3330847
H	3.30434107	9.18112367	11.9330429
H	4.24718546	10.7068286	11.9642827
N	6.48757995	7.55077652	8.60822887
O	6.77786372	7.76357282	6.31641266
O	4.62121228	9.5821068	9.60334673
O	5.37256718	8.961169	11.6541141
C	8.18141704	4.4167567	7.51771004
C	9.525927	3.79126844	7.83706748
H	10.3217266	4.49033362	7.53756335
H	9.6658109	2.86344542	7.26740359
C	9.45719657	3.57971968	9.35306947
H	10.4124714	3.74247149	9.86731176
H	9.10227408	2.56845505	9.58488576
C	8.35784514	4.58530141	9.80034137
H	7.74464611	4.18206673	10.6125943
C	9.0177488	5.86578945	10.2966773
C	9.65723332	7.06867055	12.2427488
H	9.55503655	6.93363165	13.3233005
H	9.18928225	8.00924047	11.9261761

H	10.7135391	7.06382394	11.9467344
N	7.5455972	4.81943305	8.60748764
O	7.7552852	4.5226783	6.31613805
O	9.58039412	6.68679605	9.59343884
O	8.96392469	5.94138301	11.6478597
C	3.11883347	6.89594784	7.52264256
C	1.77446337	7.52055985	7.8443672
H	0.97855563	6.82109329	7.54602062
H	1.63311043	8.44839265	7.27511144
C	1.84565009	7.73184629	9.36039031
H	0.89134297	7.56831552	9.87615999
H	2.20028186	8.74328822	9.5920735
C	2.94630139	6.72676958	9.80552826
H	3.56078731	7.13066365	10.6164505
C	2.28884151	5.44556091	10.3032794
C	1.66099448	4.23813352	12.2500212
H	1.77044318	4.36968056	13.3302741
H	2.12916757	3.29985767	11.9268771
H	0.60266473	4.24137148	11.9612621
N	3.75641842	6.49292565	8.61118768
O	3.54345451	6.79088539	6.32047263
O	1.72430622	4.62455081	9.60160835
O	2.3473786	5.36905206	11.654193
H	4.4764165	0.98474346	7.54041545
H	2.85049327	1.6455246	7.2779476
H	6.50114588	6.2461533	13.8294926
H	5.71204551	4.63762943	13.8328366
H	4.71331334	6.1248723	13.8236614

74

Coordinates from ORCA-job [BiRh(MEPY)$_4$]

Single point energy: -29287.406796620849

C	4.35603858	3.17007722	7.565822
C	3.72295255	1.83399198	7.8944181
C	3.59926301	1.87704763	9.42301026
H	3.78359893	0.91073538	9.90810002
H	2.60489297	2.23256871	9.71550008
C	4.64503532	2.95836885	9.8347714
H	4.29579005	3.56842316	10.6783718
C	5.93575432	2.26025489	10.2496158
C	7.18017902	1.49865019	12.1262329
H	7.0672937	1.53935709	13.2133489
H	8.12858607	1.95745882	11.8211252
H	7.13631372	0.46326827	11.7667115
Bi	5.64962368	5.65784998	6.07680603
N	4.82477248	3.77895745	8.64063075
O	4.41582804	3.62486578	6.36791764

O	6.71269577	1.70953803	9.48962335
O	6.06327034	2.26021619	11.5963591
Rh	5.65267103	5.6566138	8.66239122
C	6.94243783	8.14642634	7.5643023
C	7.57018073	9.48518271	7.89339048
H	6.89959506	10.2872441	7.54895702
H	8.52830198	9.60389796	7.3710936
C	7.70607151	9.43455142	9.4205809
H	7.53138715	10.3987205	9.91341024
H	8.70115663	9.07139216	9.70153104
C	6.66037205	8.35452109	9.83426249
H	7.00983781	7.74444402	10.6777441
C	5.37034612	9.05333708	10.2504626
C	4.1293252	9.81658859	12.1286631
H	4.2444719	9.7775029	13.2156053
H	3.18090516	9.35612508	11.8261028
H	4.17112027	10.8515708	11.7677277
N	6.47951573	7.53422859	8.63990372
O	6.88027309	7.69301965	6.3660807
O	4.59064238	9.60123673	9.49129719
O	5.2460686	9.05572438	11.5975397
C	8.14006147	4.364107	7.56222211
C	9.4786185	3.73525552	7.89012089
H	10.2809638	4.40413611	7.54304158
H	9.59516463	2.77600663	7.36940537
C	9.43050259	3.6022804	9.41765056
H	10.3958184	3.77644187	9.90842336
H	9.06625302	2.60834238	9.7012995
C	8.35282594	4.65042712	9.83115684
H	7.74403265	4.30386142	10.6767319
C	9.05448404	5.94030281	10.2430049
C	9.82462434	7.18350423	12.1170039
H	9.78909724	7.0697873	13.2042201
H	9.36385158	8.13188308	11.8147854
H	10.8583616	7.14045322	11.7526686
N	7.53029305	4.82960922	8.63812791
O	7.68452484	4.42430957	6.36470666
O	9.60077183	6.71827473	9.48090728
O	9.06109757	6.0666987	11.5898846
C	3.16329436	6.94997878	7.56769858
C	1.82496123	7.57788164	7.89827901
H	1.02246595	6.90882115	7.55185367
H	1.70700416	8.53752809	7.37862957
C	1.87541458	7.70938756	9.42586208
H	0.91092889	7.53450176	9.91800693
H	2.23980513	8.7031824	9.70979686
C	2.95406309	6.66102966	9.83659275

H	3.563926	7.00686165	10.6817338
C	2.25306224	5.37062631	10.2479016
C	1.48143364	4.12792683	12.1215801
H	1.51520431	4.24235374	13.2087822
H	1.94348841	3.17973372	11.8206847
H	0.44820806	4.16983999	11.755663
N	3.77485208	6.48353958	8.64214996
O	3.61704798	6.89101776	6.36944459
O	1.70794917	4.59207688	9.48560307
O	2.24486961	5.24495167	11.5948896
H	4.38378653	1.02838616	7.53976263
H	2.75949871	1.72554583	7.37957262